Maciej Paszynski
Amanda S. Barnard
Yongjie Jessica Zhang (Eds.)

LNCS 15912

Computational Science – ICCS 2025 Workshops

25th International Conference
Singapore, Singapore, July 7–9, 2025
Proceedings, Part VI

6 Part VI

ICCS 2025

Springer

Lecture Notes in Computer Science **15912**

The series Lecture Notes in Computer Science (LNCS), including its subseries Lecture Notes in Artificial Intelligence (LNAI) and Lecture Notes in Bioinformatics (LNBI), has established itself as a medium for the publication of new developments in computer science and information technology research, teaching, and education.

LNCS enjoys close cooperation with the computer science R & D community, the series counts many renowned academics among its volume editors and paper authors, and collaborates with prestigious societies. Its mission is to serve this international community by providing an invaluable service, mainly focused on the publication of conference and workshop proceedings and postproceedings. LNCS commenced publication in 1973.

Maciej Paszynski · Amanda S. Barnard ·
Yongjie Jessica Zhang
Editors

Computational Science – ICCS 2025 Workshops

25th International Conference
Singapore, Singapore, July 7–9, 2025
Proceedings, Part VI

Springer

Editors
Maciej Paszynski
AGH University of Krakow
Krakow, Poland

Amanda S. Barnard
Australian National University
Canberra, ACT, Australia

Yongjie Jessica Zhang
Carnegie Mellon University
Pittsburgh, PA, USA

ISSN 0302-9743 ISSN 1611-3349 (electronic)
Lecture Notes in Computer Science
ISBN 978-3-031-97572-1 ISBN 978-3-031-97573-8 (eBook)
https://doi.org/10.1007/978-3-031-97573-8

This Springer imprint is published by the registered company Springer Nature Switzerland AG
The registered company address is: Gewerbestrasse 11, 6330 Cham, Switzerland

Preface

Welcome to the Workshops on Computational Science, which were co-organized with the 25th International Conference on Computational Science (ICCS - https://www.iccs-meeting.org/iccs2025/), held on July 7–9, 2025 at the Nanyang Technological University (NTU), Singapore.

This 25th edition in Singapore marked our return to a fully in-person event. Although the challenges of our present times are manifold, we have always tried our best to keep the ICCS community as dynamic, creative, and productive as possible. We are proud to present the proceedings you are reading as a result.

ICCS 2025 was jointly organized by Nanyang Technological University, the A*STAR Institute of High Performance Computing, the University of Amsterdam, and the University of Tennessee.

Considered one of the most developed countries in the world, the island country of Singapore is a major aviation, financial, and maritime shipping hub in Asia. Singapore is multilingual, multiethnic, and multicultural, and as such a very popular, safe tourism destination.

NTU Singapore is a public university ranked among the world's best, with 35,000 students, and home to the world-renowned autonomous National Institute of Education and S. Rajaratnam School of International Studies. In addition to many research institutes and centers at the university, college, and school levels, NTU also hosts two National Research Foundation (NRF) and Ministry of Education (MOE) Research Centers of Excellence, namely the Singapore Center for Environmental Life Sciences Engineering (SCELSE) and the Institute for Digital Molecular Analytics & Science (IDMxS), and 11 Corporate Labs in partnership with various industries. ICCS 2025 took place on the One-north campus.

The Institute of High Performance Computing (IHPC) is a national research institute under the Agency for Science, Technology and Research (A*STAR), dedicated to advancing science and technology through computational modeling, simulation, AI, and high-performance computing. With a multidisciplinary team of scientists and engineers, IHPC drives innovation across sectors such as advanced manufacturing, microelectronics, sustainability, maritime, and biomedical sciences. It leads Singapore's national efforts in hybrid quantum-classical computing and digital twin platforms, and partners extensively with industry and government agencies to translate deep tech into real-world impact.

The Workshops on Computational Science are a set of thematic workshops organized by experts in a particular area of Computational Science. These workshops are specifically intended to provide a forum for the discussion of novel and more focused topics in the field of Computational Science among an international group of researchers, and to strengthen the application of Computational Science in particular disciplines.

We are proud to note that this 25th edition of ICCS, with 23 workshops (the Workshops on Computational Science), one co-located event (the Asian Network of Complexity Scientists Workshop), and over 300 participants, kept to the tradition and high standards of previous editions.

The theme for 2025, "**Making Complex Systems tractable through Computational Science**", highlighted the role of Computational Science in tackling the complex problems of today and tomorrow.

ICCS is well known for its lineup of keynote speakers. The keynotes for 2025 were:

- **Johan Bollen**, Indiana University Bloomington, USA
- **Jack Dongarra**, University of Tennessee, USA
- **Mile Gu**, Nanyang Technological University, Singapore
- **Erika Fille Legara**, Center for AI Research | Asian Institute of Management, Philippines
- **Yong-Wei Zhang**, Institute of High Performance Computing, A*STAR, Singapore

This year, the Workshops on Computational Science registered 322 submissions, of which 137 were accepted as full papers, and 32 as short papers. There were on average 2.7 single-blind reviews per submission.

We would like to thank all committee members from the main track and workshops for their contribution to ensuring a high standard for the accepted papers. We would also like to thank *Springer, Elsevier,* and *Intellegibilis* for their support. Finally, we appreciate all the local organizing committee members for their hard work in preparing this conference.

We hope you enjoyed the conference and the beautiful country of Singapore.

July 2025

Maciej Paszynski
Amanda S. Barnard
Yongjie Jessica Zhang

Organization

Program Committee Chair – Workshops on Computational Science

Maciej Paszynski	AGH University of Krakow, Poland

Program Committee – Workshops on Computational Science

Amanda S. Barnard	Australian National University, Australia
Yongjie Jessica Zhang	Carnegie Mellon University, USA

Program Committee Chairs – ICCS Conference

Peter M. A. Sloot	University of Amsterdam, The Netherlands
Jack J. Dongarra	University of Tennessee, USA
Michael H. Lees	University of Amsterdam, The Netherlands
David Abramson	University of Queensland, Australia
Wentong Cai	Nanyang Technological University, Singapore
Cheong Siew Ann	Nanyang Technological University, Singapore
Su Yi	Institute for High Performance Computing, A*Star, Singapore

Local Program Committee at NTU Singapore

Ee Hou Yong	Nanyang Technological University, Singapore
Kang Hao	Nanyang Technological University, Singapore

Publicity Chairs

Leonardo Franco	University of Málaga, Spain
Muhamad Azfar Ramli	Institute for High Performance Computing, A*Star, Singapore

Impact Chair

Valeria Krzhizhanovskaya	University of Amsterdam, The Netherlands

Outreach Chair

Alfons Hoekstra	University of Amsterdam, The Netherlands

Workshop Chairs

Advances in High-Performance Computational Earth Sciences: Numerical Methods, Frameworks & Applications – IHPCES

Takashi Shimokawabe	University of Tokyo, Japan
Kohei Fujita	University of Tokyo, Japan
Dominik Bartuschat	FAU Erlangen-Nürnberg, Germany

Artificial Intelligence Approaches for Network Analysis – AIxNA

Marianna Milano	University Magna Graecia of Catanzaro, Italy
Pietro Hiram Guzzi	University Magna Graecia of Catanzaro, Italy
Giuseppe Agapito	University Magna Graecia of Catanzaro, Italy
Pietro Cinaglia	University Magna Graecia of Catanzaro, Italy

Artificial Intelligence and High-Performance Computing for Advanced Simulations – AIHPC4AS

Maciej Paszynski	AGH University of Krakow, Poland
Maciej Woźniak	AGH University of Krakow, Poland
Victor Calo	Curtin University, Australia
David Pardo	Basque Center for Applied Mathematics, Spain
Quanling Deng	Australian National University, Australia

Biomedical and Bioinformatics Challenges for Computer Science – BBC

Mario Cannataro	University Magna Graecia of Catanzaro, Italy
Giuseppe Agapito	University Magna Graecia of Catanzaro, Italy
Mauro Castelli	NOVA IMS, Universidade Nova de Lisboa, Portugal
Riccardo Dondi	Università degli Studi di Bergamo, Italy
Rodrigo Weber dos Santos	Universidade Federal de Juiz de Fora, Brazil
Italo Zoppis	University of Milano-Bicocca, Italy

Computational Diplomacy and Policy – CoDiP

Michael Lees	University of Amsterdam, Netherlands
Roland Bouffanais	University of Geneva, Switzerland
Brian Castellani	University of Durham, UK

Computational Health – CompHealth

Sergey Kovalchuk	Huawei, Russia
Georgiy Bobashev	RTI International, USA
Anastasia Angelopoulou	University of Westminster, UK

Computational Modeling and Artificial Intelligence for Social Systems – CMAISS

Tanzhe Tang	University of Amsterdam, Netherlands
Jaeyoung Kwak	Nanyang Technological University, Singapore
Takashi Kamihigashi	Kobe University, Japan
Thomas Feliciani	Politecnico di Milano, Italy

Computational Optimization, Modelling and Simulation – COMS

Xin-She Yang	Middlesex University London, UK
Slawomir Koziel	Reykjavik University, Iceland
Leifur Leifsson	Purdue University, USA

Computational Science and AI for Addressing Complex and Dynamic Societal Challenges Equitably – CASCADE

Ilkay Altintas	University of California, San Diego, USA
Manish Parashar	University of Utah, USA
David Abramson	Monash University, Australia
Melissa Floca	UC San Diego, USA

Computer Graphics, Image Processing and Artificial Intelligence – CGIPAI

Andres Iglesias Prieto	Universidad de Cantabria, Spain
Farhan Mohamed	Universiti Teknologi Malaysia, Malaysia
Chan Vei Siang	Universiti Teknologi Malaysia, Malaysia
Lihua You	Bournemouth University, UK
Akemi Galvez-Tomida	University of Cantabria, Spain

Computing and Data Science for Materials Discovery and Design – CDMDD

Ulf Schiller	University of Delaware, USA
Derek Groen	Brunel University London, UK
Xiao Xue	University College London, UK

Large Language Models and Intelligent Decision-Making within the Digital Economy – LLM-IDDE

Wei Li	National University of Singapore, Singapore
Luyao Zhu	Nanyang Technological University, Singapore
Yi Qu	Chinese Academy of Sciences, China
Muyang Li	University of Chinese Academy of Sciences, China
Yunlong Mi	University of Chinese Academy of Sciences, China

Machine Learning and Data Assimilation for Dynamical Systems – MLDADS

Rossella Arcucci	Imperial College London, UK
Sibo Cheng	ENPC, France

Multi-Criteria Decision-Making: Methods, Applications, and Innovations – MCDM

Wojciech Sałabun	National Institute of Telecommunications, Poland
Jarosław Wątróbski	University of Szczecin, Poland

(Credible) Multiscale Modelling and Simulation – MMS

Derek Groen	Brunel University London, UK
Diana Suleimenova	Brunel University London, UK
Bartosz Bosak	PSNC, Poland

Numerical Algorithms and Computer Arithmetic for Computational Science – NACA

Paweł Gepner	Warsaw University of Technology, Poland
Ewa Deelman	USC Information Sciences Institute, USA
Hatem Ltaief	King Abdullah University of Science and Technology, Saudi Arabia

Quantum Computing – QCW

Katarzyna Rycerz	AGH University of Technology, Poland
Marian Bubak	AGH University of Krakow, Poland and University of Amsterdam, Netherlands

Quantum-Enhanced Agents and Recurrent Computation – QuARC

Mile Gu	Nanyang Technological University, Singapore

Retrieval-Augmented Generation – RAGW

Aleksander Smywiński-Pohl	AGH University of Krakow, Poland
Magdalena Król	AGH University of Krakow, Poland

Simulations of Flow and Transport: Modeling, Algorithms and Computation – SOFTMAC

Shuyu Sun	King Abdullah University of Science and Technology, Saudi Arabia
Jingfa Li	Yangtze University, China
James Liu	Colorado State University, USA

Smart Systems: Bringing Together Computer Vision, Sensor Networks and Artificial Intelligence – SmartSys

Pedro J. S. Cardoso	University of the Algarve, Portugal
Roberto Lam	University of the Algarve, Portugal
Jânio Monteiro	University of the Algarve, Portugal
João M. F. Rodrigues	University of the Algarve, Portugal
Jaime A. Martins	University of the Algarve, Portugal

Solving Problems with Uncertainty – SPU

Vassil Alexandrov	Hartree Centre STFC, UK
Aneta Karaivanova	IPP-BAS, Bulgaria

Teaching Computational Science – WTCS

Evguenia Alexandrova	STFC - Hartree Centre, UK
Tseden Taddese	Hartree Centre - STFC, UK

Reviewers

Zeeshan Abbas	Sungkyunkwan University, South Korea
David Abramson	Monash University, Australia
Tesfamariam Mulugeta Abuhay	University of Gondar, Ethiopia
Giuseppe Agapito	Università Magna Graecia Catanzaro, Italy
Adriano Agnello	STFC Hartree Centre, UK
Elisabete Alberdi	University of the Basque Country UPV/EHU, Spain
Vassil Alexandrov	Hartree Centre STFC, UK
Evguenia Alexandrova	STFC - Hartree Centre, UK
Rayner Alfred	Universiti Malaysia Sabah, Malaysia
Shaukat Ali	Simula Research Laboratory and Oslo Metropolitan University, Norway
Ilkay Altintas	University of California, San Diego, USA
Julen Alvarez-Aramberri	University of the Basque Country (UPV/EHU), Spain
Domingos Alves	University of São Paulo, Brazil
Sergey Alyaev	NORCE, Norway
Anastasia Anagnostou	Brunel University, UK
Anastasia Angelopoulou	University of Westminster, UK
Hideo Aochi	BRGM, France
Rossella Arcucci	Imperial College of London, UK
Paula Bajdor	Częstochowa University of Technology, Poland
Krzysztof Banaś	AGH University of Krakow, Poland
Luca Barillaro	Magna Graecia University of Catanzaro, Italy
Dominik Bartuschat	FAU Erlangen-Nürnberg, Germany

Pouria Behnoudfar	Curtin University, Australia
Jörn Behrens	University of Hamburg, Germany
Gebrail Bekdas	Istanbul University, Turkey
Mehmet Ali Belen	Iskenderun Technical University, Turkey
Sana Ben Abdallah Ben Lamine	University of Manouba, Tunisia
Stefano Beretta	San Raffaele Telethon Institute for Gene Therapy, Italy
Benjamin Berkels	RWTH Aachen University, Germany
Gabriele Bertoli	University of Florence, Italy
John Betts	Monash University, Australia
Kishor Bharti	National University of Singapore, Singapore
Asniyani Nur Haidar Binti Abdullah	Universiti Teknikal Malaysia Melaka, Malaysia
Piotr Biskupski	IBM, Poland
Georgiy Bobashev	RTI International, USA
Klavdiya Bochenina	ITMO University, Russia
Carlos Bordons	University of Seville, Spain
Kamil Bortko	West Pomeranian University of Technology in Szczecin, Poland
Bartosz Bosak	PSNC, Poland
Lorella Bottino	University Magna Graecia Catanzaro, Italy
Roland Bouffanais	University of Geneva, Switzerland
Marian Bubak	AGH Krakow, Poland and University of Amsterdam, Netherlands
Keith Butler	University College London, UK
Aleksander Byrski	AGH University of Krakow, Poland
Cristiano Cabrita	Universidade do Algarve, Portugal
Xing Cai	Simula Research Laboratory, Norway
Carlos T. Calafate	Universitat Politècnica de València, Spain
Victor Calo	Curtin University, Australia
Almudena Campuzano	University of Amsterdam, Netherlands
Mario Cannataro	University Magna Graecia of Catanzaro, Italy
Karol Capała	AGH University of Krakow, Poland
Pedro J. S. Cardoso	Universidade do Algarve, Portugal
Brian Castellani	University of Durham, UK
Mauro Castelli	NOVA IMS, Universidade Nova de Lisboa, Portugal
Nicholas Chancellor	Durham University, UK
Prasenjit Chatterjee	MCKV Institute of Engineering, India
Boyang Chen	Imperial College London, UK
Sibo Cheng	ENPC, France
Su-Fong Chien	MIMOS Berhad, Malaysia

Marta Chinnici	ENEA - Italian National Agency for New Technologies, Energy and Sustainable Economic Development, Italy
Witold Chmielarz	University of Warsaw, Poland
Bastien Chopard	University of Geneva, Switzerland
Maciej Ciesielski	University of Massachusetts, USA
Pietro Cinaglia	University Magna Graecia of Catanzaro, Italy
Noélia Correia	Universidade do Algarve, Portugal
Adriano Cortes	University of Rio de Janeiro, Brazil
Ana Cortes	Universitat Autònoma de Barcelona, Spain
Enrique Costa-Montenegro	Universidad de Vigo, Spain
David Coster	Max Planck Institute for Plasma Physics, Germany
Carlos Cotta	Universidad de Málaga, Spain
Matteo Croci	Basque Center for Applied Mathematics, Spain
Daan Crommelin	CWI Amsterdam, Netherlands
Attila Csikasz-Nagy	King's College London, UK/Pázmány Péter Catholic University, Hungary
António Cunha	UTAD, Portugal
Pawel Czarnul	Gdańsk University of Technology, Poland
Pasqua D'Ambra	IAC-CNR, Italy
Dong Dai	University of Delaware, USA
Lisandro Dalcin	KAUST, Saudi Arabia
Haluk Damgacioglu	Medical University of South Carolina, USA
Bhaskar Dasgupta	University of Illinois Chicago, USA
Subhasis Dasgupta	University of California, San Diego, USA
Ewa Deelman	USC Information Sciences Institute, USA
Quanling Deng	Australian National University, Australia
Muhammet Deveci	National Defense University, Turkey
Jean Dezert	Onera, France
Jacek Długopolski	AGH University of Science and Technology, Poland
Riccardo Dondi	Università degli Studi di Bergamo, Italy
Rafal Drezewski	AGH University of Krakow, Poland
Hans du Buf	University of the Algarve, Portugal
Witold Dzwinel	AGH University of Science and Technology, Poland
Rob E. Loke	Amsterdam University of Applied Sciences, Netherlands
Wouter Edeling	Vrije Universiteit Amsterdam, Netherlands
Nahid Emad	Paris-Saclay University, France
Christian Engelmann	ORNL, USA
Aniello Esposito	Hewlett Packard Enterprise, Switzerland

Fedra Rosita Falvo	University Magna Graecia of Catanzaro, Italy
Thomas Feliciani	Politecnico di Milano, Italy
Jinyuan Feng	Research Center on Fictitious Economy & Data Science, China
Anna Fernandez	Basque Center for Applied Mathematics, Spain
Nicola Ferrier	Argonne National Laboratory, USA
Melissa Floca	University of California San Diego, USA
Marcin Fojcik	Western Norway University of Applied Sciences, Norway
Piotr Frąckiewicz	Pomeranian University, Poland
Alberto Freitas	University of Porto, Portugal
Kohei Fujita	University of Tokyo, Japan
Takeshi Fukaya	Hokkaido University, Japan
Wlodzimierz Funika	AGH University of Krakow, Poland
Ernst Fusch	Siemens Labs, Siemens AG, Germany
Teresa Galvão	University of Porto, Portugal
Akemi Galvez-Tomida	University of Cantabria, Spain
Luis Garcia-Castillo	Universidad Carlos III de Madrid, Spain
Bartłomiej Gardas	Jagiellonian University, Poland
Piotr Gawron	Nicolaus Copernicus Astronomical Centre, Polish Academy of Sciences, Poland
Bernhard Geiger	Know-Center GmbH, Austria
Paweł Gepner	Warsaw University of Technology, Poland
Maziar Ghorbani	Brunel University London, UK
Alexandrino Gonçalves	Polytechnic University of Leiria, Portugal
Simon Goodchild	STFC, UK
Yuriy Gorbachev	Soft-Impact LLC, Russia
Pawel Gorecki	University of Warsaw, Poland
Derek Groen	Brunel University London, UK
Mile Gu	Nanyang Technological University, Singapore
Joel Guerreiro	University of the Algarve, Portugal
Manish Gupta	Harish-Chandra Research Institute, India
Piotr Gurgul	Snapchat, Switzerland
Oscar Gustafsson	Linköping University, Sweden
Pietro Hiram Guzzi	University Magna Graecia of Catanzaro, Italy
Zulfiqar Habib	COMSATS University Islamabad, Lahore Campus, Pakistan
Laura Harbach	Brunel University London, UK
Mohamed Hassan	Virginia Tech, USA
Alexander Heinecke	Intel Parallel Computing Lab, USA
Teiko Heinosaari	University of Jyväskylä, Finland

Marcin Hernes	Wrocław University of Economics and Business, Poland
Maximilian Höb	Leibniz-Rechenzentrum der Bayerischen Akademie der Wissenschaften, Germany
Xiao Hou	Beihang University, China
Huda Ibeid	Intel Corporation, USA
Andres Iglesias Prieto	Universidad de Cantabria, Spain
Alireza Jahani	Brunel University London, UK
Jaroslaw Jankowski	West Pomeranian University of Technology, Poland
Peter Janku	Tomas Bata University in Zlín, Czechia
Jiří Jaroš	Brno University of Technology, Czechia
Hang-Hyun Jo	Catholic University of Korea, South Korea
Takashi Kamihigashi	Kobe University, Japan
John Kang	San Diego State University, USA
Aneta Karaivanova	IPP-BAS, Bulgaria
Haruo Kobayashi	Gunma University, Japan
Łukasz Kobyliński	Institute of Computer Science, Polish Academy of Sciences, Poland
Marcel Koch	KIT, Germany
Bartłomiej Kocot	AMD, USA
Ivana Kolingerova	University of West Bohemia, Czechia
Joanna Kołodziejczyk	National Institute of Telecommunications, Poland
Georgy Kopanitsa	Tomsk Polytechnic University, Russia
Sergey Kovalchuk	Huawei, Russia
Slawomir Koziel	Reykjavik University, Iceland
Marek Kozłowski	OPI PIB, Poland
Ronald Kriemann	Max Planck Institute for Mathematics in the Sciences, Germany
Magdalena Król	AGH University of Krakow, Poland
Valeria Krzhizhanovskaya	University of Amsterdam, Netherlands
Marek Kubalcik	Tomas Bata University in Zlín, Czechia
Sebastian Kuckuk	Friedrich-Alexander-Universität Erlangen-Nürnberg, Germany
Krzysztof Kurowski	Poznań Supercomputing and Networking Center, Poland
Halim Kusumaatmaja	Durham University, UK
Marcin Kuta	AGH University of Science and Technology, Poland
Jaeyoung Kwak	Nanyang Technological University, Singapore
Roberto Lam	ISE - Universidade do Algarve, Portugal
Marek Lampart	VŠB-Technical University of Ostrava, Czechia

Ilaria Lazzaro	Università degli studi Magna Graecia di Catanzaro, Italy
Paola Lecca	Free University of Bozen-Bolzano, Italy
Michael Lees	University of Amsterdam, Netherlands
Leifur Leifsson	Purdue University, USA
Kenneth Leiter	Army Research Laboratory, USA
Yu Leng	Los Alamos National Laboratory, USA
Paulina Lewandowska	IT4Innovations National Supercomputing Center, Czechia
Muyang Li	University of Chinese Academy of Sciences, China
Wei Li	National University of Singapore, Singapore
Jingfa Li	Yangtze University, China
Tomer Libal	University of Luxembourg, Luxembourg
Che Liu	Imperial College London, UK
Zhao Liu	National Supercomputing Center in Wuxi, China
James Liu	Colorado State University, USA
Marcelo Lobosco	Federal University of Juiz de Fora, Brazil
Jay Lofstead	Sandia National Laboratories, USA
Chu Kiong Loo	University of Malaya, Malaysia
Marcin Łoś	AGH University of Krakow, Poland
Hatem Ltaief	King Abdullah University of Science and Technology, Saudi Arabia
Stefan Luding	University of Twente, Netherlands
Piotr Luszczek	University of Tennessee Knoxville, USA
Pedro M. M. Guerreiro	Universidade do Algarve, Portugal
Raghu Machiraju	Ohio State University, USA
Peyman Mahouti	Yildiz Technical University, Turkey
Krzysztof Małecki	West Pomeranian University of Technology, Poland
Alexander Malyshev	UiB, Norway
Anirban Mandal	Renaissance Computing Institute, USA
Livia Marcellino	University of Naples Parthenope, Italy
Tomas Margalef	Universitat Autònoma de Barcelona, Spain
Osni Marques	Lawrence Berkeley National Laboratory, USA
Ignacio Martinez-Moyano	Argonne National Laboratory, USA
Maria Chiara Martinis	Università Magna Graecia di Catanzaro, Italy
Jaime A. Martins	University of the Algarve, Portugal
Michele Martone	Max-Planck-Institut für Plasmaphysik, Germany
Pawel Matuszyk	Baker Hughes Inc., USA
Valerie Maxville	Curtin University, Australia
Francesca Mazzia	Università di Bari Aldo Moro, Italy

Wagner Meira Jr.	Universidade Federal de Minas Gerais, Brazil
Roderick Melnik	Wilfrid Laurier University, Canada
Ivan Merelli	Institute for Biomedical Technologies - National Research Council, Italy
Yunlong Mi	University of Chinese Academy of Sciences, China
Jakub Mielczarek	Jagiellonian University, Poland
Marianna Milano	Università Magna Græcia di Catanzaro, Italy
Jaroslaw Miszczak	Institute of Theoretical and Applied Informatics, Polish Academy of Sciences, Poland
Farhan Mohamed	Universiti Teknologi Malaysia, Malaysia
Mohd Khalid Mokhtar	Universiti Teknikal Malaysia Melaka, Malaysia
Fernando Monteiro	Polytechnic Institute of Bragança, Portugal
Jânio Monteiro	University of the Algarve, Portugal
Andrew Moore	University of California Santa Cruz, USA
Anabela Moreira Bernardino	Polytechnic Institute of Leiria, Portugal
Eugénia Moreira Bernardino	Polytechnic Institute of Leiria, Portugal
Leonid Moroz	Warsaw Technology University, Poland
Dariusz Mrozek	Silesian University of Technology, Poland
Peter Mueller	IBM Zurich Research Laboratory, Switzerland
Judit Munoz-Matute	University of the Basque Country, Spain
Ikmal Faiq Albakri Mustafa Albakri	Universiti Teknikal Malaysia Melaka, Malaysia
Hiromichi Nagao	University of Tokyo, Japan
Fallah Najjar	Al-Furat Al-Awsat Technical University, Iraq
Kengo Nakajima	University of Tokyo, Japan
Philipp Neumann	Helmut-Schmidt-Universität, Germany
Sinan Melih Nigdeli	Istanbul University, Turkey
Anita Nikolich	University of Illinois Urbana-Champaign, USA
Hitoshi Nishizawa	Sony Research Labs., Japan
Joseph O'Connor	University of Edinburgh, UK
Lidia Ogiela	AGH University of Krakow, Poland
Ángel Javier Omella	University of the Basque Country (UPV/EHU), Spain
Kenji Ono	Kyushu University, Japan
Hiroyuki Ootomo	NVIDIA, Japan
Eneko Osaba	TECNALIA Research & Innovation, Spain
Joanna Paliszkiewicz	Warsaw University of Life Sciences, Poland
Dragan Pamučar	University of Belgrade, Serbia
George Papadimitriou	Apple, USA
Nikela Papadopoulou	University of Glasgow, UK
Manish Parashar	University of Utah, USA

David Pardo	University of the Basque Country and IKERBASQUE, Spain
Dário Passos	CENTRA-IST, Portugal
Zbigniew Pastuszak	Maria Curie-Skłodowska University, Poland
Anna Paszynska	Jagiellonian University, Poland
Maciej Paszynski	AGH University of Krakow, Poland
Abani Patra	Tufts University, USA
Lukasz Pawela	Institute of Theoretical and Applied Informatics, Polish Academy of Sciences, Poland
Sara Perez Carabaza	Universidad de Cantabria, Spain
Piotr Pęzik	University of Łódź, Poland
Frank Phillipson	TNO, Netherlands
Anna Pietrenko-Dabrowska	Gdańsk University of Technology, Poland
Armando Pinho	University of Aveiro, Portugal
Yuri Pirola	Università degli Studi di Milano-Bicocca, Italy
Ollie Pitts	Imperial College London, UK
Beth Plale	Indiana University, USA
Robert Platt	Imperial College London, UK
Paweł Pławiak	Cracow University of Technology, Poland
Michal Pluhacek	AGH University of Krakow, Poland
Paweł Poczekajło	Koszalin University of Technology, Poland
Valeria Popello	University Magna Graecia of Catanzaro, Italy
Cristina Portales	Universidad de Valencia, Spain
Simon Portegies Zwart	Leiden University, Netherlands
Anna Procopio	Università Magna Graecia di Catanzaro, Italy
Małgorzata Przybyła-Kasperek	Uniwersytet Śląski w Katowicach, Poland
Ubaid Ali Qadri	Science and Technology Facilities Council, UK
Yipeng Qin	Cardiff University, UK
Yi Qu	Chinese Academy of Sciences, China
Andrianirina Rakotoharisoa	Imperial College London, UK
Raul Ramirez	Tecnológico de Monterrey, Mexico
Célia Ramos	University of the Algarve, Portugal
Georgia Ray	Imperial College London, UK
Robin Richardson	Netherlands eScience Center, Netherlands
Heike Riel	IBM Research - Zurich, Switzerland
João M. F. Rodrigues	Universidade do Algarve, Portugal
Daniel Rodriguez	University of Alcalá, Spain
Marcin Rogowski	Saudi Aramco, Saudi Arabia
Sergio Rojas	Monash University, Australia
Albert Romkes	South Dakota School of Mines and Technology, USA
Tomasz Rybotycki	IBS PAN, CAMK PAN, AGH, Poland

Katarzyna Rycerz	AGH University of Technology, Poland
Emre Sahin	UKRI STFC Hartree Centre, UK
Wojciech Sałabun	National Institute of Telecommunications, Poland
Özlem Salehi	Özyeğin University, Turkey
Ayşin Sancı	altinay, Turkey
Allah Bux Sargano	COMSATS University Islamabad, Lahore Campus, Pakistan
Jaromir Savelka	Carnegie Mellon University, USA
Robert Schaefer	AGH University of Krakow, Poland
Ulf Schiller	University of Delaware, USA
Tapan Senapati	Southwest University, China
Paulina Sepúlveda-Salas	Pontificia Universidad Católica de Valparaíso, Chile
Marzia Settino	Universita Magna Graecia Catanzaro, Italy
Mostafa Shahriari	Basque Center for Applied Mathematics, Spain
Pengyuan Shao	Imperial College London, UK
Takashi Shimokawabe	University of Tokyo, Japan
Bhargav Sriram Siddani	Lawrence Berkeley National Laboratory, USA
Marcin Sieniek	Google Brain, USA
Haozhen Situ	South China Agricultural University, China
Leszek Siwik	AGH University of Krakow, Poland
Grażyna Ślusarczyk	Jagiellonian University, Poland
Maciej Smołka	AGH University of Krakow, Poland
Michalis Smyrnakis	STFC, UK
Aleksander Smywiński-Pohl	AGH University of Krakow, Poland
Isabel Sofia Brito	Instituto Politécnico de Beja, Portugal
Chengxi Song	University of Chinese Academy of Sciences, China
Robert Staszewski	University College Dublin, Ireland
Željko Stević	University of East Sarajevo, Bosnia and Herzegovina
Magdalena Stobinska	University of Gdansk and Institute of Physics, Polish Academy of Sciences, Poland
Barbara Strug	Jagiellonian University, Poland
Karol Struniawski	Warsaw University of Life Sciences - SGGW, Poland
Diana Suleimenova	Brunel University London, UK
Shuyu Sun	King Abdullah University of Science and Technology, Saudi Arabia
Martin Swain	Aberystwyth University, UK
Tseden Taddese	Hartree Centre - STFC, UK
Claude Tadonki	Mines ParisTech/CRI - Centre de Recherche en Informatique, France

Chi Wee Tan	Tunku Abdul Rahman University of Management and Technology, Malaysia
Tanzhe Tang	University of Amsterdam, Netherlands
Andrew Tangarra	Centre for Quantum Technologies, Singapore
Osamu Tatebe	University of Tsukuba, Japan
Michela Taufer	University of Tennessee Knoxville, USA
Jamie Taylor	CUNEF Universidad, Spain
Andrei Tchernikh	CICESE Research Center, Mexico
Marco ten Eikelder	TU Darmstadt, Germany
Kasim Terzic	University of St Andrews, UK
Jannis Teunissen	Centrum Wiskunde & Informatica, Netherlands, KU Leuven, Belgium
Jayne Thompson	National University of Singapore, Singapore
Sue Thorne	UKRI Science and Technology Facilities Council, UK
Vinod Tipparaju	ByteDance, USA
Pawel Topa	AGH University of Science and Technology, Poland
Ola Torudbakken	Meta, Norway
Paolo Trunfio	University of Calabria, Italy
Eirik Valseth	South Dakota School of Mines and Technology, USA
Aleksandra Vatian	ITMO University, Russia
Chan Vei Siang	Universiti Teknologi Malaysia, Malaysia
Milana Vuckovic	European Centre for Medium-Range Weather Forecasts, UK
Jianwu Wang	University of Maryland, Baltimore County, USA
Shaoni Wang	University of Groningen, Netherlands
Peng Wang	NVIDIA, China
Ximing Wang	Nanyang Technological University, Singapore
Jarosław Wąs	AGH University of Krakow, Poland
Jarosław Wątróbski	University of Szczecin, Poland
Rodrigo Weber dos Santos	Universidade Federal de Juiz de Fora, Brazil
Mei Wen	National University of Defense Technology, China
Wendy Winnard	UKRI STFC, UK
Konrad Wojtasik	Politechnika Wrocławska, Poland
Maciej Wołoszyn	AGH University of Science and Technology, Poland
Maciej Woźniak	AGH University of Krakow, Poland
Michał Wroński	NASK National Research Institute, Poland
Dunhui Xiao	Tongji University, China
Huilin Xing	University of Queensland, Australia

Xiao Xue	University College London, UK
Jiayu Xue	UCAS, China
Yani Xue	Brunel University London, UK
Xin-She Yang	Middlesex University, UK
Lihua You	Bournemouth University, UK
Sebastian Zając	SGH Warsaw School of Economics, Poland
Małgorzata Zajęcka	AGH University of Krakow, Poland
Gabor Závodszky	University of Amsterdam, Netherlands
Justyna Zawalska	ACC Cyfronet AGH, Poland
Wei Zhang	Huazhong University of Science and Technology, China
Tianchi Zhao	University of Chinese Academy of Sciences, China
Lei Zheng	University of Chinese Academy of Sciences, China
Luyao Zhu	Nanyang Technological University, Singapore
Kewei Zhu	University College London, UK
Beata Zielosko	University of Silesia in Katowice, Poland
Ewa Ziemba	University of Economics in Katowice, Poland
Italo Zoppis	University of Milano-Bicocca, Italy
Chiara Zucco	Università degli Studi “Magna Graecia” di Catanzaro, Italy
Pavel Zun	ITMO University, Russia
Karol Życzkowski	Jagiellonian University, Poland

Contents – Part VI

Smart Systems: Bringing Together Computer Vision, Sensor Networks and Artificial Intelligence

Formal Security Analysis of the Authentication Protocol in Smart Cities Using AVISPA 3
Hyewon Park and Yohan Park

Automatic Help Summoning Through Speech Analysis on Mobile Devices 18
Bożena Małysiak-Mrozek, Paweł Wojaczek, Krzysztof Tokarz, Vaidy Sunderam, Dariusz Mrozek, and Jean-Charles Lamirel

Leveraging Graph Digital Twin for Fault Detection and Improved Power Grid Stability in Smart Cities 33
Anubhav Mendhiratta, Craig Fernandes, Dharini Hindlatti, Divyansh Vinayak, and Chandrashekhar Pomu Chavan

PEMS-API: Malware Classification Using Parameter-Enhanced Multi-dimensional API Sequence Features 48
Han Miao, Wen Wang, Wanqian Zhang, and Feng Liu

The Effectiveness of Visual Attention Patterns in the Process of Spatial Exploration in a 3D Video Game Environment 63
Bartosz Krukowski, Mateusz Zawisza, Aneta Wiśniewska, Adam Wojciechowski, and Rafał Szrajber

A New Way to Generate Urban Environments for Video Games Using the Architectural Impression Curve Method 78
Andrzej Sasinowski, Aneta Wiśniewska, Jarosław Andrzejczak, Adam Wojciechowski, and Rafał Szrajber

Enhancing Learning in Augmented Reality (AR): A Deep Learning Framework for Predicting Memory Retention in AR Environments 92
Onyeka J. Nwobodo, Godlove Suila Kuaban, Kamil Wereszczyński, and Krzysztof A. Cyran

Solving Problems with Uncertainty

Unified and Diverse Coalition Formation in Dispersed Data Classification – A Conflict Analysis Approach with Weighted Decision Trees 109
Małgorzata Przybyła-Kasperek and Jakub Sacewicz

From Uncertainty to Semantics in Self-reported Data: An Empirical Analysis 125
Salvatore F. Pileggi and Gnana Bharathy

Uncertainties in Modeling Psychological Symptom Networks: The Case of Suicide 140
Valeria Epelbaum, Sophie Engels, Rory O'Connor, Denny Borsboom, Derek De Beurs, and Valeria Krzhizhanovskaya

Making Astrometric Solver Tractable Through In-Situ Visual Analytics 154
Konstantin Ryabinin, Wolfgang Löffler, Olga Erokhina, Gerasimos Sarras, and Michael Biermann

Scheduling in Workflow-as-a-Service Model with Pre-parameterized DAG Using Inaccurate Estimates 168
Victor Toporkov, Dmitry Yemelyanov, and Artem Bulkhak

Global Sensitivity Analysis for a Mathematical Model of the General Escape Theory of Suicide 183
Sophie Engels, Valeria Epelbaum, Shirley B. Wang, Derek de Beurs, and Valeria Krzhizhanovskaya

Multidimensional Granular Approach to Solving Fuzzy Complex System of Linear Equations 198
Marek Landowski

An Algorithm for Calculating the Multidimensional Solution of the Fuzzy Sylvester Matrix Equation 213
Marek Landowski

Modelling Extreme Uncertainty: Queues with Pareto Inter-arrival Times and Pareto Service Times 222
Raul Ramirez-Velarde, Cristobal Pareja-Flores, Neil Hernandez-Gress, and Laura Hervert-Escobar

Teaching Computational Science

Best Practices in Teaching Digitization and Process Automation - A Case Study of Warsaw University of Technology 239
Wojtachnik Robert, Gavkalova Nataliia, Krawiec Jerzy, and Martin John

Contrast Computation for Improved Visibility and User Experience in Educational Interfaces 254
Agnieszka Olejnik-Krugly, Anna Lewandowska, Maja Dzisko, and Jarosław Jankowski

The Role of Sustainability Competences for IT Systems Engineers 269
Aleksander Buczacki, Bartlomiej Gladysz, Aldona Kluczek, Krzysztof Krystosiak, Krzysztof Ejsmont, Izabela Malenczyk, Rodolfo Haber Guerra, Erika Palmer, and Tim van Erp

Smart Product-Service System for Intelligent Welding System 285
Mariusz Salwin and Tomasz M. Chmielewski

The Use of Artificial Intelligence and Virtual Computer Laboratories to Develop Computer Science Education 305
Andrzej Kamiński, Martyna Wybraniak-Kujawa, Sergio Iserte, and Jerzy Krawiec

Exploring AI Applications in Business: Case Studies on Key Competencies for Professionals 320
Aleksandra Kopyto, Mahtab Afsari, and Bartosz Wachnik

The Use of the Chat GPT to Solve Mathematical Programming Tasks: A Didactic Experiment with the Participation of Warsaw University of Life Sciences Students 333
Włodzimierz Wojas and Piotr Stachura

Service-Oriented Architecture: Learning with Generative AI and AWS 347
Marcela Castro León, Dolores Rexachs, and Emilio Luque

Author Index 355

Smart Systems: Bringing Together Computer Vision, Sensor Networks and Artificial Intelligence

Formal Security Analysis of the Authentication Protocol in Smart Cities Using AVISPA

Hyewon Park and Yohan Park(✉)

School of Computer Engineering, Keimyung University, Daegu, Republic of Korea
wldnjsfuf@stu.kmu.ac.kr, yhpark@kmu.ac.kr

Abstract. Smart cities optimize traffic management and vehicle communication through Intelligent Transportation Systems (ITS), with Vehicular Ad-hoc Networks (VANET) serving as a core infrastructure. In these environments, security vulnerabilities can severely impact the smart city traffic system, leading to traffic congestion, blockage of emergency vehicle routes, and disruption of autonomous driving systems. Unfortunately, identifying security vulnerabilities of the system in VANET is complex due to various attack types and the dynamic nature of the network, requiring systematic verification techniques for effective analysis. Recently, Nath et al. proposed an authentication protocol for VANETs using LWE-based lattice signatures and tokens, however the protocol has not been sufficiently validated. This study utilizes AVISPA (Automated Validation of Internet Security Protocols and Applications) to analyze Nath et al.'s protocol. AVISPA, an automated security verification tool based on the Dolev-Yao(DY) attacker model, is effective in assessing various threats such as replay attacks and man-in-the-middle attacks, making it ideal for evaluating security in the VANET environment. The security analysis reveals that the protocol is vulnerable to multiple attacks due to the lack of message freshness verification and user authentication. To address these vulnerabilities, we propose countermeasures to enhance message freshness verification and user authentication mechanisms, and validate the improved protocol's security through AVISPA simulation. Finally, we verify the security of the authentication scheme which is applied the countermeasures through AVISPA. The result shows that the security of smart city vehicular networks can be strengthened through AVISPA-based security verification and this can provide valuable insights for designing security protocols in smart cities.

Keywords: Intelligent Transportation System · Vehicular Ad-hoc Networks · Lattice-based cryptography · security protocol analysis · AVISPA simulation · sybil attack · eclipse attack

1 Introduction

Smart cities achieve efficient urban operations through Intelligent Transportation Systems (ITS), which optimize traffic management and facilitate seamless

M. Paszynski et al. (Eds.): ICCS 2025 Workshops, LNCS 15912, pp. 3–17, 2025.
https://doi.org/10.1007/978-3-031-97573-8_1

vehicle communication [6]. Vehicular Ad-hoc Networks (VANET) play a critical role in the transportation infrastructure of smart cities, enabling real-time data exchange between vehicles (V2V) and between vehicles and infrastructure (V2I). This allows for the optimization of traffic flow, accident prevention, and the enhancement of emergency response systems [14]. Furthermore, VANET is also employed in various user-centric services such as road traffic load balancing, 3D navigation, and in-vehicle entertainment services [9].

However, if security vulnerabilities exist in VANET, a smart city's traffic management system could be significantly affected by malicious actors. For instance, replay attack or sybil attack [4] could disseminate false traffic information, leading to large-scale congestion or malfunctioning emergency vehicle priority systems. Additionally, an eclipse attack [8] that isolates a specific vehicle from the network could mislead autonomous vehicles into making incorrect decisions, potentially resulting in severe accidents. Thus, ensuring the security of VANET in smart cities is not only essential for traffic management but also crucial for maintaining overall urban stability and trust. To address these security challenges, robust authentication mechanisms are required, and it is critical to assess whether existing approaches provide sufficient security in VANET environments.

The previously proposed authentication methods in the VANET environment provide security using cryptographic algorithms based on mathematical challenges such as the discrete logarithm problem or integer factorization, like Rivest-Shamir-Adleman (RSA) and Elliptic-Curve Cryptography (ECC) [5,18,21]. However, with advancements in quantum algorithms, their vulnerabilities have become increasingly apparent [7,19]. To address this issue, Nath et al. (2024) [15] proposed an authentication scheme that integrates a lattice-based signature mechanism based on the Learning With Errors (LWE) problem and a token-based authentication approach. This scheme claims to enhance anonymity using pseudo-identities and to enable fast authentication via a token-based mechanism. However, our analysis reveals that this approach is vulnerable to various attacks, including replay attack, impersonation attack, insider attack, table leakage attack, denial-of-service (DoS) attack, eclipse attack, and sybil attack.

In this paper, we review the lattice-based authentication protocol proposed by Nath et al. and conduct a formal simulation analysis using the Automated Validation of Internet Security Protocols and Applications (AVISPA) [1] version 1.6 tool. This formal analysis method is effective for evaluating protocol security [10,11,16,17,20]. Finally, we demonstrate that this scheme is not suitable for real-world VANET environments and provide recommendations to address its vulnerabilities and enhance security.

2 Preliminaries

2.1 System Model

In a VANET environment, authentication and message exchange involve trusted entities such as the Trusted Authority (TA), Road Side Unit (RSU), and

Onboard Unit (OBU). The TA oversees information exchange and ensures secure communication over wireless media after vehicle registration. The RSU serves as infrastructure, managing vehicle authentication and parameters, while the OBU utilizes these functions to communicate with RSUs or other vehicles. In a high-speed vehicular environment, authentication must occur with minimal delay, necessitating advanced security designs. The overall system model is shown in Fig. 1.

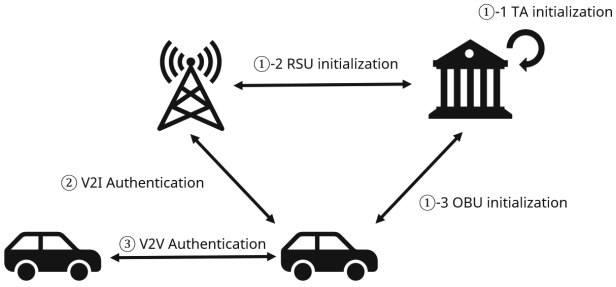

Fig. 1. System model.

2.2 Threat Model

Nath et al. conducted a security analysis using the Dolev-Yao (DY) [3] and Canetti-Krawczyk (CK) [2] attacker models. The attackers in the DY and CK models possess the following capabilities:

- The attacker can eavesdrop, intercept, modify, delete, and manipulate messages transmitted over public channels.
- The attacker may guess the legitimate user's identity or password but cannot accurately guess both simultaneously.
- The attacker can compromise security by launching impersonation attack, replay attack, and man-in-the-middle attack.
- These models assume perfect cryptographic primitives, meaning encrypted messages are infeasible to decrypt without the corresponding key.
- The attacker can leak certain secret information, such as temporary nonces and session keys.

2.3 Lattice-Based Cryptography

Lattice-based cryptography provides strong resistance against quantum attacks due to the computational hardness of solving problems like the Shortest Vector Problem (SVP) and Learning With Errors (LWE) [12]. These problems are

computationally hard even for quantum computers, making lattice-based cryptography a promising alternative to classical public-key systems. A widely used encryption method relies on the LWE problem, where messages are encoded using a random matrix A, a secret key sek, and an error term e [13].The encryption process follows:

$$c = (A, \lfloor A \cdot sek + e + \text{encode}(m) \rceil) . \tag{1}$$

For decryption:

$$m = \text{decode}(\lfloor g \rceil - A \cdot sek). \tag{2}$$

Here, $\lfloor . \rceil$ denotes a rounding function that maps a point $a \in \mathbb{R}^n$ onto a lattice code $(\wedge, \lfloor . \rceil_\wedge)$:

$$a = \lfloor a \rceil_\Lambda + [a]_\Lambda, \tag{3}$$

where $\lfloor a \rceil_\Lambda \in \wedge$ is the quantized lattice point and $[a]_\Lambda \in \mathcal{V}_\wedge$ represents the rounding error. This transformation ensures efficient message encoding with minimal decoding errors.

2.4 AVISPA

To formally verify the proposed protocol, we utilize AVISPA [1], a widely used tool for security assessment. AVISPA is a well-known simulation tool for verifying the security of internet protocols and applications, particularly effective in evaluating vulnerabilities such as replay attack and man-in-the-middle attack. This tool employs code written in the High-Level Protocol Specification Language (HLPSL) and utilizes four backend models: Constraint-Logic-Based Attack Searcher (CL-AtSE), On-the-Fly Model Checker (OFMC), SAT-Based Model Checker (SATMC), and Tree-Automata-Based Protocol Analyzer (TA4SP). To assess the security properties of the protocol, the HLPSL code is first converted into an intermediate format using the HLPSL2IF translator, after which the backend models perform the verification.

3 Review of Nath et al.'s Scheme

This section provides an overview of the model proposed by Nath et al. The scheme is divided into three processes: the initialization phase, authentication in V2I (authentication for token issuance), and authentication in V2V and V2I(authentication for communication).

3.1 System Initialization

This section outlines the initialization process for each entity involved in the system. Before mutual authentication and message exchange, every entity must undergo an initialization phase. Once a vehicle completes the registration process with the TA, the TA generates and periodically updates a Reg_{PID} table containing the vehicle's master public key and pseudo-ID. This table is maintained in the RSU. By maintaining this table, the need for digital certificate exchange between the RSU and OBU is eliminated. The details are as follows.

TA Initialization. The TA, equipped with high computational capabilities, selects and distributes the necessary parameters for secure key exchange among the entities. First, it selects two distinct matrices, $A \in \mathbb{Z}_q^{m \times n}$ and $A' \in \mathbb{Z}_q^{m \times n}$. Then, it chooses a secret key sek from the distribution $\mathbb{Z}_q^{x^m}$ and computes the public key $Pub = A'.sek$. Subsequently, the TA selects a lattice code pair $X, (\lfloor . \rceil)_X$ for error correction and another lattice code pair $Y, (\lfloor . \rceil)_Y$ for quantization. Next, it selects two hash functions: $H_1 : \mathbb{Z}_q^m \rightarrow \mathbb{Z}_q$ and $H_2 : 0, 1^{-} \mathbb{Z}_q$. Finally, it sets the public parameters as $m, n, q, A, Pub, H_1, H_2$.

RSU Initialization. The r-th RSU is identified by its unique identity, RSU_r. Under the supervision of the TA, the RSU selects its secret key $rsek_r$ from $x^m \in \mathbb{Z}_q$ and computes its public key as $rpub_r = A'.rsek_r$. The RSU_r receives from the TA the identities and public keys of nearby RSUs (e.g., RSU_s, RSU_t), along with the lattice code pairs $X, (\lfloor . \rceil)_X$, $Y, (\lfloor . \rceil)_Y$, and the hash functions H_1 and H_2. Finally, the RSU stores its key pair $(rsek_r, rpub_r)$, the error term $(err \rightarrow x^n)$, and the lattice codes $X, (\lfloor . \rceil)_X$, $Y, (\lfloor . \rceil)_Y$ in inactive memory. The public parameters are then set as $\{RSU_r, A, rpub_r, H_1, H_2\}$.

OBU Initialization. The i-th vehicle, or OBU_i, must undergo a registration process through the TA. The OBU_i receives the following parameters from the TA: the real identity $real_i$, the master secret key $msek_{vi}$, the master public key $mpub_{vi} = A.msek_{vi}$, the secret key sek_{vi}, the public key $pub_{vi} = A'.sek_{vi}$, the pseudo-identity $PID_i = \langle PID_{i1}, PID_{i2} \rangle$, where $PID_{i1} = H_1(real_i)$ and $PID_{i2} = real_i \oplus H_1(sek)$, and the list of active RSUs within a specific region, $List_{RSU}$. Next, the OBU_i stores the hash functions H_1, H_2 and the lattice codes $X, (\lfloor . \rceil)_X$, $Y, (\lfloor . \rceil)Y$ in non-volatile memory, and sets $\{PID_i, A, pub_{vi}, H_1, H_2\}$ as the public parameters.

3.2 Authentication in V2I

Before communicating with other vehicles, a fully registered OBU must receive a token from the RSU. The authentication and token exchange process between the RSU and OBU is illustrated in Fig. 2, and the detailed procedure is as follows.

First, the j-th RSU, denoted as RSU_j, broadcasts a beacon message containing its identity RSU_j and public key $rpub_j$. Upon receiving the broadcasted message, OBU_i verifies whether RSU_j is listed in $List_{RSU}$. If the verification is successful, OBU_i generates a timestamp t_i and constructs a message $M1 = \{PID_i, t_i, RSU_j\}$, where PID_i is its pseudo-identity, and sends it as a response.

Next, RSU_j checks whether PID_i exists in the Reg_{PID} table. If a match is found, it retrieves the master public key of the corresponding OBU_i, denoted as $mpub_{vi}$, and computes $h_0 = H_1(mpub_{vi})$. Then, using the identities and public keys of neighboring RSUs aligned in a straight path, it generates the token as $\rho = H_2(RSU_j || rpub_j || RSU_k || rpub_k || RSU_l || rpub_l || \Delta t)$.

RSUj		OBUi
	broadcast $RSU_j, rpub_j \longrightarrow$	
		check RSU_j in $List_{RSU}$ generate timestamp t_i
	$\longleftarrow PID_i, t_i, RSU_j$	
check PID_i in Reg_{PID} calculate $h_0 = H_1(mpub_{vi})$ $\rho = H_2(RSU_j \|\| rpub_j \|\| RSU_k \|\| rpub_k \|\| RSU_l \|\| rpub_l \|\| \Delta t)$ $\mathbb{C} = encrypt(\rho)$		
	$h_0, A, \mathbb{C} \longrightarrow$	
		calculate $h'_0 = H_1(mpub_{vi})$ check $h_0 = h'_0$ $decrypt(\mathbb{C}) = \rho$

Fig. 2. V2I Authentication phase of Nath et al.'s scheme.

The RSU then encrypts the generated token using the master public key of OBU_i, computing $\mathbb{C} = encrypt(\rho)$, and transmits $\{h_0, A, \mathbb{C}\}$ to OBU_i.

Upon receiving $\{h_0, A, \mathbb{C}\}$, OBU_i computes $h'_0 = H_1(mpub_{vi})$ using its own master public key and verifies whether $h_0 = h'_0$. If the verification succeeds, OBU_i decrypts $\mathbb{C}$ using its master secret key to obtain $\rho = decrypt(\mathbb{C})$.

3.3 Authentication in V2V and V2I

Once OBU_j obtains the token ρ from a nearby RSU, it becomes eligible to communicate with other vehicles. To initiate communication with another vehicle, OBU_j follows the process outlined below.

First, OBU_j computes $\gamma_j = mesk_{vj}.\rho$ and generates a timestamp t_j. It then performs a hash operation on the message msg, ρ, and t_j to compute $\beta_j = H_2(msg||\rho||t_j||PID_{j1})$. Subsequently, it generates the signature as $sign_j = \beta_j + \gamma_j$.

Next, OBU_j constructs the message containing the destination information $dest$ and the message $MSG = \{msg, PID_j, sign_j, \beta_j, mpub_{vj}, t_j\}$. This message is then broadcasted over the wireless communication medium to be received by OBU_k.

Upon receiving $\{dest, MSG\}$, OBU_k verifies the timestamp t_j and computes $\beta_k = H_2(msg||\rho||t_j||PID_{j1})$ using the received information. It then checks whether $\beta_k = \beta_j$. If the values match, OBU_k verifies OBU_j's signature using the equation $A.sign_j = A.\beta_k + mpub_{vj}.\rho$. If the signature verification is successful, OBU_k considers the message from OBU_j to be valid. Otherwise, it discards the message.

This authentication process is not limited to a single vehicle. It is performed dynamically during V2V communication, allowing multiple vehicles to exchange messages simultaneously. Additionally, vehicles can transmit messages to the RSU, which can verify the authenticity of these messages using the previously described verification process.

4 Security Weakness of Nath et al.'s Scheme

This section demonstrates that Nath et al.'s scheme is vulnerable to replay attack, impersonation attack, insider attack, table leakage attack, DoS attack, eclipse attack, and sybil attack. The vulnerabilities are analyzed using both formal and informal methods.

4.1 Formal Analysis Using AVISPA Tool

HLPLS Specifications. To verify the security of the protocol, HLPSL code was written for each entity involved in the communication process. The code is categorized based on the roles of the entities: TA (Fig. 3 (a)), RSU (Fig. 3 (b)), and OBU (Fig. 3 (c)). Finally, the session and environment details are shown in Fig. 3 (d).

The registration process for RSUs and OBUs corresponds to transitions 1 and 2 in the code. To ensure that the registered public keys can be effectively utilized in the protocol, each entity (TA, RSU, and OBU) receives its public key as a parameter. The public keys of TA, RSU, and OBU are denoted as PK_t, PK_r, PK_i, respectively, while the master public key of OBU is represented as MPK_i. In transition 1 of the RSU, $SND(RSU_j, PK_r)$ signifies the stage in the V2I authentication process where the RSU broadcasts its information. After receiving this message, the OBU sends an authentication request message PID_i, t_i, RSU_j to the RSU, which corresponds to $SND(Ti', PIDi1, PIDi2, RSUj')$ in transition 3. Upon receiving this message, the RSU generates a token, encrypts it, and transmits it to the OBU. This process occurs in transition 4, and the transmission to the OBU is represented as $SND(H1(MPK_i), Token', Token_{MPK_i})$. Finally, the process in which the OBU receives the encrypted message is described in transition 5. To evaluate the protocol's security, authentication is performed using witness() and request() functions during the message transmission and reception process. The protocol identifiers $auth_1, auth_2,$ and $auth_3$ are used in conjunction with witness() and request() to verify whether the authentication process is correctly executed. Lastly, the code defined in the Goal section is used to verify that the protocol's overall authentication process is properly conducted.

Simulation Results. The results of executing the AVISPA simulation on the previously defined HLPSL code are shown in Fig. 4. The simulation results confirm that the scheme proposed by Nath et al. is not secure against replay attacks and man-in-the-middle (MITM) attacks. The specific points where issues arise can be identified in the Goal section. This analysis allows for the identification of authentication vulnerabilities within the protocol and provides valuable insights for developing security enhancements.

```
role
role_TA(TA:agent,RSU:agent,OBU:agent,PKt:public_key,MPKi:public_key,PKi:public_key,PKr:public_key,Key_set_TA_RSU:(symmetric_key) set,Key_set_TA_OBU:(symmetric_key) set,SND,RCV:channel(dy))
played_by TA
def=
  local

State:nat,Reali:text,PIDi1:text,A:text,NN:text,MM:text,QQ:text,PIDi2:text,Key_2:symmetric_key,Key_1:symmetric_key
  init
    State := 0
  transition
    1. State=0 /\ RCV(start) =|> State':=1
    /\ A':=new() /\ QQ':=new() /\ NN':=new() /\ MM':=new()
    /\ Key_1':=new() /\
Key_set_TA_RSU':=cons(Key_1',Key_set_TA_RSU)
    /\ SND({MM'.NN'.QQ'.A'.PKt}_Key_1')

    /\ Reali':=new() /\ PIDi2':=new() /\ PIDi1':=new() /\ Key_2':=new()
    /\ Key_set_TA_OBU':=cons(Key_2',Key_set_TA_OBU)
    /\ SND({MM'.NN'.QQ'.A'.PKt.MPKi.PKi.PIDi1'.PIDi2'.Reali'}_Key_2')
end role
```

(a) TA's role.

```
role
role_RSU(TA:agent,RSU:agent,OBU:agent,PKt:public_key,MPKi:public_key,PKi:public_key,PKr:public_key,Key_set_TA_RSU:(symmetric_key) set,SND,RCV:channel(dy))
played_by RSU
def=
  local

State:nat,QQ:text,MM:text,NN:text,A:text,RSUj:text,PIDi1:text,Ti:text,PIDi2:text,Token:text,H:hash_func,Key_1:symmetric_key
  init
    State := 0
  transition
    1. State=0 /\ in(Key_1',Key_set_TA_RSU)
    /\ RCV({MM'.NN'.QQ'.A'.PKt}_Key_1') =|> State':=1
    /\ Key_set_TA_RSU':=delete(Key_1',Key_set_TA_RSU)

    /\ SND(RSUj.PKr)
    /\ witness(RSU,OBU,auth_1,RSUj)

    4. State=1 /\ RCV(Ti'.PIDi1'.PIDi2'.RSUj) =|> State':=2
    /\ request(RSU,OBU,auth_2,PIDi1')
    /\ Token':=H(RSUj.PKr.Ti')
    /\ SND(H(MPKi).Token'.{Token'}_MPKi)
    /\ witness(RSU,OBU,auth_3,Token')
end role
```

(b) RSU's role.

```
role
role_OBU(TA:agent,RSU:agent,OBU:agent,PKt:public_key,MPKi:public_key,PKi:public_key,PKr:public_key,Key_set_TA_OBU:(symmetric_key) set,SND,RCV:channel(dy))
played_by OBU
def=
  local

State:nat,Reali:text,A:text,NN:text,MM:text,QQ:text,RSUj:text,PIDi1:text,Ti:text,PIDi2:text,Token:text,H:hash_func,Key_1:symmetric_key
  init
    State := 0
  transition
    2. State=0 /\ in(Key_1',Key_set_TA_OBU)
    /\ RCV({MM'.NN'.QQ'.A'.PKt.MPKi.PKi.PIDi1'.PIDi2'.Reali'}_Key_1')
=|> State':=1
    /\ Key_set_TA_OBU':=delete(Key_1',Key_set_TA_OBU)

    3. State=1 /\ RCV(RSUj'.PKr) =|> State':=2
    /\ request(OBU,RSU,auth_1,RSUj)
    /\ Ti':=new()
    /\ SND(Ti'.PIDi1.PIDi2.RSUj')
    /\ witness(OBU,RSU,auth_2,PIDi1)

    5. State=2 /\ RCV(H(MPKi).Token'.{Token'}_MPKi) =|> State':=3
    /\ request(OBU,RSU,auth_3,Token')
end role
```

(c) OBU's role.

```
role
session(TA:agent,RSU:agent,OBU:agent,PKt:public_key,MPKi:public_key,PKi:public_key,PKr:public_key,Key_set_TA_RSU:(symmetric_key) set,Key_set_TA_OBU:(symmetric_key) set)
def=
  local
    SND3,RCV3,SND2,RCV2,SND1,RCV1:channel(dy)
  composition

role_OBU(TA,RSU,OBU,PKt,MPKi,PKi,PKr,Key_set_TA_OBU,SND3,RCV3) /\
role_RSU(TA,RSU,OBU,PKt,MPKi,PKi,PKr,Key_set_TA_RSU,SND2,RCV2) /\
role_TA(TA,RSU,OBU,PKt,MPKi,PKi,PKr,Key_set_TA_RSU,Key_set_TA_OBU,SND1,RCV1)
end role


role environment()
def=
  const

pki:public_key,pkt:public_key,trust:agent,hash_0:hash_func,obu:agent,rsu:agent,mpki:public_key,pkr:public_key,auth_1:protocol_id,auth_2:protocol_id,auth_3:protocol_id
  intruder_knowledge = {trust,rsu,obu,pkt,mpki,pki,pkr}
  composition
    session(trust,rsu,obu,pkt,mpki,pki,pkr,{},{})
end role

goal
  authentication_on auth_1
  authentication_on auth_2
  authentication_on auth_3
end goal

environment()
```

(d) Session, Environment, and Goal.

Fig. 3. HLPSL code.

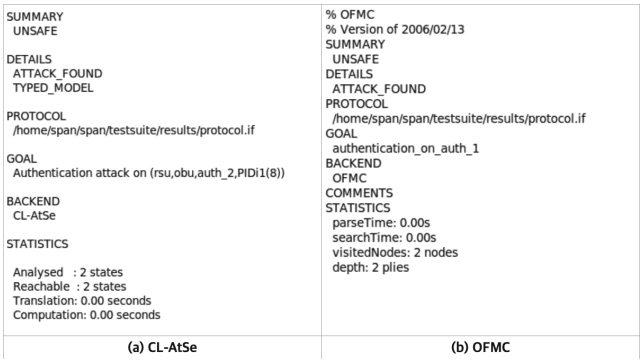

Fig. 4. AVISPA execution results.

4.2 Informal Analysis

This section demonstrates, through logical security analysis, that the scheme proposed by Nath et al. is vulnerable to replay attack, impersonation attack, insider attack, table leakage attack, DoS attack, eclipse attack, and sybil attack.

Replay attack

1. An attacker may capture and replay broadcast messages originating from RSU_j. OBU_i cannot verify the generation time of the broadcast message or authenticate its sender. As a result, the attacker can impersonate RSU_j through a replay attack.
2. An attacker can record the message M_1 sent by OBU_i, modify only the timestamp, and replay it. RSU_j does not verify the sender of message M_1. Consequently, the attacker can impersonate OBU_i using a replay attack.

Impersonation attack

1. An attacker can generate a broadcast message for RSU_j using publicly available information, such as RSU_j and $rpub_j$. OBU_i cannot verify the sender of the broadcast message, making it possible for the attacker to impersonate RSU_j.
2. An attacker can generate message M_1 using publicly available information, such as PID_i and RSU_j. RSU_j is unable to distinguish the actual sender of message M_1, allowing the attacker to impersonate OBU_i.

Insider Attack. A malicious user who has completed the legitimate registration process can obtain $mpub_{vi}$ through V2V communication. Using the acquired master public key of another vehicle, the attacker can generate $h_0, A, \mathbb{C}$ and send them to the OBU_i. Since OBU_i cannot verify the sender of the received message, the attacker can impersonate RSU_j.

Table Leakage Attack. An attacker can compromise the stored table of RSU_j and obtain critical parameters. Using the extracted values, including $mpub_{vi}$, RSU_j, and $rpub_j$, the attacker can generate $h_0, A, \mathbb{C}$ and send them to OBU_i. Since OBU_i cannot verify the sender of the received message, the attacker can impersonate RSU_j.

DoS attack

1. An attacker can record and replay the broadcast message from RSU_j or generate a new broadcast message using publicly available information, then repeatedly send it to OBU_i. Since OBU_i does not perform message verification, it is vulnerable to DoS attack.
2. An attacker can record and replay message M_1 sent by OBU_i or generate a new one, then repeatedly send it to RSU_j. Since RSU_j does not verify incoming messages, it is susceptible to DoS attack.

Eclipse Attack. An attacker capable of impersonating RSU_j can generate and transmit a manipulated token ρ to OBU_i. Since OBU_i cannot detect the alteration, it proceeds with V2V communication using the compromised token. As a result, OBU_i with the manipulated token is unable to communicate with legitimate vehicles and becomes isolated within the network. In smart city environments, this type of attack could have severe consequences by isolating emergency vehicles, preventing them from receiving critical updates on optimal routes, or delaying first responders. This could directly impact urban safety and traffic management efficiency.

Sybil attack

1. An OBU that has received a manipulated token from an attacker impersonating RSU_j may also receive a V2V message $dest, MSG$ from a fake vehicle created by the attacker. In this case, the OBU authenticates the fake vehicle's message using the compromised token. Since OBU_i cannot distinguish between legitimate and fake vehicles, it accepts $dest, MSG$ from the fake vehicle as valid information.
2. A malicious user who has completed legitimate registration can utilize a token obtained through the V2I process along with fabricated vehicle information to generate $dest, MSG$ and send it to OBU_i. Since OBU_i verifies messages solely based on the received information and token, it cannot determine whether the sender is a real or fake vehicle. Consequently, OBU_i accepts $dest, MSG$ from the fake vehicle as legitimate.

In large-scale smart cities, a sybil attack can significantly disrupt intelligent traffic management systems by allowing attackers to manipulate traffic data, leading to artificial congestion, inefficient routing, and delays in automated traffic flow optimization.

5 Security Fixes

The scheme proposed by Nath et al. demonstrates significant security vulnerabilities primarily due to the lack of message freshness verification and absence of user authentication mechanisms. As a result of these weaknesses, an attacker can ultimately isolate users from the legitimate network and force them to accept only manipulated information. These critical security flaws are discussed in detail in Sect. 4.

Nath et al. claimed that their scheme enables fast and secure communication using tokens. However, the absence of message freshness checks, and the lack of a user authentication mechanism leaves the entire network highly vulnerable. Therefore, it is essential to design a method that ensures message freshness and incorporates a user authentication process to enhance network security.

To address the security issues identified in the protocol by Nath et al., we propose the following key guidelines.

Solution 1. According to Sect. 3.2, RSU_j transmits only its identity and public key during broadcasting. To prevent RSU_j impersonation attack, a timestamp and a signature mechanism can mitigate various attack. The detailed process is as follows.

RSU_j generates a timestamp t_j and signs it using its secret key $rsek_j$ to create the signature value $tsign_j = t_j + rsek_j$. Then, RSU_j constructs the broadcast message as $\{RSU_j, rpub_j, tsign_j, t_j\}$.

Upon receiving the broadcasted message, OBU_i first checks the freshness of the message using t_j. It then verifies the signature by computing $A.tsign_j = A.t_j + rpub_j$. Through this process, OBU_i can defend against replay attack, RSU impersonation attack, and DoS attack. The generated signature value remains valid for a certain period during RSU broadcasting and is updated when the token is refreshed.

Solution 2. In the process described in Sect. 3.2, when OBU_i sends message M_1, the sender cannot be authenticated, and RSU_j does not verify the timestamp upon receiving M_1. As a result, the freshness of the message cannot be ensured. To address this issue, a timestamp signing mechanism similar to the previous solution can be incorporated. The detailed method is as follows.

OBU_i selects a timestamp t_i and applies a digital signature using its master secret key $msek_{vi}$, producing $tsign_i = t_i + msek_{vi}$. It then constructs the message $M_1 = \{PID_i, t_i, tsign_i, RSU_j\}$ and transmits it to RSU_j.

Upon receiving the message, RSU_j verifies the freshness of the message by checking the timestamp t_i and then validates the signature by computing $A.tsign_i = A.t_i + mpub_{vi}$. Through this process, RSU_j can resist replay attack, OBU impersonation attack, and DoS attack.

Solution 3. In Sect. 3.2, RSU_j generates the message $\{h_0, A, C\}$ and sends it to OBU_i. Upon receiving this message, OBU_i decrypts it to obtain the token. However, there is no procedure to verify the freshness of the message, and there

```
role
role_TA(TA:agent,RSU:agent,OBU:agent,PKt:public_key,MPKi:public_key,PKi:public_key,PKr:public_key,Key_set_TA_RSU:(symmetric_key) set,Key_set_TA_OBU:(symmetric_key) set,SND,RCV:channel(dy))
played_by TA
def=
        local

State:nat,Reali:text,PIDi1:text,A:text,NN:text,MM:text,QQ:text,PIDi2:text,Key_2:symmetric_key,Key_1:symmetric_key
init
    State := 0
transition
    1. State=0 /\ RCV(start) =|> State':=1
    /\ A':=new() /\ QQ':=new() /\ NN':=new() /\ MM':=new()
    /\ Key_1':=new() /\
Key_set_TA_RSU':=cons(Key_1',Key_set_TA_RSU)
    /\ SND({MM'.NN'.QQ'.A'.PKt}_Key_1')

    /\ Reali':=new() /\ PIDi2':=new() /\ PIDi1':=new() /\ Key_2':=new()
    /\ Key_set_TA_OBU':=cons(Key_2',Key_set_TA_OBU)
    /\ SND({MM'.NN'.QQ'.A'.PKt.MPKi.PKi.PIDi1'.PIDi2'.Reali'}_Key_2')
end role
```

(a) TA's role.

```
role
role_RSU(TA:agent,RSU:agent,OBU:agent,PKt:public_key,MPKi:public_key,PKi:public_key,PKr:public_key,Key_set_TA_RSU:(symmetric_key) set,SND,RCV:channel(dy))
played_by RSU
def=
        local

State:nat,QQ:text,MM:text,NN:text,A:text,Tj2,Tj1,RSUj:text,PIDi1:text,Ti:text,PIDi2:text,Token:text,H:hash_func,Key_1:symmetric_key
        init
    State := 0
        transition
    1. State=0 /\ in(Key_1',Key_set_TA_RSU)
    /\ RCV({MM'.NN'.QQ'.A'.PKt}_Key_1') =|> State':=1
    /\ Key_set_TA_RSU':=delete(Key_1',Key_set_TA_RSU)

    /\ Tj1':=new()
    /\ SND(Tj1'.RSUj.PKr.{Tj1'}_inv(PKr))
    /\ witness(RSU,OBU,auth_1,Tj1')

    4. State=1 /\ RCV(Ti'.PIDi1.PIDi2.RSUj.{Ti'}_inv(PKi)) =|> State':=2
    /\ request(RSU,OBU,auth_2,Ti')
    /\ Tj2':=new()
    /\ Token':=H(RSUj.PKr.Ti')
    /\ SND({H(Tj2'.Token')}_inv(PKr).Tj2'.{Token'}_MPKi)
    /\ witness(RSU,OBU,auth_3,Token')
end role
```

(b) RSU's role.

```
role
role_OBU(TA:agent,RSU:agent,OBU:agent,PKt:public_key,MPKi:public_key,PKi:public_key,PKr:public_key,Key_set_TA_OBU:(symmetric_key) set,SND,RCV:channel(dy))
played_by OBU
def=
        local

State:nat,Reali:text,A:text,NN:text,Tj2,Tj1,MM:text,QQ:text,RSUj:text,PIDi1:text,Ti:text,PIDi2:text,Token:text,H:hash_func,Key_1:symmetric_key
        init
    State := 0
        transition
    2. State=0 /\ in(Key_1',Key_set_TA_OBU)
    /\ RCV({MM'.NN'.QQ'.A'.PKt.MPKi.PKi.PIDi1'.PIDi2'.Reali'}_Key_1')
=|> State':=1
    /\ Key_set_TA_OBU':=delete(Key_1',Key_set_TA_OBU)

    3. State=1 /\ RCV(Tj1'.RSUj.PKr.{Tj1'}_inv(PKr)) =|> State':=2
    /\ request(OBU,RSU,auth_1,Tj1')
    /\ Ti':=new()
    /\ SND(Ti'.PIDi1.PIDi2.RSUj.{Ti'}_inv(PKi))
    /\ witness(OBU,RSU,auth_2,Ti')

    5. State=2 /\ RCV({H(Tj2'.Token')}_inv(PKr).Tj2'.{Token'}_MPKi) =|
> State':=3
    /\ request(OBU,RSU,auth_3,Token')
end role
```

(c) OBU's role.

```
role
session(TA:agent,RSU:agent,OBU:agent,PKt:public_key,MPKi:public_key,PKi:public_key,PKr:public_key,Key_set_TA_RSU:(symmetric_key) set,Key_set_TA_OBU:(symmetric_key) set)
def=
        local
    SND3,RCV3,SND2,RCV2,SND1,RCV1:channel(dy)
        composition

role_OBU(TA,RSU,OBU,PKt,MPKi,PKi,PKr,Key_set_TA_OBU,SND3,RCV3) /\
role_RSU(TA,RSU,OBU,PKt,MPKi,PKi,PKr,Key_set_TA_RSU,SND2,RCV2) /\
role_TA(TA,RSU,OBU,PKt,MPKi,PKi,PKr,Key_set_TA_RSU,Key_set_TA_OBU,SND1,RCV1)
end role

role environment()
def=
        const

pki:public_key,pkt:public_key,trust:agent,hash_0:hash_func,obu:agent,rsu:agent,mpki:public_key,pkr:public_key,auth_1:protocol_id,auth_2:protocol_id,auth_3:protocol_id
    intruder_knowledge = {trust,rsu,obu,pkt,mpki,pki,pkr}
    composition
    session(trust,rsu,obu,pkt,mpki,pki,pkr,{},{})
end role

goal
    authentication_on auth_1
    authentication_on auth_2
    authentication_on auth_3
end goal

environment()
```

(d) Session, Environment, and Goal.

Fig. 5. HLPSL code reflecting the solutions.

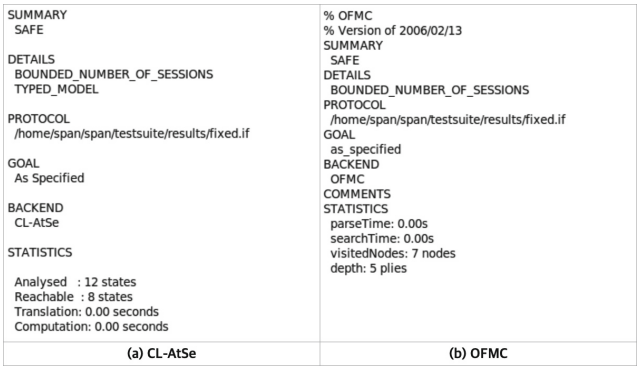

Fig. 6. AVISPA execution results reflecting the solutions.

is a lack of validation to ensure that RSU_j is the actual sender. This results in vulnerabilities to insider attack and table leakage attack. Additionally, since there is no mechanism to confirm that the sender is a legitimate RSU, there is a risk that OBU_i might receive a manipulated token without detecting it. As a result, the network becomes highly susceptible to severe security threats such as sybil attack and eclipse attack. To mitigate this risk, a procedure for OBU_i to verify RSU_j is necessary. The process is as follows:

First, RSU_j generates the token ρ, then encrypts it using OBU_i's master public key $mpub_{vi}$ to produce $\mathbb{C} = encrypt(\rho)$. Next, RSU_j generates a timestamp t_{j2} and calculates the signature for the token as $rsign_j = H_1(\rho||t_{j2}) + rsek_j$. Then, RSU_j sends $\{A, \mathbb{C}, rsign_j, t_{j2}\}$ to OBU_i.

Upon receiving the message, OBU_i first verifies the freshness of the message using the timestamp t_{j2}. Then, using its master secret key $msek_{vi}$, OBU_i decrypts $\mathbb{C}$ to obtain the token ρ. Afterward, to confirm that the token indeed came from RSU_j, the signature is verified using $A.rsign_j = A.H_1(\rho||t_{j2}) + rpub_j$. If the signature verification is successful, OBU_i can be confident that the token it received is the latest token sent by RSU_j, thus ensuring resistance against Sybil and Eclipse attacks.

Figure 5 presents the HLPSL code incorporating the proposed solutions. *Solution* 1 is applied in Transition 1 of the RSU, where an additional component, $\{Tj1'\}\_inv(PKr)$, is included in the broadcast message. Unlike the original protocol, this addition enables the OBU to verify that the broadcast message was indeed generated by the RSU. *Solution* 2 is implemented in Transition 3 of the OBU. In contrast to the original protocol, the message sent to the RSU now includes $\{Ti'\}\_inv(PKi)$. This modification allows the RSU to confirm that the message was generated by the OBU. *Solution* 3 is applied in Transition 4 of the RSU. Unlike the original approach, this solution utilizes a timestamp and a token to generate the signature $\{H(Tj2'.Token')\}\_inv(PKr)$ before transmission. This ensures that the OBU can verify that both the message and the token originated from the RSU. Figure 6 presents the AVISPA simulation results for the HLPSL code incorporating these solutions. The results confirm

that the enhanced protocol is resistant to replay attacks and man-in-the-middle attacks.

6 Conclusion and Future Works

This study analyzes the security of VANET, a core infrastructure in smart city traffic systems. To evaluate the security of the lattice-based authentication protocol proposed by Nath et al., both formal analysis using AVISPA and informal logical analysis were conducted.

The analysis revealed that the protocol is vulnerable to various security threats, including replay attacks, impersonation attacks, and insider attacks, due to the lack of message freshness verification and absence of user authentication. In particular, through AVISPA verification, the study analyzed and validated how these vulnerabilities could be exploited in real attack scenarios.

To address these issues, this study proposes security improvements that strengthen message freshness verification and user authentication to ensure secure authentication in the smart city VANET environment. AVISPA-based validation confirmed that the proposed improvements effectively resolved existing vulnerabilities and demonstrated security against major attacks. This demonstrates the effectiveness of AVISPA verification in addressing security issues in smart city VANET environments.

Future work will focus on optimizing the proposed authentication framework for high mobility smart city environments to ensure faster and more secure communication. Additionally, performance and security validation under various network conditions will be conducted to develop a VANET authentication framework that is practically applicable.

Acknowledgments. This work was supported by the Bisa Research Grant of Keimyung University in 2024 under Project 20240618.

Disclosure of Interests. The authors have no competing interests to declare that are relevant to the content of this article.

References

1. Armando, A., et al.: The AVISPA tool for the automated validation of internet security protocols and applications. In: Etessami, K., Rajamani, S.K. (eds.) CAV 2005. LNCS, vol. 3576, pp. 281–285. Springer, Heidelberg (2005). https://doi.org/10.1007/11513988_27
2. Canetti, R., Krawczyk, H.: Universally composable notions of key exchange and secure channels. In: Knudsen, L.R. (ed.) EUROCRYPT 2002. LNCS, vol. 2332, pp. 337–351. Springer, Heidelberg (2002). https://doi.org/10.1007/3-540-46035-7_22
3. Dolev, D., Yao, A.: On the security of public key protocols. IEEE Trans. Inf. Theory **29**(2), 198–208 (1983)
4. Douceur, J.R.: The sybil attack. In: International Workshop on Peer-to-Peer Systems, pp. 251–260. Springer (2002)

5. Dwivedi, S.K., Amin, R., Vollala, S., Das, A.K.: Design of blockchain and ECC-based robust and efficient batch authentication protocol for vehicular AD-HOC networks. IEEE Trans. Intell. Transp. Syst. (2023)
6. Elassy, M., Al-Hattab, M., Takruri, M., Badawi, S.: Intelligent transportation systems for sustainable smart cities. Transp. Eng. **16**, 100252 (2024)
7. Grover, L.K.: A fast quantum mechanical algorithm for database search. In: Proceedings of the Twenty-Eighth Annual ACM Symposium on Theory of Computing, pp. 212–219 (1996)
8. Heilman, E., Kendler, A., Zohar, A., Goldberg, S.: Eclipse attacks on {Bitcoin's}{peer-to-peer} network. In: 24th USENIX Security Symposium (USENIX Security 15), pp. 129–144 (2015)
9. Hussein, N.H., Yaw, C.T., Koh, S.P., Tiong, S.K., Chong, K.H.: A comprehensive survey on vehicular networking: communications, applications, challenges, and upcoming research directions. IEEE Access **10**, 86127–86180 (2022)
10. Ju, S., Park, H., Son, S., Kim, H., Park, Y., Park, Y.: Blockchain-assisted secure and lightweight authentication scheme for multi-server internet of drones environments. Mathematics **12**(24), 3965 (2024)
11. Kim, M., Park, K., Park, Y.: A reliable and privacy-preserving vehicular energy trading scheme using decentralized identifiers. Mathematics **12**(10), 1450 (2024)
12. Micciancio, D., Regev, O.: Lattice-based cryptography. In: Post-Quantum Cryptography, pp. 147–191. Springer (2009)
13. Micciancio, D., Schultz-Wu, M.: Error correction and ciphertext quantization in lattice cryptography. In: Annual International Cryptology Conference, pp. 648–681. Springer (2023)
14. Naeem, M.A., Chaudhary, S., Meng, Y.: Road to efficiency: V2V enabled intelligent transportation system. Electronics **13**(13), 2673 (2024)
15. Nath, H.J., Choudhury, H.: LbPV: lattice-based privacy-preserving mutual authentication scheme for VANET. Comput. Electr. Eng. **120**, 109765 (2024)
16. Park, H., Son, S., Park, Y., Park, Y.: Provably quantum secure three-party mutual authentication and key exchange protocol based on modular learning with error. Electronics **13**(19), 3930 (2024)
17. Park, K., Lee, J., Das, A.K., Park, Y.: BPPS: blockchain-enabled privacy-preserving scheme for demand-response management in smart grid environments. IEEE Trans. Dependable Secure Comput. **20**(2), 1719–1729 (2022)
18. Shayea, G.G., Mohammed, D.A., Abbas, A.H., Abdulsattar, N.F.: Privacy-aware secure routing through elliptical curve cryptography with optimal rsu distribution in vanets. Designs **6**(6), 121 (2022)
19. Shor, P.W.: Algorithms for quantum computation: discrete logarithms and factoring. In: Proceedings 35th Annual Symposium on Foundations of Computer Science, pp. 124–134. IEEE (1994)
20. Yu, S., Lee, J., Sutrala, A.K., Das, A.K., Park, Y.: LAKA-UAV: Lightweight authentication and key agreement scheme for cloud-assisted unmanned aerial vehicle using blockchain in flying AD-HOC networks. Comput. Netw. **224**, 109612 (2023)
21. Zhu, D., Guan, Y.: Secure and lightweight conditional privacy-preserving identity authentication scheme for VANET. IEEE Sens. J. **24**(21), 35743–35756 (2024)

Automatic Help Summoning Through Speech Analysis on Mobile Devices

Bożena Małysiak-Mrozek[1], Paweł Wojaczek[2], Krzysztof Tokarz[3], Vaidy Sunderam[4], Dariusz Mrozek[2(✉)], and Jean-Charles Lamirel[5]

[1] Department of Distributed Systems and Informatic Devices, Silesian University of Technology, Akademicka 16, 44-100 Gliwice, Poland
[2] Department of Applied Informatics, Silesian University of Technology, Akademicka 16, 44-100 Gliwice, Poland
dariusz.mrozek@polsl.pl
[3] Department of Graphics, Computer Vision and Digital Systems, Silesian University of Technology, Akademicka 16, 44-100 Gliwice, Poland
[4] Department of Computer Science, Emory University, Atlanta, GA 30322, USA
[5] Synalp team, LORIA, Nancy - University of Strasbourg, Strasbourg, Grand Est, France

Abstract. The aging population has led to an increasing number of elderly individuals living alone, making it crucial to address their need for prompt and effective emergency assistance. Older adults, often facing physical limitations or illnesses, require reliable systems for immediate help during life-threatening situations. To meet this need, smart devices like emergency call systems are being developed, enhancing seniors' safety and improving health and social care responses. Our research explores how passive and active speech analysis on mobile devices can support automatic emergency assistance. We show that this can be achieved on Edge devices using tiny machine learning (ML) models for wake-word detection, speech-to-text conversion, and intention recognition, paving the way for safer, smarter living environments for seniors.

Keywords: Internet of Things · older adults · Natural Language Processing · intention recognition · speech analysis

1 Introduction

The aging society, characterized by a growing proportion of older individuals in the population, is a global phenomenon [18]. Advances in healthcare have improved living conditions, enabling more people to reach old age [1]. For the first time, projections suggest that the global population over 65 could soon exceed the number of children under 5 [26]. This trend spans all regions worldwide [18].

In 2021, 761 million people worldwide were over 65, including 155 million aged 80 or older (Table 1). By 2050, these numbers are expected to rise to 1.6 billion and 459 million, respectively. Older individuals constituted 9% of the global population in 2021, a figure projected to reach 16% by 2050—meaning

M. Paszynski et al. (Eds.): ICCS 2025 Workshops, LNCS 15912, pp. 18–32, 2025.
https://doi.org/10.1007/978-3-031-97573-8_2

Table 1. The number of older people in the global society in 2021 and 2050 [28].

Year	2021	2050
The number of people over 65 years old	761 million	1.6 billion
The number of people over 80 years old	155 million	459 million
Percentage of people over 65 years old in total population	9%	16%

one in six people will be elderly. Additionally, life expectancy for those over 65 is expected to increase from 82 years in 2021 to 84 years by 2050 in more developed regions [28]. Older people who live alone form a social group that requires special attention, support, and care from others due to their health and physical conditions. It may seem natural that this care can be provided by their relatives, such as children or grandchildren, or if they do not have any, siblings, or people from extended family. Statistical analyses have shown that, for the most part, even when adult children no longer live with their parents, they still live close to their place of residence, which certainly makes it easier for them to provide help to their parents [27]. Elderly people can also benefit from the help of employed home caregivers. Various types of social services, helping the elderly, charities, and self-help groups, are also being established.

Nevertheless, the above-mentioned forms of assistance are often not practiced continuously at any time of the day or night. Therefore, devices that enable reliably calling for help at any time are needed, especially in situations of immediate life-threatening risk caused by illness or accident. These may be electronic devices, edge Internet of Things (IoT) solutions, or smartphones that enable remote notification of appropriate people or services about the need to provide help. The introduction of these solutions becomes a key element in caring for the health of seniors, providing support for their families and caregivers, and contributing to an improvement in the quality of life within an aging society.

This paper shows how the automatic call for help (ACH) can be initialized through passive and active voice analysis on a mobile device. Section 3 discloses the general idea and architecture of ACH with voice analysis models. Section 4 describes the algorithm designed to perform this process, and Sect. 5 explains the created experimental environment with the ML models used for particular phases of ACH. In Sect. 6, we experimentally test wake-up keyword detection and voice-to-text transcription for various noise conditions. We also verify the effectiveness of different ML-based intention recognition models operating at edge devices and those provided as web services. Our experiments confirm that ACH can be efficiently performed with tiny ML models designed for smartphones.

2 Related Works

In today's society, where caring for the elderly and disabled plays a key role, the use of smart technologies to create devices that enable calling for help has become indispensable. These devices are intended to ensure a quick response in

emergency situations and provide a sense of security for both people in need of support and their caregivers [3]. The number of devices was developed and described in the literature. They are usually equipped with a wearable IoT device with a set of sensors and a stationary receiver with internet connectivity. The stationary device can be a mobile phone, like in PhystioDroid created by Banos et al. [7], or a separate device, like in the system developed by Lersilp et al. [17]. The carried device can have a form of the wristband [17], the belt mounted at the waist level [30], or chest level [7]. Sensors can be integrated with the wheelchair [14] or with the user's clothes [13]. Wearable devices contain mainly sensors for body temperature, movements, heart rate, blood pressure and haemoglobin oxygen saturation SpO2. Critical features are the ability of the fall detection [16,23] and the alarm trigger, which can have a form of a large red SOS button [2,17]. In a more advanced system, the emergency situation can be cancelled by a voice command or confirmed by the command or lack of it, causing the notification of relatives or medical services.

There is a group of systems relying on speech recognition technology, which makes it easier to operate with, especially for people with lower digital technology skills, since speech is the most natural way of communicating between people. Such systems usually consist of two main modules - Automatic Speech Recognition (ASR) and then Natural Language Understanding (NLU) [8]. ASR systems can recognise separate words, while more advanced NLU systems try to understand their meaning when spoken in conjunction with other words. NLU is still a complex task for computers [9], especially in an emergency situation, when patients may not be able to speak clearly. Additional information can be obtained with emotion detection [11]. The availability of high computing power and artificial intelligence (AI) services in computing clouds has enabled the creation of voice recognition systems in the form of voice assistants. These are currently Apple's Siri [6], Microsoft Cortana (2014), Amazon Alexa (2014), and Google Assistant (2016). One of the newest achievements in this area is the OpenAI Whisper [24]. Research shows that it can even successfully recognise the speech for dysarthric patients [29]. Currently, the NLP in the cloud is more effective than voice recognition technology built into end devices [6], but constant development and miniaturisation of microcontrollers enable progress in voice recognition on the Edge. In 2021, Mrozek et al. [20] also investigated ASR approaches available in the cloud. However, their usage was highly dependent on the availability of cloud services and stable Internet access. The current work describes the system that moves this process to the Edge, which is essential in situations of lack or poor Internet connection. However, we also compare the Edge-based models with the external, cloud-based ones.

3 General Idea of Calling for Help

Our idea for calling for help in dangerous situations that may occur in seniors' lives assumes the use of a smartphone to monitor the surrounding speech in standby mode and wake up and react only when a monitored person (senior)

utters a call for help. Although not every senior may have one, smartphones are increasingly used by this group of people. As electronic devices, today's smartphones not only provide connectivity in terms of voice and data transmission but are also powerful enough to perform sophisticated computational operations, such as data analysis involving ML-based inference. This analysis may cover ASR and NLU, as shown in Fig. 1. Some of these processes can also be optionally implemented by invoking external services. However, such a flow requires a stable internet connection, additional GSM data transmission from a mobile device (such as a smartphone) to these services, and the constant availability of external services. Therefore, local, edge-based help summoning should work more efficiently and support real-time reactions in the event of danger. This will be verified experimentally (Sect. 6). In an emergency, the smartphone calls the caregiver or informs him of what happened. Another argument for using smartphones is that they can detect dangerous situations (e.g., falls) automatically based on built-in IMU sensors. This enables the integration of various monitoring approaches into a single mobile device, suitable for use in both smart home environments and outdoors in smarter cities.

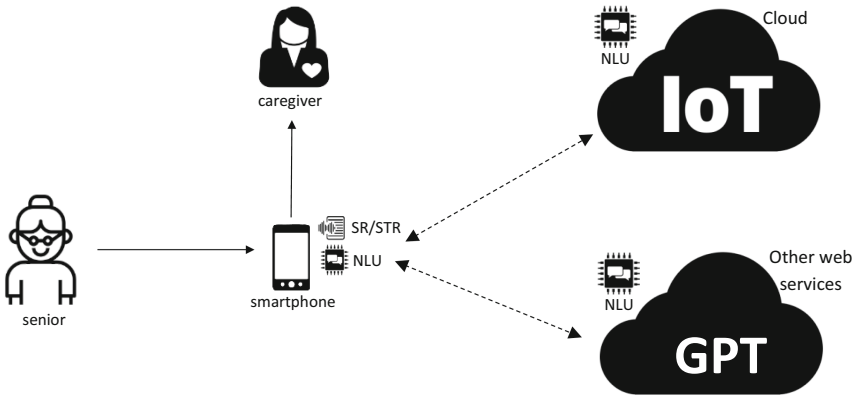

Fig. 1. General architecture of the senior monitoring environment with automatic help summoning through speech analysis on a mobile device.

4 Speech Stream Processing for Help Summoning

Every day, people speak on many topics, formulating sentences consisting of words that create a logical sequence of statements. Each statement can, therefore, be treated as a stream of sentences and the words that compose them. Let S be a statement stream with n sentences s spoken by a person:

$$S = \{s_i | i = 1 \dots n, n \in \mathbb{N}^+\}. \tag{1}$$

Each sentence $s_i \in S$ consists of a different number of words w:

$$s_i =< w_1, w_2, \ldots, w_m >, \tag{2}$$

where $w_1, w_2, \ldots, w_m$ are particular words and m is a (varying) number of words in a sentence.

Calling for help using smart devices that analyze speech consists of several stages. The first one assumes that the intention to call for help appears after saying a special wake-up keyword w_k.

$$s_i =< w_1, w_2, \ldots, [w_k], \ldots, w_m >, \tag{3}$$

where $[w_k]$ denotes that the keyword may appear optionally in a sentence. However, once it appears as a spoken word, it starts the second and the third stages of the analysis for the rest of the statement stream:

$$S' = \{< w_k, w_{k+1} \ldots, w_m >, s_{i+1}, \ldots s_n\}. \tag{4}$$

The process is, therefore, carried out in three stages, as shown in Fig. 2. In the idle state, the device listens for the user to say a defined keyword, monitoring the signal from the device's built-in microphone. For the purposes of this work, we chose the word *help*. It is easily recognized, short, characterized by clear sound, and commonly used in situations requiring urgent intervention or support. After detecting the utterance of a keyword, the application enters the active state in which it transcribes the words spoken by the user, transforming speech into text.

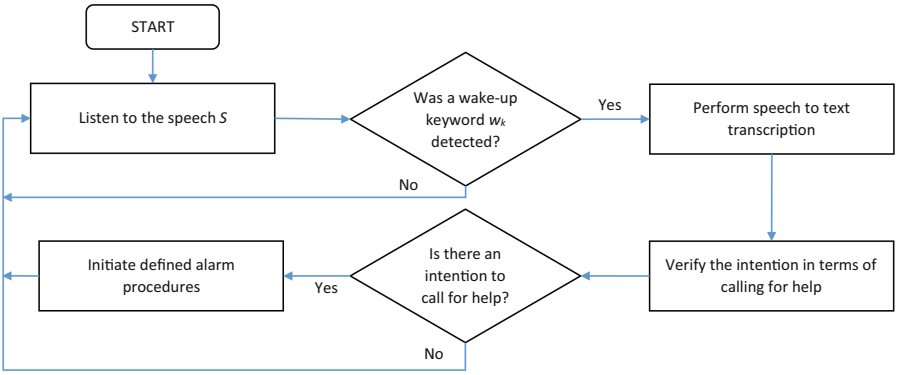

Fig. 2. General algorithm of automatic help summoning through speech analysis on a mobile device.

In such a form, the transcribed speech can be classified more effectively using computer technology. Transcription continues until the user stops speaking any more words for a defined period. The final stage covers the classification of the user's statements to recognize the intention to call for help. The application

determines whether the user had actual intention to call for help or whether his statement was accidental or unrelated to an emergency situation. The classification process relies on analyzing the content of the transcript and defining the probability of an alarm situation occurring. If a true intention to call for help is detected, the device is ready to initiate defined alarm procedures, e.g., to inform the appropriate emergency services about the location and nature of the reported event or to record this fact in a database available to the user's caregivers. Otherwise, the device remains idle, ready for any further sound signals.

5 Experimental Environment and Methods

To investigate the automatic call for help, we developed a mobile application for a smartphone (Dart programming language and Flutter framework) with a backend layer implementing the speech analysis algorithm presented in Fig. 2 and a frontend to visually observe the results of the analysis.

For keyword detection, we considered several solutions, including Pocketsphinx [15], Mycroft Precise, Snowboy, and Porcupine Wake Word by Picovoice, and finally selected and tested the last one as it fitted our requirements. The capability of detecting the wake word to stitch into active mode is particularly valuable in voice-controlled applications and devices, offering a seamless and efficient means of interaction [21]. The Porcupine supports multiple languages, many target platforms, operating systems, and programming languages, which allows building models optimized for a given device. In our case, we created an Android model, and we trained it to detect the wake-up keyword *help*. Then, we could process voice data fully locally on the device without the use of external servers or services. This locality eliminated the impact of network delays, access interruptions, or bandwidth limitations on the quality of voice analysis.

For the second stage of the speech analysis, i.e., speech-to-text transcription, we considered several, mainly open-source toolkits and libraries, including Kaldi [22], DeepSpeech engine by Mozilla [12], Pocketsphinx [15], and Vosk [4]. Based on the comparisons of the quality and performance reported in [25], we focused on Kaldi and Vosk and finally chose Vosk, which supports over 20 languages and allows building small models (approx. 50MB) intended for use on smartphones and single-board computers such as Raspberry Pi. They require relatively little computing power and memory to operate [5].

For the fundamental stage of detecting the intention to call for help in the user's statements, we tested six analytical solutions. For local intent detection, we created three different models using the TensorFlow Lite (TFLite) library. Additionally, we created a fourth model using a light embedding approach. These models have been optimized to operate on devices with limited resources and low energy consumption, such as portable devices, smartphones, microcontrollers, and embedded systems.

The first model (*TF simple*) is a simple sequential model acting as a classifier composed of several layers (Fig. 3a). The initial layer is the *TextVectorization*, tasked with transforming the text into a sequence of token indices. The next one,

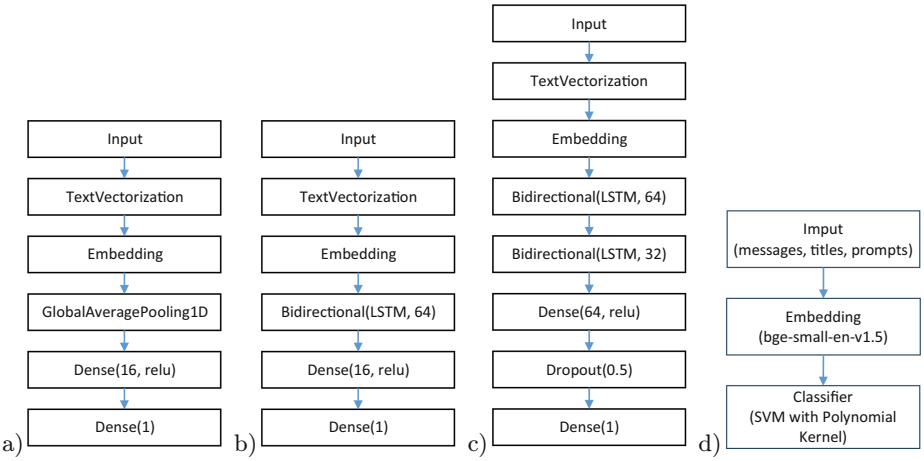

Fig. 3. Local inference models for intent detection: (a) simple, (b) 1-layer Bidirectional LSTM, (c) 2-layer Bidirectional LSTM, and (d) Embed&Class.

the *Embedding* layer, holds a vector for each word. Upon invocation, it transforms sequences of word indices into sequences of vectors. The *GlobalAveragePooling1D* layer produces a constant-length output vector for each example by computing the average across the sequence dimension. This approach allows the model to manage variable-length input data in a straightforward manner, which is crucial given the varying number of words in input statements. The constant-length output vector is passed through a fully connected *Dense* neural network layer with 16 hidden units. The final *Dense* layer is fully connected with a single output node. The second model (*TF 1-layer Bi-LSTM*, Fig. 3b) is slightly more complicated and uses the bidirectional LSTM recurrent neural network and fixed-length representation of text in the *Embedding*. The third model (*TF 2-layer Bi-LSTM*, Fig. 3c) differs from the second one by adding one more recurrent bidirectional LSTM layer directly after the first existing bidirectional LSTM layer and the *Dropout* layer, which helps prevent overfitting. The fourth model, we named Embed&Class, operates in a different way. In the first, embeddings are produced by the use of the Qdrant FastEmbed library[1], a library designed for fast embedding and which can rely on lightweight quantized language models based on Transformers, like bge-small-en-v1.5, a small-scale English text embedding model developed by BAAI (Beijing Academy of Artificial Intelligence). This approach is then combined with a standard SVM classifier that operates directly on the generated embedding vectors to detect intentions. The SVM model is trained using a 10-fold cross-validation process. Input embedding vectors used for learning are normalized. As parameters, the SVM uses a ridge logistic regressor for data calibration, a polynomial kernel, and a C value of 1.

[1] https://github.com/qdrant/fastembed.

As an external tool for intent recognition and the fifth analytical solution, we tested Azure Cognitive Services. It is a set of cloud services available in Microsoft Azure that enable the integration of artificial intelligence and machine learning across applications. These services offer pre-trained models for processing text, video, and speech data, as well as services for analyzing geospatial data. The default, pre-trained model has been tuned by us to the problem of calling for help. Specifically, the model was tuned to assign the sentence to one of two classes - the class of sentences containing or not the intention of calling for help.

As the last analytical approach, we also tested the external GPT-3.5 (Generative Pre-trained Transformer 3.5) service by OpenAI. It provided a stable (at the time of system implementation) and advanced language model based on the Transformer architecture, a neural network specifically designed to process sequences of data, such as text.

6 Experiments

All three stages of the speech analysis were experimentally tested on Samsung S20 with Android 13 using the implemented mobile application to assess the feasibility of performing automated calling for help at the Edge.

6.1 Wake-Up Keyword Detection

To assess the quality of wake-up word detection, we utilized a dataset comprising 300 voice recordings in WAV format, with a sampling frequency of 16 kHz. The dataset was balanced, comprising 150 speech recordings with the *help* wake-up word among other sentences spoken, and 150 recordings without the wake-up word. The dataset was created based on sentences from the Kaggle *Medical Speech, Transcription, and Intent* dataset [19] with audio statements related to typical medical symptoms along with their transcriptions. Since this dataset does not contain any sentences with the wake-up word, based on its content, we recorded 300 statements with ten 60+ volunteers speaking 30 selected sentences that contained or did not contain the wake-up word from a distance of 40 cm.

The detection process was treated as a two-class classification problem, where the output of the detector was a logical value indicating whether it recognized the keyword in the recording or not. Based on the obtained confusion matrix, where a *True Positive* was a correctly detected recording with the wake-up word, while the *True Negative* was a correctly detected recording without a wake-up word, we calculated the values of performance metrics, including accuracy, precision, recall, and F1-score (Table 2). The research was carried out on original recordings and the recordings with white noise added. The maximum amplitude of the recording was assumed as the default value for the maximum noise amplitude. We also tested the recordings with added noise of the amplitudes reduced by 20, 40, and 60 dB compared to the default value.

As can be observed, the accuracy of detecting the wake-up word was the highest for the original sound and is as high as 98%. As white noise is added,

Table 2. Performance of the wake-up word detection

	Accuracy	Precision	Recall	F1-score
Original sound	0.980	0.993	0.967	0.980
With white noise (−60 dB)	0.963	1.000	0.927	0.962
With white noise (−40 dB)	0.943	1.000	0.887	0.940
With white noise (−20 dB)	0.827	1.000	0.653	0.790
With white noise (−0 dB)	0.500	N/A	0.000	N/A

the accuracy decreases, but for noise with an amplitude reduced by 60 and 40 dB, the detector still achieves satisfactory results above 94%. Adding noise with an amplitude reduced by 20 dB causes a significant deterioration of the model's accuracy, which drops to 82.7%. The effect of adding noise with the default amplitude is the complete cessation of detection of the wake-up word, as evidenced by an accuracy value of 50% combined with a sensitivity (recall) of zero. Precision values of 1 in most analyzed cases suggest that the model is never triggered by phrases not containing the *help* word. The exception is only one case for the original sound, which contributed to the precision value in this case being 0.993. However, this is still a very high value. The key metric in the context of the considered application of the detector is sensitivity (recall). It tells us what proportion of real distress calls were correctly detected. For the original sound, the value of this metric reached 0.967. This is a satisfactory result. The sensitivity for recordings with added noise is slightly worse. However, for a noise amplitude reduced by 60 dB, the model still achieves a value exceeding 90%. As the amplitude of the added noise increases, the sensitivity value decreases, and for noise with an amplitude reduced by 20 dB, the software detects only about two-thirds of the distress calls. Adding noise at the default high amplitude means that the wake-up word is not detected in any of the test recordings, as evidenced by a sensitivity value of zero. The values of the F1-score, which is the harmonic mean of precision and sensitivity, also show similar behavior and decrease as the amplitude of the added noise increases. However, it is worth noting that the noise values corresponding to the two highest considered amplitudes are rarely encountered in real-life conditions.

6.2 Transcription of the Speech

To examine the accuracy of the transcriptions of the statements, we used prepared recordings and reference data in the form of transcriptions of the spoken sentences. The research was carried out on 1,200 recordings, which included 30 statements for each of the two classes - statements with the intention to call for help and neutral statements, recorded twice by 10 people. The statements with the intention to call for help or containing descriptions of medical symptoms along with their transcription were taken from the KAGGLE *Medical Speech, Transcription, and Intent* dataset [19]. The neutral sentences were taken from

the KAGGLE *TED Talks Transcripts for NLP* dataset containing transcripts of talks given on various topics at TED scientific conferences [10]. The recordings were provided as input to the Vosk model, which produced their transcriptions. Transcriptions from the Vosk model were compared to reference transcripts to determine their accuracy. For this purpose, we used the following quality measures:

– *Word Error Rate* (WER) - the ratio of the total number of word errors (substitutions S, deletions D, or insertions I) to the number of words N in the reference transcription:

$$WER = \frac{S + D + I}{N}, \tag{5}$$

– *Sentence Error Rate* (SER) - the percentage of transcripts containing at least one incorrect word:

$$SER = \frac{F}{M}, \tag{6}$$

where S is the number of words replaced with other words relative to the reference transcription, D is the number of words omitted (deleted) relative to the reference transcription, I is the number of words inserted additionally to the reference transcription, N is the total number of words in the reference transcription, F is the number of transcriptions containing at least one incorrect word, M is the total number of transcriptions. Particular ratios of S/N, D/N, and I/N in our experiments are presented in Table 3.

When assessing the transcription quality, we did not consider capitalization and punctuation. Each transcription was changed to all lowercase letters, and punctuation was removed completely. Similarly to the wake-up word detection, experiments were performed on original recordings and recordings with added white noise. By default, the maximum amplitude of the noise was assumed to be equal to the maximum amplitude of the original recording. Additionally, we analyzed the recordings with additional noise, whose amplitudes were reduced by 20, 40, and 60 decibels compared to the default value.

For original sound, the speech-to-text transcription with the Vosk model achieved very good results (Table 4). The mean value of the WER error is 9.228%, and the standard deviation is 13.635%. Noteworthy is the median value of zero. This proves that a large group of recordings was transcribed flawlessly. Taking into account the specificity of the WER metric and its lowest possible value equal to zero, at least half of all recordings belong to this group.

As the amplitude of noise added to recordings changes, the ratios of substitutions, deletions, and insertions to the total words in the reference transcription also change. Higher noise amplitude increases deletions and substitutions (except at maximum amplitude) while reducing insertions (Table 3). Substitutions and deletions had the most significant impact on the WER metric. For original recordings and those with −60 dB noise, substitutions contributed about 0.06 to the ratio, with deletions three to four times lower. In contrast, for noise levels at

Table 3. The ratio of the number of substitutions S, deletions D and insertions I to the number of all words in the reference transcript (μ - mean, σ - standard deviation)

	S		D		I	
	μ	σ	μ	σ	μ	σ
Original sound	0.063	0.107	0.016	0.044	0.012	0.046
With the white noise (−60 dB)	0.064	0.105	0.019	0.051	0.012	0.042
With the white noise (−40 dB)	0.079	0.129	0.094	0.244	0.010	0.036
With the white noise (−20 dB)	0.207	0.191	0.293	0.330	0.007	0.035
With the white noise (−0 dB)	0.119	0.077	0.879	0.077	0.000	0.000

Table 4. WER values for the speech-to-text transcription

	WER		
	Mean (%)	Standard deviation (%)	Median (%)
Original sound	9.228	13.635	0,000
With white noise (−60 dB)	9.520	13.236	0.000
With white noise (−40 dB)	18.368	27.102	9.100
With white noise (−20 dB)	50.737	33.952	50.000
With white noise (−0 dB)	99.907	0.737	100.000

−40, −20, and 0 dB, deletions had a greater influence. Substitution ratios ranged from 0.079 to 0.207, while deletion ratios spanned 0.094 to 0.879. Insertions had minimal impact on WER, regardless of noise level. The average insertion ratio was a maximum of 0.012, indicating the model rarely added unnecessary words to the transcription.

The SER error value increased with higher noise amplitude (Table 5). For original recordings, the SER was 7.917%, meaning 1,105 out of 1,200 recordings were transcribed correctly. Low-amplitude noise had little impact on results, with significant discrepancies only at noise levels of −40 dB or higher. Even with SER below 20%, these transcriptions can still aid in detecting intent to call for help when better-quality recordings are unavailable. However, the highest noise levels (−0 dB and −20 dB) produced the worst results, making transcriptions under these conditions unsuitable for emergency call procedures.

6.3 Detecting Intentions to Call for Help

For intention detection, we used the same transcription set as the previous experiment, dividing it 80:20 into balanced training and test sets with utterances expressing or not expressing the intent to call for help. Several models were trained and tested, including TF Simple, TF 1-layer Bi-LSTM, TF 2-layer Bi-LSTM, Embed&Class, Azure Cognitive Services, and GPT 3.5. The Embed&Class model uses three different kinds of input leading to three vari-

Table 5. SER values for the speech-to-text transcription ($M = 1200$)

	The number of transcripts containing at least one incorrect word F	SER (%)
Original sound	95	7.917
With white noise (−60 dB)	99	8.250
With white noise (−40 dB)	230	19.167
With white noise (−20 dB)	788	65.667
With white noise (−0 dB)	1200	100.000

ations, standard rough sentences (Embed&Class), rough sentences with metadata like message titles, if available (Embed&Class-T), or messages titles and intention prompts, if available (Embed&Class-TP). The task was treated as a two-class classification, where models identified whether a statement indicated the intent to call for help. Test set utterances were classified by the models, and results were compared with reference data to build confusion matrices and calculate metrics, including accuracy, precision, sensitivity, and F1-score. We also measured the classification times for each model (see Table 6).

Table 6. Classification performance and time while detecting the intention to call for help (μ_T - mean execution time, σ_T - standard deviation)

	Accuracy	Precision	Sensitivity	F1-score	μ_T (s)	σ_T (s)
TF simple	0.900	0.910	0.887	0.899	0.038	0.012
TF 1-layer Bi-LSTM	0.887	0.869	0.912	0.890	0.044	0.003
TF 2-layer Bi-LSTM	0.894	0.889	0.900	0.894	0.042	0.005
Embed&Class	0,997	0,997	0.995	0,997	0.030	0.004
Embed&Class-T	0,998	0,998	0.997	0,998	0.031	0.004
Embed&Class-TP	1.000	1.000	1.000	1.000	0.032	0.004
Azure Cognitive Services	0.981	0.975	0.988	0.981	0.207	0.038
GPT 3.5	0.881	0.867	0.900	0.883	0.795	0.219

The accuracy of local TensorFlow models working on the edge device did not exceed 90%. Among them, the *TF simple* model had the highest precision, making it the most effective at identifying emergency calls, though it detected about 1 in eleven calls incorrectly. The *1-layer Bi-LSTM* model achieved the highest sensitivity, but cases of missed emergency calls remain. Differences in F1-scores among these models were minimal. GPT 3.5 performed the worst among remote models, with an accuracy of 88.1% and the lowest precision and F1-score. In contrast, Azure Cognitive Services delivered better results, with a 98.1% accuracy. However, the best results are obtained by the local Embed&Class models

that outperform all models, even remote prompt-based ones, with a minimum of 99.7% accuracy. Although simpler than the local TensorFlow models, these models even reaches 100% accuracy whenever additional metadata are used for learning (Embed&Class-TP).

Inference times for statement classification were shortest with TensorFlow and Embed&Class models running locally on the edge device, averaging 30–44 milliseconds, enabling near-instant detection of help intent. Remotely invoked models were slower due to communication delays. GPT 3.5 had the worst performance, averaging nearly 800 milliseconds, with some cases taking up to 2,334 milliseconds—about 20 times slower than local models. Azure Cognitive Services performed better, with an average classification time of 207 milliseconds, a reasonable result for a cloud-based solution requiring internet access. While both remote services are acceptable for this application, their differing speeds may affect user experience.

7 Discussion and Concluding Remarks

Our experiments demonstrated that we can successfully perform automatic help calls through speech and text data analysis at the Edge. An interesting finding from these experiments is that lightweight AI/ML models running on Edge devices may outperform remote prompt-based models for this specific task, whilst working locally on smartphones. This not only accelerates the initiation of help requests or caregiver alerts while challenging previous results, such as those presented in [20], which suggested that cloud-based services often offer better accuracy, but also highlights how these services can be hindered by limited or delayed internet connectivity.

The rapid evolution of language models, including their lighter versions, is significantly transforming this landscape, notably enhancing the efficiency and accuracy of local approaches. These advancements ensure continuous, unobtrusive, and discreet monitoring of seniors, enhancing their sense of security without infringing on their independence. In fact, local solutions may even strengthen their autonomy by reducing the reliance on remote systems. Regardless of the approach used—whether local Edge-based, remote cloud-based, or hybrid—all of them contribute to enhancing the lives of older adults by making smart technologies accessible across generations and promoting their inclusion in modern society.

Acknowledgments. This paper was supported by the Reactive Too project that has received funding from the European Union's Horizon 2020 Research, Innovation and Staff Exchange Programme under the Marie Skłodowska-Curie Action (Grant Agreement No871163), the pro-quality grant (02/100/RGJ25/0041) of the Rector of the Silesian University of Technology (SUT), Gliwice, Poland, Statutory Research funds of the Department of Applied Informatics at SUT (grants No 02/100/BK_25/0044). Scientific work published as part of an international project co-financed by the program of the Minister of Science and Higher Education entitled "PMW" in the years 2021–2025; contract no. 5169/H2020/2020/2.

References

1. Global health and aging, Technical report 7737, World Health Organization (2011)
2. Aakesh, U., Rajasekaran, Y., Bethanney Janney, J.: Wristband for elderly individuals: Esp-32 and Arduino Nano enabled solution for health monitoring and tracking. In: 2023 IEEE Asia-Pacific Conference on Geoscience, Electronics and Remote Sensing Technology (AGERS), pp. 26–33 (2023)
3. Cook, A.M., Polgar, J.M.: Assistive Technologies: Principles and Practice. Elsevier, St. Louis, Missouri, P.E. (2016)
4. AlphaCephei: Vosk speech recognition (2024). https://alphacephei.com/vosk/
5. AlphaCephei: Vosk speech recognition models (2024). https://alphacephei.com/vosk/models/
6. Austerjost, J., et al.: Introducing a virtual assistant to the lab: a voice user interface for the intuitive control of laboratory instruments. SLAS Technol. Transl. Life Sci. Innov. **23**(5), 476–482 (2018)
7. Banos, O., Villalonga, C., Damas, M., Gloesekoetter, P., Pomares, H., Rojas, I.: PhysioDroid: combining wearable health sensors and mobile devices for a ubiquitous, continuous, and personal monitoring. Sci. World J. **2014**, 1–11 (2014). https://doi.org/10.1155/2014/490824
8. Bhosale, S., Sheikh, I., Dumpala, S.H., Kopparapu, S.K.: Transfer learning for low resource spoken language understanding without speech-to-text. In: 2019 IEEE Bombay Section Signature Conference (IBSSC), pp. 1–5 (2019)
9. Braines, D., O'Leary, N., Thomas, A., Harborne, D., Preece, A.D., Webberley, W.M.: Conversational homes: a uniform natural language approach for collaboration among humans and devices. Int. J. Intell. Syst. **10**(3), 223–237 (2017)
10. Corral Jr., M.: TED talks transcripts for NLP (2020). https://www.kaggle.com/datasets/miguelcorraljr/ted-ultimate-dataset
11. de Velasco, M., Justo, R., Antón, J., Carrilero, M., Torres, M.I.: Emotion detection from speech and text. In: Proceedings of the IberSPEECH 2018, pp. 68–71 (2018)
12. Hannun, A.Y., et al.: Deep speech: scaling up end-to-end speech recognition. arXiv preprint arXiv:1412.5567 (2014)
13. Hosseinzadeh, M., et al.: An elderly health monitoring system based on biological and behavioral indicators in internet of things. J. Ambient Intell. Humaniz. Comput. **14**, 5085–5095 (2023)
14. Hou, L., Latif, J., Mehryar, P., Zulfiqur, A., Withers, S., Plastropoulos, A.: IoT based smart wheelchair for elderly healthcare monitoring. In: 2021 IEEE 6th International Conference on Computer and Communication Systems (ICCCS), pp. 917–921 (2021)
15. Huggins-Daines, D., Kumar, M., Chan, A., Black, A., Ravishankar, M., Rudnicky, A.: PocketSphinx: a free, real-time continuous speech recognition system for handheld devices. In: 2006 IEEE International Conference on Acoustics Speech and Signal Processing Proceedings, vol. 1, p. I (2006)
16. Jain, R., Semwal, V.B.: A novel feature extraction method for preimpact fall detection system using deep learning and wearable sensors. IEEE Sens. J. **22**(23), 22943–22951 (2022)
17. Lersilp, S., Putthinoi, S., Lerttrakarnnon, P., Silsupadol, P.: Development and usability testing of an emergency alert device for elderly people and people with disabilities. Sci. World J. **2020**, 1–7 (2020)
18. Sabri, S.M., Annuar, N., Rahman, N.L.A., Musairah, S.K., Mutalib, H.A., Subagja, I.: Major trends in ageing population research: a bibliometric analysis from 2001 to 2021. Proceedings **82**, 19 (2022)

19. Mooney, P.: Medical speech, transcription, and intent (2019). https://www.kaggle.com/datasets/paultimothymooney/medical-speech-transcription-and-intent
20. Mrozek, D., Kwaśnicki, S., Sunderam, V., Małysiak-Mrozek, B., Tokarz, K., Kozielski, S.: Comparison of speech recognition and natural language understanding frameworks for detection of dangers with smart wearables. In: Paszynski, M., Kranzlmüller, D., Krzhizhanovskaya, V.V., Dongarra, J.J., Sloot, P. (eds.) ICCS 2021. LNCS, vol. 12745, pp. 471–484. Springer, Cham (2021). https://doi.org/10.1007/978-3-030-77970-2_36
21. Picovoice: Porcupine wake word (2024). https://picovoice.ai/platform/porcupine/
22. Povey, D., et al.: The kaldi speech recognition toolkit. In: IEEE 2011 Workshop on Automatic Speech Recognition and Understanding (2011)
23. Qian, Z., et al.: Development of a real-time wearable fall detection system in the context of internet of things. IEEE Internet Things J. **9**(21), 21999–22007 (2022)
24. Radford, A., Kim, J.W., Xu, T., Brockman, G., McLeavey, C., Sutskever, I.: Robust speech recognition via large-scale weak supervision. In: Proceedings of the 40th International Conference on Machine Learning. ICML'23, JMLR.org (2023)
25. Trabelsi, A., Warichet, S., Aajaoun, Y., Soussilane, S.: Evaluation of the efficiency of state-of-the-art speech recognition engines. Procedia Comput. Sci. **207**, 2242–2252 (2022)
26. United Nations: Department of Economic and Social Affairs, Population Division: World Population Ageing 2019. United Nations, New York (2020)
27. United Nations: Department of Economic and Social Affairs, Population Division: World Population Ageing 2020 Highlights: Living arrangements of older persons. United Nations, New York (2020)
28. United Nations: Department of Economic and Social Affairs, Population Division: World Social Report 2023: leaving no one behind in an ageing world. United Nations, New York (2023)
29. Vinotha, R., Hepsiba, D., Vijay Anand, L., D.: Leveraging openai whisper model to improve speech recognition for dysarthric individuals. In: 2024 Asia Pacific Conference on Innovation in Technology (APCIT), pp. 1–5 (2024)
30. Zhang, Q., Ren, L., Shi, W.: HONEY: a multimodality fall detection and telecare system. Telemed. J. e-Health Off. J. Am. Telemed. Assoc. **19**(5), 415–429 (2013)

Leveraging Graph Digital Twin for Fault Detection and Improved Power Grid Stability in Smart Cities

Anubhav Mendhiratta(✉), Craig Fernandes, Dharini Hindlatti, Divyansh Vinayak, and Chandrashekhar Pomu Chavan

Deptartment of CSE, PES University, Bangalore, Karnataka, India
{pes2202100830,pes2202100820,pes2202100100,pes2202100809}@pesu.pes.edu, cpchavan@pes.edu

Abstract. Despite the critical role played by power grids in smart cities, traditional systems often detect issues too late leading to costly outages and safety risks. This paper presents a novel approach by leveraging graph-based digital twins created with the help of Microsoft Azure IoT TwinMaker to enable an always-on view of real-time power grids. For one to derive a virtual model of this grid that reflects what happens in its counterpart in the physical plane, digital twins have this application. Simulation of the grid's behavior helps reveal existing problems to operators without affecting the infrastructure. The system incorporates advanced machine learning techniques, including a genetic algorithm, which can predict failures in advance by taking realtime and previously recorded data from the digital twin. This approach is proactive, thereby preventing disruptions and operational risks. It ensures scalability and efficient processing of large datasets when running machine learning models in the cloud on Microsoft Azure, thus adapting the system to the complex needs of modern power grids in smart cities. Using machine learning in the digital twin rather than in the physical grid minimizes real-world testing and avoids unanticipated downtime, thereby saving costs. This approach not only enhances the accuracy of fault detection but also improves the lasting ability and steadiness of the grid. The solution aims to support the rising energy demands of smart cities by offering a scalable, cost-effective, and reliable way of managing power grids.

Keywords: Digital Twin · Smart Cities · Fault Detection · Power Grid Stability · Graph Digital Twin · TPOT · Machine Learning · Azure IoT TwinMaker

1 Introduction

The increasing complexity and strong demand for a stable power supply in smart cities call for innovative approaches to the management of grids. This project aimed at addressing these issues in light of using digital twin technology, specifically in graph-based digital twins, to generate real-time dynamic models for key

M. Paszynski et al. (Eds.): ICCS 2025 Workshops, LNCS 15912, pp. 33–47, 2025.
https://doi.org/10.1007/978-3-031-97573-8_3

components of the power grid. A graph-based digital twin mirrors the very intricate interconnections associated with the grid and could potentially be utilized to gain further insights into its operations [1].

A key feature of this project is the graph-based representation of various components of the power grid, which means intuitive modeling can be represented if there are relationships amongst various parts of the grid. Hence, it should be possible to create mappings of interaction between the interactions between the generators and critical nodes with transformers when considering the complexity of mapping it into a graph-based model of a digital twin for the power grid [2]. This approach gives a better insight into the behavior of the grid, thus fast detection of faults, downtime, and inefficiencies. Additionally, with graph theory, algorithms are developed to detect anomalies and faults, thus improving the stability and resilience of the grid.

The rich dataset feeds into the digital twin, which allows the machine learning models to make predictions based on the analyzed patterns [3].

At the heart of our predictive capabilities lies the use of machine learning algorithms specifically, a genetic algorithm, to predict potential faults [4]. Such algorithms analyze the collected data and ensure optimized functioning of the grid by detecting weaknesses before they develop into large failures.

The scope of this project extends beyond the mere detection of faults. Our system is built to make power grids more interoperable in smart cities, compatible with the existing infrastructure of a smart city [5]. That is, our solution can be integrated with other digital systems in the city, such as transportation, communication, and water supply networks, making the urban environment more connected and efficient. Such an approach would, therefore, be crucial in offering solutions to the existing particular challenges in smart cities, where different systems must be interconnected and function in harmony with each other seamlessly.

The rest of this paper is organized as follows: Sect. 2 covers related work and technologies. Section 3 presents the system architecture and methodology. Section 4 discusses the machine learning techniques used. Section 5 provides experimental results and analysis. Finally, Sect. 6 concludes the paper with a summary and future directions.

2 Related Work

2.1 Power Grid Monitoring Systems

Continuous and stable operation of electric networks calls for power grid monitoring systems. It enables the operators to monitor the actual performance of the grid, detect anomalies, and take corrective actions to avoid or minimize outages. In modern power grids where the coalition of renewable sources of energy, electric vehicles, and smart technologies has increased the complexity, effective monitoring systems are in demand. While the approaches used in monitoring traditional power grids have been perfected with time, they are limited and prevent them from effectively preventing failures and interruptions [6]. Traditional approaches followed along with their limitations are as follows.

Supervisory Control and Data Acquisition (SCADA) Systems. The most common technology applied in power grid monitoring is the Supervisory Control and Data Acquisition (SCADA) system. Supervisory Control and Data Acquisition systems are centralized networks that collect data from sensors dispersed throughout the grid and give real-time information to operators. These systems monitor a range of parameters, such as voltage levels, current flow, and equipment status, and help operators manage grid operations. However, the SCADA system often requires operator intervention to make decisions and tends to respond rather than predict. Above all, SCADA systems do not have a robust predictive ability, which in turn reduces its capability to find slight signs of potential failure before time, which sadly is absent in SCADA systems [7].

Limitations:

- The primary focus of SCADA systems is monitoring real-time conditions and typically do not analyze historical data or simulate future scenarios, which would reduce their ability to provide predictive insights.
- Some of the known vulnerabilities of centralised SCADA architecture include the problem of single points of failure, and may not be competent enough to handle modern distributed energy resources (DERs).
- SCADA systems are often dependent on human interpretation of the data they provide, which inevitably leads to delays in taking corrective actions and potential missed opportunities for proactive maintenance.

Phasor Measurement Units (PMUs). Phasor-Measurement Units (PMUs) are the time-synchronized measurements of electrical waves all over the power grid. It provides very accurate monitoring of the stability of the grid. The PMUs detect the disturbances that are in the grid, identify the weak points, and determine the overall performance of the grid. PMUs give real-time data but they do not predict failures for the future based on the pattern that has occurred [8].

Limitations:

- The high expenses associated with PMU installation limit their deployment, particularly in older or underfunded infrastructures.
- Despite the accuracy of PMUs in detecting disturbances, they do not offer predictive insights and therefore cannot prevent issues before they occur.
- The large volume of data generated by PMUs can overwhelm traditional data processing systems, resulting in inefficiencies in extracting actionable insights.

Periodic Manual Inspections and Maintenance. Another traditional method of monitoring power grids is through periodic manual inspection and maintenance. Utility companies schedule routine inspections of major grid components, such as transformers, transmission lines, and substations. Field technicians evaluate the condition of these components and make necessary repairs. This method can identify any visible wear or damage but is time-consuming,

labor-intensive, and prone to human error. Furthermore, the use of scheduled maintenance increases the chances of missing issues that develop between inspection periods [9].

Limitations:

- Manual inspections require significant time, labor, and financial resources.
- The infrequency of inspections could indicate that early signs of equipment deterioration can be missed, resulting in unforeseen failures.
- Human error during inspections could potentially lead to inaccurate assessments and increased operational risks.

Event-Driven Fault Detection. Traditional power grids rely on event-driven fault detection systems, which detect alarms and initiate protective actions in the event of certain occurrences, like short circuits or overloads. Such systems use protective relays and circuit breakers to get to a faulty component by detecting anomalies. However, an event-driven system can only react after an event has happened and cannot prevent a disruption from happening. While these help reduce the impact of faults, they do not offer predictive capabilities or early warnings [10].

Limitations:

- These systems can only react to predefined thresholds or conditions, which could potentially result in overlooking early-stage issues and not triggering immediate alarms.
- Relying on event-driven systems can often result in prolonged downtime since operators work to restore grid operations after a fault has occurred.

2.2 Digital-Twin Technology in Smart-Cities

Digital-twin technology, that is based on virtual representations of physical assets and systems, is considered a transformational solution for managing complex urban environments [11]. The integration of digital twins within smart cities further improves infrastructure by providing real-time monitoring, simulation, and optimization.

Existing Implementations of Digital Twins. Digital twins technology has been implemented with success in various smart city initiatives around the world in different infrastructure sectors [12]. Singapore and Dubai, for example, use digital twins to manage their urban planning and development. The Virtual Singapore project utilizes a detailed digital twin of the city to propagate urbanised planning, optimize resource allocation, and enhance public safety.

In the same vein, cities like Helsinki have utilized digital twins to enhance public transportation. The concept of developing real-time models of transport networks assists planners in analyzing traffic patterns and optimizing routes and service delivery [13].

Applications of Digital-Twins in Power Systems. Digital-twins in the power system are mainly advantageous in providing an improved monitoring and predictive maintenance approach and also enhancing the decision-making process [14].It is thus possible to respond more rapidly to abnormal conditions, hence decreasing the likelihood of an outage.

Application of digital-twins in power systems also extended towards predictive maintenance. Utilities can identify patterns of potential equipment failures through analysis of data from digital twins. This helps reduce unplanned downtime, prolong asset life, and save on maintenance costs. Through digital twins, the planning and optimization of energy resources can be properly improved. Utilities can plot different scenarios or conditions.This capability results in better decision-making regarding the resources that should be allocated.

Digital twin technology is, therefore, a key component in developing smart cities, offering innovative methods in urban infrastructure management [15],thus promising to transform the very way utilities operate in order to assure a more resilient and efficient energy grid.

2.3 Machine-Learning for Fault Detection

The integration of Machine-Learning (ML) techniques into power grid systems has significantly advanced the field of fault detection. Machine learning algorithms, based on vast amounts of operational data, can detect patterns and anomalies that may signify potential faults in grid infrastructure. Traditional fault detection methods, often based on threshold-based approaches, lack the adaptability and predictive power of machine learning [16]. Utilities are therefore looking at a myriad of machine learning approaches for the improvement of fault detection.

Previous Approaches Using Machine Learning in Grid Systems. There are previous studies that have demonstrated the use of machine-learning for fault-detection in power systems [17]. Most popularly, supervised learning algorithms, including support-vector machines (SVM), decision trees, and random forests, are utilized. All these algorithms are trained from historical fault data to identify different types of anomalies that may lead to failures. For instance, [18] used random forests to analyze outage history data, and they received better accuracy in detecting faults than traditional methods. Similarly, deep models like neural networks have been used on power grid data to model intricate relationships present within the data for better fault detection related to equipment degradation.

Another approach is through unsupervised learning methods, namely, clustering algorithms and anomaly detection methods. Such methods do not necessarily make use of labeled data, hence particularly useful in identifying faults that are previously unseen [19].

Despite such promising results, these approaches have several challenges. Among them are data quality and data quantity, model-interpretability, and

the ability of machine learning systems to interface with existing infrastructure for fault detection in power grids.

Genetic Algorithms and Their Role in Optimization and Prediction. Genetic algorithms (GAs) are a strong optimization technique that has its inspiration in the principles of natural selection. In machine learning for fault detection, GAs can be applied for optimizing the parameters of the model, feature selection, and the overall architecture of the predictive models. The natural tendency of GAs to efficiently explore an extensive search space makes them highly suited to identifying optimal configurations in complex systems.

Genetic algorithms also serve another role in power systems: the optimization of machine learning models.For example, one possible application of GAs is to seek the best hyperparameters for machine learning models that would result in better predictive accuracy and robustness when performing fault detection tasks [20]. The hybrid GAs combined with machine learning improve the rate of fault detection as well as model efficiency to significant extents.

GAs may also be useful in determining which of the features are most contributing in predicting faults, thereby making significant power systems information about overwhelming volumes of data that might be produced [21]. Hence, the complexity of the model is reduced because it is based on a smaller number of more important features.

3 Methodology

3.1 Dataset

This study uses electrical grid stability simulated data to improve the proposed model's robustness in real-time fault detection and stability assessment within power grid systems. The dataset is specifically designed for the local stability analysis of a 4-node star system and contains over 60,000 labeled instances, representing a wide variety of grid conditions. It is multivariate, complete (no missing values), and serves as a crucial foundation for training and evaluating learning algorithms in predicting grid steadiness [22].

The variables included in the dataset offer valuable insights into the behavior of grid participants and their responses under varying conditions. Key columns include:

- **Reaction Times** $(\tau_1, \tau_2, \tau_3, \tau_4)$: Represent the reaction times of the four participants in response to fluctuating electricity prices. These are critical in understanding how the system might respond to disturbances that influence overall stability.
- **Mechanical Power** (p_1, p_2, p_3, p_4): Indicate the mechanical power generated (positive) or absorbed (negative) by each participant. Power dynamics play a vital role in maintaining a balanced and stable grid.

- **Price Elasticity Coefficients** (g_1, g_2, g_3, g_4): Represent the price elasticity of each participant, helping estimate how responsive they are to price fluctuations and how that affects grid stability.
- **Stability Indicator** (*stab*): A numerical value measuring grid stability, with negative values indicating stable states and positive values indicating instability. This is the primary prediction target.
- **Categorical Stability Status** (*stabf*): Derived from the *stab* column, this categorical label classifies grid states as either "stable" or "unstable," aiding in classification tasks and model evaluation.

The dataset was generated using the methodology outlined in "Taming Instabilities in Power Grid Networks by Decentralized Control" (Benjamin Schafer, Carsten Garbow), which emphasizes decentralized control strategies to mitigate instabilities in power grid systems. This makes it highly aligned with our focus on digital twin-driven analysis and control.

Despite its usefulness, the dataset is simulated and represents an idealized version of a power grid, limited to a simplified 4-node star topology. This abstraction, while beneficial for initial algorithm development and theoretical analysis, does not fully capture the complexities, noise, and unpredictability of real-world power grid data. Real-world systems often involve higher node counts, nonlinear behaviors, communication delays, and missing or corrupted sensor data. These challenges can significantly affect model performance and generalizability. Therefore, while this dataset provides a strong baseline for experimentation and validation, future work must incorporate real-time, real-world datasets—potentially sourced from smart grid testbeds or utility partners—to ensure scalability, reliability, and practical applicability of the proposed digital twin approach.

This dataset will be used in model training to simulate a variety of scenarios and assess the impact of various parameters on grid stability. The large volume of labeled data enables the development of robust machine learning models, which can later be validated against real-time data generated by the digital twin of the power grid. This two-step approach helps bridge the gap between simulation and practical deployment, enhancing predictive accuracy and operational resilience for smarter, more stable grid infrastructure.

3.2 Digital-Twin Model

The digital-twin concept to be implemented for our power grid system is through the platform Azure Digital Twins. It is the platform from which holistic digital representations of physical environments can be created. The methodology, therefore, makes use of both the control plane and the data plane APIs to efficiently manage all the resources, models, and relationships in the Azure ecosystem.

Control Plane. The control plane contains the resource manager APIs, which are employed to manage all the Azure resources that are associated with Azure Digital Twins. It includes those functionalities concerned with creating and deleting full instances of digital twins. It is also concerned with managing endpoints.

Data Plane. In contrast, it is the control plane that focuses on API requests related to operations on models, digital twins, relationships, and event routes within the Azure Digital Twins instance itself. The key components for the data plane are:

- **Event Routes:** Event routes are significant in the flow of digital twin data through the Azure Digital Twins graph and to endpoints to forward the data to downstream services for further processing.
- **Jobs:** The data plane supports the management of long-running jobs.
- **Models:** Custom definitions describe specific entities in an environment, such as generators, sensors, and consumers, and each type of entity has a corresponding model.
- **Query:** Querying capabilities will allow users to query the Azure Digital Twins graph regarding properties, models, and relationships.
- **Twins:** Finally, there are requests for managing the digital twins. These requests denote instances of a model reflecting specific entities within the environment. For example, in a single model of the Generator, multiple digital twins can be there, namely, Generator A, Generator B, and Generator C.

This design we would implement using the Azure Digital Twins Command Line Interface (CLI) to manage user roles. For example, we add a role assignment for a "SAZURE USER" user assigned to the "Azure Digital Twins Data Owner" role in the instance of the "powergrid" Digital Twin of the resource group "azure-digital-twins-training". This would be the role assignment that would ensure that the users, once assigned, are enabled with the right permissions to do most things within the digital twin environment. Also, User Access Control (UAC) settings on this storage account are enforced to limit access to only twin owners; they can read and write, upload, or execute data in the account.

By integrating all these components and methodologies into our digital twin system, it should become a powerful tool for realtime monitoring and speculative analysis of the power-grid.

3.3 Machine Learning Workflow

Our workflow is to make our model robust, scalable, and optimized for use in real-time applications. This process involves several very crucial stages: data preprocessing, feature extraction, model training, and finally, the deployment on Microsoft Azure.

Model Training and Deployment on Microsoft Azure. We used an AutoML framework called TPOT (Tree-based Pipeline Optimization Tool) that aims at designing machine learning pipelines in a rather automatic way, through automated optimization. TPOT will discover the best-performing pipeline by searching over numerous configurations of models, preprocessing steps, and

hyperparameters without much need for a human (Fig. 1). GAs encode possible solutions as chromosomes and iteratively evolve those solutions to maximize a predefined fitness function.

The TPOT optimization process involves several key parameters:

- **Generations:** We set the number of generations to 5, meaning TPOT iteratively improves the population of pipelines over five cycles and enhances their performance at each stage.
- **Population Size:** In each generation, it evaluates a diverse set of 20 pipelines. That means that during optimization, there is a large variety of models considered.
- **Cross-Validation (cv=5):** TPOT uses 5-fold cross-validation for evaluation, which ensures consistency and reliability in the performance of pipelines over different subsets of the training data.

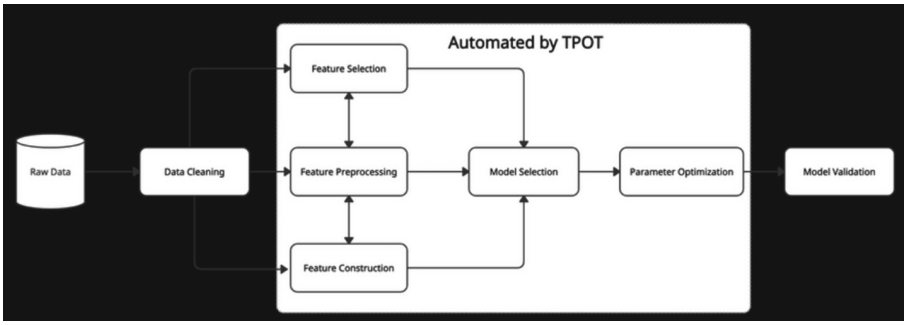

Fig. 1. Model Architecture.

Cloud-Based Processing and Scaling. We then deploy the optimal model on Microsoft Azure, where the power of cloud-based processing and scaling can be unleashed. The Azure platform offers necessary resources for handling large amounts of data and real-time computations, which is indispensable for our application's necessities. Utilizing Azure's robust infrastructure ensures that the model can work efficiently regardless of the loads and varying conditions, thereby ensuring fault detection in the power grid system in a timely and proactive manner.

Figure 2 shows a fully realized project of a complete Digital Twin solution that will build and deploy on the asset site. Data collection, preprocessing, feature engineering, model training, and real-time fault detection are incorporated within the architecture. Deployed on the Azure cloud platform, integration to multiple assets and systems in real-time, provides this capability for predictive maintenance.

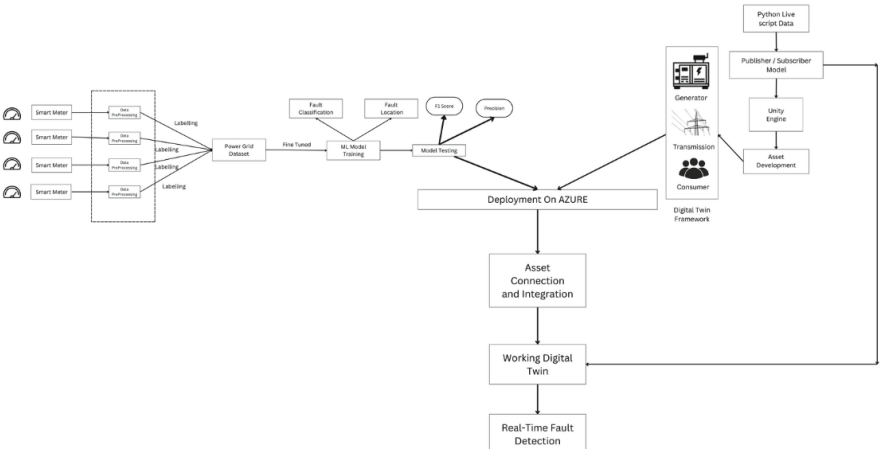

Fig. 2. High Level Workflow.

4 Results and Discussion

4.1 Benefits of Graph Digital-Twin in Smart-Cities

Implementing a graph digital-twin for the smart power grid system introduces a more advanced approach to monitoring and managing city-wide infrastructure. This setup is crucial for managing the complexity of urban energy systems and supports the integration of the power grid with other smart city infrastructures, such as transportation and emergency response systems.

Graph digital twins enhance resilience by offering a real-time understanding of the relationships between different components in the power grid. In the event of a fault, the graph structure enables the system to quickly identify impacted nodes and reroute power, maintaining supply to critical services. Additionally, by simulating various fault conditions, operators can proactively strengthen the network's resilience. The digital twin approach thus enables a shift from reactive to proactive grid management, helping to prevent issues before they escalate.

Figure 3 illustrates the final graph digital twin of a smart power grid system. Each node in the graph represents a specific component of the power grid, including city plants, delivery substations, domestic consumers, farm consumers, industrial consumers, and various energy sources like industrial plants, solar plants, and wind plants. The edges between the nodes indicate power lines that connect these components, showing the flow of electricity across the system. This visual setup helps monitor and manage the interactions between different elements of the power grid, enhancing stability and efficiency.

4.2 Fault Detection Performance

The fault detection capabilities of our model, optimized using TPOT, were evaluated with several key metrics, which include among others precision, recall,

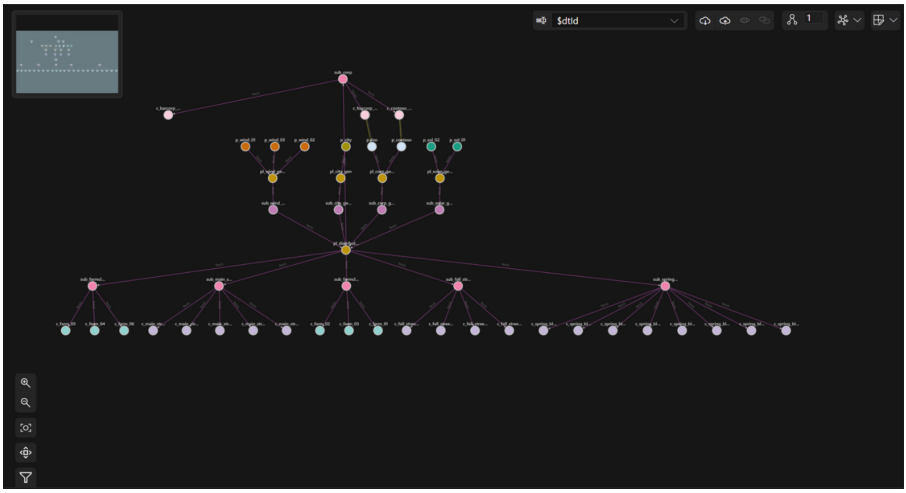

Fig. 3. Graph Digital Twin of Smart Power Grid implemented on Microsoft Azure.

F1-score, and accuracy. These metrics help predict the model's performance in accurately detecting faults within the power grid. The model achieved high precision, ensuring that instances identified as faulty are indeed faulty, thus minimizing false positives. High recall values demonstrate the model's effectiveness in identifying nearly all actual faults, ensuring that potential issues are caught before escalation.

The F1-score produces a balanced metric, integrating precision and recall to reflect the model's robustness across different fault scenarios. A high F1-score confirms that the model performs consistently well, even in complex situations. Additionally, the model attained an overall accuracy of 98.6%, indicating its high reliability in classifying instances within the dataset accurately. When compared to baseline models, this optimized approach demonstrated significant improvements in fault detection accuracy, supporting the utility of graph digital twins combined with advanced machine learning techniques for effective fault management in smart power grids.

The confusion-matrix displayed in Fig. 4 provides an in-depth evaluation of the model's fault detection performance, illustrating how well the model classifies stable and unstable states within the power grid system. Here's a breakdown of the matrix components:

1. **True Positives (TP)**: There are 1,260 instances in the bottom-right cell where the model correctly identified faults (labeled as "1") when they actually occurred. This reflects the model's ability to detect faulty conditions accurately.
2. **True Negatives (TN)**: The top-left cell shows 1,257 instances where the model accurately classified the stable state (labeled as "0"). These are cases where no faults occurred, and the model correctly identified them as such.

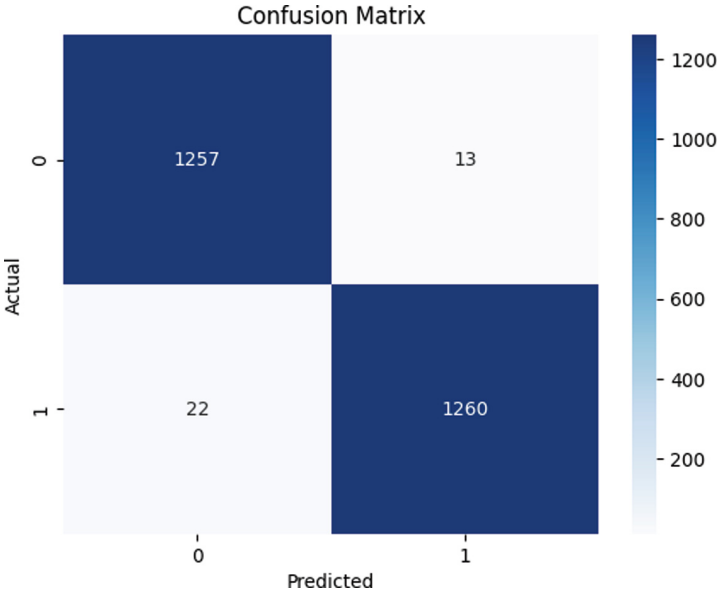

Fig. 4. Confusion Matrix of TPOT Model.

3. **False Positives (FP)**: In the top-right cell, there are 13 instances where the model incorrectly classified a stable condition as a fault. This represents the cases where the model generated a false alarm, identifying a fault when there was none.
4. **False Negatives (FN)**: The bottom-left cell shows 22 instances where the model failed to detect an actual fault, misclassifying it as a stable condition. These instances represent missed fault detections, which could potentially impact grid stability if faults go undetected.

The low false positive rate suggests minimal disruption from unnecessary alarms, while the low false negative rate indicates reliability in capturing most actual faults, supporting the model's application in real-time fault detection and grid stability enhancement.

TPOT Performance Analysis. As evidenced by the classifier performance summary in Fig. 5, TPOT demonstrates superior performance among all evaluated classifiers. With a baseline accuracy of 98.3% and a tuned accuracy of 98.6%, TPOT achieved the highest performance metrics in the comparative analysis. The 0.3% improvement through optimization, while modest, represents significant enhancement given the already exceptional baseline performance. In comparison, other classical machine learning approaches showed lower performance levels: Support Vector Classifier achieved 97.3% after tuning with a 0.6% improvement, Gradient Boosting Classifier reached 95.5% with a 1.5% improve-

ment, Random Forest Classifier attained 92.4% with a 0.4% increase, and K-Nearest Neighbors Classifier achieved 90.4% with a 1.2% improvement. The substantial performance gap between TPOT and simpler models like Logistic Regression, which achieved 81.5% accuracy, underscores TPOT's effectiveness in automated machine learning optimization. TPOT's superior performance can be attributed to its automated pipeline optimization capabilities, which include comprehensive feature preprocessing, model selection, and hyperparameter tuning. The high baseline accuracy demonstrates TPOT's capability to establish strong initial configurations without extensive manual tuning, making it particularly suitable for immediate deployment in fault detection systems.All the preceding classical classifier performance were computed on the same azure instance as the GA algorithm for comparable results.

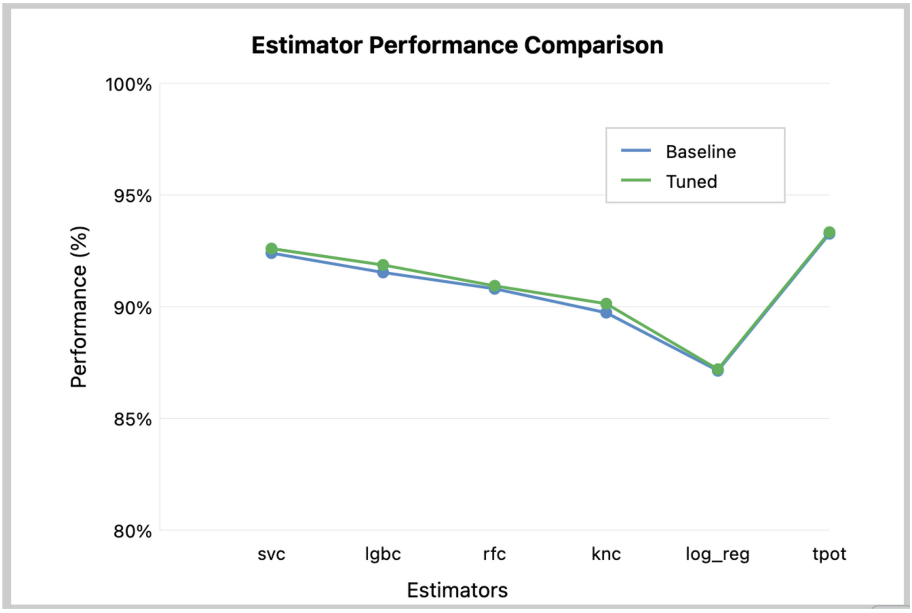

Fig. 5. Estimator Performance Comparison.

5 Conclusion and Future Work

We propose a new approach in this research for the improvement of fault detection and stability of power grids by graph digital twins and advanced machine learning techniques. A full-scale digital twin of the power grid was developed with the use of Microsoft Azure IoT TwinMaker to enable real-time monitoring and predictive analysis. Substantive accuracy improvements in the detection of faults were also derived through the deployment of the classifier models

optimized using TPOT and cloud-based processing. These improvements can facilitate the enhancement of the reliability as well as efficiency of a power grid system. Such research, therefore, serves as a basis for identifying and establishing the potential benefits and application areas of using a combination of digital-twin technology with machine-learning in a smart city context for the proper handling of challenges in its management of power infrastructure.

More lines of future work open up in the subsequent avenues. More and more components of the smart grid can be integrated into the digital twin model. In particular, renewable energy sources and storage systems might be included to give a holistic view of the dynamics of the grid. Future research can focus on the inclusion of realtime data feeds from IoT devices that might eventually enhance the response capabilities of the fault detection algorithms.

Another important aspect of future work will be the validation of the proposed models using real-world operational data. This includes exploring potential collaborations with utility companies, smart grid pilot projects, or national power system research initiatives to gain access to authentic grid data. Such validation will ensure the proposed model can generalize beyond simulated environments and operate reliably under real-world grid conditions.

While our current work demonstrates enhanced fault detection capabilities, ensuring overall grid stability—especially with the integration of intermittent renewable sources—remains a complex challenge. To address this, future extensions of our model will incorporate dynamic load balancing algorithms and predictive analytics that consider fluctuations in renewable input. Coupling digital twins with energy storage modeling and real-time demand-response mechanisms will allow for better simulation of these scenarios, supporting a more stable and adaptive grid in the presence of renewable generation.

References

1. Hashmi, R., Liu, H., Yavari, A.: Digital twins for enhancing efficiency and assuring safety in renewable energy systems: a systematic literature review. Energies **17**(11), 2456 (2024)
2. Nakarmi, U.: Reliability Analysis of Power Grids and its Interdependent Infrastructures: An Interaction Graph-Based Approach. University of South Florida (20200
3. Cao, H., Zhang, D., Yi, S.: Real-time machine learning-based fault detection, classification, and locating in large scale solar energy-based systems: digital twin simulation. Sol. Energy **251**, 77–85 (2023)
4. Sulaiman, A., et al.: Artificial intelligence-based secured power grid protocol for smart city. Sensors **23**(19), 8016 (2023)
5. Mouftah, H.T., Erol-Kantarci, M., Rehmani, M.H. (eds.): Transportation and Power Grid in Smart Cities: Communication Networks and Services. Wiley (2018)
6. Aguero, J.R., Takayesu, E., Novosel, D., Masiello, R.: Modernizing the grid: challenges and opportunities for a sustainable future. IEEE Power Energ. Mag. **15**(3), 74–83 (2017)
7. Sayed, K., Gabbar, H.A.: SCADA and smart energy grid control automation. In: Smart Energy Grid Engineering, pp. 481–514. Academic Press (2017)

8. Biswal, C., Sahu, B.K., Mishra, M., Rout, P.K.: Real-time grid monitoring and protection: a comprehensive survey on the advantages of phasor measurement units. Energies **16**(10), 4054 (2023)
9. Gill, P.: Electrical Power Equipment Maintenance and Testing. CRC Press (2016)
10. Vemulapalli, G.: Architecting for real-time decision-making: building scalable event-driven systems. Int. J. Mach. Learn. Artif. Intell. **4**(4), 1–20 (2023)
11. Mazzetto, S.: A review of urban digital twins integration, challenges, and future directions in smart city development. Sustainability **16**(19), 8337 (2024)
12. El-Hajj, M.: Leveraging digital twins and intrusion detection systems for enhanced security in IoT-based smart city infrastructures. Electronics **13**(19), 3941 (2024)
13. Ferré-Bigorra, J., Casals, M., Gangolells, M.: The adoption of urban digital twins. Cities **1**(131), 103905 (2022)
14. Shen, Z., Arraño-Vargas, F., Konstantinou, G.: Artificial intelligence and digital twins in power systems: trends, synergies and opportunities. Digital Twin **1**(3), 11 (2023)
15. Agostinelli, S.: Optimization and management of microgrids in the built environment based on intelligent digital twins (2024)
16. Ahmad, T., Madonski, R., Zhang, D., Huang, C., Mujeeb, A.: Data-driven probabilistic machine learning in sustainable smart energy/smart energy systems: key developments, challenges, and future research opportunities in the context of smart grid paradigm. Renew. Sustain. Energy Rev. **1**(160), 112128 (2022)
17. Hussain, N., Nasir, M., Vasquez, J.C., Guerrero, J.M.: Recent developments and challenges on AC microgrids fault detection and protection systems - a review. Energies **13**(9), 2149 (2020)
18. Zhang, D., Han, X., Deng, C.: Review on the research and practice of deep learning and reinforcement learning in smart grids. CSEE J. Power Energy Syst. **4**(3), 362–370 (2018)
19. Usama, M., et al.: Unsupervised machine learning for networking: techniques, applications and research challenges. IEEE Access **14**(7), 65579–65615 (2019)
20. Fei, S.W., Zhang, X.B.: Fault diagnosis of power transformer based on support vector machine with genetic algorithm. Expert Syst. Appl. **36**(8), 11352–11357 (2009)
21. Bouktif, S., Fiaz, A., Ouni, A., Serhani, M.A.: Optimal deep learning lstm model for electric load forecasting using feature selection and genetic algorithm: comparison with machine learning approaches. Energies **11**(7), 1636 (2018)
22. Bashir, A.K., et al.: Comparative analysis of machine learning algorithms for prediction of smart grid stability. Int. Trans. Electr. Energy Syst. **31**(9), e12706 (2021)

PEMS-API: Malware Classification Using Parameter-Enhanced Multi-dimensional API Sequence Features

Han Miao[1,2], Wen Wang[1(✉)], Wanqian Zhang[1], and Feng Liu[1]

[1] Institute of Information Engineering, CAS, Beijing, China
{miaohan,wangwen,zhangwanqian,liufeng}@iie.ac.cn
[2] School of Cyber Security, University of Chinese Academy of Sciences, Beijing, China

Abstract. The abuse of encryption and obfuscation in malware poses a significant threat to cybersecurity. Dynamic API call sequences, which directly reflect malware behavior and are hard to falsify, offer more robust and reliable features for classification and detection than static ones. Based on our analysis, we identify the following key characteristics in API call sequences: (1) The implementation of malicious functionality often involves the allocation and interaction of resources. API calls to the same resource object, such as files or registries, typically exhibit contextual dependencies, regardless of whether they are adjacent; (2) Multi-process interleaved execution is common in malware, and API sequences can be organized by execution order or process grouping. The sorting method can impact model performance, especially for multi-process malware; (3) API sequences often contain many consecutive repeated API names, but their parameters may differ. Therefore, we can distinguish these repeated calls by their parameters, rather than simply removing redundancy through truncation. Based on these observations, we propose a malware classification ensemble model that integrates multi-dimensional API sequence features. Specifically, we train separate classification models based on three different feature perspectives: the API resource graph, multi-process API sequence representation, and parameter-enhanced API name sequences. The outputs of these three base models are then aggregated using K-Nearest Neighbors (KNN) soft voting. Training and evaluation on three classification tasks demonstrate that the three base models outperform existing API sequence-based detection techniques, and the ensemble model further enhances the detection performance.

Keywords: Malware Classification · API Sequence · Neural Networks

1 Introduction

The rampant use of encryption and obfuscation techniques in malware poses significant challenges for detection and comprehension. Malware authors employ these techniques to conceal their true intentions and evade analysis, making

M. Paszynski et al. (Eds.): ICCS 2025 Workshops, LNCS 15912, pp. 48–62, 2025.
https://doi.org/10.1007/978-3-031-97573-8_4

it extremely difficult for security researchers to understand and mitigate the threats. Running malware in controlled sandbox environments and analyzing the generated API call sequences has become a widely adopted approach in the field of malware detection. API calls provide direct insights into the underlying behavior of malware. By examining these API call traces, analysts can gain valuable intelligence about the functionality, goals, and potential impact of the malware.

There are numerous malware detection methods that utilize dynamic behavioral features, which can be categorized into the three types: API sequences-based models [2,3,9,17,20,21], API graph-based models [5–7,11,18] and API arguments enhanced model [7,16,22]. API2Vec [5] and API2Vec++ [6] consider the relationships between processes by constructing process relationship graphs and leveraging NLP techniques to represent API sequences. [7,11] also construct graph models to describe API call relationships and further employ pattern recognition and deep learning techniques for malware detection. However, most methods above adopt a single feature perspective and have a relatively coarse granularity, primarily focusing on the names of API sequences and statistic features of API arguments. This would result in a partial representation of the API sequence, focusing only on a subset of the information. To extract more implicit information from API sequence parameters, we have made several observations based on extensive analysis. The findings are as follows:

Resource Allocation and Interaction: Malicious functionality in malware often requires the allocation and interaction of various system resources. API calls that operate on the same resource object, such as files or registries, typically exhibit contextual dependencies, even if they are not adjacent in the sequence. This is particularly important in the analysis of malware, as understanding the context of resource interactions can provide valuable insights into its behavior. Ignoring these dependencies may lead to a less accurate representation of the malware's dynamic execution.

Multi-process Interleaved Execution: Malware often executes across multiple processes that interleave their activities. In such scenarios, the API sequences can be organized in two primary ways: by the order of execution or by grouping based on the process. The method of sorting API calls can significantly affect the performance of classification models, especially those that rely on the order of sequence. When applied to multi-process malware, models that depend heavily on the sequence order may experience a performance decline, as the interleaved nature of the processes introduces complexity that is not adequately captured by a simple linear sequence. This observation underscores the need for more sophisticated approaches to handling multi-process malware and highlights the importance of considering process grouping in the analysis.

Consecutive Repeated API Calls with Varying Parameters: API sequences often contain consecutive repeated API calls, where the API names

are the same, but their parameters may differ. These repeated calls, while seemingly redundant, can provide important contextual information. Rather than simply applying a truncation method to eliminate redundancy, distinguishing these repeated calls based on their parameters can provide additional insights into the functionality of the malware. By considering the variation in parameters, we can more accurately capture the underlying behavior of the malware, as different parameters may represent different stages or types of malicious activity.

Based on these three observations, we propose a malware classification ensemble model that integrates multi-dimensional features from API sequences. Our approach incorporates three distinct perspectives of API sequence features: the API resource graph, which models the interactions and dependencies between API calls and resource objects; the multi-process API sequence representation, which accounts for the interleaved execution of multiple processes; and the parameter-enhanced API name sequences, which distinguishes repeated API calls by considering their parameters. To combine the outputs of these models, we use K-Nearest Neighbors (KNN) soft voting, which allows us to leverage the strengths of each individual model and make a more robust classification decision.

The contributions in this paper are as follows:

- We propose a malware classification ensemble model that combines multi-perspective API sequence features: API resource graph, multi-process API sequence representation, and parameter-enhanced API name sequences. Both individual models and the ensemble model achieve outstanding results in classification tasks.
- We first propose using the handle parameter, which uniquely identifies resource objects, to build the API resource graph. This approach is more accurate and efficient compared to the previous method, which relied on identifying objects through strings.
- We first propose using API parameters to address the issue of redundant repetition in API sequences.
- We first propose a cross-attention-based Multi-process API Sequence Representation method and a process state transition graph to address the representation challenge of multi-process malware.

2 Related Work

2.1 API Sequence-Based Malware Detection

Sequence-based malware detection [2–4,8,12] utilizes deep learning to directly extract features from API call sequences for malware detection. Various methods have been proposed in this domain: Kwon et al. [13] and Yazi et al. [14]apply LSTM to capture API calling patterns for classification, while Tobiyama et al. [15] use an RNN for feature extraction, followed by CNN classification of the generated feature images. ASSCA [16] employs a bidirectional residual network to classify API sequences, removing redundant information. Additionally, Li et

al. [17] utilize Bi-LSTM to capture and combine intrinsic API sequence features. While sequence-based methods are simple and do not require extensive prior knowledge, they face challenges: long sequences can obscure key malicious behavior features, adversarial malware can insert noise APIs to evade detection, and these methods often require large datasets while struggling to exploit API relationships effectively.

2.2 API Graph-Based Malware Detection

Researchers have proposed graph-based malware detection methods to model the behavior of APIs using graphs [7,11,18], then apply Graph Neural Networks (GNNs) for feature extraction in malware detection. API2Vec [5] and API2Vec++ [6] designs Temporal Process Graphs (TPG) and Temporal API Property Graphs (TAPG) to model inter- and intra-process behaviors for detection and using random walk to extract meta path to represent the API sequence for classification. DMalNet [7] converts API call sequences into call graphs to model API relationships and enhance malware classification. MINES [11] extracted the API existence feature of malware by graph contrastive learning between two API graphs. Graph-based approaches generally outperform sequence-based methods by using GNNs to capture the complex behavior of software through API relationships. However, these methods often fail to fully account for the diverse API relationships, as they typically focus on only one type of relationship.

2.3 API Arguments Enhanced Methods

DMDS [7] firstly propose a feature engineering method by utilizing a feature hashing trick to encode the API call arguments. CTIMD [10] integrates Cyber Threat Intelligence (CTI) to enhance sequence learning with runtime parameters. DMalNet [7] and Malatt [8] both used feature encoder that uses different encoding strategies according to the characteristics of different types of data to represent API names and arguments as semantic feature vectors in their works. These methods enhance the model's expressive power and feature information by incorporating parameters, yielding relatively good results. However, using specific parameter values, such as IP addresses and file paths, may reduce the model's generalization ability and make it more vulnerable to evasion attacks.

3 Methodology

As shown in Fig. 1, our approach to malware detection encompasses multiple perspectives and leverages advanced techniques to capture intricate details and behavioral patterns. The proposed method consists of four key components:

3.1 API Resource Graph

Motivation. The implementation of malicious functions requires resource management, allocation, and interaction through APIs, such as reading and writing

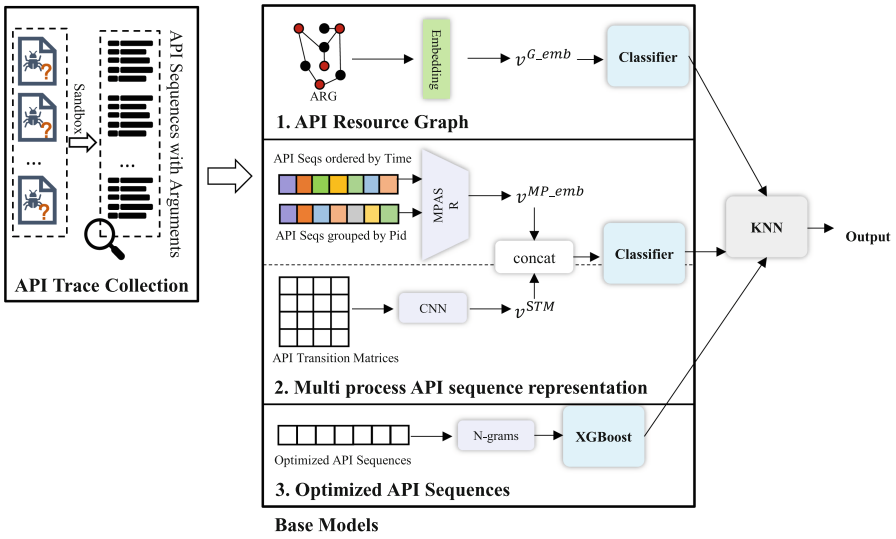

Fig. 1. System architecture of PEMS-API.

files, reading and writing registry, etc. The interactions between processes and resources are quite different between malicious and benign programs.

The challenge to construct API Resource Graph is identifying resource nodes. Different resource nodes may have different representations in various APIs. For example, a file node can be represented as absolute path or file name, among others. Recognizing resources by strings like file path or file name may result in multiple duplicate resource nodes. API Resources Graph constructed by Heternet [18] remains the problem.

In the Windows operating system, handles are unique 32-bit or 64-bit unsigned integers used to identify objects created or used by applications. These objects include windows, modules, threads, processes, files, mutexes, sockets, and more. Within the same process, the mapping between objects and handles is one-to-one, regardless of the object type. Therefore, by examining the handles present in the API call parameters, we can identify the different objects involved in the program's execution. As shown in Fig. 2, resource objects could be identified from API arguments.

For the same reason, socket is also an important identifiers for network objects in a program. Under the assumption that handles and socket serve as bridges connecting API calls and resources, we can construct dependencies between discrete APIs by leveraging the affinity of resource.

The Framework of classifier based on is shown in (Fig. 3).

Graph Construction. The constructed ARG can be represented as:

$$G = (V_{\text{API}} \cup V_{\text{Resource}}, E) \tag{1}$$

```
{
    "category": "filesystem",
    "status": true,
    "api": "NtCreateFile",
    "arguments": {
        "file_handle": "0x00000000000000ac",
        "desired_access": "0x80100080",
        "file_attributes": 0,
        "create_disposition": 1,
        "create_options": 0,
        "share_access": 5,
        "filepath": "C:\\Windows\\System32\\en-US\\wshtcpip.dll.mui",
        "filepath_r": "\\??\\C:\\Windows\\System32\\en-US\\wshtcpip.dll.mui",
        "status_info": 1}
},
```


Add an edge in ARG(api→handle id)

NtCreateFile → 0x00000000000000ac

Fig. 2. An Example of API and corresponding arguments.

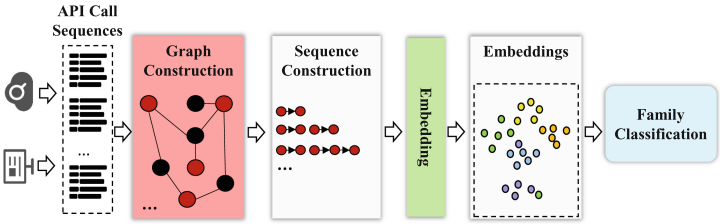

Fig. 3. Overview of classifier based on ARG.

where V_{API} contains the API nodes, V_{Resource} contains the resource object nodes, and E contains the edges representing interactions between the APIs and the resources.

The set V_{Resource} contains objects that are identified through the parameters of API calls. Specifically, the resource objects are extracted from parameters such as: file_handle, key_handle,process_handle, socket. These parameters correspond to specific system resources, such as open files, registry keys, processes, and network sockets.

From the perspective of API Resource Graph, we gain valuable insights into the behavior and resource usage patterns of the program. The ARG allows us to analyze the dependencies between API calls and the resources they access, providing a comprehensive view of the program's execution flow.

By focusing on resource usage in API arguments, we can uncover hidden dependencies and interactions that may not be visible through API name sequence alone. The ARG enables us to identify suspicious or malicious resource usage patterns.

Graph Representation. We adopted a simple yet effective method to represent the Application Resource Graph (ARG). For each object node, we gather all adjacent API nodes and order them chronologically, forming a set of API paths.

To obtain meaningful representations, we use Doc2Vec [21] to learn embeddings for both the API paths and individual APIs from a large corpus. Each path

and API is represented as a 64-dimensional vector, capturing their interactions with resources. This approach enables effective analysis and comparison of API behaviors.

Let P represent the set of paths. For the i-th path p_i and a specific API p_j^i within p_i, we first collect the context APIs within a window of size C, denoted as $\delta = \{p_{j-C}^i, \ldots, p_{j-1}^i, p_{j+1}^i, \ldots, p_{j+C}^i\}$. The representation of p_j^i is then computed as the embedding of p_i combined with the embeddings of the APIs in δ, given by:

$$E(p_j^i) = W \cdot \frac{1}{2C+1} \left(E(p_i) + \sum_{k \in \delta} E(p_k^i) \right) \tag{2}$$

where $E(\cdot)$ denotes the embedding function for an API or path, and W is the weight matrix learned during training.

The objective is to minimize the following loss function, which represents the average negative log-likelihood of each API across all paths:

$$-\frac{1}{N_p} \sum_{i=0}^{N_p} \frac{1}{N_{p_i}} \sum_{j=0}^{N_{p_i}} \log P(p_j^i | \delta, p_i) \tag{3}$$

Here, N_p is the total number of paths in P, N_{p_i} is the length of path p_i, and $P(p_j^i|\delta, p_i)$ represents the probability of a context API p_j^i given the current API p_i and its surrounding context δ. This formulation aims to optimize the embeddings by minimizing the log-likelihood of context API predictions within the defined window.

3.2 Multi Process API Sequence Representation

Motivation. Multi-process and inter-process interactions are major characteristics of malware behavior, such as process injection attacks, process replacement attacks, and others. Existing methods rarely capture the process-related profiles of API sequences. Typically, past approaches organize API sequences as a single, long sequence, ignoring the fact that they may contain multiple distinct functional processes and subsequences. In this section, we organize the input API sequence in two ways: a globally ordered sequence and process-grouped sequences, illustrated in Fig. 4. The global API sequence is first sorted by time and then divided into blocks based on process. Each block can be seen as accomplishing an independent function. As illustrated in the figure below, this clearly exhibits a hierarchical structure: API words, API groups (sentences), and complete API sequences (documents). Furthermore, to directly express the process structural information, we propose the concept of a Process State Transition Graph (PSTG) and utilize a convolutional network to obtain the transition matrix representation. The architecture of Multi process API sequence representation is shown in Fig. 4.

Based on the above insights, we propose the Multi-process API Sequence Representation (MPASR) method. The overall structure of the method is shown

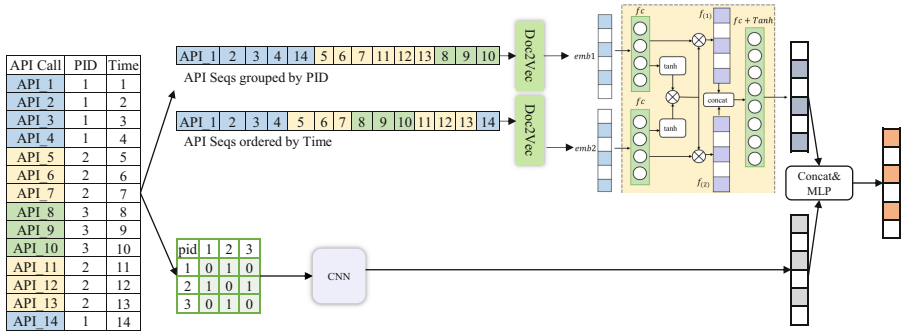

Fig. 4. Architecture of Multi process API sequence representation.

in the diagram below. It includes two primary modules: the *Cross-Attention-based Semantic Representation Module* and the *Process State Transition Structure Graph Module*. These modules extract the semantic information from the API sequence and the process structural information, respectively, and serve as input for the final deep learning classifier.

Cross-Attention-Based Semantic-Aware Modeling. In the semantic-aware module, we propose a cross-attention-based multi-process API sequence semantic enhancement representation learning. This approach has several advantages. First, grouping the API sequences by process allows the sequence to be represented from the perspective of individual processes. Second, cross-attention enhances the feature representation. Third, the Doc2Vec representation can effectively handle longer API sequences.

Semantic-Aware Encoder. We analogize API subsequences to sentences and view the complete API sequences as documents. Therefore, Doc2Vec is an efficient representation method that aligns with this characteristic. Based on this, we obtain the representations of the two types of API sequences using Doc2Vec. The relevant mathematical expressions have been presented above.

Cross-Attention Semantic Enhancement. As shown in the Fig. 4, after obtaining the embeddings of the API call sequences under two organizational structures, the cross-attention mechanism is applied to establish connections between the two API sequences, thereby enhancing the semantic representation of the multi-process API sequences. In the figure, emb_1 represents the embedding of the API sequence sorted by execution time, and emb_2 represents the embedding of the API sequence grouped by process ID and then sorted by the first appearance time of each process. The cross-attention module consists mainly of three fully connected layers: l_1, l_2, and l_3, with parameter matrices defined as $W_1 \in \mathbb{R}^{d_f \times d_{f_1}}$, $W_2 \in \mathbb{R}^{d_f \times d_{f_2}}$, and $W_3 \in \mathbb{R}^{d_{f_a} \times d_{f_h}}$, where d represents the feature vector dimensions, and d_{f_1} and d_{f_2} are equal, representing the output dimensions of fully connected layers l_1 and l_2, respectively. d_{f_a} denotes the dimension of the attention

features after concatenation, and d_{f_h} represents the output feature dimension of the linear layer l_3. First, we obtain f_1 and f_2 as latent features from the intermediate layer, and the calculation is as follows:

$$f_1 = f \cdot W_1, \quad f_2 = f \cdot W_2 \tag{4}$$

where $\cdot$ denotes matrix multiplication. Specifically, we apply the activation function tanh to map the intermediate feature values to the range $(-1, +1)$, obtaining the corresponding feature sign vectors v_1 and v_2 to represent the latent feature values. Finally, the feature vector α is obtained by multiplying the two sign vectors as shown below:

$$\alpha = v_{s_1} \cdot v_{s_2} \tag{5}$$

After obtaining α, we combine it with the latent feature vectors f_{a_1} and f_{a_2}. The two new feature vectors are concatenated into a high-dimensional vector and passed as input to the final linear layer l_3. The output f_h is the final output after the cross-attention operation, as shown in the following equation:

$$f_h = \text{Concat}(\alpha f_1, \alpha f_2) \cdot W_3 \tag{6}$$

Finally, the embeddings enhanced by cross-attention retain the information of the original two types of API sequences while also capturing the representations of API calls related to inter-process interactions.

Process State Transition Graph. The Process State Transition Graph (PSTG) is constructed based on the time-ordered API sequence. We further divide the sequence into blocks based on the process ID, encoding each block with its corresponding process number. A directed edge is drawn between adjacent blocks based on their sequence in the API flow. The resulting structure captures the transitions between processes, providing a state transition matrix, shown in Fig. 4. In the time-ordered API sequences, there may be cases where API sequences are interleaved. Let the state transition matrix be T. If two APIs are adjacent in execution order but belong to different processes, a process state transition occurs, and we update $T_{i,j}$ += 1, where i and j are the indices of the two processes involved in the context switch. Note that the process index is different from the PID—it starts from 0, with the first encountered process labeled as 0, and so on. This approach helps reduce the dimensionality of the state transition matrix.

After getting the state transition matrix $PTSG$, we use ResNet [23] to process it. ResNet facilitates efficient information transmission through shortcut connections. We employ an 11-layer ResNet with 3 residual blocks. All convolution kernels have a size of 3×3, as we aim to capture subtle changes in the graph. Next, we use a global max pooling layer to compute the embedding of the state transition graph. Specifically, the embedding of the state transition graph is given by:

$$\mathbf{e_{PTSG}} = Maxpooling(\text{ResNet}(PTSG)) \tag{7}$$

We only apply pooling methods in the last layer to handle varying input sizes.

3.3 Arguments Enhanced API Sequences

By analyzing the API sequences and their parameters, we found that malicious software's dynamic API call sequences often contain many repeated API names, but with different parameters. Previous methods treated these as noise and simplified the sequences by removing duplicates. Based on this insight, we propose a set of heuristic strategies based on parameter content to optimize the representation of API sequences. As shown in the Fig. 5, 'LdrGetProcedureAddress' is used for loading functions at runtime and typically appears consecutively in the sequence. Its parameter, 'function_name', indicates the function whose address needs to be obtained. Therefore, we replace the original API sequence with 'API_function_name'. Similarly, we use 'sleep_dwMilliseconds' instead of 'sleep', and 'NtDelayExecution_DelayInterval' instead of 'NtDelayExecution'.

The benefit of this approach is that it enriches the representation of the API sequences without reducing the model's generalization ability or causing adversarial detection.

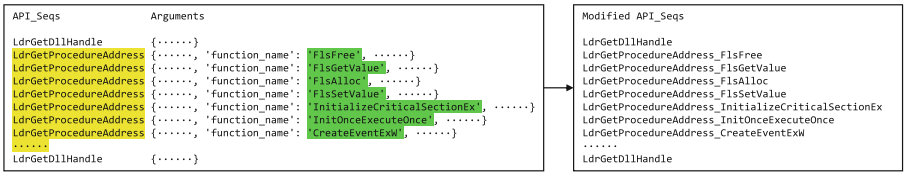

Fig. 5. Example of simplifying a repeated API subsequence based on parameters.

After getting modified API sequences, we use N-grams to represent the sequence and apply machine learning techniques for classification. First, we extract N-grams from the API sequences. N-grams are contiguous sequences of N items from a given sample of text, and they are used to capture local patterns in the API sequences. We choose the most frequent N-grams in the training data to construct feature vectors for each sample. Specifically, for each API sequence, we compute a feature vector where each element corresponds to the frequency of a particular N-gram in that sequence. Then, we select features with mutual information to gain the top K_2 most relevant features, where mutual information $I(X, Y)$ between features X and label Y is defined as:

$$I(X,Y) = \sum_{x \in X} \sum_{y \in Y} p(x,y) \log \frac{p(x,y)}{p(x)p(y)} \tag{8}$$

The top K_2 features are selected based on the highest mutual information scores. After selecting the features, we apply the XGBoost classifier to train a model on the selected features.

3.4 Ensemble Learning

After obtaining the results from the three models, we use ensemble learning to enhance the performance of the classification model, improving its accuracy and robustness by combining the predictions from multiple models. Ensemble learning, using the voting method, integrates these outputs to provide a final prediction. The voting method can be classified into hard voting (majority vote) and soft voting (based on class probabilities). Here, K-Nearest Neighbors (KNN) is used for soft voting. For optimal performance, the base models should meet two conditions: 1. Similar accuracy: Models should have comparable accuracy to avoid one dominating the voting process. 2. Low homogeneity: Models should be diverse to capture different aspects of the data, providing complementary insights that enhance overall performance.

4 Experiments

4.1 Experimental Setup

Dataset. In our paper, both API name sequences and called arguments of dynamic execution are required. Although there are some publicly available API sequences dataset, they are not suitable for our approach due to the absence of API arguments. Thus, we collect malware and goodware from various sources by ourselves and execute each sample in cuckoo sandbox [19] environment for 2 min. Then, we get API call sequences and arguments from the dynamic execution logs. Finally, the experiment was conducted on a dataset containing 19088 malware from 62 families and 11030 goodware. Malware are categorized into 12 classes based on attack intent and techniques. We construct three classification tasks—malware family classification, malware functionality classification and malware detection.

Evaluation Metrics. We evaluate our method and compared methods using five widely used metrics, including Accuracy and F1-Score.

$$Accuracy = \frac{TP + TN}{TP + TN + FP + FN} \tag{9}$$

$$Precision = \frac{TP}{TP + FP} \tag{10}$$

$$Recall = \frac{TP}{TP + FN} \tag{11}$$

$$F1 - Score = 2 \times \frac{\text{Precision} \times Recall}{Precision + Recall}, \tag{12}$$

where TP and TN are correct detections of positives and negatives, while FN and FP are misclassified positive and negative samples, respectively.

4.2 Results and Analysis

Comparative Results. The comparative results are presented in Table 1. The following observations can be made from the experimental results:

Firstly, in the comparison of individual models, MPAR achieved the best performance in terms of the metrics. ARG and Modified_API also outperformed most other models. Although these methods only extract partial features of the API sequences, such as resource dependency information, process semantics and structural information of the API sequences, and the existence information of optimized APIs containing parameter information, they still perform well, indicating that these partial features are useful for classification tasks. MalAtt exhibits comparable performance to the three standard models we proposed; however, considering that it integrates static opcode information, which is vulnerable to code obfuscation attacks, its performance will degrade significantly when samples are obfuscated. Additionally, the graph-based method API2Vec did not perform as expected. We believe this could be due to the large number of duplicate nodes hindering the random walk process from exploring more diverse paths. Furthermore, methods that incorporate parameter information (such as DMDS, MalAtt, Dmalnet, and Agrawal et al.) generally outperform methods that rely solely on the API name sequence. Finally, we observed that as the complexity of the classification task increases and the number of categories grows, classification performance tends to decrease, as capturing more intricate details becomes necessary to further distinguish between samples.

Table 1. Comparisons of different models on three tasks. The best results are in boldface.

Model	Family Classification		Function Classification		Malware Detection		Inference Time (ms/sample)
	Accuracy	F1-Score	Accuracy	F1-Score	Accuracy	F1-Score	
API2Vec [5]	0.7651	0.7134	0.8017	0.7533	0.8929	0.8552	919.9
DMDS [7]	0.8937	0.8383	0.917	0.8443	0.9314	0.882	21.2
TextCNN [9]	0.613	0.5847	0.6521	0.6019	0.7244	0.6915	19.8
Agrawal et al. [1]	0.9087	0.9182	0.9331	0.924	0.9551	0.9291	34.5
MalAtt [8]	0.9126	0.9122	0.9363	0.9166	0.972	0.9481	28.3
Dmalnet [7]	0.9136	0.9097	0.9214	0.9138	0.9371	0.9257	20
MPAR	0.9213	0.9057	0.9372	0.9237	0.9796	0.9556	21.1
ARG	0.9157	0.91	0.9353	0.9113	0.9543	0.9342	25.3
Modified_API	0.9172	0.891	0.9297	0.9077	0.9712	0.9466	**18.5**
ARG+MPAR	0.9382	0.9191	0.949	0.9345	0.9874	0.9565	46.7
ARG+Modified_API	0.9255	0.9032	0.9448	0.9179	0.9836	0.9546	39.8
Modified_API+MPAR	0.9318	0.9089	0.9417	0.9111	0.9866	0.9547	44.2
Ensemble Model	**0.9411**	**0.9373**	**0.9574**	**0.9411**	**0.9884**	**0.9579**	65.4

Ablation Study. To evaluate the contribution of each model to overall accuracy, we compared individual models as well as their pairwise combinations. Among the individual models, Multi-process API Sequence Representation (MPAR) achieved the highest accuracy, followed by API Resource Graph (ARG). As illustrated in Fig. 1,when ARG and MPAR were used together, the accuracy on the family classification task increased by 0.169% compared to using MPAR alone. We hypothesize that although there is a large accuracy gap between the two base models, their low homogeneity allows for performance improvement when combined. No combination led to a decrease in accuracy, which we attribute to the low homogeneity and relatively small accuracy differences between the three models, making this an ideal scenario for deep ensemble learning. When all three models were used together, the accuracy improved by as much as 1.98%.

Additionally, we explored whether optimizing the processing of API sequences through parameter tuning enhances classification performance, and how different API sorting strategies influence the results. We also assessed whether our cross-attention mechanism offers superior performance compared to simply concatenating the two embeddings. As illustrated in Fig. 6, the optimized API sequences yielded better results than the original sequences when used as input. Moreover, the cross-attention-based API sequence representation method outperformed both individual API sequences and the concatenated version of the two sequences, which aligns with our expectations.

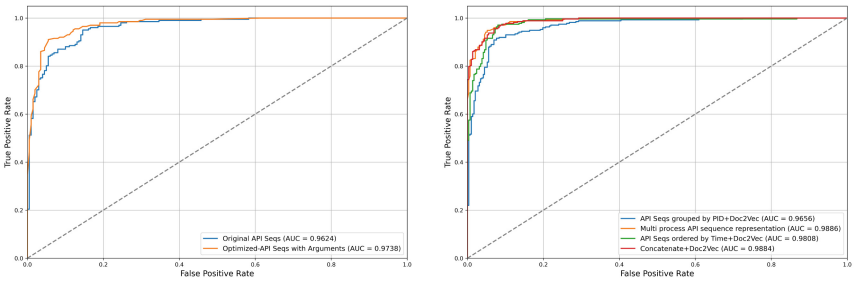

(a) ROC of methods with different API processing strategies

(b) ROC of methods with different API Sequence order

Fig. 6. Comparison of ROC Curves.

Inference Time Overhead. The inference time overhead of this method comes from three components: ARG, MPAR, and Modified_API. The experiments were conducted on an Ubuntu (20.04.2 LTS) server with a 32-core AMD EPYC 9654 96-Core Processor and 120GB of RAM. The average processing time per sequence for each of the three components was 21.1 ms, 26.3 ms, and 18.5 ms, respectively, while the time for processing with the three models combined was 65.4 ms. In comparison, API2Vec, DMDS, TextCNN, Agrawal et al., MalAtt, and

Dmalnet took 919.9 ms, 21.2 ms, 19.8 ms, 34.5 ms, 28.3 ms, and 20 ms, respectively, to process one sequence. Although our method takes relatively longer, the 65.4 ms detection time is still reasonable. Therefore, we believe this method is feasible for malware detection in real-world scenarios.

5 Conclusion

This paper proposes a hybrid model that combines deep learning and machine learning, leveraging ensemble learning to integrate different deep learning base models and obtain final results through a voting mechanism. The model extensively explores API information from three aspects: API resource graphs, multi process API sequence representation, and arguments Enhanced API sequence n-grams. These heterogeneous pieces of information are integrated to further improve accuracy. We evaluated the model on a large dataset composed of real-world software. Experimental results show that the proposed model outperforms other comparison models in terms of accuracy and f1 score.

Acknowledgments. This work was supported by the Program with No. E3YY-131112.

References

1. Agrawal, R., Stokes, J.W., Marinescu, M., Selvaraj, K.: Neural sequential malware detection with parameters. In: 2018 IEEE International Conference on Acoustics, Speech and Signal Processing (ICASSP), pp. 2656–2660. IEEE (2018)
2. Li, C., Zheng, J.: API call-based malware classification using recurrent neural networks. J. Cyber Secur. Mob. **10**(3), 617–640 (2021)
3. Catak, F.O., Yazı, A.F., Elezaj, O., Ahmed, J.: Deep learning based sequential model for malware analysis using windows exe API calls. PeerJ Comput. Sci. **6**, e285 (2020)
4. Demirkıran, F., Çayır, A., Ünal, U., Dağ, H.: An ensemble of pre-trained transformer models for imbalanced multiclass malware classification. arXiv preprint arXiv:2112.13236 (2021)
5. Cui, L., Cui, J., Ji, Y, Hao, Z., Li, L., Ding, Z.: API2Vec: learning representations of API sequences for malware detection. In: Proceedings of the 32nd ACM SIGSOFT International Symposium on Software Testing and Analysis (ISSTA 2023), pp. 261–273 (2023). https://doi.org/10.1145/3597926.3598054
6. Cui, L., et al.: API2Vec++: boosting API sequence representation for malware detection and classification IEEE Trans. Softw. Eng. **50**(8), 2142–2162 (2024). https://doi.org/10.1109/TSE.2024.3422990
7. Li, C., et al.: DMalNet: dynamic malware analysis based on API feature engineering and graph learning. Comput. Secur. **122**, 102872 (2022). https://doi.org/10.1016/j.cose.2022.102872
8. Bao, H., et al.: Stories behind decisions: towards interpretable malware family classification with hierarchical attention. Comput. Secur. **144**, 103943 (2024). https://doi.org/10.1016/j.cose.2024.103943

9. Qin, B., Wang, Y., Ma, C.: API call based ransomware dynamic detection approach using TextCNN. In: 2020 International Conference on Big Data, Artificial Intelligence and Internet of Things Engineering (ICBAIE), Fuzhou, China, pp. 162–166 (2020). https://doi.org/10.1109/ICBAIE49996.2020.00041
10. Chen, T., Zeng, H., Lv, M., Zhu, T.: CTIMD: cyber threat intelligence enhanced malware detection using API call sequences with parameters. Comput. Secur. **136**, 103518 (2024). https://doi.org/10.1016/j.cose.2023.103518
11. Wu, P., Gao, M., Sun, F., Wang, X., Pan, L.: Multi-perspective API call sequence behavior analysis and fusion for malware classification. Comput. Secur. **148**, 104177 (2025). https://doi.org/10.1016/j.cose.2024.104177
12. Kolosnjaji, B., Zarras, A., Webster, G.D., Eckert, C.: Deep learning for classification of malware system call sequences. In: Advances in Artificial Intelligence, pp. 137–149 (2016)
13. Kwon, I., Im, E.G.: Extracting the representative API call patterns of malware families using recurrent neural network. In: International Conference on Research in Adaptive and Convergent Systems, pp. 202–207 (2017)
14. Yazi, A.F., Catak, F.O., Gul, E.: Classification of methamorphic malware with deep learning (LSTM). In: IEEE Signal Processing and Communications Applications Conference, pp. 1–4 (2019)
15. Tobiyama, S., Yamaguchi, Y., Shimada, H., Ikuse, T., Yagi, T.: Malware detection with deep neural network using process behavior. In: IEEE Annual Computer Software and Applications Conference, pp. 577–582. COMPSAC (2016)
16. Lu, X., Jiang, F., Zhou, X., Yi, S., Sha, J., Li, P.: ASSCA: API sequence and statistics features combined architecture for malware detection. Comput. Netw. **157**, 99–111 (2019)
17. Li, C., Lv, Q., Li, N., Wang, Y., Sun, D., Qiao, Y.: A novel deep framework for dynamic malware detection based on API sequence intrinsic features. Comput. Secur. **116**, 102686 (2022). https://doi.org/10.1016/j.cose.2022.102686
18. Song, R., Li, L., Cui, L., Liu, Q., Gao, J.: Binary malware detection via heterogeneous information deep ensemble learning. In: 2023 IEEE 29th International Conference on Parallel and Distributed Systems (ICPADS), Ocean Flower Island, China, pp. 1147–1156 (2023). https://doi.org/10.1109/ICPADS60453.2023.00168
19. Cuckoo Sandbox. https://cuckoosandbox.org/. Accessed 27 Feb 2025
20. Mikolov, T., Chen, K., Corrado, G., Dean, J.: Efficient estimation of word representations in vector space. arXiv preprint arXiv:1301.3781 (2013)
21. Le, Q., Mikolov T.: Distributed representations of sentences and documents. In: International Conference on Machine Learning, pp. 1188–1196. PMLR (2014)
22. Javan, N.T., Mohammadpour, M., Mostafavi, S.: Enhancing malicious code detection with boosted N-gram analysis and efficient feature selection. IEEE Access **12**, 147400–147421 (2024). https://doi.org/10.1109/ACCESS.2024.3476164
23. He, K., Zhang, X., Ren, S., Sun, J.: Deep residual learning for image recognition. In: Proceedings of the IEEE Conference on Computer Vision and Pattern Recognition, pp. 770–778 (2016)

The Effectiveness of Visual Attention Patterns in the Process of Spatial Exploration in a 3D Video Game Environment

Bartosz Krukowski, Mateusz Zawisza, Aneta Wiśniewska, Adam Wojciechowski, and Rafał Szrajber(✉)

Institute of Information Technology, Lodz University of Technology, 215 Wólczańska Street, 90-924 Lodz, Poland
rafal.szrajber@p.lodz.pl
https://it.p.lodz.pl/

Abstract. This study examines the effectiveness of visual navigation cues in guiding player movement within 3D virtual environments. Using experimental levels with lighting contrast and object geometry cues at three intensity levels, the research identifies the minimum cue strength needed to influence player navigation effectively. Differences in cue responsiveness between casual and advanced players were also analyzed. The findings reveal threshold values for subtle yet effective navigation methods, providing practical insights for level designers. These results can enhance the development of user-friendly and engaging game environments, catering to players of varying skill levels.

Keywords: wayfinding · video game · environment · visual cues

1 Introduction

In contemporary society, video games have become a highly popular form of entertainment, catering to players of all ages and skill levels. Game development studios strive to make their products accessible to a broad audience. In recent years, major industry players have demonstrated a comprehensive approach to accessibility by integrating features designed to support individuals with disabilities, including those with visual or motor impairments. A critical component of modern games is the exploration of three-dimensional spaces. If a level designed by developers is overly simplistic, players may derive little satisfaction from discovering objectives such as exits or hidden treasures. Conversely, levels that are excessively complex or poorly designed can lead to frustration, disorientation, and disengagement. To balance these extremes, level designers have developed principles and methodologies [8,14], often through iterative processes, to craft environments that are both engaging and navigable. This study explores methods for guiding players in virtual environments, focusing on how

M. Paszynski et al. (Eds.): ICCS 2025 Workshops, LNCS 15912, pp. 63–77, 2025.
https://doi.org/10.1007/978-3-031-97573-8_5

various navigational cues influence movement and decision-making. The research aims to evaluate specific types of cues integrated into game environments and determine the minimum intensity required to effectively direct player behavior without compromising immersion. The findings presented in this paper are intended to provide practical insights for level designers, aiding in the creation of virtual spaces that are both challenging and accessible, enhancing the overall player experience.

2 Related Works

As the gaming industry has advanced, designers have developed well-established methods to effectively guide players and direct them along intended paths. Over time, these methods have evolved into structured design patterns, akin to those introduced by Christopher Alexander in the field of architecture [1]. These patterns systematically define specific problems, propose solutions, and outline the potential outcomes of their application. The increasing number and refinement of these patterns correlate directly with the growing body of research dedicated to their efficacy and impact on players' experiences during gameplay. Experimental studies aim to validate the effectiveness of these methods, providing empirical evidence to support their use in game design.

An important area of this research focuses on the influence of visual attention patterns on players' exploratory behavior and decision-making. A notable contribution to this field is the work of Barney [2], which adapts the concept of pattern language to address design challenges in games, encompassing both mechanical and environmental aspects. The author elaborates on how to construct custom pattern languages derived from established game productions and apply them to game development. Ongoing studies by various research teams continue to assess the effectiveness and efficiency of these patterns, contributing to a deeper understanding of their role in enhancing player engagement and navigation within virtual environments.

The use of various elements such as light, motion, color, and sound to guide players within virtual environments is comprehensively discussed in the study by Hoeg [5]. The research involved the creation of an advanced level designed to simulate a segment of a first-person shooter game. Participants navigated through a building with the objective of locating and rescuing hostages. The environment was carefully constructed to include decision points during corridor exploration, allowing the study to assess whether specific methods effectively captured players' attention, influencing their choice between two available paths. The findings identified light as one of the most impactful techniques for influencing player decision-making.

Player decision-making influenced by contrast is examined in detail by Winn [15]. The authors argue that the proper interpretation of this effect is to answer the question, "Where should the player go?" rather than "Where must the player go?" Their research highlights the effectiveness of contrast created through increased lighting or brightening of the main path. The results confirmed that

contrast significantly influences player behavior, as also supported by Liszio [9], who categorizes contrast among the most effective yet minimally intrusive navigation methods. These techniques aim to naturally draw the player's gaze toward a specific object or path.

Winters [16] further explored the role of form contrast in guiding player navigation. Post-experiment interviews revealed that all participants identified contrast as a key factor influencing their decisions, underscoring its importance in virtual environment design.

The challenges of guiding players using lightened paths can be effectively addressed through contrast-based methods, as exemplified by techniques employed at Disneyland and described by Rogers [13]. In his lecture, Rogers demonstrates how park visitors are guided using environmental light and contrast. The park's design features a well-lit central castle, towering over its surroundings and visible from a distance. As the park prepares to close, lighting in areas farther from the castle is gradually dimmed, increasing the contrast between the central castle and its surroundings. This technique naturally draws visitors' attention to the castle, subtly encouraging them to move toward it.

The influence of contrast on decision-making during exploration was also studied by Marples [10] in the context of player navigation within a maze. Participants began at the edge of the level, with the objective of reaching a large central figure. The maze featured bifurcations offering only two paths at each decision point, where contrasting cues were employed. The results demonstrated a significant reduction in navigation time when contrasting paths were used, nearly halving the completion time compared to levels without these cues. This highlights the efficacy of contrast in directing players toward their objectives.

Lighting has been further analyzed in studies [7,12]. Petersson [12] examined the visibility of visual cues in a 3D platform-adventure game, concluding that lighting-based cues held players' attention the longest. Knez [7] explored lighting contrast involving warm and cold colors, finding a strong player preference for warm lighting, which was chosen significantly more often, reinforcing its utility in navigation design.

Understanding how the human mind perceives space and responds to visual cues can have practical applications beyond virtual environments, including the design of public spaces. In a study by Irshad et al. [6], researchers examined the impact of navigational cues on individuals' vital parameters and mental states in high-stress situations. Participants were tasked with escaping a flooded area to reach safety. The study divided participants into three groups: one without any navigational cues, another with evacuation signs, and a third group with illuminated signs. The findings revealed that navigating without wayfinding cues significantly increased difficulty, stress, and tension. These results underscore the importance of visual attention patterns not only in aiding navigation but also in mitigating emotional strain during critical situations.

Moura et al. [11] compiled a taxonomy of recurring navigational prompts in games, categorizing them into direct methods, such as compasses or maps, and subtler approaches. Among these were markers—elements designed to draw

attention by contrasting with the game environment. Markers could range from abstract forms, such as glowing arrows, to more integrated elements, like distinctively colored paths that blend seamlessly with the game world.

Markers associated with spatial navigation are further explored in a review by Yesiltepe et al. [17], which refers to them as landmarks. This work emphasizes two key aspects of landmarks: visibility and salience. The study found that the effectiveness of landmarks is maximized when they are placed strategically along routes and at decision points, such as intersections, reinforcing their critical role in wayfinding.

The study by Gomez et al. (2021) [3] utilized established level design patterns to investigate their influence on player curiosity. The authors identified four distinct patterns: reaching extreme points, removing visual obstructions, introducing out-of-place elements, and enhancing spatial understanding. Among these, the out-of-place element, represented by stacked stones and stones arranged in a spiral pattern across the grass, emerged as the pattern most frequently visited by players.

Compared to the existing studies, our approach introduces a more systematic assessment of cue intensity by testing each method at three levels of strength within a controlled and uniform 3D environment. Unlike prior works that often examined isolated cues or relied on real-game scenarios with multiple variables, our study isolates the effect of visual attention patterns in a neutral setting, enabling clearer attribution of player behavior to specific design elements. A key advantage of this approach is its ability to identify threshold values for cue effectiveness, offering actionable insights for level designers. On the other hand, the highly controlled nature of the environment may limit ecological validity, as real-world game levels typically feature more complex and diverse visual stimuli. Future work should aim to validate these findings in more varied and immersive game contexts.

3 Methodology

The research methodology employed in this study utilizes an open-level design to assess the impact of selected player guidance techniques. The openness of the environment is intended to facilitate unrestricted exploration by the player, thereby enabling the evaluation of the methods' effectiveness in more dynamic and unpredictable contexts.

Participants are required to progress through a series of sequential maps (stages), with each stage evaluating the efficacy of a single visual method. Each method is tested three times, with the stages arranged in a manner that exposes the player to each method initially in its weakest form, followed by its stronger and, finally, its most robust variant. Consequently, each participant navigates a total of 18 maps. In each level, the player's objective is to locate a hidden portal that will advance them to the subsequent stage. Within the narrative framing of the study, the player assumes the role of a wandering mage traversing mysterious, floating forest islands in search of magical portals. The guidance methods are

applied in such a way as to subtly suggest the portal's location, thus influencing the player's navigation decisions.

The study begins with an introductory level, which is excluded from the analysis. This introductory phase serves to familiarize participants with the basic controls, allow them to get used to the environment, and provide an introduction to the narrative while clarifying the purpose of the game. Participants are not informed about the experimental aims or specific research focus. Instead, they are told that their objective is to locate all the portals, thereby completing all the levels presented in the study.

3.1 Environment

The design of the environment for exploration was primarily guided by two key principles: the environment had to be open to allow for free and the maps needed to be highly homogeneous—that is, stripped of any visual variety or distinctive elements (such as colors, shadows, or complex models) that could unintentionally draw the player's attention and influence decision-making. For the target environment, a forested area on an island floating in a vacuum was selected. To ensure maximal environmental simplicity, a single tree model, a few mushroom models, and a single grass texture were utilized in the construction. Additionally, the environment was intentionally stripped of color to eliminate the possible influence of color on players' decision-making. In line with this approach, the environment was also devoid of any directional light sources, relying instead on sterile ambient lighting. Consequently, the generation of shadows for all objects within the scene was disabled.

The study was designed to test all visual cues within an identical environment. For each stage of the study, the only variables that changed were the starting position of the player, the position of the portal (the target the player was tasked with reaching), and the specific visual pattern being tested, along with its designated strength. The starting positions for each level were determined such that, in the initial frame, the tested method was always visible to the player. The ideal condition for the test assumed that the player would immediately notice the relevant method and proceed towards it as soon as they began the stage. The distances between the starting and ending points for levels testing varying intensities of the same method were kept consistent.

The primary aim of the study is to replicate, as closely as possible, the conditions that gamers encounter during typical gameplay. To achieve this, the study was framed as a game that participants were asked to play through. As detailed in a previous section, the study begins with an introductory level to provide context for the game's narrative and familiarize participants with the controls. By presenting the player with a clear in-game objective, the study aims to simulate real gameplay experiences, which, as indicated by previous research [3,12], can influence player decisions and behaviors without negatively impacting the integrity of the experiment.

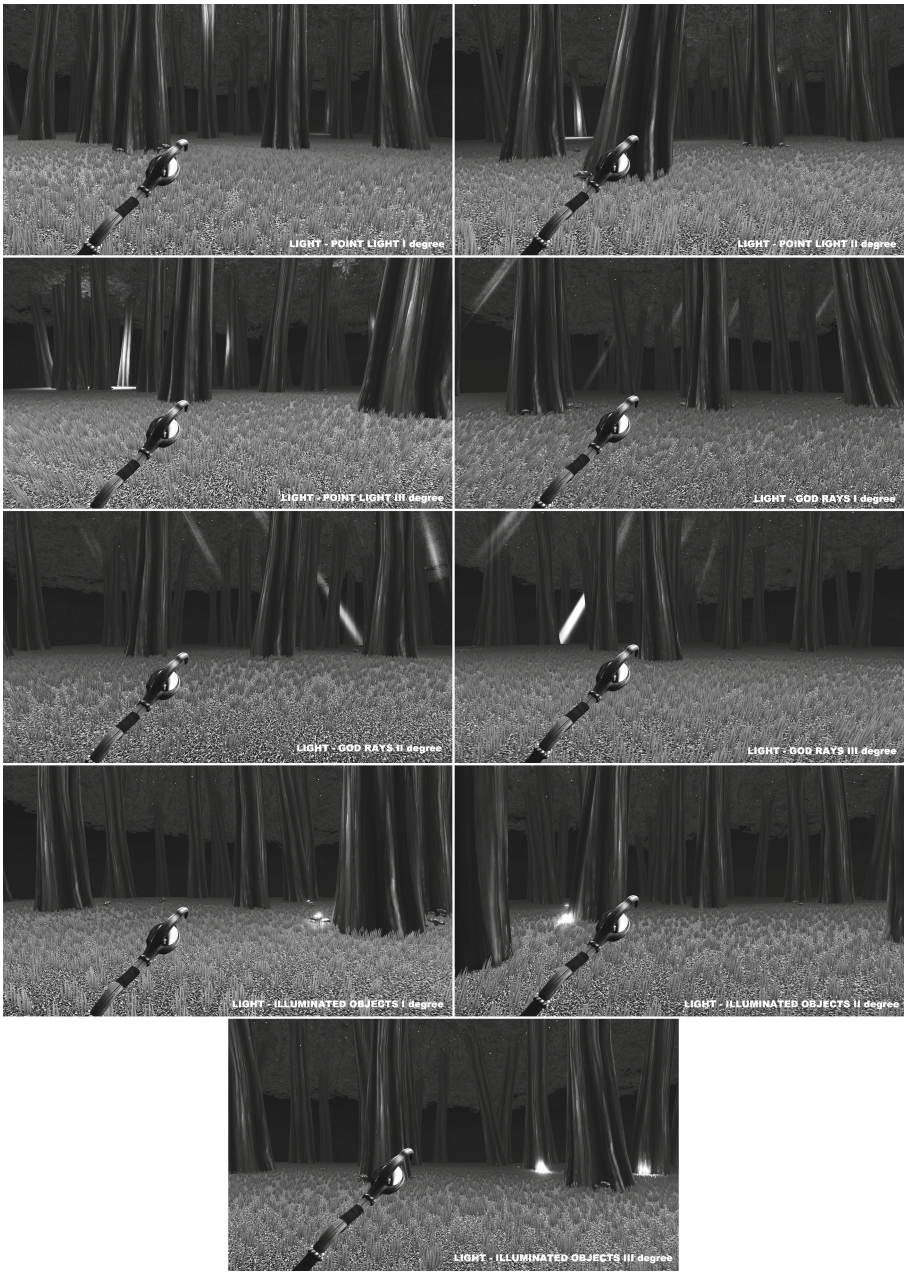

Fig. 1. Views from starting points on levels implementing light methods.

3.2 Methods

Two types of visual cues were used in the work. One based on light and the other based on geometry. Each type has three variations in three degrees of intensity. Both types will be explained below.

Light. The light-based visual cues employed in this study consisted of point lights, god rays, and illuminated objects distributed along the path. Further descriptions of the lighting parameters will be provided in terms of the contrast between the environment and the light, quantified as a percentage based on the color brightness derived from the lightness parameter in the HSL model. Given that the environment was devoid of color, the hue and saturation parameters remained constant at 0, with only the lightness parameter being relevant for contrast calculations. For instance, the color notation (0,0,14) in the HSL model would be represented as 14% brightness.

Each level incorporating a point light features a designated illuminated spot for the player to reach. In the case of god rays, these rays are directed towards the target spot. For the illuminated object variant, small glowing mushroom models were placed along the path, with their arrangement guiding the player to the destination (Fig. 1). For each of the methods tested, three levels of intensity were applied, determined by the corresponding difference in brightness between the light source and its immediate surroundings. These intensity levels are differentiated by increasing contrast values, as presented in Table 1.

Table 1. The difference in pixel brightness between a particular variant and the surroundings expressed as a percentage in light method. The difference in models between a particular variant in geometry method.

Light			
–	Point light	God rays	Illuminated objects
I degree	6%	5%	6%
II degree	11%	9%	12%
III degree	21%	20%	27%
Geometry			
–	Rotation	Scale	Shape
I degree	15°	scale x2	4 branches
II degree	30°	scale x3	8 branches
III degree	60°	scale x4	16 branches

Geometry. The visual cue variants based on geometry involve modifying a parameter of a tree object commonly used in the environment. The parameters

subject to modification include rotation, scale, and shape of the object. The specific values for each of these altered parameters are detailed in Table 1.

In levels associated with the study of the effect of object rotation on player navigation, a single tree is distinguished by its tilt angle. The tilted object is rotated along a single axis such that it aligns with the player's initial viewpoint. The tilt angle for the pattern in its first degree is set to 15°, with subsequent tilt angles doubling the previous value.

Levels featuring the scale-related variant include a single tree that has been enlarged. The default scale for all other trees is set to 1. The pattern strength for I degree is defined by a scale value that is twice the size of the default tree's scale. Subsequent degrees of intensity increase linearly by one unit.

The stages of the study examining the impact of object shape on player behavior each feature a single tree with modifications to its geometric shape, specifically in relation to the branches. To ensure that the modified tree stands out in contrast to the simple trunks of other trees, all non-pattern trees in these levels have a single branch. I Degree of the pattern strength involves four branches evenly distributed on each side of the tree. In subsequent degrees, the number of branches doubles with each increase (Fig. 2).

3.3 Collected Data

For the purposes of this study, a player tracking system was developed, drawing inspiration from, among other sources, a data collection system described in research on visual attention in interactive environments, particularly in relation to task performance [4]. During the exploration of each level, data samples are collected at regular intervals, recording the following information: the player's position, the camera's rotation, and whether the object implementing the method under study was within the player's view. The data gathered through this process enables the precise reconstruction of each participant's gameplay, allowing for a comprehensive and unrestricted analysis. Upon completion of the study, which involves navigating and completing all the designed levels, participants are also required to fill out a questionnaire intended to complement and further inform the study's findings.

4 Participants

The survey included 36 participants: 26 men and 10 women. Most respondents (83.3%) were aged 21–25, followed by 8.3% aged 26–30, 5.6% aged 16–20, and 2.8% aged 31–35. Weekly time spent playing computer games varied: 41.7% played 10–20 hours, 30.6% played less than 5 h, 16.7% played 5–10 hours, and 11.1% played more than 20 h.

Participants were categorized into two groups based on gaming activity: casual gamers (up to 10 h/week, 47% of respondents) and hardcore gamers (more than 10 h/week, 53% of respondents).

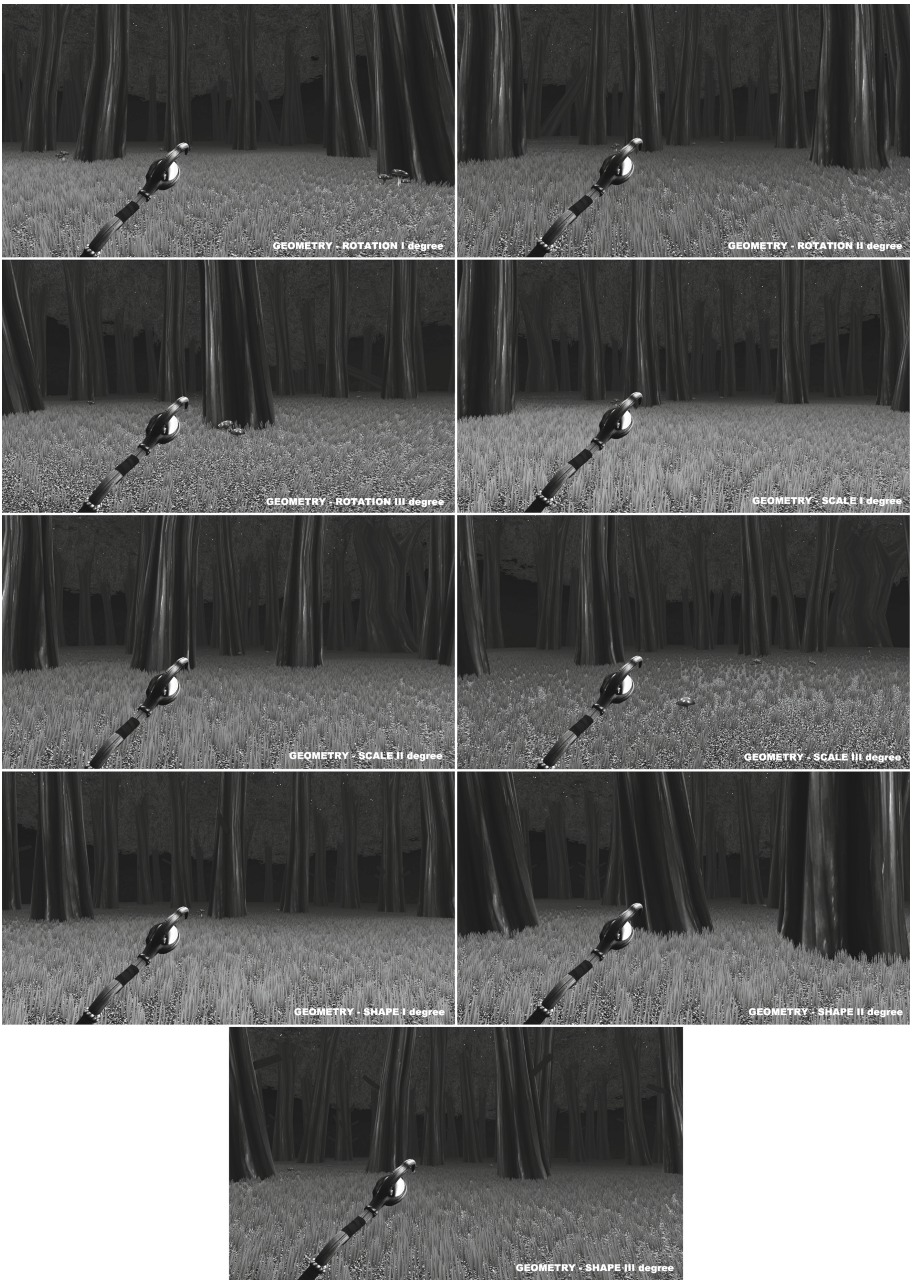

Fig. 2. Views from starting points on levels implementing geometry methods.

5 Results

In response to the first optional question of the questionnaire, which asked participants to identify the methods they noticed, 34 out of 36 respondents provided answers. The methods noticed by the participants were categorized as follows: Illuminated objects: Noticed by 25 participants; God rays: Noticed by 23 participants; Point light: Noticed by 13 participants; Rotation: Noticed by 32 participants; Scale: Noticed by 28 participants; Shape: Noticed by 20 participants.

As evident from these responses, the most frequently noticed method was the rotation variant.

During the exploration of each level, data samples were collected at regular intervals, documenting the player's position, camera rotation, and the visibility of the method on the player's screen. For this study, samples were collected every half second.

To assess the visibility of each method during the test, a parameter was developed. This visibility parameter represents the total duration (in percentage) that the method was visible in the central area of the participant's screen during a given level. All samples collected throughout the test are included in the calculation. This approach allows for the determination of the cumulative time that the method was visible while the participant progressed through the level. A summary of all the results collected during the survey can be found in Table 2.

6 Discussion

This chapter analyzes the collected data through graphical maps of player routes and calculated parameters, evaluating the impact of each method and variant.

6.1 Light

The point light variant showed increasing effectiveness with higher degrees of implementation. At the weakest level (I), visibility was only 63.5%, with many participants failing to notice the contrasting light source, resulting in arbitrary exploration. Level II demonstrated a significant improvement, achieving a 92.7% visibility rate, with most participants immediately navigating toward the illuminated portal. Level III results were comparable to level II, confirming the method's reliability at higher strengths. The god ray variant was initially less effective, with a level I visibility rate of 59.3%, as participants often failed to detect the subtle light beams. Level II visibility improved to 85.5%, and level III reached 96.1%, demonstrating its effectiveness when implemented with stronger contrast. The illuminated objects variant proved the least effective of the light-based methods. Visibility ranged from 70.5% at level I to 79.6% at level III, with only minor improvements across variants. Players frequently overlooked the illuminated objects, resulting in disorganized navigation and minimal impact on exploration.

Table 2. A table summarizing the results for each Light and Geometry variant and degree of strength. Visibility is the average percentage of how long the method was visible on the users' screen. While time is the average of the times of each user.

Point light					Rotation				
I degree	Visibility	σ	Time	σ	I degree	Visibility	σ	Time	σ
all players	63.5%	2.5	21.5 s	3.2	all players	55.9%	1.9	49.4 s	4.7
casual	57.7%	3.7	27.3 s	6.7	casual	53.7%	2.2	53.4 s	5.3
hardcore	68.1%	2.8	17 s	1.5	hardcore	57.9%	1.4	45.9 s	4
II degree	Visibility	σ	Time	σ	II degree	Visibility	σ	Time	σ
all players	92.7%	1.4	11.6 s	1.4	all players	80%	1.9	24.6 s	1.7
casual	93.7%	1.5	14.8 s	3	casual	80.7%	1.9	24 s	1.1
hardcore	92%	2.1	9.2 s	0.2	hardcore	79.4%	1.9	25.2 s	2.1
III degree	Visibility	σ	Time	σ	III degree	Visibility	σ	Time	σ
all players	85.6%	1.5	9.3 s	0.5	all players	88%	1.7	26.3 s	1.7
casual	84.2%	2.1	10.7 s	0.9	casual	87.2%	1.6	28.3 s	1.6
hardcore	86.6%	2.1	8.2 s	0.2	hardcore	88.7%	1.7	24.5 s	1.8
God rays					Scale				
I degree	Visibility	σ	Time	σ	I degree	Visibility	σ	Time	σ
all players	59.3%	4.4	25.3 s	2.8	all players	53.5%	2.1	69.9 s	6.3
casual	61%	6.9	25 s	3.8	casual	49.9%	2.2	89.8 s	6.4
hardcore	58%	5.7	25.6 s	4.1	hardcore	56.8%	2	52.1 s	5.6
II degree	Visibility	σ	Time	σ	II degree	Visibility	σ	Time	σ
all players	85.5%	2.8	13.2 s	1	all players	68%	2.1	60 s	17.2
casual	85.3%	4.1	15.6 s	1.6	casual	65.4%	2.1	99.3 s	24.4
hardcore	85.7%	3.9	11.3 s	1.1	hardcore	70.4%	2.1	24.9 s	1.5
III degree	Visibility	σ	Time	σ	III degree	Visibility	σ	Time	σ
all players	96.1%	1.5	10.3 s	0.9	all players	87.7%	1.3	28.8 s	2.8
casual	96.6%	1.6	12.2 s	1.9	casual	88.2%	1.4	34 s	4
hardcore	98.7%	2.3	8.8 s	0.1	hardcore	87.1%	1.2	24.1 s	0.5
Illuminated objects					Shape				
I degree	Visibility	σ	Time	σ	I degree	Visibility	σ	Time	σ
all players	70.5%	3.8	26.1 s	5.8	all players	44.1%	1.6	68.7 s	5.1
casual	69.7%	6	35.9 s	11	casual	44.4%	1.6	66.7 s	4.7
hardcore	71%	4.8	18.3 s	5.1	hardcore	43.8%	1.7	70.4 s	5.3
II degree	Visibility	σ	Time	σ	II degree	Visibility	σ	Time	σ
all players	79%	3.7	28.2 s	7.3	all players	56.1%	2.1	57.8 s	5.8
casual	71.7%	5.9	32.1 s	11.8	casual	59.5%	2.2	60.1 s	6
hardcore	84.8%	4.3	25.2 s	9.1	hardcore	53%	1.9	55.6 s	4.4
III degree	Visibility	σ	Time	σ	III degree	Visibility	σ	Time	σ
all players	79.6%	2.5	21.6 s	13.4	all players	73.9%	2.5	30.6 s	3.2
casual	75.3%	4.3	38.9 s	29.9	casual	76%	2.5	35.9 s	3.8
hardcore	83%	2.7	8 s	0.9	hardcore	72%	2.6	25.9 s	2.4

6.2 Geometry

The rotation variant demonstrated clear improvements in effectiveness with increasing degrees. At level I, visibility was 55.9%, and players often failed to notice the leaning object. At level II, visibility rose to 80%, with clearer navigation paths emerging. Level III achieved 88% visibility, demonstrating strong influence on player behavior. The scale variant followed a similar pattern, with visibility improving from 53.5% at level I to 87.7% at level III, suggesting it became effective only at its strongest implementation. The shape variant was the least impactful. Visibility ranged from 44.1% at level I to 56.1% at level II, with minimal improvements even at level III. The added branches to differentiate the object failed to consistently attract attention, highlighting the method's limited salience.

6.3 Impact of the Player Type

The influence of player experience was analyzed by comparing casual and hardcore players. For point light, hardcore players completed levels faster, averaging one-third less time than casual players at level I, though visibility rates were 10% lower, reflecting their focused navigation. At levels II and III, results were similar for both groups, with visibility exceeding 90% and differences primarily in completion times. The god ray method showed similar trends across groups, with both casual and hardcore players achieving high visibility rates at stronger levels, though hardcore players consistently completed levels more quickly.

The illuminated objects variant revealed marked differences: hardcore players completed level I nearly twice as fast as casual players, and their performance continued to improve across variants, while casual players struggled to interpret the method effectively. For geometry-based cues, hardcore players generally outperformed casual players in both completion time and navigation efficiency. However, at the strongest level of the shape variant, casual players unexpectedly outperformed hardcore players, achieving better visibility and faster completion times. This suggests that the shape-based method may be less intuitive for experienced players, potentially due to over-exploration or misinterpretation of cues.

These findings emphasize the importance of tailoring navigation methods to account for player experience and highlight the effectiveness of stronger visual cues in guiding both casual and hardcore players.

7 Conclusions

The objective of this study was to evaluate and compare the effectiveness of visual methods for guiding player behavior during exploratory tasks. The survey, conducted with 36 participants, demonstrated that the influence of these methods on players' decision-making is significantly affected by the strength of the visual cues.

The effectiveness of light-based methods was quantified through the difference in average pixel brightness between the highlighted area intended to attract the

player's attention and its surrounding environment. A critical threshold for contrast was identified at 10% brightness difference in the HSL color model, beyond which a notable improvement in players' navigation behavior was observed. This finding aligns with values reported in existing literature, where contrast has been analyzed in the context of other visual guidance techniques.

Parametric and visual analysis of player movement routes revealed that the most effective geometric method was rotation, followed by scale, while shape-based methods had the least influence. Furthermore, thresholds were identified for the strength of these geometric methods, indicating when they begin to meaningfully impact players' attention. For instance, the rotation method proved effective at a 30-degree tilt, while the scale method only became impactful at its maximum strength, where objects were six times larger than others in the scene. Shape-based methods, even at their strongest degree, did not reliably assist in player navigation.

A comparison of results across casual and experienced players reinforced the universality of these visual methods. Both groups responded similarly to the tested techniques, suggesting their applicability across different player demographics.

It is important to note the potential influence of player curiosity during initial levels, which may diminish the observed effectiveness of weaker variants of the methods. This curiosity-driven exploration could obscure the methods' true impact at lower intensities.

An important limitation of the study design is the fixed order in which cue intensities were presented—each method was always tested from weakest to strongest. While this approach reflects a natural learning curve and ensures that stronger cues are not prematurely introduced, it may also introduce an order effect. Specifically, participants may become increasingly familiar with the game mechanics or the visual language of the environment as they progress, potentially improving their ability to detect cues regardless of their strength. Additionally, the initial exposure to weaker cues may have been influenced by elevated curiosity and exploratory behavior, which could obscure the actual effectiveness of these cues. Counterbalancing the order of intensity levels across participants would have mitigated these effects and strengthened the validity of the results, although it would have introduced additional complexity into the experimental design. Future studies may consider randomized or balanced cue sequences to better isolate the impact of cue strength from learning or habituation effects.

Finally, the use of a controlled, homogeneous environment in this study allows for the generalization of results to other settings with different environmental elements. Future research could explore the applicability of these findings in more varied contexts, offering additional insights into the robustness of these visual guidance techniques.

While the results presented in this study are promising, it is essential to consider certain limitations that may affect the validity of the findings. One potential threat to internal validity is the influence of participants' prior gaming experience or expectations, which may have shaped how they perceived and

responded to the cues. Although the test environment was intentionally simplified to control for external variables, the stylized and homogeneous design may reduce ecological validity compared to real-world game settings, where players encounter more complex visual and narrative contexts. Additionally, the short duration of the experimental sessions may not fully capture how players adapt to visual cues over extended gameplay. Future research should aim to validate these findings in more immersive and varied environments, incorporating longer play sessions and more diverse participant groups to strengthen the generalizability of the conclusions.

Acknowledgements. This article has been completed while the third author was the Doctoral Candidate in the Interdisciplinary Doctoral School at the Lodz University of Technology, Poland.

References

1. Alexander, C.: A Pattern Language: Towns, Buildings, Construction. Oxford University Press (1977)
2. Barney, C.: Pattern Language for Game Design. CRC Press (2020)
3. Gómez-Maureira, M.A., Kniestedt, I., Van Duijn, M., Rieffe, C., Plaat, A.: Level design patterns that invoke curiosity-driven exploration: an empirical study across multiple conditions. Proc. ACM Hum.-Comput. Interact. **5**(CHI PLAY), 1–32 (2021)
4. Hadnett-Hunter, J., Nicolaou, G., O'Neill, E., Proulx, M.: The effect of task on visual attention in interactive virtual environments. ACM Trans. Appl. Percept. (TAP) **16**(3), 1–17 (2019)
5. Hoeg, T.: The invisible hand: Using level design elements to manipulate player choice. Masters of Interactive Technology in Digital Game Development with a Specialization in Level Design, Guildhall at Southern Methodist University (2008)
6. Irshad, S., Perkis, A., Azam, W.: Wayfinding in virtual reality serious game: an exploratory study in the context of user perceived experiences. Appl. Sci. **11**(17), 7822 (2021)
7. Knez, I., Niedenthal, S.: Lighting in digital game worlds: effects on affect and play performance. CyberPsychology & Behav. **11**(2), 129–137 (2008)
8. Kremers, R.: Level Design: Concept, Theory, and Practice. CRC Press (2009)
9. Liszio, S., Masuch, M.: Lost in open worlds: design patterns for player navigation in virtual reality games. In: Proceedings of the 13th International Conference on Advances in Computer Entertainment Technology, pp. 1–7 (2016)
10. Marples, D., Gledhill, D., Carter, P.: The effect of lighting, landmarks and auditory cues on human performance in navigating a virtual maze. In: Symposium on Interactive 3D Graphics and Games, pp. 1–9 (2020)
11. Moura, D., El-Nasr, M.S.: Design techniques for planning navigational systems in 3-d video games. Comput. Entertainment (CIE) **12**(2), 1–25 (2015)
12. Petersson, E., Helgesson, F.: Visual attention in level design for a 3d adventure platform game-analyzing visual cues in a 3d environment (2018)
13. Rogers, S.: Everything i learned about level design i learned from disneyland. In: Game Developers Conference (2009)

14. Totten, C.W.: Architectural Approach to Level Design. CRC Press (2019)
15. Winn, B.M., Peng, W., Pfeiffer, K.: Player guiding in an active video game. In: 2011 IEEE International Games Innovation Conference (IGIC), pp. 107–108. IEEE (2011)
16. Winters, G.J., Zhu, J.: Guiding players through structural composition patterns in 3d adventure games. In: FDG (2014)
17. Yesiltepe, D., Conroy Dalton, R., Ozbil Torun, A.: Landmarks in wayfinding: a review of the existing literature. Cogn. Process. **22**, 369–410 (2021)

A New Way to Generate Urban Environments for Video Games Using the Architectural Impression Curve Method

Andrzej Sasinowski, Aneta Wiśniewska, Jarosław Andrzejczak, Adam Wojciechowski, and Rafał Szrajber(✉)

Institute of Information Technology, Lodz University of Technology, 215 Wólczańska Street, 90-924 Lodz, Poland
aneta.wisniewska@dokt.p.lodz.pl, rafal.szrajber@p.lodz.pl
http://it.p.lodz.pl

Abstract. One of the most important elements influencing the perception of the game is a properly designed space that accompanies the gameplay. Designing a level in such a way that it provides the viewers with the impressions assumed by the designer at a given moment of the game, and thus becomes visually engaging or merely a background, is a task requiring adequate preparation, experience, and many simulations. We have proposed a new way of generating urban space using the architectural method of the impression curve. In developing the tool, we defined the individual values of the impression curve in spatial form and its accompanying relationship, so that the game environment corresponds to the user's experience at the adopted scale. We analyzed the levels, generated with our tool based on the defined impression curves, by a group of users who produced their impression curves as part of their exploration of the space. Our method indicated a different take on modular and generative spatial design than has been done to date, and the effectiveness of the proposed solution. Our discovery will allow further development of the use of the impression curve method in video games and link it to currently studied methods of the gameplay curve or audio curve, as components responsible for the appropriate control of player engagement and activity.

Keywords: Virtual environment · Level design · Impression curve · Urban space generation

1 Introduction

Level design is a fundamental and intricate phase in the game development process, playing a crucial role in shaping the player's experience. The virtual environment, within which a game unfolds, is not merely a background element but an active component that significantly influences both narrative delivery and

M. Paszynski et al. (Eds.): ICCS 2025 Workshops, LNCS 15912, pp. 78–91, 2025.
https://doi.org/10.1007/978-3-031-97573-8_6

player immersion. The deliberate structuring of space to evoke specific emotions, guide the player's perception, and align with gameplay objectives is a complex challenge. Achieving the desired effect requires careful planning, extensive design work, and a deep understanding of spatial composition.

Traditionally, game levels and environments intended to facilitate storytelling or enhance player experience are manually crafted by skilled level designers. This approach ensures that every detail—from layout and lighting to object placement—contributes to the intended gameplay dynamics and emotional impact. When designing a level tailored to a specific game concept, mechanics, or playstyle, numerous factors must be analyzed and seamlessly integrated into a coherent framework [18]. The interplay of aesthetics, functionality, and player psychology dictates the success of the final design.

In recent years, the field of Procedural Content Generation (PCG), including the automated creation of game levels, has been gaining traction as an alternative or complementary approach to manual design. The advancement of PCG techniques has led to the development of various algorithms and methods capable of generating diverse virtual spaces. However, despite the progress in this domain, algorithmically generated environments frequently fall short in delivering the depth of immersion achieved by handcrafted levels. Many procedural techniques focus on efficiency and variability but often lack the nuanced spatial storytelling elements that define high-quality level design [6].

The present study explores whether it is feasible to develop a tool that integrates spatial characteristics defined by the Kazimierz Wejchert impression curve as a guiding parameter for procedural environment generation. To achieve this, a generator was designed based on a modular system structured around an urbanized setting—specifically, a street environment. The generated virtual space was composed of individual modules that reflected values corresponding to the impression curve scale, thereby aiming to replicate human spatial perception in a controlled manner.

To validate this approach, a series of test environments were procedurally generated, each structured to align with varying impression curve values. Subsequently, experimental tests were conducted to assess the effectiveness of the method and verify whether it successfully produces immersive, perception-driven spatial compositions. The findings contribute to the ongoing discourse on bridging procedural generation techniques with human-centered design principles, offering insights into the potential for more immersive and narratively cohesive automated level design.

2 Related Works

Since the designed tool incorporates subjective parameters such as emotions and impressions, it becomes essential to establish a quantifiable framework that translates these intangible experiences into measurable values. One of the methodologies introduced in architectural studies that aligns with this need is the impression curve, a concept developed by Kazimierz Wejchert [20]. This

tool is based on a ten-grade scale used to assess variations in spatial perception over time or distance, typically presented in graphical form. By assigning specific characteristics and spatial features to numerical values, Wejchert's approach provides a structured method for analyzing urban environments, with particular emphasis on streets as dynamic, spatiotemporal sequences.

The impression curve has traditionally been employed to evaluate the attractiveness and perceptual qualities of streets, public spaces, and other elements of urban landscapes. It has been widely used in architecture and urban planning as a means to analyze human reactions to spatial arrangements and their aesthetic impact [3,9]. Furthermore, it has found application in real estate valuation, where spatial perception plays a role in determining property desirability [12]. Despite its broad use in the analysis of real-world environments, the application of the impression curve to virtual spaces remains a relatively unexplored domain [16]. Early research efforts in this field, as presented in [14,15], provided the first indications that the impression curve could serve as a valuable tool in the design and evaluation of digital environments. More recent studies further support this idea, demonstrating that it is possible to apply the impression curve in the assessment of virtual spaces at various stages of level design in video games [2]. This highlights its potential as a quantitative method for evaluating spatial immersion and user experience in digital environments.

Architecture and level design share many common principles and design methodologies, as indicated in [17]. The author of this study not only identifies the parallels between these fields but also explores the transfer of architectural concepts and spatial planning techniques to the design of virtual environments. One of the key factors influencing the level of immersion in a video game is spatial simulation [13]. In both real-world and digital environments, individuals instinctively construct cognitive maps of their surroundings, gradually memorizing distinctive elements and using them for navigation. This process, fundamental to human spatial perception, is equally applicable to virtual worlds, where the arrangement of objects, pathways, and landmarks influences how players interact with and explore their surroundings. The way in which space is structured significantly impacts the player's ability to navigate and their motivation to explore, reinforcing the importance of intentional level design.

A well-designed game environment, much like an urban setting, can subtly guide player movement and encourage exploration through careful placement of visual cues and suggestive design elements. A clear example of this approach is Disneyland, where architectural and spatial design are deliberately employed to direct visitors' paths and enhance their overall experience [11]. Similarly, in video game level design, the application of architectural knowledge enables the creation of spaces that feel realistic, engaging, and intuitive to explore. Beyond realism, this approach allows games to serve as immersive representations of distant, lost, or even entirely fictional locations, reinforcing the idea that video games can act as experiential tools for exploring environments that might otherwise be inaccessible [10].

The studies presented above underscore the significant impact of architectural techniques on increasing player immersion and shaping the perceptual experience of digital spaces. Prior research confirms that the impression curve can be successfully applied to the evaluation and validation of virtual worlds, offering a structured and quantifiable method for assessing spatial design and user engagement. By integrating architectural analysis with level design methodologies, future research can further refine these approaches, bridging the gap between real-world spatial perception and the immersive potential of digital environments.

3 Modular Approach

The problem of generating urban spaces can be divided into four stages, each of which is carried out using different methods: space planning, which involves the division into streets and designated areas for buildings, the generation of the external appearance of buildings, the internal spatial division of structures, and the distribution of details and furnishings within the generated environment [4]. These stages contribute to the overall realism and functionality of the virtual space. However, evaluation criteria typically focus on aspects such as realism, scale, variety, performance, or algorithm control, while the degree of player immersion is often not taken into account [7]. Most research in this area emphasizes the development of techniques for procedurally generating cities and buildings, analyzing performance, the degree of control over the process, and the runtime efficiency of algorithms. While these aspects are essential for optimizing generation methods, they do not sufficiently address the influence of the generated space on gameplay and player experience, as seen in studies such as [1,8,19]. In this paper, the criteria for verifying the performance of the system will be based on how closely the players' impressions, expressed on the ten-point scale of the impression curve, correspond to those assumed at the stage of space generation.

The layout and generation of buildings are carried out using two primary methods: employing objects that represent entire building models or constructing objects from smaller modules. Another possible approach involves algorithms that directly operate on a grid-based system [1]. The first method is the most straightforward in terms of implementation but is also the most time-consuming. Designing an entire building as a single model requires considerable manual effort, particularly when a diverse set of structures is needed to maintain the visual variety of the environment. While procedural algorithms can modify the geometry of pre-existing models to introduce variation, they do not provide complete control over the resulting forms. This limitation is problematic for an urban environment generator that relies on specific perceptual guidelines, such as the impression curve, as an input factor. To address this issue, the modular approach to building generation was adopted.

Authors in [5] classified modular construction methods based on the type of modules used, identifying three main categories. The first type consists of small,

indivisible modules that serve a specific function but cannot exist independently within a scene. Examples of such modules include windows, pillars, or doors, which must be combined with other elements to create a complete structure. The second type, referred to as the "box" concept, defines modules as larger architectural units that incorporate a greater level of detail and do not necessarily require integration with additional components. Some of these modules can function as standalone objects, appearing in the generated environment without further modification. The third type is a hybrid approach that combines elements of the first two categories, offering larger modular components composed of smaller, indivisible objects. Although this method allows for the creation of complex and unique architectural forms, it also presents challenges related to computational efficiency and design constraints.

For the design of the urban space generator, the "box" concept was selected due to its ability to balance control over architectural details, the level of variation in structures, and the efficiency of module creation. Research conducted in [5] indicates that this approach provides an optimal compromise between maintaining a detailed and recognizable architectural style while allowing for procedural diversity in the generated space. By adopting this method, the generator can produce urban environments that align with predefined perceptual expectations, ensuring that the spatial experience conforms to the intended values of the impression curve. This structured approach facilitates the creation of immersive and coherent virtual spaces while maintaining a level of flexibility that supports both design efficiency and user engagement.

4 Methodology

The aim of the research was to verify the performance of the generator and the modular structure for defining space developed within it, as well as to verify the application of the impression curve as a set of data shaping a reliable space at the stage of advanced blockout without human intervention. To the generator, 49 base modules were prepared, which were then additionally modified by adding additional decorative elements, thus obtaining 210 modules that will be used to generate buildings. Based on the quantisation of grades prepared by Kazimierz Wejchert in [20], individual modules received scores. To further reduce the probability of the occurrence of a sense of boredom with the environment, which is reflected in the scale by a downgrading, an additional system based on probability was used, according to which a given module can be assigned multiple assessments with a numerical chance of their occurrence within a given rating. This allowed the scores to be blurred in such a way that modules designed for lower scores could also appear within higher scores, but with correspondingly lower probability. This allowed more realism and more modules to be matched to a particular grade. The division of modules according to their function was also introduced - base or ground level (always present and being level 0), floors (levels above 0), roof/ceiling (being the tip of the building). A given module has a selected value of the impression curve based on its complexity. Examples of designed modules can be seen in Fig. 1.

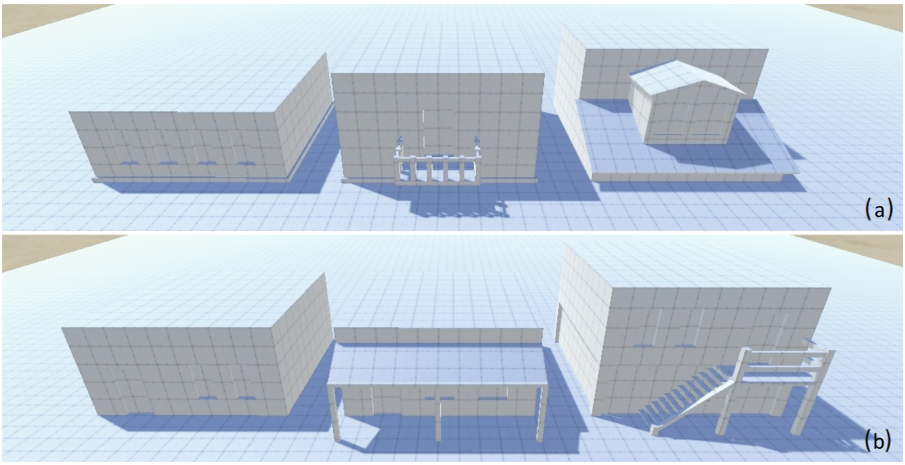

Fig. 1. (a) Examples of modules serving as a base, (b) examples of modules serving as floors. Examples of modules from which buildings are constructed.

As the impression curve tool works best with linear spaces, the street was used as a form of urban environment. Twenty-two street structure templates were also designed and assigned to specific grades based on theories from the field of architecture. All models are based on simple geometry only, as it is already possible to use the impression curve at this level design stage [2]. Additional input for the application was also the determination of the acceptable quantity of one module. This allows adjustment of how many times the same modules can be used in a particular grade. Lower grades had larger values, while higher grades had smaller and smaller values, to avoid a situation where many modules are repeated and create a feeling of monotony.

A test application was prepared for the research. The character, which is controlled by the player, uses a first-person camera. To maintain the linearity of the test, additional restrictions were introduced so that the user can only move along a dedicated section of the street, even if the street has additional openings or branches. Each level consists of generated sections of street and is on average 50 units in length, with an evaluation of the environment taking place halfway through. The player moves at a speed of 5 units per second - so assuming the player does not stop and moves in the right direction all the time, they reach the next point in about 10 s.

The environment has three levels (referred to as L1, L2 and L3 hereafter), different impression curves were used to generate each level. All three streets consist of 7 fragments generated by the program and evaluated during the experiment. The values of the impression curve from which each level was created are as follows: L-1 - 1, 3, 4, 4, 5, 3, 2; L-2 - 4, 3, 5, 6, 6, 8, 7; L-3 - 4, 5, 7, 9, 10, 8, 5. The choice of three levels with slightly different values and curve shapes allows the different courses of the impression curve to be examined.

5 Generator Implementation

The functioning of the generator is based on a structured data system in the form of an object that stores information about all predefined modules. Each module is characterized by a set of parameters that determine its properties and placement rules within the generated environment. These parameters include the type of module, its dimensions, window styles, and specific impression curve values within which the module can appear, along with the associated probability (weight) for each value. Additionally, the structure contains information about whether the module has alternative versions, which may differ in terms of detail, as well as which walls of the module contain additional decorative elements such as windows, balconies, or protruding architectural features. The module manager also incorporates a set of predefined street templates, each of which has associated ratings that determine its probability of selection. Within each street template, there are designated building placement areas that include constraints on the types of modules that can be selected for that location. These constraints specify the allowable module sizes and define which walls of the buildings can contain decorative elements. By enforcing these constraints, the system ensures that adjacent buildings do not have overlapping side-wall decorations, preventing visual inconsistencies and maintaining architectural coherence in the generated environment.

The generator operates by processing the impression curve values provided as input and selecting corresponding street templates based on their assigned evaluation scores. Once a street template is chosen, the system proceeds to generate buildings within the designated areas by sequentially selecting their base, main structure, and roof. At each step of this process, only modules that are compatible with the given evaluation criteria and impression curve values are considered. Additionally, the probability weight assigned to each module influences its likelihood of being selected, meaning that modules with higher weights for a particular impression curve value have a greater chance of being used in the final generated environment.

To maintain variety and prevent excessive repetition of specific modules within a single street, the generator tracks the number of times each module has been selected. This mechanism ensures that no module appears more frequently than permitted by the predefined program parameters for a given impression curve evaluation. The described sequence of operations is applied iteratively to each of the impression curve values provided as input to the generator, resulting in a procedurally assembled urban space that aligns with the intended spatial perception and design objectives.

6 Procedure

There were 36 participants in the study, the vast majority of whom (n = 33) were aged between 16 and 27 years old. Each participant knew the basics of computer use, was familiar with computer games and common control schemes.

The experiment was conducted remotely. An important assumption was that the subject had no information regarding the impression curves used to generate the levels, and each level was passed only once without repeating the experiment.

At the beginning of the test, an introductory screen was displayed to familiarize the participant with the details of the experiment. The message provided information regarding the number of levels, the purpose of each level, and a brief explanation of the evaluation procedure. Additionally, the participant was informed about the evaluation scale, with an important clarification that a score of 1 corresponds to a simple and uninteresting environment, while a score of 10 represents a highly engaging space rich in detail and architectural dominants.

Once the participant acknowledged the message, they were allowed to explore the virtual street environment. Upon reaching the designated evaluation point, movement was restricted, although the participant retained the ability to look around freely. The evaluation process commenced as soon as the participant confirmed their readiness by pressing the designated button. Following the evaluation, movement was re-enabled, allowing the participant to continue exploring.

Reaching the end of the street triggered progression to the next level. In cases where the completed stage was the final one, a concluding screen was displayed. Upon completion of the experiment, a CSV file was generated, recording the participant's ratings for each of the three tested levels. Examples of the generated street segments evaluated during the study can be seen in Fig. 2.

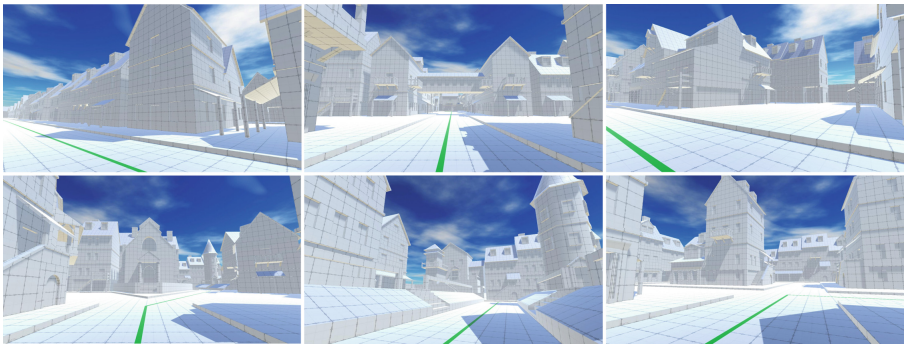

Fig. 2. Sample screenshots showing street fragments that were generated with the implemented system and were evaluated during the study. Fragments generated sequentially from grades: 4, 8, 6, 9, 10, 8. Screenshots from the application showing the generated street sections.

7 Results

Before the results could be analyzed, they had to be properly processed so that comparisons could be made between the results and the values used in the generator. The impression curve represents subjective values of impressions, but

according to research, individual elements in space influence the observers' feelings to the same or similar extent. This means that it is possible to use individual impression curve plots to prepare an averaged result [2,20].

measuring point	1	2	3	4	5	6	7
L-1							
original value	1	3	4	4	5	3	2
average	3.81	4.58	5.64	5.42	6.33	4.42	3.53
standard deviation	1.647	1.498	1.566	1.479	1.528	1.422	1.481
L-2							
original value	4	3	5	6	6	8	7
average	5.11	4.44	6.28	6.92	6.81	7.75	7.11
standard deviation	1.021	1.257	1.304	1.320	1.350	1.441	1.429
L-3							
original value	4	5	7	9	10	8	5
average	5.11	5.5	6.75	9.14	8.81	8.44	6.42
standard deviation	1.286	1.236	1.187	0.787	1.023	1.383	1.233

Fig. 3. Summary of the values used to generate the street, the mean scores of the experimental participants and the standard deviation for each level.

Due to the inherently subjective nature of the experiment, the ratings provided by individual participants exhibited variations both in scale and in the range of values used. Some participants utilized the entire spectrum of available ratings, while others predominantly assigned lower or higher scores, limiting their evaluations to a narrower subset of the scale. Additionally, there were noticeable differences in the way ratings fluctuated throughout the experiment. In many cases, participants provided scores that followed a relatively stable and linear pattern of increase or decrease. However, for some individuals, the assigned ratings appeared more inconsistent, with abrupt changes in values, leading to greater fluctuations between subsequent evaluations.

To analyze the collected data, the mean and standard deviation were calculated for each evaluation point across all three tested levels. The summary of the original values used for generating the street fragments, along with the computed statistical measures, is presented in Fig. 3. The observed standard deviations confirm the diversity in rating tendencies among participants, reflecting the subjective differences in how individuals perceived and evaluated the generated spaces. Notably, the standard deviations appear to be higher for the first level, which may indicate that participants initially lacked a clear reference point for how to appropriately distribute their ratings along the scale. As the experiment progressed, this variability tended to stabilize, suggesting that participants gradually developed a more consistent internal framework for assessing the environments. This pattern highlights the importance of contextual familiarity in subjective evaluations, where early assessments may be influenced by uncertainty or a lack of comparative reference, gradually adjusting as users gain

more experience with the task. Examples of the street sections evaluated by participants, representing the lowest, intermediate, and highest grades used in the experiment, are shown in Fig. 4.

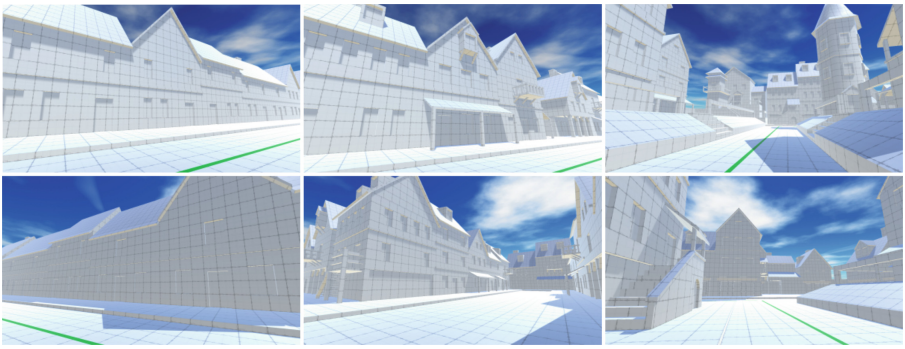

Fig. 4. Examples of points where participants in the study were asked to evaluate the space. All of the points presented were then used in the questionnaire. Extracts with the lowest, intermediate and highest grade are presented. The fragments generated sequentially from the grades: 1, 5, 10, 1, 5, 10. Screenshots from the application showing the generated street sections.

8 Discussion

The impression curve is a tool influenced by the subjective feelings and predispositions of the observer. Depending on the individual, the rating scale may vary and be used to a different extent. This means that as a criterion by which to confirm the effectiveness of the implemented generator, it cannot be used only whether the average of the samples observed during the experiment is close to the original value of the curve at a given point (Fig. 5).

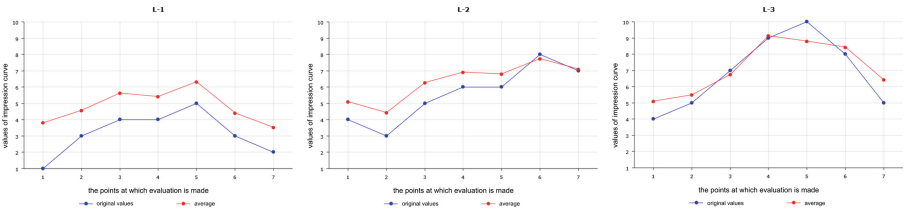

Fig. 5. Comparison of the course of the original impression curve and the average impression curve for the conducted research.

In this regard, additional criteria have also been adopted in terms of which the effectiveness of the solution will be tested:

- The same trend of ratings between points was observed. This means that the monotonicity of the averaged curve is the same as the impression curve from which the level was generated.
- The numerical change in mean scores between points is like the numerical change in scores from the impressions curve used.
- The global extremes are at the same points.

Figure 6 highlights where the trend of the averaged curve differs from that assumed. However, it is worth noting that two of these differences relate to two street sections that were generated using the same value. The system used the same values, which means that the user had to travel twice as long a route generated using the same rules and the same pool of available modules for the grade. The author in [20] pointed out that a lack of change in the structure of the space or in the amount of detail negatively influences the feeling, so that a decrease in such places, although different in trend from the assumed one, is not accepted as an anomaly.

section	1 – 2	2 – 3	3 – 4	4 – 5	5 – 6	6 – 7
L-1						
trend - original curve	increase	increase	**constant**	increase	decrease	decrease
trend - averaged curve	increase	increase	**decrease**	increase	decrease	decrease
L-2						
trend - original curve	decrease	increase	increase	**constant**	increase	decrease
trend - averaged curve	decrease	increase	increase	**decrease**	increase	decrease
L-3						
trend - original curve	increase	increase	increase	**increase**	decrease	decrease
trend - averaged curve	increase	increase	increase	**decrease**	decrease	decrease

Fig. 6. Comparison of the trend between individual points between the original and the averaged impression curve.

Analysing the change in scores between individual sections of the averaged impression curve against the change in values for the original curve allows us to see how effective and accurate the implemented system is in controlling the player's feelings. The calculated numerical changes are shown in Fig. 7. A difference of at least 0.5 was taken as the difference between the expected value and the averaged value, which can be considered significant. This is due to the previously mentioned elements such as different rating scales among users. The first point where the calculated difference is relatively large is the very beginning of the first level. This is most likely since the players had no reference point at the beginning of the experiment and each participant took a different input threshold for the ratings. The largest discrepancy in the change in the value of the ratings between the different points was observed in the third level, which contained not only the highest ratings but also the largest increases or decreases

section	1 – 2	2 – 3	3 – 4	4 – 5	5 – 6	6 – 7
L-1						
change in grades- original curve	**2**	1	0	1	-2	-1
change in grades - averaged curve	**0.77**	01.06	-0.22	0.91	-1.91	-0.89
difference (absolute value)	**1.23**	0.06	0.22	0.09	0.09	0.11
L-2						
change in grades- original curve	-1	2	1	0	**2**	-1
change in grades - averaged curve	-0.67	1.84	0.64	-0.11	**0.94**	-0.64
difference (absolute value)	0.33	0.16	0.36	0.11	**1.06**	0.36
L-3						
change in grades- original curve	**1**	**2**	2	**1**	**-2**	**-3**
change in grades - averaged curve	**0.39**	**1.25**	2.39	**-0.33**	**-0.37**	**-2.02**
difference (absolute value)	**0.61**	**0.75**	0.39	**1.33**	**1.63**	**0.98**

Fig. 7. Comparison of the numerical change of scores between the different points. A positive value means an increase by a given value, while a negative value means a decrease.

between them. One reason may be the assumed length of the street, which was too short to express such large differences in player sentiment when the ratings are already at a high level. This also means that the system should not only take into account the mere trend between grades through a different pool of modules, the frequency and multiplicity of their occurrence or the structure of the space, but should also take into account the intensity of change.

While this study focused exclusively on the spatial geometry of urban environments, it is important to acknowledge that additional factors such as lighting, textures, sound design, and gameplay context also significantly influence the player's perception of space. These elements were intentionally excluded to isolate the effects of spatial structure, but their impact has been described in prior work, particularly in [2]. This provides a foundation for future studies aiming to integrate multiple sensory and contextual elements into impression-based procedural generation.

9 Conclusions

The research presented here indicates that implementing an urban space generator using impression curve values as input is possible, and furthermore, using geometry alone to represent urban objects is sufficient to predict the player's feelings, confirming previous research in this area. Further improvements to the performance of the system and additional research could be conducted. Some of the potential improvements that were highlighted after analyzing the results include:

- Considering the values of the previous street fragment for additional space modifications to create smoother transitions and maintain continuity between segments.
- Implementing additional rules for the generator when the impression curve used as input contains several consecutive points with the same value to avoid repetitive spatial structures.

– Generating additional decorations and environmental elements for higher-rated segments to enhance detail richness and improve player perception of space.

An important addition to the research will be an analysis of the influence of player characteristics, such as player type and player motivation and prior experience with design or architecture, on the alignment of the assigned ratings with the shape of the original impression curve. Understanding these variations could provide insights into how different users perceive and evaluate virtual spaces, potentially refining the application of impression curves in procedural urban environment generation. This direction represents an opportunity for further development in integrating architectural principles into virtual spatial design.

References

1. Alkaim, A.: Procedural generation for architecture (2015)
2. Andrzejczak, J., Osowicz, M., Szrajber, R.: Impression curve as a new tool in the study of visual diversity of computer game levels for individual phases of the design process. In: International Conference on Computational Science, pp. 524–537. Springer (2020)
3. Antoszczyszyn, M.: Methodology of spatial perception and proxemics learning in szczecin architecture faculty. Gen. Prof. Educ. **2018**(1), 7–16 (2018)
4. Cogo, E., Prazina, I., Hodzic, K., Haseljic, H., Rizvic, S.: Survey of integrability of procedural modeling techniques for generating a complete city. In: 2019 XXVII International Conference on Information, Communication and Automation Technologies (ICAT), pp. 1–6. IEEE (2019)
5. Fenech, B., Carter, J.: Approaches to modular construction for real-time game environments. University of the Sunshine Coast, Queensland, Technical Report (2017)
6. Johnson, M.R.: Integrating procedural and handmade level design. In: Level Design Processes and Experiences, pp. 217–242. AK Peters/CRC Press (2017)
7. Kelly, G., McCabe, H.: A survey of procedural techniques for city generation. ITB J. **14**(3), 342–351 (2006)
8. Kim, J.S., Kavak, H., Crooks, A.: Procedural city generation beyond game development. SIGSPATIAL Special **10**(2), 34–41 (2018)
9. Mordwa, S.: Krzywa wrażeń dla ulicy piotrkowskiej w Łodzi (2009)
10. Porreca, R., Geropanta, V., Abril, K., Giordanelli, D.: Gaming as a disembodied experience of the city: from assassin's creed to'smart learner'. SCIRES-IT-SCIentific RESearch Inf. Technol. **10**(2), 117–130 (2020)
11. Rogers, S.: Everything i learned about level design i learned from disneyland. In: Game Developers Conference (2009)
12. Senetra, A., et al.: Wpływ metodyki oceny walorów krajobrazowych na wyniki szacowania nieruchomości. Acta Scientiarum Polonorum Administratio Locorum **9**(2), 113–128 (2010)
13. Swink, S.: Game Feel: a Game Designer's Guide to Virtual Sensation. CRC Press (2008)
14. Szrajber, R.: Impression curve and the gameplay curve as an attempt to record the player's experience (2014)

15. Szrajber, R.: Architecture in video games - seeing or experiencing (2017)
16. Szrajber, R.: Architecture in virtual worlds as a field of research. In: Badania Interdyscyplinarne w Architekturze 2, vol. 1, pp. 55–66. Silesian University of Technology, Wydzial Architektury Politechniki Slaskiej (2017)
17. Totten, C.W.: Architectural Approach to Level Design. CRC Press (2019)
18. Upton, B.: Pt and the play of stillness. In: Level Design Processes and Experiences, pp. 185–204. AK Peters/CRC Press (2017)
19. Viitanen, H.: Procedural city generation tool with unity game engine (2016)
20. Wejchert, K.: Elementy kompozycji urbanistycznej. Arkady (1984)

Enhancing Learning in Augmented Reality (AR): A Deep Learning Framework for Predicting Memory Retention in AR Environments

Onyeka J. Nwobodo[1(✉)], Godlove Suila Kuaban[2], Kamil Wereszczyński[1], and Krzysztof A. Cyran[1]

[1] Department of Computer Graphics, Vision and Digital Systems, Silesian University of Technology, Akademicka 2A, 44-100 Gliwice, Poland
{onyeka.nwobodo,kamil.wereszczynski,krzysztof.cyran}@polsl.pl
[2] Institute of Theoretical and Applied Informatics, Polish Academy of Sciences, Baltycka 5, 44–100 Gliwice, Poland
gskuaban@iitis.pl

Abstract. The integration of Artificial Intelligence (AI) with Augmented Reality (AR) has transformed human-computer interaction, offering new opportunities for immersive learning and cognitive assessment. However, the relationship between user engagement in AR environments and memory retention remains underexplored. This study proposes an AI-driven framework for predicting memory retention using behavioural interaction data captured through Microsoft HoloLens 2 sensors. The model estimates the likelihood of object recall in AR-based learning environments by analyzing key interaction metrics such as gaze duration, interaction frequency, revisit counts, and head movement stability. To validate the AI predictions, we compared model-generated retention scores with user-reported recall, demonstrating a strong alignment between predicted and actual memory performance. Our findings align with established cognitive theories, indicating that increased interaction and attentional engagement enhance memory retention. Furthermore, comparisons with prior research on perceptual judgments and spatial memory reinforce the model's effectiveness in capturing real-world cognitive processes. This study introduces a scalable, non-invasive approach to cognitive modeling, bridging AI-driven analytics with AR-based learning. The results have broad implications for education, medical training, AR-based flight simulation training, and workforce development, where optimizing learning efficiency is crucial. By leveraging AI for real-time memory prediction, this research paves the way for more adaptive and personalized AR learning experiences.

Keywords: Augmented reality · Artificial intelligence · Memory retention · Gaze duration · Deep learning · Behavioral interaction

M. Paszynski et al. (Eds.): ICCS 2025 Workshops, LNCS 15912, pp. 92–106, 2025.
https://doi.org/10.1007/978-3-031-97573-8_7

1 Introduction

The integration of Artificial Intelligence (AI) and Augmented Reality (AR) has ushered in a new age of human-computer interaction, with significant implications for cognitive science and education. AR integrates digital content with the real world, creating immersive environments that transform how individuals interact with complex information [1]. However, the effect of AR on memory retention, a key factor in learning effectiveness, remains insufficiently explored. This gap in knowledge presents a significant challenge, as memory retention is essential for the long-term success of educational and training interventions.

A study by Chen et al. [2] examined using Microsoft HoloLens for learning anatomy and physiology, comparing AR-based instruction to traditional PowerPoint lectures. Their findings revealed that while AR learning methods improved student engagement and reduced test anxiety, they did not significantly enhance memory recall compared to conventional methods. This highlights the need to refine AR-based learning frameworks to improve long-term retention and recall rather than focusing solely on engagement. Similarly, Gargrish et al. [3] investigated an AR-based Geometry Learning Assistant and found that while AR enhanced student engagement and visualization skills, it did not significantly improve long-term memory retention. Makhataeva et al. [4] developed the ExoMem framework, integrating computer vision and AI-driven spatial localization to augment memory. Their study found that AR significantly reduced cognitive load, improved accuracy, and enhanced performance in object-location memory tasks, with participants making 7.52 times fewer errors and completing tasks 27% faster. While highlighting AR's potential for memory augmentation, the study primarily focused on spatial cognition rather than general memory retention.

Beyond education, AI-driven AR systems have shown significant advancements in manufacturing applications, where AR reduces cognitive load by providing real-time task-related information without disrupting user focus [5]. Traditional AR methods in manufacturing rely on non-AI strategies for detection, tracking, and camera calibration, limiting their adaptability to dynamic environments. AI integration in AR has enhanced real-time adaptability through deep learning, object tracking, and ontology-based knowledge representation, providing a more scalable and practical solution across multiple domains. The potential of AI-enhanced AR systems in adaptive learning environments remains an underexplored area that can benefit from these innovations.

Memory retention is a multifaceted process influenced by cognitive, sensory, and environmental factors [6]. Research in cognitive psychology has established that attentional engagement plays a pivotal role in memory encoding, with increased interaction and focus on stimuli leading to stronger memory traces [7]. Traditional methods for studying memory, such as eye-tracking and electroencephalography (EEG), have provided valuable insights into the relationship between gaze fixation and knowledge retention. However, these methods face significant limitations in dynamic environments, particularly AR settings. For instance, while eye-tracking can identify objects of focus, it cannot capture

the underlying cognitive processes or perceptions [8]. Similarly, movement artefacts often contaminate EEG data, complicating analysis and interpretation [9]. Given these challenges, there is a need for innovative, non-invasive approaches that seamlessly integrate with AR technologies.

Recent studies have explored AI-based models for predicting memory retention, primarily relying on physiological signals such as pupil dilation, heart rate variability, and EEG data [10]. While promising, these approaches rely heavily on biometric data, limiting their scalability and practicality in real-world applications. This research proposes a novel AI-driven memory prediction framework that utilizes behavioural interaction data exclusively captured within AR environments. By focusing on metrics such as gaze duration, interaction frequency, revisit counts, and head movement stability, the framework offers a practical and scalable solution for predicting memory retention.

The key Contributions of this Research are as Follows:

- Development of an AI-driven memory prediction model trained on the Microsoft HoloLens 2 sensor data.
- Design of a computational framework for non-invasive cognitive modeling in AR environments.
- A comparative analysis of AI model predictions against user-reported memory retention demonstrates the model's accuracy and reliability.

This study significantly advances personalized learning and adaptive educational systems by bridging the gap between AI-driven cognitive models and AR-based learning environments. The proposed framework addresses a critical gap in the literature by introducing a scalable, non-invasive solution for real-time memory prediction. This innovation enables the development of more effective and engaging learning experiences. The findings have broad implications across multiple domains, including education, medical training, and workforce development, where optimizing learning efficiency and outcomes is essential.

2 Related Works

Memory retention has been widely studied using eye-tracking and electroencephalography (EEG) techniques to analyze the relationship between gaze fixation and cognitive load [11]. Prior research has demonstrated that gaze duration and pupil dilation correlate with attentional focus, a key factor in memory formation [12]. Kolnes et al. [13] further expanded on this by showing that pupil dilation reflects the breadth of attention, underscoring its utility in assessing cognitive dynamics.

EEG was also used to analyze the relation between brainwave activity and reaction time [14] and mental fatigue [15] in flight simulator sessions. EEG studies highlight theta and gamma oscillations as keys to memory encoding and retrieval. Theta activity in the medial temporal lobe (MTL) and neocortex correlates with memory accuracy and confidence, while theta-gamma phase-amplitude coupling (PAC) supports detailed memory representations [16].

Wynn et al. [17] found that parietal theta power correlates with memory confidence, while frontal and parietal gamma oscillations support memory accuracy and decision-making. Increased gamma power during retrieval facilitates pattern completion and neocortical information reinstatement.

Recent research has extended these findings to augmented reality (AR) environments, where physiological measurements, including EEG and eye-tracking, are used to assess cognitive load during AR-based learning and training. However, these methods face challenges in dynamic environments due to signal contamination and practical limitations. Studies suggest that AI-based behavioural analysis offers a scalable alternative for predicting memory retention without requiring intrusive biometric data. Suzuki et al. [18] systematically reviewed physiological methods in AR, identifying EEG and eye-tracking as the most prevalent techniques for assessing cognitive load. Their findings emphasize that a multi-method approach integrating EEG, eye-tracking, and self-rating scales enhances assessment reliability. Vortmann et al. [19] demonstrated that EEG and eye-tracking can distinguish attention between real and virtual objects in AR, achieving 77% accuracy using machine learning. These studies highlight the potential of EEG-based brain-computer interfaces (BCIs) to adapt AR content in real-time, enhancing cognitive training and educational tools.

Gargrish et al. [20] found that AR-based geometry learning significantly improved memory retention compared to interactive simulation (IS) methods. Over two months, AR students showed higher retention scores (12.24 post-learning, 11.76 after one week, 11.32 after two months) versus IS students (9.64, 8.00, 6.44). The immersive, interactive nature of AR enhanced engagement, visualization of abstract concepts, and long-term memory consolidation. Shen et al. [21] further advanced this field by developing a memory augmentation agent using machine learning and natural language encoding: their system, which uses large vision language models, encoded and retrieved egocentric video data from AR headsets. Using the QA-Ego4D dataset, it achieved a BLEU score of 8.3, a metric to evaluate text quality against human references, outperforming previous models (3.4–5.8). A user study showed that the agent enhanced episodic memory recall, surpassing human performance in retrieving spatial and event-based details.

While these advancements demonstrate the potential of AR for memory retention, practical challenges persist in implementing these techniques in real-world applications. Both Suzuki et al. [18] and Vortmann et al. [19] highlight the need for lightweight, non-invasive EEG solutions that can be seamlessly integrated into AR headsets. Building on these studies, our research leverages Microsoft HoloLens 2 sensors to analyze user retention through gaze duration, interaction frequency, revisit counts, and head movement stability metrics. Our work goes beyond traditional AR by using deep learning to model memory retention, an area that has been largely unexplored in prior research. Unlike studies relying on physiological signals, we leverage behavioral data for a more accessible, contact-free approach, making it more practical for real-world education and training.

3 Material And Methodology

This study presents an AI-based framework for predicting memory retention in augmented reality (AR) environments using deep neural networks (DNN) trained on behavioural interaction metrics. The proposed model is designed to process behavioural data, including gaze duration, interaction frequency, revisit count, and head movement stability, which is captured using Microsoft HoloLens 2 sensors. By leveraging deep learning, this model learns patterns in user interaction behavior and predicts the likelihood of remembering specific objects.

3.1 Experimental Setup

The study was designed to develop and validate an AI-based model for predicting memory retention in augmented reality (AR) environments using behavioural data captured through Microsoft HoloLens 2 sensors. The AR environment was developed using Unity 3D and integrated with the Microsoft HoloLens 2 platform. The environment consists of interactive learning tasks designed to simulate real-world educational scenarios, as illustrated in Fig. 1.

Participants: Thirty-six participants with varying augmented reality knowledge were recruited for the study. Before the experiment, participants received a briefing on the study objectives and provided informed consent.

Procedure: The study was conducted in a controlled AR environment using Microsoft HoloLens 2 to evaluate memory retention through interactive object engagement. Each participant was given the HoloLens 2 headset, which was carefully adjusted to ensure proper fit and calibration. Before beginning the experiment, participants received a brief explanation of the study objectives and were given instructions on interacting with the AR environment. Once the experiment started, various virtual objects were instantiated and positioned within the participant's field of view. Participants were instructed to click on each object to reveal its name, which was displayed in a text field within the AR interface. They were also encouraged to revisit and interact with objects multiple times to reinforce memory retention. This process was designed to simulate real-world learning and recall mechanisms.

Throughout the interaction phase, the system continuously recorded the following behavioural data:

Object Name: The specific object that the participant interacted with. **Interaction frequency:** The number of times a participant clicked on each object. **Revisit count:** The number of times a participant returned to a previously interacted object. **Head movement stability:** Quantified as the variance of head rotation and position over a fixed time window, used to assess attentional focus and cognitive engagement. The interaction phase lasted for five minutes, during which participants could freely explore the AR environment and interact with the objects as they wished. This ensured that participants had adequate exposure to all objects and could reinforce their memory through repeated interactions.

After the interaction phase, participants received a brief 5-minute pause before completing a free recall form, where they listed objects remembered from the session. No object lists or prompts were provided, ensuring unbiased memory retrieval. No false recalls occurred, though some participants omitted objects, reflecting natural variability. These responses served as ground truth for evaluating the predictions of the AI model.

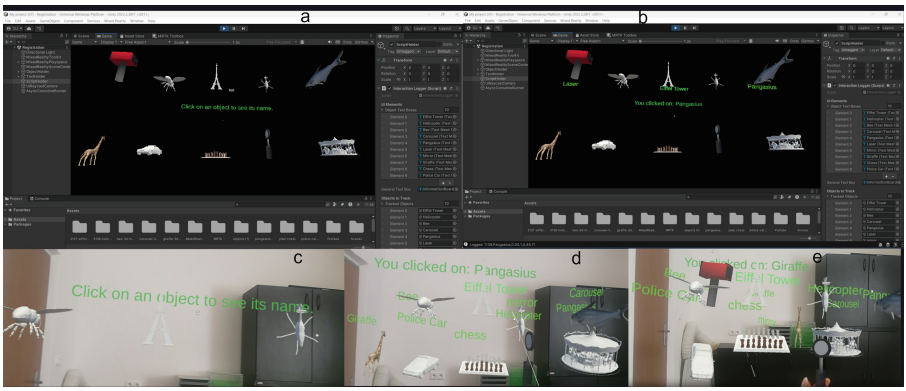

Fig. 1. (a-b) shows the user interface design in Unity for the AR-based memory retention experiment using Microsoft HoloLens 2. (c-e) illustrates the user interactions with objects in the world.

3.2 AI Model Training and Prediction Using Deep Neural Networks (DNN)

This study adopts an efficient approach for predicting memory retention by encoding image identity through category embeddings rather than processing raw image data. The proposed model receives two distinct inputs: behavioural features and object categories. The behavioural features comprise gaze duration, interaction count, revisit frequency, and head movement, which indicate user engagement within the augmented reality environment. The object category is represented as an integer and mapped into a continuous vector space via an embedding layer. This enables the model to learn dense semantic representations of object classes such as “Bee” or “Carousel.”

As illustrated in Fig. 2, these two input streams are concatenated and processed through a fully connected neural network of two hidden dense layers with ReLU activation functions, followed by a dense softmax output layer. Dropout layers are incorporated to mitigate overfitting and enhance generalization. The final layer of the model is a softmax classifier that outputs one of four memory states: Strong Recall, Weak Recall, Cognitive Overload, or Lack of Engagement. The detailed configuration of the model layers is presented in Table 1.

To enhance model performance, Bayesian Optimization is employed to fine-tune key hyperparameters, including learning rate, number of units in each dense layer, batch size, and early stopping patience. The model is trained using the Adam optimizer with categorical cross-entropy as the loss function. Early stopping based on validation loss ensures robust generalization.

This approach offers a lightweight yet semantically rich solution by leveraging category embeddings instead of visual feature extraction. It maintains the

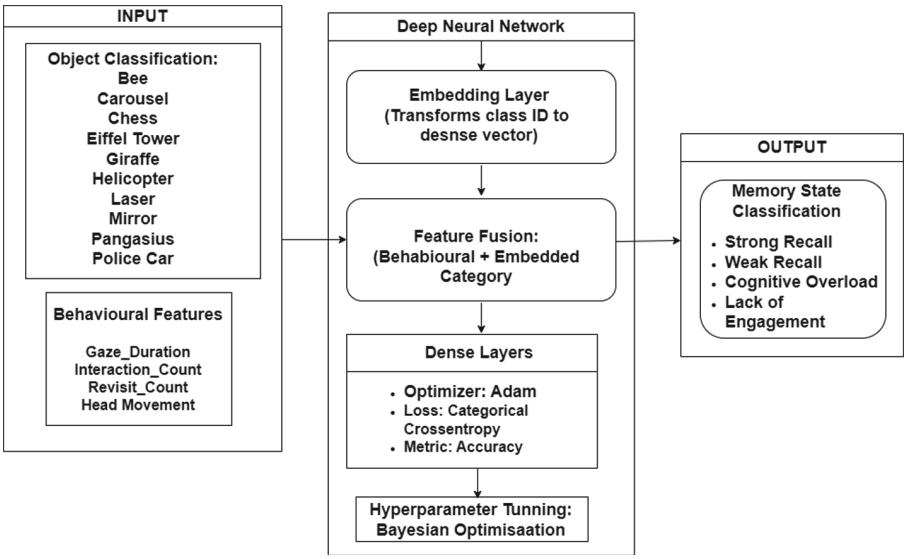

Fig. 2. An overview of the deep learning framework for memory state classification using behavioral features and embedded object categories. Outputs correspond to four memory states, with model parameters optimized via Bayesian optimization.

Table 1. Model architecture summary.

Layer (type)	Output Shape	Param #	Connected To
input_layer_3 (InputLayer)	(None, 1)	0	–
embedding_1 (Embedding)	(None, 1, 4)	40	input_layer_3[0][0]
input_layer_2 (InputLayer)	(None, 4)	0	–
flatten_1 (Flatten)	(None, 4)	0	embedding_1[0][0]
concatenate_1 (Concatenate)	(None, 8)	0	input_layer_2[0][0], flatten_1[0][0]
dense_3 (Dense)	(None, 20)	180	concatenate_1[0][0]
dropout_2 (Dropout)	(None, 20)	0	dense_3[0][0]
dense_4 (Dense)	(None, 30)	630	dropout_2[0][0]
dropout_3 (Dropout)	(None, 30)	0	dense_4[0][0]
dense_5 (Dense)	(None, 4)	124	dropout_3[0][0]

Table 2. Categorization of memory states by the AI model based on user interaction metrics.

Predicted Memory State	AI Interpretation (Based on User Interaction Metrics)
Strong Recall	High interaction counts and long gaze duration indicate deep engagement [7]. Frequent revisits reinforce memory encoding, and stable head movement reflects focused attention [12].
Weak Recall	Low interaction counts and short gaze duration suggest brief engagement [12]. Few revisits and stable head movement indicate passive involvement.
Cognitive Overload	Moderate interaction with high revisit counts and frequent gaze shifts implies cognitive strain [13]. Unstable head movement reflects difficulty processing multiple stimuli [18].
Lack of Engagement	Very low interaction, minimal revisits, short gaze duration, and unstable head movement suggest low attention and disengagement [12,18].

capacity to capture object identity while ensuring scalability and practicality for deployment in real-world augmented reality learning environments (Table 2).

4 Results and Discussions

The proposed deep neural network model was evaluated using the accuracy of training, validation, and loss metrics. As shown in Fig. 3, the model demonstrated stable convergence across training epochs. It achieved a final training and validation accuracy of 0.94 and 0.93, respectively, indicating strong predictive performance on the held-out validation data. The accuracy curves rapidly increased during the initial training epochs, followed by convergence beyond epoch 80. This trend suggests that the model effectively learned representations from the behavioural interaction features: gaze duration, interaction count, revisit frequency, and head movement alongside the embedded object categories. Correspondingly, both training and validation loss decreased steadily, stabilizing below 0.2, indicating efficient minimization of prediction error. In addition to classification accuracy and loss, the model achieved a mean absolute error (MAE) of 0.14 and a mean squared error (MSE) of 0.404 on the validation set. These low error values indicate that the predicted memory states closely align with the true labels. The results confirm the model's suitability for generalization and effectiveness in memory state classification using embedded object categories and behavioural interaction features. The observed learning behaviour supports the model's potential application in real-time augmented reality (AR)-based learning environments for personalized memory prediction.

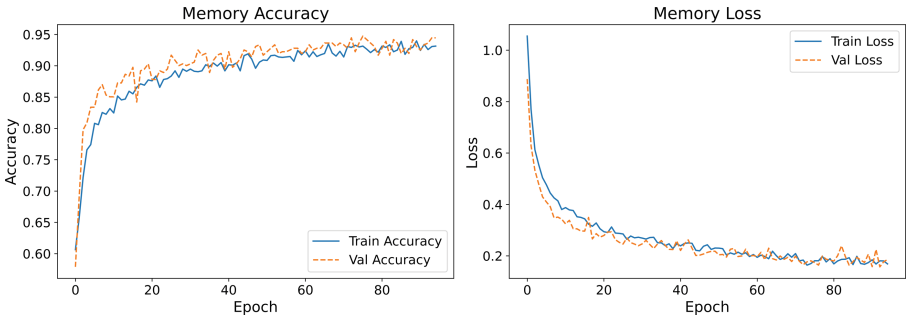

Fig. 3. Training and validation accuracy (left) and loss (right) curves of the deep neural network for memory state classification. The model shows consistent convergence across epochs, indicating effective learning and generalization.

Key interaction metrics: Gaze duration, interaction frequency, revisit count, and head movement stability were analysed for their influence on predicted retention scores (Fig. 4). The results show a strong correlation between engagement and memory retention, with higher scores linked to prolonged gaze, frequent interactions, and revisits. Head movement stability appeared most frequently, likely due to its continuous tracking of subtle attentional shifts. Additionally, gaze duration may influence head stability, as sustained visual focus tends to reduce head movement [12], highlighting the interplay of these features in the model's interpretation of cognitive engagement.

A detailed breakdown of the predicted and true memory states across different objects is presented in Fig. 5. The grouped bar chart reveals that Chess recorded the highest number of predictions and true instances of lack of engagement, followed by Police Car, Pangasius, and Mirror. At the same time, several objects, such as Bee, Laser, and Police Car, also exhibit a considerable number of strong recall cases across both predictions and true states. While this may initially appear contradictory, it reflects the model's instance-based classification, which evaluates each object interaction independently. These outcomes are informed by distinct behavioural features such as gaze duration, interaction frequency, revisit counts, and head movement stability, captured in real-time through the Microsoft HoloLens 2. Thus, depending on their unique engagement profiles during the interaction, the same object may elicit divergent participant memory state outcomes. For example, users who demonstrated sustained attention and multiple revisits were likely associated with strong recall, while others showing minimal gaze or interaction with the same object often aligned with a lack of engagement. The behavioural variability explains the coexistence of predicted and true memory state discrepancies for a single object. In some cases, memory states observed in the true states were not predicted, and vice versa, highlighting the model's sensitivity to subtle behavioural cues that may not always align with labeled outcomes. Additionally, objects like the Carousel and Police Car showed more frequent weak recall. Meanwhile, cognitive overload

remained relatively limited, occasionally appearing in objects such as the Giraffe, Eiffel Tower, and Helicopter. The results reinforce the model's ability to capture and differentiate memory outcomes based on users' heterogeneous behavioural interactions.

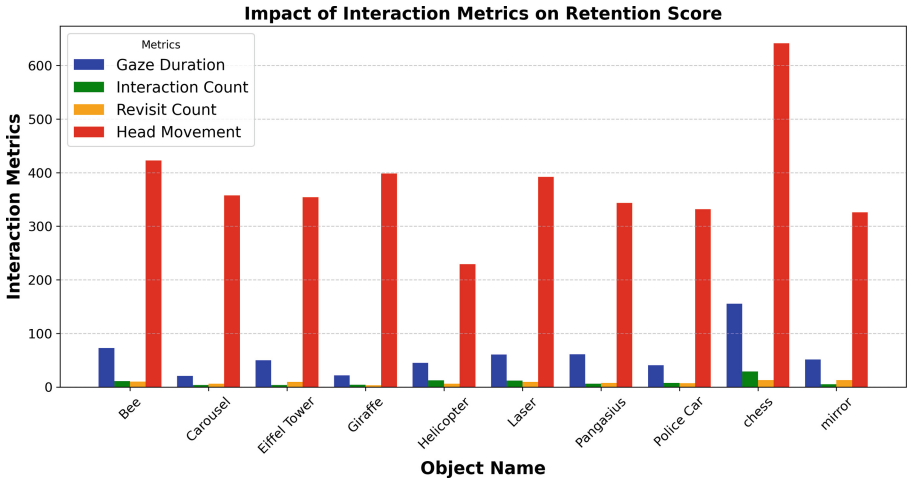

Fig. 4. Impact of interaction metrics: gaze duration, interaction count, revisit count, and head movement on memory retention for different objects.

4.1 Memory State Prediction and User Recall

To evaluate how closely the AI model's memory state predictions reflect actual human memory, we analyzed the predicted memory outcomes for objects that participants recalled after interacting with the AR environment. This comparison provides an empirical basis for assessing the model's cognitive alignment with user recall behaviour.

Figure 6 presents a grouped bar chart showing the AI-predicted memory states: Strong Recall, Weak Recall, Cognitive Overload, and Lack of Engagement for objects listed in the user feedback. Overlaid on the chart is a black line indicating the frequency with which users recalled each object. In Fig. 6, Eiffel Tower was the most frequently recalled object, followed by Pangasius and Laser. The AI model also predicted these objects with a high number of Strong Recall and lower Weak Recall classifications, demonstrating a precise alignment between predicted memory strength and participant recall. In contrast, Giraffe, Helicopter, and Mirror had the lowest user recall frequencies. The model accurately captured this in the Giraffe case, which received no Strong Recall predictions, only Weak Recall, Lack of Engagement, and Cognitive Overload classifications. This reflects a strong match between the AI's prediction and actual

human memory performance, suggesting that the model could infer the object's low memorability based on user interaction features. Although user recall was similarly low for Helicopter and Mirror, the model still predicted some level of Strong Recall. This indicates a partial misalignment and suggests that while the model may have detected surface-level engagement behaviors (e.g., prolonged viewing or revisits), these interactions alone may not always lead to successful long-term recall [12].

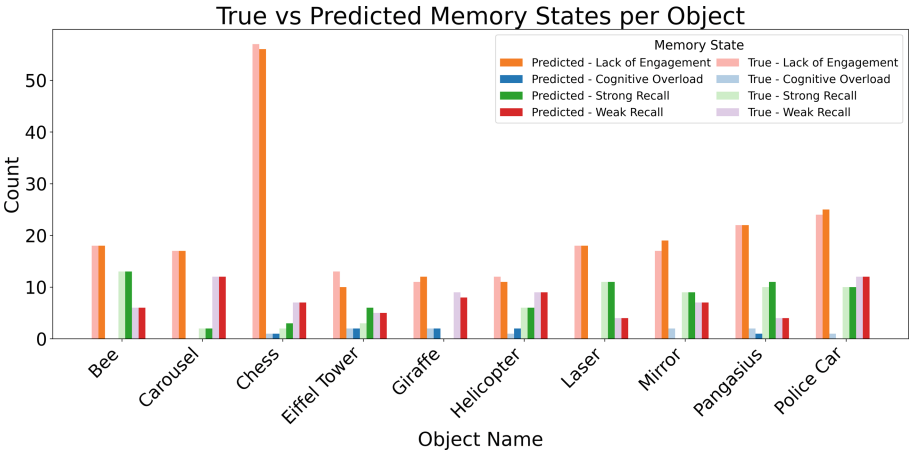

Fig. 5. Grouped bar chart showing AI-predicted and true memory states across objects based on interaction metrics. The distribution reflects object-specific engagement patterns captured during AR experiences.

Our findings align with research by Mynick et al. [22], which suggests that memory is predictive in perceptual judgments, particularly in immersive environments. Their study found that individuals use memory-based expectations to anticipate visual scenes, enhancing perception and recall efficiency. This supports our observation that users also frequently recalled objects with high AI-predicted retention scores, reinforcing that memory-driven expectations influence engagement and recall patterns.

Similarly, research on spatial memory in augmented reality (AR) environments by Maidenbaum et al. [23] further strengthens this relationship. Their study demonstrated that AR-based spatial memory tasks improve recall accuracy and engagement compared to traditional memory tests, emphasizing the role of interactive and immersive experiences. These findings are consistent with our results, where frequently interacted objects, such as the Eiffel Tower, Laser, and Pangasius, were not only the most accurately recalled by users but also closely aligned with the AI model's predictions.

Furthermore, both studies suggest that familiarity and prior exposure to objects enhance recall accuracy. Mynick et al. [22] highlight that learned envi-

ronments contribute to faster and more precise recall. This aligns with our observation that AI-predicted memory retention closely mirrored user-reported recall patterns. Maidenbaum et al. [23] extend this idea by demonstrating that spatial engagement and movement enhance memory encoding. This supports our finding that increased interaction frequency and prolonged gaze duration correlate with stronger recall probabilities.

These results validate the AI model's ability to predict memory retention by replicating known cognitive processes. The observed alignment between user feedback and AI predictions suggests that AI-driven memory prediction models can effectively simulate real-world memory retention processes, particularly in AR-based learning and interactive environments.

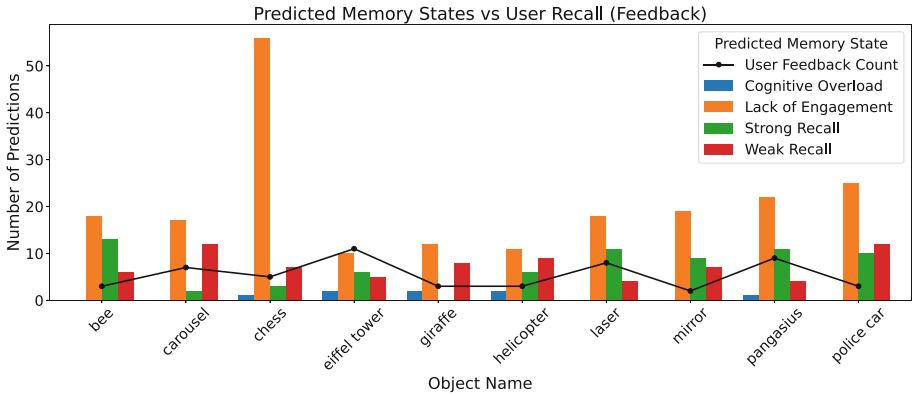

Fig. 6. Comparison of AI-predicted memory states and actual user recall frequencies for recalled objects. The bars represent the predicted memory classification per object, while the black line indicates user recall frequency based on post-interaction feedback.

4.2 Statistical Analysis

We conducted repeated-measures ANOVAs with Tukey HSD post hoc tests at the 5% significance level. Normality was confirmed via Q-Q plots (Fig. 7), validating the ANOVA assumptions by showing that residuals approximated a normal distribution. A one-way ANOVA was conducted to examine differences in interaction features across the ten object categories. The dataset consisted of 1,804 object-level interaction samples (N = 1794).

The results indicated statistically significant differences among objects for all four dependent variables. Interaction Count showed a significant effect, $F(9, N) = 54.48, p < 0.001$. Similarly, significant effects were observed for Revisit Count, $F(9, N) = 15.74, p < 0.001$, Head Movement, $F(9, N) = 36.60, p < 0.001$, and Gaze Duration, $F(9, N) = 65.71, p < 0.001$. Given these significant results, a post-hoc Tukey's Honest Significant Difference (HSD) test was performed to

determine which objects differed significantly. The analysis included ten distinct objects: Bee, Chess, Pangasius, Mirror, Laser, Eiffel Tower, Helicopter, Giraffe, Carousel, and Police Car.

The Tukey HSD test revealed multiple significant pairwise differences across all dependent variables. Objects with high interaction counts demonstrate significantly different engagement levels, particularly between Chess and Bee ($p < 0.001$). Revisit Count was significantly higher for Mirror and Chess compared to other objects, indicating strong user retention. This finding aligns with the visualization presented in Fig. 4, which illustrates the impact of interaction metrics on retention scores, highlighting the increased revisit count for Chess and Mirror. Head movement significantly differed between Pangasius and Helicopter, suggesting varying levels of physical engagement. Gaze Duration showed marked differences, with Bee and Chess receiving more visual attention than other objects.

These findings suggest that object type significantly influences user engagement, memory retention, and interaction behaviour. The results show that specific objects elicit distinct cognitive and physical responses, supporting the hypothesis that object features impact user interaction patterns.

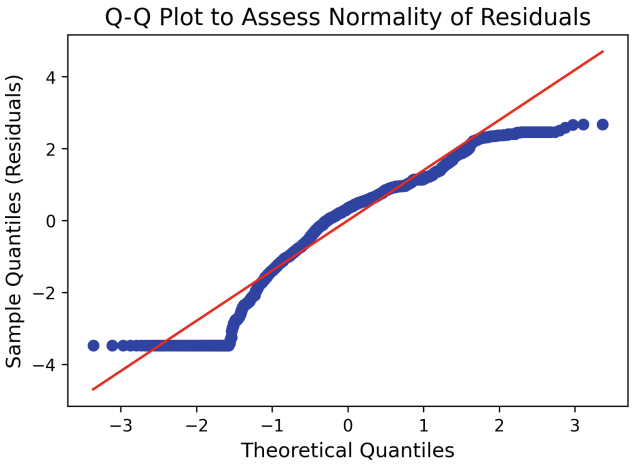

Fig. 7. Q-Q Plot to Assess Normality of Residuals. The points align closely with the theoretical quantiles, indicating approximate normality.

5 Conclusion

This study introduced an AI-driven framework for predicting memory retention in augmented reality (AR) environments using behavioural interaction data captured via Microsoft HoloLens 2 sensors. The proposed model estimated the likelihood of object recall by analyzing key interaction metrics such as gaze duration, interaction frequency, revisit counts, and head movement stability. The

results revealed a strong correlation between engagement and memory retention, aligning with cognitive theories and validating the effectiveness of AI-driven approaches in modeling attention and recall. Statistical analysis, supported by ANOVA and Tukey HSD tests, confirmed significant differences in user interaction patterns across objects, highlighting the role of attentional engagement in memory encoding.

These findings demonstrate the potential of AI-enhanced AR learning systems to improve educational and training outcomes and provide a strong foundation for future work to explore comparative modeling baselines and expand predictive robustness. The results align with prior research on perceptual judgments and spatial memory, supporting that memory-driven expectations influence engagement behaviour in AR. Additionally, the framework offers a more accessible, contact-free alternative for assessing memory processes, bridging the gap between machine learning and human cognition.

This work has important implications for domains such as education, medical training, and workforce development, where optimizing learning efficiency is critical. Future research may build on this by integrating cognitive or physiological signals to complement behavioural data and deploying the framework in real-world settings to evaluate its practical impact. These steps will further validate its potential as a personalized and adaptive learning tool.

Acknowledgement. This publication was supported by the Department of Computer Graphics, Vision and Digital Systems, under statute research project (2025), Silesian University of Technology (Gliwice, Poland).

Conflict of Interest. The authors declare no conflict of interest.

References

1. Nwobodo, O.J., Kuaban, G.S., Kukuczka, T., Wereszczyński, K., Cyran, K.: Analysis of marker and slam-based tracking for advanced augmented reality (AR)-based flight simulation. In: International Conference on Computational Science, pp. 208–222, Springer (2024)
2. Zhang, L., Luczak, T., Smith, E., Burch, R.F., et al.: Using microsoft hololens to improve memory recall in anatomy and physiology: a pilot study to examine the efficacy of using augmented reality in education. J. Educ. Technol. Dev. Exchange (JETDE) **12**(1), 2 (2019)
3. Gargrish, S., Kaur, D.P., Mantri, A., Singh, G., Sharma, B.: Measuring effectiveness of augmented reality-based geometry learning assistant on memory retention abilities of the students in 3d geometry. Comput. Appl. Eng. Educ. **29**(6), 1811–1824 (2021)
4. Makhataeva, Z., Akhmetov, T., Varol, H.A.: Augmented-reality-based human memory enhancement using artificial intelligence. IEEE Trans. Hum.-Mach. Syst. **53**(6), 1048–1060 (2023)
5. Sahu, C.K., Young, C., Rai, R.: Artificial intelligence (AI) in augmented reality (AR)-assisted manufacturing applications: a review. Int. J. Prod. Res. **59**(16), 4903–4959 (2021)

6. Eysenck, M.W., Keane, M.T.: Cognitive Psychology: A Student's Handbook. Psychology Press (2020)
7. Unsworth, N., Miller, A.L.: An examination of individual differences in levels of processing, Memory, pp. 1–12 (2024)
8. Li, Y.F., Lye, S.W., Rajamanickam, Y.: Assessing attentive monitoring levels in dynamic environments through visual neuro-assisted approach, Heliyon, vol. 8, no. 3 (2022)
9. Nolte, D., et al.: Combining EEG and eye-tracking in virtual reality: Obtaining fixation-onset event-related potentials and event-related spectral perturbations. Attent. Percept. Psychophysics 1–21 (2024)
10. Kalafatovich, J., Lee, M., Lee, S.-W.: Prediction of memory retrieval performance using ear-eeg signals. In: 2020 42nd Annual International Conference of the IEEE Engineering in Medicine & Biology Society (EMBC), pp. 3363–3366. IEEE (2020)
11. Gorin, H., Patel, J., Qiu, Q., Merians, A., Adamovich, S., Fluet, G.: A review of the use of gaze and pupil metrics to assess mental workload in gamified and simulated sensorimotor tasks. Sensors **24**(6), 1759 (2024)
12. Binetti, N., Harrison, C., Coutrot, A., Johnston, A., Mareschal, I.: Pupil dilation as an index of preferred mutual gaze duration. Royal Soc. Open Sci. **3**(7), 160086 (2016)
13. Kolnes, M., Uusberg, A., Nieuwenhuis, S.: Broadening of attention dilates the pupil. Attent. Percept. Psychophys. **86**(1), 146–158 (2024)
14. Binias, B., Myszor, D., Binias, S., Cyran, K.A.: Analysis of relation between brainwave activity and reaction time of short-haul pilots based on EEG data. Sensors **23**(14), 6470 (2023)
15. Binias, B., Myszor, D., Niezabitowski, M., Cyran, K.A.: Evaluation of alertness and mental fatigue among participants of simulated flight sessions. In: 2016 17th International Carpathian Control Conference (ICCC), pp. 76–81. IEEE (2016)
16. Bybee, C., Belsten, A., Sommer, F.T.: Cross-frequency coupling increases memory capacity in oscillatory neural networks, *arXiv preprint*arXiv:2204.07163 (2022). arXiv:2204.07163
17. Wynn, S.C., Townsend, C.D., Nyhus, E.: The role of theta and gamma oscillations in item memory, source memory, and memory confidence. Psychophysiology e14602 (2024)
18. Suzuki, Y., Wild, F., Scanlon, E.: Measuring cognitive load in augmented reality with physiological methods: a systematic review. J. Comput. Assist. Learn. **40**(2), 375–393 (2024)
19. Vortmann, L.-M., Schwenke, L., Putze, F.: Using brain activity patterns to differentiate real and virtual attended targets during augmented reality scenarios. Information **12**(6), 226 (2021)
20. Gargrish, S., Mantri, A., Kaur, D.P.: Evaluation of memory retention among students using augmented reality based geometry learning assistant. Educ. Inf. Technol. **27**(9), 12891–12912 (2022)
21. Shen, J., Dudley, J.J., Kristensson, P.O.: Encode-store-retrieve: Augmenting human memory through language-encoded egocentric perception. In: 2024 IEEE International Symposium on Mixed and Augmented Reality (ISMAR), pp. 923–931. IEEE (2024)
22. Mynick, A., Steel, A., Jayaraman, A., Botch, T.L., Burrows, A., Robertson, C.E.: Memory-based predictions prime perceptual judgments across head turns in immersive, real-world scenes. Curr. Biol. **35**(1), 121–130 (2025)
23. Maidenbaum, S., Patel, A., Garlin, I., Jacobs, J.: Studying spatial memory in augmented and virtual reality, bioRxiv, p. 777946 (2019)

Solving Problems with Uncertainty

Unified and Diverse Coalition Formation in Dispersed Data Classification – A Conflict Analysis Approach with Weighted Decision Trees

Małgorzata Przybyła-Kasperek(✉) and Jakub Sacewicz

Institute of Computer Science, University of Silesia in Katowice, Będzińska 39, 41-200 Sosnowiec, Poland
{malgorzata.przybyla-kasperek,jakub.sacewicz}@us.edu.pl

Abstract. The paper delves into the challenge of classification using dispersed data gathered from independent sources. The examined approach involves local models as ensembles of decision trees or random forests constructed based on local data. In the proposed model, a conflict analysis is used to identify the coalitions of local models. Two variants of forming coalitions were checked – unified and diverse – and two different strategies for generating final decisions were explored, allowing one or two of the strongest coalitions to make decisions. The diverse coalition approach is a wholly new and innovative strategy. The methods were tested and compared with corresponding accuracy-based weighted variants. The proposed approach improves classification performance, with weighted variants outperforming unweighted ones in balanced accuracy. Diverse model coalitions are especially effective for challenging and heterogeneous datasets.

Keywords: Dispersed data · Conflict analysis · Decision trees · Random forests · Ensembles of classifiers · Weighted Method

1 Introduction

In today's digitalized world, adapting systems to local markets, such as healthcare, banking, and mobile applications, has led to the proliferation of dispersed data. Unlike centralized data systems, where information is gathered in a single repository, dispersed data exists in multiple and diverse environments—from cloud servers to users' private devices—autonomously gathered without any structural unification. This trend, driven by factors such as law, data security, and the resulting aleatoric uncertainty due to variability and inconsistency across sources, presents both opportunities and challenges that machine learning methods should address, underscoring the growing importance of this research topic.

The topic of dispersed data is most frequently discussed in the distributed learning paradigms [3,19], which insists on training a group of models separately.

M. Paszynski et al. (Eds.): ICCS 2025 Workshops, LNCS 15912, pp. 109–124, 2025.
https://doi.org/10.1007/978-3-031-97573-8_8

Then, various fusion methods, including hierarchical [10] and parallel [2,15] variants, use the local predictions in final decision-making. However, the process of making decisions based on ensemble outputs introduces a degree of epistemic uncertainty, especially when the models exhibit conflicting predictions due to insufficient or unrepresentative data in local tables. This uncertainty necessitates robust frameworks to reconcile differences and ensure reliable classification outcomes. The focus is on the diversity among base classifiers [9,11]. The effectiveness of the global model depends on the method applied to those local classifiers [6,7]. Mostly, the dependencies between local models are not considered while generating the final prediction. However, that information, in many cases, is crucial and plays a significant role in improving classification quality. Those relations should be taken into account using the selected fusion method. In distributed learning, cooperation, and conflict recognition are rarely applied. Early Artificial Intelligence (AI) conflict studies focused on decision support systems, exploring disputes, identifying key issues, and forming potential coalitions. Various tools have been introduced to analyze conflicts and propose solutions [5]. Nowadays, where there are many multi-agent systems, we can also check their dependencies. Examining them manually, especially when many are dynamic and complex, may be ineffective, burdensome, and unscalable. In this paper, the Pawlak conflict model [12,13] is considered. The simple model based on rough set theory [14] also gives great insight and understanding of any conflict. The theoretical foundation of rough set theory provides a tool for addressing uncertainty in classification. Rough set theory facilitates the analysis of imprecise or incomplete information by partitioning data into lower and upper approximations, effectively managing uncertainty and conflict in decision-making. The model has been further investigated by many researchers [16,17,22], as with some of its developments – the three-way decision theory proposed by Yao [21], with further study by other researchers [20].

This study also uses Pawlak's model to create a dynamic system in which coalitions of local classifiers are formed. Decision trees and random forests are used as local models, two different variants of creating coalitions are analyzed, and two methods of choosing coalitions (unified and diverse) are used. Additionally, all variants are compared with their weighted variants, where the weights are assigned to each local model based on its accuracy. To the best of our knowledge, the conjunction of forming coalitions with Pawlak's model with weighted models has never been considered before and compared. The paper shows that, mostly, variants with weights perform better than their corresponding variants. Also, which of the variants of generating and selecting coalitions performs better depends on the chosen data set.

The paper's contribution is as follows. Introduction of hierarchical decision tree frameworks for dispersed data. Integration of Pawlak's conflict model to dynamically form coalitions of local models. Exploration of two types of coalitions: unified and diverse. Investigation of two decision strategies: using one or two strongest coalitions. Analysis of the performance of weighted vs. unweighted coalitions. The paper is structured as follows: Sect. 2 presents the theoretical

foundations of the analysis models. Section 3 introduces the methodology, compares results, and discusses findings. The conclusion provides a summary.

2 Methods

Dispersed data is characterized by inconsistencies in structure among different local data sets. One possible approach to address this issue, which also allows data protection, is to deal with each data set in isolation. This is done by generating local models for each local table. In this paper, the ensembles of decision trees or random forests are built. In the following step, we utilize the conflict analysis model to establish coalitions. The process is done for each object dynamically, resulting in different sets of coalitions. Eventually, based on generated coalitions, selected models pass a vote to make the final decision. More formally, we have access to local decision tables represented as $D_i = (U_i, A_i, d)$ for $i \in 1, \ldots, n$. In this context, U_i represents the universe, a set of objects; A_i is a set of conditional attributes describing features of the objects; and d denotes the decision attribute, which represents labels. Although some elements may be shared, the objects or attributes may vary. So, the experimental part includes two versions of dispersed data (sets of local tables) – those in which attributes are dispersed and those in which objects are dispersed.

There are various widely known approaches to building local models. This study focuses on a tree-based approach, and we use the decision tree and the random forest models. The models are created using Python with classes from the Skit-learn library (DecisionTreeClassifier or RandomForestClassifier). In future works, we will test other models, as well as the combination of different models, to see if it would result in an improvement in classification quality. For the decision tree, no parameters are specified. For random forest, four different values are selected for the number of estimators: 10, 20, 50, 100. Each local model is trained on a separate data set.

Such ensembles of trees generated based on all local tables make a prediction for the test object $\hat{x}$. The prediction is represented as a vector $[\mu_{i,1}(\hat{x}), \ldots, \mu_{i,c}(\hat{x})]$ with dimension c equal to the number of decision classes. The value $\mu_{i,j}(\hat{x})$ is the number of votes cast for decision class j by the random trees in the ensemble. In the paper, we use two approaches – weighted and unweighted methods. During data preprocessing, for weighted approaches, the weights for each local model were calculated with a validation set created randomly with a predefined seed from the test set in a stratified way. In the literature, in most cases, the final decision is made with simple or weighted voting [18] or another fusion method [6]. The novelty of this work is using prediction vectors in conjunction with the conflict analysis method. This method is used to find coalitions that influence the final decision. Two types of local models' coalitions are considered in this study: coalitions of local models with similar opinions and coalitions of local models with diverse opinions are considered. Both approaches are relevant and based on different justifications. The first approach seeks consensus opinions, assuming that the majority of local models are

accurate and make correct decisions. The second emphasizes diversity, drawing on the ensemble of classifiers principle, which suggests that varied local models enhance classification quality. For the task of creating those coalitions, Pawlak's conflict model [12,13] is applied.

In Pawlak's conflict analysis model, information about the conflict situation is stored in an information system $S = (LM, V)$, where LM is a set of local models, and V is a set of decision attribute values. Function $v : LM \rightarrow \{-1, 0, 1\}$ for each $v \in V$ and $i \in LM$ is defined

$$v(i) = \begin{cases} 1 & \text{if the coordinate } \mu_{i,v}(\hat{x}) \text{ for decision } v \text{ in the prediction vector of} \\ & \text{model } i \text{ has the maximum value of all coordinates in this vector.} \\ 0 & \text{if the coordinate } \mu_{i,v}(\hat{x}) \text{ for decision } v \text{ in the prediction vector of} \\ & \text{model } i \text{ is this vector's second highest of all coordinates.} \\ -1 & \text{in other cases} \end{cases} \tag{1}$$

That is a way of storing opinions of local models on the test object. For each model, the decision with the most significant support is assigned the value 1, which is interpreted as supporting the decision by the model. The next most supported decision is assigned the value 0, which means the model is neutral to this decision. We assign the value -1 for all other decisions, which means the model is against them. A conflict function is applied in the next step of the Pawlak conflict analysis model. The conflict function $\rho : LM \times LM \rightarrow [0, 1]$ is defined as follows:

$$\rho(i, j) = \frac{card\{v \in V : v(i) \neq v(j)\}}{card\{V\}}, \tag{2}$$

where $card\{V\}$ is the cardinality of the set of decision classes and $i, j \in LM$.

For unified coalitions, set $X \subseteq LM$ is a coalition of local models if for every $i, j \in X$ we have $\rho(i, j) < 0.5$. The coalition will include those local models for which the opinion is consistent in more than half of the decision classes. The conditions are opposite in diverse coalitions; they include local models inconsistent with more than half of the decision classes. Coalitions do not have to be disjoint sets. One local model can belong to many coalitions simultaneously, reflecting real arrangements in everyday life. Algorithm 1 presents a pseudo-code for determining coalitions.

Once the coalitions are generated, the next step is to make a final decision using them. This work explores four different approaches combined with both ways of creating coalitions described above.

The first approach assumes using the **two strongest coalitions** (in terms of the number of models in the coalition). The chosen coalitions are the ones with the maximum number of members. In situations where there are coalitions with the size of the second strongest coalition, those coalitions are also considered. Then, the prediction vectors of all chosen models are added, and a single prediction vector is formed. If some models are part of many coalitions, their vectors are included every time they occur. Finally, the decision with the biggest score is made – the decision with the largest value of the coefficient of the joint

Algorithm 1: Create Coalitions

```
Data: S = (LM, V)
Result: Coalition_set
1  begin
2      Coalition_set ← empty list;                    // Initialize an empty list
3      Boolean ← TRUE;
4      foreach X ⊆ LM do
5          foreach i, j ∈ X do
6              if ρ(i, j) >= 0.5 then
                   // for unified coalitions or ρ(i, j) <= 0.5 for diverse coalitions
7                  Boolean = FALSE
8          if Boolean = TRUE then
9              Coalition_set ← X
10 return Coalition_set
```

prediction vector. The second approach is analogous to the previous one, except that we choose only **one most strongest coalition**, which will decide.

Both **weighted** approaches work analogously to unweighted ones. Besides that, each local model's prediction vector is multiplied by the weight, equal to the model's accuracy, estimated by evaluating the model using the validation set. Before testing the global model, the test set is stratified into test and validation sets with proportions of 0.5 to 0.5.

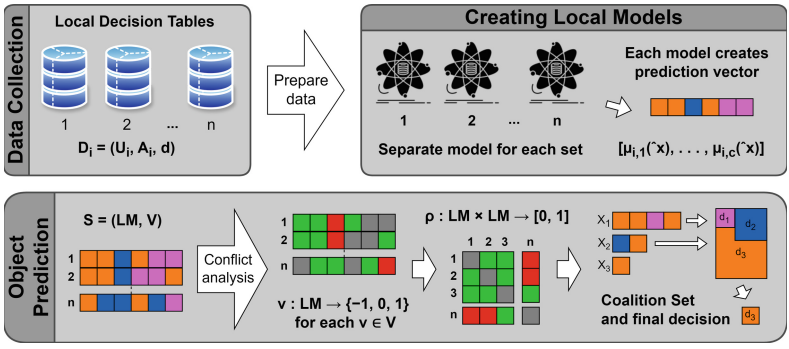

Fig. 1. Model generation stages.

Figure 1 shows the proposed hierarchical framework with conflict analysis for ensembles of local models (decision trees of random forests), presenting stages discussed above. At the beginning, the dispersed data are given. For each local table, we build a separate predictive model. During the classification stage, we retrieve the prediction vector from every local model. Those vectors are next

used to create an information system representing the conflict situation. Then, the coalitions are formed, and depending on the method, one or some of them are selected to make the final decision. The last step is to calculate the score for each decision class and choose the one with the highest score.

3 Data Sets and Experimental Results

The study evaluated approaches using three datasets from the UC Irvine Machine Learning Repository [1,8,23] and one empirical dataset [4]. The Avian Influenza dataset tracks global human infections from 12 countries, organized into four tables by region (e.g., Egypt, Vietnam, Indonesia) with region-specific attributes. Its structure supports predictive modeling and epidemiological research to understand avian influenza's impact on health. The Car Evaluation dataset includes six categorical features (e.g., price, maintenance, doors, capacity, luggage size, safety) and classifies cars into four categories, making it suitable for machine learning evaluation. The Lymphography dataset classifies lymphatic diseases using features like node appearance and histological findings to aid medical diagnosis. The Vehicle Silhouettes dataset distinguishes vehicle types based on shape features from silhouettes. Dataset characteristics are summarized in Table 1.

Table 1. Data set characteristics

Data set	# The training set	# The test set	# Conditional attributes	Attributes type	# Decision classes	Source
Avian influenza	205	89	5	Categorical and Integer	4	[4]
Car evaluation	1210	518	6	Categorical	4	[1]
Lymphography	104	44	18	Categorical	4	[23]
Vehicle Silhouettes	592	254	18	Integer	4	[8]

The research investigates two different methodologies concerning data dispersion with respect to both attribute and object dispersion. All datasets within the UCI repository were consolidated into one table, which was subsequently dispersed across various local tables (3, 5, 7, 9, and 11 local tables for each dataset). For the Lymphography and the Vehicle Silhouettes, attributes were dispersed randomly across the tables. Efforts were made to balance the number of attributes allocated to each table. The same objects are present in all tables, but their identifiers were omitted to simulate a real-world scenario where recognizing identical objects across tables is not possible. The Car dataset was dispersed relative to the objects. This means that the objects were divided among the tables in a stratified and random manner, and all attributes were included in each table. The Avian dataset was collected in 12 countries and divided into four local tables based on what country the object comes from. Local tables include countries like Egypt, Vietnam, Indonesia, and others were created. Each table contains conditional attributes and objects from specific countries.

The evaluation insists on repeating a test 10 times to check the stability of all methods. Despite the random behavior of some approaches, to make the results reproducible, the set of 10 seeds was randomly chosen, and each test was conducted with its assigned seed, starting from learning local models on local tables, generating validation sets, and ending on generating global decisions by all approaches.

The assessment of classification quality relied on the test set with various accuracy measures: Classification Accuracy (Acc), Accuracy's standard deviation (Acc SD), Recall, Precision (Prec.), balanced accuracy (BAcc), balanced accuracy standard deviation (BAcc SD), and F1 measure (F1). This study uses two methods to calculate the F1 measure: weighted and macro.

The results are summarized in Figs. 2, 3, 4 and 5, presenting averaged metric values from all 10 achieved metrics with standard deviation for accuracy and balanced accuracy. Each dataset, characterized by varying degrees of dispersion, is evaluated using three approaches: without coalitions, with coalitions representing agents' agreement, and with coalitions representing agents' disagreement. The following notations are used:

- Probability Sum; normal – Local classifiers (random forest or decision tree) independently predict; their prediction vectors are summed, and the decision with the highest value is selected;
- Probability Sum; weighted – Similar to normal, but classifiers are weighted by accuracy estimated on a validation set (split from the test set);
- Unified groups; one strongest – Coalitions are formed based on prediction vectors using classical Pawlak's approach. The strongest coalition's summed vectors determine the decision;
- Unified groups; two strongest – Extends the above by considering the two strongest coalitions;
- Unified groups; weighted one strongest/weighted two strongest – Combines the above with accuracy-based weighting of coalition vectors;
- Diverse groups; one strongest/two strongest/weighted one strongest/weighted two strongest – Forms coalitions of local models with conflicting predictions (vector distance greater than 0.5). Variants include one/two strongest or weighted coalitions.

Additionally, various numbers of estimators were tested for the random forest classifier, specifically 10, 20, 50, and 100. The tables present the best result achieved, along with the corresponding number of estimators that produced this outcome. For each dataset, the table indicates the best result obtained.

Based on the results in Figs. 2, 3, 4 and 5, we can draw the following conclusions. The Avian Influenza dataset showed its highest performance using the random forest (RF) classifier with the 'Diverse groups' approach. This result suggests that conflicting classifiers through coalition formation improve predictive accuracy. We believe that this is due to the variety of approaches taken, as differing perspectives significantly impact quality. The ability to aggregate diverse predictions likely mitigates inconsistencies caused by object dispersion across

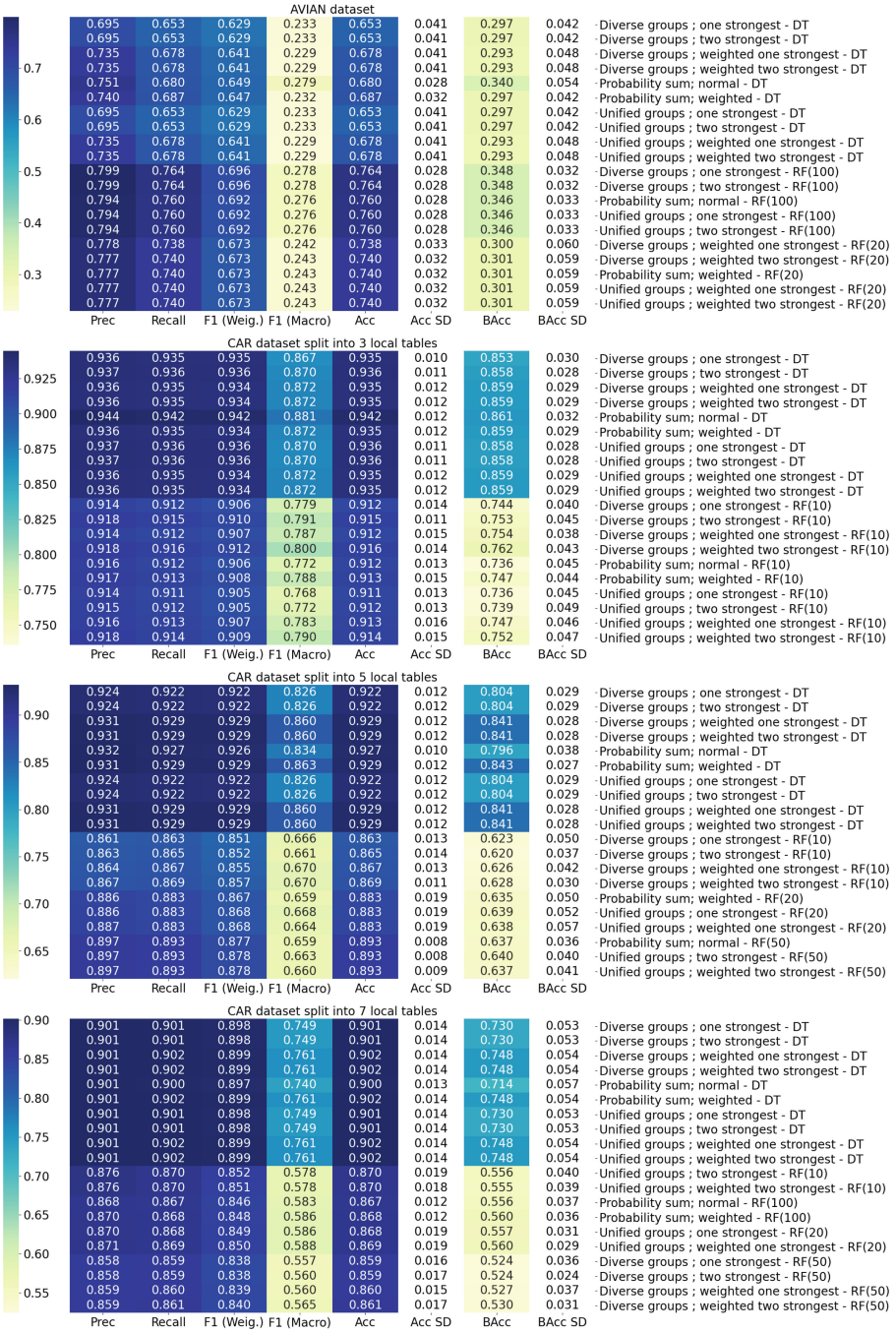

Fig. 2. Results of precision (Prec.), recall, F-measure (F-m.), balanced accuracy (*bacc*) and classification accuracy (*acc*) for the considered approaches Part 1. RF is the abbreviation Random Forest and DT for Decision Tree.

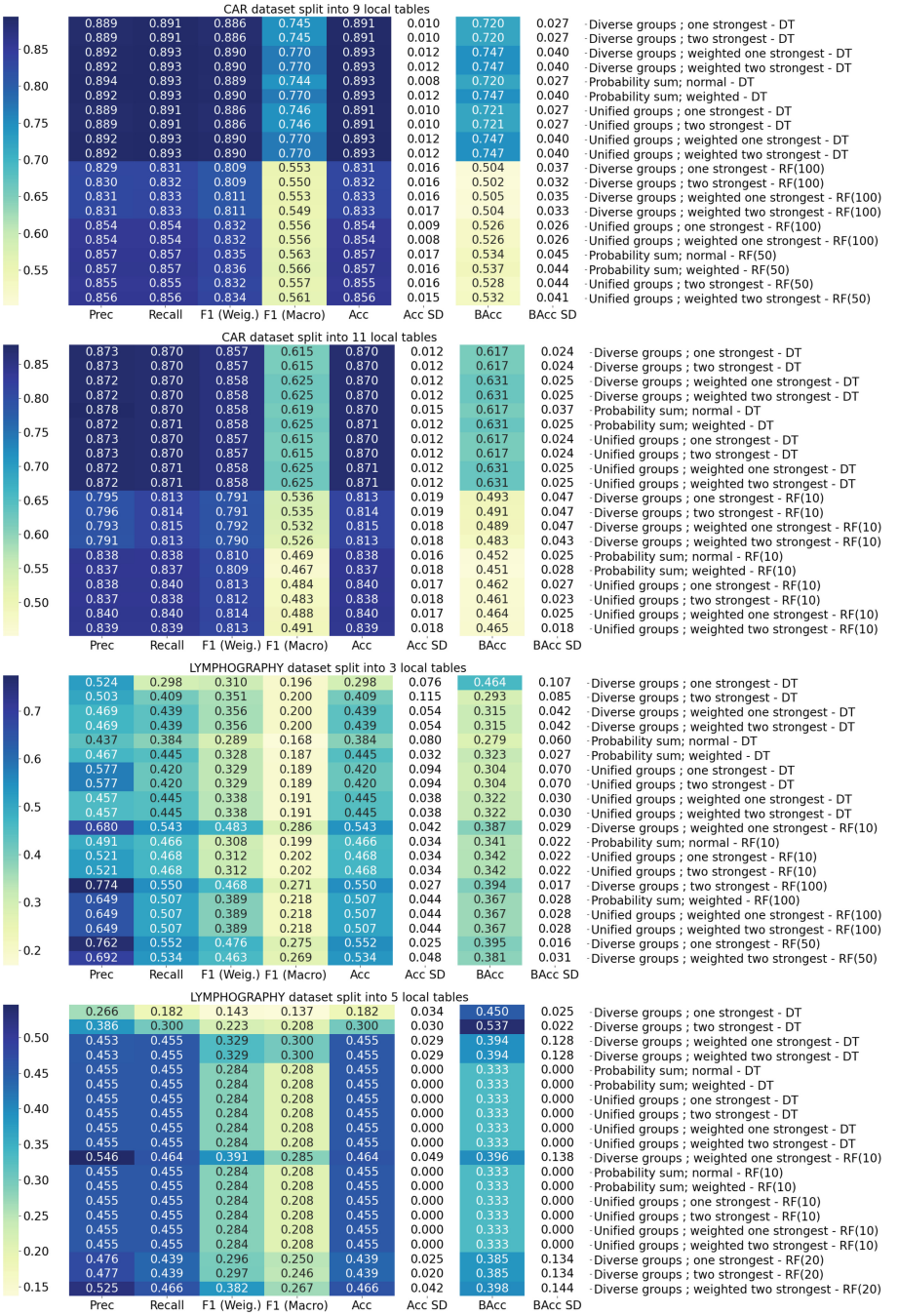

Fig. 3. Results of precision (Prec.), recall, F-measure (F-m.), balanced accuracy (*bacc*) and classification accuracy (*acc*) for the considered approaches Part 2. RF is the abbreviation Random Forest and DT for Decision Tree.

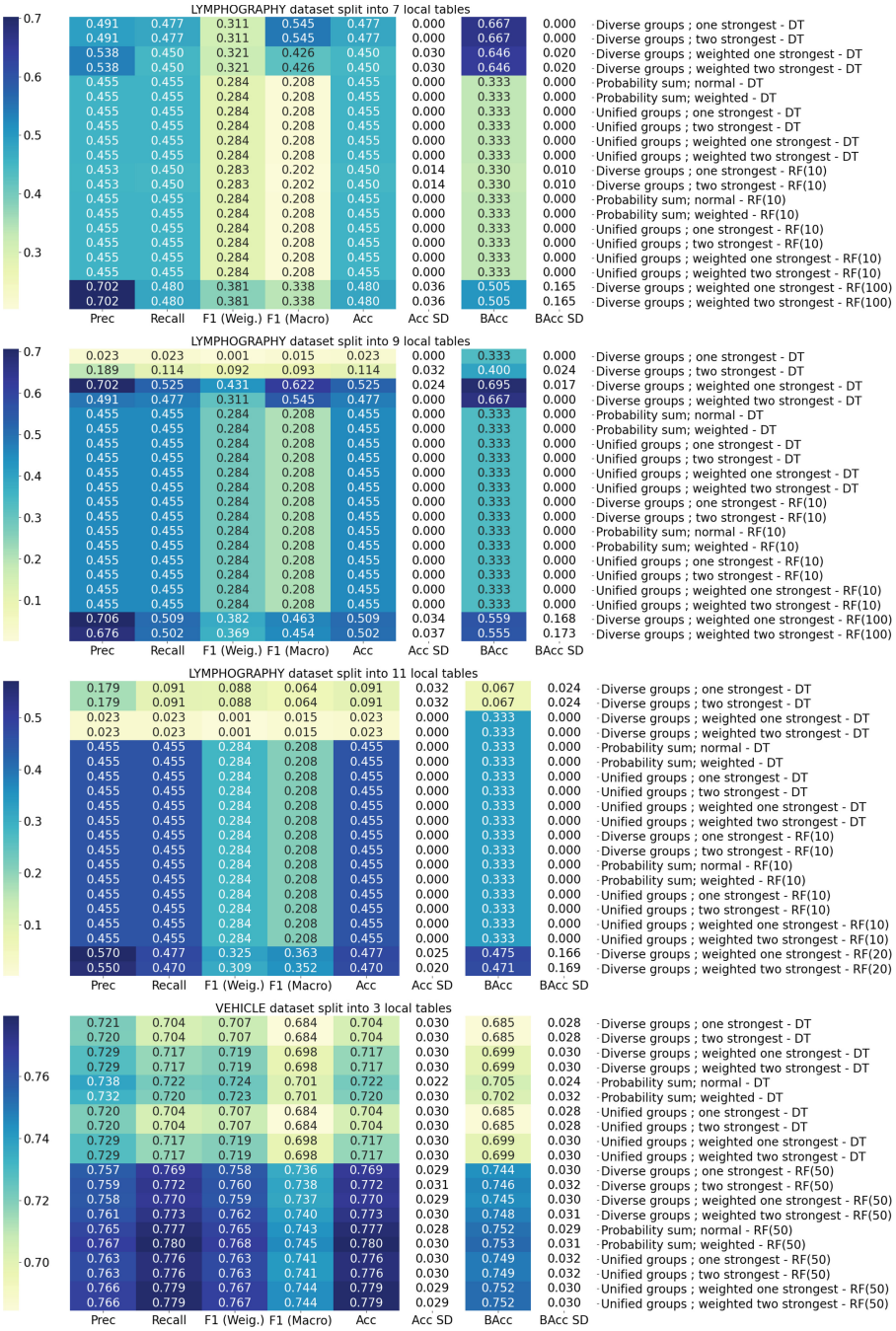

Fig. 4. Results of precision (Prec.), recall, F-measure (F-m.), balanced accuracy (*bacc*) and classification accuracy (*acc*) for the considered approaches Part 3. RF is the abbreviation Random Forest and DT for Decision Tree.

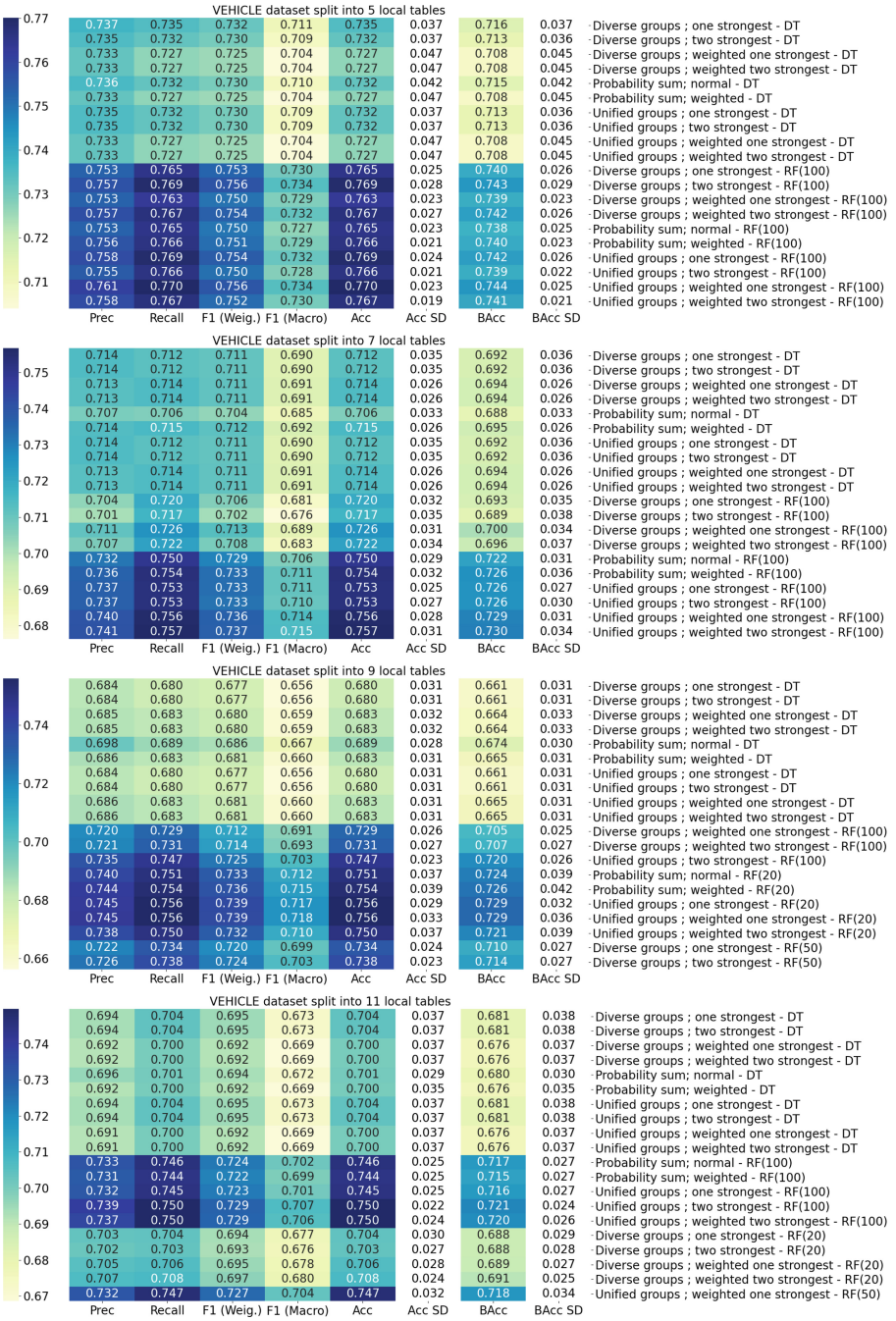

Fig. 5. Results of precision (Prec.), recall, F-measure (F-m.), balanced accuracy (*bacc*) and classification accuracy (*acc*) for the considered approaches Part 4. RF is the abbreviation Random Forest and DT for Decision Tree.

multiple tables (countries). The decision tree (DT) classifier using the 'Unified groups' or 'Diverse groups' approach consistently gives the best results for most versions of dispersion. The Car Evaluation dataset has categorical features, making it well-suited for decision trees. Interestingly, for the Car dataset, the 'Probability Sum' approach, without coalitions, also often produces good results (for dispersion 3LT, 7LT, 9LT). It is also worth noting that, for this dataset, the use of weights does not lead to any improvements. The Lymphography dataset, characterized by complex medical features, performed best when using weighted random forests in the 'Diverse groups' configuration. This suggests that classifier weighting based on validation set accuracy compensates for prediction conflicts. However, results were generally lower due to the dataset's challenging nature. Given that decision trees sometimes obtain the highest prediction quality (especially for 9LT), it is important to emphasize that accurate weighting and conflict resolution are crucial for this dataset. For the Vehicle Silhouettes dataset, the best-performing approach was random forests with weighted and sometimes unweighted 'Unified groups'.

In general, random forests consistently outperformed decision trees in datasets with numerical or complex features, such as Vehicle Silhouettes and Lymphography. In contrast, decision trees excelled in the Car Evaluation dataset due to its well-defined categorical attributes. It could also be a result of a number of features selected to build trees. By default, a single decision tree uses all features, while in a random forest, the square root of the number of features. Higher dispersion levels negatively impacted all approaches, especially in complex datasets like Lymphography. Approaches utilizing weighted classifiers or diverse coalition strategies mitigated this decline. Forming coalitions among classifiers with conflicting predictions improved results, emphasizing the value of ensemble diversity. Applying classifier accuracy-based weights led to better results in most cases.

Statistical tests were performed to confirm the observed validities and balanced accuracy values were used for comparison. At first, the balanced accuracy values of all twenty approaches were compared – so twenty dependent samples each containing of 16 observations were created, representing the results for each dataset and dispersion version. Since the balanced accuracy is ratio-scaled and normal distribution is not confirmed, also the samples are small the Friedman test was used to determine whether the differences in balanced accuracy values among the approaches were statistically significant. The Friedman test indicated that there is no statistically significant difference in mean balanced accuracy among the twenty approaches, $\chi^2(15, 19) = 9.58, p = 0.96$. A comparative box plot illustrating the balanced accuracy results for the twenty methods is provided in Fig. 6. Although the statistical test did not confirm the significance of the mean differences for such a large number of samples, the graph clearly shows that the results for the weighted approaches are significantly higher than those for the other methods. Therefore, further statistical tests were conducted.

Next, we analyze the differences in average balanced accuracy among the four approaches: unified groups unweighted and weighted, diverse groups unweighted

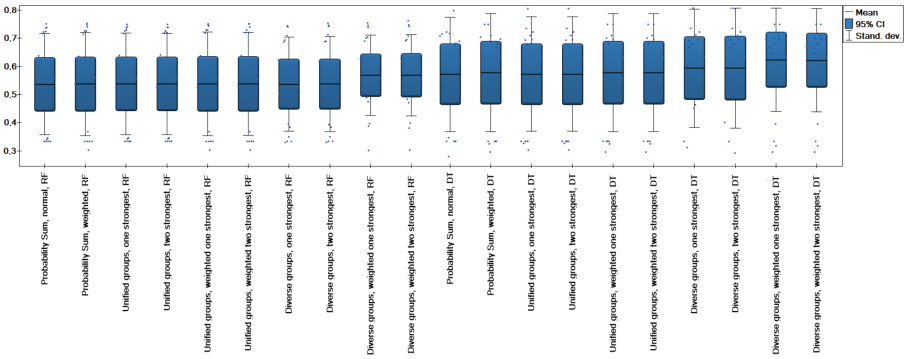

Fig. 6. Comparison of balanced accuracy obtained for all analyzed approaches.

and weighted. This time, the results were organized into 4 dependent groups, each containing 64 observations. Similarly, the Friedman test was conducted on balanced accuracy values. The test confirmed a statistically significant difference in the averages among at least two of the approaches, $\chi^2(64, 3) = 17.75, p = 0.0005$. To pinpoint the specific differences, a post-hoc Dunn-Bonferroni test was performed, with the significant results highlighted in blue in Table 2. The test revealed significant differences between the unweighted and weighted approaches. A comparative box plot (Fig. 7) shows that the balanced accuracy results are slightly better for weighted than unweighted approaches. This was also confirmed by the Wilcoxon test (p-value 0.0001) for results organized into two groups – unweighted and weighted approaches – with 128 observations in each. It was checked analogously with the Wilcoxon test (p-value 0.17) that the division into approaches with different methodologies for forming coalitions – unified groups and diverse groups – does not bring significant differences. However, when we analyzed individual data sets, it was apparent that sometimes the approach with consensus coalitions is better, while for difficult data sets, the approach with incompatible coalitions is better. Thus, the effectiveness of the coalition formation approach depends on the dataset. However, in general, it can be concluded that weighted approaches yield better results.

Table 2. p-values for the post-hoc Dunn Bonferroni test for appeoaches: unified groups unweighted and weighted; diverse groups unweighted and weighted

p-value	Unified groups	Unified groups weighted	Diverse groups	Diverse groups weighted
Unified groups		0.04	1	0.04
Unified groups. weighted	0.04		0.03	1
Diverse groups	1	0.03		0.03
Diverse groups. weighted	0.04	1	0.03	

In conclusion, the results indicate the importance of classifier accuracy-based weighting for dispersed data. Diverse coalition strategies, which group classifiers with conflicting predictions, proved particularly effective for datasets with complex features or high dispersion, such as Lymphography and Vehicle Silhouettes. In contrast, unified coalition approaches often performed better in datasets with categorical features, exemplified by the Car Evaluation dataset. Overall, the findings emphasize the critical role of classifier diversity and weighting in achieving robust predictive performance across varied datasets.

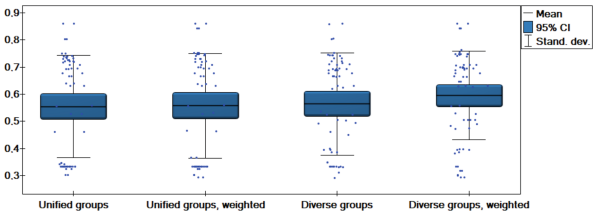

Fig. 7. Comparison of balanced accuracy obtained for approaches: unified groups unweighted and weighted; diverse groups unweighted and weighted.

4 Conclusion

This paper proposes a hierarchical classification model based on dispersed data. Decision trees and random forests were used with conflict model analysis. For the first time, a model with diverse coalitions was used in conjunction with the sum method. In addition to that, the weighted variants were introduced and compared with the unweighted ones. In this work, tests were made on sixteen different dispersed datasets, some with respect to objects and others with respect to attributes. The results were compared with other known literature methods: the sum and weighted sum methods with trees or random forest methods.

The proposed approach yields better results for most of the tested data sets. It was also statistically proven that in terms of classification quality, determined by balanced accuracy measure, weighted variants provide better classification quality than corresponding variants without assigning weights for local models. Also, which method of creating coalitions is better depends on the data set—coalitions of diverse models enhance classification quality for more challenging and diverse data sets.

In future work, the k-nearest neighbors, AdaBoost classifiers, and multilayer perceptrons are planned to be used as local classifiers in conjunction with the conflict analysis and coalition formation method and with other methods of determining differences among local models. The plans also includes features importance and their similarity between coalitions.

References

1. Bohanec, M.: Car Evaluation. UCI Machine Learning Repository (1997). https://doi.org/10.24432/C5JP48
2. Czarnowski, I.: Weighted ensemble with one-class classification and over-sampling and instance selection (WECOI): an approach for learning from imbalanced data streams. J. Comput. Sci. **61**, 101614 (2022). ISSN 1877–7503
3. Czarnowski, I., Jędrzejowicz, P.: Ensemble online classifier based on the one-class base classifiers for mining data streams. Cybern. Syst. **46**(1–2), 51–68 (2015)
4. Fiebig, L., Soyka, J., Buda, S., Buchholz, U., Dehnert, M., Haas, W.: Avian influenza A(H5N1) in humans - line list (2011). http://dx.doi.org/10.25646/7661 Accessed 15 Feb 2024
5. Giordano, R., Passarella, G., Uricchio, V.F., Vurro, M.: Integrating conflict analysis and consensus reaching in a decision support system for water resource management. J. Environ. Manage. **84**(2), 213–228 (2007)
6. Kashinath, S.A., et al.: Review of data fusion methods for real-time and multi-sensor traffic flow analysis. IEEE Access **9**, 51258–51276 (2021)
7. Kuncheva, L.I.: Combining Pattern Classifiers: Methods and Algorithms. Wiley (2014)
8. Mowforth, P. Shepherd, B.: Statlog (Vehicle Silhouettes) [Dataset]. UCI Machine Learning Repository. https://doi.org/10.24432/C5HG6N
9. Nam, G., Yoon, J., Lee, Y., Lee, J.: Diversity matters when learning from ensembles. Adv. Neural. Inf. Process. Syst. **34**, 8367–8377 (2021)
10. Ng, W.W., Zhang, J., Lai, C.S., Pedrycz, W., Lai, L.L., Wang, X.: Cost-sensitive weighting and imbalance-reversed bagging for streaming imbalanced and concept drifting in electricity pricing classification. IEEE Trans. Industr. Inf. **15**(3), 1588–1597 (2018)
11. Ortega, L.A., Cabañas, R., Masegosa, A.: Diversity and generalization in neural network ensembles. In: International Conference on Artificial Intelligence and Statistics, pp. 11720–11743. PMLR (2022)
12. Pawlak, Z.: Some remarks on conflict analysis. Eur. J. Oper. Res. **166**, 649–654 (2005)
13. Pawlak, Z.: Conflict analysis. In: Proceedings of the Fifth European Congress on Intelligent Techniques and Soft Computing (EUFIT 1997), Aachen, Germany, pp. 1589–1591, 8–12 September 1997
14. Pawlak, Z.: Rough sets. Int. J. Comput. Inf. Sci. **11**, 341–356 (1982)
15. Pławiak, P., Abdar, M., Pławiak, J., Makarenkov, V., Acharya, U.R.: DGHNL: a new deep genetic hierarchical network of learners for prediction of credit scoring. Inf. Sci. **516**, 401–418 (2020)
16. Przybyła-Kasperek, M., Sacewicz, J.: Ensembles of random trees with coalitions-a classification model for dispersed data. Procedia Comput. Sci. **246**, 1599–1608 (2024)
17. Przybyła-Kasperek, M., Wakulicz-Deja, A.: A dispersed decision-making system-the use of negotiations during the dynamic generation of a system's structure. Inf. Sci. **288**, 194–219 (2014)
18. Tasci, E., Uluturk, C., Ugur, A.: A voting-based ensemble deep learning method focusing on image augmentation and preprocessing variations for tuberculosis detection. Neural Comput. Appl. **33**(22), 15541–15555 (2021)
19. Verbraeken, J., Wolting, M., Katzy, J., Kloppenburg, J., Verbelen, T., Rellermeyer, J.S.: A survey on distributed machine learning. ACM Comput. Surv. **53**(2), 1–33 (2020)

20. Li, X., Yan, Y.: A dynamic three-way conflict analysis model with adaptive thresholds. Inf. Sci. **657** (2024)
21. Yao, Y.: Three-way decisions with probabilistic rough sets. Inf. Sci. **180**(3), 341–353 (2010)
22. Gillani, Z., Bashir, Z., Aquil, S.: A game theoretic conflict analysis model with linguistic assessments and two levels of game play. Inf. Sci. **677**, 120840 (2024). ISSN 0020–0255
23. Zwitter, M., Soklic, M.: Lymphography. UCI Machine Learning Repository (1988). https://doi.org/10.24432/C54598

From Uncertainty to Semantics in Self-reported Data: An Empirical Analysis

Salvatore F. Pileggi(✉) and Gnana Bharathy

School of Computer Science, Faculty of Engineering and IT, University of Technology Sydney, Sydney, Australia
{SalvatoreFlavio.Pileggi,Gnana.Bharathy}@uts.edu.au

Abstract. Survey data often presents uncertainty because of missing values or situations that do not allow the measure of a given variable, for instance inability/reluctance to answer. On the other side, the sensitivity of questions may affect the quality of data, as well as its reliability and interpretation. Intuitively, uncertainty in such kind of data could be related to some kind of criticality, more concretely to topic sensitivity in this specific case. This paper reports an empirical study conducted on a subset of the World Values Survey (WVS) aimed at the assessment of the relationship between uncertainty and topic sensitivity in survey data. The experiment shows a fundamental convergence and, although results cannot be generalised because of the limited number of experiments conducted, it establishes the fundamentals for a more systematic approach in the context of the current technological landscape, which offers the capabilities to enable human-centric and fully automated solutions. Last but not least, the critical analysis looking at current limitations has defined a roadmap to further enhance the proposed method aiming at a broader and more consolidated experimental and validation framework.

Keywords: Knowledge Engineering · Data Engineering · Data Quality · Sensitive Data · Uncertainty · Self-reported Data · Human-centric AI

1 Introduction

Uncertainty in its different forms (e.g. aleatory and epistemic [12]) is inherent in a computational world [4]. While potentially any kind of data may present some degree of uncertainty, in a data-intensive society uncertainty tends to be associated mostly with the complexity of a given domain and related applications, such as, among very many, Big Data Analytics [8] and business [2]/economic [6] complexity.

While apparently less critical, also survey data may present uncertainty. That is normally because of missing data and is related more or less directly to the inability/reluctance of participants to answer. A well-designed survey should

M. Paszynski et al. (Eds.): ICCS 2025 Workshops, LNCS 15912, pp. 125–139, 2025.
https://doi.org/10.1007/978-3-031-97573-8_9

offer the possibility to disclose such situations in context (e.g. "*Prefer not to answer*"), as well as such situations should be transparently reported with proper codes in the resulting dataset to contribute to assure a proper quality standard.

On the other side, questions on sensitive topics are relatively common and often critical [19] as it is widely accepted that the sensitivity of questions may affect the quality of data, as well as its reliability and interpretation. However, the intrinsic complexity of topic sensitivity has not been widely studied across the different dimensions and variety of possible contexts [17]. Literature proposes some works on specific methods to address sensitive topics (e.g. [16]).

The huge body of knowledge in literature on uncertainty addresses multiple perspectives [12], from a more conceptual/philosophic view to solutions across the different domains. However, at the very best of our knowledge, there is a fundamental lack of study on the relationship between uncertainty and topic sensitivity in survey data. An interesting study on the topic links sensitive topics to resulting measures or estimations [18], discussing the facto a conceptual relationship.

In order to contribute to bridge such a research gap, this study empirically approaches the issue looking at the following research goals:

RG-1. Empirical assessment of the relationship between uncertainty and topic sensitivity in survey data.
RG-2. Systematic context-specific topic sensitivity assessment.
RG-3. Establish the fundamentals for a systematic validation of the relationship between uncertainty and topic sensitivity in survey data.

The current approach intrinsically relies on the potential of the modern AI technology. However, the focus is on systematic, transparent and reliable human-centric AI solutions [11], which may eventually be customised and tuned by human inputs within explainable environments [21].

Structure of the paper. The core part of the paper is structured in three sections that respectively address the methodological aspects (Sect. 2), an empirical analysis of a relevant case study (Sect. 3) and a critical discussion of the results looking at main limitations and future research (Sect. 4).

2 Methodology and Approach

A workflow-based representation of the adopted methodology is proposed in Fig. 1. As shown, the input for the iterative process is survey data, meaning a dataset composed of a number of survey questions and their measure.

As a very first step, questions are processed to extract the main topic. In the context of this work, such a step is not required as the considered case study [13] includes a conceptualisation. More in general, topics can be extracted from input questions by adopting automatic tools (e.g. BERT [10] based). The output for this step is an aligned set of relevant concepts [7], each one associated with one or more questions.

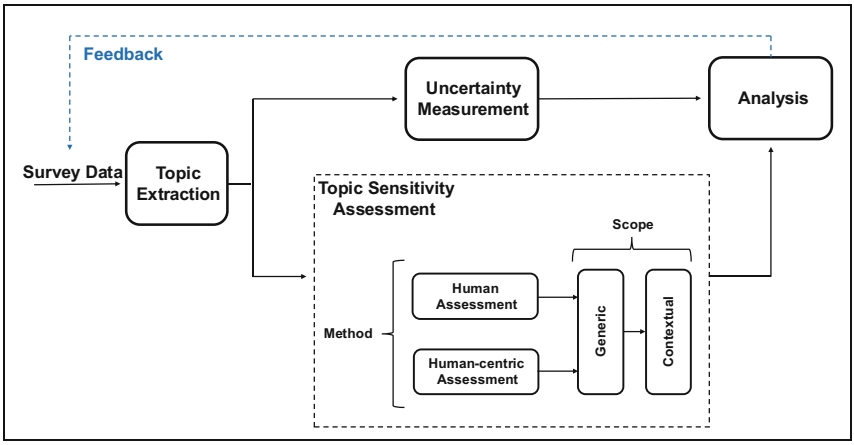

Fig. 1. Methodology overview.

The conceptualization is followed by two independent processes, which aim to (*i*) quantify data uncertainty (Sect. 3.1) and (*ii*) assess topic sensitivity (Sect. 3.2) respectively. Uncertainty is semantically associated with missing values or situations that do not allow the measure of a given variable (for instance inability/reluctance to answer), while topic sensitivity is a much more abstracted concept as per common meaning. To remark that uncertainty in this specific case can be measured according to objective criteria; on the contrary, the assessment of sensitivity is contextual and, in general terms, subject to bias and multiple interpretations. Therefore, topic sensitivity is assessed by adopting different methods (human and human-centric) with a progressive scope refinement, from generic to contextual.

Finally, the output of the mentioned processes are object of analysis to estimate the potential convergence between uncertainty and topic sensitivity.

3 Empirical Analysis: A Case Study

The empirical analysis object of this paper is performed on a subset of the *World Values Survey (WVS)* [9]. It is characterised by a relatively low dimensionality and includes a conceptualization [13].

A reduced dimensionality (16 features) is more suitable to this initial study, as it allows a more intelligible framework of analysis. Moreover, a consolidated conceptualization contributes in a determinant way to effectively design and incorporate systematic methods in scope.

3.1 Uncertainty Analysis

In the context of this specific case study, uncertainty is associated with missing values or values that do not allow the measure of a given variable.

The *World Values Survey (WVS)* [9], which underpins the case study object of analysis, has been designed according to high-quality standards and, indeed, specific codes are available to flag the different situations that may lead to such computational uncertainty. They include *Don't know* (code = −1), *No answer/refused* (code = −2), *Not applicable* (value code = −3), *Missing* (code = −5), in addition to the value −4 which, at the best of authors understanding, is not associated to any specific meaning. In general terms, positive values are associated with computationally valid answers.

As such a fine-grained classification is not relevant for the conducted study, main statistics (reported in Fig. 2) simply refer to the uncertainty resulting by the combination of all mentioned codes. The considered dataset is composed of 94278 rows, including a 77.23% of complete rows and a 22.77% with at least one negative code (uncertainty). The breakdown by feature in the same figure shows a significantly higher amount of uncertainty for the variable *Q36*.

From a code perspective, to remark that there is no entry with code −3 (associated with *Not applicable*); on the other side, a high number of rows present at least one variable with code −1 (*Don't know*) or −4 code (unknown meaning), 13.1% and 11.8% respectively; finally, a relatively small number of rows (4.1% and 2.6%) is associated with some code −2 or −5.

An overview of uncertainty (scaled in the range 0–3) is proposed in Fig. 3a, while Fig. 3b presents the same view excluding variables with an amount of uncertainty significantly higher than others (*Q36* in this specific case).

In order to provide a consistent overview of the uncertainty in presence of those numerical patters, a semi-quantitative approach is adopted: given a range of values x_i and a range for feature scaling $[u_{min}, u_{max}]$, the higher value of the range (u_{max}) is reserved to values significantly higher than others ($x_k = u_{max}$, $\forall k, i : x_k >> x_i$), while all other values are scaled assuming a range $[u_{min}, u_{max} - 1]$. Such an approximation is acceptable in this specific context as the original numerical patterns are still present in the figure but they are mitigated. In this specific case, the variable *Q36* is associated with 3 and all other features are scaled between 0 and 2 (Fig. 4).

3.2 Topic Sensitivity Assessment

This sub-section deals with topic sensitivity and its assessment. Such an assessment is addressed by adopting different methods and assumes a different scope - i.e. generic and contextual.

Human Assessment. In general terms, the assessment of the sensitivity of a given topic depends on several factors, including, among others, phrasing, context, audience, respondent, as well as cultural, social and political environment. Additionally, it may be intrinsically subjective, if not biased, and hard to generalise.

In this sense, in addition to evidence-based research, a collaborative approach aimed at establishing shared views on the model of shared meaning-making [1]

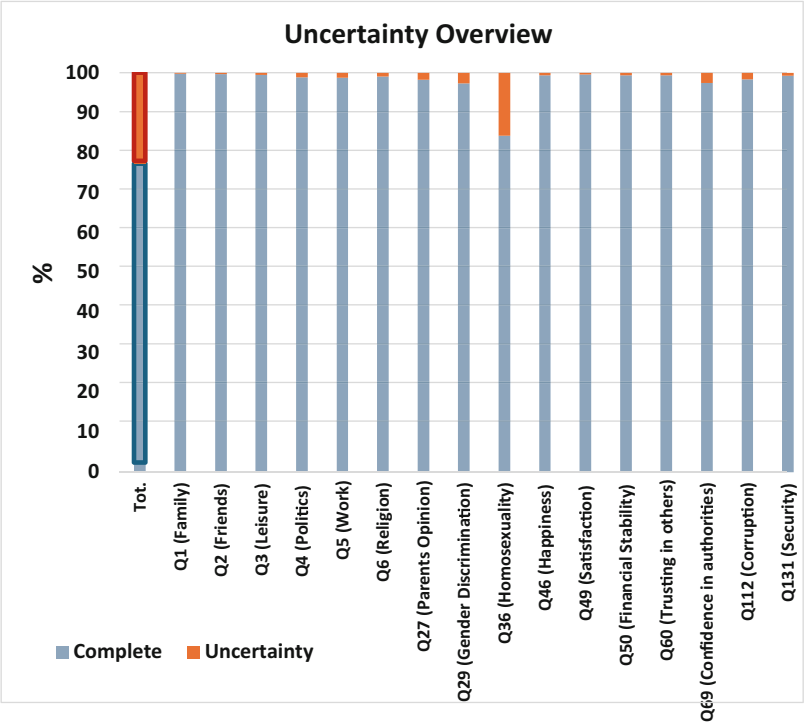

Fig. 2. Uncertainty overview. The first bar (*Tot.*) reports the number of rows with uncertainty; the other bars provides a view by feature.

may positively contribute. However, a collaborative method should be properly designed according to a number of principles to address the inherent sociocultural complexity. It may be hard to enable in practice.

In this work, a human assessment of topic sensitivity is performed according to a simplified approach that relies on common knowledge. Under the assumption that any topic my be potentially sensitive depending on the context, looking at the topics in the case study from a generic perspective, *Politics*, *Religion*, *Gender Discrimination*, *Homosexuality*, *Confidence in authorities* and *Corruption* are definitely critical, with *Work* that may present some intrinsic sensitivity in multiple context. Looking more specifically at the nature of the WVS and the actual questions (contextual assessment), the number of high-sensitive topics is probably lower as questions on politics, work and religion aim to generically measure their relevance as a value for respondents. An overview is reported if Fig. 5a

The proposed analysis is evidently qualitative and, indeed, tends to be "radical" by focusing on the identification of the most critical topics.

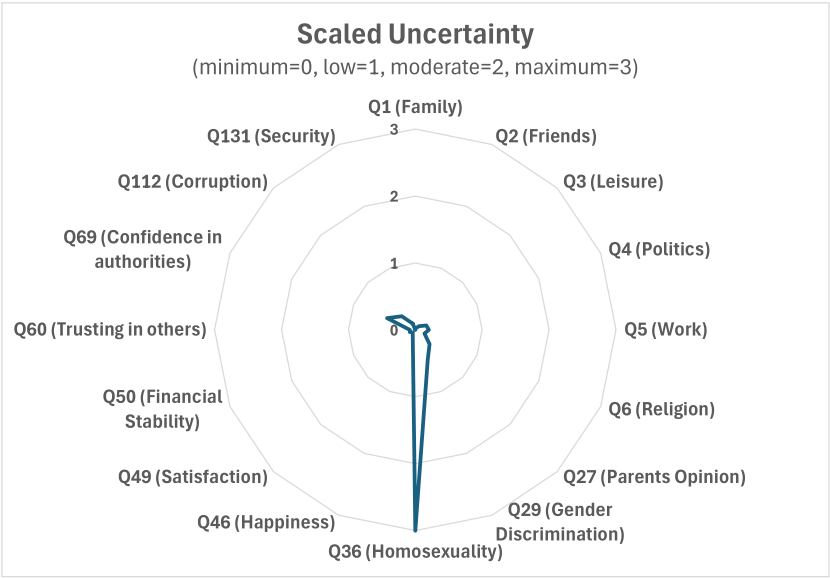

(a)

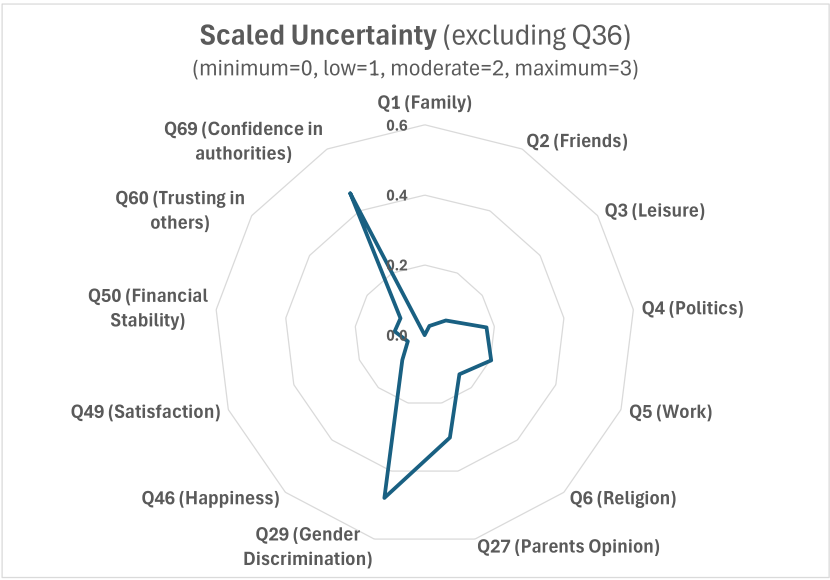

(b)

Fig. 3. Uncertainty overview scaled between 0 and 3. One of the feature (Q36) presents a significantly higher value.

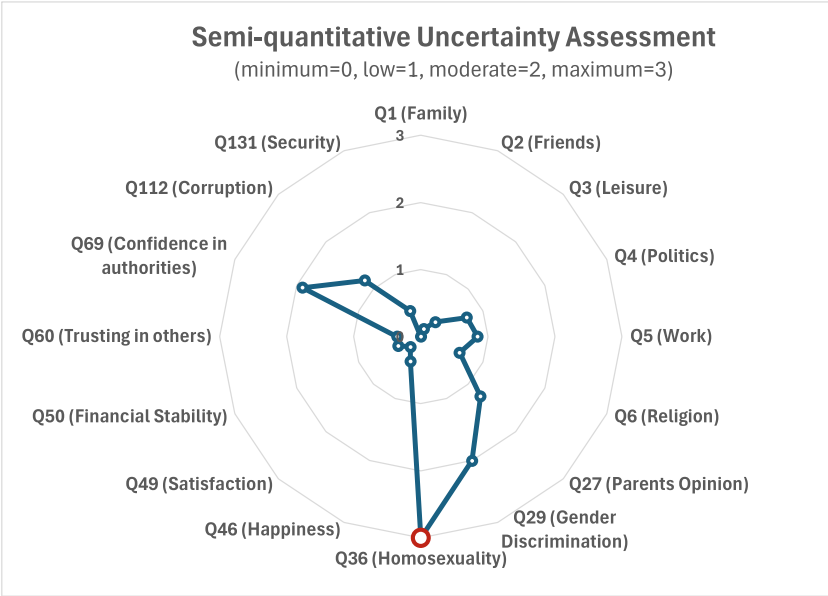

Fig. 4. Semi-quantitative view of uncertainty.

Human-Centric Approach. In a context of huge proliferation of AI technology, in this specific case, a simplified understanding of a human-centric approach [5] assumes a close collaboration between humans and AI to solve a given problem [14]. It may realistically reflect many everyday life situations in the current technological landscape.

More concretely, topic sensitivity has been assessed with the support of WhatsGPT[1] and key human inputs in terms of prompt engineering and refinement of the results.

The input for the assessment of the sensitivity of a given topic X is the following query:

```
How sensitive is a question on
X
in a survey
from 0 (minimum) to 3 (maximum)?
```

In addition to explanations and other information, the response to such a query includes a variable number of example survey questions on the topic with a related sensitivity score. The average score on the returned examples estimates the generic sensitivity of the topic. The contextual assessment assumes a further level of analysis as a subset of example questions is selected to match the actual case study context. For instance, 5 out of 7 example questions on homosexuality

[1] WhatsGPT - https://www.whatsgpt.me, accessed on 16 January 2025.

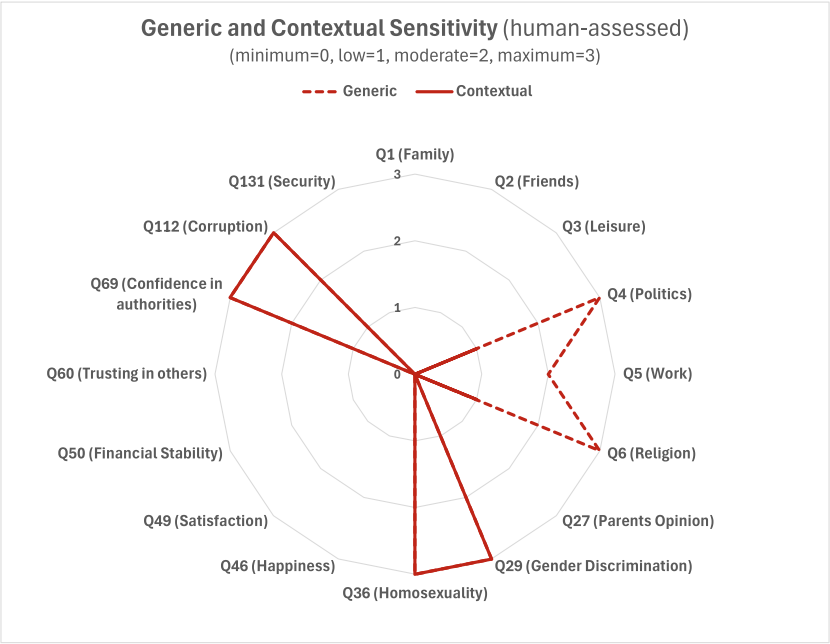

(a)

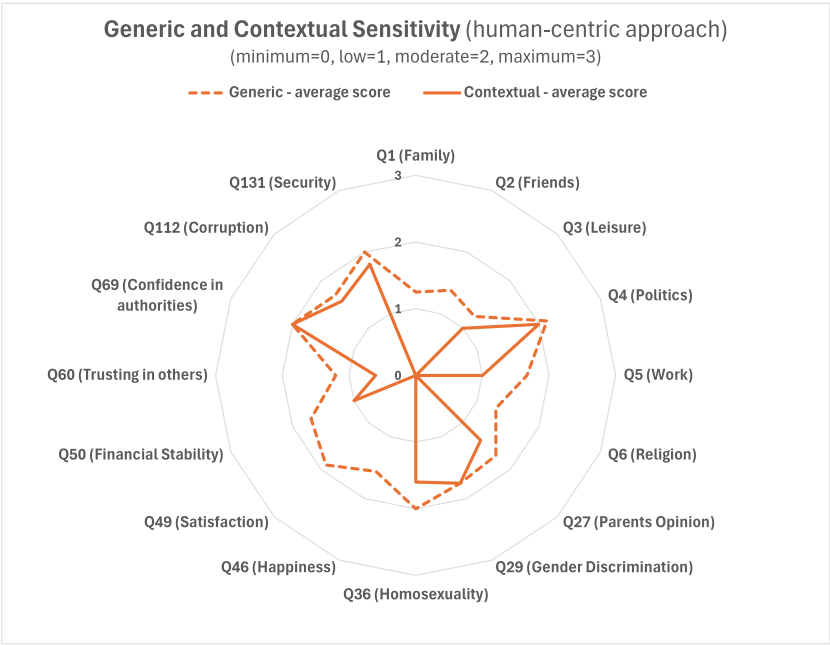

(b)

Fig. 5. Sensitivity assessment, including a human assessment and a human-centric approach.

have been selected looking at the more specific meaning of the question in the dataset, which is on homosexuality acceptance in this specific case.

The human-centric analysis is summarised in Table 1. To note that, due to the generality of the topic and the relatively specific context, a contextual assessment for *Q29* adopting the proposed method was unsuccessful as the example questions are not conceptually aligned with the actual application in the dataset.

A graphical overview is proposed in Fig. 5b

Table 1. Human-centric assessment.

	Generic		Contextual		
Variable	Samples	Av. score	Samples	Av. score	**Context**
Q1 (Family)	8	1.25	1	0	Value
Q2 (Friends)	8	1.38	1	0	Value
Q3 (Leisure)	8	1.25	1	1	Value
Q4 (Politics)	8	2.13	1	2	Value
Q5 (Work)	9	1.67	1	1	Value
Q6 (Religion)	10	1.3	1	0	Value
Q27 (Parents Opinion)	10	1.7	8	1.38	Value
Q29 (Gender Discrimination)	8	1.75	*0*	*1.75*[a]	Opinion
Q36 (Homosexuality)	7	2	5	1.6	Acceptance
Q46 (Happiness)	9	1.56	2	0	Perception
Q49 (Satisfaction)	10	1.9	1	0	Perception
Q50 (Financial Stability)	10	1.7	2	1	Perception
Q60 (Trusting in others)	10	1.2	5	0.6	Opinion
Q69 (Confidence in authorities)	8	2	1	2	Opinion
Q112 (Corruption)	10	1.7	7	1.57	Perception
Q131 (Security)	10	2	5	1.8	Perception

[a] Same as for generic assessment due to a lack of examples relevant to the specific context.

3.3 From Uncertainty to Semantics

The quantitative estimation of the convergence between uncertainty and sensitivity adopts the *Euclidean Distance*. Assuming two points $p = [p_1, p_2, ..., p_i, ..., p_n]$ and $q = [q_1, q_2, ..., q_i, ..., q_n]$ in the Euclidean n-space, the distance between such points is defined as in Eq. (1).

$$d(p, q) = \sqrt{\sum_{i=1}^{n} (q_i - p_i)^2} \tag{1}$$

Results are reported in Table 2 and point out two clear independent patterns, including (*i*) a significantly lower distance for the contextual approach regardless of the adopted method and (*ii*) human-centric approach slightly more effective to approximate experimental measurements.

A visual representation is provided in Figs. 6 and 7, for the human and the human-centric approach respectively.

Table 2. Results summary in terms of Euclidean Distance.

Assessment Method	Assessment Scope	Distance
Human	Generic	4.46
Human	Contextual	2.96
Human-centric	Generic	4.22
Human-centric	Contextual	2.70
Hybrid	Generic	4.82
Hybrid	Contextual	1.94

Last but not least, a hybrid approach resulting from the two methods (average values) is proposed. Numerical values are in Table 2 and a visual representation is in Fig. 8. While the generic assessment for the hybrid approach presents the higher distance from experimental data, its fine-tuned version (contextual) outperforms both underlying methods. It provides significant insight for the future evolution of the system and its automation.

4 Current Limitations and Outline of Future Research

The empirical assessment has provided valuable insight, in line with the predefined research goals. The results achieved establish a grounding framework to enable in fact a systematic evidence-based approach.

However, such a result should be considered looking at current limitations to define a roadmap for future research:

- *Scale*. While the conducted experiment involves a large dataset, the analysis has been conducted at a reduced dimensionality. The current focus on topics over specific question intrinsically enable a scalable framework of analysis.

- *Data source*. The experiment is currently related to one single dataset. Extending the empirical assessment to multiple datasets in a diverse and multi-disciplinary context is a key factor to consolidate a systematic and generic approach, as well as to identify peculiarities and possible limitations.

- *Bias*. As extensively discussed in the paper, there is an intrinsic risk of bias to assess the sensitivity of a given topic. Such a quantification inherently

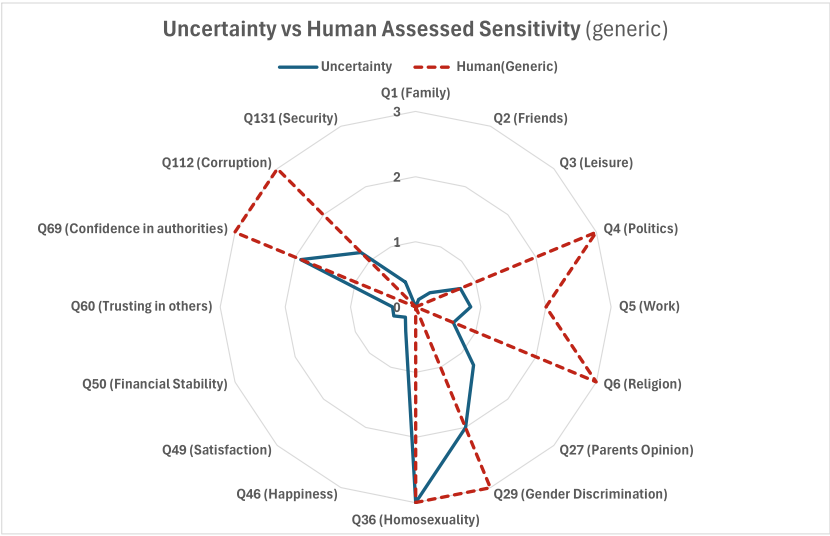

(a)

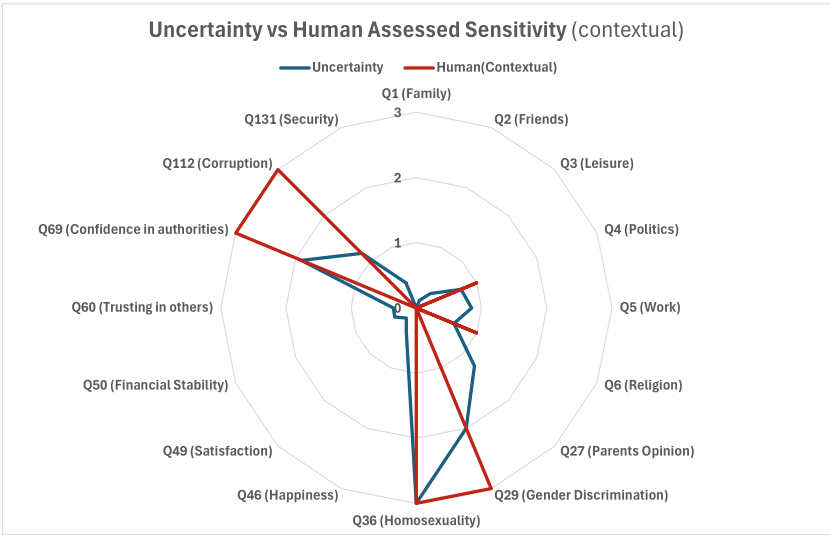

(b)

Fig. 6. Uncertainty and human-assessed sensitivity, including a generic and contextual analysis.

presents a certain degree of complexity, as it may depend on different contextual factors. The simplified approach adopted in this paper should be further enhanced through more consistent mitigation strategies (for both human and AI bias [15]) based on formal analysis frameworks.

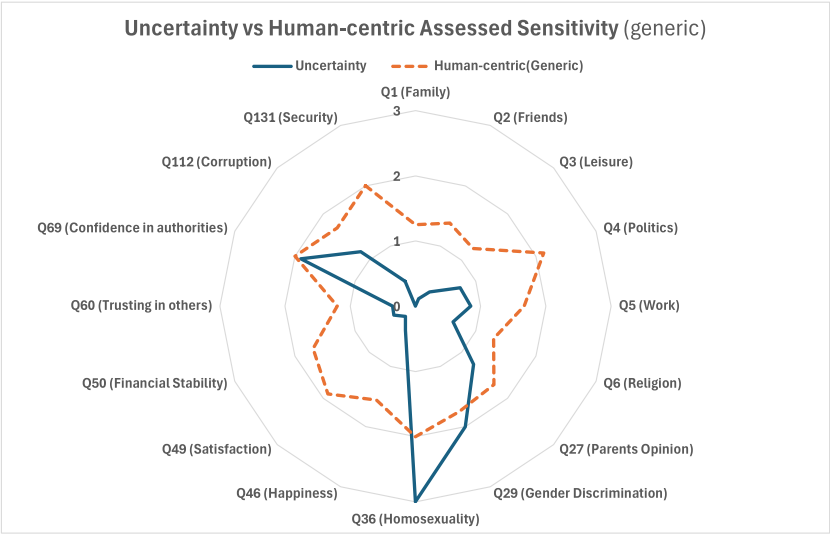

(a)

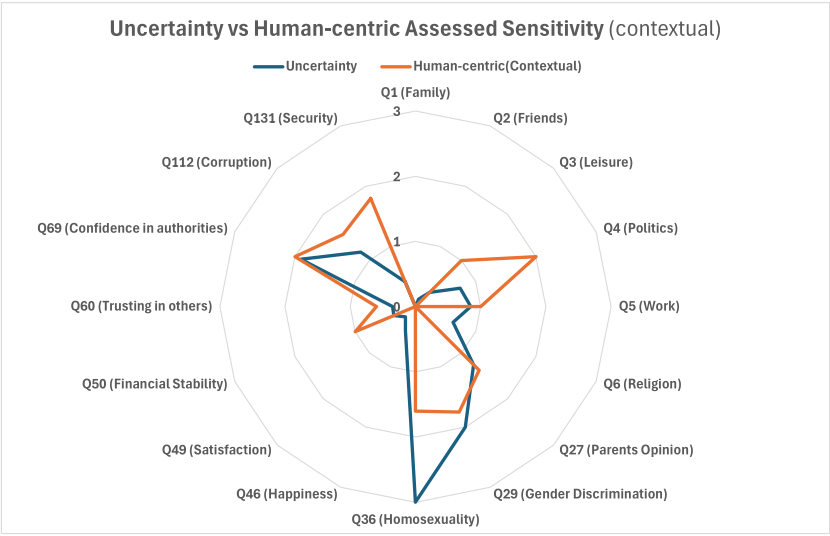

(b)

Fig. 7. Uncertainty and sensitivity (assessed according to a human-centric approach). It includes generic and contextual analysis.

– *Interaction with AI.* The human-centric approach is valuable in the context of this work and, more in general, critical in the modern technological landscape. In this specific case, a consistent approach requires a more sophisticated interaction model [3] to further enhance the reliability and effectiveness of sys-

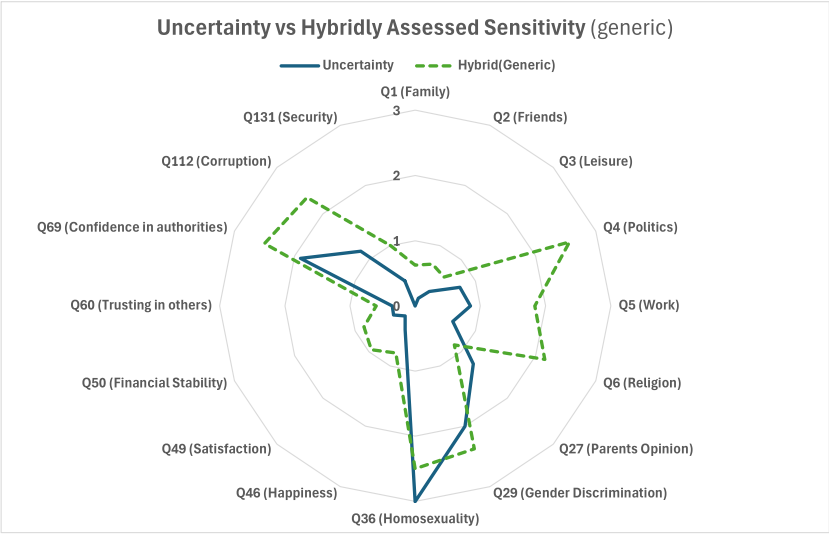

(a)

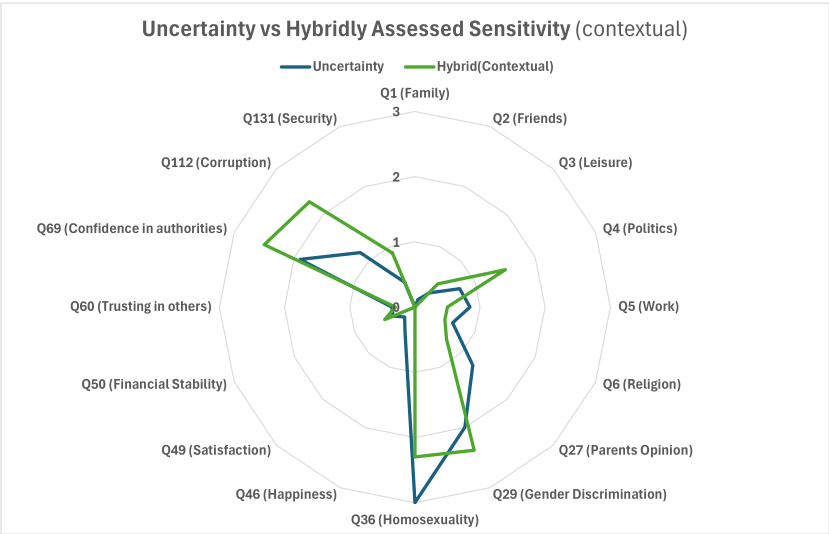

(b)

Fig. 8. Uncertainty and sensitivity assessed according to a hybrid approach.

tematic solutions. Additionally, the stability of the output and the impact of different tools as a function of the input (e.g. Prompt Engineering [20]) should be carefully assessed.

– *Assessment metrics.* In generic terms, the assessment metrics are simple to prioritize intelligible analysis and interpretations. While this is an unquestionable advantage, additional metrics are required to support the evolution of the system toward automation.

– *Automated approach.* More in general, the synthesis and the validation of fully-automated solutions require additional experimentation and testing, in line with the previous discussion points.

5 Conclusions

This empirical work has provided valuable insight to assess the relationship between uncertainty and topic sensitivity in survey data, showing a relatively clear convergence. Although the current experimentation (limited to one single case study) doesn't allow the generalisation of the results, it establishes the fundamentals for a more systematic approach in the context of the current technological landscape, which offers the capabilities to enable human-centric and fully automated solutions. Additionally, the critical analysis looking at current limitations has defined a roadmap to further enhance the proposed method aiming at a broader and more consolidated experimental and validation framework.

References

1. Aldemir, T., Borge, M., Soto, J.: Shared meaning-making in online intergroup discussions around sensitive topics. Int. J. Comput.-Support. Collab. Learn. **17**(3), 361–396 (2022)
2. Altig, D., Barrero, J.M., Bloom, N., Davis, S.J., Meyer, B., Parker, N.: Surveying business uncertainty. J. Econometrics **231**(1), 282–303 (2022)
3. Amershi, S., et al.: Guidelines for human-AI interaction. In: Proceedings of the 2019 Chi Conference on Human Factors in Computing Systems, pp. 1–13 (2019)
4. Bossaerts, P., Yadav, N., Murawski, C.: Uncertainty and computational complexity. Philos. Trans. R. Soc. B **374**(1766), 20180138 (2019)
5. Bryson, J.J., Theodorou, A.: How society can maintain human-centric artificial intelligence. In: Toivonen, M., Saari, E. (eds.) Human-Centered Digitalization and Services. TSS, vol. 19, pp. 305–323. Springer, Singapore (2019). https://doi.org/10.1007/978-981-13-7725-9_16
6. Cascaldi-Garcia, D., et al.: What is certain about uncertainty? J. Econ. Lit. **61**(2), 624–654 (2023)
7. Chuang, J., Gupta, S., Manning, C., Heer, J.: Topic model diagnostics: assessing domain relevance via topical alignment. In: International Conference on Machine Learning, pp. 612–620. PMLR (2013)
8. Hariri, R.H., Fredericks, E.M., Bowers, K.M.: Uncertainty in big data analytics: survey, opportunities, and challenges. J. Big Data **6**(1), 1–16 (2019). https://doi.org/10.1186/s40537-019-0206-3
9. JD Systems Institute & WVSA: European Values Study and World Values Survey: Joint EVS/WVS 2017-2022 Dataset (Joint EVS/WVS), Dataset Version 4.0.0 (2022). https://doi.org/10.14281/18241.21

10. Kenton, J.D.M.W.C., Toutanova, L.K.: BERT: pre-training of deep bidirectional transformers for language understanding. In: Proceedings of NAACL-HLT, vol. 1. Minneapolis, Minnesota (2019)
11. Lepri, B., Oliver, N., Pentland, A.: Ethical machines: the human-centric use of artificial intelligence. IScience **24**(3), 102249 (2021)
12. Li, Y., Chen, J., Feng, L.: Dealing with uncertainty: a survey of theories and practices. IEEE Trans. Knowl. Data Eng. **25**(11), 2463–2482 (2012)
13. Pileggi, S.F.: A hybrid approach to analysing large scale surveys: individual values, opinions and perceptions. SN Soc. Sci. **4**(8), 144 (2024)
14. Pileggi, S.F.: Ontology in hybrid intelligence: a concise literature review. Future Internet **16**(8), 1–19 (2024)
15. Roselli, D., Matthews, J., Talagala, N.: Managing bias in AI. In: Companion Proceedings of the 2019 World Wide Web Conference, pp. 539–544 (2019)
16. Rosenbaum, A., Rabenhorst, M.M., Reddy, M.K., Fleming, M.T., Howells, N.L.: A comparison of methods for collecting self-report data on sensitive topics. Violence Vict. **21**(4), 461–471 (2006)
17. Roster, C.A., Albaum, G., Smith, S.M.: Topic sensitivity and internet survey design: a cross-cultural/national study. J. Mark. Theory Pract. **22**(1), 91–102 (2014)
18. Tourangeau, R., Groves, R.M., Redline, C.D.: Sensitive topics and reluctant respondents: demonstrating a link between nonresponse bias and measurement error. Public Opin. Q. **74**(3), 413–432 (2010)
19. Tourangeau, R., Yan, T.: Sensitive questions in surveys. Psychol. Bull. **133**(5), 859 (2007)
20. Velásquez-Henao, J.D., Franco-Cardona, C.J., Cadavid-Higuita, L.: Prompt engineering: a methodology for optimizing interactions with AI-language models in the field of engineering. Dyna **90**(SPE230), 9–17 (2023)
21. Xu, F., Uszkoreit, H., Du, Y., Fan, W., Zhao, D., Zhu, J.: Explainable AI: a brief survey on history, research areas, approaches and challenges. In: Tang, J., Kan, M.-Y., Zhao, D., Li, S., Zan, H. (eds.) NLPCC 2019. LNCS (LNAI), vol. 11839, pp. 563–574. Springer, Cham (2019). https://doi.org/10.1007/978-3-030-32236-6_51

Uncertainties in Modeling Psychological Symptom Networks: The Case of Suicide

Valeria Epelbaum[1,2,3(✉)], Sophie Engels[1], Rory O'Connor[4], Denny Borsboom[1], Derek De Beurs[2,3], and Valeria Krzhizhanovskaya[1,3]

[1] Computational Science Lab, Informatics Institute, Faculty of Science, The University of Amsterdam, Amsterdam, The Netherlands
{V.Epelbaum,S.L.Engels,D.Borsboom,V.Krzhizhanovskaya}@uva.nl
[2] Faculty of Social and Behavioural Sciences, The University of Amsterdam, Amsterdam, The Netherlands
D.deBeurs@uva.nl
[3] Centre for Urban Mental Health, The University of Amsterdam, Amsterdam, The Netherlands
[4] Suicidal Behaviour Research Lab, School of Health and Wellbeing, University of Glasgow, Glasgow G12 8TA, UK
rory.oconnor@glasgow.ac.uk

Abstract. In psychological research, network models are widely used to study symptoms of mental health disorders. However, these models often fail to account for uncertainty, leading to potentially misleading inferences. To address this issue, this study examines the robustness of psychological networks by analyzing a dataset of risk factors for suicidal behavior with multiple network algorithms. We compare two causal discovery algorithms—Hill Climbing (HC) and TABU search—and the Gaussian Graphical Model (GGM), a widely used statistical network model in psychology. Uncertainty is assessed along two dimensions: (1) the impact of noise, by introducing varying levels of white noise into the dataset, and (2) the effect of sample size reduction, by systematically decreasing the number of observations. Our results indicate that both HC and TABU search are highly sensitive to noise and sample size, with HC slightly outperforming TABU in terms of precision and recall. GGM performance declines gradually with increasing noise and sample size reduction, leading to sparser networks. For all algorithms, recall declined at a faster rate than precision. Finally, we examine the robustness of edges leading to suicidal ideation, finding that the edge from Depression to suicidal ideation remains relatively stable across conditions. This is a promising result, since many suicide interventions are based on treating depressive mood. Our results emphasize the importance of considering uncertainty in network-based psychological research, particularly when applying causal discovery algorithms.

Keywords: Uncertainty Quantification · Suicidal Behaviour · Causal Discovery Algorithms · Gaussian Graphical Model

M. Paszynski et al. (Eds.): ICCS 2025 Workshops, LNCS 15912, pp. 140–153, 2025.
https://doi.org/10.1007/978-3-031-97573-8_10

1 Introduction

In the last decade, network models have gained increasing popularity in the social and behavioral sciences. For instance, in psychology, they are particularly valuable for modeling complex interactions between symptoms [3]. The most commonly used approach are undirected network models, where edges represent conditional independence relationships between variables. These are typically estimated using statistical models, such as Gaussian Graphical Models (GGMs), which infer edges based on partial correlations [9]. More recently, there has been a growing interest in causal discovery algorithms [12,16]. These methods are often used to estimate directed networks, typically as Directed Acyclic Graphs (DAGs). Unlike GGMs, which capture associative patterns, DAGs attempt to infer causal structures using, for instance, score- or constraint-based methods.

Recently, increasing attention has been given to the replicability and robustness of network models, with researchers questioning the extent to which reliable inferences can be drawn from estimated networks [10]. Much of this work has focused on measurement-related uncertainty, such as how different response scales or node aggregation methods influence network structures. For example, [14] showed that using aggregated variables, whether through latent factors or mean scores, improved the performance compared to single-indicator models.

While this line of research addresses uncertainty on a measurement related level, it does not focus on uncertainty arising directly from the data, which can be an especially big issue in psychology [10]. For instance, most psychological data sets have small sample sizes to begin with. Additionally, some participants might misinterpret the asked questions or answer dishonestly, for example due to stigma. As a consequence, the data can become very noisy, which can manifest as spurious or missing relationships in networks. This is particularly concerning in clinical psychology, where network models are increasingly used to identify key symptoms or potential targets for interventions. While multiple studies have investigated the role of sample size [9,14], other data-related sources of uncertainty, for instance noise, have not been studied in a psychological context yet. Thus, this study aims to address this gap by evaluating the performance of various network algorithms using a real data set. Specifically, two sources of data uncertainty will be examined: noise and sample size reduction.

To examine these effects of uncertainty, this study uses a cross-sectional dataset derived from [19]. The original authors studied risk factors for suicidal ideation through the lens of the Integrated Motivational Volitional theory (IMV) of suicidal behavior. According to that theory, suicidal thoughts arise from the interaction of different factors such as entrapment or defeat [19]. Previously, [7] already used this data to construct various networks using statistical models, such as GGM. Using this data set, the present study systematically introduces two types of data uncertainty—noise, and sample size—and assesses their impact on both directed and undirected network estimation. Additionally, the robustness of the causal edges leading towards suicidal thoughts, under both noise and data reduction, will be examined.

1.1 Background and Related Work

Background. Most undirected networks in psychology are based on the pairwise Markov random field (PMRF). In these models, when two variables are connected, it implies conditional dependence, while the absence of an edge signifies conditional independence given all other variables in the network. When the data follows a multivariate Gaussian distribution, the appropriate PMRF model is a GGM, described in more detail in Sect. 2.2.

A directed acyclcial graph (DAG) is a graph $G = (V, E)$, where $V = V_1, ...V_n$ represents a set of random variables, also referred to as nodes, and E is a set of directed edges. In this context, an edge from variable A to B ($A \rightarrow B$), indicates that variable A is considered a potential cause of variable B. However, to make this kind of conclusions, causal discovery algorithms are usually based on certain assumptions, such as faithfulness. An in-depth review of them is beyond the scope of this paper, but see [13] for a more detailed discussion.

There are multiple approaches to learn a DAG from a data set. For example, score-based algorithms approach this problem from a machine-learning perspective: they search the space of potential DAG structures to determine the one that reduces the score of a loss function.

Related Work. In computational science, uncertainty in DAGs has been assessed across multiple levels. For instance, there are many proposed extensions and algorithms that take uncertainty into account [2]. Another strategy is to induce noise directly into the data. For example, [6] compared different DAG algorithms on noisy real-world data. Using multiple empirical networks as different case studies, they induced noise by adding missing/incorrect values or merging variables. They conclude that evaluation based on synthetic data can overestimate performance by anywhere from 10% up to 50%. [1] arrives at a similar conclusion.

Both of these studies compared the noisy graph to a reference network, which was either constructed by the authors themselves (e.g., via simulations) or supplied by experts. However, in social and behavioral sciences, such use of reference networks is rare: graphs are most commonly only learned from the data. Thus, to make our study more realistic, we directly learn the graph from the data, rather than relying on pre-constructed reference graphs.

2 Methodology

For each type of uncertainty, a single experiment will be conducted, resulting in two experiments in total. Each of them will feature all the algorithms described below, and will be run over 500 iterations. Following this, the frequency of edges leading to suicidal ideation identified by the different algorithms will be assessed under two conditions: varying noise levels and sample size. Thus, an edge is considered robust if it appears consistently, even under high noise and reduced sample size.

The analysis is conducted in R, using the R studio environment [15]. For the undirected networks, the package *bootnet* is used [9], while the DAGs were constructed using *bnlearn* [17]. Further, *tidyverse* was used to clean the data and visualize the results [20].

2.1 Data Description

The data comes from a population-based study on wellbeing, and is described in detail elsewhere [7]. Briefly, variables from the IMV theory were measured using various psychological questionnaires in the general population. For example, a question from the Barret Impulsivity scale (BIS), assessing Impulsivity, reads: "I act on impulse", and can be answered on a scale from 1 (not at all) to 4 (always). For a full overview of all the questionnaires and variables see [7].

To conduct further analysis, a common practice is to create sum scores for each questionnaire, i.e. to sum up all the observations for each individual per variable. For example, the BIS questionnaire consists of 30 questions. For each participant, all 30 scores were added up, reducing the amount of data from 30 raw scores to 1 sum score. For the current analysis, only participants experiencing suicidal ideation were used ($n = 333$), as otherwise the distribution of the variables would be non-Gaussian. Further, as the different questions were measured on different scales, all the scores were normalized to a 0 to 100 scale.

2.2 Algorithms for Constructing Networks from Data

Networks are constructed using multiple algorithms. Undirected, statistical graphs were computed using a GGM, one of the most commonly used algorithms in Psychology [9]. The edges in a GGM represent partial correlation coefficients. To enforce sparsity in the network structure, the Graphical Least Absolute Shrinkage and Selection Operator (glasso) was applied, which imposes a penalty on the inverse covariance matrix, driving small partial correlations to zero [9].

For the DAGs, both the Hill Climbing (HC) and TABU algorithm are used. HC is a score-based algorithm, relying on a greedy search strategy. It starts off with an empty graph and makes local moves such as adding/removing an edge that lower a scoring function. Once a move does not improve the score, the algorithm terminates, which can result in it getting stuck in a local minimum. To avoid this problem, an extension of this algorithm was created that allows lower scoring moves. This extension is called TABU search. For both algorithms, the default scoring option of the Bayesian Information Criterion (BIC) will be used.

Each algorithms depends on a set of hyperparameters. For example, for TABU, the number of recent moves can be modified. This kind of memory serves the purpose of not revisiting older moves again. In our experiments, we used all the default settings, as outlined in Table 1.

Table 1. Software and Hyperparameters for each algorithm.

Algorithm	Software	Default Hyperparameters
Gaussian Graphical Model (GGM)	bootnet	gamma = 0.5, number of tested lambda values = 100, Ratio of lowest lambda value compared to maximal lambda = 0.01
Hill Climbing (HC)	bnlearn	random restarts = 0, scores = BIC
TABU Search	bnlearn	tabu list = 10, escapes = 10, scores = BIC

2.3 Data Augmentation

The data was modified in two different ways. First, white noise was induced in the data set. Using a fixed amplitude α, we add an absolute noise level $\alpha\%$ (in percentage points of the normalized 0–100 scale) by drawing from:

$$\delta_i \sim \text{Uniform}([-\alpha, +\alpha])$$

where δ_i refers to the added noise to the ith observation. Thus, the noisy ith observation x_i^{noisy} is defined as:

$$x_i^{\text{noisy}} = x_i + \delta_i$$

with x_i being the original, i.e. unmodified, observation. For example, if the noise amplitude is $\alpha = 10$, then $\delta_i \in [-10, +10]$, so a point at $x_i = 50$ is perturbed somewhere in $[40, 60]$. Thus, as δ_i has the same range for every observation, the variance of the added noise is constant across all observation (i.e. *homoscedastic*) - a condition necessary for the GGM. Since the range of the data is bounded between 0 and 100, values above or below these thresholds are clipped. Second, data quantity was compromised. Here, rows of the observed data were randomly removed according to a percentage. For example, if this quantity percentage is 20%, then 67 randomly chosen rows would be removed, and the graph would be estimated based on the remaining 266 observations instead of 333.

2.4 Evaluation Metrics

Evaluation in this context refers to how well the graph based on modified data performs in comparison to the graph learned from the original non-modified data. It should be noted, that in this sense, there is no "ground truth" network, since the true model is not known when working with an empirical data set. As the main goal is to estimate the impact of noise relative to the original data, the network learned from the non-augmented data will be used as a "reference".

Subsequently, the graph based on the non-augmented data will be referred as the original graph. A similar use of reference graphs was also previously done by [13], who evaluated different DAG algorithms on empirical data sets without knowing the true underlying structure. Their study, however, relied on an fMRI data set and one composed of cause–effect pairs—both of which differ substantially from the types of data typically encountered in clinical psychology. Our use of reference graphs also implies that for all three algorithms, the baseline graphs will be different. Three scoring metrics are calculated for each experiment:

1. Precision: Measures the proportion of predicted edges that are actually present in the original graph. It is calculated by dividing the True Positive rate (TP) by the sum of TP and False Positives (FP).
2. Recall: Measures how many true edges from the original graph are successfully recovered by the noisy graph. It is calculated by dividing TP by the sum of TP and False negatives (FN).
3. F1: The F1 score is the harmonic mean between Recall and Precision, and is a commonly used metric in the field of DAGs. It is defined as:

$$\text{F1} = \frac{2 * \text{Precision} * \text{Recall}}{\text{Precision} + \text{Recall}}$$

Even though the F1 score is the mean of both precision and recall, it can still be informative to look at all three scores. The reason is that a low F1 score does not tell us whether it is low due to recall or precision.

3 Results

3.1 Baseline Results

Figure 1 displays the baseline graphs. The GGM is very densely connected compared to the HC and the TABU algorithm: the average degree for the GGM is appoximately 9, while for HC and Tabu it is approximatly 2. On the other side, the HC and the TABU algorithms do not differ much. The main differences appear to be the direction of the edges. For instance, in the HC algorithm, feelings of defeat (Def) lead to stress (Str), while in the TABU graph this direction is reversed. The centrality measures degree and betweenness are shown in Table 2. Despite these structural differences, the nodes connected to suicidal ideation appear consistent across the algorithms: suicidal ideation is linked to thwarted belongingness, depression, mental well-being, and feelings of defeat. These associations are supported by prior empirical research [5]. Other empirically supported links, such as those between depression and perceived burdensomeness or impulsivity, are also present [7].

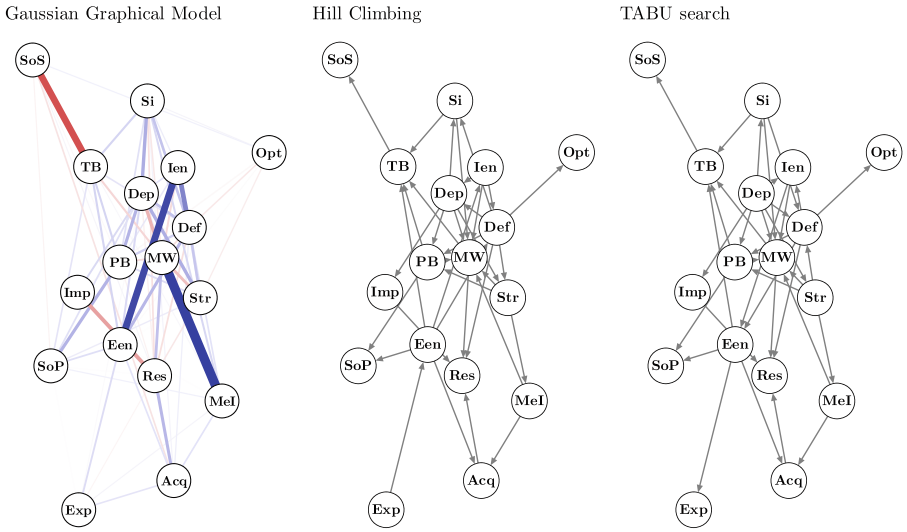

Fig. 1. Baseline graphs for the three algorithms. In the Gaussian graphical model, edge thickness reflects the strength of the partial correlation. Blue edges represent positive relationships, while the red ones the negative. Since Hill Climbing and TABU are structure learning algorithms, no edge weights are assigned. The symptoms are described in Table 2. (Color figure online)

3.2 Uncertainty: Data Noise

Figure 2 shows the results for noisy data. Overall, the impact of noise is quite significant: 20% noise already results in a F1 value of less than 0.8. HC slightly outperforms TABU search, both in regards to precision and recall. The added noise also had a higher impact on recall compared to precision, meaning that the noisy graph is less prone to false positive edges, but misses many edges that were present in the original graph (high false negative).

For the GGM, the performance gradually decreases up until 50% noise. After that, a slight increase in precision can be observed. A potential reason for this could be that the graph is becoming more sparse: the original graph contains 75 edges on average, which decreases to 59 edges for 50% noise, and further drops to 30 edges for 80% noise. As the number of the detected edges declines, so does the number of false positives. This decrease is happening at a faster rate compared to the decline in true positives, leading to an increase in precision[1].

This pattern is also visualized in Fig. 3. The edges detected under higher levels of noise are usually around nodes with high centrality, such as feelings of defeat (Def) or Perceived Burdensomeness (PB) in the example of Fig. 3.

[1] From 50% to 80% noise, the true positives drop by $\approx 46\%$, while the false positives drop by $\approx 63\%$.

Table 2. Degree centrality (C_D) and betweenness centrality (C_B) of nodes for GGM, Hill Climbing, and TABU graphs. The term in the bracket of the Node column refers to the abbreviation used in the plotted graphs.

Node	C_D GGM	C_D HC	C_D Tabu	C_B GGM	C_B HC	C_B Tabu
Depression (Dep)	12	7	7	40	7	0
Perceived Burdensomeness (PB)	12	6	6	18	7	6
Defeat (Def)	11	8	8	46	18	15
Resilience (Res)	11	4	4	34	0	0
Suicidal Thoughts (Si)	10	4	4	4	2	1
External Entrapment (Een)	10	6	6	34	15	13
Stress (Str)	10	5	5	4	8	1
Mental Well-being (MW)	9	8	8	54	10	9
Social Perfectionism (SoP)	9	2	2	0	0	0
Mental Imagery (MeI)	9	3	3	0	4	1
Thwarted Belongingness (TB)	8	5	5	26	10	9
Internal Entrapment (Ien)	8	4	4	30	4	2
Optimism (Opt)	7	1	1	0	0	0
Acquired Capabilities (Acq)	7	3	3	4	2	2
Social Support (SoS)	7	1	1	4	0	0
Exposure to Suicide (Exp)	6	1	1	0	0	0
Impulsivity (Imp)	4	2	2	0	1	0

3.3 Uncertainty: Data Quantity

Figure 2 shows the results for reducing the data quantity. As the sample size decreases, both precision and recall decline, with recall exhibiting a higher decrease across all three algorithms. HC and TABU perform similarly, though HC consistently outperforms TABU by a small margin. This is not surprising, since TABU can be viewed as an extension of HC. The performance of the GMM gradually decreases as well, but at a smaller rate compared to the causal discovery algorithms. Similar to the noise experiment, the GGM becomes sparser as the sample size decreases. While the retained edges are largely correct, many true edges from the original graph are omitted, likely due to the loss of power (see Fig. 4). This results in a relatively high precision and low recall. Notably, when 80% of the data is missing, the graph is estimated to be empty in approximately 8% of the cases. When 90% of the data is missing, the graph is empty every time.

3.4 Uncertainty: Causal Edges Leading to Suicidal Ideation

In the baseline HC graph two edges lead to suicidal ideation: depression and defeat, while in the TABU graph only depression leads to suicidal ideation.

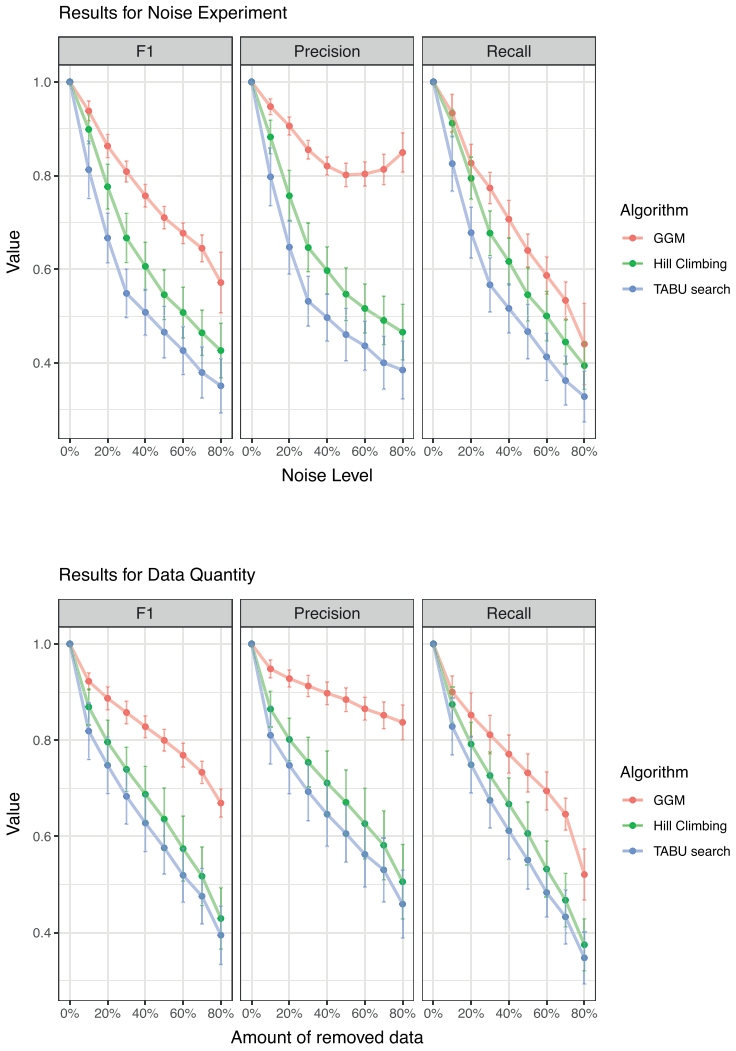

Fig. 2. Simulation results for all the evaluated uncertainty types across the causal discovery algorithms. The first plot depicts the results when adding noise and the second one for the reduction of the sample size. The errorbars correspond to the IQR range of observed values.

Figure 5 depicts the frequency of the edges across various noise levels and sample sizes (over 500 iterations). Depression → Suicidal ideation appears to be relatively robust across both noise and sample size reductions. At 40% noise, the edge was found in approximately 75% of the cases in both HC and TABU algorithms, while for 80% noise, it was slightly below 50%. A similar pattern is observed when reducing the sample size.

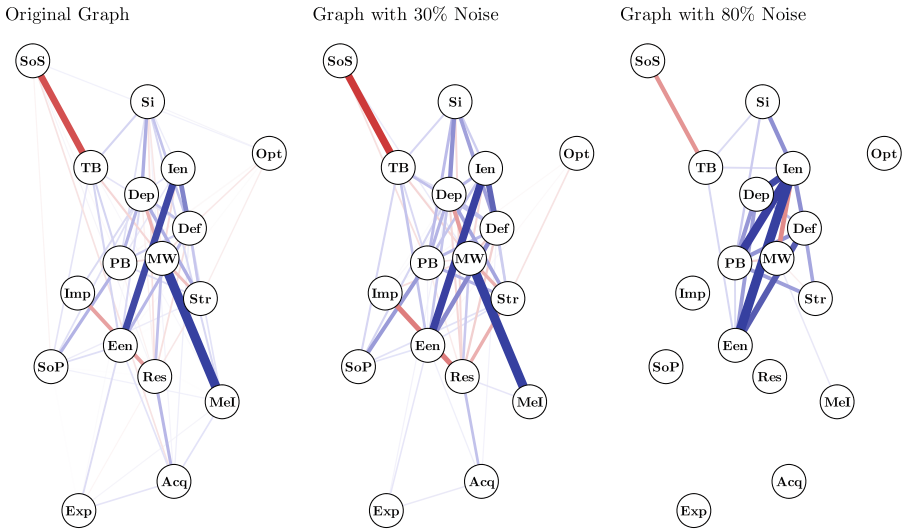

Fig. 3. GGM graph examples with noise. The graph on the left is the original graph, learned from the unmodified data, while the graph in the middle was learned with 30% noise and the one on the right with 80% noise. For node legend see Table 2.

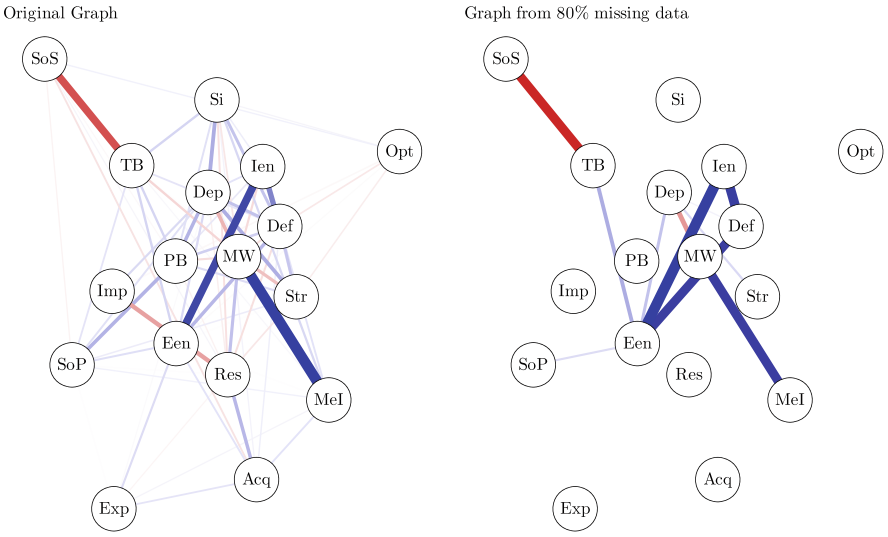

Fig. 4. GGM graph examples with compromised sample size. The graph on the left is the original graph, learned from the unmodified data, while the graph on the right was learned with data with 80% missing observations, meaning only 67 rows of observations were used instead of the full 333. For node legend see Table 2.

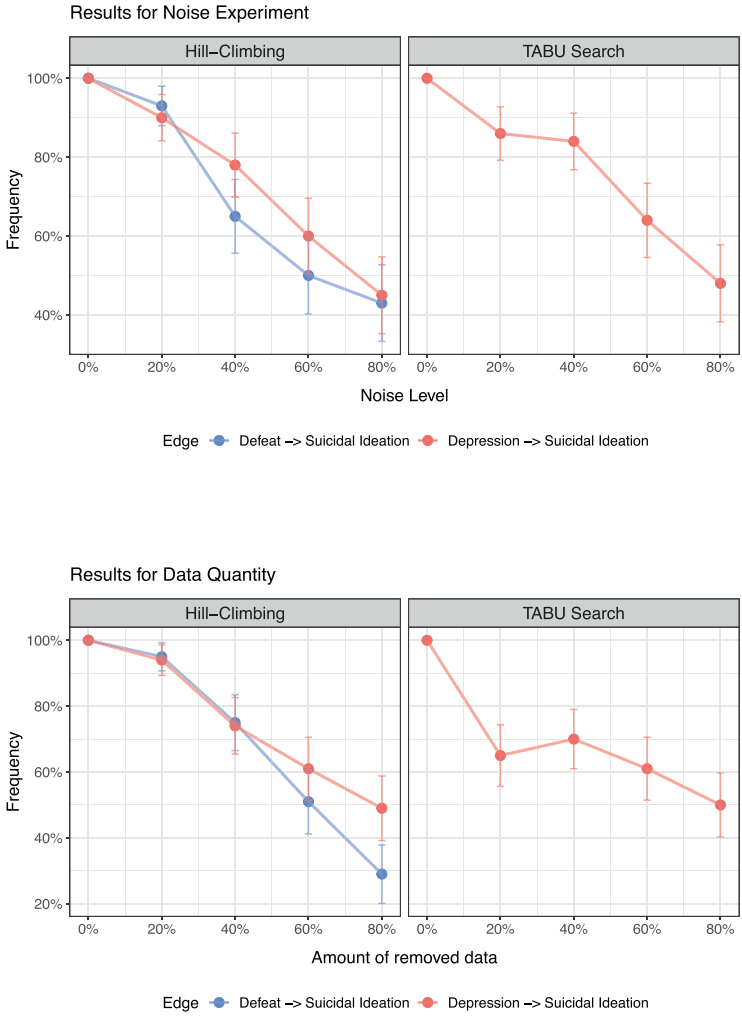

Fig. 5. Results for the experiments of the robustness of the edges leading to suicidal ideation for the Hill Climbing and TABU algorithm. The top plot depicts the results for the noise experiment and the bottom plot for the sample size. The y-axis refers to the frequency in percentage of the observed edges, averaged across all the observations. The error bars represent 95% confidence intervals.

The edge Defeat → Suicidal ideation is also relatively stable in the HC algorithm, although less than Depression → Suicidal ideation. From 20% noise onward, the frequency of this edge declines faster than for Depression → Suicidal ideation, so that at 60% noise, it is only present in half of the cases. When reducing the sample size, a similar trend is observed: up until 40% of the data is removed, both edges are present in over 70% of the cases, but when 60% of the

data is removed, Defeat → Suicidal is present in only half of the cases. For the TABU algorithm, this edge was not examined, since it was not present in the baseline graph in Fig. 1.

4 Conclusion

This study examined the impact of data-related uncertainty—specifically noise and data reduction—on the estimation of psychological networks. Overall, we found that the network structures were highly sensitive. Both HC and TABU search in particular were especially affected, with HC slightly outperforming TABU search. The GGM graphs mostly became very sparse, with high noise or data reduction resulting only in few estimated edges.

Among the edges leading to suicidal ideation, the edge from depression to suicidal thoughts remained consistently detectable across both noise and sample size. This is a promising result, implying that intervening on depressive mood could lead to changes in suicidal thinking. Indeed, there are multiple trials suggesting that targeting depressive symptoms can lead to lower suicidal ideation [11,18]. There are also specific suicide interventions, such as PROSPECT-an intervention for elderly people- whose main goal is to target depressive symptoms [4]. For a review of depression-based suicide interventions see [8].

Lastly, although this study is one of the first to examine data-related uncertainty in a psychological data set, there are a few limitations. For instance, we examined only one data set, meaning that for slightly different data, the results could be very different. Additionally, we examined only the network structure and did not analyze the parameter weights. Since determining the structure of a graph is typically the first step before estimating parameters, it is arguably a more critical aspect. Nevertheless, future research should further investigate the influence of data-related uncertainty on the edge weights. Despite these limitations, our study represents an important first step in exploring the impact of data-related uncertainties within a real psychological dataset. By highlighting the sensitivity of network structures to noise and data reduction, it lays the groundwork for future research aimed at improving network estimation methods in the context of psychological data.

Acknowledgments. This study was supported by the Research priority area Urban Mental Health of the University of Amsterdam, within the project "Understanding the Dynamics of Suicide: An Agent-Based Modeling Approach to Inform Intervention Strategies in an Urban Context".

Disclosure of Interests. The authors have no competing interests to declare that are relevant to the content of this article.

References

1. Beretta, S., Castelli, M., Goncalves, I., Henriques, R., Ramazzotti, D.: Learning the structure of Bayesian networks: a quantitative assessment of the effect of different algorithmic schemes (2018). https://doi.org/10.48550/arXiv.1704.08676. arXiv:1704.08676 [cs]
2. Bhattacharya, R., Nabi, R., Shpitser, I., Robins, J.M.: Identification in missing data models represented by directed acyclic graphs. In: Proceedings of The 35th Uncertainty in Artificial Intelligence Conference, pp. 1149–1158. PMLR, August 2020. https://proceedings.mlr.press/v115/bhattacharya20b.html. iSSN: 2640-3498
3. Borsboom, D.: A network theory of mental disorders. World Psychiatry **16**(1), 5–13 (2017). https://doi.org/10.1002/wps.20375. https://onlinelibrary.wiley.com/doi/abs/10.1002/wps.20375. _eprint: https://onlinelibrary.wiley.com/doi/pdf/10.1002/wps.20375
4. Bruce, M.L., Pearson, J.L.: Designing an intervention to prevent suicide: PROSPECT (Prevention of Suicide in Primary Care Elderly: Collaborative Trial). Dialogues Clin. Neurosci. **1**(2), 100–112 (1999). https://www.ncbi.nlm.nih.gov/pmc/articles/PMC3181574/
5. Cleare, S., Wetherall, K., Eschle, S., Forrester, R., Drummond, J., O'Connor, R.C.: Using the integrated motivational-volitional (IMV) model of suicidal behaviour to differentiate those with and without suicidal intent in hospital treated self-harm. Prev. Med. **152**, 106592 (2021)
6. Constantinou, A.C., Liu, Y., Chobtham, K., Guo, Z., Kitson, N.K.: Large-scale empirical validation of Bayesian network structure learning algorithms with noisy data. Int. J. Approximate Reasoning **131**, 151–188 (2021). https://doi.org/10.1016/j.ijar.2021.01.001. https://www.sciencedirect.com/science/article/pii/S0888613X21000025
7. De Beurs, D., et al.: Exploring the psychology of suicidal ideation: a theory driven network analysis. Behav. Res. Therapy **120**, 103419 (2019). https://doi.org/10.1016/j.brat.2019.103419
8. Dueweke, A.R., Bridges, A.J.: Suicide interventions in primary care: a selective review of the evidence. Families Syst. Health **36**(3), 289–302 (2018). https://doi.org/10.1037/fsh0000349
9. Epskamp, S., Borsboom, D., Fried, E.I.: Estimating psychological networks and their accuracy: a tutorial paper. Behav. Res. Methods **50**(1), 195–212 (2018). https://doi.org/10.3758/s13428-017-0862-1
10. Huth, K.B.S., Keetelaar, S., Sekulovski, N., van den Bergh, D., Marsman, M.: Simplifying Bayesian analysis of graphical models for the social sciences with easybgm: a user-friendly R-package. Adv./Psychol. **2**, e66366 (2024). https://doi.org/10.56296/aip00010. https://advances.in/psychology/10.56296/aip00010/
11. Lapierre, S., et al.: A systematic review of elderly suicide prevention programs. Crisis **32**(2), 88–98 (2011). https://doi.org/10.1027/0227-5910/a000076. https://econtent.hogrefe.com/doi/10.1027/0227-5910/a000076
12. McNally, R.J., Heeren, A., Robinaugh, D.J.: A Bayesian network analysis of posttraumatic stress disorder symptoms in adults reporting childhood sexual abuse. Eur. J. Psychotraumatol. **8**(sup3), 1341276 (2017). https://doi.org/10.1080/20008198.2017.1341276. https://www.ncbi.nlm.nih.gov/pmc/articles/PMC5632780/
13. Niu, W., Gao, Z., Song, L., Li, L.: Comprehensive review and empirical evaluation of causal discovery algorithms for numerical data, September 2024. https://doi.org/10.48550/arXiv.2407.13054. http://arxiv.org/abs/2407.13054 [cs] version: 2

14. de Ron, J., et al.: Quantifying and addressing the impact of measurement error in network models. Behav. Res. Therapy **157**, 104163 (2022). https://doi.org/10.1016/j.brat.2022.104163. https://www.sciencedirect.com/science/article/pii/S0005796722001346
15. RStudio Team: R: A Language and Environment for Statistical Computing (2020). http://www.rstudio.com/
16. Schutzeichel, F., et al.: Life meaning and feelings of ineffectiveness as transdiagnostic factors in eating disorder and comorbid internalizing symptomatology - a combined undirected and causal network approach. Behav. Res. Therapy **172**, 104439 (2024). https://doi.org/10.1016/j.brat.2023.104439
17. Scutari, M.: Learning Bayesian networks with the **bnlearn***R* package. J. Stat. Softw. **35**(3) (2010). https://doi.org/10.18637/jss.v035.i03. http://www.jstatsoft.org/v35/i03/
18. Sufrate-Sorzano, T., et al.: Interventions of choice for the prevention and treatment of suicidal behaviours: an umbrella review. Nurs. Open **10**(8), 4959–4970 (2023). https://doi.org/10.1002/nop2.1820. https://onlinelibrary.wiley.com/doi/10.1002/nop2.1820
19. Wetherall, K., et al.: From ideation to action: differentiating between those who think about suicide and those who attempt suicide in a national study of young adults. J. Affect. Disord. **241**, 475–483 (2018). https://doi.org/10.1016/j.jad.2018.07.074. https://linkinghub.elsevier.com/retrieve/pii/S0165032718312898
20. Wickham, H., et al.: Welcome to the Tidyverse. J. Open Source Softw. **4**(43), 1686 (2019). https://doi.org/10.21105/joss.01686

Making Astrometric Solver Tractable Through In-Situ Visual Analytics

Konstantin Ryabinin(✉), Wolfgang Löffler, Olga Erokhina, Gerasimos Sarras, and Michael Biermann

Astronomisches Rechen-Institut, Center for Astronomy of Heidelberg University, Mönchhofstr. 12–14, 69120 Heidelberg, Germany
{konstantin.riabinin,olga.erokhina,gerasimos.sarras}@uni-heidelberg.de,
{loeffler,biermann}@ari.uni-heidelberg.de

Abstract. In astronomy, precise determination of stellar positions, proper motions, and parallaxes based on space telescope observations is a Big Data problem. It requires a dedicated software solver running on a high-performance computer to analyse billions of input data records and produce an output stellar catalogue. The solution process relies on a sophisticated model to calibrate out the distortions, which are inevitably presented in the raw input data due to the imperfections of the telescope. After the solution is calculated, its quality must be assessed for physical correctness, scientific value, and possible ways of calibration model improvement. The tools for the solution quality assessment are as important as the solver itself and contribute to the solver's tractability by unveiling the path to fine-tuning the solving process. In our previous work, we created a high-performance astrometric solver AJAS suited for the Japan Astrometry Satellite Mission for INfrared Exploration (JASMINE). In the present work, we foster AJAS tractability by integrating it with the ontology-driven visual analytics platform SciVi leveraging the principles of multi-purpose ontology-driven API for in-situ data processing. This integration provides users with high-level management tools for AJAS computation jobs and high-level visual data mining tools for AJAS solutions. All these tools can be configured via a graphical user Web interface, extended in Jupyter Notebooks, and executed on the same computing resource as AJAS, which minimises the data transfer. In this paper, we elaborate on the technical details of the above-mentioned tools and demonstrate their capabilities on the real examples of the AJAS solution quality assessment.

Keywords: Astrometry · Data Fitting · Visual Analytics · Ontology Engineering · Big Data

1 Introduction

Astrometry is a branch of astronomy aiming to precisely determine stellar parameters like position, proper motion, and parallax based on raw telescope obser-

M. Paszynski et al. (Eds.): ICCS 2025 Workshops, LNCS 15912, pp. 154–167, 2025.
https://doi.org/10.1007/978-3-031-97573-8_11

vations. Accurate values of these parameters are crucial for fundamental astronomical and astrophysical studies of the structure and history of the Milky Way Galaxy [7].

An astrometric solver is a complex software pipeline tackling a Big Data problem with uncertainties. It reveals the stellar parameters based on a massive amount of observational data, which contain uncertainties in the form of various distortions and noise caused by the imperfections of the telescope optics, detector electronics, etc. To reach its scientific aim, an astrometric solver must be performant, numerically accurate, and provide tools for assessing and alleviating uncertainties propagated from the input data to the output.

In our research work, we contribute to the development of the astrometric solver for the Japan Astrometry Satellite Mission for INfrared Exploration (JASMINE) [10]. For JASMINE, a thorough exploration of the crowded area of the Milky Way centre is planned, which involves about 115 thousand stars with 9.2 billion observations. For this purpose we have developed at the Institute for Computational Astronomy (Astronomisches Rechen-Institut, ARI) of Heidelberg University, Germany, the ARI JASMINE Astrometric Solver (AJAS) suited for massively parallel high-performance computers [14,15].

For AJAS, we managed to solve the Big Data processing issue by proposing a dedicated software architecture and utilising state-of-the-art approaches to build high-performance applications. This allows AJAS to handle the expected full-scale JASMINE mission's data within 8.5 h on a cluster with 5000 CPU cores. In this paper, we propose an approach of making the AJAS tractable by the in-situ visual analytics platform SciVi [4] allowing for monitoring and assessing the solution outcome.

The key contributions of the paper are the following:

1. Bridging astrometry with in-situ visual analytics.
2. Developing the in-situ toolset for assessing the astrometric solution quality for AJAS.
3. Extending the smart interoperability of the SciVi visual analytics platform to better handle the in-situ processing cases.
4. Developing a high-performance data access library for AJAS solutions.

2 Methodology

In general, an astrometric observation o is the centroid with particular coordinates $(\kappa; \mu)$ of a stellar image taken by a telescope at a particular moment of time. The set of observations can be expressed as a function $\boldsymbol{o} = f(\boldsymbol{p})$, where $\boldsymbol{p}$ is a vector of model parameters describing, on the one hand, the best knowledge of the locations and motions of the stars on the celestial sphere, and, on the other hand, the best knowledge of the spatial orientation and imaging properties of the telescope used for making these observations. The function f has a complicated nature incorporating a lot of effects including, for example, relativistic effects such as aberration and light bending as well as image distortions

of the optical and electronic imaging system. Therefore, f is not fully known and cannot be expressed analytically nor inverted to straightforwardly get $\boldsymbol{p}$. Instead, an optimisation task arises to find the best fit of $\boldsymbol{p}$ by minimising the residuals $\boldsymbol{o} - \boldsymbol{c}$, where $\boldsymbol{c} = g(\boldsymbol{p})$ is a vector of predicted observations and g is a model of f. To adequately model the unknown f function by the g function, a calibration model is introduced that is supposed to describe the differences between the imaging properties of the ideally specified nominal telescope and the actually implemented telescope. The calibration model spawns its own nuisance parameters, which are included in the optimisation process as an integral part of $\boldsymbol{p}$.

The data fitting procedure is based on the least squares approach involving linearisation of g and subsequent solving of the linear equations system. This procedure has two major problems to tackle. The first problem is a Big Data issue concerning the size of the system. It depends on the particularities of the astrometric mission, but even for relatively small missions, the number of equations goes into the billions. The second problem is the quality of the calibration model. To approximate f by g within the target accuracy, the calibration model needs to be properly fine-tuned. These two problems impose challenging requirements the software astrometric solver should meet: it should be very high-performant, flexible, and tractable. It should also contain tools to assess the accuracy and correctness of the solution, and to appraise the ability of the calibration model to absorb systematic distortions.

3 Related Work

The JASMINE astrometric problem is formulated adopting the experience from the ESA Hipparcos [5] and ESA Gaia [7] space astrometry missions and solved by AJAS utilising the direct approach [14] similarly to the Gaia One Day Astrometric Solution (ODAS) [11]. This means that the system of equations for the least squares data fitting is solved in one go, without iterations, by inverting its reduced normal matrix $\boldsymbol{\mathcal{M}}$. Since $\boldsymbol{\mathcal{M}}$ by its nature is rank-deficient [14], AJAS leverages singular value decomposition to calculate its pseudo-inverse $\boldsymbol{\mathcal{M}}^{+}$. Computations rely on the state-of-the-art libraries ScaLAPACK [1] and EigenExa [16] for number crunching and MPI for inter-process communication. Along with that, hand-crafted optimisations for matrix operations are implemented by considering the peculiarities of the matrix structure and fine-tuning for data locality, efficient multithreading, CPU cache usage, and vectorisation [14].

The JASMINE problem is driven by data. This means that data access and storage are the main bottlenecks of the solver. While running, AJAS scans hundreds of gigabytes and produces terabytes of data, moreover the general data access pattern is highly random and very cache-unfriendly by its nature. A thorough inspection of the AJAS solution requires access to all the data generated during the calculations. For the traditional posthoc analysis made in software like TOPCAT [17], which is very popular among astronomers, it would be necessary to download the corresponding set of files from the cluster to gain local

access. Even the bare minimum subset for the meaningful analysis (for example, the array of solution residuals) is more than 100 gigabytes. This, in turn, would mean spending drastically more time for network communication, than the solving process takes, and potentially abusing the connection channel. Besides that, handling the required data volume locally imposes severe requirements on the performance of a local machine. The natural way to tackle this problem is going for the so-called *in-situ* techniques, which "attempt to avoid the overhead of fully loading and indexing the data in a database management system and improve performance by progressively building an index during data exploration" [12].

In-situ visualisation and analytics is a broad umbrella term that encloses the entire paradigm of processing data as it is generated [2,3]. H. Childs et al. propose an elaborated taxonomy of in-situ systems and define classification criteria to derive a dedicated type for an arbitrary in-situ system [2]. The main idea of in-situ processing is twofold: the data can be processed before their generation is finished, and data transferring overhead is minimised.

Recently, one of the popular and flexible ways of organising in-situ data processing is Jupyter running on the side of a high-performance computer and exposing a Python interpreter to the user via a Web browser [9,18]. Analysis within Jupyter Notebooks gives all the freedom of Python scripting but requires corresponding programming skills from the scientist. In contrast, scientific visualisation systems like ParaView and VisIt provide in-situ processing capabilities with a high-level graphical user interface, smoothing the learning curve but constraining the scientists by a predefined set of analytical tools [3].

To balance between these two approaches, we leverage the in-situ visual analytics for AJAS with the ontology-driven platform SciVi [4,13]. SciVi can run in userspace on high-performance computers, exposes a Web interface, and provides an intuitive visual programming language based on data flow diagrams for defining visual analytics pipelines using a set of predefined operators. The defined pipelines can then be either executed directly within SciVi or automatically transformed into the Jupyter Notebooks. The latter allows for the extension of SciVi operators in Python should they not be enough for advanced analytics beyond the main expected analytical scenarios. Along with that, it is very easy to extend SciVi with new operators written in Python, C++, and JavaScript, making them immediately available in the SciVi Web GUI.

SciVi also can be seamlessly integrated with AJAS supplying settings parameters directly to AJAS modules and allowing the monitoring of intermediate AJAS state on the fly.

4 AJAS Job Management

Typically, AJAS runs on a CPU cluster as a job that is first submitted to the specific execution queue. The job defines the requested resources (including amount of RAM, number of cluster nodes and CPU cores, time limit, etc.), the runtime environment, and the configuration of AJAS (including paths to input and output data, multithreading parameters, etc.). Traditionally, a job is described and

submitted manually, which requires an understanding of the cluster architecture and knowledge of the specific notation supported by the particular queue manager. The monitoring of the execution is then also manual by requesting the job status, while no information about the actual AJAS progress can be retrieved. In this sense, the job submission preparations might be tedious and the tractability of AJAS is limited.

The SciVi system overcomes this hurdle. For AJAS and the cluster, on which AJAS should run, ontological profiles are created and saved in the SciVi knowledge base. The AJAS ontological profile (see Fig. 1) describes the AJAS settings and output data types. The cluster ontological profile (see Fig. 2) describes resource limits and available queue types, as well as provides a job template for the queue manager and the job status retrieving commands. By parsing these profiles, SciVi automatically builds an intuitive user interface for creating the AJAS jobs and monitoring their state. Only high-level settings are exposed to the interface, for example, paths to input and output data and the type of queue to submit the job to. The low-level settings like multithreading options ("Number of Building Threads" and "Number of Summation Threads") are calculated automatically to gain maximal performance. The process grid ("Number of Processes" and "Number of CPU Cores per Process") and time limit settings are customizable but SciVi automatically calculates default values for them based on the chosen input data and queue type. The formulas to calculate the defaults are a part of the AJAS ontological profile (contained in the "AJAS Job" implementation). The service outputs "Start Date" and "Progress" allow monitoring of the particular AJAS job status in realtime.

5 AJAS Solution Analysis

Another part of the demanded AJAS tractability is tuning the solving process and the calibration model based on the solution quality assessment.

The solution analysis consists of two main steps: automatic generation of a standard report and custom data mining. The standard report contains a set of visual and numerical metrics, which, based on our experience, are needed to estimate the solution quality. Custom data mining relies on the interactive SciVi capabilities. The data mining is applicable only if a standard report indicates some solution problems, and it aims to unveil the causes of these problems.

The list of metrics for the standard report and the palette of tools for the custom data mining are still incomplete and are a matter of extension when the real JASMINE mission data will be available. So, here we describe only three items to demonstrate the idea of our visual analytics pipeline: plotting the spectrum of $\boldsymbol{\mathcal{M}}$, fitting the Gaussian function to the distribution of astrometric residuals, and plotting the map of uncertainties in the stellar parameters. The presented analytical examples are demonstrated on the test cases, which contain 10 thousand stars and 800 million observations and are solved for two astrometric parameters (stellar position).

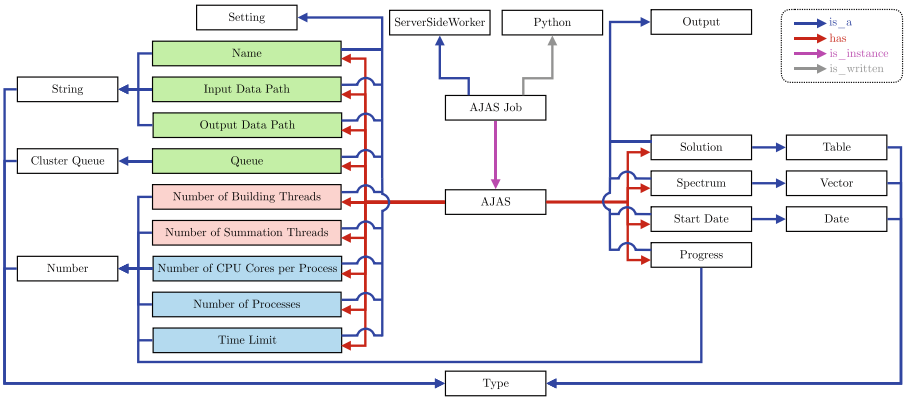

Fig. 1. A fragment of AJAS ontological profile. For the nodes, green highlights the settings given by the user, blue highlights customizable settings which have computable default values, red highlights settings which are determined automatically. (Color figure online)

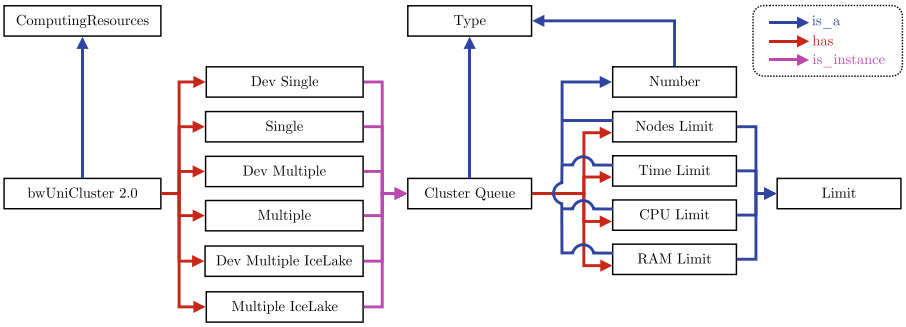

Fig. 2. A fragment of bwUniCluster 2.0 (the cluster available for academic use for the universities of Baden-Württemberg, Germany) ontological profile.

5.1 Plotting the Spectrum of $\mathcal{M}$

The mathematical foundation of AJAS has been elaborated in [14]. The main idea is to solve the linearised system

$$\mathcal{D}\boldsymbol{x} = \boldsymbol{o} - \boldsymbol{c}, \tag{1}$$

where $\mathcal{D} = (\mathcal{CS})$, $\mathcal{C}$ is the matrix of the Jacobian derivatives of the calibration model, $\mathcal{S}$ is is the matrix of the Jacobian derivatives of the stellar parameters, $\boldsymbol{o}$ is the vector of observations, $\boldsymbol{c}$ is the vector of predicted observations. These predictions are made for the given observation model represented by the derivatives in $\mathcal{D}$ and the initial guess of the calibration and stellar parameters $\boldsymbol{p}$. Then, $\boldsymbol{x}$ is a vector of updates for $\boldsymbol{p}$.

The system (1) is overdetermined and the normal matrix $\boldsymbol{\mathcal{N}} = \boldsymbol{\mathcal{D}}^{\mathsf{T}}\boldsymbol{\mathcal{D}}$ is rank-deficient, so we use the least squares fitting to resolve $\boldsymbol{x}$. For this, the pseudo-inverse matrix $\boldsymbol{\mathcal{N}}^{+}$ must be found, which is computationally not possible because of the huge size of $\boldsymbol{\mathcal{N}}$. Instead, a reduced normal matrix $\boldsymbol{\mathcal{M}}$ is calculated by forward-eliminating parts of $\boldsymbol{\mathcal{C}}$ [14]. The $\boldsymbol{\mathcal{M}}$ matrix is then almost two orders of magnitude smaller than $\boldsymbol{\mathcal{N}}$ and can be inverted in reasonable time by the singular value decomposition:

$$\boldsymbol{\mathcal{M}}^{+} = \boldsymbol{\mathcal{Z}}\boldsymbol{\mathcal{E}}^{-1}\boldsymbol{\mathcal{Z}}^{\mathsf{T}}, \tag{2}$$

where $\boldsymbol{\mathcal{Z}}$ is a matrix of eigenvectors and $\boldsymbol{\mathcal{E}}$ is a diagonal matrix of singular values (non-zero eigenvalues) of $\boldsymbol{\mathcal{M}}$.

The eigenvalue spectrum of $\boldsymbol{\mathcal{M}}$ gives information about the degeneracy of the system. Because of its inherent rank deficiency, the eigenvalue spectrum of $\boldsymbol{\mathcal{M}}$ will always contain zero eigenvalues. These can, however, be eliminated by appropriately constraining the system. If not eliminated by constraints, these algebraically but not necessarily numerically zero eigenvalues pose a problem. In addition, more eigenvalues may become numerically small when there are not enough observations to determine the corresponding model parameter, contributing to the same problem. Once inverted in (2), these near zero eigenvalues will become large and numerically destroy the solution. To prevent this, they have to be zeroed out in $\boldsymbol{\mathcal{E}}^{-1}$.

Logarithmic spectrum plots (Fig. 3) help to inspect the consistency of input data and the numerical stability of the solution. For example, the top plot in Fig. 3 shows that the spectrum has several very small eigenvalues spanning the spectrum's dynamic range from 10^{-10} to 10^{8}, which is beyond the range of 64-bit floating point data type. This indicates the numerical instability and degeneracy of the system. The degeneracy comes from the fact that the system has the freedom to either calibrate the observations, bringing them to the predicted stellar positions, or to update the stellar positions, bringing them to the observations. To restrict this freedom, the set of stars is used, whose parameters are known with high precision. These stars come from the Gaia DR3 catalogue [6]. For them, extra summands are put to the $\boldsymbol{\mathcal{S}}$ block of the system's design matrix $\boldsymbol{\mathcal{D}}$ reinforcing the weight of corresponding Jacobian derivatives. The improvement of the spectrum in this case is shown in the bottom plot in Fig. 3.

In some cases, zero and also negative eigenvalues may pop up. To stick with the logarithmic scale, absolute values of eigenvalues are taken, and those, which were negative, are then marked red in the plot and a corresponding legend appears explaining the meaning of colours.

5.2 Fitting a Gaussian to the Residuals

If all systematic uncertainties have been accounted for by the calibration model, the residuals $\boldsymbol{r} = \boldsymbol{o} - \boldsymbol{c} - \boldsymbol{\mathcal{D}}\boldsymbol{x}$ should have a perfect Gaussian distribution reflecting the remaining, purely random observational noise. If the distribution of $\boldsymbol{r}$ differs from Gaussian, it means, that the utilised calibration model was unable to

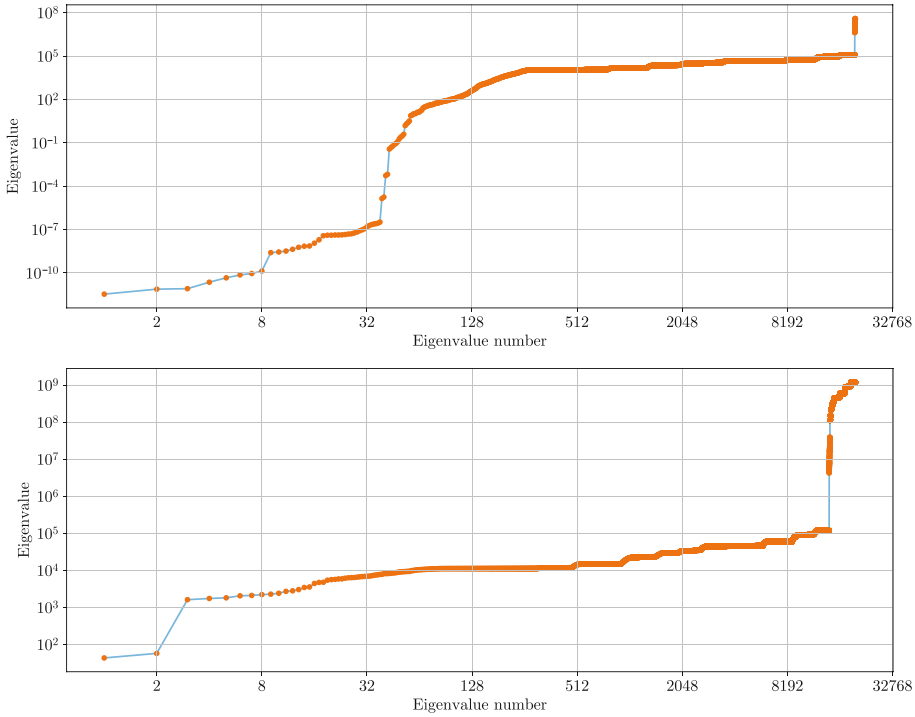

Fig. 3. Plot of the $\mathcal{M}$ spectrum drawn by SciVi using matplotlib [8]. Top: the $\mathcal{S}$ block of the system's design matrix $\mathcal{D}$ is *not* reinforced by the stars from the Gaia DR3 catalogue, bottom: the $\mathcal{S}$ block *is* reinforced.

absorb all the systematic errors of the observations, for example, optical distortions introduced by the telescope, geometrical imperfections of the focal plane, etc. In this case, $\boldsymbol{x}$ is not the desired astrometric solution and the calibration model has to be improved. Finding the way to that improvement is a challenge. The first step in that way is the identification of the observations, which deviate the distribution from the Gaussian. The common characteristics of these observations will then give a hint, which effects are missing in the calibration model.

To allow this type of analysis, the histogram of residuals is built and the Gaussian curve is fitted to it. There are also tools, which provide the possibility to perform this operation on an arbitrary subset of observations. Figure 4 demonstrates the corresponding visualisation results for two cases. Both plots show residuals in one direction (η) of the field-of-view reference system (FoVRS). The top plot corresponds to the case when the calibration model is unable to absorb all systematic distortions. Two problems are immediately seen: the goodness of fit for the Gaussian curve is not high enough, just 0.97, and, more importantly, the Gaussian distribution is not centred at zero ($\mu = 10^{-9}$). The bottom plot shows the case when all the systematic distortions are removed. The goodness

of fit for the Gaussian curve is almost exactly 1.0 and it is centred at zero ($\mu = 10^{-14}$), which reflects the pure random observational noise.

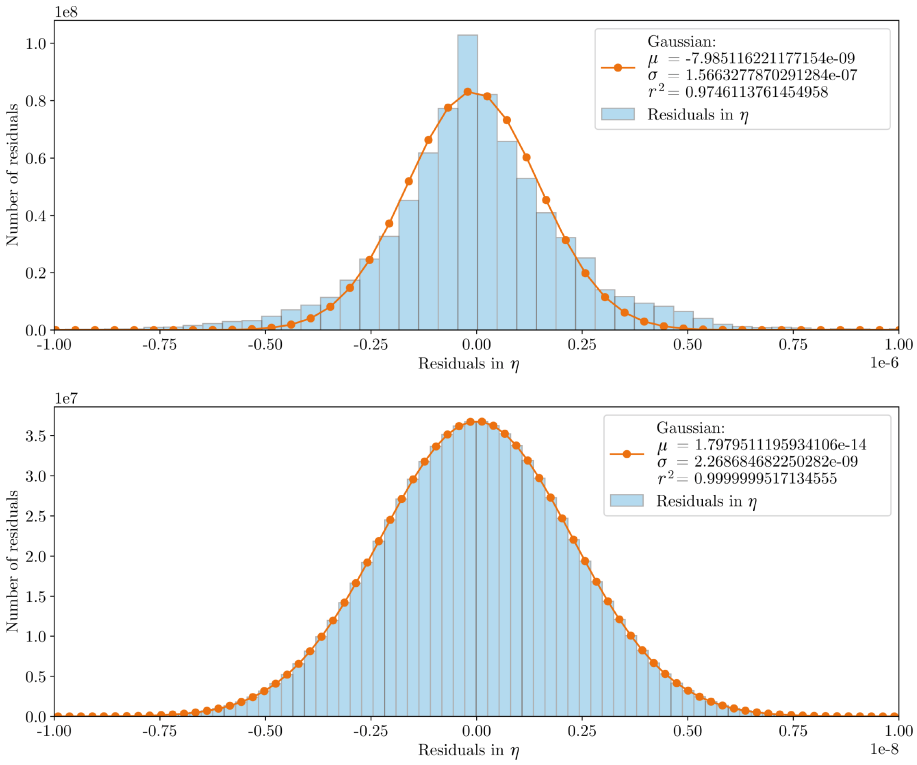

Fig. 4. Fitting the Gaussian curve to the histogram of residuals drawn by SciVi using matplotlib. Top: systematic remains in the residuals, bottom: systematic is fully removed. Note, that the axes of both plots have different scales.

5.3 Plotting the Stellar Uncertainties

The pseudo-inverse matrix $\mathcal{M}^+$ is a covariance matrix for the $\mathcal{S}$ block of (1), which means, its main diagonal contains standard errors of the stellar parameters. The square roots of these elements represent corresponding uncertainties, which, in turn, can be used for the solution quality assessment. To visually inspect them, we plot them as a colour-coded stellar map (see Fig. 5). The dots correspond to the stars drawn in the International Celestial Reference System (ICRS), and the colours represent uncertainties of a chosen stellar parameter (for example, one of the position coordinates). This representation way highlights the sky regions, which are covered worse than others by observations. Based on this

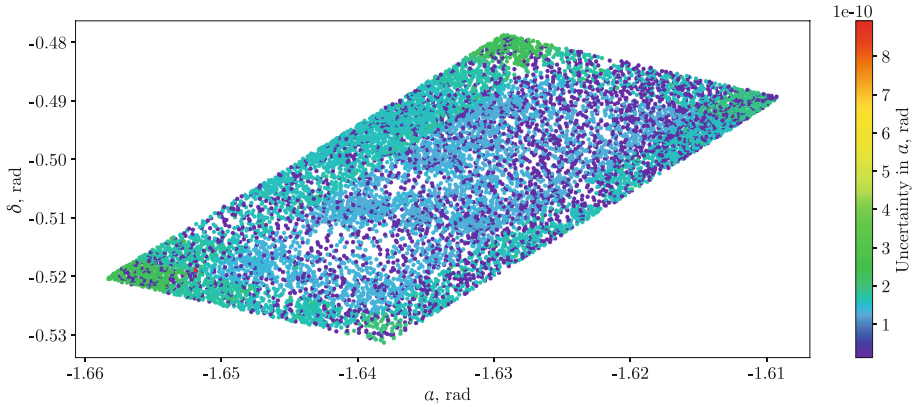

Fig. 5. Map of stellar uncertainties of the first position coordinate in ICRS drawn in SciVi using matplotlib.

information, the observation strategy of the satellite can be amended to improve coverage of these problematic regions.

In this example, four categories of stars can be visually distinguished according to the uncertainty of the α coordinate (one angular position coordinate in ICRS):

1. Stars with very low uncertainty are highlighted with a violet colour. As mentioned in Sect. 5.1, these stars have a very good initial guess of their position because they are taken from the Gaia DR3 catalogue and used to resolve the degeneracy between the calibration model and stellar positions. As can be seen in Fig. 5, they are distributed pretty evenly over the JASMINE target region, providing good coverage of the observed field.
2. Stars with acceptably low uncertainty are highlighted with a blue colour. These are the majority of stars inside the JASMINE target region, which have been observed a sufficient number of times to obtain a high-quality astrometric solution.
3. Stars with higher uncertainty are highlighted with a greenish and green colours. These stars are on the border (especially in the corners) of the JASMINE target region, so they are observed fewer times, which slightly worsens the quality of the astrometric solution for them.
4. A single star located approximately at $(-1.652; -0.519)$ with very high uncertainty is highlighted with a red colour. This star has only 59 observations, while the others have, on average, 77 thousand observations (almost four orders of magnitude more). Therefore, the solution of this star should be used with caution. However, since in this category there is only one star out of 10 thousand observed in this test case, the overall quality of the solution is considered high.

As an improvement for this visualization type, we plan to implement the ability to query and plot corresponding observations for chosen stars on demand.

Plotting all observations at once is pointless, but showing individual observations for specific stars at the appropriate zoom level might be helpful for inspecting the astrometric solution.

In the future, we are also interested in finding a presentation form for the off-diagonal elements of $\mathcal{M}^+$, which express the covariances of different stellar and higher-order calibration parameters.

5.4 Organizing the Custom Visual Analytics in SciVi

The standard report gives an overview of the whole solution, but if problems are identified, more fine-grained manual analysis is needed. SciVi allows the user to customize the analytical pipeline defining particular data flow diagrams (DFDs), which declare querying, transforming, and visualizing appropriate subsets of data.

Let us assume for example that the fitting of the Gaussian curve to the whole set of residuals leads to unsatisfactory results. It means that the input data contain systematic distortion that was not absorbed by the calibration model. To identify which observations introduce this distortion, different subsets of the solution should be investigated individually. Figure 6 demonstrates the DFD describing a custom visual analytics pipeline. The AJAS solution is filtered to extract its subset according to the given criteria specified in the settings of the "Filter" operator. These settings are not shown in the diagram as they are displayed separately in the SciVi user interface when the user clicks on this operator. Then, a histogram is created and a Gaussian curve is fitted to it. Then, both the histogram and the curve are plotted, joined together and displayed to the user.

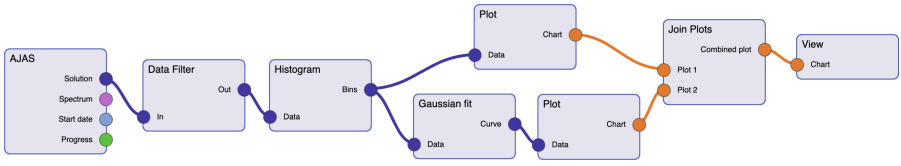

Fig. 6. DFD of a custom visual analytics pipeline in SciVi.

Each operator has its own ontological profile (like, for example, the one for AJAS is shown in Fig. 1). This profile specifies the inputs, outputs, and settings of the operator along with its implementation and the computing resource it should be executed on. Based on this information, SciVi maintains the graphical user interface of the operator, its appearance in the DFD, and its interoperability with other operators within the pipeline defined by DFD.

In the DFD from Fig. 6, all the operators except for the "View" are specified to run on the server (supercomputer) side to have direct access to the data. The "View" operator combines two actions: rendering of the plot, which is also

performed on the server side, and displaying the rendering result to the user, which happens on the client side (in the user's Web browser). The ontological profile of the compound "View" operator is shown in Fig. 7. Here, suboperators "Render" and "Display" are linked to "View" as its parts, and the output of "Render" is declared to be used as an input of "Display", while "Render" is linked to the server side and "Display" is linked to the client side. The data transfer between them is managed by SciVi automatically.

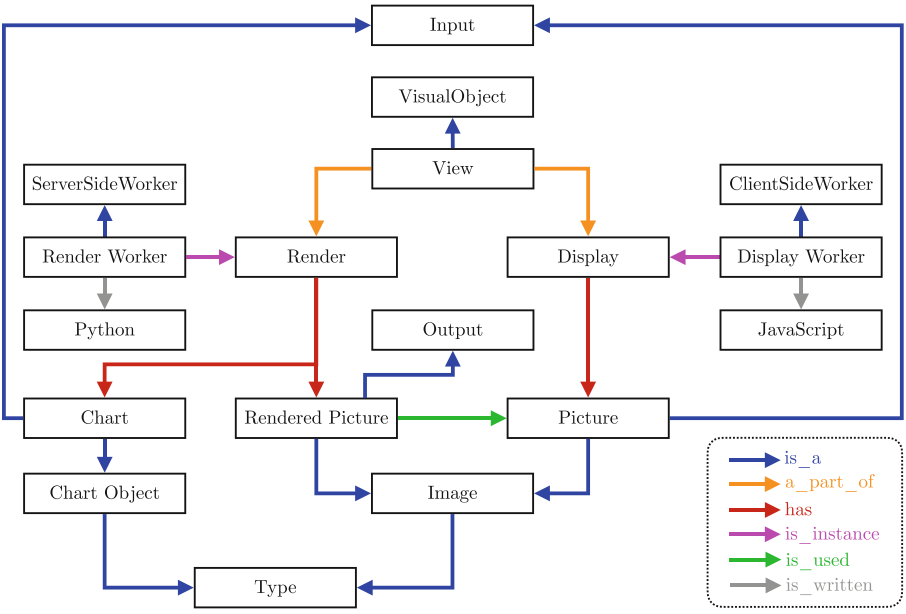

Fig. 7. Ontological profile of the "View" operator.

The concept of compound operators is new to SciVi and is first introduced in this work. It is a further improvement of the smart interoperability introduced in [13]. Smart interoperability allows different operators within the same DFD to run on different computing resources and freely exchange the data with minimal transmission overhead. However, each regular operator is tied to its computing resource. The compound operators generalise the smart interoperability approach to the cases, where a single operator is distributed over several different computing resources. This makes SciVi DFDs more versatile, efficient, and concise.

All the AJAS-related server-side SciVi operators rely on the Rapid ACCess Operations On Numerical Solutions (RACCOONS) library. We developed this library in C++ and created a binding to Python. Its core implements a multithreaded data querying engine and its Python interface provides `pandas`-like access to the AJAS solution. The querying engine supports lazy caching and on-

demand indexing of data, which optimises the analytics process when the user issues requests for data of a similar nature.

Since SciVi operators are internally implemented in Python, it was for us straightforward to implement the automatic dumping of any particular SciVi visual analytics pipeline to a Jupyter Notebook. This feature allows the user to customise the pipeline even further and build upon it more complicated processing machinery using Python.

6 Conclusion

We integrate the ontology-driven visual analytics platform SciVi with AJAS using the principles of a multipurpose ontology-driven API and run them on the same computing resource to avoid unnecessary data transfer. Within the SciVi environment, we developed a set of tools providing both automatic and human-in-the-loop operation controls, which enable AJAS tractability via in-situ visualisation and analytics. SciVi exposes these tools via a Web interface and automatically generates for them an intuitive graphical user interface that allows the users to build data processing pipelines using a visual programming language based on data flow diagrams. These tools facilitate starting AJAS on a cluster, monitoring its progress, and extensive analysis of its output. Advanced visual analytics helps to assess the quality of astrometric solutions produced by AJAS, identify the issues and find out the ways to corresponding improvements via the fine-tuning of the AJAS solving process.

Data processing pipelines created in SciVi can be automatically converted into Jupyter Notebooks and then further customized in Python.

We demonstrate the SciVi capabilities on three examples of analysing $\mathcal{M}^+$ spectrum, astrometric system's residuals, and astrometric parameters' uncertainties. This list, however, is still incomplete to fully assess the quality of the astrometric solution, so, a part of future work is to extend this toolset with other instruments and metrics. Another direction of improvement is the optimisation of the RACCOONS library that provides efficient access to the AJAS data.

Acknowledgments. This work was financially supported by the German Aerospace Agency (Deutsches Zentrum für Luft- und Raumfahrt e.V., DLR) through grant 50OD2201. The authors acknowledge support by the state of Baden-Württemberg through bwHPC. The authors also thank the National Astronomical Observatory of Japan (NAOJ) for fruitful discussions about the mission specifics.

References

1. Blackford, L.S., et al.: ScaLAPACK Users' Guide. Society for Industrial and Applied Mathematics, Philadelphia, PA (1997)
2. Childs, H., et al.: A terminology for in situ visualization and analysis systems. Int. J. High Perform. Comput. Appl. **34**(6), 676–691 (2020). https://doi.org/10.1177/1094342020935991

3. Childs, H., Bennett, J.C., Garth, C.: In Situ Visualization for Computational Science. Springer, Cham (2022)
4. Chuprina, S., Ryabinin, K., Koznov, D., Matkin, K.: Ontology-driven visual analytics software development. Program. Comput. Softw. **48**, 208–214 (2022). https://doi.org/10.1134/S0361768822030033
5. ESA: The Hipparcos and Tycho Catalogues. ESA SP-1200 (1997). https://www.cosmos.esa.int/web/hipparcos/catalogues
6. Collaboration Gaia et al.: Gaia data release 3 - mapping the asymmetric disc of the milky way. Astron. Astrophys. **674**, A37 (2023). https://doi.org/10.1051/0004-6361/202243797
7. Collaboration Gaia et al.: The Gaia mission. Astron. Astrophys. **595**, A1 (2016). https://doi.org/10.1051/0004-6361/201629272
8. Hunter, J.D.: Matplotlib: a 2D graphics environment. Comput. Sci. Eng. **9**(3), 90–95 (2007). https://doi.org/10.1109/MCSE.2007.55
9. Ibrahim, S., Stitt, T., Larsen, M., Harrison, C.: Interactive in situ visualization and analysis using ascent and Jupyter. In: Proceedings of the Workshop on In Situ Infrastructures for Enabling Extreme-Scale Analysis and Visualization, ISAV 2019, pp. 44–48. Association for Computing Machinery, New York, NY, USA (2020). https://doi.org/10.1145/3364228.3364232
10. Kawata, D., et al.: JASMINE: near-infrared astrometry and time-series photometry science. Publ. Astron. Soc. Japan **76**(3), 386–425 (2024). https://doi.org/10.1093/pasj/psae020
11. Löffler, W., et al.: The one-day astrometric solution for the Gaia mission. Astron. Astrophys. (in preparation)
12. Papastefanatos, G., Alexiou, G., Bikakis, N., Maroulis, S., Stamatopoulos, V.: VisualFacts: a platform for in-situ visual exploration and real-time entity resolution. In: EDBT/ICDT Workshops (2022). https://api.semanticscholar.org/CorpusID:248893496
13. Ryabinin, K., Chuprina, S., Labutin, I.: Tackling IoT interoperability problems with ontology-driven smart approach. In: Rocha, A., Isaeva, E. (eds.) Perm Forum 2021. LNNS, vol. 342, pp. 77–91. Springer, Cham (2022). https://doi.org/10.1007/978-3-030-89477-1_9
14. Ryabinin, K., Sarras, G., Löffler, W., Olga, E., Biermann, M.: AJAS: a high performance direct solver for advancing high precision astrometry. J. Comput. Sci. (2025). https://doi.org/10.1016/j.jocs.2025.102554
15. Ryabinin, K., Sarras, G., Löffler, W., Erokhina, O., Biermann, M.: Satellite telescope self-calibration through precise stellar data mining. Front. Artif. Intell. Appl. **398**, 248–254 (2024). https://doi.org/10.3233/FAIA241425
16. Sakurai, T., Futamura, Y., Imakura, A., Imamura, T.: Scalable eigen-analysis engine for large-scale eigenvalue problems. In: Sato, M. (ed.) Advanced Software Technologies for Post-Peta Scale Computing, pp. 37–57. Springer, Singapore (2019). https://doi.org/10.1007/978-981-13-1924-2_3
17. Taylor, M.: TOPCAT: working with data and working with users (2017). https://arxiv.org/abs/1711.01885
18. Tsai, S.R., Schive, H.Y., Turk, M.: Libyt: a tool for parallel in situ analysis with YT, Python, and Jupyter. In: Proceedings of the Platform for Advanced Scientific Computing Conference. PASC 2024. Association for Computing Machinery, New York, NY, USA (2024). https://doi.org/10.1145/3659914.3659939

Scheduling in Workflow-as-a-Service Model with Pre-parameterized DAG Using Inaccurate Estimates

Victor Toporkov(✉), Dmitry Yemelyanov, and Artem Bulkhak

National Research University "MPEI", Moscow, Russia
{ToporkovVV,YemelyanovDM,BulkhakAN}@mpei.ru

Abstract. Workflow is currently the most common execution model for composite applications across multiple disciplines: seismology (CyberShake), bioinformatics (Epigenomics, SIPHT), astrophysics (Montage), gravitational wave physics (LIGO), hydro and aerodynamics, quantum chemistry, nanotechnology, hydrometeorology, modeling of social systems and transport infrastructure. The workflow is usually a collection of interrelated tasks within the directed acyclic graph (DAG) model parameterized by a priori, usually inaccurate, user estimates for tasks (relative computational or data transfer volumes, execution durations etc.). In this work, we propose an approach for scheduling science-intensive applications within the framework of the concept of Workflow-as-a-Service (WaaS). The proposed scheduling model is built based on the critical jobs' method, which allows us to obtain the deadlines for completing each of the workflow tasks under given efficiency criteria and inaccurate user estimates. This schedule must consider the actual dynamics of the WaaS resources' utilization and lifecycle of virtual machines (VMs). To solve this problem, we propose a novel procedure to group and assign workflow tasks to VMs instances provided by the Infrastructure as a Service (IaaS) provider.

Keywords: Cloud Computing · Scientific Workflow · Scheduling · Inaccurate Estimates · Critical Job · Task · Batch · Hungarian algorithm

1 Introduction

Many well-known scientific-intensive projects, such as Montage, CyberShake, Epigenomics, SIPHT, and LIGO are implemented as workflows [1–16]. IaaS allows a Workflow Management System (WMS) to access a practically unlimited pool of virtualized resources on a "pay-per-use" basis. To date, there are a huge number of workflow management systems [17]. They include ASKALON, Galaxy, HyperFlow, Kepler, Pegasus, Taverna, CloudBus and several others. The paradigm of WaaS makes it possible to implement effective mechanisms for managing continuous flows of diverse types of jobs in cloud computing. However, this raises a few fundamental problems associated with organizing the scheduling of the heterogeneous job-flows and composite applications.

M. Paszynski et al. (Eds.): ICCS 2025 Workshops, LNCS 15912, pp. 168–182, 2025.
https://doi.org/10.1007/978-3-031-97573-8_12

The main purpose of the presented solution is the implementation of WaaS platforms for monitoring, processing requests, scheduling, and managing heterogeneous cloud resources, and in particular, the dynamic creation and removal of VMs and containers for their efficient assignment to various workflows tasks.

The proposed solution intends to take into account a number of important aspects: 1) the presence of multiple IaaS providers and different types of resources; 2) geographic distribution of data centers; 3) heterogeneity of workflows; 4) the need to implement the "pay-per-use" model for a specific system user; 5) finally, solving the problem of an efficient deploying of VMs and providing many containers ready for multi-threaded environment on physical servers.

The rest of this paper is organized as follows. Section 2 reviews work that is related to our discussion. Section 3 presents the critical jobs' method (CJM) method for scheduling science-intensive applications and its implementation. Sections 4 and 5 introduce strategies and a general optimization scheme for VMs allocation. Sections 6 and 7 contain software implementation details and workflows scheduling results obtained for the considered algorithms. Section 8 summarizes the paper.

2 Related Works

The development of cloud technologies and WMS has given new impetus to research in the field of workflow scheduling in various applications. In particular, one of the areas of research is related to the active development of a paradigm in cloud computing WaaS [1–16].

As a rule, in known scheduling algorithms, the total cost of executing a workflow is used as one of the optimization criteria or restrictions [1–6, 13]. The work [1] proposes an approach to scheduling workflows in a container cloud environment for the WaaS model. The paper [2] introduces the use of a workflow broker based on a combination of on-demand and spot resource instances to minimize flow execution costs while meeting deadline constraints. The authors of [4] propose a time- and budget-aware dynamic workflow scheduling (DDBWS) algorithm designed specifically for WaaS environments. DDBWS schedules workflows by solving the problem of packing multiple resources. Unlike existing algorithms, it simultaneously considers the processor and memory demands of tasks. The proposed algorithm can significantly reduce the total number of rented VMs. In [6], the results of expanding the functionality of WMS CloudBus to process multiple workflows are presented and a prototype of a WaaS cloud platform for applications in the field of bioinformatics is proposed. A budget-constrained resource scheduling algorithm for multiple workflows (EBPSM) is implemented. In [13], a scheduling method is proposed that can reduce monetary costs and complete the work process within the minimum execution time. To analyze the performance of the proposed algorithm, an experiment is carried out in the WorkflowSim environment, and the results are compared with existing well-known algorithms - HEFT and DHEFT.

One of the main challenges of workflow scheduling is to make it energy efficient for cloud providers [3, 14, 16]. To date, formal formulations of workflow scheduling problems in scientific applications with several criteria are known [7, 8]. Artificial intelligence methods are increasingly being used in workflow scheduling tasks [5, 9, 10].

An important issue is representing the workflow model as a DAG. In a number of applications, loops are present naturally. In some known WMS (Pegasus. Apache Airflow, Taverna, Kepler) palliative techniques are used. This results in increased planning time.

In this work, in contrast to the studies discussed above, we propose innovative technologies and tools for scheduling and managing workflows of varying complexity and structure, considering many factors affecting the efficiency of using cloud platform resources, and the simultaneous passage of workflows on WaaS platforms.

3 Workflow Scheduling with Critical Jobs' Method

3.1 Critical Jobs' Method

The core of WaaS system is obviously the algorithm for processing and scheduling the workflows. Although there are many approaches to this problem, including classical ones and presented in the above section, we begin our consideration with the Critical Jobs' Method (CJM). The main important feature of CJM is the possibility to prepare ***a reference scheduling plan*** and define execution ***deadlines*** for each task of the workflow using ***a priori, usually inaccurate, user estimates***.

More formally, the CJM algorithm solves the following problem. The workflow of data-dependent tasks can be represented with DAG, the vertices of which correspond to tasks and data transfers (Fig. 1). The processing of the flow of independent tasks is implemented in groups, in which the tasks are ordered by priorities. A ***job*** is a sequence of tasks (a path on the DAG). Let G be a parameterized workflow graph with various levels of parallelism of its partially ordered tasks. The partial order relation on the set $T = J \cup D$ of tasks and data transfers is defined with a DAG, where a subset J correspond to computational tasks, and a subset D - to the data transfers between the tasks. The set of oriented edges of the graph represents information and logical connections and dependencies. The graph is parameterized by a priori estimates of relative computational or data transfer volumes v_{ik}, execution durations t_{ik}^0 for tasks $j_i \in J$, $i = 1, \ldots, n$, on the corresponding resource type $k \in K$, K is a number of resource types, and n is a number of tasks. Examples of these parameters for graph from Fig. 1 on four types of resources are given in Table 1.

We define the distribution r of resources between tasks in J over a period of time $[0, t^*]$ as follows:

$$r = \{(a_i, b_i, t_i), i = 1, .., n, a_i = k \vee k^\circ, k = 1, .., K, k^\circ \in \{1, .., K\}, b_i \in [0, t^*)\}, \tag{1}$$

where a_i is a parameter determining the assignment of a task $j_i \in J$ to the corresponding resource; b_i and t_i are, respectively, the start time and execution duration of the task $j_i \in J$ on the resource, the type of which is determined by the assignment a_i.

In (1), $a_i = k$ if a task $j_i \in J$ is tied to a so-called base resource, the level (for example, the number of processors) of which is limited and depends on the capabilities of the task parallelization system, the cost of using the resource of the type k, and a number of other factors.

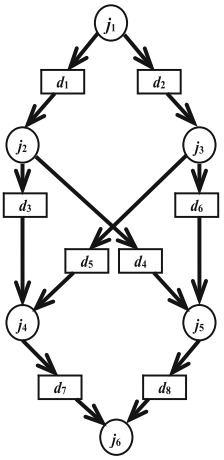

Fig. 1. Example of workflow DAG

In the event of a conflict between parallel tasks from J, competing for the same resource of type k, taking into account the scalability of the computing environment, a resource of type $k^\circ \in \{1, .., K\}$ is introduced that is not inferior in its characteristics to the basic one, and at the same time $a_i = k^\circ$. This may be, for example, an additional processor node of the same type k or an unused base node of the type $k^\circ \neq k$.

Table 1. Examples of parameterization for tasks $j_1, \ldots, j_6$

Parameters	j_1	j_2	j_3	j_4	j_5	j_6
t^0_{i1}	2	3	1	2	1	2
t^0_{i2}	4	6	2	4	2	4
t^0_{i3}	6	9	3	6	3	6
t^0_{i4}	8	12	4	8	4	8
v_{ik}	20	30	10	20	10	20

Let us assume that restrictions (deadlines) are configured for completion times of individual tasks and jobs, i.e. sequences $j_{i_1}, .., j_{i_L}$ of informationally or logically related tasks $1 \leq i_1 \leq \cdots \leq i_L \leq n$ that make up the job:

$$t^*_g - t_g \geq 0, t^*_h - \sum\nolimits_h t_h \geq 0, g, h \in \{1, .., n\}, \tag{2}$$

where t_g, t_h - completion times of tasks $j_g, j_h \in J$, and t^*_g, t^*_h - deadlines for task j_g and the job containing the task j_h.

One example of a scheduling criterion is the function of a workflow completion cost:

$$CF = \sum\nolimits_{i=1}^{n} \lceil \frac{v_{ik}}{t_{ik}} \rceil, t_{ik} \geq t^0_{ik}, \tag{3}$$

where v_{ik} - is the relative computational volume of task j_i; t_{ik} - is the time allocated for executing a task j_i on a processor of type k; n - is the number of tasks; $\lceil \cdot \rceil$ denotes the nearest integer that is not less than the value $\frac{v_{ik}}{t_{ik}}$ of the cost of executing the i-th task.

Resource allocation (1) is admissible if constraints (2) are met and the corresponding optimality criterion is defined, for example (3).

A ***critical job*** is a sequence of tasks (containing unassigned tasks) with the largest sum of specified prior execution estimates using ***the best combination of resources***. Let us assume the durations of all data transfers $d_1, \ldots, d_8$ in the workflow model G (see Fig. 1 and Table 1) are equal to one unit of time. Let $t^* = 20$ be the deadline for completing the workflow. Let us rank critical jobs according to the values of their a priori maximin duration: $(j_1, d_1, j_2, d_3, j_4, d_7, j_6)$; $(j_1, d_1, j_2, d_4, j_5, d_8, j_6)$; $(j_1, d_2, j_3, d_5, j_4, d_7, j_6)$; $(j_1, d_2, j_3, d_6, j_5, d_8, j_6)$. For the above-mentioned works, this indicator is respectively equal to 12, 11, 10 and 9 units of time (Fig. 2).

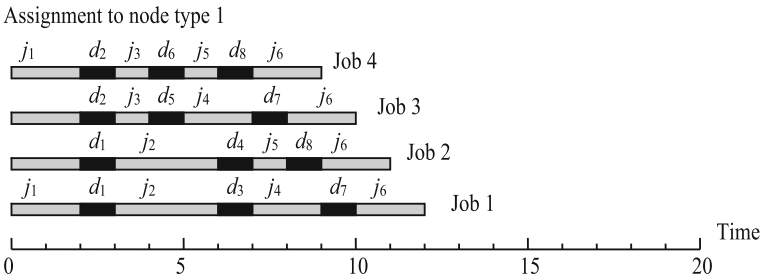

Fig. 2. Ranking of critical jobs when assigned to the first node

Then the first critical job in terms of duration corresponds to the path $(j_1, d_1, j_2, d_3, j_4, d_7, j_6)$. It is a priori maximin duration is 12 time units (see Table 1). After the assignment of tasks to this sequence, the next considered job is $(j_1, d_1, j_2, d_4, j_5, d_8, j_6)$ since tasks d_4, j_5, d_8 have not been assigned yet and the a priori duration of the job is 11 time units. The resource allocation for the subsequence (d_4, j_5, d_8) must account for the assignment results of the previous critical job. More detailed information on CJM scheduling, collision resolution and formalization based on dynamic programming schemes is presented in the paper [18].

The iterative application of this procedure with conflict resolution between parallel tasks competing for the same resource, in accordance with (1), is the essence of the ***critical jobs' method***. Based on this method, it is possible to construct a scheme for the sequential formation of reference (optimal) and suboptimal schedules for a given efficiency criterion. Let the criterion for the efficiency of resource use be given as a cost function (3). The CF takes the closest to t_{ik} duration estimate t_{ik}^0 that determines the type k of resource being used (slot set or node). The Gantt chart shown in Fig. 3, represents the result of workflow scheduling for graph from Fig. 1 on four types of resources are given in Table 1.

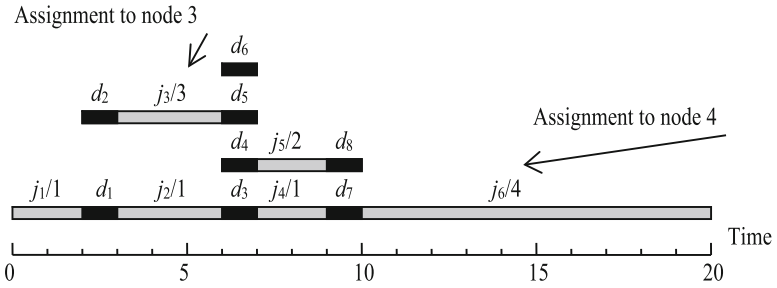

Fig. 3. Gantt chart of workflow scheduling

3.2 Critical Jobs' Method Modification

Firstly, we list major features and limitations of the original CJM:

- the method is designed to schedule a single static workflow;
- the point of the base method is to use a multiphases procedure, which identifies the next critical job and resolves possible conflicts (collisions) with previously assigned tasks over a shared resource;
- it allows to obtain optimal and close to optimal plans for specified restrictions on the total cost or task execution time for a single workflow.

Considering the dynamic workflow processing environment, the basic CJM algorithm is available to process incoming workflow jobs individually at the moment of the arrival to the platform. The main problem that arises is the dynamic component of the system and compliance with the relevant requirements for the quality of service of each workflow. In the base implementation of CJM at the conflict resolution stage, it is proposed to reduce the bipartite graph of a "multilayer" collision to a bipartite graph of a "two-layer" collision by sequentially viewing adjacent pairs of the graph vertices (tasks) and selecting vertices with the required weight. Thus, each scheduling of the next critical job may cause a conflict with the previous allocation. Further it can lead to collisions between parallel tasks and jobs of multiple simultaneously processing workflows.

Thus, in our dynamic model, for all arriving workflow jobs we implement only the first CJM stage of planning time ranges for performing critical job tasks according to budget and time user restrictions for the whole workflow. These calculations can be made simultaneously for multiple different workflows without any conflicts for the resources. The resulting time ranges represent execution recommendations and deadlines for each task which should be further handled by the cloud resource assignment module.

While developing the method, several statements have been made.

1) Since only resource types are considered at CJM planning stage, and not their specific instances, there are no conflicts within a job, a workflow, or many workflows. Therefore, the conflict resolution process is not included in the modified CJM but is transferred to the stage of assigning tasks to specific instances of VMs.
2) The modified CJM builds a workflow execution plan based on a priori time estimates of task execution from given resource types and the data transfer time between workflow tasks. Information about the amount of data transmitted and the time of

each data transaction is recorded in the result of the CJM operation and passed to the assignment module.

3) At the stage of scheduling a critical job and calculating the additive separable criterion, in the case of several identical values of the criterion, we settle on the first one. At this stage it is important to select the optimal value, regardless of the specific assignment for resource types.

In the result, the modified CJM is applied for each new workflow that arrives on the WaaS platform, and as the output it provides the following: time ranges of the workflow tasks execution; tasks' volume and execution requirements; data volumes and the data transfer dependencies between the tasks of the workflow.

4 The General Optimization Scheme of the Virtual Resources Allocation

4.1 Virtual Resources Allocation Strategies

One of the most important problems arose when scheduling and executing many computational tasks from the workflows is the effective allocation and management of VMs. By managing VMs, we mean determining the moments of start (creation) and finish (stopping, releasing) of individual VMs and containers, as well as the assignment and the execution order of ready-to-run computational tasks. We propose several strategies for managing VMs to execute workflow tasks.

Firstly, one can create a new dedicated VM specifically to execute each individual task and release it when the task is completed. This ***greedy*** but flexible strategy allows us to strictly match VM types and lifetime with the tasks' requirements, especially in conditions when the time required to create and shut down VM is much less compared to the average task execution time. However, the VM creation and preparation time includes time to configure the necessary software environment and the time to copy and receive the required input data. The shutdown/cleanup time may increase due to the need to save and copy the calculation results to the next task of the global data storage (e.g., Amazon 3s).

Secondly, one can maintain some dynamically changing pool of constantly active VMs and distribute ready-to-run tasks between them (the so-called ***control strategy***). The pool dynamics implies a decrease and an increase in the number of active machines, depending on the computing needs at a certain time. With this approach, it may be possible to schedule and assign tasks more efficiently by matching tasks' requirements with already active VMs and sometimes skip the data transfer routines. For example, when two consecutive (data-dependent) tasks are executed on the same VM, then the operation of copying and transferring data is not required. On the other hand, due to the specifics and variety of workflow structures, as well as their variable number, it is not always possible to ensure full and constant loading of the entire pool of active VMs. Thus, some of the VMs will be idle from time to time, thereby reducing the usefulness and cost-effectiveness of this approach. In addition, a certain difficulty lies in designing an algorithm for efficiently assigning tasks to available VMs.

Thirdly, there is a ***mixed strategy***, when some basic minimum pool of active VMs is maintained during the execution of workflows, but additional dedicated VMs can be created to account for all unassigned ready-to-run tasks.

Since the implementation of the first greedy approach is trivial but does not provide clear mechanisms to optimize the use of virtual resources, a control strategy is further considered in this paper.

4.2 High-Level Optimization Scheme

To implement the control strategy, we propose the following general algorithm scheme.

1) As input data the algorithm receives execution time plans for the individual tasks, data transfer volumes between them, as well as available types of VMs. The task execution plan is the time interval expected for its actual execution (i.e. the earliest start time and the latest completion time). It is assumed that these time ranges are passed from modified CJM implementation and maintain the relationship of continuity and sequence of execution in the initial workflows.
2) At the first stage, the input task flow is divided into parallel execution batches. The main requirement for dividing is that all tasks in one batch must be independent (there must be no data dependencies between them) and can be performed in parallel, taking into account the execution plan. Thus, the entire set of tasks is divided into many consecutive groups-batches. Tasks with data dependency should be in different, sequential (although not necessarily adjacent) parallel execution batches. The dividing into batches can be performed dynamically, taking into account the constantly incoming tasks. It is enough to operate with two parallel execution bacthes to implement the general optimization scheme.
3) At the second stage, the algorithm performs sequential scheduling and task assignment of each batch to the virtual resources. To achieve this, the problem of the minimum perfect matching (assignment problem) is solved using the Hungarian (Kuhn-Munkres) algorithm [19].

5 Algorithms to Group Tasks into Parallel Batches

5.1 Generalization and Input Data

The important initial step for efficient VM allocation and processing is to determine the number of simultaneously required VMs at any given time. This number depends on the structure of workflows, the relationships between tasks, the time of their execution, the history of assignment to VMs, etc. Thus, it should be determined dynamically in the runtime. For this purpose, we propose and study two different algorithms of grouping workflow tasks into batches. Each batch should contain tasks which can be executed in parallel without breaking data dependencies and local deadlines.

Firstly, we proposed and implemented the algorithm Follow The Leader (FTL) [19]. The main idea behind FTL is to preserve the following invariant *given the batch start time and tasks' deadlines, no two tasks in the batch can be executed sequentially even on the fastest VM*. Thus, FTL determines the minimum required parallelism level of

the incoming task flow at any given time. The result of its work can be further used for predicting and dynamic management of multiple VMs.

FTL algorithm receives a set of computational tasks t_i and a list of available VM types Vm_r^j. Every task t_i contains the following information: its own computational volume Vp^i (which is necessary to predict the time of its execution Te^i on each type of VM), the amount of input Vin^i and output $Vout^i$ data, and the relationship of precedence with parent and children tasks. In addition, an expected execution interval is defined for each task (the earliest start time tr^i and the deadline for completion Td^i) at the stage of preprocessing by the CJM module. Based on the early start time values tr^i, the execution time Te^i on the given virtual machine and the deadline for completion Td^i, two additional characteristics can be computed separately: the earliest completion time $mint_f^i = tr^i + Te^i$ and the latest start time $maxt_s^i = Td^i - Te^i$.

5.2 ASAP Algorithm

However, despite the implementation of the above-described invariant, FTL algorithm tends to save and minimize average demand for VMs and to postpone the execution of all tasks closer to their deadlines. These features may lead to an increase in the required VM performance and may result in parent and child tasks not being included in adjacent packages. In turn, this may prevent the reuse of execution data when performing parent and child tasks on the same VM instance. Thus, as an alternative to FTL we considered the more straightforward algorithm described in [6]. The basic idea of this algorithm is to execute each task as soon as possible when all parent tasks are finished. Each task is placed into the batch following the batch containing its last parent task. We call this algorithm ASAP. Thus, in contrast to FTL, ASAP strives to execute all tasks immediately when ready, without considering local deadlines. However, looking ahead, this policy of placing tasks into batches as early as possible turns out to be more suitable and flexible for the VM assignment stage.

Another important numerical metric of the batch grouping quality is the number N_{pc} of parent and child tasks in adjacent batches. Generally, such groupings may allow us to save time on data transfers due to reuse of VMs, their internal data storage and configurations. Table 2 shows N_{pc} provided by FTL and ASAP algorithms for different workflows. The results in Table 2 demonstrate the general advantage of the ASAP algorithm over FTL in terms of N_{pc} even for small workflows consisting of 50 tasks. On the other hand, the batch grouping result strongly depends on the workflow structure and the given task deadlines. The greatest advantage is demonstrated in heterogeneous workflows with tasks of varying duration. However, for MONTAGE workflow consisting of 1000 tasks, ASAP and FTL algorithms provided identical batch groupings with $N_{pc} = 834$. As a result, ASAP algorithm generally demonstrates more efficient results because it groups tasks into batches more tightly and allows for resource reuse during the workflow execution.

Table 2. Number N_{pc} provided by FTL and ASAP algorithms for different workflows

Algorithm	LIGO50	GENOME50	CYBERSHAKE50	MONTAGE1000
FTL	31	15	29	834
ASAP	38	48	45	834

5.3 Dynamic VM Allocation

Next, we discuss the problem of efficient resources allocation and assignment for each batch of parallel execution retrieved with FTL algorithm. It should be noticed that this assignment operation implicitly assumes the possibility of disabling unnecessary VMs.

The VMA (VM Allocation) algorithm is proposed to solve this problem, based on the Hungarian Kuhn-Munkres algorithm (Kuhn, H.W., 1955) to find a perfect matching in a bipartite graph $G = (T, R, E)$, where T is the set of batch B tasks, R is the set of available resources, and E is the set of edges between T and R. The edge between the task from T and the resource from R means that the task can be executed on the corresponding VM in compliance with all requirements. The edge weight is a target optimization criterion of this assignment and scheduling in general. By these means we can optimize VMs total usage cost, tasks' execution runtimes, data transfers time, etc. [19].

6 Software Implementation and Analysis

In developing the software implementation of the proposed algorithms, the following basic assumptions were made.

Firstly, in the current implementation, it is assumed that the expected task execution time on some instance of VM can be calculated as the ratio of the task computational volume to a given performance characteristic of the VM. This assumption is optional and is made for greater clarity of the model, input data and calculations. In future versions of the program, it is assumed to provide a more flexible calculation of task execution time, for example, based on a given matrix of correspondence between tasks and types of available VMs.

The second assumption is there is global data storage with sufficient volume for simultaneous storage of all intermediate data necessary for transfer between the tasks. At the same time, the calculated data transfer rate remains the same in parallel copying of output data from a set of completed tasks. This assumption is necessary to simplify calculations in cases where the sequential tasks are executed with some acceptable delay, and it is more beneficial to copy output data to a centralized storage, rather than keep it on a VM until the next task is started. This assumption can be justified in scenarios where the volume of transferred data does not exceed a certain critical value, and centralized, possibly cloud storage implements effective balancing of requests between several nodes.

Thirdly, the developed program solution does not implement a single best-case processing scenario for all possible workflows but provides a set of configuration parameters to tailor processing for a specific scheduling scenario. These parameters are primarily

aimed at minimizing the schedule calculation time, which can grow cubically relative to the set of elements in the parallel batch.

An important stage is the preparation of data for the assignment problem and Hungarian algorithm: calculating the edges' cost of the considered bipartite graph. Thus, it is necessary to precalculate the expected result and parameters (including the target criterion) for each pair between the tasks T and VMs R.

Each pair of a task t_i and a VM VM^j can be considered independently. The execution plan of each pair may include VM waiting (idle) time, preparation time, actual task execution runtime (based on the task computational volume Vp^i and VM performance P^j) and release time. VM preparation time includes the time to create a new machine and the time to copy the necessary data from the previous related task. Data can be copied either directly from the VM on which the previous task was executed, or from global storage. If the current task is scheduled to be performed on the same instance of VM, then data transfer is not required. Based on the preparation time of the VM and the task execution time, the required usage time of the VM and the corresponding economic cost are calculated.

7 Workflow Scheduling Optimization Results

7.1 Optimization Results

To demonstrate the optimization capabilities of the presented algorithm, we conducted a series of scheduling experiments on many real workflows, including GENOME, LIGO, CYBERSHAKE, SIPHT, MONTAGE and their intersecting combinations.

Table 3 shows the main execution characteristics of LIGO workflows in different optimization scenarios. The results were obtained with developed software in Python 3 environment, CPU Core i5, and 8 GB RAM. The presented results show significant optimization potential realized by selecting the required criterion for in the implemented algorithm.

Table 3. LIGO Workflow Optimization Results

Optimization	Total VM Cost	Total Runtime, sec	Total VM Time, sec
Cost minimization	**12740**	4260	4328
Cost maximization	**13057**	4576	4754
Runtime minimization	12929	**4180**	4310
Runtime maximization	12769	**4757**	4840
VM time minimization	12743	4200	**4269**
VM time maximization	12952	4823	**4980**

7.2 Comparison of VM Allocation Strategies

In this experiment series we study VM allocation efficiency provided by the following strategies and algorithms.

1. **Greedy strategy** creates a new dedicated VM for each workflow task. VM type is selected to optimize the global scheduling criterion while meeting the execution time deadline. VM usage may require additional uptime to receive data transfers required for the task execution.
2. **Control strategy** is represented with the proposed **VMA** algorithm: VM assignment procedure optimizes global criteria given the deadline constraints for workflow tasks grouped in batches.

Testing was carried out based on a workload consisting of 100 independent workflows. The workflow instances were built based on real scientific applications (Montage, Cybershake, Genome, LIGO, SIPHT) and contain 50 vertices each. The execution deadline for each individual workflow was generated randomly between the fastest (using highest performance VMs) and the slowest (using the least performance VMs) possible execution times. The deadline limit determines the base execution plan and therefore affects the allocation variants and strategies. These workflows differ in their structure, required computational and data transfers volumes. For example, the average execution time of Montage workflow is 100 s, while Cybershake on average requires 30000 s. So, workflows with larger computational volumes may have a greater impact on the simulation results.

The following environment configuration parameters were studied:

- the arrival rate of workflows to the WaaS platform (quantity per minute);
- time intervals required to create and initialize and to release the VM.

It is worth to mention CJM scheduling step allows us to specify a specialized optimization criterion for each received workflow. This optimization will generally affect deadlines for the tasks of the workflow.

However, only one common optimization criterion can be used in VMA during the actual VM allocation. To support specific optimization criteria for input workflows it is possible to run several instances of VMA algorithms, each processing workflow matching one particular global criterion.

Table 4 contains total results of the workload execution depending on the workflow arrival rate (from 0.5 to 100 workflows per minute). Firstly, we note that Greedy execution results do not depend on the workflow arrival rate: all VMs are created and tailored for specific tasks, so the absolute start time of the task does not affect the choice of the VM type. On the other hand, VMA scheduling directly depends on the density of the incoming tasks. So, based on the workflow arrival rate and the composition of the parallel batches, VMA allocated 5–20% less VM instances by reusing them to execute several consecutive tasks. This strategy resulted in nearly 5% advantage over the Greedy strategy by the total VM cost criterion. Total tasks' execution time remained nearly constant as it depends on the pre-configured deadlines specific to each workflow and independent from the arrival rate.

Table 4. Algorithms' comparison depending on workflow arrival rate

Workflow Arrival Rate (per minute)	Algorithm	Total Task Execution Time, sec	Total VM Cost	# of Created VMs
0.5	VMA	409280	13226	3912
1	VMA	409486	13277	4116
2	VMA	409602	13316	4334
6	VMA	409601	13279	4503
12	VMA	409586	13257	4574
60	VMA	409578	13168	4619
100	VMA	409596	13168	4633
*	**Greedy**	**409650**	**13906**	**4955**

Table 5 contains total results of the workload execution depending on the time required to create and initialize and to release (destroy) VM. This parameter affects the result of both VMA and Greedy algorithms, as total cost directly depends on total VM usage time, including periods of VM initialization and release.

Based on the results obtained, VMA allocated 16% less VM instances to execute the same amount of tasks, resulting in an up to 10% advantage over Greedy algorithms by the total cost criterion. Sa expected, the advantage increases with increasing VM creation and initialization time.

Table 5. Algorithms comparison depending on VM initialization and release time

VM Init/Release Time	Algorithm	Total Task Execution Time, sec	Total Cost	# of Created VMs
0/0	VMA	391361	10878	4175
0/0	Greedy	391559	10885	4955
10/1	VMA	391297	11009	4127
10/1	Greedy	391559	11053	4955
100/10	VMA	391449	12144	4125
100/10	Greedy	391559	12557	4955
300/30	VMA	391453	14576	4134
300/30	Greedy	391559	15899	4955
500/50	VMA	391413	17076	4118
500/50	Greedy	391559	19242	4955

Overall, the following main conclusions can be drawn from the comparison results:

- both VMA and Greedy algorithms meet workflow deadlines in 100% of simulation experiments; total cost optimization implies approximate equality in terms of total time criterion;
- VMA exploits the possibility of reusing VMs, minimizing VMs initialization time and data transfer times between data-dependent tasks; in this way VMA at average allocates 10–15% less VM instances, resulting in 5% less total VM usage cost.

8 Conclusion and Future Work

In this work, a multi-module procedure was proposed and implemented for scheduling and executing multiple independent workflows. For this purpose, several modifications of the CJM were implemented, including the possibility of time modeling to receive and schedule a set of workflows that are spaced in time.

The resource assignment stage allows us to optimize many global characteristics of cloud resource usage. The proposed solution manages the pool of active VMs by defining for each instance the creation, preparation, utilization, data transfer and shutdown intervals. The developed solution has been evaluated on several examples of real-world workflows. It is worth emphasizing once again that in many respects the results of this work were obtained based on a study of both classical and highly specialized optimization algorithms.

The main limiting factor is the high (cubic) computational complexity of the solution relative to the parallelism degree of the incoming task flow [19]. Thus, there is a natural limitation in the size of workflows, the scheduling of which can be completed in a feasible time. Future work will concern problems of scheduling algorithms complexity in scalable WaaS platforms.

Acknowledgments. This work was supported by the Russian Science Foundation (project no. 22–21-00372, https://rscf.ru/en/project/22-21-00372/).

References

1. Karmakar, K., Tarafdar, A., Das, R.K., et al.: Cost-efficient workflow as a service using containers. J. Grid Comput. **22**, 40 (2024). https://doi.org/10.1007/s10723-024-09745-7
2. Taghavi, B., Zolfaghari, B., Abrishami, S.: A cost-efficient workflow as a service broker using on-demand and spot instances. J Grid Comput. **21**, 40 (2023). https://doi.org/10.1007/s10723-023-09676-9
3. Tarafdar, A., Karmakar, K., Khatua, S., Das, R.K.: Energy-efficient scheduling of deadline-sensitive and budget-constrained workflows in the cloud. In: Goswami, D., Hoang, T.A. (eds.) ICDCIT 2021. LNCS, vol. 12582, pp. 65–80. Springer, Cham (2021). https://doi.org/10.1007/978-3-030-65621-8_4
4. Saeedizade, E., Ashtiani, M.: DDBWS: a dynamic deadline and budget-aware workflow scheduling algorithm in workflow-as-a-service environments. J. Supercomput. **77**(12), 14525–14564 (2021)

5. Qin, Y., Wang, H., Yi, S., Li, X., Zhai, L.: An energy-aware scheduling algorithm for budget-constrained scientific workflows based on multi-objective reinforcement learning. J. Supercomput. **76**(1), 455–480 (2020)
6. Hilman, M.H., Rodriguez, M.A., Buyya, R.: Workflow-as-a-service cloud platform and deployment of bioinformatics workflow applications (2020). 30 p. https://www.researchgate.net/scientific-contributions/Maria-A-Rodriguez-2114894132
7. Tarafdar, A., Karmakar, K., Das, R.K., Khatua, S.: Multi-criteria scheduling of scientific workflows in the workflow as a service platform. Comput. Electr. Eng. **105**, 108458 (2023)
8. De Maio, V., Kimovski, D.: Multi-objective scheduling of extreme data scientific workflows in Fog. Future Gener. Comput. Syst. **106**, 171–184 (2020)
9. Li, H., Wang, Y., Huang, J., Fan, Y.: Mutation and dynamic objective-based farmland fertility algorithm for workflow scheduling in the cloud. J. Parallel Distrib. Comput. **164**, 69–82 (2022). https://doi.org/10.1016/j.jpdc.2022.02.005
10. Gu, Y., Cao, J., Qian, S., Zhu, N., Guan, W.: MANSOR: a module alignment method based on neighbor information for scientific workflow. Concurr. Comput. Pract. Exp. **36**(10), e7736 (2024). https://doi.org/10.1002/cpe.7736
11. Ahmad, Z., Nazir, B., Umer, A.: A fault-tolerant workflow management system with quality-of-service-aware scheduling for scientific workflows in cloud computing. Int. J. Commun. Syst. **34**(1), 4649 (2021)
12. Burkat, B., et al.: Serverless containers–rising viable approach to scientific workflows. In: 17th International Conference on eScience (eScience), pp. 40–49. IEEE (2021)
13. Karmakar, K., Das, R.K., Khatua, S.: Resource scheduling for tasks of a workflow in cloud environment. In: Hung, D., D'Souza, M. (eds.) ICDCIT 2020. LNCS, vol. 11969, pp. 214–226. Springer, Cham (2020). https://doi.org/10.1007/978-3-030-36987-3_13
14. Ranjan, R., Thakur, I.S., Aujla, G.S., Kumar, N., Zomaya, A.Y.: Energy-efficient workflow scheduling using container-based virtualization in software-defined data centers. IEEE Trans. Ind. Inform. **16**(12), 7646–7657 (2020)
15. Silva, R.F., Pottier, L., Coleman, T., Deelman, E., Casanova, H.: WorkflowHub: community framework for enabling scientific workflow research and development. In: 2020 IEEE/ACM Workflows in Support of Large-Scale Science (WORKS), pp. 49–56. IEEE (2020)
16. Medara, R., Singh, R.S.: A review on energy-aware scheduling techniques for workflows in IaaS clouds. Wirel. Pers. Commun. **125**, 1545–1584 (2022). https://doi.org/10.1007/s11277-022-09621-1
17. Amstutz, P., Mikheev, M., Crusoe, M.R., Tijanić, N., Lampa, S., et al.: Existing Workflow systems. Common Workflow Language wiki, GitHub (2024). https://s.apache.org/existing-workflow-systems. Accessed 18 Aug 2024
18. Toporkov, V., Yemelyanov, D.: Micro-scheduling for dependable resources allocation. In: Bocewicz, G., Pempera, J., Toporkov, V. (eds.) Performance Evaluation Models for Distributed Service Networks. SSDC, vol. 343, pp. 79–103. Springer, Cham (2021). https://doi.org/10.1007/978-3-030-67063-4_5
19. Toporkov, V., Yemelyanov, D., Bulkhak, A., Pirogova, M.: Job batch scheduling in workflow-as-a-service platforms. In: Sokolinsky, L., Zymbler, M., Voevodin, V., Dongarra, J. (eds.) PCT 2024. CCIS, vol. 2241, pp. 65–79. Springer, Cham (2024). https://doi.org/10.1007/978-3-031-73372-7_5

Global Sensitivity Analysis for a Mathematical Model of the General Escape Theory of Suicide

Sophie Engels[1(✉)], Valeria Epelbaum[1,3], Shirley B. Wang[2], Derek de Beurs[1,3], and Valeria Krzhizhanovskaya[1,3]

[1] University of Amsterdam, Amsterdam, Netherlands
{S.L.Engels,V.Epelbaum,D.deBeurs,V.Krzhizhanovskaya}@uva.nl
[2] Yale University, New Haven, USA
Shirley.Wang@yale.edu
[3] Centre for Urban Mental Health, University of Amsterdam, Amsterdam, Netherlands

Abstract. This study explores a formalized dynamical systems model of the General Escape Theory of Suicide using Sobol and PAWN global sensitivity analyses. The findings highlight the importance of self-feedback loops, the effect of stressors on aversive internal states, and the interaction effects between aversive internal states and the urge to escape on suicidal ideation and non-suicidal escape behaviors. Time-dependent sensitivity analysis also reveals the long-term stability of parameter importance over time. These results hold potential for informing clinical interventions by identifying the most important influences for individual suicidal ideation.

Keywords: Sensitivity Analysis · Dynamical Systems · Uncertainty Quantification · Sobol Sensitivity Indices · PAWN Sensitivity Indices

1 Introduction

Suicide is a major global public health problem, with over 700.000 deaths a year [9]. Suicidal behavior is conceptualized as the result of the complex interaction between many different variables [2]. An influential review article stated that the prediction of suicidal ideation and behaviors has not improved over the last 50 years [3]. Within the field of suicide prevention, a novel route to better understand and study this complexity is by working with mathematical models. These formalized models force researchers and clinicians to make any assumptions about the relation of different factors explicit and allow them to test more vigorously what the theory proposes to predict.

In their paper "Mathematical and Computational Modeling of Suicide as a Complex Dynamical System," Wang et al. [15] developed a mathematical model of suicidal thoughts as a system of differential equations. Taking inspiration from

M. Paszynski et al. (Eds.): ICCS 2025 Workshops, LNCS 15912, pp. 183–197, 2025.
https://doi.org/10.1007/978-3-031-97573-8_13

applications of nonlinear dynamical systems theory, their model presents suicidal ideation as a system of interacting subcomponents, such as stressors, aversive internal states, suicidal thoughts, and escape behaviors. The advantage of such an approach is the ability to test predictions made by verbal theories, which have generally dominated suicide research in psychology. This model is built from the newly proposed General Escape Theory of Suicide by Millner et al. [8]. The formalization of this theory as a mathematical model then forces the developer to make choices about the type of interactions between subcomponents and the values of self-feedback loop and interaction parameters [15]. The simulated data provides insight into whether or not the mathematical model reflects the expected emergent behavior associated with the phenomena. In particular, the simulation provides evidence for the rapid-onset and high variability of suicidal thoughts in response to random stressors and heightened aversive internal states.

Methods for global sensitivity analysis are useful in understanding which parameters are influencing particular outputs from a model. It explores the effects of changes in all parameters across the entire parameter space, thereby also investigating parameter-interaction effects on the final outcome variable measured [10]. Conducting a sensitivity analysis for the suicide model by Wang et al. [15] is essential to understanding how the parameter choices affect the model outcomes, which may provide insights into how to improve model parsimony or where the mathematical and verbal model may not align (i.e. if the verbal model posits that a particular parameter is extremely important but has little effect on the outcome in the simulation). In this project, Sobol sensitivity and PAWN sensitivity analyses were conducted to explore these questions.

1.1 The Model

The model by Wang et al. [15] defines stressors (S_t) with a Brownian motion equation, including both the deterministic drift parameter μ, the stochastic volatility parameter σ, and the regulating effect of externally-focused strategies, modulated by parameter f_1. Next, the change in a patient's aversive internal state (A) is increased by the stressor according to another parameter, a, and a logistic growth term with a carrying capacity of K_2. We also assume that the aversive internal state is reduced by suicidal thoughts and escape behaviors according to parameters d_2 and e_5, since these can have a functional purpose as a reprieve from the aversive feelings. Finally, aversive internal state is improved by the effect of internally-focused strategies according to parameter g_2. The change in the urge to escape (U) is governed by a negative self-feedback loop and positive influence of the aversive internal state, controlled by parameter b_3. They define the change in suicidal thoughts (T) as a sigmoidal function which has a negative self-feedback loop and whose structure is dictated by two parameters, c_{41} and c_{42}, which determines the steepness and midpoint of the sigmoidal curve respectively. The change in escape behavior (X) is defined nearly identically, with parameters c_{51} and c_{52}. The change in externally-focused strategies (E) and internally-focused strategies (I) are also governed by a logistic equation, plus a positive impact of aversive internal states (regulated by parameters b_6

and b_7, respectively)and a negative impact of the urge to escape (with parameters c_6 and c_7 for externally and internally focused strategies). The equations governing the model can be found below.

$$S_t = S_0 e^{\left(\mu - \frac{\sigma^2}{2}\right)t + \sigma W_t - f_1 E}, \tag{1}$$

$$\frac{dA}{dt} = b_2 A\,(K_2 - A) + a_2 S - d_2 T - e_2 X - g_2 I, \tag{2}$$

$$\frac{dU}{dt} = -c_3 U + b_3 A, \tag{3}$$

$$\frac{dT}{dt} = -d_4 T + \frac{1}{1 + e^{-c_{41}(U - c_{42})}}, \tag{4}$$

$$\frac{dX}{dt} = -e_5 X + \frac{1}{1 + e^{-c_{51}(U - c_{52})}}, \tag{5}$$

$$\frac{dE}{dt} = f_6 E\,(K_6 - E) + b_6 A - c_6 U, \tag{6}$$

$$\frac{dI}{dt} = g_7 I\,(K_7 - I) + b_7 A - c_7 U \tag{7}$$

1.2 Global Sensitivity Analysis

While local sensitivity analyses investigate the effect of changes in a single variable on the model output, global sensitivity analysis, all parameters are varied across the defined parameter space at the same time to investigate both parameters' single and interaction based effects [16]. In this paper, we will focus on two prominent methods: Sobol sensitivity analysis, a variance-based method, and PAWN sensitivity analysis, a moment-independent method.

Sobol Sensitivity Analysis. Sobol sensitivity analysis decomposes the model output variance into sensitivity indices for each parameter, allowing for an interpretation of how much a particular output's variability can be attributed to a particular parameter or parameter interaction [13]. First, we choose reasonable parameter ranges which are then sampled using a Sobol sequence, a quasi-random sequence that more efficiently covers the parameter space than completely random methods such as Monte Carlo. The model is then run for each combination of parameter values. From here, first-order and higher-order sensitivity indices are calculated for each parameter.

If we define $X = (X_1, ..., X_n)$ as an input vector with n parameters, and $f(X) = Y$ as the model output, then the variance of the average of that model output for all possible parameter values provides a useful measure of model variability as a result of that parameter set. We are particularly interested in the variance of the average across all possible values of X_i to avoid any dependence on the value of X_i in the parameter space. For ease of interpretation, we can define $\mu_{X_i} = E(Y|X_i)$ as the conditional expectation when the parameter X_i is

fixed and $\mu_{X_{\sim i}} = E(Y|X_{\sim i})$ as the expectation when all other parameters are held constant except X_i, as per standard convention.

The first-order sensitivity index is then described in Sobol [13] as the proportion of the total variance that can be explained by variation in the parameter set X_i, i.e.

$$S_i = \frac{V(\mu_{X_i}(Y))}{V(Y)}, 0 \leq S_i \leq 1. \tag{8}$$

This provides the main effect of the particular parameter X_i on the output variability of the model. If this value is high, we can assume a strong, direct effect of this parameter on the variability in the model output. We can similarly extend this to second-order indices, where we explore the variance in model output as a result of all other variables while two particular parameters are fixed. This can be depicted with the following equation, adapted from Sobol [13],

$$S_{i,j} = \frac{V(\mu_{X_{\sim i,j}}(Y)) - V(\mu_{X_i}(Y)) - V(\mu_{X_j}(Y))}{V(Y)}. \tag{9}$$

If the second-order sensitivity index for a particular parameter combination is high, we can assume a strong interaction effect between these two parameters on the output. Given that there are 24 parameters to investigate, looking at all possible interaction levels would be unrealistic and computationally demanding. Therefore, we can use the total-order sensitivity index as a metric for these higher-order interactions. The total-order sensitivity index describes the proportion of variance caused by that particular parameter while all other parameters are fixed. From the Law of Total Variance, we know that

$$\frac{E_{X_{\sim i}}(V_{X_i}(Y|X_{\sim i}))}{V(Y)} + \frac{V_{X_{\sim i}}(E_{X_i}(Y|X_{\sim i}))}{V(Y)} = 1. \tag{10}$$

Hence, the first term in the above expression encapsulates total-order sensitivity, as it averages across all other parameters, the conditional variance caused by the parameter of interest. Therefore, the total-order sensitivity index of a particular parameter, X_i, can be described in the following equation (once again adapted from Sobol [13]),

$$S_{T_i} = 1 - \frac{V(\mu_{X_{\sim i}}(Y))}{V(Y)}. \tag{11}$$

A high total-order index for a parameter implies it has a strong overall effect, which includes its interaction and main effects. This would imply that if first or second-order indices for a parameter were low, but total-order indices were high, then the model output was likely due to higher-order interactions between multiple parameters and the parameter of interest.

PAWN Sensitivity Analysis. In situations where output distributions are highly skewed or bimodal, variance decomposition techniques may not provide the most reliable estimates of sensitivity indices. Another approach is PAWN, which is moment independent [10]. Rather than measuring changes in variability, it measures distributional changes in the output. After sampling for parameter combinations, the model is evaluated and its overall cumulative distribution function (CDF) is calculated without any parameter held constant, representing the baseline distribution of the output. Then, each parameter is sampled for a particular conditioning value, X_i. The model is then evaluated for random samples of all other parameters for each conditioned value of X_i. The output CDF for each conditioned value of X_i is compared to the original, overall output CDF using the Kolmogorov-Smirnov statistic. This statistic is then used to calculate the sensitivity index for the overall effect of that parameter on the output, akin to the Sobol total-order sensitivity index [11]. However, this calculation cannot capture first or second-order variance decomposition. As a result, we will use PAWN to verify the robustness of our result from the Sobol sensitivity analysis.

2 Methods Implementation

2.1 Model Implementation

The model implementation is the same as the version published by Wang et al. [15], which can be found at https://github.com/ShirleyBWang/math_model_suicide. As in the original paper, the simulation length was two weeks, calculated as $(15 \cdot 1440)$ min in 15 days, with increments of 0.01. The only adjustment made is the use of the Python compiler library, Numba, which uses a different random number generator [6]. Given the numerical nature of the model itself, Numba lends itself well to speeding the model evaluations, reducing a single model run from 0.3 s to 0.002 s.

Additionally, for the time-dependent sensitivity analysis, the seed for the model was set to compare sensitivity for different output values for a particular run. This output was chosen for its medial variability in output values,

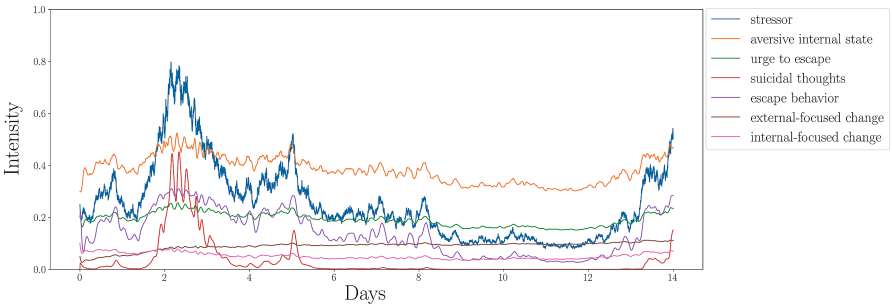

Fig. 1. Simulation output for Numba seed 504 from the model provided in Wang et al. [15].

lending itself to interesting interpretations whilst not being overly complex. A visualization of this output can be found in Fig. 1.

2.2 Sensitivity Analysis Implementation

The sensitivity analysis was implemented using SALib (version 1.5.0) [5], a Python library designed for the task. All documentation for library can be found at https://salib.readthedocs.io/en/latest/index.html. The `saltelli()` function from the `sample` package was used to sample the parameter space according to the Saltelli algorithm, which reduces error associated with the Sobol sequence used for quasi-random sampling of parameter space [12]. The analyze() functions from packages `sobol` and `pawn` were utilized to estimate the sensitivity indices. The number of conditioning intervals used for the PAWN analysis was dependent on the sample size, with the number of conditioning intervals being roughly 1% of the sample size for reliable convergence [1]. Additionally, the NumPy library (version 1.26.4) [4] and Pandas library (version 2.2.2) [7] were employed for data manipulation and analysis. Finally, MatPlotLib (version 3.8.0) [14] was imported for visualizations.

3 Results and Discussion

3.1 Maximum Model Output Sensitivity Analysis

We first plotted the output distributions for runs with 2^{10} parameter space samples to determine the appropriateness of the sensitivity analysis method. From Fig. 2, we notice that the output distributions for the maximum of suicidal thoughts and the maximum escape behavior are highly right-skewed, meaning that comparison of variance-based sensitivity results with moment-independent, PAWN sensitivity indices is useful in confirming results. The distribution of aversive internal state model outputs is relatively evenly distributed, indicating that we can rely on the results of variance-based, Sobol analysis results for this output.

We notice similar results reflected in convergence graphs for both Sobol total-order indices and PAWN indices (seen in Fig. 3 and Fig. 4 respectively). Increasing the number of parameter space samples for aversive internal state model outputs does not significantly improve the convergence of sensitivity indices. However, overall, we notice that the total-order sensitivity indices for any of the three outputs does not substantially change for more than 2^{16} samples, with only a minor reduction in the confidence interval. For PAWN indices, little information is gained past 2^{10} parameter space samples, since values have already converged. Hence, further analyses for maxima of model outputs were conducted with 2^{17} parameter samples for Sobol indices and 2^{14} parameter samples for PAWN indices.

The PAWN approach to sensitivity indices captures a more general effect of each parameter on the model output distribution, which may include some higher-order interactions with other parameters. We can then compare the

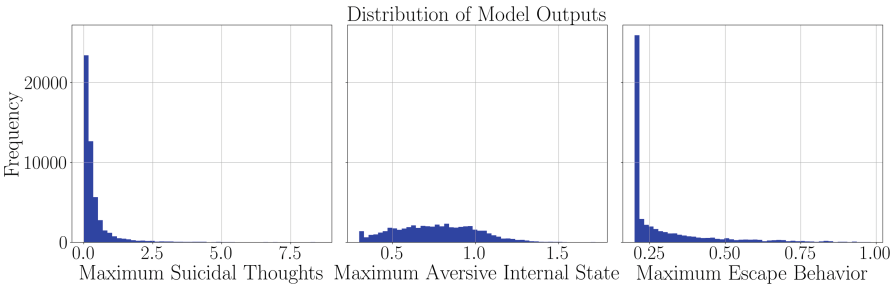

Fig. 2. Output distributions for maximum each output variable from model runs (suicidal thoughts, aversive internal state, and escape behavior) with 2^{10} parameter space samples.

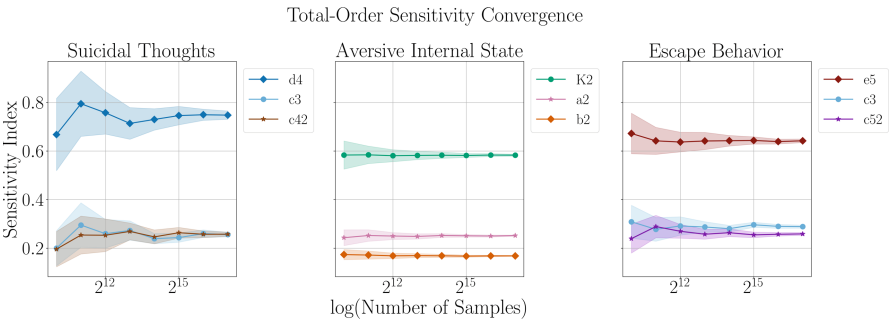

Fig. 3. Sobol total-order index values for the three highest sensitivity indices for the maximum of each model output (suicidal thoughts, aversive internal state, and escape behavior) for an increasing number of parameter space samples with 95% confidence.

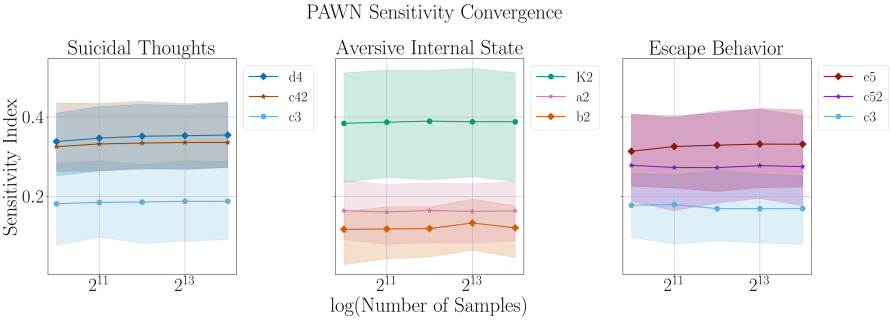

Fig. 4. PAWN sensitivity index values for the three highest sensitivity indices for the maximum of each model output (suicidal thoughts, aversive internal state, and escape behavior) for an increasing number of parameter space samples with the coefficient of variation as error.

PAWN sensitivity indices and the total-order Sobol sensitivity indices to evaluate the robustness of the results, found in Fig. 5. As illustrated in both the convergence plots and the side-by-side total-order and PAWN sensitivity plots, we notice that the only disagreement between the two methods is between the relative importance of the self-feedback loop parameters and c_{42} and c_{52}, which control the horizontal placement of the midpoint of the sigmoidal curves for suicidal thoughts and escape behaviors respectively. The two sensitivity analysis methods cannot be compared exactly, since they rely on two distinct measurements. However, the disagreement between relative importance of the midpoints of the sigmoidal curves indicates that these parameters have a greater impact on the asymmetric distributional changes on the model output than the overall variance in the model output. Regardless, the methods agree on which parameters remain the most important to the model outputs, regardless of their original distribution.

As mentioned in Sect. 1.2, the main effects of each parameter can be captured with first-order Sobol sensitivity indices, shown in Fig. 6. These agree with the highest total-order sensitivity indices for each model output. The most relevant parameters that contribute to variance in the maximum of suicidal thoughts are d_4 (the self-feedback loop of suicidal thoughts), c_{42} (the midpoint of the sigmoidal curve for suicidal thoughts), b_3 (the effect of the aversive internal state on the change in the urge to escape), c_3 (the self-feedback loop on the urge to escape) and K_2 (the carrying capacity of the aversive internal state) with the self-feedback loop having the greatest impact. For aversive internal state, the most influential parameters are overwhelmingly K_2 (the carrying capacity for aversive internal state), b_2 (the self-feedback loop on aversive internal states), and a_2 (the effect of stressors on the change in aversive internal states). For escape behavior, the most important parameters identified are e_5 (the self-feedback loop of escape behaviors), c_{52} (the midpoint of the sigmoidal curve for escape behavior), and once again c_3, b_3, and K_2.

The high relevance of the self-feedback loops associated with each maximum for the outcome variable relates to the nonlinear effect of feedback on the system. All of the self-feedback loops have negative effects on their respective output, dampening the state's proportional effect on the rate of change of its output. Therefore, as these values decrease, the exponential effect of the model output state is strengthened, and that particular variable can maximize at a higher peak. This can lead to greater variability in model outputs as a result of changes to any of their respective self-feedback loops.

In comparison to the total-order Sobol indices seen in Fig. 5, the same parameters of importance are highlighted for all model outputs in Fig. 6. However, for the maximum of suicidal thoughts and escape behavior, the first-order sensitivity indices generally have much lower indices than their total-order counterparts. This indicates a high amount of second-order or higher-order interactions for each of these variables. However, the values of the sensitivity indices for maximum of aversive internal state are almost identical to their total-order sensitivity indices, indicating that the vast majority of variance in model output is due to

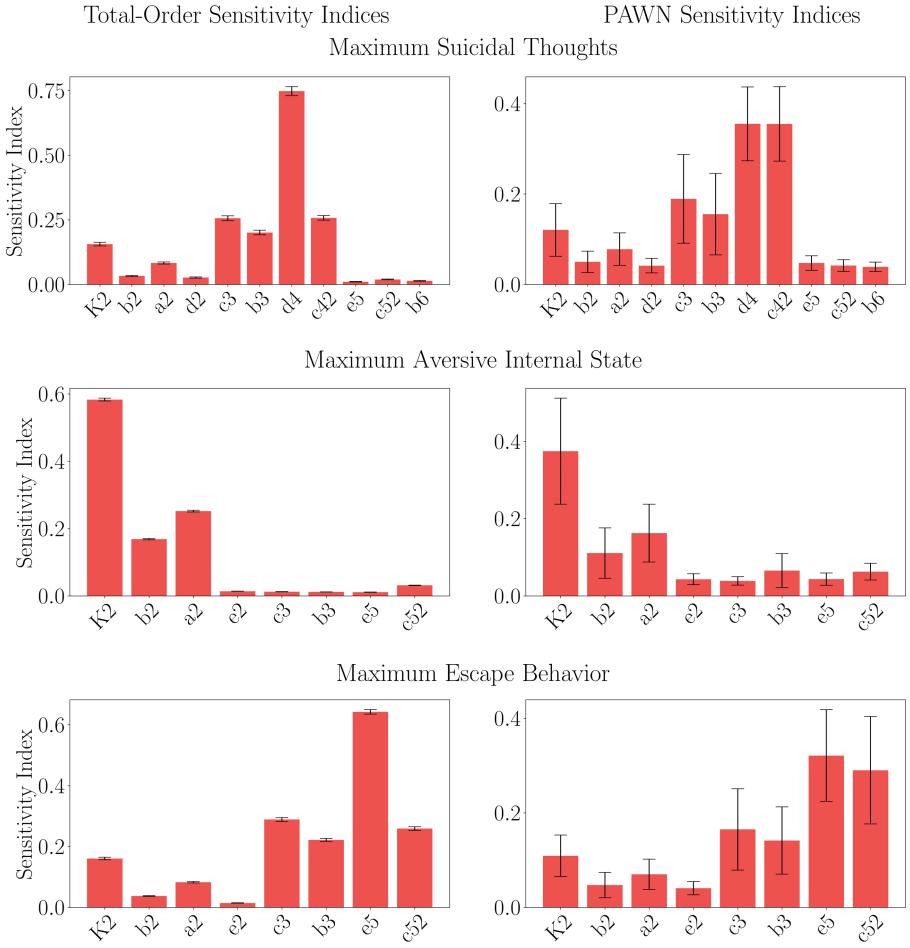

Fig. 5. Total-order Sobol sensitivity indices (left) and PAWN sensitivity indices (right) for the maximum of the specified model output. Error for Sobol indices is measured as a 95% confidence interval and the coefficient of variation as error for PAWN indices. Only parameters with an index greater than 0.01 are visualized for ease of reading. Sobol sensitivity indices were calculated with 2^{17} samples, compared with PAWN sensitivity indices calculated with 2^{14} samples.

the individual effect of each of these parameters with minimal reliance on higher-order interactions. This begs the question as to which particular interactions are relevant for the model outputs. As expected, the only second-order parameter interaction with a sensitivity index greater than 0.01 is between b_2 and a_2, since a_2 is the effect of stressors on the change in aversive internal state, which in turn directly effects the self-feedback loop parameter b_2.

For maximum escape behavior and the maximum of suicidal thoughts, there are more interesting second-order interaction dynamics, particularly between

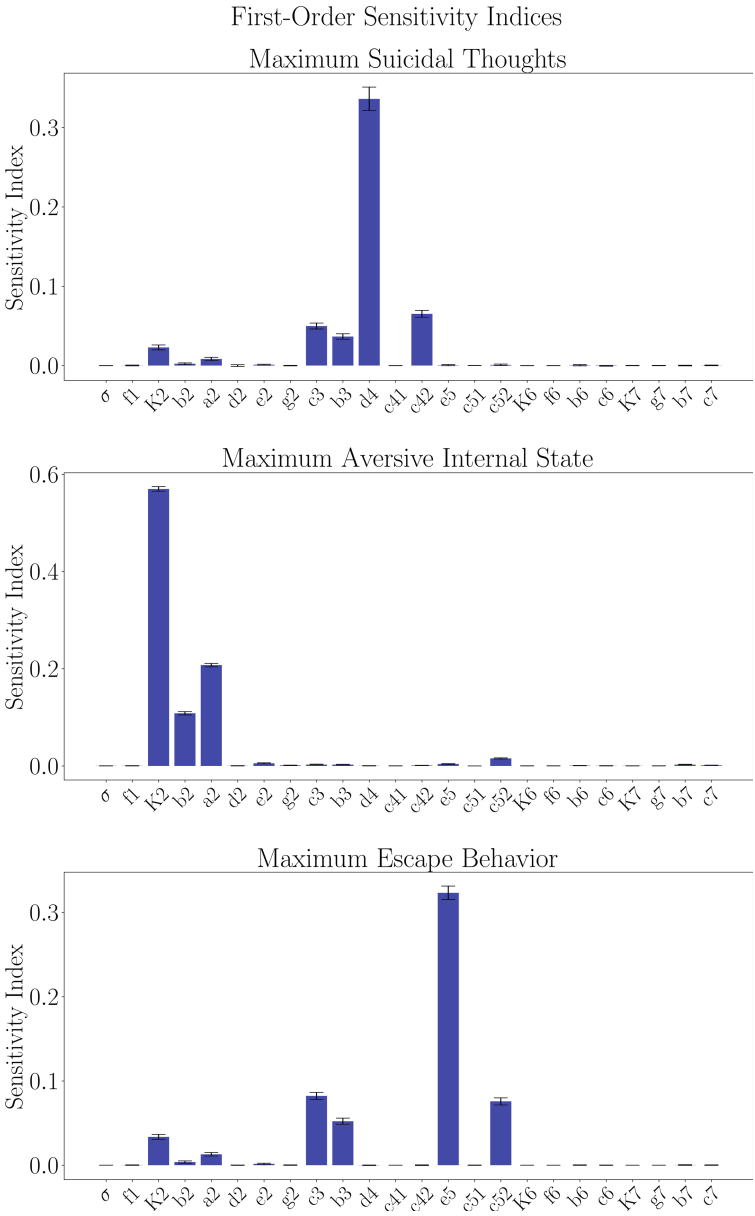

Fig. 6. First-order Sobol sensitivity indices for all parameters for the maximum of each model output.

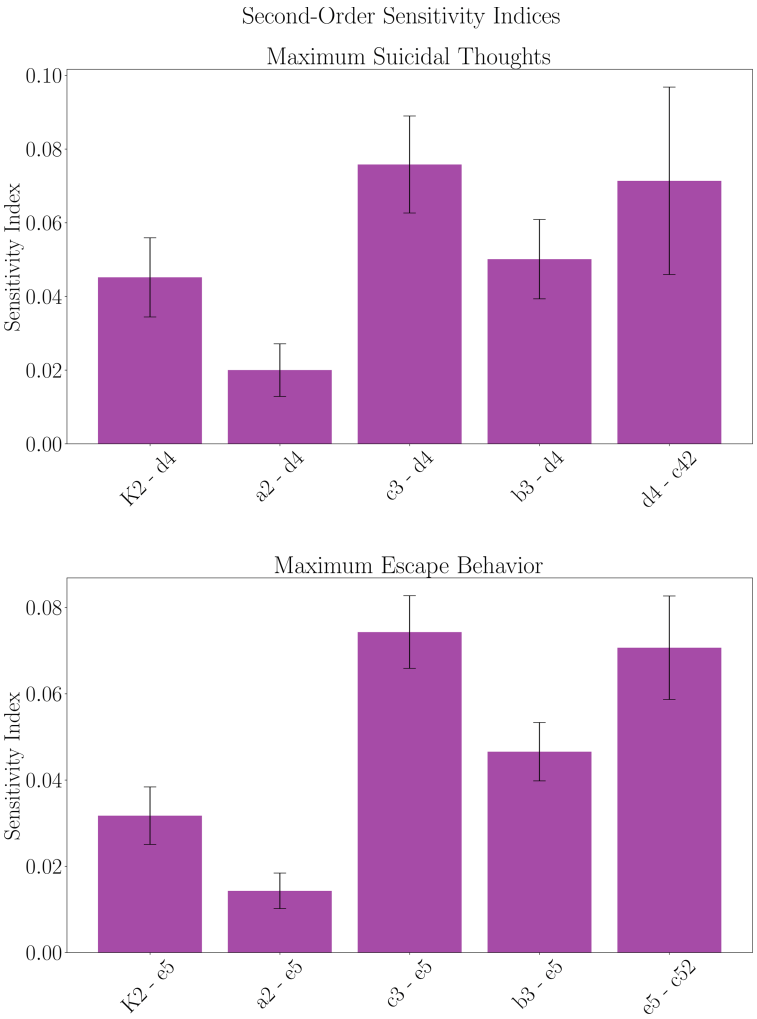

Fig. 7. Second-order Sobol sensitivity indices for parameters with indices greater than 0.01 for the maximum of suicidal thoughts and escape behaviors.

parameters governing self-feedback loops. The results of the second-order Sobol sensitivity analyses are found in Fig. 7.

We notice that all of the most relevant parameter interactions for a particular model output involve the parameter associated with its self-feedback loop. For the maximum of suicidal thoughts and escape behavior, this is d_4 and e_5 respectively. We also notice the high relevance of K_2, a_2, b_3, and particularly c_3 (the parameter associated with the self-feedback loop for the urge to escape). This highlights, once again, the impact of exponential growth for self-feedback loops between coupled states. Since the urge to escape has a positive, nonlinear effect

on both suicidal thoughts and escape behaviors, any exponential growth that results from lowering c_3 will greatly impact the results of both escape behaviors and suicidal thoughts. The cascading effect of variables is also highlighted, as K_2 is the carrying capacity for aversive internal state, a_2 is the positive effect of stressors on aversive internal state, and b_3 is the positive effect aversive internal state on the urge to escape. This in turn feeds both escape behaviors and suicidal thoughts, whose state will dictate their growth rate as a result of their self-feedback loops. We again notice the high importance of interactions with c_{42} and c_{52}: since these parameters control the placement of these sigmoidal curves, changes in these parameters will affect the threshold of urge to escape at which either escape behaviors or suicidal thoughts will sharply increase. Small perturbations in the parameters introduce nonlinearities that, when combined with their own self-feedback loops, will starkly affect the model output.

3.2 Time-Dependent Sensitivity Analysis

In order to assess any changes in parameter influence over the two-week simulation, a sensitivity analysis for all three model outputs was conducted each day of the simulation output found in Fig. 1. This particular realization of the model was chosen for its sufficiently fluctuating dynamics, particularly its peak in stressors between the second and third day of the simulation and trough at day 11. In Fig. 8, we see the results for the first-order and total-order sensitivity indices for the five highest sensitivity indices for each model output with 2^{16} samples. For both types of sensitivity indices, we notice a general trend of stability in the value of sensitivity indices over the course of the simulation. The general stability of sensitivity indices over the course of the simulation, despite fluctuations in variable outputs, indicates that the choice of simulation realization seen in Fig. 1 does not influence the sensitivity analysis output. The individual influence of d_4 (self-feedback loop of suicidal thoughts) decreases over the course of the simulation, while its interactions remain highly relevant throughout for suicidal thoughts. This indicates that while d_4 may have a direct importance in the trajectory of suicidal thoughts initially, its interactions with parameters governing aversive internal state or urge to escape maintain the overall influence of the self-feedback loop on the suicidal thoughts output. The self-feedback loop governed by d_4 may also diminish in individual importance as the system stabilizes and suicidal thoughts decrease.

For aversive internal state, higher-order interactions involving b_6 (effect of aversive internal states on external-focused strategies), c_3 (self-feedback loop on urge to escape), b_3 (effect of aversive internal states on change in urge to escape), and c_6 (effect of urge to escape on external-focused strategies) all increase slightly on the second day of the simulation when stressors inflate, before remaining relatively constant for the remainder of the simulation. As stressors spike in the early part of the simulation, aversive internal state and the urge to escape temporarily amplify each other. This highlights the interaction between mediating parameters like b_3 and c_3 that capture the reinforcing loop where higher aversive states drive a greater urge to escape. This sharp increase in stressors also drives the

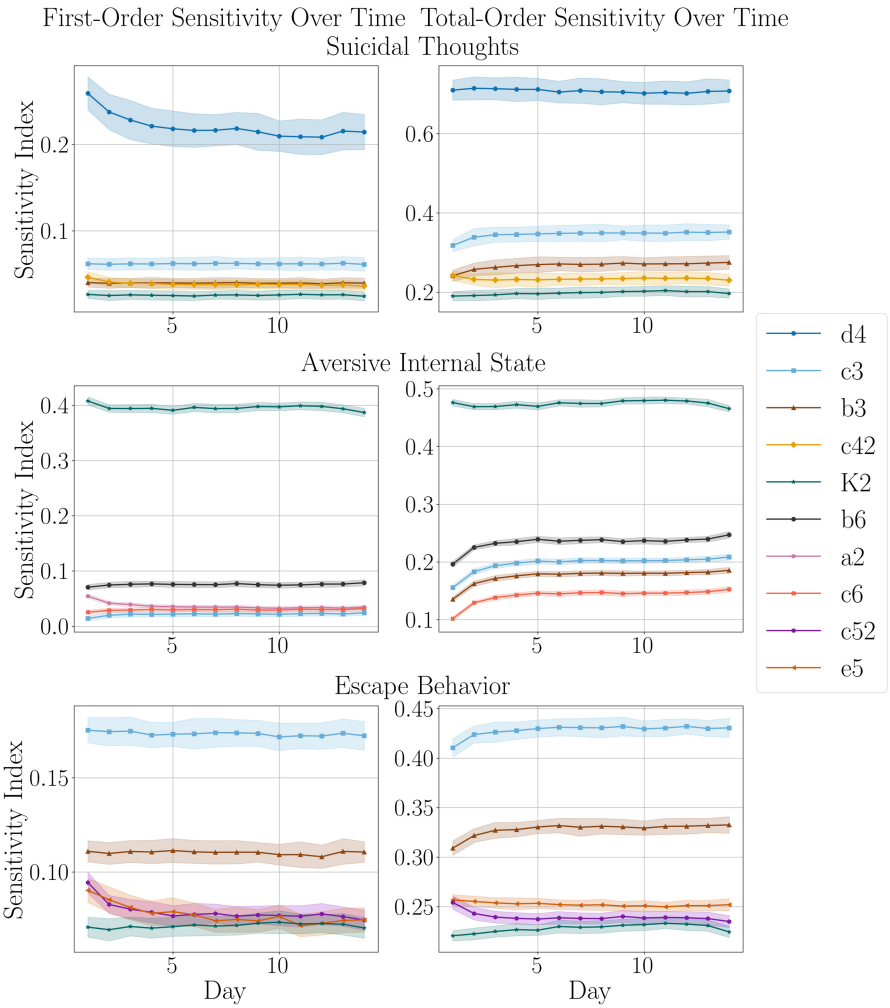

Fig. 8. The five highest first and total-order sensitivity indices for each model output on each day of the simulation.

activation of externally based strategies as a result of increased aversive internal state and the urge to escape, which underscores the importance of parameter interactions involving b_6 and c_6. We also notice that a_2 (the positive effect of aversive internal states on change in urge to escape) has a modest individual influence on aversive internal state. In this way, it acts as a bridge between aversive internal state and the urge to escape, but does not amplify the reinforcing loop between the two states.

We see a similar trend for higher-order interactions with c_3 and b_3 for escape behavior, and a slight decline in interaction importance for c_{52} following the first

day of the simulation and a modest increase in interaction importance for K_2. This is likely due to the fact that c_{52} (the midpoint of the sigmoidal curve for escape behavior) strongly influences the sharp increase of escape behaviors by interacting with the variable's self-feedback loop when stressors are high in the early days of the simulation. Interactions with the carrying capacity for aversive internal state (K_2) increase in relevance as the simulation proceeds, indicating greater reliance on K_2 as a regulating mechanism for aversive internal state.

4 Conclusion and Future Work

Results from a sensitivity analysis of the General Escape model of suicidal thoughts by Wang et al. [15] highlight the importance of parameters governing self-feedback loops, carrying capacities for aversive internal states, and the downregulation of cascading effects of stressors on escape behaviors and suicidal thoughts. The results also indicate that the relative influence of these parameters are stable throughout the simulation. Interaction effects between aversive internal state and the urge to escape were also found to greatly impact the model output. Future research should validate these model findings with clinical data and explore individual differences to refine the model's applicability to intervention strategies.

Acknowledgments. This study was supported by the Research priority area Urban Mental Health of the University of Amsterdam, within the project "Understanding the Dynamics of Suicide: An Agent-Based Modeling Approach to Inform Intervention Strategies in an Urban Context".

Disclosure of Interests. The authors have no competing interests to declare that are relevant to the content of this article.

References

1. Colucci, S., Papale, P.: Deep magma transport control on the size and evolution of explosive volcanic eruptions. Front. Earth Sci. **9** (2021). https://doi.org/10.3389/feart.2021.681083
2. de Beurs, D., et al.: A network perspective on suicidal behavior: understanding suicidality as a complex system. Suicide Life-Threat. Behav. **51**(1), 115–126 (2021). https://doi.org/10.1111/sltb.12676
3. Franklin, J.C., et al.: Risk factors for suicidal thoughts and behaviors: a meta-analysis of 50 years of research. Psychol. Bull. **143**(2), 187–232 (2017). https://doi.org/10.1037/bul0000084
4. Harris, C.R., et al.: Array programming with NumPy. Nature **585**, 357–362 (2020). https://doi.org/10.1038/s41586-020-2649-2
5. Herman, J., Usher, W.: SALib: an open-source python library for sensitivity analysis. J. Open Source Softw. **2**(9) (2017). https://doi.org/10.21105/joss.00097
6. Lam, S.K., Pitrou, A., Seibert, S.: Numba: a LLVM-based python JIT compiler. In: Proceedings of the Second Workshop on the LLVM Compiler Infrastructure in HPC. LLVM 2015. Association for Computing Machinery, New York, NY, USA (2015). https://doi.org/10.1145/2833157.2833162

7. McKinney, W.: Data structures for statistical computing in Python. In: van der Walt, S., Millman, J. (eds.) Proceedings of the 9th Python in Science Conference, pp. 56–61 (2010). https://doi.org/10.25080/Majora-92bf1922-00a
8. Millner, A.J., Robinaugh, D.J., Nock, M.K.: Advancing the understanding of suicide: the need for formal theory and rigorous descriptive research. Trends Cogn. Sci. **24**(9), 704–716 (2020). https://doi.org/10.1016/j.tics.2020.06.007
9. World Health Organization: Technical report (2021). https://www.who.int/news-room/fact-sheets/detail/suicide
10. Puy, A., Lo Piano, S., Saltelli, A.: A sensitivity analysis of the pawn sensitivity index. Environ. Model. Softw. **127**, 104679 (2020). https://doi.org/10.1016/j.envsoft.2020.104679
11. Roy, D.D.: Global sensitivity analysis - how to perform comprehensive, efficient, and robust global sensitivity analysis? June 2024
12. Saltelli, A., et al.: Global Sensitivity Analysis. The Primer. Wiley (2007). https://doi.org/10.1002/9780470725184
13. Sobol, I.: Global sensitivity indices for nonlinear mathematical models and their monte Carlo estimates. Math. Comput. Simul. **55**(1–3), 271–280 (2001). https://doi.org/10.1016/s0378-4754(00)00270-6
14. Team, The Matplotlib Development: Matplotlib: visualization with Python (2023). https://doi.org/10.5281/ZENODO.8347255
15. Wang, S.B., Robinaugh, D., Millner, A., Fortgang, R., Nock, M.: Mathematical and computational modeling of suicide as a complex dynamical system, September 2023. https://doi.org/10.31234/osf.io/b29cs
16. Zhang, X., Trame, M., Lesko, L., Schmidt, S.: Sobol sensitivity analysis: a tool to guide the development and evaluation of systems pharmacology models. CPT Pharmacometrics Syst. Pharmacol. **4**(2), 69–79 (2015). https://doi.org/10.1002/psp4.6

Multidimensional Granular Approach to Solving Fuzzy Complex System of Linear Equations

Marek Landowski(✉)

Faculty of Computer Science and Telecommunications, Maritime University of Szczecin, Waly Chrobrego 1-2, 70-500 Szczecin, Poland
m.landowski@pm.szczecin.pl

Abstract. The paper describes a multidimensional approach to solving a fuzzy complex linear system (FCLS). Together with the definition of arithmetic operations on complex fuzzy numbers with a horizontal granular membership function, the properties of these basic arithmetic operations are given and proven. Using the horizontal membership function of the fuzzy number and its counterpart in the complex number space, a multidimensional full granule of solution of FCLS was obtained. There are many methods in the scientific literature that generate results that are not full solutions of FCLS. The examples presented show that the use of the horizontal approach generates a full solution and indicate differences with the results obtained from other methods cited in the article. Furthermore, with granular approach the solution of the full FCLS was calculated.

Keywords: Fuzzy complex number · Horizontal complex fuzzy membership function · Fuzzy complex linear system · Uncertainty theory · Artificial intelligence

1 Introduction

Fuzzy set was proposed by Zadeh [31]; subsequently, a fuzzy number as a fuzzy subset on the real line, with arithmetic on fuzzy numbers, called fuzzy arithmetic, were introduced [8,10,19,22]. A fuzzy complex number (FCN) was defined by Backley [6,7]; Ramot et al. [29,30] also present concept of the FCN. In many papers the definition of FCN was used e.g. [3,11,13,18,28].

In this paper the multidimensional horizontal approach to the FCN is used to solve fuzzy complex system of linear equations. The horizontal membership function (HMF) of the fuzzy set and its arithmetic was introduced by Piegat for the first time was presented in [25]. The concept of the HMF is based on relative distance measure interval arithmetic (RDMIA) [24,26,27]. In this approach, the entire problem space is considered, where the solution is a multidimensional information granule. RDMIA uses the approach of defining the interval $[x_1, x_2]$

M. Paszynski et al. (Eds.): ICCS 2025 Workshops, LNCS 15912, pp. 198–212, 2025.
https://doi.org/10.1007/978-3-031-97573-8_14

as a value of the form $\lambda x_1 + (1-\lambda)x_2$, where $\lambda \in [0,1]$. Such a definition of the interval was given by Zimmermann 1985 [32] and Klir and Yuan 1995 [20]. The HMF concept has been used in scientific works, e.g. for solving differential equations [21], as well as for studying the stability of fuzzy linear dynamic systems [23] and many others.

Determining full and correct solution of the fuzzy complex linear system (FCLS) is still very interesting for the research community. In problems of real life, variables usually are uncertain. For researchers of many fields of science, such as economy, medicine, engineering, mathematics or physics, it is very important to find a solution of the FCLS. The papers where the real fuzzy linear system is solved are [1,2,5,9,12,16,17]. Also, there are methods for solving FCLS and their application. Raheooy et al. in [28] applied FCLS to circuit analysis, while Jahantigh et al. in [18] proposed a numerical procedure to find the solution of FCLS. Behera and Chakraverty in [3,4] describe a method for solving FCLS; later Ghanbari [13] published its modified version. Recently, Guo and Zhang in [14] wrote about minimal solution of FCLS. Farahani et al. in [11] solved FCLS using eigenvalue method. Moreover, Han and Guo in [15] discussed the numerical procedure for solution of FCLS.

The fuzzy complex linear system (FCLS) in [3] is defined as $[C][\tilde{Z}] = [\tilde{W}]$, where: $[C]$ - the $n \times n$ matrix of crisp complex coefficients; $[\tilde{W}]$ - the $n \times 1$ matrix of fuzzy complex numbers; and $[\tilde{Z}]$ - unknown fuzzy complex numbers. The full fuzzy complex linear system (FFCLS) is defined as a FCLS where the matrix of coefficients $[C]$ is a matrix of fuzzy complex numbers $[\tilde{C}]$.

On the presented examples it was shown that results generated by methods in the cited papers are not full solutions of the FCLS. It was proved by generating the crisp solution of the crisp complex linear system (CCLS) from FCLS which does not belong to the set of results of the cited papers. Therefore, there is a need to find a method that will generate a full solution of the FCLS. To fill this gap, the HMF and its arithmetic is used.

The method with fuzzy complex number (FCN) and its horizontal membership function (HMF) presented in the paper allows to generate crisp sets of the dependent solutions, the granule of solution. With the solution expressed in the form of granule of information it can be determined if any crisp solution is possible or not. Three examples analyzed in the paper were taken from [3,4,11,15,28]. The last example presents application of the HMF to find the solution of the full fuzzy complex linear system.

The multidimensional granular complex HMF approach provides solutions that satisfy fuzzy complex linear systems. It is shown on examples that the methods from the cited articles do not generate a full FCLS solution, the results are overestimated or underestimated. The obtained multidimensional solution by HMF is an information granule of the full set of solutions that satisfies FCLS (FFCLS) and its equivalent forms.

The rest of the paper is organized as follows: in Sect. 2 the theoretical foundation of the fuzzy complex number with horizontal membership function and its arithmetic with basic algebraic properties are given. In Sect. 3 the numeri-

cal examples are considered, where the fuzzy complex linear systems are solved. Section 4 presents some conclusions.

Abbreviations: FCN - fuzzy complex number, CCLS - crisp complex linear system, FCLS - fuzzy complex linear system, FFCLS - full fuzzy complex linear system, HMF - horizontal membership function.

2 Theoretical Foundations

This section presents the theoretical foundations of the fuzzy complex number, horizontal fuzzy number, horizontal fuzzy complex number and horizontal fuzzy complex arithmetic used in the paper for solving fuzzy complex linear system.

Let us introduce the following notations: E_1 is a set of fuzzy numbers on the real numbers $\mathbb{R}$, and $u_{\tilde{x}}^{\mu} = (\underline{u}_{\tilde{x}}^{\mu}, \overline{u}_{\tilde{x}}^{\mu})$ is μ-cut level of $\tilde{x} \in E_1$, $\mu \in [0,1]$.

Definition 1 *[12] (Fuzzy number). An arbitrary fuzzy number is an ordered pair of functions* $(\underline{u}^{\mu}, \overline{u}^{\mu})$, $0 \le \mu \le 1$, *which satisfy the following requirements:*

1. $\underline{u}^{\mu}$ *is a bounded left continuous nondecreasing function over* $[0,1]$.
2. $\overline{u}^{\mu}$ *is a bounded left continuous nonincreasing function over* $[0,1]$.
3. $\underline{u}^{\mu} \le \overline{u}^{\mu}$, $0 \le \mu \le 1$.

Definition 2 *[3] (Fuzzy complex number). An arbitrary fuzzy complex number is written as* $\tilde{z} = \tilde{p} + i\tilde{q}$, *where* $\tilde{p} = [\underline{p}^{\mu}, \overline{p}^{\mu}]$ *and* $\tilde{q} = [\underline{q}^{\mu}, \overline{q}^{\mu}]$, $0 \le \mu \le 1$.

For fuzzy complex number $\tilde{z} = \tilde{p} + i\tilde{q}$, $\tilde{p}$ is called the real part ($Re(\tilde{z})$) and $\tilde{q}$ is called the imaginary part ($Im(\tilde{z})$). A μ-level of an arbitrary fuzzy complex number can be written as $\tilde{z}^{\mu} = [\underline{p}^{\mu}, \overline{p}^{\mu}] + i[\underline{q}^{\mu}, \overline{q}^{\mu}] = [\underline{p}^{\mu} + i\underline{q}^{\mu}, \overline{p}^{\mu} + i\overline{q}^{\mu}]$.

Definition 3 *[21,25] (Horizontal membership function). Let* $\tilde{u} : [a,b] \subseteq \mathbb{R} \to [0,1]$ *be a fuzzy number. The horizontal membership function* $u^{gr} : [0,1] \times [0,1] \to [a,b]$ *is a representation of* $\tilde{u}(x)$ *as* $u^{gr}(\mu, \alpha_u) = x$ *in which "gr" stands for the granule of information included in* $x \in [a,b]$, $\mu \in [0,1]$ *is the membership degree of* x *in* $\tilde{u}(x)$, $\alpha_u \in [0,1]$ *is called RDM variable, and* $u^{gr}(\mu, \alpha_u) = \underline{u}^{\mu} + (\overline{u}^{\mu} - \underline{u}^{\mu})\alpha_u$.

The horizontal membership function presented by granule of information of fuzzy number $\tilde{u}$ is denoted in [21] as $\mathcal{H}(\tilde{u}) = u^{gr}(\mu, \alpha_u)$.

Definition 4 *[23]. The horizontal membership function of the fuzzy complex number* $\tilde{z} = \tilde{p} + i\tilde{q}$ *is denoted by* $\mathcal{H}(\tilde{z}) = z^{gr}(\mu, \alpha_p, \alpha_q)$ *and defined as* $\mathcal{H}(\tilde{z}) = \mathcal{H}(\tilde{p}) + i\mathcal{H}(\tilde{q})$. *Therefore,* $Re(\mathcal{H}(\tilde{z})) = \mathcal{H}(Re(\tilde{z}))$ *and* $Im(\mathcal{H}(\tilde{z})) = \mathcal{H}(Im(\tilde{z}))$.

For example, the fuzzy complex number with nonlinear borders $\tilde{z}^{\mu} = \tilde{p}^{\mu} + i\tilde{q}^{\mu} = [3 + \mu^2, 5 - \sqrt{\mu}] + i[4 + \mu^3, 7 - \mu^2]$, $\mu \in [0,1]$, has a complex granular form of membership function as: $z^{gr}(\mu, \alpha_p, \alpha_q) = 3 + \mu^2 + \alpha_p(2 - \sqrt{\mu} - \mu^2) + i[4 + \mu^3 + \alpha_q(3 - \mu^2 - \mu^3)]$, where μ, α_p, $\alpha_q \in [0,1]$. The fuzzy complex number $\tilde{z}^{\mu}$ with nonlinear boundaries together with variables α_p and α_q generating the information granule is presented in 3D space in Fig. 1.

The definition of the span of the complex information granule $z^{gr}(\mu, \alpha_p, \alpha_q)$ is as follows.

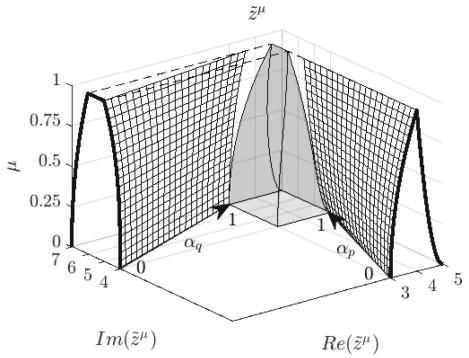

Fig. 1. Fuzzy complex number $\tilde{z}^\mu = \tilde{p}^\mu + i\tilde{q}^\mu = [3 + \mu^2, 5 - \sqrt{\mu}] + i[4 + \mu^3, 7 - \mu^2]$, $\mu \in [0, 1]$ and variables $\alpha_p, \alpha_q \in [0, 1]$ generating the information granule.

Definition 5. *The fuzzy complex number $\tilde{z} = \tilde{p} + i\tilde{q}$ can be represented by the span of its horizontal membership function $\mathcal{H}(\tilde{z}) = z^{gr}(\mu, \alpha_p, \alpha_q)$, by the formula (1),*

$$\tilde{z}^\mu = \mathcal{H}^{-1}(z^{gr}(\mu, \alpha_p, \alpha_q)) = \left[\inf_{\gamma \geq \mu} \min_{\alpha_p} z^{gr}(\gamma, \alpha_p), \sup_{\gamma \geq \mu} \max_{\alpha_p} z^{gr}(\gamma, \alpha_p)\right] + i\left[\inf_{\gamma \geq \mu} \min_{\alpha_q} z^{gr}(\gamma, \alpha_q), \sup_{\gamma \geq \mu} \max_{\alpha_q} z^{gr}(\gamma, \alpha_q)\right] \tag{1}$$

Definition 6. *Let $\tilde{z}_1 = \tilde{p}_1 + i\tilde{q}_1$ and $\tilde{z}_2 = \tilde{p}_2 + i\tilde{q}_2$ are the fuzzy complex numbers, with the horizontal membership functions $\mathcal{H}(\tilde{z}_1) = \mathcal{H}(\tilde{p}_1) + i\mathcal{H}(\tilde{q}_1)$ and $\mathcal{H}(\tilde{z}_2) = \mathcal{H}(\tilde{p}_2) + i\mathcal{H}(\tilde{q}_2)$. Denotes $\odot$ as a one of four basic arithmetic operations $\{+, -, \times, /\}$. Therefore, $\tilde{z}_1 \odot \tilde{z}_2$ is a fuzzy complex number such that $\mathcal{H}(\tilde{z}_1 \odot \tilde{z}_2) = \mathcal{H}(\tilde{p}_1) \odot \mathcal{H}(\tilde{p}_2) + i(\mathcal{H}(\tilde{q}_1) \odot \mathcal{H}(\tilde{q}_2))$, operation / occurs only if $0 \notin \mathcal{H}(\tilde{z}_2)$.*

For fuzzy numbers whose horizontal membership functions are as in Definition 4 the basic algebraic properties hold.

Lemma 1. *Let $\tilde{z}_1$, $\tilde{z}_2$ and $\tilde{z}_3$ are fuzzy complex numbers with horizontal membership functions $\mathcal{H}(\tilde{z}_1)$, $\mathcal{H}(\tilde{z}_2)$ and $\mathcal{H}(\tilde{z}_3)$. The FCN with HMF addition and multiplication are commutative and associative, equations in (2) are true,*

$$\begin{aligned} &\tilde{z}_1 + \tilde{z}_2 = \tilde{z}_2 + \tilde{z}_1, \\ &\tilde{z}_1\tilde{z}_2 = \tilde{z}_2\tilde{z}_1, \\ &\tilde{z}_1 + (\tilde{z}_2 + \tilde{z}_3) = (\tilde{z}_1 + \tilde{z}_2) + \tilde{z}_3, \\ &\tilde{z}_1(\tilde{z}_2\tilde{z}_3) = (\tilde{z}_1\tilde{z}_2)\tilde{z}_3. \end{aligned} \tag{2}$$

Lemma 2. *The FCN with HMF has identity elements under addition and multiplication that are crisp values 0 and 1, respectively. Equations in (3) hold for any FCN $\tilde{z}$ with HMF $\mathcal{H}(\tilde{z})$,*

$$\begin{aligned} &0 + \tilde{z} = \tilde{z} + 0 = \tilde{z}, \\ &1 \cdot \tilde{z} = \tilde{z} \cdot 1 = \tilde{z}. \end{aligned} \tag{3}$$

It is easy to show that Lemma 1 and 2 hold, so the proof is left to the reader.

Lemma 3. *The FCN* $\tilde{z} = \tilde{p} + i\tilde{q}$ *with HMF* $\mathcal{H}(\tilde{z}) = z^{gr}(\mu, \alpha_p, \alpha_q) = \underline{p}^{\mu} + \alpha_p(\overline{p}^{\mu} - \underline{p}^{\mu}) + i[\underline{q}^{\mu} + \alpha_q(\overline{q}^{\mu} - \underline{q}^{\mu}]$, *where* $\mu, \alpha_p, \alpha_q \in [0, 1]$, *has an additive inverse element (4),*

$$-z^{gr}(\mu, \alpha_p, \alpha_q) = -[\underline{p}^{\mu} + \alpha_p(\overline{p}^{\mu} - \underline{p}^{\mu})] - i[\underline{q}^{\mu} + \alpha_q(\overline{q}^{\mu} - \underline{q}^{\mu})]. \tag{4}$$

Proof. $z^{gr}(\mu, \alpha_p, \alpha_q) + (-z^{gr}(\mu, \alpha_p, \alpha_q)) = [\underline{p}^{\mu} + \alpha_p(\overline{p}^{\mu} - \underline{p}^{\mu}) + i[\underline{q}^{\mu} + \alpha_q(\overline{q}^{\mu} - \underline{q}^{\mu})]] + [-[\underline{p}^{\mu} + \alpha_p(\overline{p}^{\mu} - \underline{p}^{\mu})] - i[\underline{q}^{\mu} + \alpha_q(\overline{q}^{\mu} - \underline{q}^{\mu})]] = \underline{p}^{\mu} + \alpha_p(\overline{p}^{\mu} - \underline{p}^{\mu}) + i[\underline{q}^{\mu} + \alpha_q(\overline{q}^{\mu} - \underline{q}^{\mu})] - [\underline{p}^{\mu} + \alpha_p(\overline{p}^{\mu} - \underline{p}^{\mu})] - i[\underline{q}^{\mu} + \alpha_q(\overline{q}^{\mu} - \underline{q}^{\mu})] = 0$ □

Lemma 4. *For the FCN* $\tilde{z} = \tilde{p} + i\tilde{q}$ *with HMF* $H(\tilde{z}) = z^{gr}(\mu, \alpha_p, \alpha_q) = \underline{p}^{\mu} + \alpha_p(\overline{p}^{\mu} - \underline{p}^{\mu}) + i[\underline{q}^{\mu} + \alpha_q(\overline{q}^{\mu} - \underline{q}^{\mu})]$, $0 \notin z^{gr}(\mu, \alpha_p, \alpha_q)$, *where* $\mu, \alpha_p, \alpha_q \in [\overline{0}, 1]$, *there exists a multiplicative inverse element given by (5),*

$$1/z^{gr}(\mu, \alpha_p, \alpha_q) = \frac{\underline{p}^{\mu} + \alpha_p(\overline{p}^{\mu} - \underline{p}^{\mu}) - i[\underline{q}^{\mu} + \alpha_q(\overline{q}^{\mu} - \underline{q}^{\mu})]}{[\underline{p}^{\mu} + \alpha_p(\overline{p}^{\mu} - \underline{p}^{\mu})]^2 + [\underline{q}^{\mu} + \alpha_q(\overline{q}^{\mu} - \underline{q}^{\mu})]^2}. \tag{5}$$

Proof. $z^{gr}(\mu, \alpha_p, \alpha_q) \cdot (1/z^{gr}(\mu, \alpha_p, \alpha_q))$
$= [\underline{p}^{\mu} + \alpha_p(\overline{p}^{\mu} - \underline{p}^{\mu}) + i[\underline{q}^{\mu} + \alpha_q(\overline{q}^{\mu} - \underline{q}^{\mu})]] \cdot \frac{\underline{p}^{\mu} + \alpha_p(\overline{p}^{\mu} - \underline{p}^{\mu}) - i[\underline{q}^{\mu} + \alpha_q(\overline{q}^{\mu} - \underline{q}^{\mu})]}{[\underline{p}^{\mu} + \alpha_p(\overline{p}^{\mu} - \underline{p}^{\mu})]^2 + [\underline{q}^{\mu} + \alpha_q(\overline{q}^{\mu} - \underline{q}^{\mu})]^2}$
$= \frac{[\underline{p}^{\mu} + \alpha_p(\overline{p}^{\mu} - \underline{p}^{\mu})]^2 + [\underline{q}^{\mu} + \alpha_q(\overline{q}^{\mu} - \underline{q}^{\mu})]^2}{[\underline{p}^{\mu} + \alpha_p(\overline{p}^{\mu} - \underline{p}^{\mu})]^2 + [\underline{q}^{\mu} + \alpha_q(\overline{q}^{\mu} - \underline{q}^{\mu})]^2} = 1$ □

Lemma 5. *The distributive law (6) holds for any FCN* $\tilde{z}_1 = \tilde{p}_1 + i\tilde{q}_1$, $\tilde{z}_2 = \tilde{p}_2 + i\tilde{q}_2$ *and* $\tilde{z}_3 = \tilde{p}_3 + i\tilde{q}_3$ *with* $\mathcal{H}(\tilde{z}_1) = z_1^{gr}(\mu, \alpha_{p_1}, \alpha_{q_1})$, $\mathcal{H}(\tilde{z}_2) = z_2^{gr}(\mu, \alpha_{p_2}, \alpha_{q_2})$ *and* $\mathcal{H}(\tilde{z}_3) = z_3^{gr}(\mu, \alpha_{p_3}, \alpha_{q_3})$,

$$\tilde{z}_1(\tilde{z}_2 + \tilde{z}_3) = \tilde{z}_1\tilde{z}_2 + \tilde{z}_1\tilde{z}_3 \tag{6}$$

Proof. $\mathcal{H}(\tilde{z}_1)(\mathcal{H}(\tilde{z}_2) + \mathcal{H}(\tilde{z}_3)) = [\underline{p}_1^{\mu} + \alpha_{p_1}(\overline{p}_1^{\mu} - \underline{p}_1^{\mu}) + i[\underline{q}_1^{\mu} + \alpha_{q_1}(\overline{q}_1^{\mu} - \underline{q}_1^{\mu})]] \cdot \{[\underline{p}_2^{\mu} + \alpha_{p_2}(\overline{p}_2^{\mu} - \underline{p}_2^{\mu}) + i[\underline{q}_2^{\mu} + \alpha_{q_2}(\overline{q}_2^{\mu} - \underline{q}_2^{\mu})]] + [\underline{p}_3^{\mu} + \alpha_{p_3}(\overline{p}_3^{\mu} - \underline{p}_3^{\mu}) + i[\underline{q}_3^{\mu} + \alpha_{q_3}(\overline{q}_3^{\mu} - \underline{q}_3^{\mu})]]\} = [\underline{p}_1^{\mu} + \alpha_{p_1}(\overline{p}_1^{\mu} - \underline{p}_1^{\mu}) + i[\underline{q}_1^{\mu} + \alpha_{q_1}(\overline{q}_1^{\mu} - \underline{q}_1^{\mu})]] \cdot [\underline{p}_2^{\mu} + \alpha_{p_2}(\overline{p}_2^{\mu} - \underline{p}_2^{\mu}) + i[\underline{q}_2^{\mu} + \alpha_{q_2}(\overline{q}_2^{\mu} - \underline{q}_2^{\mu})]] + [\underline{p}_1^{\mu} + \alpha_{p_1}(\overline{p}_1^{\mu} - \underline{p}_1^{\mu}) + i[\underline{q}_1^{\mu} + \alpha_{q_1}(\overline{q}_1^{\mu} - \underline{q}_1^{\mu})]] \cdot [\underline{p}_3^{\mu} + \alpha_{p_3}(\overline{p}_3^{\mu} - \underline{p}_3^{\mu}) + i[\underline{q}_3^{\mu} + \alpha_{q_3}(\overline{q}_3^{\mu} - \underline{q}_3^{\mu})]] = \mathcal{H}(\tilde{z}_1)\mathcal{H}(\tilde{z}_2) + \mathcal{H}(\tilde{z}_1)\mathcal{H}(\tilde{z}_3)$,
where $\mu, \alpha_{p_1}, \alpha_{p_2}, \alpha_{p_3}, \alpha_{q_1}, \alpha_{q_2}, \alpha_{q_3} \in [0, 1]$. □

Lemma 6. *The cancellation law for addition (7) holds in the FCN with HMF arithmetic,*

$$\tilde{z}_1 + \tilde{z}_3 = \tilde{z}_2 + \tilde{z}_3 \Rightarrow \tilde{z}_1 = \tilde{z}_2, \tag{7}$$

where $\tilde{z}_1 = \tilde{p}_1 + i\tilde{q}_1$, $\tilde{z}_2 = \tilde{p}_2 + i\tilde{q}_2$ *and* $\tilde{z}_3 = \tilde{p}_3 + i\tilde{q}_3$ *are FCN with HMF:* $\mathcal{H}(\tilde{z}_1) = z_1^{gr}(\mu, \alpha_{p_1}, \alpha_{q_1})$, $\mathcal{H}(\tilde{z}_2) = z_2^{gr}(\mu, \alpha_{p_2}, \alpha_{q_2})$ *and* $\mathcal{H}(\tilde{z}_3) = z_3^{gr}(\mu, \alpha_{p_3}, \alpha_{q_3})$.

Proof. $\tilde{z}_1 + \tilde{z}_3 = \tilde{z}_2 + \tilde{z}_3$;
$[\underline{p}_1^{\mu} + \alpha_{p_1}(\overline{p}_1^{\mu} - \underline{p}_1^{\mu}) + i[\underline{q}_1^{\mu} + \alpha_{q_1}(\overline{q}_1^{\mu} - \underline{q}_1^{\mu})]] + [\underline{p}_3^{\mu} + \alpha_{p_3}(\overline{p}_3^{\mu} - \underline{p}_3^{\mu}) + i[\underline{q}_3^{\mu} + \alpha_{q_3}(\overline{q}_3^{\mu} - \underline{q}_3^{\mu})]] = [\underline{p}_2^{\mu} + \alpha_{p_2}(\overline{p}_2^{\mu} - \underline{p}_2^{\mu}) + i[\underline{q}_2^{\mu} + \alpha_{q_2}(\overline{q}_2^{\mu} - \underline{q}_2^{\mu})]] + [\underline{p}_3^{\mu} + \alpha_{p_3}(\overline{p}_3^{\mu} - \underline{p}_3^{\mu}) + i[\underline{q}_3^{\mu} + \alpha_{q_3}(\overline{q}_3^{\mu} - \underline{q}_3^{\mu})]]$;
Adding $-\tilde{z}_3$ on both sides, we have:
$\underline{p}_1^{\mu} + \alpha_{p_1}(\overline{p}_1^{\mu} - \underline{p}_1^{\mu}) + i[\underline{q}_1^{\mu} + \alpha_{q_1}(\overline{q}_1^{\mu} - \underline{q}_1^{\mu})] = \underline{p}_2^{\mu} + \alpha_{p_2}(\overline{p}_2^{\mu} - \underline{p}_2^{\mu}) + i[\underline{q}_2^{\mu} + \alpha_{q_2}(\overline{q}_2^{\mu} - \underline{q}_2^{\mu})]$;
$\tilde{z}_1 = \tilde{z}_2$,
where $\mu, \alpha_{p_1}, \alpha_{p_2}, \alpha_{p_3}, \alpha_{q_1}, \alpha_{q_2}, \alpha_{q_3} \in [0, 1]$. □

Lemma 7. *For any FCN* $\tilde{z}_1 = \tilde{p}_1 + i\tilde{q}_1$, $\tilde{z}_2 = \tilde{p}_2 + i\tilde{q}_2$ *and* $\tilde{z}_3 = \tilde{p}_3 + i\tilde{q}_3$ *with HMF* $\mathcal{H}(\tilde{z}_1) = z_1^{gr}(\mu, \alpha_{p_1}, \alpha_{q_1})$, $\mathcal{H}(\tilde{z}_2) = z_2^{gr}(\mu, \alpha_{p_2}, \alpha_{q_2})$ *and* $\mathcal{H}(\tilde{z}_3) = z_3^{gr}(\mu, \alpha_{p_3}, \alpha_{q_3})$, *if* $0 \notin \tilde{z}_3$, *the cancellation law for multiplication (8) holds in the FCN with HMF arithmetic,*

$$\tilde{z}_1\tilde{z}_3 = \tilde{z}_2\tilde{z}_3 \Rightarrow \tilde{z}_1 = \tilde{z}_2. \tag{8}$$

Proof. $\tilde{z}_1 \cdot \tilde{z}_3 = \tilde{z}_2 \cdot \tilde{z}_3$;
$[\underline{p}_1^\mu + \alpha_{p_1}(\overline{p}_1^\mu - \underline{p}_1^\mu) + i[\underline{q}_1^\mu + \alpha_{q_1}(\overline{q}_1^\mu - \underline{q}_1^\mu)]] \cdot [\underline{p}_3^\mu + \alpha_{p_3}(\overline{p}_3^\mu - \underline{p}_3^\mu) + i[\underline{q}_3^\mu + \alpha_{q_3}(\overline{q}_3^\mu - \underline{q}_3^\mu)]] =$
$[\underline{p}_2^\mu + \alpha_{p_2}(\overline{p}_2^\mu - \underline{p}_2^\mu) + i[\underline{q}_2^\mu + \alpha_{q_2}(\overline{q}_2^\mu - \underline{q}_2^\mu)]] \cdot [\underline{p}_3^\mu + \alpha_{p_3}(\overline{p}_3^\mu - \underline{p}_3^\mu) + i[\underline{q}_3^\mu + \alpha_{q_3}(\overline{q}_3^\mu - \underline{q}_3^\mu)]]$;
Multiplying by $1/\tilde{z}_3$ both sides, we have:
$\underline{p}_1^\mu + \alpha_{p_1}(\overline{p}_1^\mu - \underline{p}_1^\mu) + i[\underline{q}_1^\mu + \alpha_{q_1}(\overline{q}_1^\mu - \underline{q}_1^\mu)] = \underline{p}_2^\mu + \alpha_{p_2}(\overline{p}_2^\mu - \underline{p}_2^\mu) + i[\underline{q}_2^\mu + \alpha_{q_2}(\overline{q}_2^\mu - \underline{q}_2^\mu)]$;
$\tilde{z}_1 = \tilde{z}_2$,
where $\mu, \alpha_{p_1}, \alpha_{p_2}, \alpha_{p_3}, \alpha_{q_1}, \alpha_{q_2}, \alpha_{q_3} \in [0, 1]$. □

The special cases of the fuzzy complex number (FCN) are triangular and trapezoidal FCNs. In the following two remarks, the triangular and trapezoidal FCNs granular approaches are defined.

Remark 1 (Triangular horizontal fuzzy complex membership function). A triangular fuzzy complex number $\tilde{v}^\mu = [a_1 + (b_1 - a_1)\mu, c_1 - (c_1 - b_1)\mu] + i[a_2 + (b_2 - a_2)\mu, c_2 - (c_2 - b_2)\mu]$ in the granular notation has a form of (9), where μ, α_p, $\alpha_q \in [0, 1]$, see Fig. 2.

$$\begin{aligned} v^{gr}(\mu, \alpha_p, \alpha_q) = {} & a_1 + (b_1 - a_1)\mu + [c_1 - a_1 - \mu(c_1 - a_1)]\alpha_p \\ & + i[a_2 + (b_2 - a_2)\mu + [c_2 - a_2 - \mu(c_2 - a_2)]\alpha_q] \end{aligned} \tag{9}$$

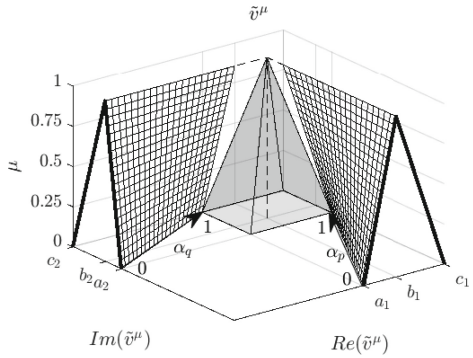

Fig. 2. Triangular fuzzy complex number $\tilde{v}^\mu = [a_1 + (b_1 - a_1)\mu, c_1 - (c_1 - b_1)\mu] + i[a_2 + (b_2 - a_2)\mu, c_2 - (c_2 - b_2)\mu]$, $\mu \in [0, 1]$ and variables $\alpha_p, \alpha_q \in [0, 1]$ generating the information granule.

Remark 2 (Trapezoidal horizontal fuzzy complex membership function). A trapezoidal fuzzy complex number $\tilde{w}^{\mu} = [a_1 + (b_1 - a_1)\mu, d_1 - (d_1 - c_1)\mu] + i[a_2 + (b_2 - a_2)\mu, d_2 - (d_2 - c_2)\mu]$ in the granular notation has a form of (10), where μ, α_p, $\alpha_q \in [0, 1]$, see Fig. 3.

$$w^{gr}(\mu, \alpha_p, \alpha_q) = a_1 + (b_1 - a_1)\mu + [d_1 - a_1 - \mu(d_1 - a_1 + b_1 - c_1)]\alpha_p + i[a_2 + (b_2 - a_2)\mu + [d_2 - a_2 - \mu(d_2 - a_2 + b_2 - c_2)]\alpha_q] \tag{10}$$

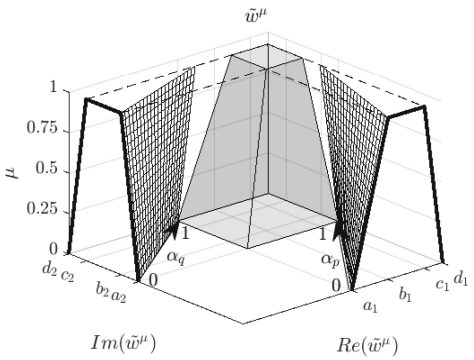

Fig. 3. Trapezoidal fuzzy complex number $\tilde{w}^{\mu} = [a_1 + (b_1 - a_1)\mu, d_1 - (d_1 - c_1)\mu] + i[a_2 + (b_2 - a_2)\mu, d_2 - (d_2 - c_2)\mu]$, $\mu \in [0, 1]$ and variables $\alpha_p, \alpha_q \in [0, 1]$ generating the information granule.

3 Examples of the FCLS Solved with the Granular Fuzzy Complex Membership Function

In this section three examples from [3,4,11,14,15,28] using horizontal approach to fuzzy complex numbers are solved. The last example presented in the paper - Example 3 - considers the full fuzzy complex linear system and its multidimensional granular solution.

Moreover, in the presented examples it was shown that the cited papers do not provide a full solution. On the basis of the fuzzy complex linear system (FCLS), infinitely many crisp complex linear systems (CCLS) can be generated. To show that results obtained in [3,4,11,13–15,28] are not full solutions, the CCLS generated from the analyzed examples of FCLS are examined, i.e. for support when $\mu = 0$. If the methods give a full solution, then the solution of the CCLS should be included in the result of the FCLS, for the same constant $\mu = 0$.

3.1 Examples

Example 1 (Example 1 [3,4], example 4.1 [15], example 1 [14], example 5.1 [11]). Let us consider the fuzzy complex linear system (11).

$$\begin{aligned} \tilde{z}_1 - \tilde{z}_2 &= [\mu, 2-\mu] + i[1+\mu, 3-\mu] \\ \tilde{z}_1 + 3\tilde{z}_2 &= [4+\mu, 7-2\mu] + i[\mu-4, -1-2\mu] \end{aligned} \tag{11}$$

The FCLS (11) in granular notation has a form of (12),

$$\begin{aligned} z_1^{gr} - z_2^{gr} &= \mu + (2-2\mu)\alpha_{p_1} + i(1+\mu+(2-\mu)\alpha_{q_1}) \\ z_1^{gr} + 3z_2^{gr} &= 4+\mu+(3-3\mu)\alpha_{p_2} + i(-4+\mu+(3-3\mu)\alpha_{q_2}) \end{aligned} \tag{12}$$

where $\mu, \alpha_{p_1}, \alpha_{p_2}, \alpha_{q_1}, \alpha_{q_2} \in [0,1]$.

With basic algebraic operations the multidimensional granular solution was obtained, formula (13),

$$\begin{aligned} z_1^{gr}(\mu, \alpha_{p_1}, \alpha_{p_2}, \alpha_{q_1}, \alpha_{q_2}) &= (4+6\alpha_{p_1}+3\alpha_{p_2}+\mu(4-6\alpha_{p_1}-3\alpha_{p_2}))/4 \\ &\quad + i(-1+6\alpha_{q_1}+3\alpha_{q_2}+\mu(4-6\alpha_{q_1}-3\alpha_{q_2}))/4 \\ z_2^{gr}(\mu, \alpha_{p_1}, \alpha_{p_2}, \alpha_{q_1}, \alpha_{q_2}) &= (4-2\alpha_{p_1}+3\alpha_{p_2}+\mu(2\alpha_{p_1}-3\alpha_{p_2}))/4 \\ &\quad + i(-5-2\alpha_{q_1}+3\alpha_{q_2}+\mu(2\alpha_{q_1}-3\alpha_{q_2}))/4 \end{aligned} \tag{13}$$

where $\mu, \alpha_{p_1}, \alpha_{p_2}, \alpha_{q_1}, \alpha_{q_2} \in [0,1]$.

The granular solution (13) satisfies the FCLS (11). Substituting the obtained solution for $\tilde{z}_1$ and $\tilde{z}_2$ in the FCLS, we have:

$\tilde{z}_1 - \tilde{z}_2 = [(4+6\alpha_{p_1}+3\alpha_{p_2}+\mu(4-6\alpha_{p_1}-3\alpha_{p_2}))/4 + i(-1+6\alpha_{q_1}+3\alpha_{q_2}+\mu(4-6\alpha_{q_1}-3\alpha_{q_2}))/4] - [(4-2\alpha_{p_1}+3\alpha_{p_2}+\mu(2\alpha_{p_1}-3\alpha_{p_2}))/4 + i(-5-2\alpha_{q_1}+3\alpha_{q_2}+\mu(2\alpha_{q_1}-3\alpha_{q_2}))/4] = 2\alpha_{p_1}+\mu(1-2\alpha_{p_1}) + i(1+2\alpha_{q_1}+\mu(1-2\alpha_{q_1})) = r+(2-2\mu)\alpha_{p_1} + i(1+\mu+(2-2\mu)\alpha_{q_1}) = [\mu, 2-\mu] + i[1+\mu, 3-\mu]$;

$\tilde{z}_1 + 3\tilde{z}_2 = [(4+6\alpha_{p_1}+3\alpha_{p_2}+\mu(4-6\alpha_{p_1}-3\alpha_{p_2}))/4 + i(-1+6\alpha_{q_1}+3\alpha_{q_2}+\mu(4-6\alpha_{q_1}-3\alpha_{q_2}))/4] + 3[(4-2\alpha_{p_1}+3\alpha_{p_2}+\mu(2\alpha_{p_1}-3\alpha_{p_2}))/4 + i(-5-2\alpha_{q_1}+3\alpha_{q_2}+\mu(2\alpha_{q_1}-3\alpha_{q_2}))/4] = 4+3\alpha_{p_2}+\mu(1-3\alpha_{p_2}) + i(-4+3\alpha_{q_2}+\mu(1-3\alpha_{q_2})) = 4+\mu+(3-3\mu)\alpha_{p_2} + i(-4+\mu+(3-3\mu)\alpha_{q_2}) = [4+\mu, 7-2\mu] + i[\mu-4, -1-2\mu]$.

The granular solution also satisfies equivalent form (14) of the FCLS (11).

$$\begin{aligned} \tilde{z}_1 - [\mu, 2-\mu] - i[1+\mu, 3-\mu] &= \tilde{z}_2 \\ \tilde{z}_1 - [4+\mu, 7-2\mu] - i[\mu-4, -1-2\mu] &= -3\tilde{z}_2 \end{aligned} \tag{14}$$

Substituting multidimensional granular solution (13) into FCLS (14), we have:

$\tilde{z}_1 - [\mu, 2-\mu] - i[1+\mu, 3-\mu] = [(4+6\alpha_{p_1}+3\alpha_{p_2}+\mu(4-6\alpha_{p_1}-3\alpha_{p_2}))/4 + i(-1+6\alpha_{q_1}+3\alpha_{q_2}+\mu(4-6\alpha_{q_1}-3\alpha_{q_2}))/4] - [\mu+(2-2\mu)\alpha_{p_1} + i(1+\mu+(2-2\mu)\alpha_{q_1})] = (4-2\alpha_{p_1}+3\alpha_{p_2}+\mu(2\alpha_{p_1}-3\alpha_{p_2}))/4 + i(-5-2\alpha_{q_1}+3\alpha_{q_2}+\mu(2\alpha_{q_1}-3\alpha_{q_2}))/4 = \tilde{z}_2$;

$\tilde{z}_1 - [4+\mu, 7-2\mu] - i[\mu-4, -1-2\mu] = [(4+6\alpha_{p_1}+3\alpha_{p_2}+\mu(4-6\alpha_{p_1}-3\alpha_{p_2}))/4 + i(-1+6\alpha_{q_1}+3\alpha_{q_2}+\mu(4-6\alpha_{q_1}-3\alpha_{q_2}))/4] - [4+\mu+(3-3\mu)\alpha_{p_2} + i(-4+\mu+(3-3\mu)\alpha_{q_2})] = (-12+6\alpha_{p_1}-9\alpha_{p_2}-6\mu\alpha_{p_1}+9\mu\alpha_{p_2})/4 + i(15+6\alpha_{q_1}-9\alpha_{q_2}-6\mu\alpha_{q_1}+9\mu\alpha_{q_2})/4 = -3[(4-2\alpha_{p_1}+3\alpha_{p_2}+\mu(2\alpha_{p_1}-3\alpha_{p_2}))/4 + i(-5-2\alpha_{q_1}+3\alpha_{q_2}+\mu(2\alpha_{q_1}-3\alpha_{q_2}))/4] = -3\tilde{z}_2$.

Similarly, it can be shown that the obtained granular solution satisfies other equivalent forms of the FCLS.

The span of the granular solution (13) in the form of fuzzy complex numbers presents (15) and graphically in Fig. 4,

$$\begin{aligned} \tilde{z}_1^{\mu} &= \mathcal{H}^{-1}(z_1^{gr}(\mu, \alpha_{p_1}, \alpha_{p_2}, \alpha_{q_1}, \alpha_{q_2})) = [1+\mu, 3.25-1.25\mu] \\ &\quad + i[-0.25+\mu, 2-1.25\mu], \\ \tilde{z}_2^{\mu} &= \mathcal{H}^{-1}(z_2^{gr}(\mu, \alpha_{p_1}, \alpha_{p_2}, \alpha_{q_1}, \alpha_{q_2})) = [0.5+0.5\mu, 1.75-0.75\mu] \\ &\quad + i[-1.75+0.5\mu, -0.5-0.75\mu], \end{aligned} \tag{15}$$

where $\mu \in [0,1]$.

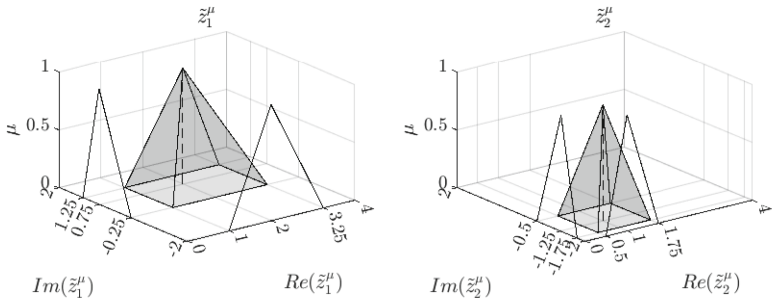

Fig. 4. Spans of complex granule of solution of fuzzy complex system of linear equations, Example 1.

The next Example 2 taken from [11,28] considers a simple RLC circuit where both current and source are fuzzy.

Example 2 (Example 2 [28], example 5.5 [11]). Let us consider the FCLS (16) for RLC circuit presented in Fig. 5.

$$\begin{aligned} (10-7.5i)\tilde{z}_1 + (-6+5i)\tilde{z}_2 &= [4+\mu, 6-\mu] + i[-1+\mu, 1-\mu] \\ (-6+5i)\tilde{z}_1 + (16+3i)\tilde{z}_2 &= [-2+\mu, -\mu] + i[-3+\mu, -1-\mu] \end{aligned} \tag{16}$$

where $\mu \in [0,1]$.

FCLS (16) in the granular notation has a form (17)

$$\begin{aligned} (10-7.5i)z_1^{gr} + (-6+5i)z_2^{gr} &= 4+\mu+\alpha_{p_1}(2-2\mu) + i[-1+\mu+\alpha_{q_1}(2-2\mu)] \\ (-6+5i)z_1^{gr} + (16+3i)z_2^{gr} &= -2+\mu+\alpha_{p_2}(2-2\mu) + i[-3+\mu+\alpha_{q_2}(2-2\mu)] \end{aligned} \tag{17}$$

where $\mu, \alpha_{p_1}, \alpha_{p_2}, \alpha_{q_1}, \alpha_{q_2} \in [0,1]$.

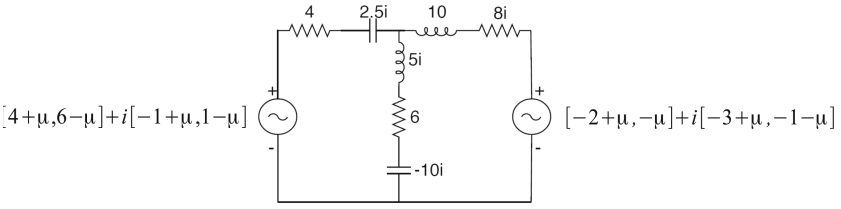

Fig. 5. A simple RLC circuit where both current and source are fuzzy [11,28].

The multidimensional granular form of solution is presented by (18).

$$\begin{aligned}
&z_1^{gr}(\mu,\alpha_{p_1},\alpha_{p_2},\alpha_{q_1},\alpha_{q_2})\\
&=\{21232\alpha_{p_1}+9432\alpha_{p_2}-7956\alpha_{q_1}+5420\alpha_{q_2}+28880\\
&\quad+\mu(14064-21232\alpha_{p_1}-9432\alpha_{p_2}+7956\alpha_{q_1}-5420\alpha_{q_2})\\
&\quad+i[7956\alpha_{p_1}-5420\alpha_{p_2}+21232\alpha_{q_1}+9432\alpha_{q_2}-3432\\
&\quad+\mu(16600-7956\alpha_{p_1}+5420\alpha_{p_2}-21232\alpha_{q_1}-9432\alpha_{q_2})]\}\\
&\quad/121249\\
&z_2^{gr}(\mu,\alpha_{p_1},\alpha_{p_2},\alpha_{q_1},\alpha_{q_2})\\
&=\{9432\alpha_{p_1}+15520\alpha_{p_2}+5420\alpha_{q_1}+7890\alpha_{q_2}-11201\\
&\quad+\mu(19131-9432\alpha_{p_1}-15520\alpha_{p_2}-5420\alpha_{q_1}-7890\alpha_{q_2})\\
&\quad+i[9432\alpha_{p_1}-7890\alpha_{p_2}-5420\alpha_{q_1}+15520\alpha_{q_2}-30946\\
&\quad+\mu(5821+5420\alpha_{p_1}+7890\alpha_{p_2}-9432\alpha_{q_1}-15520\alpha_{q_2})]\}\\
&\quad/121249
\end{aligned} \tag{18}$$

Obtained multidimensional solution (18) satisfies the considered FCLS and its equivalent forms. It can be proved similarly as in Example 1.

The span of the multidimensional granular solution expressed in the form of the FCN is presented by formula (19) and in Fig. 6

$$\begin{aligned}
\tilde{z}_1^{\mu}&=\mathcal{H}^{-1}(z_1^{gr}(\mu,\alpha_{p_1},\alpha_{p_2},\alpha_{q_1},\alpha_{q_2}))=[0.1726+0.1816\mu,0.5358-0.1816\mu]\\
&\quad+i[-0.0730+0.1816\mu,0.2902-0.1816\mu]\\
\tilde{z}_2^{\mu}&=\mathcal{H}^{-1}(z_2^{gr}(\mu,\alpha_{p_1},\alpha_{p_2},\alpha_{q_1},\alpha_{q_2}))=[-0.0924+0.1578\mu,0.2232-0.1578\mu]\\
&\quad+i[-0.3650+0.1578\mu,-0.0494-0.1578\mu]
\end{aligned} \tag{19}$$

Example 3. Let us consider the full fuzzy complex linear system (20).

$$\begin{aligned}
([\mu,2-\mu]+i[\mu,2-\mu])\tilde{z}_1+([-3+\mu,-1-\mu]+i[5+\mu,7-\mu])\tilde{z}_2\\
=[-11+\mu,-9-\mu]+i[11+\mu,13-\mu],\\
([-8+\mu,-6-\mu]+i[-5+\mu,-3-\mu])\tilde{z}_1+([\mu,2-\mu]+i[\mu,2-\mu])\tilde{z}_2\\
=[-3+\mu,-1-\mu]+i[-9+\mu,-7-\mu].
\end{aligned} \tag{20}$$

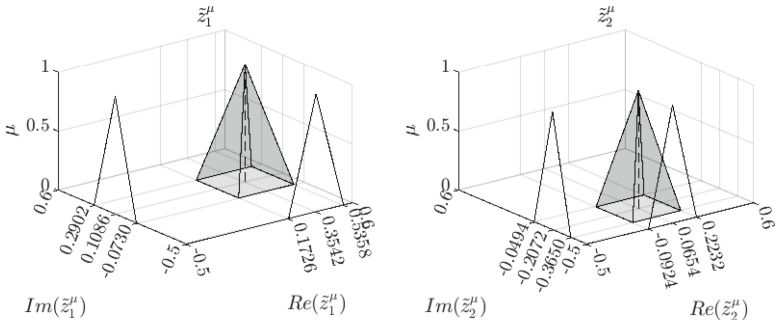

Fig. 6. Span of the multidimensional granule of solution $\tilde{z}_1^\mu$ and $\tilde{z}_2^\mu$ from Example 2.

Fuzzy complex linear system (20) in multidimensional granular notation has a form of (21),

$$\begin{aligned}
[\mu + \alpha_{p_1}(2-2\mu) \; &+i[\mu + \alpha_{q_1}(2-2\mu)]]z_1^{gr} \\
&+[-3+\mu+\alpha_{p_2}(2-2\mu)+i[5+\mu+\alpha_{q_2}(2-2\mu)]]z_2^{gr} \\
&=-11+\mu+\alpha_{p_3}(2-2\mu)+i[-5+\mu+\alpha_{q_3}(2-2\mu)], \\
[-8+\mu+\alpha_{p_4}(2 \; &-2\mu)+i[-5+\mu+\alpha_{q_4}(2-2\mu)]]z_1^{gr} \\
&+[\mu+\alpha_{p_5}(2-2\mu)+i[\mu+\alpha_{q_5}(2-2\mu)]]z_2^{gr} \\
&=-3+\mu+\alpha_{p_6}(2-2\mu)+i[-9+\mu+\alpha_{q_6}(2-2\mu)],
\end{aligned} \tag{21}$$

where $\mu, \alpha_{p_1}, \ldots, \alpha_{p_6}, \alpha_{q_1}, \ldots, \alpha_{q_6} \in [0,1]$.

The granule of determinant $d^{gr}(\mu, \alpha_p, \alpha_q)$ of the coefficients of uncertain values of the FCLS (21) is equal as in Eq. (22),

$$\begin{aligned}
d^{gr}(\mu, \alpha_p, \alpha_q) = \; &[\mu + \alpha_{p_1}(2-2\mu) + i[\mu + \alpha_{q_1}(2-2\mu)]] \\
&\cdot [\mu + \alpha_{p_5}(2-2\mu) + i[\mu + \alpha_{q_5}(2-2\mu)]] \\
&-[-3+\mu+\alpha_{p_2}(2-2\mu)+i[5+\mu+\alpha_{q_2}(2-2\mu)]] \\
&\cdot [-8+\mu+\alpha_{p_4}(2-2\mu)+i[-5+\mu+\alpha_{q_4}(2-2\mu)]],
\end{aligned} \tag{22}$$

where $\alpha_p = \{\alpha_{p_1}, \ldots, \alpha_{p_6}\}$, $\alpha_q = \{\alpha_{q_1}, \ldots, \alpha_{q_6}\}$ and μ, α_{p_1}, …, α_{p_6}, α_{q_1}, …, $\alpha_{q_6} \in [0,1]$.

Equation (23) and Fig. 7 present the span of the determinant $d^{gr}(\mu, \alpha_p, \alpha_q)$ for border values of the variables $\alpha_p = \{\alpha_{p_1}, \ldots, \alpha_{p_6}\}$, $\alpha_q = \{\alpha_{q_1}, \ldots, \alpha_{q_6}\}$, $0 \notin d^{gr}(\mu, \alpha_p, \alpha_q)$.

$$\tilde{d}^\mu = \mathcal{H}^{-1}(d^{gr}(\mu, \alpha_p, \alpha_q)) = [-63+25\mu, -17-21\mu] + i[15+21\mu, 61-25\mu], \tag{23}$$

where $\mu \in [0,1]$.

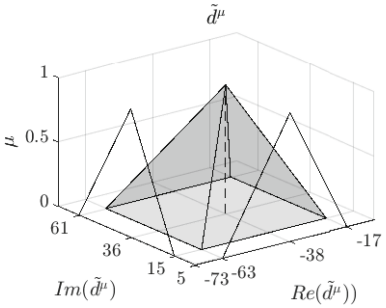

Fig. 7. Span of determinant $\tilde{d}^{\mu}$.

With basic algebraic operations, the multidimensional granular solution of the FCLS (21) equals as presented with Eq. (24)

$$\begin{aligned}
z_1^{gr}\ (\mu,\alpha_p,\alpha_q) &= \{[-11+\mu+\alpha_{p_3}(2-2\mu)+i[-5+\mu+\alpha_{q_3}(2-2\mu)]] \\
&\cdot[\mu+\alpha_{p_5}(2-2\mu)+i[\mu+\alpha_{q_5}(2-2\mu)]]-[-3+\mu+\alpha_{p_2}(2-2\mu) \\
&+i[5+\mu+\alpha_{q_2}(2-2\mu)]]\cdot[-3+\mu+\alpha_{p_6}(2-2\mu) \\
&+i[-9+\mu+\alpha_{q_6}(2-2\mu)]]\}/d^{gr}(\mu,\alpha_p,\alpha_q)) \\
z_2^{gr}\ (\mu,\alpha_p,\alpha_q) &= \{[\mu+\alpha_{p_1}(2-2\mu)+i[\mu+\alpha_{q_1}(2-2\mu)]] \\
&\cdot[-3+\mu+\alpha_{p_6}(2-2\mu)+i[-9+\mu+\alpha_{q_6}(2-2\mu)]] \\
&-[-11+\mu+\alpha_{p_3}(2-2\mu)+i[-5+\mu+\alpha_{q_3}(2-2\mu)]] \\
&\cdot[-8+\mu+\alpha_{p_4}(2-2\mu)+i[-5+\mu+\alpha_{q_4}(2-2\mu)]]\}/d^{gr}(\mu,\alpha_p,\alpha_q))
\end{aligned} \tag{24}$$

where $\alpha_p=\{\alpha_{p_1},\ldots,\alpha_{p_6}\}$, $\alpha_q=\{\alpha_{q_1},\ldots,\alpha_{q_6}\}$ and $\mu,\alpha_{p_1},\ldots,\alpha_{p_6},\alpha_{q_1},\ldots,\alpha_{q_6}\in[0,1]$.

To prove that the obtained solution satisfies the FCLS and its equivalent forms, the granular solution should be used in the place of variables in the system, similarly as in the Example 1.

The span of the granular solution (24) is presented in Fig. 8. The spans in Fig. 8 were calculated for border values $\{0,1\}$ of the horizontal variables and $\mu\in[0:0.2:1]$. In this example the left and the right sides of the spans of the solution are nonlinear.

Approximations of the spans by the triangular fuzzy complex number using the supports and the cores of the spans are presented with the Eq. (25),

$$\begin{aligned}
\tilde{z}_1^{\mu} &= \mathcal{H}^{-1}(z_1^{gr}(\mu,\alpha_p,\alpha_q)) = [0.1584+0.8416\mu,2.0902-1.0902\mu] \\
&\quad +i[0.0338+0.9662\mu,2.3312-1.3312\mu], \\
\tilde{z}_2^{\mu} &= \mathcal{H}^{-1}(z_2^{gr}(\mu,\alpha_p,\alpha_q)) = [0.9292+1.0708\mu,3.1375-1.1375\mu] \\
&\quad +i[-0.1315+1.1315\mu,2.5344-1.5344\mu],
\end{aligned} \tag{25}$$

where $\mu\in[0,1]$.

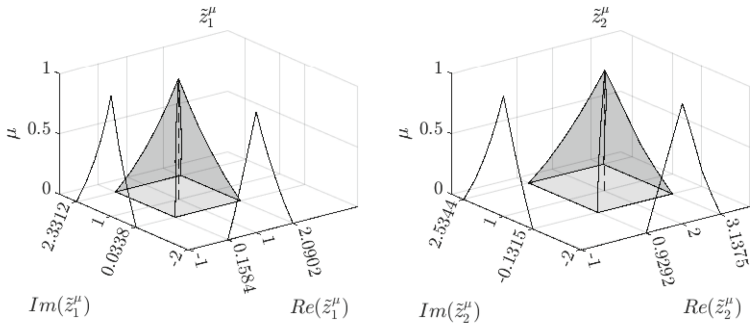

Fig. 8. The span of the multidimensional granular solution from Example 3.

3.2 Comparison of Results

Let us consider the solution obtained in Example 1. The fuzzy complex numbers (15) are different than the results with the method provided by the authors in [3,4,11,14,15].

From the FCLS in example 1 [3,4], example 4.1 [15], example 5.1 [11] and example 1 [14], for $\mu = 0$ the CCLS (26) can be obtained:

$$\begin{aligned} z_1 - z_2 &= 2 + 3i, \\ z_1 + 3z_2 &= 7 - i, \end{aligned} \tag{26}$$

where the crisp solution equals: $z_1 = 3.25 + 2i$ and $z_2 = 1.25 - i$. Unfortunately, the crisp solution z_1 does not belong to the solution of the FCLS presented in [3,4,11,14,15], for $\mu = 0$ we have: $z_1 = 3.25 + 2i \notin \tilde{z}_1(\mu = 0) = [1.375, 2.875] + i[0.125, 1.625]$. It shows that results presented in [3,4,14,15] are not a full solution.

With the multidimensional granular solution (13) using the horizontal variables all pairs of the crisp complex solutions can be generated. For example, for $\mu = 0$ and $\alpha_{p_1} = \alpha_{p_2} = \alpha_{q_1} = \alpha_{q_2} = 1$ the crisp solution of the crisp complex linear system (26) can be obtained.

Let us analyze solution of Example 2. The solution (18) obtained with multidimensional horizontal approach is different than results calculated in papers [11,28]. Let us consider the CCLS (27) from FCLS (16), where $\mu = 0$

$$\begin{aligned} (10 - 7.5i)z_1 + (-6 + 5i)z_2 &= 4 + i \\ (-6 + 5i)z_1 + (16 + 3i)z_2 &= -2 - 3i \end{aligned} \tag{27}$$

Crisp solution of the CCLS (27) equals: $z_1 = 0.1726 + 0.1468i$, $z_2 = -0.0477 - 0.1774i$. Value z_1 does not belong to the results in [11,28], for $\mu = 0$ we have: $z_1 = 0.1726 + 0.1468i \notin \tilde{z}_1(\mu = 0) = [0.3164, 0.3920] + i[0.0708, 0, 1464]$. So the results in [11,28] are not full solutions.

The crisp solution of CCLS (27) belongs to the direct solution with HFCN (18), it can be obtained for $\mu = \alpha_{p_1} = \alpha_{p_2} = \alpha_{q_2} = 0$ and $\alpha_{q_1} = 1$.

4 Conclusions

The paper presents a multidimensional approach to solving fuzzy systems of linear equations using fuzzy complex numbers (FCN) and their horizontal membership functions (HMF). It is also proved that defined operations on FCNs with HMFs hold basic algebraic properties. With arithmetic on the fuzzy complex numbers with HMFs the fuzzy complex linear systems (FCLS) were solved. Obtained solution is a granule of information expressed in the form of the formula. What is more, it was shown that the multidimensional solution satisfies the FCLS and its equivalent forms. With a multidimensional solution it is possible to generate any crisp solution. This feature helps to prove that presented results obtained in the cited papers [3,4,11,15,28] are not full solutions of the FCLS. With a multidimensional solution, a crisp solution of the FCLS was generated, which is not present in the results obtained with the methods used in cited papers.

Presented approach of the complex horizontal fuzzy membership function and their arithmetic can be used in many problems of granular computations.

References

1. Abbasbandy, S., Alavi, M.: A method for solving fuzzy linear systems. Iran. J. Fuzzy Syst. **2**(2), 37–43 (2005)
2. Behera, D., Chakraverty, S.: A new method for solving real and complex fuzzy systems of linear equations. Comput. Math. Model. **23**(4), 507–518 (2012)
3. Behera, D., Chakraverty, S.: Solving fuzzy complex system of linear equations. Inf. Sci. **277**, 154–162 (2014)
4. Behera, D., Chakraverty, S.: Erratum to Solving fuzzy complex system of linear equations. [Inf. Sci. **277**, 154–162 (2014)]. Inf. Sci. **369**, 788–790 (2016)
5. Boroujeni, M., Basiri, A., Rahmany, S., Valibouze, A.: Solving fuzzy systems in dual form using Wu's method. Int. J. Fuzzy Syst. **17**(2), 170–180 (2015)
6. Buckley, J.J.: Fuzzy complex numbers. Fuzzy Sets Syst. **33**(3), 333–345 (1989)
7. Buckley, J.J.: Fuzzy complex analysis II: integration. Fuzzy Sets Syst. **49**(2), 171–179 (1992)
8. Chang, S., Zadeh, L.A.: On fuzzy mapping and control. IEEE Trans. Systems Man. Cybernet. **2**, 30–34 (1972)
9. Dehghan, M., Hashemiand, B., Ghatee, M.: Computational methods for solving fully fuzzy linear systems. Appl. Math. Comput. **179**, 328–343 (2006)
10. Dubois, D., Prade, H.: Operations on fuzzy numbers. Int. J. Systems Sci. **9**, 613–626 (1978)
11. Farahani, H., Nehi, H.M., Paripour, M.: Solving fuzzy complex system of linear equations using eigenvalue method. J. Intell. Fuzzy Syst. **31**(3), 1689–1699 (2016)
12. Friedman, M., Ming, M., Kandel, A.: Fuzzy linear systems. Fuzzy Sets Syst. **96**, 201–209 (1998)
13. Ghanbari, M.: A discussion on "solving fuzzy complex system of linear equations." Inf. Sci. **402**, 165–169 (2017)
14. Guo, X., Zhang, K.: Minimal solution of complex fuzzy linear systems. Adv. Fuzzy Syst. **9**, 1–9 (2016)

15. Han, Y., Guo, X.: Complex fuzzy linear systems. Int. J. Eng. Appl. Sci. **3**, 30–34 (2016)
16. Jafari, H., Saeidy, M., Vahidi, J.: The Homotopy analysis method for solving fuzzy system of linear equations. Int. J. Fuzzy Syst. **11**(4), 308–313 (2009)
17. Jafarian, A., Nia, S.: On the solution of nonlinear fuzzy equation systems by fuzzy neural network method. Int. J. Fuzzy Syst. **15**(3), 376–380 (2013)
18. Jahantigh, M.A., Khezerloo, S., Khezerloo, M.: Complex fuzzy linear systems. Int. J. Ind. Math. **2**, 21–28 (2010)
19. Kaufmann, A., Gupta, M.M.: Introduction to Fuzzy Arithmetic: Theory and Applications. Van Nostrand Reinhold Co., New York, N.Y. (1985)
20. Klir, G.J., Yuan, B.: Fuzzy Sets and Fuzzy Logic: Theory and Applications. Prentice Hall, Upper Saddle River, NJ (1995)
21. Mazandarani, M., Pariz, N., Kamyad, A.V.: Granular differentiability of fuzzy-number-valued functions. IEEE Trans. Fuzzy Syst. **26**(1), 310–323 (2018)
22. Mizumoto, M., Tanaka, K.: The four operations of arithmetic on fuzzy numbers. Syst. Comput. Controls **7**, 73–81 (1976)
23. Najariyan, M., Zhao, Y.: On the stability of fuzzy linear dynamical systems. J. Franklin Inst. **357**, 5502–5522 (2020)
24. Piegat, A., Landowski, M.: Two interpretations of multidimensional RDM interval arithmetic - multiplication and division. Int. J. Fuzzy Syst. **16**, 488–496 (2013)
25. Piegat, A., Landowski, M.: Horizontal membership function and examples of its applications. Int. J. Fuzzy Syst. **17**, 22–30 (2015)
26. Piegat, A., Landowski, M.: Is an interval the right result of arithmetic operations on intervals? Int. J. Appl. Math. Comput. Sci. **27**(3), 575–590 (2017)
27. Piegat, A., Landowski, M.: On fuzzy RDM-arithmetic. In: Kobayashi, S., Piegat, A., Pejaś, J., El Fray, I., Kacprzyk, J. (eds.) ACS 2016. AISC, vol. 534, pp. 3–16. Springer, Cham (2017). https://doi.org/10.1007/978-3-319-48429-7_1
28. Rahgooy, T., Yazdi, H.S., Monsefi, R.: Fuzzy complex system of linear equations applied to circuit analysis. Int. J. Comput. Electr. Eng. **1**, 1793–8163 (2009)
29. Ramot, D., Milo, R., Friedman, M., Kandel, A.: Complex fuzzy sets. IEEE Trans. Fuzzy Syst. **10**, 171–186 (2002)
30. Ramot, D., Friedman, M., Langholzn, G., Kandel, A.: Complex fuzzy logic. IEEE Trans. Fuzzy Syst. **11**, 450–461 (2003)
31. Zadeh, L.A.: Fuzzy sets. Inf. Control **8**, 338–353 (1965)
32. Zimmermann, H.J.: Fuzzy Set Theory - and Its Applications. Springer, New York (1985)

An Algorithm for Calculating the Multidimensional Solution of the Fuzzy Sylvester Matrix Equation

Marek Landowski(✉)

Faculty of Computer Science and Telecommunications, Maritime University of Szczecin, Waly Chrobrego 1-2, 70-500 Szczecin, Poland
m.landowski@pm.szczecin.pl

Abstract. The paper presents a multidimensional horizontal approach to solving the fuzzy Sylvester matrix equation (FSME). The use of the horizontal membership function (HMF) of the fuzzy set allows for generating a granule of information about the FSME solution. The paper presents an algorithm for solving FSME using HMF, which generates a full FSME solution. The solution obtained using the given algorithm differs from the results presented in the cited articles. The calculated granule of the FSME solution contains solutions that do not occur in the results obtained in the analyzed examples, therefore these results are underestimated.

Keywords: Fuzzy Sylvester matrix equation · Horizontal membership function · Uncertainty theory · Artificial intelligence

1 Introduction

Finding a solution to the fuzzy Sylvester matrix equation (FSME) is still being attempted by many scientists. The basic matrix Sylvester equation has the form $AX + XB = C$, where $A \in \mathbb{R}^{m\times m}$, $B \in \mathbb{R}^{m\times m}$, and $C \in \mathbb{R}^{n\times m}$, [5]. In this paper we will consider the FSME, which is the basic Sylvester matrix equation with fuzzy values. Fuzzy sets were proposed by Zadeh [11] and they model uncertainty in the form of a membership function $\mu : X \to [0, 1]$. The notation $\mu_A(x)$ represents the degree of membership of variable $x \in X$ to concept A.

Solutions to the FSME using different methods can be found in the articles [1–3,9,10]. In this paper, we propose the use of horizontal fuzzy set membership functions to solve the FSME. The horizontal membership function (HMF) of a fuzzy set was proposed by Piegat [8]. The HMF is a multidimensional approach to uncertainty modeling. It allows to represent the membership of a fuzzy set using a multidimensional information granule by introducing an additional variable called the relative distance measure (RDM) variable [7]. This theory is based on the notation of the interval as $\lambda x_1 + (1 - \lambda)x_2$, where $\lambda \in [0, 1]$, which is also described in the books [4,12].

M. Paszynski et al. (Eds.): ICCS 2025 Workshops, LNCS 15912, pp. 213–221, 2025.
https://doi.org/10.1007/978-3-031-97573-8_15

The main contribution of the article is the use of a multidimensional horizontal approach to the solution of the FSME, the proposal of an algorithm for calculating the solution of the FSME, and the demonstration that the methods presented in the cited articles do not provide a complete solution. The complete solution can be obtained by a method that does not rely only on the boundary values of the fuzzy number in arithmetic operations.

The rest of the paper is organized as follows: In Sect. 2, the theoretical background of FSME, horizontal membership function and the algorithm for calculating the FSME solution using HMF are presented. In Sect. 3, the FSME is calculated based on the proposed algorithm. In Sect. 4, conclusions from the presented research are given.

2 Theoretical Foundations

The fuzzy Sylvester matrix equation (FSME) has a form (1).

$$A\tilde{X} + \tilde{X}B = \tilde{C} \tag{1}$$

where $A = [a_{ij}] \in \mathbb{R}^{n\times n}$, $B = [b_{ij}] \in \mathbb{R}^{m\times m}$ and $\tilde{C} = [\tilde{c}_{ij}]$ is $n \times m$ matrix of fuzzy number, [2].

The equivalent form of the FSME has the form (2), [2].

$$(I_m \otimes A + B^T \otimes I_n)vec(\tilde{X}) = vec(\tilde{C}) \tag{2}$$

where I_k is $k \times k$ identity matrix, vec is a vectorization of matrix, $vec(\tilde{X})$ and $vec(\tilde{C})$ are $nm \times 1$ matrices, operation $\otimes$ is the Kronecker product, and B^T is transpose of a matrix B.

Definition 1. *[6, 8] (Horizontal membership function) Let* $\tilde{u} : [a, b] \subseteq \mathbb{R} \rightarrow [0, 1]$ *be a fuzzy number. The horizontal membership function* $u^{gr} : [0, 1]\times[0, 1] \rightarrow [a, b]$ *is a representation of* $\tilde{u}(x)$ *as* $u^{gr}(\mu, \alpha_u) = x$ *in which "gr" stands for the granule of information included in* $x \in [a, b]$, $\mu \in [0, 1]$ *is the membership degree of* x *in* $\tilde{u}(x)$, $\alpha_u \in [0, 1]$ *is called RDM variable, and* $u^{gr}(\mu, \alpha_u) = \underline{u}^{\mu} + (\overline{u}^{\mu} - \underline{u}^{\mu})\alpha_u$.

The horizontal membership function presented by granule of information of fuzzy number $\tilde{u}$ is denoted in [6] as $\mathcal{H}(\tilde{u}) = u^{gr}(\mu, \alpha_u)$.

Definition 2. *[6] The span of the information granule of the horizontal membership function* $\mathcal{H}(\tilde{u}) = u^{gr}(\mu, \alpha_u)$ *of* $\tilde{u}(x) \in E_1$ *is obtained as the* μ*-level sets of the vertical membership function of* $\tilde{u}(x)$*, using (12),*

$$\mathcal{H}^{-1}(u^{gr}(\mu, \alpha_u)) = \tilde{u}^{\mu} = \left[\inf_{\beta\geq\mu}\min_{\alpha_u} u^{gr}(\beta, \alpha_u), \sup_{\beta\geq\mu}\max_{\alpha_u} u^{gr}(\beta, \alpha_u)\right] \tag{3}$$

Let $\tilde{v}$ and $\tilde{w}$ are the fuzzy numbers, with the horizontal membership functions $\mathcal{H}(\tilde{v})$ and $\mathcal{H}(\tilde{w})$. Denotes $\odot$ as a one of four basic arithmetic operations $\{+, -, \times, /\}$. Therefore, $\tilde{v} \odot \tilde{w}$ is a fuzzy number such that $\mathcal{H}(\tilde{v} \odot \tilde{w}) = \mathcal{H}(\tilde{v}) \odot \mathcal{H}(\tilde{w})$, operation / occurs only if $0 \notin \mathcal{H}(\tilde{w})$, [6,8].

For arithmetic operations on fuzzy numbers with a horizontal membership function, the following basic algebraic properties hold, [6]:

1. $\tilde{u} - \tilde{v} = -(\tilde{v} - \tilde{u})$,
2. $\tilde{u} - \tilde{u} = 0$,
3. $\tilde{u}/\tilde{u} = 1$,
4. $(\tilde{u} + \tilde{v})\tilde{w} = \tilde{u}\tilde{w} + \tilde{v}\tilde{w}$.

Algorithm 1 presents the steps for calculating the solution of the fuzzy Sylvester matrix equation using horizontal membership function.

Algorithm 1. Algorithm for calculating the Sylvester fuzzy matrix equation $A_{n\times n}\tilde{X}_{n\times m} + \tilde{X}_{n\times m}B_{m\times m} = \tilde{C}_{n\times m}$

1. Check whether the matrices A and $-B$ do not share any eigenvalue. If they do, then STOP - fuzzy Sylvester matrix equation has no unique solution. Otherwise, Step 2.
2. Using the Kronecker product and the vectorization operator vec write the Sylvester equation in the form $(I_m \otimes A_{n\times n} + B^T_{m\times m} \otimes I_n)_{nm\times nm} vec(\tilde{X})_{nm\times 1} = vec(\tilde{C})_{nm\times 1}$, where I_k is $k \times k$ identity matrix.
3. Write down the elements of matrix $vec(\tilde{C})$ as arbitrary fuzzy numbers. Then rewrite the obtained equation using the horizontal membership function for matrix $vec(\tilde{C})$.
4. Calculate a granule of solution of the equation using basic arithmetic operations on fuzzy numbers with horizontal membership function.
5. Find the span of the granule of solution obtained in Step 4. Obtained fuzzy numbers represents minimum and maximum values of the multidimensional granule of solution.

3 Numerical Examples

Example 1. (Example 4.3 in [2]) Let us consider a fuzzy Sylvester matrix equation $A\tilde{X} + \tilde{X}B = \tilde{C}^{\mu}$, as in (4).

$$\begin{bmatrix} -1.2 & 0.2 \\ 0.8 & -1.2 \end{bmatrix} \begin{bmatrix} \tilde{x}_{11} & \tilde{x}_{12} \\ \tilde{x}_{21} & \tilde{x}_{22} \end{bmatrix} + \begin{bmatrix} \tilde{x}_{11} & \tilde{x}_{12} \\ \tilde{x}_{21} & \tilde{x}_{22} \end{bmatrix} \begin{bmatrix} 1.2 & 0.6 \\ 0.4 & 1.2 \end{bmatrix} = \begin{bmatrix} (120 + 12\mu, 144 - 12\mu) & (100 + 11\mu, 122 - 11\mu) \\ (100 + 12\mu, 124 - 12\mu) & (160 + 16\mu, 192 - 16\mu) \end{bmatrix} \tag{4}$$

where $\mu \in [0,1]$.

Considered the Sylvester Eq. (4) has a unique solution because matrices A and $-B$ do not share any eigenvalue.

Using the Kronecker product notation and the vectorization operator vec let us write the Eq. (4) in the form (5).

$$\left(\begin{bmatrix} 1 & 0 \\ 0 & 1 \end{bmatrix} \otimes \begin{bmatrix} -1.2 & 0.2 \\ 0.8 & -1.2 \end{bmatrix} + \begin{bmatrix} 1.2 & 0.6 \\ 0.4 & 1.2 \end{bmatrix}^T \otimes \begin{bmatrix} 1 & 0 \\ 0 & 1 \end{bmatrix} \right) vec(\tilde{X}) = vec(\tilde{C}^{\mu}) \tag{5}$$

where

$$vec(\tilde{X}) = \begin{bmatrix} \tilde{x}_{11} \\ \tilde{x}_{21} \\ \tilde{x}_{12} \\ \tilde{x}_{22} \end{bmatrix}, vec(\tilde{C}^{\mu}) = \begin{bmatrix} (120 + 12\mu, 144 - 12\mu) \\ (100 + 12\mu, 124 - 12\mu) \\ (100 + 11\mu, 122 - 11\mu) \\ (160 + 16\mu, 192 - 16\mu) \end{bmatrix}, \mu \in [0,1].$$

Rewriting $vec(\tilde{C}^{\mu})$ using a horizontal membership function with variables μ, $\alpha_{c_{11}}$, $\alpha_{c_{12}}$, $\alpha_{c_{21}}$, $\alpha_{c_{22}} \in [0,1]$, we have multidimensional granule of information $vec(C^{gr})$ in the form:

$$vec(C^{gr}) = \begin{bmatrix} 120 + 12\mu + \alpha_{c_{11}}(24 - 24\mu) \\ 100 + 12\mu + \alpha_{c_{21}}(24 - 24\mu) \\ 100 + 11\mu + \alpha_{c_{12}}(22 - 22\mu) \\ 160 + 16\mu + \alpha_{c_{22}}(32 - 32\mu) \end{bmatrix}$$

With operation of Kronecker product and the multidimensional granular vector $vec(C^{gr})$ the Eq. (5) is equivalent to fuzzy matrix Eq. (6).

$$\begin{bmatrix} 0 & 0.2 & 0.4 & 0 \\ 0.8 & 0 & 0 & 0.4 \\ 0.6 & 0 & 0 & 0.2 \\ 0 & 0.6 & 0.8 & 0 \end{bmatrix} \begin{bmatrix} x_{11}^{gr} \\ x_{21}^{gr} \\ x_{12}^{gr} \\ x_{22}^{gr} \end{bmatrix} = \begin{bmatrix} 120 + 12\mu + \alpha_{c_{11}}(24 - 24\mu) \\ 100 + 12\mu + \alpha_{c_{21}}(24 - 24\mu) \\ 100 + 11\mu + \alpha_{c_{12}}(22 - 22\mu) \\ 160 + 16\mu + \alpha_{c_{22}}(32 - 32\mu) \end{bmatrix} \tag{6}$$

where $\mu, \alpha_{c_{11}}, \alpha_{c_{12}}, \alpha_{c_{21}}, \alpha_{c_{22}} \in [0,1]$

The solution to Eq. (6) is a multidimensional information granule of the form (7).

$$\begin{aligned} x_{11}^{gr}(\mu, \alpha_{c_{11}}, \alpha_{c_{12}}, \alpha_{c_{21}}, \alpha_{c_{22}}) &= 250 + 25\mu + (-60\alpha_{c_{21}} + 110\alpha_{c_{12}})(1 - \mu) \\ x_{21}^{gr}(\mu, \alpha_{c_{11}}, \alpha_{c_{12}}, \alpha_{c_{21}}, \alpha_{c_{22}}) &= -400 - 40\mu + (-240\alpha_{c_{11}} + 160\alpha_{c_{22}})(1 - \mu) \\ x_{12}^{gr}(\mu, \alpha_{c_{11}}, \alpha_{c_{12}}, \alpha_{c_{21}}, \alpha_{c_{22}}) &= 500 + 50\mu + (180\alpha_{c_{11}} - 80\alpha_{c_{22}})(1 - \mu) \\ x_{22}^{gr}(\mu, \alpha_{c_{11}}, \alpha_{c_{12}}, \alpha_{c_{21}}, \alpha_{c_{22}}) &= -250 - 20\mu + (180\alpha_{c_{21}} - 220\alpha_{c_{12}})(1 - \mu) \end{aligned} \tag{7}$$

It is easy to show that the obtained granular solution (7) satisfies the system of Eq. (4). Substituting the solution (7) into the matrix Eq. (4) we have:

$$
\begin{aligned}
L &= \begin{bmatrix} -1.2 & 0.2 \\ 0.8 & -1.2 \end{bmatrix} \begin{bmatrix} x_{11}^{gr}(\mu, \alpha_{c_{11}}, \alpha_{c_{12}}, \alpha_{c_{21}}, \alpha_{c_{22}}) & x_{12}^{gr}(\mu, \alpha_{c_{11}}, \alpha_{c_{12}}, \alpha_{c_{21}}, \alpha_{c_{22}}) \\ x_{21}^{gr}(\mu, \alpha_{c_{11}}, \alpha_{c_{12}}, \alpha_{c_{21}}, \alpha_{c_{22}}) & x_{22}^{gr}(\mu, \alpha_{c_{11}}, \alpha_{c_{12}}, \alpha_{c_{21}}, \alpha_{c_{22}}) \end{bmatrix} \\
&+ \begin{bmatrix} x_{11}^{gr}(\mu, \alpha_{c_{11}}, \alpha_{c_{12}}, \alpha_{c_{21}}, \alpha_{c_{22}}) & x_{12}^{gr}(\mu, \alpha_{c_{11}}, \alpha_{c_{12}}, \alpha_{c_{21}}, \alpha_{c_{22}}) \\ x_{21}^{gr}(\mu, \alpha_{c_{11}}, \alpha_{c_{12}}, \alpha_{c_{21}}, \alpha_{c_{22}}) & x_{22}^{gr}(\mu, \alpha_{c_{11}}, \alpha_{c_{12}}, \alpha_{c_{21}}, \alpha_{c_{22}}) \end{bmatrix} \begin{bmatrix} 1.2 & 0.6 \\ 0.4 & 1.2 \end{bmatrix} \\
&= \begin{bmatrix} 120 + 12\mu + \alpha_{c_{11}}(24 - 24\mu) & 100 + 11\mu + \alpha_{c_{12}}(22 - 22\mu) \\ 100 + 12\mu + \alpha_{c_{21}}(24 - 24\mu) & 160 + 16\mu + \alpha_{c_{22}}(32 - 32\mu) \end{bmatrix} \\
&= \begin{bmatrix} (120 + 12\mu, 144 - 12\mu) & (100 + 11\mu, 122 - 11\mu) \\ (100 + 12\mu, 124 - 12\mu) & (160 + 16\mu, 192 - 16\mu) \end{bmatrix} = R
\end{aligned}
$$

The span of the multidimensional granule of solution (7) in the form of matrix with fuzzy numbers is presented in Eq. (8), and also shown n Fig. 1, where $\alpha_{c_{ij}} = \{\alpha_{c_{11}}, \alpha_{c_{12}}, \alpha_{c_{21}}, \alpha_{c_{22}}\}$, and $\mu, \alpha_{c_{ij}} \in [0, 1]$.

$$
\begin{aligned}
&\begin{bmatrix} \mathcal{H}^{-1}(x_{11}^{gr}(\mu, \alpha_{c_{ij}})) & \mathcal{H}^{-1}(x_{12}^{gr}(\mu, \alpha_{c_{ij}})) \\ \mathcal{H}^{-1}(x_{21}^{gr}(\mu, \alpha_{c_{ij}})) & \mathcal{H}^{-1}(x_{22}^{gr}(\mu, \alpha_{c_{ij}})) \end{bmatrix} = \begin{bmatrix} \tilde{x}_{11}^{\mu} & \tilde{x}_{12}^{\mu} \\ \tilde{x}_{21}^{\mu} & \tilde{x}_{22}^{\mu} \end{bmatrix} \\
&= \begin{bmatrix} (190 + 85\mu, 360 - 85\mu) & (420 + 130\mu, 680 - 130\mu) \\ (-640 + 200\mu, -240 - 200\mu) & (-470 + 200\mu, -70 - 200\mu) \end{bmatrix}
\end{aligned} \tag{8}
$$

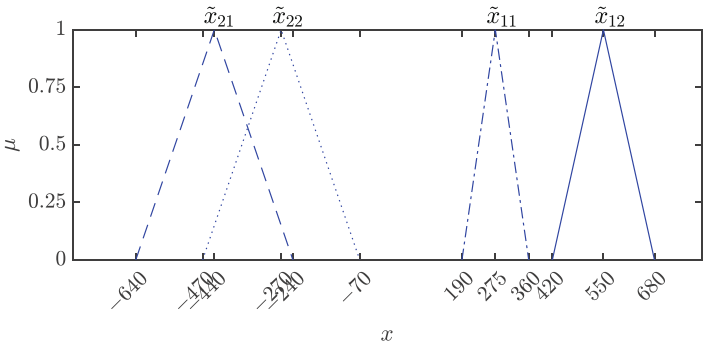

Fig. 1. Span of the multidimensional granule of solution (7).

The fuzzy numbers that are the result obtained in [2] are different from the fuzzy numbers (8) (also shown in Fig. 1). We will show that the solution in [2] is incomplete (underestimated). Let us consider one of the infinitely many solutions that can be generated from the multidimensional granule of solution (7), obtained using horizontal membership functions.

Let us consider the solution located on the support of solution (7). Substituting the values $\mu = \alpha_{c_{11}} = \alpha_{c_{12}} = \alpha_{c_{21}} = \alpha_{c_{22}} = 0$ with solution (7) we obtain the exact single solution (9).

$$
\begin{bmatrix} x_{11} & x_{12} \\ x_{21} & x_{22} \end{bmatrix} = \begin{bmatrix} 250 & 500 \\ -400 & -250 \end{bmatrix} \tag{9}
$$

Single solution (9) satisfies Sylvester matrix Eq. (4). Substituting (9) into the left side of Eq. (4) gives us a matrix that is contained in the fuzzy matrix $\tilde{C}^{\mu}$ that is the right side of Eq. (4). This substitution operation is shown below.

$$L = \begin{bmatrix} -1.2 & 0.2 \\ 0.8 & -1.2 \end{bmatrix} \begin{bmatrix} 250 & 500 \\ -400 & -250 \end{bmatrix} + \begin{bmatrix} 250 & 500 \\ -400 & -250 \end{bmatrix} \begin{bmatrix} 1.2 & 0.6 \\ 0.4 & 1.2 \end{bmatrix}$$
$$= \begin{bmatrix} 120 & 100 \\ 100 & 160 \end{bmatrix} = \tilde{C}_{(\mu=\alpha_{c_{11}}=\alpha_{c_{12}}=\alpha_{c_{21}}=\alpha_{c_{22}}=0)} = R$$

The exact single solution of (9) is not found in the solution given in Example 4.3 in [2]. This proves that the solution given in [2] is incomplete.

Example 2. (Example 4.1 in [1]) Let us consider the fuzzy Sylvester matrix equation $A\tilde{X} + \tilde{X}B = \tilde{C}^{\mu}$, $\mu \in [0,1]$, (10).

$$\begin{bmatrix} 1 & 0 \\ -1 & 1 \end{bmatrix} \begin{bmatrix} \tilde{x}_{11} & \tilde{x}_{12} & \tilde{x}_{13} \\ \tilde{x}_{21} & \tilde{x}_{22} & \tilde{x}_{23} \end{bmatrix} + \begin{bmatrix} \tilde{x}_{11} & \tilde{x}_{12} & \tilde{x}_{13} \\ \tilde{x}_{21} & \tilde{x}_{22} & \tilde{x}_{23} \end{bmatrix} \begin{bmatrix} 1 & 0 & -1 \\ 0 & -1 & 1 \\ 1 & 2 & 0 \end{bmatrix}$$
$$= \begin{bmatrix} (\mu, 2-\mu) & (-1+\mu, 1-\mu) & (1+\mu, 3-\mu) \\ (0, 1-\mu) & (0, 1-\mu) & (2\mu, 4-\mu) \end{bmatrix} \tag{10}$$

Matrices A and $-B$ do not share any eigenvalue, so the Sylvester Eq. (10) has a unique solution. Using the Kronecker product's notation and the vectorization operator *vec* the Eq. (10) has a form of (11).

$$\left(\begin{bmatrix} 1 & 0 & 0 \\ 0 & 1 & 0 \\ 0 & 0 & 1 \end{bmatrix} \otimes \begin{bmatrix} 1 & 0 \\ -1 & 1 \end{bmatrix} + \begin{bmatrix} 1 & 0 & -1 \\ 0 & -1 & 1 \\ 1 & 2 & 0 \end{bmatrix}^{T} \otimes \begin{bmatrix} 1 & 0 \\ 0 & 1 \end{bmatrix} \right) vec(\tilde{X}) = vec(\tilde{C}^{\mu}) \tag{11}$$

where

$$vec(\tilde{X}) = \begin{bmatrix} \tilde{x}_{11} \\ \tilde{x}_{21} \\ \tilde{x}_{12} \\ \tilde{x}_{22} \\ \tilde{x}_{13} \\ \tilde{x}_{23} \end{bmatrix}, vec(\tilde{C}^{\mu}) = \begin{bmatrix} (\mu, 2-\mu) \\ (0, 1-\mu) \\ (-1+\mu, 1-\mu) \\ (0, 1-\mu) \\ (1+\mu, 3-\mu) \\ (2\mu, 4-\mu) \end{bmatrix}, \mu \in [0,1].$$

With operation of Kronecker product and using a horizontal membership function with variables μ, $\alpha_{c_{11}}$, $\alpha_{c_{12}}$, $\alpha_{c_{13}}$, $\alpha_{c_{21}}$, $\alpha_{c_{22}}$, $\alpha_{c_{23}} \in [0,1]$ for the vector $vec(\tilde{C}^{\nu})$ the Eq. (11) is equivalent to fuzzy matrix Eq. (12).

$$\begin{bmatrix} 2 & 0 & 0 & 0 & 1 & 0 \\ -1 & 2 & 0 & 0 & 0 & 1 \\ 0 & 0 & 0 & 0 & 2 & 0 \\ 0 & 0 & -1 & 0 & 0 & 2 \\ -1 & 0 & 1 & 0 & 1 & 0 \\ 0 & -1 & 0 & 1 & -1 & 1 \end{bmatrix} \begin{bmatrix} x_{11}^{gr} \\ x_{21}^{gr} \\ x_{12}^{gr} \\ x_{22}^{gr} \\ x_{13}^{gr} \\ x_{23}^{gr} \end{bmatrix} = \begin{bmatrix} \mu + \alpha_{c_{11}}(2-2\mu) \\ \alpha_{c_{21}}(1-\mu) \\ -1+\mu+\alpha_{c_{12}}(2-2\mu) \\ \alpha_{c_{22}}(1-\mu) \\ 1+\mu+\alpha_{c_{13}}(2-2\mu) \\ 2\mu+\alpha_{c_{23}}(4-3\mu) \end{bmatrix} \tag{12}$$

The solution to Eq. (12) is a multidimensional information granule of the form (13).

$$\begin{aligned}
x_{11}^{gr}(\mu,\alpha_{c_{ij}}) &= 0.25+0.25\mu+(\alpha_{c_{11}}-0.5\alpha_{c_{12}})(1-\mu)\\
x_{21}^{gr}(\mu,\alpha_{c_{ij}}) &= -0.3125+0.4375\mu+(0.25\alpha_{c_{11}}+0.5\alpha_{c_{21}}+0.125\alpha_{c_{12}}\\
&\quad -0.25\alpha_{c_{22}}-0.5\alpha_{c_{13}})(1-\mu)\\
x_{12}^{gr}(\mu,\alpha_{c_{ij}}) &= 1.75+0.75\mu+(\alpha_{c_{11}}-1.5\alpha_{c_{12}}+\alpha_{c_{13}})(1-\mu)\\
x_{22}^{gr}(\mu,\alpha_{c_{ij}}) &= -1.6875+2.0625\mu+(-0.25\alpha_{c_{11}}+0.5\alpha_{c_{21}}+1.875\alpha_{c_{12}}\\
&\quad -0.75\alpha_{c_{22}}-1.5\alpha_{c_{13}})(1-\mu)+\alpha_{c_{23}}(4--3\mu)\\
x_{13}^{gr}(\mu,\alpha_{c_{ij}}) &= -0.5+0.5\mu+\alpha_{c_{12}}(1-\mu)\\
x_{23}^{gr}(\mu,\alpha_{c_{ij}}) &= 0.125+0.375\mu+(0.5\alpha_{c_{11}}-0.75\alpha_{c_{12}}+0.5\alpha_{c_{22}}+\alpha_{c_{13}})\\
&\quad \cdot(1-\mu)
\end{aligned} \tag{13}$$

where $\alpha_{c_{ij}}=\{\alpha_{c_{11}},\alpha_{c_{12}},\alpha_{c_{13}},\alpha_{c_{21}},\alpha_{c_{22}},\alpha_{c_{23}}\}$, and $\mu,\alpha_{c_{ij}}\in[0,1]$.

It is easy to show that solution (13) satisfies fuzzy Sylvester matrix Eq. (10) and its equivalent forms. The proof is analogous to that of Example 1, so we leave it to the reader.

The span of the multidimensional solution granule (13) is presented in the form of fuzzy numbers, formula (14) and graphically in Fig. 2, where $\alpha_{c_{ij}}$, $\mu\in[0,1]$.

$$\begin{aligned}
&\begin{bmatrix}\mathcal{H}^{-1}(x_{11}^{gr}(\mu,\alpha_{c_{ij}}))\ \mathcal{H}^{-1}(x_{12}^{gr}(\mu,\alpha_{c_{ij}}))\ \mathcal{H}^{-1}(x_{13}^{gr}(\mu,\alpha_{c_{ij}}))\\ \mathcal{H}^{-1}(x_{21}^{gr}(\mu,\alpha_{c_{ij}}))\ \mathcal{H}^{-1}(x_{22}^{gr}(\mu,\alpha_{c_{ij}}))\ \mathcal{H}^{-1}(x_{23}^{gr}(\mu,\alpha_{c_{ij}}))\end{bmatrix}=\\
&=\begin{bmatrix}\tilde{x}_{11}^{\mu}\ \tilde{x}_{12}^{\mu}\ \tilde{x}_{13}^{\mu}\\ \tilde{x}_{21}^{\mu}\ \tilde{x}_{22}^{\mu}\ \tilde{x}_{23}^{\mu}\end{bmatrix}=\begin{bmatrix}(-0.25+0.75\mu,1.25-0.75\mu) & \\ (-1.0625+0.6875\mu,0.5625-0.9375\mu) & \\ (0.25+2.25\mu,4.75-2.25\mu) & (-0.5+0.5\mu,0.5-0.5\mu)\\ (-4.1875+4.5625\mu,4.6875-4.3125\mu) & (0.125+1.125\mu,2.875-1.625\mu)\end{bmatrix}
\end{aligned} \tag{14}$$

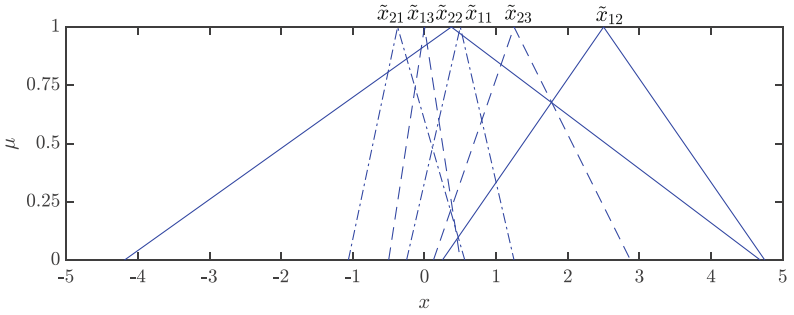

Fig. 2. Span of the multidimensional granule of solution (13).

To compare the obtained solution (13) with the solution from Example 4.1 in [1] let us generate an exact single solution. The exact single solution (15) is

the solution obtained from the multidimensional solution (13), lying on support ($\mu = 0$), for variables $\alpha_{c_{11}} = \alpha_{c_{12}} = \alpha_{c_{13}} = \alpha_{c_{21}} = \alpha_{c_{22}} = \alpha_{c_{23}} = 0$.

$$\begin{bmatrix} x_{11}\ x_{12}\ x_{13} \\ x_{21}\ x_{22}\ x_{23} \end{bmatrix} = \begin{bmatrix} 0.25 & 1.75 & -0.5 \\ -0.3125 & -1.6875 & 0.875 \end{bmatrix} \tag{15}$$

The exact single solution (15) satisfies Sylvester matrix Eq. (10), the calculations are below.

$$L = \begin{bmatrix} 1 & 0 \\ -1 & 1 \end{bmatrix} \begin{bmatrix} 0.25 & 1.75 & -0.5 \\ -0.3125 & -1.6875 & 0.875 \end{bmatrix} + \begin{bmatrix} 0.25 & 1.75 & -0.5 \\ -0.3125 & -1.6875 & 0.875 \end{bmatrix} \begin{bmatrix} 1 & 0 & -1 \\ 0 & -1 & 1 \\ 1 & 2 & 0 \end{bmatrix}$$
$$= \begin{bmatrix} 0 & -1 & 1 \\ 0 & 0 & 0 \end{bmatrix} = \tilde{C}_{(\mu=\alpha_{c_{11}}=\alpha_{c_{12}}=\alpha_{c_{13}}=\alpha_{c_{21}}=\alpha_{c_{22}}=\alpha_{c_{23}}=0)} = R$$

Single solution (15) is not included in the result obtained in Example 4.1 in [1]. This proves that the result obtained in [1] is not a full solution of the fuzzy Sylvester matrix Eq. (10).

4 Conclusions

The article presents an algorithm for calculating the solution of the FSME. The algorithm uses the horizontal membership function of the fuzzy set. The obtained solution of the FSME is a multidimensional information granule from which any single exact solution can be determined. The presented examples show that using the information granule, a solution can be generated that is not found in the results obtained by other methods from the cited articles. Application of the algorithm with HMF gives a full solution of the FSME.

References

1. Guo, X.-B.: Approximate solution of fuzzy Sylvester matrix equations. In: 2011 Seventh International Conference on Computational Intelligence and Security on Proceedings, pp. 53–56. IEEE, Sanya, China (2011)
2. He, M., Jiang, H., Liu, X.: General strong fuzzy solutions of fuzzy Sylvester matrix equations involving the BT inverse. Fuzzy Sets Syst. **480**(108862), 1–20 (2024)
3. He, Q., Hou, L., Zhou, J.: The solution of fuzzy Sylvester matrix equation. Soft. Comput. **22**, 6515–6523 (2018)
4. Klir, G.J., Yuan, B.: Fuzzy Sets and Fuzzy Logic: Theory and Applications. Prentice Hall, Upper Saddle River, NJ (1995)
5. Laub, A.J.: Matrix Analysis for Scientists and Engineers. SIAM, Philadelphia, PA (2005)
6. Mazandarani, M., Pariz, N., Kamyad, A.V.: Granular differentiability of fuzzy-number-valued functions. IEEE Trans. Fuzzy Syst. **26**(1), 310–323 (2018)
7. Piegat, A., Landowski, M.: Two interpretations of multidimensional RDM interval arithmetic: multiplication and division. Int. J. Fuzzy Syst. **15**(4), 486–496 (2013)

8. Piegat, A., Landowski, M.: Horizontal membership function and examples of its applications. Int. J. Fuzzy Syst. **17**, 22–30 (2015)
9. Sadeghi, A., Ahmad, I.M., Ahmad, A., Abbasnejad, M.E.: A note on solving the fuzzy Sylvester matrix equation. J. Comput. Anal. Appl. **15**(1), 10–22 (2013)
10. Salkuyeh, D.K.: On the solution of the fuzzy Sylvester matrix equation. Soft. Comput. **15**(5), 953–961 (2011)
11. Zadeh, L.A.: Fuzzy sets. Inf. Control **8**, 338–353 (1965)
12. Zimmermann, H.J.: Fuzzy Set Theory - and Its Applications. Springer Science+Business Media New York (1985)

Modelling Extreme Uncertainty: Queues with Pareto Inter-arrival Times and Pareto Service Times

Raul Ramirez-Velarde[1](✉), Cristobal Pareja-Flores[2], Neil Hernandez-Gress[1], and Laura Hervert-Escobar[1]

[1] Tecnologico de Monterrey, Eugenio Garza Sada 2501 Sur, Col. Tecnológico, 64849 Monterrey, N.L., Mexico
rramirez@tec.mx

[2] Departamento de Sistemas Informáticos y Computación, Facultad de Estudios Estadísticos, Universidad Complutense de Madrid, 28040 Madrid, Spain

Abstract. When an operational parameter presents extremely high variability, uncertainty becomes extreme. Long-tail probability distributions can be used to model such uncertainty. We present a queuing system in which extreme uncertainty is modelled using long-tail probability distributions. There have been many queuing analyses for a single server queue fed by an M/G/traffic process, in which G is a Pareto distribution, that focus on certain limiting conditions. In this paper, we present a mathematical model to solve an infinite queuing system with one server where the inter-arrival time between jobs follows a Pareto probability distribution with shape parameter α and a scale parameter A. The system service time is also a Pareto probability distribution with shape parameter β and scale parameter B. We call this the P/P/1 queuing model.

Keywords: Extreme uncertainty · Pareto queues · long-tails

1 Introduction

When an operational parameter presents extremely high variability, uncertainty becomes extreme. Long-tail probability distributions can be used to model such uncertainty. Many real-world systems exhibit extreme variability, where rare but significant events dominate system behaviour. Earthquakes, wildfires, and floods follow long-tailed distributions, with unpredictable inter-arrival times and durations. Similar patterns appear in network traffic, where bursts of data cause congestion, and in financial markets, where sudden crashes disrupt stability. Cybersecurity threats and human communication also display heavy-tailed activity, making prediction and management challenging.

This paper models a P/P/1 queuing system, where both inter-arrival and service times follow Pareto distributions, capturing extreme uncertainty. We provide mathematical formulations and simulations to analyse the system's behaviour, offering insights relevant to telecommunications, disaster response, and computational workload management.

M. Paszynski et al. (Eds.): ICCS 2025 Workshops, LNCS 15912, pp. 222–235, 2025.
https://doi.org/10.1007/978-3-031-97573-8_16

In this paper we will discuss a queuing system with the following characteristics:

- The inter-arrival time between jobs has a Pareto probability distribution with shape parameter α and a scale parameter A.
- The service time has a Pareto probability distribution with shape parameter β and scale parameter B.
- The queue is infinite.
- There is only one server.

We will call this the P/P/1 queuing system.

The probability distribution for random variable that represents the inter-arrivals time is defined by the Pareto I probability distribution with shape parameter α, and location parameter A:

$f(t) = \alpha\left(\frac{t}{A}\right)^{-\alpha-1}$, with $E[t] = \frac{\alpha A}{\alpha-1}$. The corresponding survival function is:

$$S(t) = 1 - F(t) = \left(\frac{t}{A}\right)^{-\alpha} \tag{1}$$

The probability distribution for the service time is also distributed as a Pareto I random variable with β as shape parameter and B as scale parameter.

$g(t) = \beta\left(\frac{t}{B}\right)^{-\beta-1}$, with $E[t] = \frac{\beta B}{\beta-1}$. The corresponding survival function is:

$$Z(t) = 1 - F(t) = \left(\frac{t}{B}\right)^{-\beta} \tag{2}$$

2 Previous Work

Many simulation studies have been undertaken to evaluate the performance of queueing systems with heavy-tail distributed inter-arrival times, execution times and transfer times. In this section, we review some of the most relevant work in this area, focusing on studies that have used the Pareto distribution to model heavy-tailed distributions.

Fischer and Cart [1] studied the properties and use of the Pareto distribution to model a M/Pareto/1 queue and a Pareto/M/1 queue. They showed that both systems can be used to model the transmission of information in a network, with the former being more suitable for switched networks and the latter being more suitable for packet transmission.

To overcome the difficulties of simulating systems with heavy-tailed distributions, Argibay Losada et al. [2] proposed a method to speed up simulations. They used M/G/1 systems as workbenches and showed that their method could significantly reduce the simulation time. Gross et al. [3] investigated the difficulties of simulating queues with Pareto service. They considered truncated Pareto service and showed that it can lead to significant errors in the estimation of queue performance. Koh and Kim [4] studied the queue performance of Pareto/M/1/k using simulations. They investigated the queue behaviour with Pareto inter-arrival distribution and showed that the asymptotic and exact loss probabilities can be significantly different.

Fischer et al. [5] studied the one-parameter, two-parameter, and three-parameter Pareto distributions. They showed that the two-parameter Pareto distribution can result in lower congestion than the one-parameter Pareto distribution. Inmaculada et al. [6] derived estimators for the truncated Pareto distribution. They also investigated the distribution properties and illustrated its applicability in practice. Albrecher et al. [7] investigates parameter estimation for tempered Pareto-type distribution tempered with a general Weibull distribution in risk management and insurance, offering improved methods for parameter estimation.

Recent studies have further explored the impact of heavy-tailed distributions on queuing systems. Jiang et al. [8] quantified the efficiency of parallelism in systems prone to failures and exhibiting power law processing delays and channel availability. They characterized the performance of redundant and split parallelism schemes in terms of the power law exponent and delay distribution tail asymptotics.

Building on these results, we model both service times and arrival times as Pareto random variables, without truncation, and derive exact and asymptotic queuing behaviour models for a single server and investigate the resulting probability distributions.

3 Modelling Heavy Tails

A heavy-tailed distribution is a distribution, for which the tail is heavier than any exponential tail. In this distribution, the probability of observing a value far from the median is greater than it would be in the normal distribution. That is, the probability of extreme values is non-negligible.

More precisely, a distribution of a random variable X with function f, and cumulative function

$$F(x) = P[X \leq x],$$

where $P[X]$ is the corresponding probability density function, is said to be heavy right tailed if $\lim_{x\to\infty} e^{\varphi x} F(x) = \infty$, for any $\varphi > 0$. It tends to have infinite moments, such as infinite variance [9].

Note, that a moment is infinite, if the integral that defines the statistical moment converges too slowly to be integrated (divergent), therefore, the moment does not exist. Since, a heavy-tailed distribution is also a long-tailed distribution, it follows that

$$\lim_{x\to\infty} P[X > x + t | X > x] = 1, \text{ or, equivalently, } \lim_{x\to\infty} \frac{F(x+t)}{F(x)} = 1, \text{ for any } t > 0.$$

Intuitively, equation states that if x exceeds some large value, then it is equally likely that it will exceed an even larger value as well. For our problem domain, it means that if the system executing a task spends large amount of time, probably it will spend longer time to complete it [10].

3.1 Probability Distribution of Jobs on System

Let us start by investigating the probability that certain time lag, say the inter-arrival time (but it could also have been the execution time) will persist further into the future less

than Δt units of time given the fact that we know it will persist more than τ time units. Assume $\Delta t \ll 1$, thus there cannot happen more than one event in Δt. Also, assume that the time is discrete, and the time slot is the smallest time interval considered in the system, for instance, seconds.

In other words, we wish to find out $P[t < \tau + \Delta t | t > \tau]$. For a Pareto r.v., $P[t < \tau + \Delta t] = 1 - \left(\frac{\tau+\Delta t}{A}\right)^{-\alpha}$. $P[t > \tau] = \left(\frac{\tau}{A}\right)^{-\alpha}$. Now, the probability $P[t < t + \Delta t \text{ and } t > \tau] = \left(\frac{\tau}{A}\right)^{-\alpha} - \left(\frac{\tau+\Delta t}{A}\right)^{-\alpha}$.

Therefore, $P[t < t + \Delta t | t > \tau] = \frac{\left(\frac{\tau}{A}\right)^{-\alpha} - \left(\frac{\tau+\Delta t}{A}\right)^{-\alpha}}{\left(\frac{\tau}{A}\right)^{-\alpha}} = 1 - \left(1 + \frac{\Delta t}{\tau}\right)^{-\alpha}$. We observe that the corresponding survival function $\psi_{arr}(\Delta t) = P[t > \tau + \Delta t | t > \tau] = \left(1 + \frac{\Delta t}{\tau}\right)^{-\alpha}$ is a Lomax probability distribution, for which a power series approximation exists. Also, $\psi_{ser}(\Delta t) = \left(1 + \frac{\Delta t}{\tau}\right)^{-\beta}$ for the service time.

Since A is the minimum time for t, let us fix τ as A for inter-arrival times and B for service times, to address the general cases, as in any given moment an event will always have existed for at least A (or B) units of time before persisting into the future.

Recall that $e^x = 1 + x + \frac{x^2}{2} + \frac{x^3}{6} + \ldots$ and that $(1 + x)^p = 1 + px + \frac{p(p-1)}{2}x^2 + \ldots$. In a Markovian queueing system with survival probability $F(t) = e^{-\lambda \Delta t} = 1 - \lambda \Delta t + \frac{(\lambda \Delta t)^2}{2} - \ldots$, we approximate $P[\textit{No event}] = P[\Delta t > \tau] \approx 1 - \lambda \Delta t$, and under the assumption that only one event can occur in the period Δt, $P[\textit{One event}] = P[t < \tau] \approx \lambda \Delta t$ [11].

Similarly, with Pareto times:

$$P[\textit{No event}] = P[\Delta t > \tau] = \left(1 + \frac{\Delta t}{A}\right)^{-\alpha} \approx 1 - \frac{\alpha \Delta t}{A} \tag{3}$$

and

$$P[\textit{One event}] = P[\Delta t < \tau] = 1 - \left(1 + \frac{\Delta t}{A}\right)^{-\alpha} \approx \frac{\alpha \Delta t}{A} \tag{4}$$

Now we solve the state probabilities for the queueing system. Let $p_i(t)$, the probability that there are i jobs at time t. Then,

$$p_0(t + \Delta t) = p_0(t)\left(1 - \frac{\alpha \Delta t}{A}\right) + p_1(t)\left(\frac{\beta \Delta t}{B}\right)$$

This means that there are two ways in which there could be zero jobs on the system, either o job arrived (and no jobs left) or there was one job and then it finished and left. With some algebra:

$\frac{p_0(t+\Delta t) - p_0(t)}{\Delta t} = p_0(t)\frac{\alpha}{A} + p_1(t)\frac{\beta}{B}$, assuming stationary and steady state probabilities $\frac{dp_i(t)}{dt} = 0$, *then*

$$p_1(t) = \frac{\alpha B}{\beta A} p_0(t)$$

For one job we have:

$$p_1(t + \Delta t) = p_0(t)\frac{\alpha \Delta t}{A} + p_2(t)\frac{\beta \Delta t}{B} + p_1(t)\left(1 - \frac{\alpha \Delta t}{A}\right)\left(1 - \frac{\beta \Delta t}{B}\right)$$

Since Δt is so small, and there cannot happen more than one event in such small period, all powers of Δt vanish:

$$p_2(t) = \left(\frac{\alpha B}{\beta A}\right)^2 p_0(t)$$

And in general,

$$p_n(t) = \left(\frac{\alpha B}{\beta A}\right)^n p_0(t) \tag{5}$$

By calling $\rho = \frac{\alpha B}{\beta A}$ and we find that $p_n = \rho^n p_0$. Also,

$$\sum_{n=0}^{\infty} p_n = \sum_{n=0}^{\infty} \rho^n p_0 = p_0\left(\frac{1}{1-\rho}\right) = 1, \text{ we find that } p_0 = 1 - \rho.$$

Therefore, the number of jobs on a Pareto queuing system still follows a geometric probability distribution $p_n = \rho^n(1-\rho)$. Then.

$$E[n] = \sum_{n=0}^{\infty} n\rho^n(1-\rho) = \frac{\rho}{1-\rho}$$

A result supported by Whitt [12]. Nevertheless, for a heavy-tailed random variable we find that the probability of no event happening in a very small Δt interval is almost one, as events tend heavily to persist into the future, or $p_0 \approx 1$. Thus empirically, a closer approximation for the expected number of jobs on the system might be (called P/P/1 Series model):

$$E[n] = \frac{\rho}{(1-\rho)^2} \tag{6}$$

And the pdf is closer to $p_n = \rho^n$

Now let us explore the probability distribution of the residence time or system time, the time a job stays on the system from entering until it has been served and then exits.

3.2 Probability Distribution of System Time of M/M/1 Queue

Let us review first the Markovian case. Let us call $f_0(t)$ the probability distribution of the time a job stays on the system when there are no other jobs on the system, that is, the execution time. Assume all execution times are i.i.d. random variables with $f_0(t) = \mu e^{-\mu t}$. If there is one job on the system when a new job arrives, then the time the arriving job stays on the system is the execution time of both jobs, that is, the addition of two exponentially distributed random variables. Then, the probability distribution of the system time of one job when there is one other job already in the system is [11]:

$$f_1(t) = \int_0^t f_0(\alpha) f_0(t-\alpha) d\alpha = \int_0^t \mu e^{-\mu\alpha} \lambda e^{-\mu(t-\alpha)} d\alpha = \mu^2 t e^{-\mu t}$$

Following on that:

$$f_2(t) = \int_0^t f_1(\alpha) f_0(t-\alpha) d\alpha = \frac{\mu^3 t^2 e^{-\mu t}}{2}$$

And in general

$f_n(t) = \frac{\mu^{n+1} t^n e^{-\mu t}}{n!}$, $f_n(t)$ is then the probability distribution of the system time when there are n jobs on the system. Recall that p_n is the probability that there are n jobs on queue. Therefore, the probability distribution of the system time of any arriving job is (with $\rho = \frac{\lambda}{\mu}$),

$$\begin{gathered} f(t) = \sum_{n=0}^{\infty} p_n f_n(t) \\ f(t) = \sum_{n=0}^{\infty} p_n f_n(t) = \sum_{n=0}^{\infty} \rho^n (1-\rho) \frac{\mu^{n+1} t^n e^{-\mu t}}{n!} = (\mu - \lambda) e^{-(\mu-\lambda)t}, \text{ and} \\ E[t] = \sum_{t=0}^{\infty} t(\mu - \lambda) e^{-(\mu-\lambda)t} dt = \frac{1}{\mu - \lambda} \end{gathered} \tag{7}$$

What are the probability distributions of the number of jobs in the system and the total system time when execution times and the inter arrival times are Pareto distributed random variables? Firstly, we will answer that question for self-similar variables. Secondly, for regular Pareto random variables.

3.3 Self-similarity and Heavy-Tails

Now, we describe how heavy-tails can cause self-similarity (fractal behaviour), and long-range dependence. Let us first assume that we deal with polynomial decay of the tail of the probability distribution, and use the Pareto Distribution as an example of heavy tailed distribution [13]:

$$\boldsymbol{P[X > x] = x^{-\alpha} L(x)},$$

where $\alpha = 1/\gamma$ is an inverse of the extreme value index γ. L is a slow varying function at infinity, that is $\lim_{x \to \infty} \frac{L(\gamma x)}{L(x)} = \mathbf{1}$, for $\boldsymbol{x > 0}$.

In non-self-similar data, the average of a series of samples tends to the population mean, as the number of samples increases [11]. That is:

$P\left[\lim_{x \to \infty} \frac{1}{n} \sum_{i=1}^{n} X_i = \mu\right] = 1$, where $\mu = E[X_i]$, $Var\left[\frac{1}{n} \sum_{i=1}^{n} X_i\right] = \frac{\sigma^2}{n}$, and σ is the standard deviation of the population.

The latter means that deviations of the sample mean with respect to the population mean decay proportionally to the size of the sample. Hence, as we aggregate data averaging larger collections, the averages become smoother, approaching the sample mean.

In [14], it is shown that in self-similar data something different happens: $Var\left[\frac{1}{n} \sum_{i=1}^{n} X_i\right] = \sigma^2 n^{-\alpha}$, where $\alpha < 1$. Hence, the sample mean converges to the population mean much slower. This implies that, with non-negligible probability, the execution time of a collection of jobs can be much larger or much smaller than the execution time computed using population mean. There is a non-negligible probability

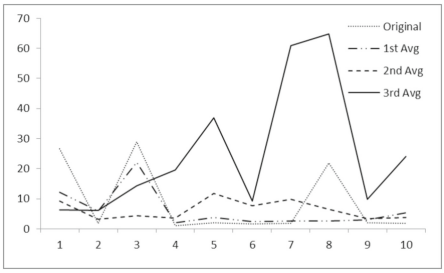

Fig. 1. Aggregation of self-similar data (Pareto distribution). Average does not smooth

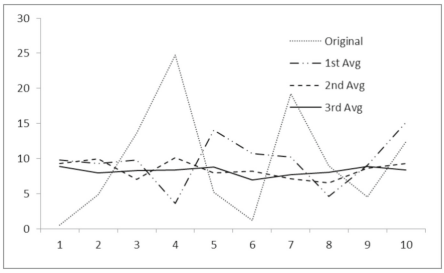

Fig. 2. Aggregation of non-self-similar data (exponential distribution). Average is smoothed

of having a exceedingly long runtime to solve the tasks, considerably longer than the population mean. It can create the self-similar profile shown in Figs. 1, 2.

There are several, not equivalent, definitions of self-similarity. The standard one states that a continuous-time process $Y = \{Y(t), t \geq 0\}$ is self-similar (with self-similarity or Hurst parameter H), if it satisfies the condition [15]:

$$Y(t) \equiv a^{-H} Y(at), \forall \mathrm{t}, \forall \mathrm{a} > 0, \text{ and } 0.5 < H < 1 \tag{8}$$

where the equality means that the expressions have equivalent probability distribution.

A process satisfying Eq. (8) can never really be stationary one as it requires that $Y(t) \equiv Y(at)$, (or rather the distribution of $\{Y(t+s) - Y(t)\}$ does not depend on t). As we show bellow, in our application, this does not hold, so we assume that $Y(t)$ has stationary increments. Let us $t = 1$ and a $= t$ in Eq. (1), thus,

$$\mathrm{Y(t)} \equiv t^H \mathrm{Y(1)}, \forall \mathrm{t}, 0.5 < H < 1.$$

Notice also, that Eq. (8) in the context of time series analysis implies that [15,16]:

$$z_n(t) = \sum i = 1^n X(i) \equiv n^H X(1) \tag{9}$$

where the equality represents equality in probability distribution and $z_n(t)$ is the accumulation process for n jobs execution time.

We assume $z_1(t)$ to be the service time for any job, that is, $f_0(t) = f(z_1(t))$ is the probability distribution of the wait when there is no job been serviced when the new job arrives. That is that wait time is only the service time for the new job, and $f_n(t) = f(z_{n+1}(t))$. Then the probability distribution of the wait time is:

$$f(t) = \sum_{n=0}^{\infty} p_n f_n(t) \tag{10}$$

With

$$f_n(t) = f(z_{n+1}(t)) = (n+1)^H f(z_1(t)) \tag{11}$$

3.4 Using Fractional Differentiation to Find the Probability Distribution of Service Time

Where $f(z_n(t))$ is the probability distribution of the system time when there are n jobs on the system and $f(z_1(t))$ is the probability distribution of the system time when there is only one job on the system, or the execution time for one job (a presumably long-tailed pdf). Thus, the probability distribution for system time is:

$$f(t) = \sum_{n=0}^{\infty} p_n f_n(t) = \sum_{n=0}^{\infty} (n+1)^H f(z_1(t))\rho^n$$

$$f(t) = f(z_1(t)) \sum_{n=0}^{\infty} (n+1)^H \rho^n$$

Recall from fractional differentiation that:

$$\frac{d^\alpha x^k}{dx^\alpha} = \frac{k!}{(k-\alpha)!} x^{k-\alpha} \tag{12}$$

Now, we use Stirling's approximation:

$$\frac{k!}{(k-\alpha)!} = \frac{k^k e^{-k}\sqrt{2\Pi k}}{(k-\alpha)^{k-\alpha} e^{-(k-\alpha)}\sqrt{2\Pi(k-\alpha)}} = \frac{k^k}{(k-\alpha)^{k-\alpha}} e^{-\alpha}\sqrt{\frac{k}{k-\alpha}}$$

For $k \gg \alpha$,

$$\frac{k^k}{(k-\alpha)^{k-\alpha}} = \left(1 - \frac{\alpha}{k}\right)^{-k} (k-\alpha)^\alpha \sim e^\alpha k^\alpha$$

With,

$$\sqrt{\frac{k}{k-\alpha}} \sim 1$$

Therefore,

$$\frac{d^\alpha x^k}{dx^\alpha} = \frac{k!}{(k-\alpha)!} x^{k-\alpha} = e^\alpha k^\alpha e^{-\alpha}(1) x^{k-\alpha} = k^\alpha x^{k-\alpha} \tag{13}$$

Since $k \gg \alpha$ is not our case, we will test the accuracy of the previous approximation for $k = -1$ and $\alpha = 1$, since $\frac{d^1 x^{-1}}{dx^1} = -\frac{1}{x^2}$. That is:

$$\begin{aligned}\frac{d^\alpha x^k}{dx^\alpha} &= \frac{dx^{-1}}{dx} = \frac{k!}{(k-\alpha)!} x^{k-\alpha} = \frac{(-1)!}{(-1-1)!} x^{-1-1} = \frac{(-1)!}{(-2)!} x^{-2} \\ &= \frac{-1^{-1}}{(-2)^{-2}} e^{-1}\sqrt{\frac{-1}{-2}}\left(x^{-2}\right) = -\frac{4\sqrt{0.5}}{e} = -1.0405 x^{-2} \sim -x^{-2}\end{aligned}$$

Or a 4% error. Now with $\alpha = H$, and $k = -1$, and considering the chain rule for differentiation, we find:

$$\frac{d^H}{da}\left(\frac{1}{1-a}\right) = \frac{d^H}{da}(1-a)^{-1} = \frac{(-1)!}{(-1-H)!}(1-a)^{-1-H}\frac{d^H}{da}(-a)$$
$$= \frac{(-1)!}{(-1-H)!}(1-a)^{-1-H}\left(\frac{1!}{(1-H)!}H(-1)\right) \sim \frac{a^{1-H}}{(1-\alpha)^{1+H}}$$

Therefore if,

$$\sum_{n=0}^{\infty} a^n = \frac{1}{1-a}$$

Then

$$\frac{d^H}{da}\sum_{n=0}^{\infty} a^n = \frac{d^H}{da}\left(\frac{1}{1-a}\right)$$

thus,

$$\sum\nolimits_{k=0}^{\infty} k^H a^{n-H} \sim \frac{a^{1-H}}{(1-\alpha)^{1+H}} \tag{14}$$

and,

$$\sum\nolimits_{n=0}^{\infty} n^H \rho^n \sim \frac{\rho}{(1-\rho)^{1+H}} \tag{15}$$

Then, the probability distribution of the system time is:

$$f(t) = f(z_1(t))\sum_{n=0}^{\infty}(n+1)^H \rho^n$$

With

$$\sum_{n=0}^{\infty}(n+1)^H \rho^n = \sum_{j=1}^{\infty} j^H \rho^{j-1} = \frac{1}{\rho}\sum_{j=0}^{\infty} j^H \rho^j$$

Then,

$$f(t) = f(z_1(t))\left(\frac{1}{\rho}\right)\left(\frac{\rho}{(1-\rho)^{1+H}}\right)$$
$$= f(t) = \frac{f(z_1(t))}{(1-\rho)^{1+H}}$$

Consequently,

$$E[t] = \frac{E[z_1(t)]}{(1-\rho)^{1+H}}$$

If $z_1(t)$ is has Pareto pdf then,

$$E[t] = \frac{\beta B}{(\beta - 1)(1 - \rho)^{1+H}} \tag{16}$$

Since Little's Law indicates that:

$$E[t] = E[n]E[arr\ time] = (E[n] + 1)E[ser\ time] \tag{17}$$

Then it follows that $E[n] = \frac{1}{(1-\rho)^{1+H}} - 1$
Therefore (called P/P/1 Frac1 model),

$$E[n] = \frac{1}{(1-\rho)^{1+H}} - 1 = \frac{1-(1-\rho)^{1+H}}{(1-\rho)^{1+H}} \approx \frac{1-(1-(1+H)\rho)}{(1-\rho)^{1+H}} = \frac{(1+H)\rho}{(1-\rho)^{1+H}} \tag{18}$$

4 Modelling Sum of Pareto Random Variables

The central limit theorem (CLT) states that, under appropriate conditions, the distribution of a normalized version of the sample mean converges to a standard normal distribution. In the same manner, the addition of random variables with α-stable (long-tailed probability distribution), when normalized, approaches a well-defined stable limiting distribution which depends on α or β [17]. This will allow us to derive a quasi-asymptotic model for our queuing system.

The Generalized Central Limit Theorem states that the properly normalized sum $S_n = \sum_i^N z_i$ of many i.i.d. Pareto r.v.s may be approximated by a stable distribution:

$$\lim_{n\to\infty} P\left[\frac{S_n - b_n}{n^{\frac{1}{\beta}} C_\beta} < \varphi\right] = F_\beta(x) \tag{19}$$

In (14) $F_\beta(x)$ is a stable distribution with indexβ. The normalization coefficient is:

$$C_\beta = \left[\Gamma(1-\alpha)\cos\left(\frac{\pi\alpha}{2}\right)\right]^{1/\beta} \tag{20}$$

The shift coefficient is:

$$b_n = \frac{n\beta}{\beta - 1} \tag{21}$$

4.1 Tail Asymptotic of Heavy-Tail Sums

According to Zaliapin et al. [18] an approximation for the upper quantiles can be obtained by noticing that the tail $1 - F_\beta(x)$ of a stable distribution has a simple asymptotic:

$$\lim_{x\to\infty} x^\beta (1 - F_\beta) = C_\alpha^{-\beta}.$$

More plainly with r.v.s with Pareto distribution:

$$\lim_{n\to\infty} P[S_n > \varphi] = \theta = \left(\frac{\varphi - b_n}{n^{\frac{1}{\beta}}}\right)^{-\beta} = n(\varphi - b_n)^{-\beta} \tag{22}$$

And thus,

$$\mathrm{P}[S_n = t] = n\beta(t - b_n)^{-\beta-1} \tag{23}$$

Recall that $(1+x)^p \sim 1+px$. Also, $(a-b)^{-\beta} = a^{-\beta}\left(1+\frac{b}{a}\right)^{-\beta} \sim a^{-\beta}\left(1+\frac{\beta b}{a}\right)$. Therefore,

$$P[S_n = t] = n\beta(t-b_n)^{-\beta-1} \sim n\beta t^{-\beta-1}\left(1+\frac{\frac{(\beta+1)n\beta}{(\beta-1)}}{t}\right) = n\beta t^{-\beta-1}\left(1+\frac{n\beta(\beta+1)}{t(\beta-1)}\right) \tag{24}$$

Therefore, the probability distribution for system time is:

$$\begin{aligned} f(t) &= \sum_{n=0}^{\infty} p_n f_n(t) = \sum_{n=0}^{\infty} p_n P\big[S_{n+1} = t\big] \\ &= \sum_{n=0}^{\infty} \rho^n(1-\rho)(n+1)\beta t^{-\beta-1}\left(1+\frac{(n+1)\beta(\beta+1)}{t(\beta-1)}\right) \\ &= (1-\rho)\beta t^{-\beta-1}\left[\sum_{n=0}^{\infty}\rho^n(n+1) + \frac{\beta(\beta+1)}{t(\beta-1)}\sum_{n=0}^{\infty}(n+1)^2\rho^n\right] \\ &= (1-\rho)\beta t^{-\beta-1}\left[\frac{1}{(1-\rho)^2} + \frac{\beta(\beta+1)}{t(\beta-1)}\left(\frac{\rho+1}{(1-\rho)^3}\right)\right] \\ f(t) &= \beta t^{-\beta-1}\left[\frac{1}{(1-\rho)} + \frac{\beta(\beta+1)}{t(\beta-1)}\left(\frac{\rho+1}{(1-\rho)^2}\right)\right] \end{aligned} \tag{25}$$

And by the Pareto scaling, if $y = Ax$, then $E\big[y\big] = AE[x]$, we have (P/P/1 Par Sum):

$$E[t] = B\left[\frac{\beta}{(1-\rho)(\beta-1)} + \frac{\beta(\beta+1)(1+\rho)}{(\beta-1)(1-\rho)^2}\right] \tag{26}$$

5 Results and Discussion

To validate the models, a discrete event simulation was carried out. The inter-arrival time of each job is Pareto I probability distribution with shape parameter α, and location parameter A, $f(t) = \alpha\left(\frac{t}{A}\right)^{-\alpha-1}$. For the simulation, $\alpha = 1.7$ and $A = 1.77059$, which makes the mean inter-arrival time of $E[arrtime] = \overline{A} = 4.3$. The probability distribution for the service time is also distributed as a Pareto I random variable with β as shape parameter and B as scale parameter, $g(t) = \beta\left(\frac{t}{B}\right)^{-\beta-1}$. For the simulation, $\beta = 1.8$ and $B = 1.51111$, which makes the mean service time of $E[servtime] = \overline{S} = 3.4$. Each run consisted of one single batch of 1,000,000 arrivals, with the results shown in Table 1. Performance measures of Table 1 were estimated using observed value means allowing for transient period.

Simulation results yield a value of W = E[t] = 74.99923 with standard deviation of 46.5673, and value of L = E[n] = 17.75728 with standard deviation of 10.68285. Results for M/G/1 model are also shown.

Table 1. Comparing the average with derived models

	Sim	M/M/1	P/P/1 Series	P/P/1 Frac1	P/P/1 Par Sum	M/G/1
Eq. ρ		$\frac{\overline{S}}{\overline{A}}$	$\frac{\alpha B}{\beta A}$	$\frac{\alpha B}{\beta A}$	$\frac{\alpha B}{\beta A}$	$\frac{\overline{S}}{\overline{A}}$
Eq. E[t]		$\frac{1}{\mu-\lambda}$	$\frac{\rho}{(1-\rho)^2}\overline{A}$	$\left(\frac{(1+H)\rho}{(1-\rho)^{1+H}}\right)\overline{A}$	$B\left[\frac{\beta}{(1-\rho)(\beta-1)} + \frac{\beta(\beta+1)(1+\rho)}{(\beta-1)(1-\rho)^2}\right]$	$\frac{\rho^2+\lambda^2\sigma^2}{2(1-\rho)} + \rho$
Eq. E[n]		$\frac{\rho}{1-\rho}$	$\frac{\rho}{(1-\rho)^2}$	$\frac{(1+H)\rho}{(1-\rho)^{1+H}}$	$\frac{B}{\overline{A}}\left[\frac{\beta}{(1-\rho)(\beta-1)} + \frac{\beta(\beta+1)(1+\rho)}{(\beta-1)(1-\rho)^2}\right]$	$\frac{\frac{\rho^2}{\lambda}+\lambda\sigma^2}{2(1-\rho)} + \frac{1}{\mu}$
ρ	0.787431	0.806037	0.790697	0.790697	0.790698	0.790698
E[t]	74.99923	17.52916	77.612345	64.738760	405.389135	51.262932
E[n]	17.75728	4.155635	18.049383	15.055525	94.2765432	11.921612

6 Discussion

In Table 1 we can see that Eq. (6), $\frac{\rho}{(1-\rho)^2}$, gives the best approximation to $E[n]$ whereas Eq. (18), $\frac{\rho}{(1-\rho)^2}\overline{A}$, gives the best approximation to $E[t]$, meaning that model P/P/1 Series is the best approximation, closely followed by the P/P/1 Frac1 model.

It is also interesting to note that the performance of the well-known M/G/1 model is much better than the M/M/1 as simulation results give $L = E[n] = 17.76$, with M/M/1 estimating $L = E[n] = 4.16$ and M/G/1 estimating $L = E[n] = 11.93$, a much better result.

Also, even though at first it appears that the P/P/1 Par Sum is way off, with a result of $L = E[n] = 94.28$, it is important to remember that it is an asymptotic model. In fact, the average maximum queue length observed, that is, maximum congestion, is $\overline{L}_{max} = 1{,}121.4$ jobs, with an all-simulations maximum of 3,438. These extremely large values result from rare, but high-impact events of extremely high service times. In these extreme cases, P/P/1 Par Sum model would yield better results.

7 Conclusion

The P/P/1 queueing system is a powerful tool for modelling a wide variety of real-world systems. In this paper, we have shown how the P/P/1 queue can be used to model systems with high variability in the inter-arrival and service times. Our results show that the P/P/1

Series model can accurately predict the mean number of jobs in the system and the mean residence time. This model assumes that the probability of no event happening in a very small Δt is almost one, as events tend heavily to persist into the future. This assumption is supported by our simulation results, which show that the P/P/1 Series model can closely approximate the mean number of jobs in the system and the mean residence time. We also find that the P/P/1 Frac1 model is also a close match with simulation results, although is fall short in estimating some parameters. Interestingly, the P/P/1 Par Sum model models better conditions in which there is congestion because the occurrence exceedingly large service time rare event.

We identify as current limitations of our work that the simulation assumes infinite queue capacity, which may not hold in real-world systems with finite resources. Also, the models rely on the assumption of steady-state conditions, which may not be valid during transient phases or under extreme variability.

Future research could explore extending this model to multi-server systems or incorporating additional real-world factors, such as varying service rates or priority queues. Also, our work will focus on the use of the P/P/1 Series model to model other real-world systems. And the use of different simulation techniques to improve the accuracy.

References

1. Fischer, M., Cart, H.: A method for analyzing congestion in Pareto and related queues. Telecommun. Rev. **10**, 15–28 (1999)
2. Argibay Losada, P., Suarez Gonzalez, A., Lopez Garcia, C., Rodriguez Rubio, R., Lopez Ardao, J.: On the simulation of queues with Pareto service. In: Proceedings of the 17th European Simulation Multiconference, Nottingham, United Kingdom (2003)
3. Gross, D., Fischer, M., Masi, D., Shorte, J.: Difficulties in simulating queues with Pareto service. In: Proceedings of the Winter Simulation Conference, New Orleans, LA, USA (2003)
4. Koh, Y., Kim, K.: Evaluation of steady-state probability of Pareto/M/1/K experiencing tail-raising effect. In: Freire, M.M., Lorenz, P., Lee, M.M.O. (eds.) HSNMC 2003. LNCS, vol. 2720, pp. 561–570. Springer, Heidelberg (2003). https://doi.org/10.1007/978-3-540-45076-4_56
5. Fischer, M., Bevilacqua Masi, D., Gross, D., Shorte, J.: One-parameter Pareto, two-parameter Pareto, three parameter Pareto: is there a modelling difference? Telecommun. Rev. **16**, 79–92 (2005)
6. Inmaculada, A., Meerschaert, M., Panorska, A.: Parameter estimation for the truncated Pareto distribution. J. Am. Stat. Assoc. **101**(473), 270–277 (2006)
7. Albrecher, H., Araujo-Acuna, J.C., Beirlant, J.: Tempered Pareto-type modelling using Weibull distributions. ASTIN Bull. J. IAA **51**(2), 509–538 (2021)
8. Jian, B., Tan, J., Shroff, N., Towsley, D.: Heavy tails in queueing systems: impact of parallelism on tail performance. J. Appl. Probab. **50**(1), 127–150 (2013)
9. Asmussen, S.: Applied Probability and Queues. Springer, New York (2003). https://doi.org/10.1007/b97236
10. Rolski, T., Schmidli, H., Schmidli, V., Teugels, J.: Stochastic Processes for Insurance and Finance. Wiley, Chichester (1999)
11. Leon-Garcia, A.: Probability, Statistics, and Random Processes for Electrical Engineering. Pearson, New York (2008)
12. Whitt, W.: The impact of a heavy-tailed service-time distribution upon the M/GI/s waiting-time distribution. Queueing Syst. **36**(1), 71–87 (2000)

13. Resnick, S.I.: Heavy tail modeling and teletraffic data. Ann. Stat. **25**(5), 1805–2272 (1997)
14. Beran, J.: Statistics for Long-Memory Processes. Taylor & Francis, New York (1994)
15. Willinger, W., Paxson, V.: Where mathematics meets the internet. Not. Am. Math. Soc. **45**, 961–970 (1998)
16. Ramirez-Velarde, R.V., Rodriguez-Dagnino, R.M.: From commodity computers to high-performance environments: scalability analysis using self-similarity, large deviations and heavy-tails. Concurr. Comput. Pract. Exp. **22**(11), 1494–1515 (2010)
17. Ramirez-Velarde, R.V., Rodriguez-Dagnino, R.M.: A gamma fractal noise source model for variable bit rate video servers. Comput. Commun. **27**(18), 1786–1798 (2004)
18. Zaliapin, I.V., Kagan, Y.Y., Schoenberg, F.P.: Approximating the distribution of Pareto sums. Pure Appl. Geophys. **162**(6–7), 1187–1228 (2005)

Teaching Computational Science

Best Practices in Teaching Digitization and Process Automation - A Case Study of Warsaw University of Technology

Wojtachnik Robert[1], Gavkalova Nataliia[1(✉)], Krawiec Jerzy[1], and Martin John[2]

[1] Faculty of Mechanical and Industrial Engineering, Warszawa University of Technology, pl. Politechniki 1, Warszawa, Poland
{robert.wojtachnik,nataliia.gavkalova,jerzy.krawiec}@pw.edu.pl
[2] School of Geography, Earth and Environmental Sciences, Faculty of Science and Engineering, University of Plymouth, Plymouth, UK
j.martin-2@plymouth.ac.uk

Abstract. This article examines recent advancements in the use of Artificial Intelligence (AI) for automation and robotics, highlighting efficiency gains across sectors. It reviews key trends, including robotic process automation in different areas and compares AI implementation frameworks such as MLOps and DevOps. The study presents educational approaches to teaching automation at Warsaw University of Technology, detailing project structures, tools and practical outcomes. Quantitative results on time savings are discussed in relation to existing research. The paper concludes with insights on incorporating AI into education to better prepare students for the digital future.

Keywords: Low/Zero-Code platforms · Warsaw University of Technology · MLOps and DevOps · digitization · automation

1 Introduction

The rapid advancement of automation technologies and Artificial Intelligence (AI) has fundamentally transformed various industries, streamlining processes and increasing operational efficiency. The integration of AI into process automation has enabled businesses to optimize workflows, reduce human intervention, and enhance accuracy across a range of applications, from manufacturing to financial services. The growing reliance on AI-driven automation has raised critical questions about how these technologies should be studied in academic settings to prepare future professionals for the evolving digital landscape.

This study explores best practices in teaching digitization and process automation, with a particular focus on the educational methodologies, which are in-use at Warsaw University of Technology. By comparing Low/Zero-Code platforms with traditional programming methods, the study aims to assess the effectiveness of different teaching

M. Paszynski et al. (Eds.): ICCS 2025 Workshops, LNCS 15912, pp. 239–253, 2025.
https://doi.org/10.1007/978-3-031-97573-8_17

approaches in equipping students with the necessary skills for AI-driven automation. As organizations increasingly adopt AI-based solutions, there is a growing demand for professionals who can efficiently implement and manage automation tools. Understanding the most effective ways to teach these skills is essential for shaping the workforce of the future.

A central objective of this study is to evaluate the effectiveness of Low/Zero-Code platforms compared to traditional programming in teaching automation and digitization. Low-Code platforms offer a visual, user-friendly interface that enables rapid application development with minimal coding expertise, making them highly accessible for non-programmers. Conversely, traditional programming methods require in-depth coding knowledge and offer greater flexibility in developing complex automation solutions. Understanding the trade-offs between these approaches is crucial for designing effective educational curricula.

This research provides an in-depth case study of Warsaw University of Technology's approach to teaching digitization and process automation. The curriculum incorporates various automation frameworks, including DevOps and MLOps, to give students a comprehensive understanding of AI-driven automation. The study outlines project structures, tools used, and practical implementations, including screenshots of student-developed automation workflows. By analyzing real-world applications of AI in automation education, the research offers valuable insights into best practices for integrating these technologies into academic programs. Moreover, the study highlights the importance of standardization and best practices in automation education. Beyond merely replacing human labor, automation involves optimizing workflows, implementing templates, and ensuring interoperability between different systems. By leveraging AI and automation frameworks, educational institutions can equip students with the competencies required for the digital age.

2 Literature Review

Previous studies have demonstrated that Low-Code platforms significantly reduce development time compared to traditional programming [1]. Our research builds on these findings by quantifying the time saved in learning automation concepts through Low-Code tools versus conventional coding methods. Preliminary results suggest that Low-Code learning is 232% faster than traditional programming, facilitating quicker upskilling and adoption of automation technologies. However, despite these advantages, we assume that Low/Zero Code approaches still require supplementation with traditional programming for more advanced and customized automation solutions.

Despite these advancements, a major challenge remains the effective training of professionals who can develop, manage, and optimize AI-driven automation tools. Research by KPMG indicates that only 51% of companies provide adequate training in automation technologies, leading to inefficiencies and suboptimal utilization of AI capabilities [2]. This gap underscores the importance of educational programs that offer practical, hands-on training in process automation, preparing students to meet industry demands. AI-powered automation has been widely adopted across industries, particularly in fields such as healthcare, finance, and logistics, where machine learning (ML) models and

robotic process automation (RPA) systems play a crucial role. Notably, methodologies like DevOps and MLOps have emerged as key frameworks for managing the lifecycle of AI-based automation solutions. Companies such as Mayo Clinic successfully integrate DevOps and MLOps principles to enhance AI-driven decision-making, demonstrating the impact of structured automation practices on organizational efficiency [3].

Using Low-Code platforms, process automation and robotization enables the rapid creation of efficient and scalable solutions [4]. Low-code programming (LCP) is an approach to software development that minimizes the need for manual coding by using visual tools, abstraction models, and methods of programming by examples and natural language programming (NLP). The faster pace of application delivery using Low-Code platforms is confirmed by research. Software development using Low-Code is approximately three times faster than using traditional coding methods [1]. Research conducted by Richardson and Rymer [5] showed that Low-Code development platforms can help accelerate enterprise development and application delivery by 5 to 10 times. An important aspect, which became actual the past few years, is also AI-driven tools usage to generate applications, analyze data, generate workflows and generate some recommendations for user [7]. Companies that use a structured approach to tool selection achieve 65% higher implementation efficiency [13]. For example, Milky Way model [20], which is an approach to analyzing and visualizing the entire organization on one page, presents the relationships between business processes, applications in a holistic and easy-to-understand way.

Rapid application development is not the only benefit of implementing Low-Code platforms. Other benefits include enhanced scalability, reduced dependency on highly specialized developers, and improved adaptability to business needs.

3 Methods and Methodology

Methods

In this study, we analyze the effectiveness of teaching digitalization by comparing two approaches: Low/Zero Code platforms and traditional programming. First, we are going to describing how we are teaching digitalization at Warsaw University of Technology based on our 6 years of experience. We will present best practices, show what applications we use, discuss the team work methods we teach, present analytical models used to collect requirements for digitalization, sample diagrams, discuss the method used to automate processes and tasks, and show how we do it using an example. Then, we will define the learning outcomes and education time and compare them to the education of programmers using classic languages such as Python.

Modern organizations must adapt to dynamic changes in the business environment, and digital transformation has become a key element of company development strategies. Digitization of operational processes allows companies to streamline operations, reduce costs and increase flexibility. According to OutSystems research [6], companies can be divided into six levels of digital maturity:

1. Unaware - 5% of companies, no digitalization activities;
2. Isolated initiatives - 19%, first experiments with digitalization;
3. Widespread digitalization - 17%, implementation of technologies in selected areas;

4. Strategic digitalization - 31%, digital solutions key to business;
5. Integrated digitalization - 10%, full integration of IT systems;
6. Continuous innovation - 18%, digital companies, constantly implementing new technologies.

The aim of the digitization project is not to create an application, but to provide a solution that provides the organization with greater efficiency through process automation and better data availability, providing better customer experience and improving cooperation between teams, which ultimately leads to increased competitiveness and innovation of the company. This is achieving digital maturity level 4, 5, 6.

Over 6 years of conducting classes on enterprise digitization, acquiring new knowledge and experience, the best practices used at the Warsaw University of Technology in teaching enterprise digitization have been developed and listed below:

– Combining application development methods and team work management (MLOps, DevOps);
– Using enterprise architecture for a comprehensive analysis of process digitization needs;
– Using Low-Code platforms, process automation and robotization to quickly create efficient and scalable solutions [4];
– Using Artificial Intelligence algorithms to generate applications, analyze data, generate workflows, generate recommendations for users and register data [7]. According to KPMG, 88% of managers believe that the integration of AI with Low-Code has huge potential [2];
– Replacing human work with the automation of processes and tasks.

According OutSystems research, 65% of enterprises need to implement at least 10 applications, and 23% need to implement more than 50 applications. Companies need to implement 58% of these applications within 3–4 months and another 23% within 5–6 months. Such a fast pace of application delivery is possible using Low-code platforms [6].

Methodology

Low-code programming (LCP) is an approach to software development that minimizes the need for manual coding by using visual tools, abstraction models, and methods of programming by examples and natural language programming (NLP). Low-Code supports digital transformation, helping to quickly reach the levels 4, 5, 6 of digital maturity.

Analysis of 24 Low/Zero-code platforms identified those that incorporate AI technology into application generation, data analysis, workflow generation, user recommendation generation, and data logging [1, 9–12]. A list of platforms implementing AI in at least two areas, and extends them with qualifications according to the Gartner report, is presented in Table 1 [9]. The table is based on the analysis mentioned above.

It should be also mentioned that although each of the applications listed in Table 1 is a Low-Code application, in the Gartner matrix they are classified into different categories: Robotic Process Automation, Low Code Application Platform, and Collaborative Work Management.

Table 1. Comparison of Low-Code Platforms

Low-code tools	Generate Apps	Data Analysis	Generate Workflow/code	Recommendations	Gartner matrix
Quickbase	✓			✓	Niche players
OutSystems	✓	✓	✓	✓	Leaders
Power Apps	✓		✓	✓	Leaders
Appian		✓	✓		Leaders
Servicenow		✓	✓		Leaders
ClickUp		✓	✓	✓	Visionaries
Make		✓	✓	✓	Visionaries
Open AI		✓	✓	✓	Visionaries

Faster pace of application delivery using Low-code platforms is confirmed by research. Software development using Low-Code is about 3 times faster than using traditional coding methods [1]. Research conducted by Richardson and Rymer showed that low-code development platforms can help accelerate enterprise development and application delivery by 5 to 10 times [5]. Rapid application development is not the only benefit resulting from the implementation of low-code platforms. Other benefits [1, 2, 8] include:

- 81% of companies consider low-code development as key to their digital strategy, 66% of companies consider this technology as key to accelerating innovation and digital transformation;
- 53% of companies notice improved operational efficiency;
- 51% of companies report improved employee productivity;
- 42% of companies indicate reduced software development costs;
- 91% of managers consider scalability as a key feature of low-code platforms;
- 42% of companies consider security risks to be the biggest;
- 43% of European companies indicate limited customization possibilities, while in the US only 32% of companies;
- 38% of companies see the risk of uncontrolled implementation of low-code applications without IT oversight (development in the shadow of IT)
- Insufficient training leads to ineffective use of these technologies. Only 51% of companies train employees.

Companies that use a structured approach to tool selection achieve 65% higher implementation efficiency [13]. When selecting tools, it is important to consider:

- Scalability – can AI, Zero/Low Code tools, automation tools grow with the company?
- Integration – do the tools work together and with existing infrastructure?
- Security – do the tools meet data protection standards?
- Cost of implementation and maintenance – what are the long-term expenses?

Due to the above criteria, ClickUp (Zero Code Platform), OpenAI (construction and training of AI models) and Make, used to automate and robotize processes and integrate all tools in the organization and build AI Agents, were selected to conduct classes on digitization at the Warsaw University of Technology.

Modern organizations, such as Mayo Clinic [3], combine the DevOps approach (agile management of software development and operations) with MLOps (lifecycle management of machine learning models) to effectively automate and integrate AI in everyday work. These experiences allow us to formulate key factors for the success of implementing AI-based process automation [3]:

- Application development by employees. This rapid development of AI at Mayo Clinic was the result of decentralizing application implementation and moving it to a place where people best understand the specifics of their work and know how to improve value delivery. The experience of Low-Code platform partners shows that delivering solutions in weekly cycles is effective [23]. Such teams should work agilely to obtain feedback and improve processes and algorithms (MLOps) every week.
- Support teams. In order for the adopted DevOps model to work and develop operations, support teams are also needed. The role of support teams is to help value stream delivery teams (DevOps) acquire missing capabilities (including knowledge, algorithms, legal regulations) through training, consultations and implementation of good practices. These can be internal or external teams.
- A team-providing infrastructure has been created. The role of this team is to reduce the cognitive load of value stream delivery teams. Low/No-Code programming platforms authorized by IT staff can help solve the risk associated with development in the shadow of the IT department. Users can build the solutions they need on platforms without constantly disturbing IT staff. The IT department controls data and applications, ensuring security and privacy.
- Data quality management. A key element of effective automation using AI is taking care of data quality. Algorithms provide only as good results as the quality of the input data. Mayo Clinic uses a "data stewardship" approach, for preparing data for analysis. In order to constantly improve data quality management processes, teams should do it in a continuous mode, i.e. work agilely. Then they introduce improvements every week.

At Warsaw University of Technology, students learn these methods in the context of a team approach to implementing automation and AI models, which reflects the real needs of the industry.

4 Results and Analysis of the Results

Enterprise Architecture (EA) management is a key aspect of IT strategy that allows organizations to better align technologies with business goals. There are several popular frameworks that help design, implement, and manage organizational architecture: Lean EA, Capstera, Gartner EA, TOGAF, Zachman Framework, FEAF and DODAF.

Table 2 [14–16, 18, 19] presents a comparison of the most popular architectural frameworks, their advantages and applications, and support for DevOps and MLOps. A rating of 0 indicates no support, 3 indicates full support.

Table 2. Comparison of architecture frameworks in the context of their applications, advantages, and support for DevOps and MLOps

Framework	Application	Advantages	DevOps support	MLOps support
Lean EA	Startups, Tech Companies, Digital Transformation	The most agile approach, supports AI and iterative changes	3	3
Capstera	Combining IT and business, e.g. fintech	Modular approach. Strategy and IT. Value streams, adaptation to changes. Ready models	3	2
Gartner EA	Connecting IT and Business: Organizations Implementing Cloud and AI	Focus on business value, flexible approach	3	2
TOGAF	Large corporations	Process structure, broad industry support	2	1
Zachman Framework	Organizations with a strong hierarchy	Comprehensive analysis of IT structure	1	0
FEAF	Public institutions, administration	Process standardization, regulatory compliance	0	0
DODAF	Defense Sector, Cybersecurity	Interoperability, process control	0	0

Since the key success factors for implementing AI-based process automation are the implementation of DevOps and MLOps [3], the best choices of architectural frameworks are Lean EA, Capstera, and Gartner EA. At the Warsaw University of Technology, students learn Lean EA and Capstera.

Using the Capster architectural framework allows you to define the structure of creating digitalization requirements. Based on the architectural framework [17], you can define models that are used at the Warsaw University of Technology in the process of learning digitalization:

- Strategic context – describes the vision, mission, strategies (increasing efficiency, development through innovation, new business models), business motivation of stakeholders, metrics and initiatives necessary to implement the company's strategy.

- Milky Way model [20] – this is an approach to analyzing and visualizing the entire organization on one page. It presents the relationships between business processes, applications in a holistic and easy-to-understand way. Building the model begins with creating a diagram with the value stream delivered as part of the Customer Journey. The map is divided into sectors: marketing and sales, service execution, after-sales service, management, product development. Business capabilities (processes, people, data and applications) should be placed in each sector. Then, you need to visualize the information flows between business capabilities (process-process, application-application and human-application). Finally, it is worth adding important elements from the Customer Journey (touchpoints, applications). The map can be made at various levels of detail of business capabilities and connections between business capabilities.
- Business services digitization – this is a model based on the Use Case model. At the center of the model is an actor (customer or partner), who uses business services. Each service is delivered by business processes (Milky Way model), which are supported by application services and applications. One application can deliver many application services. The model also shows the integrations between applications that need to be automated. This model is the basis for process digitization and defining functional requirements for applications.
- Strategic plan for business capability development – no company has an unlimited budget or time to digitize and standardize all processes at once. The key to success is wise prioritization. Some business capabilities determine competitiveness – they should be the most innovative and digitally advanced (product development, sales). Business capabilities that do not create a competitive advantage, but are essential for the smooth operation of the business should be digitized and optimized to work faster and more efficiently. Capabilities that do not create value – it is better to outsource them to external suppliers.
- Business capability maturity assessment – the model divides business capabilities into management, core and supporting. It presents an assessment of the business and technological maturity of each business capability. The model is needed to describe the required changes that must be made to increase the level of maturity of the business capability in the area of people, processes, and applications.
- Change roadmap – based on the capability assessment, you can plan the implementation of changes. This will be helped by organizing around the value stream and assigning changes to the subsequent stages of the stream of competencies, processes, applications. At each stage of value creation, teams can deliver solutions working in DevOps and MLOps.
- Data presentation – views, reports, Kanban boards, lists, dashboards help visualize data or the effects of process implementation. Users define the way of presenting data needed to implement the process and to make decisions.

Table 3 [13] shows what results can be achieved by automating tasks, processes and decision-making processes. ROI analysis will allow you to estimate the return on investment in automation in the enterprise.

Digital transformation requires rethinking traditional enterprise architecture frameworks. The framework of the future must be able to [14]:

Table 3. Impact Analysis of AI Automation Implementation

Core Application	Key Benefits	Implementation Results	Category of automation
Email Systems	Startups, Tech Companies, Digital Transformation	The most agile approach, supports AI and iterative changes	Task
Meeting Management	Combining IT and business, e.g. fintech	Modular approach. Strategy and IT. Value streams, adaptation to changes. Ready models	Task, decision
Document Processing	Connecting IT and Business: Organizations Implementing Cloud and AI	Focus on business value, flexible approach	Task
Customer Support	Large corporations	Process structure, broad industry support	Process, decision
Administrative Work/decision	Organizations with a strong hierarchy	Comprehensive analysis of IT structure	Task, decision
Robotic Process Automation	Defense Sector, Cybersecurity	Interoperability, process control	Process

- integrate digital technologies with business processes and models;
- support a customer-centric approach and create value for the customer;
- enable rapid innovation and the ability to quickly respond to market changes and implement changes agilely;
- support DevOps, MLOps, service-oriented architecture (SOA), and micro services [3].

The result of developing the architecture is knowledge about the priorities of processes for digitalization, planning the necessary changes in people, processes and applications and the way of implementing the functional requirements of the application. It is also knowledge about process automation and integration between applications and processes.

Each process consists of tasks that provide a business service. Tasks flow through subsequent process stages, which are handled by departments and within them by specific business roles. This section discusses how to automate processes, tasks, and decision-making using AI Agents and standardize processes and tasks. There are 5-step procedure for building AI Agents, which can be used during classes [21].

1. Defining the goal. The basic question in the automation process is which processes to automate? They are could be email systems, meeting management, document processing, etc. [13].

2. Technology selection. Using Low-Code platforms, platforms for process automation and robotization, and AI algorithms allows for the quick creation of efficient and scalable solutions [4]. The aforementioned solutions are used to build AI Agents. In the process of teaching digitalization at the Warsaw University of Technology, Make, OpenAI, Click Up software is used. The above-mentioned tools enable the creation of various AI Agent architectures: rule-based, using machine learning, and hybrid.
3. AI training. Using the organization's knowledge to train the model. An example of an AI Agent in a hybrid architecture is the automation of the service's mailbox. It uses AI to analyze the content of the email, categorize it, recognize sentiment, and prepare a response to the customer in the case of various scenarios. This programming is done through demonstration. The rules, on the other hand, are used to take appropriate actions such as sending a confirmation, rejecting the report, handling a repeat message for the report, creating a new report. If the AI Agent's operation is to show the results of its work to the user, then a user interface (chat, application form) should be created. For example, when handling a service box, the user interface will be a list of service requests and the ability for the service technician to handle these requests on the Kanban board.
4. Integration with other systems. Process flow digitization involves the integration of various applications or processes (business services digitization shown in the model). This can be a continuation of the process on another team's board (e.g. an order for shipment appears in the logistics department after the service has performed a repair). It can also be an import of leads from a Facebook ad or receiving/sending emails.
5. Testing and implementation – usability tests and performance optimization in accordance with the MLOps model.

Standardization of processes and tasks is also an important element of work automation, which ensures high repeatability. New possibilities of standardization appear along with new applications of Low/Zero Code [22]. How many times does each team create the same tasks from scratch (e.g. webinar organization plan, employee onboarding, recruitment)? Each time, employees define steps, assign responsible persons and estimate time. It is a waste of energy and resources. In addition, it is enough to identify repeatable processes (e.g. marketing campaign management). Then, processes should be divided into tasks and subtasks (e.g. onboarding, recruitment, webinar organization). Breaking down tasks into smaller subtasks will make it easier for employees to complete and track them. Then, for each task, the time of execution should be estimated; a responsible role and document templates (e.g. order, contract) should be assigned. Such a standardized process or task can be saved as a reusable template. Such a template can be automatically loaded when creating a new task, saving time each time the work is defined (e.g. onboarding a newly hired employee).

Research question: Which method of teaching digitization is more effective in terms of the time needed to acquire the knowledge necessary to perform process automation tasks?

The subject of the study are digitization courses conducted using Low/Zero Code and traditional methods. The subject of the study is the effectiveness of teaching digitization and the time needed to prepare for independent process automation measured by achieving the following learning abilities:

– to build DevOps teams, agile management of such a team and software development;
– to manage the MLOps machine learning lifecycle;
– to create a digitization architecture and analyze digitization needs;
– to build applications and standardize processes on the ClickUp platform;
– to integrate selected applications and automate tasks using the Make platform;
– to program AI Agents using the Make and OpenAI platforms.

A group of students of digitalization at the Warsaw University of Technology completed a course lasting 45 h of study (15 h of lectures, 15 h of exercises, and 15 h of laboratory). After completing the course, students were ready to implement process automation tasks, which they confirmed by performing a digitalization project and thus confirming the achievement of learning outcomes. The second object of the study were programming courses, the completion of which allows for the achievement of comparable learning outcomes, but using traditional programming methods. In order to identify them, a strategy of systematic search of available online courses was used, focusing on programs with the shortest duration, which at the same time ensure the achievement of all required competences. During the analysis, it was indicated that the following courses (104.5 h) should be completed:

– Agile & DevOps Leadership – IC Agile Certification (16 h)
– AI Agent Design (15 h) – maven.com
– Business Architecture Training Program (4.5 h) – Capstera
– Automation Agent (9 h) – Bots and People
– Python Developer with Django (6 0 h) - Noble Desktop

In addition, it is important to highlight the following criteria were used to select training companies:

– The company specializes in training topics and conducts training at various levels on a given topic
– The shortest training that provides the expected learning outcomes was selected.

This study aimed to compare the effectiveness of teaching digitization and process automation using Low/Zero-Code platforms and traditional programming methods. The analysis also included the time needed to train a process automation specialist. The results of the study clearly indicate that the Low/Zero-Code method is much more effective in terms of learning and implementation time. Students of the Warsaw University of Technology using Low-Code platforms achieved the required competences in 45 h, while programmers learning traditional programming languages (e.g. Python) need 104.5 h to acquire the same skills. This means that learning Low/Zero-Code was 232% faster.

5 Discussion

The use of Low/Zero-Code platforms allows for faster implementation of applications and digitalization processes, which is also confirmed by previous studies. Previous researchers showed that creating, testing and configuring software using Low-Code is 3 times faster than using traditional programming methods [1]. These results are consistent with our findings - learning, digitization and automation of processes using Low-Code is much more time-efficient.

In the context of the labor market and education, the key question is, can Low-Code replace traditional programming? Low-Code is an ideal tool for non-technical people who want to implement digitalization in companies without the need for in-depth coding knowledge. By 2026, over 80% of Low-Code tool users will not have formal programming education, which indicates the growing role of this technology in business. Companies using Low-Code can respond faster to internal or market needs and deliver solutions in a shorter time, which is key in the digital transformation strategy [9]. This is confirmed by OutSystems data - 65% of companies have to implement at least 10 applications in 3–4 months, and 23% more than 50 applications in 5–6 months in a short time. Companies at different levels of digital maturity can benefit from Low-Code, achieving their goals. Companies at maturity level 3–4 (strategic digitalization, integrated digitalization) can accelerate the implementation of digitalization in key areas. Companies at maturity level 5–6 (Continuous innovation) can use Low-Code in combination with AI for automation and intelligent data management [6].

Traditional programming still has an advantage in flexibility and customization of solutions - complex algorithms and application functions, large databases still require coding. However, advanced AI models and machine learning algorithms can already be delivered using Low/Zero Code tools, due to the possibility of using NLP.

Despite many advantages, Low-Code is not a perfect solution. KPMG reports that 42% of companies indicate security risks as a major problem, and 38% of companies see the risk of so-called “shadow IT” - uncontrolled application deployment without IT department supervision [2]. Therefore, although Low-Code is effective, it requires appropriate supervision, integration with IT and care for security. The article indicates how to solve these problems. The implementation of a DevOps team topology, which is responsible for creating value (process automation using AI supported by MLOps), support teams and platform delivery teams will certainly help in this.

6 Conclusions

Addressing the topic of the effectiveness of teaching process automation is an important topic, which is confirmed by KPMG research in 2024 [2]. According to them, only 51% of companies provide employees with appropriate training, which can lead to ineffective use of this technology. Low-Code is much more time-efficient than traditional programming, which is confirmed by both our research and previous [1]. Learning digitization using Low-Code is 232% faster than traditional programming, which allows for faster training of employees and implementation of digitization. Low-Code changes the way digitization is taught - it allows for faster implementation of solutions, but still requires supplementation with traditional programming for more complex projects.

We have shown that automation is not only about replacing human work with a machine and AI algorithms. It is also about standardization and templates that speed up the registration of tasks and the implementation of processes. Low-Code accelerates digital transformation and is particularly valuable for companies at levels 4, 5 and 6 of digital maturity [6]. Low-Code has its limitations (security, IT control), but their proper management (DevOps and MLOps team topologies) allows for the full use of the potential of this technology.

The results of this study point to several important areas for further researches:

1. Analysis of the long-term impact of Low/Zero Code education – future studies could investigate how students use the acquired skills in professional practice and whether Low/Zero Code technologies become a key element of their daily work.
2. Impact of Low-Code integration with AI – further experiments could investigate to what extent AI tools such as LLM (e.g. OpenAI, Make) can improve the efficiency of implementing digitization and automation in education and industry.
3. Comparison of different Low/Zero Code platforms – it is worth conducting a comparative analysis of different tools (e.g. ClickUp, OutSystems, Power Apps) in terms of the efficiency of teaching and implementing automation.
4. Impact of Low-Code on employees' soft skills – it is worth investigating whether Low/Zero Code education supports the development of analytical skills, creativity and teamwork in the context of managing digitization projects.

Low-Code and AI are the future of digitalization and process automation, allowing for faster implementation of changes and increasing the efficiency of the organization. However, their effective use requires an appropriate strategy, teamwork methods, methods of analyzing the needs of digitalization, training and tools that allow for the rapid creation of applications and standardization of processes, automation of processes, tasks and communication, as well as the use of AI algorithms based on NLP.

Acknowledgments. No.

Disclosure of Interests. The authors have no competing interests to declare that are relevant to the content of this article.

References

1. Trigo, A., Varajão, J., Almeida, M.: Low-code versus code-based software development: which wins the productivity game? IEEE IT Prof. **24**(5), 61–68 (2022)
2. KPMG International: Low-code adoption as a driver of digital transformation. KPMG (2024). https://hub.kpmg.de/shaping-digital-transformation-with-low-code-platforms
3. Davenport, T.H., Bean, R.: Mayo clinic's healthy model for AI success. MIT Sloan Manag. Rev. (2024). https://sloanreview.mit.edu/article/mayo-clinics-healthy-model-for-ai-success
4. Deng, X., Wang, Z., Xu, L., Zhao, J., Yin, J.: When large language models meet multi-agent systems: recent advances and future opportunities. IEEE Trans. Artif. Intell. (2024). https://doi.org/10.1109/TAI.2024.3337017
5. Richardson, C., Rymer, J.R.: Vendor landscape: the fractured, fertile terrain of low-code application platforms. Forrester (2016). https://www.forrester.com/report/vendor-landscape-thefractured-fertile-terrain-of-low-code-applicatio-plaforms/RES122549?objectid=RES122549
6. OutSystems: The State of Application Development: Is IT Ready for Disruption? (2019). https://www.outsystems.com/higher-education/-/media/1561DFEFA30542ECA8F5D63D96A855FC.ashx
7. Liu, Y., et al.: An empirical study on low-code programming using traditional vs large language model support. IEEE Trans. Softw. Eng. (2024)

8. Alsaadi, H.A., Radain, D.T., Alzahrani, M.M., Alshammari, W.F., Alahmadi, D., Fakieh, B.: Factors that affect the utilization of low-code development platforms: survey study. Rom. J. Inf. Technol. Autom. Control **31**(3), 123–140 (2021)
9. Gartner forecasts worldwide low-code development technologies market to grow 20 percent in 2023 (2022). https://www.gartner.com/en/newsroom/press-releases/2022-12-13-gartner-forecasts-worldwide-low-code-development-technologies-market-to-grow-20-percent-in-2023
10. Chirapurath, J.G.: SAP named a challenger in the 2024 Gartner Magic Quadrant for RPA. SAP News (2024). https://news.sap.com/2024/09/sap-a-challenger-2024-gartner-magic-quadrant-for-rpa
11. Dungay D.: Gartner collaborative work management magic quadrant 2024. UC Today (2025). https://www.uctoday.com/collaboration/gartner-collaborative-work-management-magic-quadrant-2024
12. Sandhu B.: SAP recognized as a visionary in the 2024 Gartner Magic Quadrant for enterprise low-code application platforms. SAP News (2024). https://news.sap.com/2024/10/sap-visionary-gartner-magic-quadrant-enterprise-low-code-application-platforms
13. Manshani, K.: AI task automation: a guide to streamlining your workday. Int. J. Comput. Eng. Technol. (IJCET) **16**(1), 628–642 (2025)
14. LeanIX: Enterprise architecture frameworks: Selecting the right EA framework (2025). https://www.leanix.net/en/wiki/ea/enterprise-architecture-frameworks#Selecting-the-right-EA-framework
15. The Open Group: TOGAF – The Open Group Architecture Framework (2024). https://www.opengroup.org/togaf
16. U.S. Department of Defense: DoD Architecture Framework (DODAF) (2025). https://dodcio.defense.gov/Library/DoD-Architecture-Framework
17. Business Architecture Framework: Capstera (2025). https://www.capstera.com/business-architecture-framework
18. Gianni, D., Lindman, N., Fuchs, J.: Complex Systems Design & Management. Proceedings of the Second International Conference on Complex Systems Design & Management CSDM 2011, Springer, Heidelberg (2011)
19. Panetto, H., Baïna, S., Morel, G.: Mapping the models onto the Zachman framework for analysing products information traceability: a case study. Int. J. Comput. Integr. Manuf. **20**(3), 239–253 (2007)
20. Nordén, C.: The milky way: map, navigate and accelerate change. Inf. Resour. Manag. (2018)
21. Wali, A., Mahamad, S., Sulaiman, S.: Task automation intelligent agents: a review. Future Internet **15**(6), 196 (2023)
22. Wojtachnik R.: Jak poukładać procesy w organizacji? Digital Passion (2025). https://digitalpassion.pl/blog/jak-poukladac-procesy-w-organizacji
23. L5.ai.: Go Live in 5 Days with ACT! (2025). https://l5.ai/act. Accessed 02 Feb 2025
24. Krishna, S.: What is artificial narrow intelligence? Venture Beat. https://venturebeat.com/ai/what-is-artificial-narrow-intelligence-ani. Accessed 02 Feb 2025
25. Russell, S.J., Norvig, P.: Artificial Intelligence: A Modern Approach, 4th edn. Hoboken, Pearson (2021). ISBN 978-0-1346-1099-3. LCCN 20190474
26. Cobbe, J., Singh, J.: Regulating Recommending: Motivations, Consideration, and Principles (2019). https://ejlt.org/index.php/ejlt/article/view/686/979
27. OSCE Non-Paper on the Impact of Artificial Intelligence on Freedom of Expression. https://www.osce.org/representative-on-freedom-ofmedia/447829. Accessed 02 Feb 2025
28. Ethics guidelines for trustworthy AI. https://ec.europa.eu/digital-single-market/en/news/ethics-guidelines-trustworthy-ai. Accessed 02 Feb 2025
29. The Most In-Demand Skills In the AI Era. https://www.youtube.com/watch?v=Kn1zdy-EutY. Accessed 02 Feb 2025

30. Outreach Redefines Sales Prospecting with Launch of AI Prospecting Agents. https://insideainews.us7.list-manage.com/track/click?u=25b85319ed833b816410d639b&id=6f736344be&e=3faed23fde. Accessed 02 Feb 2025
31. AI Revolution in EdTech: AI in Education Trends and Successful Cases. https://medium.com/sciforce/ai-revolution-in-edtech-ai-in-education-trends-and-successful-cases-7d5b7d69b77b. Accessed 02 Feb 2025

Contrast Computation for Improved Visibility and User Experience in Educational Interfaces

Agnieszka Olejnik-Krugly(✉), Anna Lewandowska, Maja Dzisko, and Jarosław Jankowski

Faculty of Computer Science and Information Technology, West Pomeranian University of Technology, Szczecin, Poland
{aolejnik,atomaszewska,mdzisko,jjankowski}@zut.edu.pl

Abstract. The effectiveness of digital learning environments depends largely on the usability and accessibility of their visual components. Contrast levels in graphical interfaces play a key role in ensuring visibility, engagement, and a positive learning experience. However, not all educational details are equally noticeable to all users. A lower contrast, if strategically applied and visually striking, can still draw attention and enhance the perception of critical information. This technique is often used in video games, where selective emphasis on certain elements directs the player's focus and improves information processing. This study examines whether high contrast alone guarantees visibility and user-friendliness in digital learning environments. Specifically, we analyze the extent to which WCAG guidelines align with educational needs and whether alternative contrast configurations can maintain readability while reducing visual fatigue. By applying these insights, educators and developers of computational science training materials can refine digital tools, enhance user engagement and improving knowledge retention among learners.

Keywords: Education systems · User experience · Contrast colors

1 Introduction

As of 2023, digital transformation has significantly influenced multiple sectors, including education. The integration of e-learning platforms, computational tools, and digital resources has heightened the importance of usability and accessibility in digital learning environments. This shift mirrors the trends observed in e-commerce, where technological advancements and internet accessibility have driven rapid expansion. Just as online sales redefine traditional shopping, digital learning is transforming educational methodologies, requiring effective, engaging, and accessible user interfaces.

The e-science market in the US was valued at nearly $400 billion in 2022 and is projected to reach $1 trillion by 2032 [3], driven by increased internet

M. Paszynski et al. (Eds.): ICCS 2025 Workshops, LNCS 15912, pp. 254–268, 2025.
https://doi.org/10.1007/978-3-031-97573-8_18

penetration, widespread use of mobile devices, and advancements in cloud-based learning systems and interactive simulations. However, accessibility remains a major challenge: According to the WebAIM annual accessibility report, only 3% of the 1.3 million analyzed websites meet the essential usability and readability standards [2].

In computational science education, the design of graphical components, including data visualizations, interactive models, and simulation tools, plays a crucial role in knowledge delivery. However, balancing engagement and cognitive load remains a challenge. Studies indicate that overly intense visuals can cause cognitive overload, reduced retention, and decreased user experience, while low-contrast designs may fail to effectively communicate key concepts [29].

The impact of visual intensity on user experience is particularly relevant in digital education, where interface design directly affects student engagement and knowledge retention. If critical content lacks sufficient emphasis, learners can overlook essential information, reducing the effectiveness of digital platforms. In contrast, excessive visual stimulation can lead to cognitive stress, making it harder for students to focus and process information efficiently [27,28]. Overly complex visuals can hinder comprehension, induce frustration, and negatively impact learning [5], while insufficient visual emphasis can cause key content to be ignored [4,11]. To optimize digital learning environments, developers must balance contrast, layout, and interactivity to ensure that visual elements enhance rather than obstruct comprehension and accessibility [36].

Although the WCAG [19] guidelines provide a framework for improving content visibility and accessibility, their adoption remains voluntary. As Fig. 1 illustrates, Case 1 represents overly intense contrast, causing irritation and cognitive strain, while Case 2 demonstrates low contrast, leading to reduced visibility and engagement. The goal is to establish Case 3, where contrast is both engaging and comfortable, optimizing learning efficiency without inducing negative cognitive effects.

This study examines whether high contrast alone is sufficient to ensure visibility and user-friendliness in digital learning environments. Specifically, we investigate whether WCAG [19] guidelines align with educational needs or if lower contrast ratios could offer comparable visibility while reducing visual fatigue. This article is a continuation of our previous work [21,22], in which we used eye-tracking technology to analyze various types of user interfaces. Our main contributions:

- Critical analysis of the applicability of WCAG [19] guidelines in educational interface design.
- Discussion on the role of visual intrusiveness, emphasizing that contrast alone does not determine usability.
- Empirical evidence showing that high contrast may improve visibility but reduce user comfort, while lower contrast can enhance readability and cognitive ease.
- Recommendations for color combinations that optimize both visibility and user-friendliness, improving the effectiveness of digital learning materials.

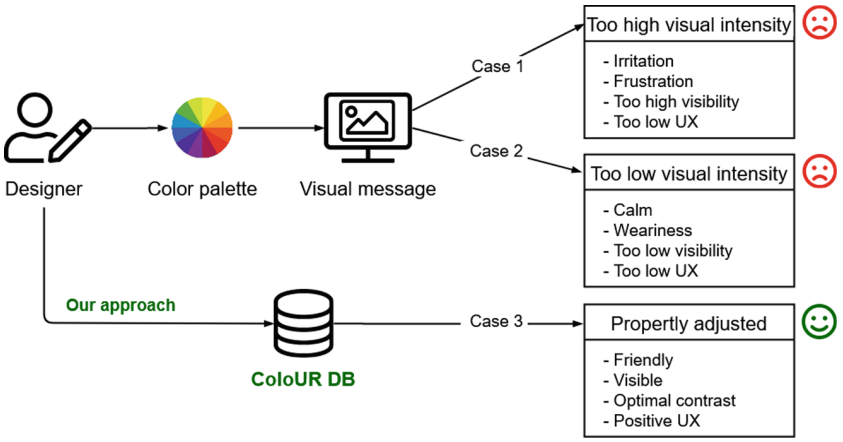

Fig. 1. A designer without support may choose colors that are either too high (Case 1) or too low (Case 2). Case 1 leads to overstimulation and irritation, while Case 2 results in reduced visibility and emotional impact. Our research aimed to develop Case 3 - a balanced approach ensuring user-friendliness, visibility, and contrast colors.

The paper is organized as follows. First, we introduce the state-of-the-art in the Related Work section. The conceptual framework and subjective experiment (which explains the subjective experimental procedure in detail) are presented in the Methods section. The results and analyses can be found in the Results section. A description of potential development directions concerning the state-of-the-art can be found in the Discussion section.

2 Related Work

Most accessibility guidelines recommend a minimum contrast ratio to enhance visibility, yet little attention is given to the potential drawbacks of excessive contrast. Research indicates that extremely high contrast can negatively impact reading experiences [20], causing visual discomfort and cognitive strain, particularly in educational contexts where students process large volumes of text and visual information over extended periods. Experimental studies have shown that a maximal contrast ratio of 21:1 is often perceived as intrusive and unfavorable. At the same time, prolonged exposure to high-contrast interfaces can reduce concentration, increase fatigue, and even lead to cybersickness [7,8]. In contrast, insufficient contrast diminishes content visibility, hindering information retention and accessibility. Both extremes—overly intense and insufficient contrast—negatively affect user engagement, as illustrated in Fig. 1. To enhance the effectiveness of graphical content in digital education, non-invasive attention-guiding techniques can help direct learners' focus toward key instructional elements [35]. Identifying entry points within an educational platform and highlighting salient areas improve user engagement and comprehension [24], while

adapting the type, intensity, or frequency of visual stimuli mitigates habituation effects [16]. A key strategy for optimizing educational visual content involves using contrast-based color combinations that enhance readability and learning outcomes [31], as contrast significantly influences cognitive processing and information retention—critical factors in digital learning environments [30].

The Importance of Contrast in the Perception of Educational Content. Contrast plays a crucial role in the visibility and clarity of educational materials, directly impacting readability and comprehension [15]. Various contrast models, such as Weber contrast [32], Michelson contrast [26], and RMS contrast [33], are applied in different contexts, posing a challenge for instructional designers. To ensure accessibility, this study follows the WCAG standard [19], which defines contrast using "relative luminance," a measure of brightness on a normalized scale from 0 (black) to 1 (white). Evaluating different contrast configurations helps identify combinations that enhance readability without causing strain. Poor contrast selection can either lead to excessive visual fatigue or reduced content visibility, hindering learning.

The Problem of Invasiveness in Educational Graphical Content. A significant challenge in designing educational graphics is avoiding excessive invasiveness, which can disrupt the learning process. Inadequate color choices may distract students, interrupt cognitive flow, and reduce focus, leading to frustration and disengagement. According to [5,36], the overuse of highly intrusive visual elements intended to capture attention is linked to declining learning efficiency and student satisfaction. Previous research that has examined the effects of intrusive elements on knowledge retention and cognitive load was investigated in [9]. Metrics have been developed to assess the level of intrusiveness [12] and have been applied in different educational contexts [25,36]. Beyond perceived intrusiveness, frequent exposure to intense visual stimuli can lead to habituation effects [18], where learners become desensitized to critical instructional graphics. This outcome is counterproductive, as it reduces engagement and prevents students from focusing on essential content. To foster an effective learning experience, designers must strike a balance between engaging graphical elements and maintaining an optimal level of cognitive load, ensuring that visual materials enhance rather than hinder comprehension.

Role of Color in Human Perception. Color plays a key role in human perception, significantly influencing our emotions, decisions, and how we perceive the world around us. Colors have the inherent ability to evoke a range of emotions and psychological states. For instance, certain colors can increase heart rate, elevate adrenaline levels, induce feelings of excitement or tranquility, stimulate concentration, or improve mood [13]. The physiological and psychological impacts of color are well-documented, illustrating how specific hues can affect human behavior and emotional responses [10].

Colors also play a crucial role in our ability to process information and understand our surroundings. Bright and contrasting colors help in the faster identification of objects, thereby improving readability and information retention. Studies have shown that using appropriate color contrasts can significantly enhance the legibility of text and the efficiency of learning materials [14,34]. This is particularly important in educational settings, where the effective use of color can facilitate better learning outcomes and comprehension.

Taking the above, there arise the research questions regarding what level of contrast in digital educational content elements attracts user attention without negatively affecting user experience. How can the lowest possible contrast be maintained while ensuring acceptable readability and user-friendliness? The motivation for this study was the significant challenge of selecting appropriate colors in educational environments, such as e-learning platforms and interactive learning materials. Improper color choices can reduce the effectiveness of information transfer and hinder the process of knowledge acquisition over time.

Therefore, we propose an approach that detects the optimal visual intensity, ensuring user-friendly and well-visible messages. It is based on selecting contrast between primary and secondary colors, where the primary color remains a fixed element of the visual message, and the secondary color serves as its complementary counterpart. Primary and secondary colors may appear in the background, images, pictograms, text, etc. The proposed approach allows for balancing user experience and visual intensity, which can support learning efficiency. Proper color selection in educational interfaces can reduce cognitive fatigue and enhance learning efficiency by optimally adjusting visual intensity to the user's level of engagement. The study results, presented in detail in the *Results* section, demonstrate that it is possible to maintain low contrast while effectively delivering content in a user-friendly manner that supports the learning process.

3 Approach and Methodology

The authors confirm that all experiments followed the relevant guidelines and regulations. All analyzed data were fully anonymized. Before the experiment, the participants provided informed written consent to have data from the perceptual experiment used in the investigation. Informed consent was obtained from all participants.

Screening Observers. The observers may have reported implausible impression scores because they misunderstood the experiment instructions or did not engage in the task and gave random answers. If the number of participants is low, it is easy to spot unreliable observers by inspecting the plots. However, when the number of observers is very high or it is difficult to examine the plots, the ITU-R.REC.BT.500 [17] standard, Annex 2.3.1, provides a numerical screening procedure. We performed this procedure on our data and found that four participants needed to be removed.

Choice of Colors for the Experiment. Color theory provides essential principles for design, including the color wheel, harmony, contrast, and contextual application. In selecting colors for our experiment, we adhered to key guidelines:

- Limited color set (maximum of 10) to maintain user focus and experimental consistency.
- Inclusion of neutral colors (white, black, gray) to balance saturated hues and provide a stable background.
- Use of highly saturated colors to enhance visual attention, based on prior research [6].
- Combination of warm and cool colors to explore their psychological impact.

Brightness and saturation variations were excluded, with all colors (except neutrals) set to 100% saturation, aligning with findings that users respond most strongly to highly saturated colors in graphical user interfaces [6].

Analysis of digital educational design trends on platforms like awwwards.com and colormatters.com highlights the increasing use of "Vibrant Colors Modulated by Neutral"—bold, saturated colors for interactive elements balanced by neutral tones for readability and engagement.

Our approach is based on the traditional color wheel, introduced by Newton (1666), which defines three primary colors (red, yellow, blue) and their secondary mixtures (orange, green, purple). This principle guided our selection of nine colors for digital learning content: red, yellow, blue, orange, green, purple, black, gray, and white. To ensure compatibility with digital displays and optimize the educational experience, colors were defined in the RGB color space—Red (255,0,0), Yellow (255,255,0), Blue (0,0,255), Orange (255,125,0), Green (0,255,0), Violet (125,0,255), Black (0,0,0), Gray (145,145,145), and White (255,255,255). These selections support contrast optimization, enhance visual hierarchy, and improve readability, ultimately reducing cognitive load and increasing accessibility in digital learning environments.

Contrast Calculation. WCAG 2.1 standard [19] defines two success criteria for contrast levels in Guideline 1.4: Minimum contrast (AA level): At least 4.5:1 (or 3:1 for large text). Increased contrast (AAA level): At least 7:1 (or 4.5:1 for large text).

Contrast is calculated numerically as a luminance ratio between two colors, based on their RGB components. The process follows these steps: (Step 1) Measure the relative luminance of each letter (unless they are all uniform) using the formula $L = 0.2126 \cdot R + 0.7152 \cdot G + 0.0722 \cdot B$ where R, G and B are defined as: if $R_{sRGB} \leq 0.03928$ then $R = R_{sRGB} \div 12.92$ else $R = ((R_{sRGB} + 0.055) \div 1.055)^{2.4}$, if $G_{sRGB} \leq 0.03928$ then $G = G_{sRGB} \div 12.92$ else $G = ((G_{sRGB} + 0.055) \div 1.055)^{2.4}$, if $B_{sRGB} \leq 0.03928$ then $B = B + sRGB \div 12.92$ else $B = ((B_{sRGB} + 0.055) \div 1.055)^{2.4}$, and R_{sRGB}, G_{sRGB}, and B_{sRGB} are defined as: $R_{sRGB} = R_{8bit} \div 255$, $G_{sRGB} = G_{8bit} \div 255$, $B_{sRGB} = B_{8bit} \div 255$. (Step 2) Measure the relative luminance of background pixels immediately next to the letter using the same formula. (Step 3) Calculate the contrast ratio using the following formula: $(L1 + 0.05) \div (L2 + 0.05)$ where L1 is the relative luminance of the lighter of the foreground or background colors, and L2 is the relative

luminance of the darker of the foreground or background colors. (Step 4) Check that the contrast ratio is equal to or greater than 7:1 It is also possible to use the Color Contrast Analyser software recommended by the WCAG (https://www.tpgi.com/color-contrast-checker).

To be able to compare results obtained for individual color pairs, data were standardized and normalized to the whole space.

Experimental Method. Our approach is based on perceptual experiments. We introduced forced-choice metrics to identify colors that match in the most noticeable way. In the following, we explain the procedure we used. In order by the *forced-choice pairwise comparison* procedure, the observers are shown a pair of images (of the same scene) corresponding to different conditions and are asked to indicate the more eye-catching image. The question that was verified through consultation with a psychologist was as follows: *Choose the color composition that you think attracts the people's attention to the poster concerning the thing you lost.* It is easier for people to answer a natural question that does not require additional knowledge. Observers are always forced to choose one image, even if they see no difference between them (hence the name "forced choice"). There is no time constraint within which one must make their decision. The method is popular, but it is highly tedious if a large number of conditions need to be compared. However, as reported in [23], it results in the smallest measurement variance and thus produces the most accurate results.

Experimental Procedure. The observers were asked to read a written instruction before every experiment. Following the recommendation ITU-R.REC.BT.500 [17], the experiment started with a training session in which observers familiarized themselves with the task, the interface, and the images displayed. To ensure that observers fully attended the experiment, three random trials were shown at the beginning of the main session without recording the results. The images were displayed in random order and with different randomizations for each session. Two consecutive trials showing the same test image were avoided if possible. If possible, two consecutive trials showing a different pair of pictograms with the same background were avoided. The experiment was carried out with the use of an eye tracker; therefore, each experiment was preceded by the calibration of the eye tracker, after which the user could start the experimental procedure.

4 Results and Analysis

The following section discusses the results of a perceptual experiment with the main goal of analyzing human preferences more related to the contrast between colors than the color itself. We want to identify the color connections that humans pay the most attention to in a positive manner. The selected colors should bring awareness to the content but without irritation or weariness. To avoid ambiguities, we created a consistent naming convention for all subsequent sections, described below.

Characteristics of the Stimulus and Experiment Conditions. To find the most eye-catching but user-friendly pairs of colors, 72 images were prepared as follows: for each of the analyzed colors (black, gray, green, blue, violet, red, orange, yellow, and white), one color was fixed as primary (and set as a background or a pictogram), and the second color for each generated pictogram was chosen from the set of remaining colors and called the secondary color. We used it as opposed to the primary color as a pictogram or a background, respectively. Example images with a black primary color are shown in Fig. 2. The images had a rectangle shape in 1:2 proportions, allowing them to better fit the display resolution. They took up 40% of the full-screen surface. The object shapes were picked such that they did not distract the user. Hence, we chose a regular rectangle shape and the widely known e-mail icon. However, colors, not shapes, were our primary focus. The choice of colors for the experiment is presented in the Methods section.

Fig. 2. The example test images used in the experiment. In the figure, the images were composed of a 'black' color set as primary for the background (top row) and for the pictogram (bottom row), and the remaining colors (blue, grey, green, orange, red, violet, white, and yellow) were set as secondary colors. We assume that the effect of contrast between two colors does not depend on whether they are used as the background or pictogram.(Color figure online)

The experiment was carried out by 35 naive observers who were confirmed to have normal or corrected-to-normal vision. The age of the observers ranged between 20 and 68 years. For additional reliability, each observer repeated each experiment three times, but no two repetitions took place on the same day in order to reduce the learning effect. According to [23], collecting 30–60 repetitions per condition is sufficient. By condition, we understand that two matched colors (pictogram and background) are represented by a pair of objects.

The images are shown on a 50% gray background, which has been recommended by the International Color Consortium (https://www.color.org/) as a background for comparing colors. The same background was used for the intervals between displayed pairs of images. The mouse cursor was reset to a neutral position after each trial. The experiment was conducted on an EIZO ColorEdge CG220 22.2-inch display, calibrated using X-Rite i1 Publish Pro 2. For optimal eye tracking, the distance from the participant's eyes to the eye tracker was set at 60 cm, as recommended by Tobii [1]. In the room, constant and uniform lighting conditions were ensured by using lamps with color temperature 5000 K (D50 standard). According to the International Color Consortium, the color observa-

tion angle was 2^o. Additionally, the surrounding light in the room was regularly controlled using a Sekonic L-478DR light meter.

For comparison, only images with the same primary color were taken. This enables reliable user comparisons, as introducing more than three colors (one primary and two secondary) would make the experiment difficult to conduct or even lead to inconsistent results.

User-Friendliness and Visibility Evaluation with Rankings. To stabilize the results between images given for the same primary color, the analysis was performed on the scores that were computed for every primary color separately. The votes received per image were first standarized. The higher the score value, the more eye-catching and user-friendly the image. After standardization, the data was normalized, allowing easier comparison of the results. The results for every primary color are depicted in Fig. 3. Every plot contains the color ranking arranged according to the four user-friendliness and visibility ranges: $< 0; 0.25)$, $< 0.25; 0.5)$, $< 0.5; 0.75)$, and $< 0.75; 1 >$. To compare the results with the typical approach given by the WCAG standard [19], contrast values were normalized as well and are displayed for the same color pairs.

During the experiment, users evaluated the colors within nine primary colors: black, gray, green, blue, violet, red, orange, yellow, and white. Each primary color was fixed as a background or pictogram, as shown in Fig. 2. The goal was to investigate whether a change (negative) in the primary color influences the user assessment of user-friendliness and visibility. The analysis of the experiment results showed that the users did not see much difference between the primary color as a background and the primary color as a pictogram (the average difference between the user responses was 0.11). Therefore, the values can be averaged. It can be assumed that we have primary and secondary colors, where the primary color can be either a background or a pictogram.

The research procedure consisted of five steps. The first step was to carry out the experiment with users according to the procedure described at the beginning of this section. The experiment was carried out under controlled laboratory conditions in a group of 41 users. Users were tasked with selecting color pairs that, according to their perception, were more user-friendly and allowed them to easily read messages. The experiment was repeated three times for each user. The collected data were subjected to statistical analysis, including standardization and normalization. This enabled their comparison and drawing objective conclusions. Afterward, ColoUR DB was created. ColoUR DB contains data on user preferences for user friendliness and visibility of primary and secondary colors. In addition, the color contrast was calculated for each pair of colors according to the WCAG [19] recommendation. The procedure for calculating the color contrast is described in the Methods section. ColoUR DB allows for grouping colors regarding user-friendliness, visibility, and color contrast, creating a color ranking within each primary color. The color ranking shows the user-friendliness, visibility, and contrast values that each color pair has achieved. Finally, we divided the scores obtained from the experiment into 4 quartiles and performed statistical analysis between them.

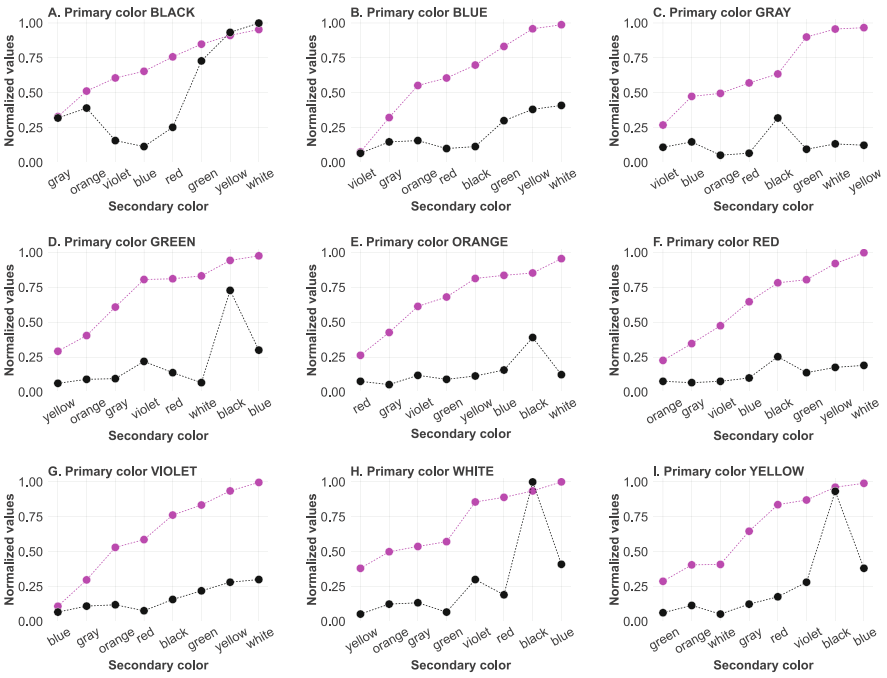

Fig. 3. Color rankings for primary and secondary colors were based on ColoUR DB. The figure presents results for nine tested colors: Black, Blue, Gray, Green, Orange, Red, Violet, White, and Yellow, ranked by user-friendliness and visibility. Each graph represents a single primary color, with secondary colors on the X-axis and normalized experimental values on the Y-axis. Two plots are shown: (1) user-perceived friendliness and visibility (pink) based on experiment data from the Results section, and (2) contrast values (black) calculated according to WCAG [19] as detailed in the Methods section.(Color figure online)

The color ranking (see Fig. 3) is ordered by user-friendliness and visibility based on user response. Results are presented for primary colors A through I, linked to a set of secondary colors (X-axis). All data have been normalized and divided into four ranges with division values 0, 0.25, 0.75, and 1 (Y axis). In the range $<0; 0.25)$, users rated pairs of primary and secondary colors as the least user-friendly and visible. In the range $<0.75; 1)$, users rated pairs of primary and secondary colors as the most user-friendly and visible. Each pair of primary and secondary colors has two values: user-friendliness and visibility (pink plot) and contrast (black plot). Discrete values are connected by a line for better data visualization. The ranking of user-friendly and visible colors does not always match that of color contrast. Primary and secondary color pairs having the highest contrast coefficients were not rated highest by users in terms of user-friendliness and visibility: see Cases C, D, E, F, H, or I in Fig. 3. On the other hand, primary and secondary color pairs with the lowest contrast coefficient

reached a high level of user-friendliness and visibility, e.g., D: Green–White; A: Black–Blue.

ColoUR Picker Tool and ColoUR DB. The research results were implemented as a tool for designers—the ColoUR Picker Tool, an application that runs in a web browser environment. The Chrome browser is recommended. The ColoUR Picker Tool allows you to select primary and secondary colors from the color wheel, set the primary color as a background or a pictogram, and visualize the remaining colors as pictograms, background, or text. Figure 4 shows example screens and the sample selection process. The results are displayed to the designer in the form of a color ranking and a user-friendliness, visibility, and contrast index. The ColoUR Picker Tool retrieves data from ColoUR DB acquired earlier during the perceptual experiment. ColoUR DB contains 72 combinations of primary and secondary colors. There are two metrics for each color pair: the contrast calculation and the user-friendliness with visibility from user responses. Normalized data is displayed on a scale from 0 to 100% for each metric. The ColoUR Picker Tool is available on Github—https://visual-communication.github.io/ColoUR-Picker.

5 Discussion

The research confirms that it is possible to find color combinations that do not necessarily have high contrast but still provide visibility and enhance the user experience in digital educational content. The conducted experiment allowed us to derive meaningful insights regarding color perception in learning environments.

Among the best combinations in terms of user-friendliness and visibility, a large number contain neutral colors. Surprisingly, user ratings were lower when the secondary color was gray. In most cases, combinations featuring gray were perceived as less user-friendly and less visible. Combinations of warm and cool colors were deemed user-friendly and visible. For user-friendliness and visibility ranges, primary and secondary color pairs, along with their reversed versions, were identified. These findings suggest that these color pairs may be universally applicable across different contexts of digital learning design.

The results indicate that visibility goals can be achieved along with user-friendliness, even when using elements with moderate contrast. For selected color pairs, even low to medium contrast resulted in a positive experience alongside effective visual performance. Avoiding excessively high contrast is justified, as previous research suggests that excessively strong contrasts may be perceived as intrusive [20]. High contrast, particularly in prolonged reading or extended interaction with content, may negatively impact the learning experience. User interface elements should be highlighted to maintain visibility for interactions lasting longer than 15 min, as excessive contrast may lead to discomfort [8]. Additionally, reducing contrast while preserving informational clarity is crucial in preventing cybersickness caused by extreme contrast levels [7].

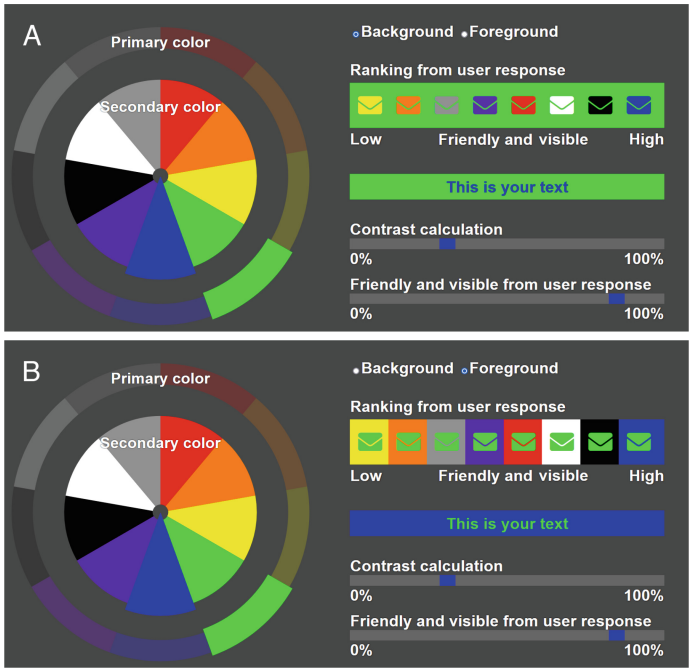

Fig. 4. The research findings are presented through the ColoUR Picker Tool. Users select primary and secondary colors via a color wheel, with a graphical analysis shown alongside. Rankings reflect user-friendliness and visibility, with pairs ordered accordingly. The tool allows toggling the primary color between background and foreground. Contrast (based on WCAG), user-friendliness, and visibility indices are displayed. Case Study: (A) Choosing green as the primary color shows compatible pairs ranked by user ratings, along with previews and metrics. The greenâĂŞblue pair, for example, received higher visibility ratings than contrast values alone suggest. (B) Switching the view places green in the foreground, enabling comparison of how color roles affect perception. (Color figure online)

Despite the practical applications of this study, certain limitations exist. The primary constraint is that an extensive set of colors may lead to cognitive overload, making it difficult for users to objectively assess differences. The experiment used a selection of 10 colors, which does not encompass the full spectrum of colors used in digital educational design. However, the findings can be applied to specific components that designers aim to highlight, such as icons, call-to-action buttons, alerts, and visual cues in educational platforms. Future studies could expand on this research by incorporating colors with varying saturation and brightness levels, broadening the scope of applicable design principles. Additionally, this experiment used images and pictograms, which prevented testing of text readability. Future research should consider text-based assessments to further refine these findings.

Research Application. The findings of this research can be applied to a wide range of digital educational materials, including graphical user interfaces for web-based learning, desktop and mobile applications, printed and digital instructional materials, and visual communication elements in e-learning environments. Designers working on digital education projects often face the challenge of choosing color schemes that both attract attention to key content areas and ensure user-friendliness, visibility, and aesthetic coherence. Use cases in digital learning environments include:

- A learning platform's design constraints may require the use of a specific accent color, such as blue. When designing text and menu icons, a designer can set blue as the primary color and use this research to select an optimal secondary color that enhances readability and user experience.
- Instructional banners and visual messages often use high-contrast colors, such as red, which may be overwhelming. Designers can select red as a primary color and pair it with a secondary color that enhances visibility while reducing contrast intensity, making the message more readable and user-friendly.
- In brand guidelines for e-learning content, logos, and graphical elements are often presented in multiple color variations. Designers can use these findings to select background colors that complement a primary logo color, such as choosing suitable secondary colors for a violet primary logo. Additionally, they can analyze how logo colors appear in negative versions and assess their visibility and user-friendliness.
- The insights from this study can also be applied to designing progress indicators in educational platforms. Color-coded feedback can enhance motivation by visually representing achievements, such as progress bars, skill levels, or reward systems. In gamification elements, selecting user-friendly yet engaging color combinations can improve user engagement, guiding learners through tasks and fostering a sense of accomplishment.

6 Conclusions and Future Work

The study confirmed that effective visibility and user-friendliness in digital educational materials can be achieved even with moderate contrast. Designers may deliberately avoid excessively high contrast, as it can negatively impact user comfort during prolonged learning sessions. Future research should encompass a broader color spectrum, including varying levels of saturation and brightness, as well as a more nuanced analysis of contrast in relation to specific content types - particularly text-heavy interfaces. This includes evaluating contrast in terms of text readability and prolonged exposure to textual content. Further experiments should also consider diverse usage contexts, including the needs of users with color vision deficiencies, and environments such as mobile applications, augmented reality, and interactive e-learning modules.

References

1. https://www.tobiipro.com/learn-and-support/learn/steps-in-an-eye-tracking-study/run/how-to-position-the-participant-and-the-eye-tracker/
2. The 2023 report on the accessibility of the top 1,000,000 home pages - https://webaim.org/projects/million/ WebAIM (2023)
3. E-learning market size - by technology (online e-learning, lms, mobile e-learning, rapid e-learning, virtual classroom, others), provider (service, content), application (corporate, academic, government) & forecast, 2023 – 2032 - https://www.gminsights.com/industry-analysis/elearning-market-size GMI215 (2023)
4. Benway, J.P., Lane, D.M.: Banner blindness: web searchers often miss "obvious" links. Itg Newsletter **1**(3), 1–22 (1998)
5. Brajnik, G., Gabrielli, S.: A review of online advertising effects on the user experience. Int. J. Hum. Comput. Int. **26**(10), 971–997 (2010)
6. Camgoz, N., Yener, C.: Effects of hue, saturation, and brightness on preference: a study on Goethe's color circle with RGB color space. In: 9th congress of the international colour association, vol. 4421, pp. 392–395. SPIE (2002)
7. Campos, F., Campos, M., Silva, T., Van Gisbergen, M.: User experience in virtual environments: relationship between cybersickness issues and the optical aspects of the image by contrast levels. In: International Conference on Intelligent Human Systems Integration, pp. 434–439. Springer (2021)
8. Chandrashekar, S., McCardle, L.: How WCAG 2.1 relates to online user experience with switch-based tools (2020)
9. Chatterjee, P.: Are unclicked ads wasted? Enduring effects of banner and pop-up ad exposures on brand memory and attitudes. J. Electron. Commerce Res. **9**(1) (2008)
10. Clarke, T., Costall, A.: The emotional connotations of color: a qualitative investigation. Color Res. Appl. **33**, 406 – 410 (2008)
11. Davies, T., Beeharee, A.: The case of the missed icon: change blindness on mobile devices. In: Proceedings of the SIGCHI Conference on Human Factors in Computing Systems., pp. 1451–1460 (2012)
12. Edwards, S.M., Li, H., Lee, J.H.: Forced exposure and psychological reactance: antecedents and consequences of the perceived intrusiveness of pop-up ads. J. Advert. **31**(3), 83–95 (2002)
13. Elliot, A., Maier, M.: Color-in-context theory. Adv. Exper. Soc. Psychol. **45**, 61–125 (2012)
14. Elliot, A.J.: Color and psychological functioning: a review of theoretical and empirical work. Front. Psychol. **6**, 368 (2015)
15. Gleitman, H., Gross, J., Reisberg, D.: Psychology. 8th Edition, W.W. Norton and Company (2011)
16. Hsieh, Y.C., Chen, K.H., Ma, M.Y.: Retain viewer's attention on banner ad by manipulating information type of the content. Comput. Hum. Behav. **28**(5), 1692–1699 (2012)
17. ITU-R.Rec.BT.500-11: Methodology for the subjective assessment of the quality for television pictures (2002)
18. Jankowski, J.: Habituation effect in social networks as a potential factor silently crushing influence maximisation efforts. Sci. Rep. **11**(1), 19055 (2021)
19. Kirkpatrick, A., Connor, J., Campbell, A., Cooper, M.: Web content accessibility guidelines - WCAG 2.1. Tech. rep., World Wide Web Consortium (W3C). https://www.w3.org (2018)

20. Kojić, T., Ali, D., Greinacher, R., Möller, S., Voigt-Antons, J.N.: User experience of reading in virtual reality—finding values for text distance, size and contrast. In: 2020 Twelfth International Conference on Quality of Multimedia Experience (QoMEX), pp. 1–6. IEEE (2020)
21. Lewandowska, A., Olejnik-Krugly, A.: Do background colors have an impact on preferences and catch the attention of users? Appl. Sci. **12**(1), 225 (2021)
22. Lewandowska, A., Olejnik-Krugly, A., Jankowski, J., Dziśko, M.: Subjective and objective user behavior disparity: towards balanced visual design and color adjustment. Sensors **21**(24), 8502 (2021)
23. Mantiuk, R.K., Tomaszewska, A., Mantiuk, R.: Comparison of four subjective methods for image quality assessment. Comput. Graph. Forum **31**(8), 2478–2491 (2012)
24. Masciocchi, C.M., Still, J.D.: Alternatives to eye tracking for predicting stimulus-driven attentional selection within interfaces. Hum. Comput. Interact. **28**(5), 417–441 (2013)
25. McCoy, S., Everard, A., Polak, P., Galletta, D.F.: The effects of online advertising. Commun. ACM **50**(3), 84–88 (2007)
26. Michelson, A.: Studies in Optics. University of Chicago science series, The University of Chicago Press (1927)
27. Moe, W.W.: A field experiment to assess the interruption effect of pop-up promotions. J. Interact. Mark. **20**(1), 34–44 (2006)
28. Nielsen, J.H., Huber, J.: The effect of brand awareness on intrusive advertising. In: Society for Consumer Psychology Conference, San Diego, CA, February 2009 (2009)
29. O'Connor, Z.: Colour, contrast and gestalt theories of perception: the impact in contemporary visual communications design. Color Res. Appl. **40**, 85–92 (12 2013)
30. Pelet, J.E., Taieb, B.: Effects of colored contrast of mobile websites on behavioral intentions. In: CARMA 2016: 1st International Conference on Advanced Research Methods in Analytics, pp. 84–91. Editorial Universitat Politècnica de València (2016)
31. Pelet, J.É., Taieb, B.: Enhancing the mobile user experience through colored contrasts. In: Encyclopedia of Information Science and Technology, Fourth Edition, pp. 6070–6082. IGI Global (2018)
32. Peli, E.: Contrast in complex images. J. Opt. Soc. Am. A **7**(10) (1990)
33. Peli, E.: Contrast in complex images. J. Optical Soc. Am. A **7**(10) (1990)
34. Sample, K.L., Henrik, H., S. Adam, B.: Components of visual perception in marketing contexts: a conceptual framework and review. J. Acad. Market. Sci. **48**, 405 – 421 (2020)
35. Turatto, M., Galfano, G.: Color, form and luminance capture attention in visual search. Vision. Res. **40**(13), 1639–1643 (2000)
36. Zha, W., Wu, H.D.: The impact of online disruptive ads on users' comprehension, evaluation of site credibility, and sentiment of intrusiveness. Am. Commun. J. **16**(2) (2014)

The Role of Sustainability Competences for IT Systems Engineers

Aleksander Buczacki[1(✉)], Bartlomiej Gladysz[1], Aldona Kluczek[1], Krzysztof Krystosiak[1,2], Krzysztof Ejsmont[1], Izabela Malenczyk[1], Rodolfo Haber Guerra[3], Erika Palmer[4], and Tim van Erp[5]

[1] Warsaw University of Technology, Narbutta 86, 02-524 Warsaw, Poland
aleksander.buczacki@pw.edu.pl
[2] Toronto Metropolitan University, 350 Victoria Street, Toronto, ON M5B 2K3, Canada
[3] Centre for Automation and Robotics (CAR), Spanish National Research Council-Technical University of Madrid (CSIC-UPM), Madrid, Spain
[4] Cornell University, Ithaca, NY 4850, USA
[5] Flinders University, Tonsley, GPO Box 2100, Adelaide, SA 5001, Australia

Abstract. Designing modern systems requires technical knowledge and sustainability competencies from engineers, as almost every system or product designed has a sustainability impact. This gained additional significance after adopting the Sustainability Development Goals in 2015 and their subsequent integration into the activities of enterprises and other entities and the products and services they offer. For this reason, the study's main goal was to determine the role of sustainability competences in activities performed by systems engineers. Sustainability competences and systems engineering competencies were analyzed. A significant overlap in many areas was found. Subsequently, the perception of these competencies by representatives of enterprises was examined. The results indicate that system engineers' perception of sustainability competences is not uniform, particularly depending on the size of the enterprise and position in the company hierarchy. Engineering team leaders and management pay more attention to soft skills. The study's results may help understand the relationships between competencies, support the development of HR processes, and entities offering training programs for employees at different career stages.

Keywords: Sustainability Competences · Systems Engineering Competencies · IT Engineers Career

1 Introduction

In an era where sustainability is becoming a critical differentiator, information technology (IT) systems engineers who implement computational science results and possess these sustainability competences (SC) might enhance their value and enable their organizations to remain competitive, responsible, and innovative [3]. Sustainability is a broad concept that includes environmental protection along with social and economic aspects, aiming to meet the needs of current and future generations without depleting natural

M. Paszynski et al. (Eds.): ICCS 2025 Workshops, LNCS 15912, pp. 269–284, 2025.
https://doi.org/10.1007/978-3-031-97573-8_19

systems [5]. It involves managing interconnected elements like energy efficiency [31], resource use, and carbon footprint [35], which is challenging, especially in complex engineering IT projects [38] or interdisciplinary projects to support the achievement of the Sustainable Development Goals (SDGs) [2].

This study directly links sustainability to characteristics that integrate environmental considerations across the entire product and system lifecycle. Designing and offering sustainable products and acting sustainably enable companies to advance in their markets. For example, sustainability is becoming a key criterion in supplier selection within global markets. With increasing emphasis on sustainable development, systems engineers are uniquely positioned to embed sustainability principles throughout the product lifecycle [14]. They coordinate cross-functional inputs, align technical requirements with sustainability goals, and ensure environmental, economic, and social impacts are considered at every stage. A systems thinking approach is increasingly necessary to address sustainability challenges, combining environmental, financial, and social objectives. Designers must integrate sustainability factors throughout the lifecycle [19]. Systems engineers, who connect the entire design and development process, need sustainability competencies and technical and project management skills. There is no universally accepted set of sustainability competencies (SC) for systems engineering education. The lack of standardized SC leads to diverse approaches [23, 29, 38], often failing to meet modern job market demands and sustainable development challenges [30]. Additionally, there is a limited understanding of how specific SC translates into organizational benefits, hindering the identification of training needs and the development of appropriate education programs [4, 29]. IT systems engineers require technical skills in computational science and systems design, along with competencies in sustainability, project management, and interdisciplinary collaboration. Balancing these areas poses significant educational and practical challenges [29].

This article identifies and analyzes sustainability-related skills critical for IT systems engineers to contribute effectively to sustainable development. It explores how incorporating sustainability competencies improves IT system design, optimizes resource efficiency, reduces environmental impact, and supports sustainable development principles. The study examines how these skills influence daily work, professional development, and competency management. In-depth interviews investigated awareness of sustainability competencies and their impact on IT systems engineers' evaluation, compensation, and promotion from personal and organizational perspectives. Publications on "systems engineering competencies" (SEC) in Scopus date back to 2005, when MITRE Corporation discussed building SEC through on-the-job activities while enhancing systems engineering training programs [39]. The topic has been widely discussed in academia and industry [18, 20]. Several authors emphasized embedding SEC in engineering education curricula [12, 28, 37, 41]. [40] presented a methodology to improve feedback between employers and education institutions. [13] addressed SEC self-improvement, and a self-assessment tool was validated by [6]. Defense departments widely use competence models in systems engineering. For instance, the Australian DoD developed a portfolio of 30 competencies [15], and the US DoD created a model with 44 competencies [42, 43]. The International Council on Systems Engineering (INCOSE) comprehensively

categorized and defined SEC into five categories: core, professional, management, technical, and integrating, with 36 detailed competencies. Each competency is described by levels of possession (awareness, supervised practitioner, practitioner, lead practitioner, expert) [16]. [18] introduced "Retirement" as a technical competency area. The framework applies to human resource management as outlined in the INCOSE Systems Engineering Handbook [17], encompassing recruitment, worker appraisals, promotions, compensation decisions, and training requirements. The framework has been successfully implemented across industries [11]. SEC considered in this research are detailed in [16] (see Table 1 for an extract).

Table 1. Systems Engineering Competencies based on [16].

Set of competencies	Description	Key Aspects
Core Systems Engineering	Utilization of systems thinking, lifecycle management, capability engineering, critical thinking, as well as systems modeling and analysis during system design and development	Systems approach, systems modeling, lifecycle
Professional	Utilization and establishment of behavioral competencies in the human resources domain, including communications, ethics, technical leadership, team dynamics management, coaching, and mentoring	Team management, ethics, communication
Technical	Engineering activities covered from the requirement definition through design, verification, and validation, as well as after transition operation and support and at the end of system retirement	Requirement management, system architecting, interface management, verification, and validation
Systems Engineering Management	Systems Engineering activities focused on planning, monitoring and control, decision management, business and enterprise integration, information management, and configuration management	Planning, monitoring and control, information management
Integrating	Incorporating project management, finance, logistics, and quality management into engineering activities	Project management, quality management

Table 2. Sustainability Competences based on [27].

Competence	Description	Key Aspects
Systems Thinking	Understanding complex interactions within systems across various domains and scales, emphasizing key dynamics, feedback loops, and systemic impacts	Comprehension, verification, systems modeling
Interdisciplinary Work	Utilization and integration of diverse disciplinary knowledge and methods to solve complex problems, emphasizing collaborative problem-solving	Knowledge evaluation, interdisciplinary integration
Anticipatory Thinking	Proactive envisioning of future scenarios and their implications, applying principles such as the precautionary approach to manage potential risks and changes	Future scenario planning, risk assessment, precautionary measures
Justice, Responsibility, and Ethics	Emphasis on ethical conduct, justice, and responsibility, focusing on the impact of actions on social and ecological systems, and the negotiation and reconciliation of diverse values and goals	Ethical integrity, social justice, responsibility for actions
Critical Thinking and Analysis	Examination and questioning of existing norms and opinions, along with reflection on personal values and an understanding of alternative viewpoints	Norm evaluation, self-reflection, external perspective analysis
Interpersonal Relations and Collaboration	Skills in participatory problem-solving and project collaboration, using effective communication, negotiation, and leadership abilities	Teamwork, communication, leadership
Empathy and Change of Perspective	Identification with and sensitivity to the needs and perspectives of others, fostering an environment where diverse opinions are valued and integrated	Compassion, empathy, diversity acceptance

(*continued*)

Table 2. (*continued*)

Competence	Description	Key Aspects
Communication and Use of Media	Effective intercultural communication and judicious use of information and communication technologies, with a focus on critical media evaluation	Media literacy, digital communication efficiency
Strategic Action	Strategic design and execution of sustainable projects and initiatives, focusing on leadership, risk management, and organizational control	Project management, strategic planning, leadership
Personal Involvement	Active engagement in sustainability efforts, marked by a willingness to innovate and self-motivate, coupled with a commitment to continuous personal and professional development	Self-motivation, initiative, continuous learning
Assessment and Evaluation	Creation of standards for assessing and evaluating projects or policies, ensuring independence from conflicts of interest and adaptability in the face of uncertain information	Independent evaluation, standards development, conflict management
Tolerance for Ambiguity and Uncertainty	Effective management of ambiguity in decision-making processes, maintaining resilience and adaptability in situations involving conflicting goals, uncertainties, or setbacks	Ambiguity management, resilience in uncertainty

SC are widely examined in academic literature on education for sustainable development. Works [1, 7, 32] define key sustainability competences and explore how higher education fosters them. A detailed picture emerges of the nature of these competences, their interrelationships, and methodologies for analysis. [32] highlights competences like critical thinking, systemic thinking, and normative skills, essential for engaging with the complexity of sustainable development. [7] builds a framework using qualitative and quantitative methods to assess how these competences interconnect, showing how their synergy enhances educational programs. The aggregation of research findings on SC was expanded by [1], identifying key competences recognized across studies and analyzing their interrelations. This review links theoretical constructs to empirical findings [3, 44, 45]. [25] summarized SC studies, synthesizing works from [22, 34, 44] and proposing 12

competences (Table 2). The discussion included teaching specific competences through particular pedagogical approaches [24, 26]. These competences, validated in international contexts, serve as a solid foundation for empirical studies and were referenced in this paper [27].

2 Methodological Approach

A research strategy of theory building from multiple cases [8], particularly using structured multiple case study, was adopted [46], focusing on a few selected cases rather than many. This research strategy provides several methodological benefits [9]. First, it allows for a more in-depth and comprehensive analysis of each case, enabling the researcher to understand the specific contexts and nuances of the phenomenon being studied [36]. Furthermore, focusing on fewer cases can enhance the reliability and contextual richness of the findings. Fewer cases emphasize understanding specific local conditions, which can lead to more credible insights [10]. This is particularly important in qualitative research, where the value often lies in capturing the depth and complexity of individual cases rather than aiming for broad generalizations. Another significant advantage of focusing on fewer cases is its utility in theory building. As [8] argues, a smaller sample size enables a more iterative data collection and analysis process, which is conducive to developing theoretical frameworks. This process helps balance between detailed case-specific analysis and drawing broader theoretical insights.

This qualitative and exploratory research aims to generate hypotheses for broader quantitative studies. Researchers selected enterprises familiar with systems engineering and willing to participate in interviews, indicating some knowledge of sustainability. Participants and cases were chosen from current and former members of the Polish Chapter of INCOSE, representing various industries (Table 3) but focusing on embedded systems development or IT systems to ensure a wide perspective for future considerations. Unlike studies involving numerous cases that simplify analysis for generalization, a limited number of cases allows preserving each context's complexity and specific traits. [36] this approach yields more meaningful conclusions by integrating contextual insights without losing individual case details. Systems engineering focuses on technical and organizational aspects. IT system engineers naturally prioritize technological advancements and, even without explicit recognition of Industry 4.0 policies, are generally familiar with the latest technologies driving this paradigm. However, their understanding of Industry 5.0 pillars—such as human-centricity, resilience, and sustainability—remains uncertain. For a successful transition to Industry 5.0, system engineers must play a crucial organizational role, recognizing how decisions in the engineering process impact these pillars. This paper examines whether system engineers are prepared for the I5.0 era, focusing on the sustainability competencies (SC) expected of them. Figure 1 depicts a three-step methodology.

First, the study examined whether prominent approaches to defining SC and SEC in IT and computational science contexts are consistent or differ. This was achieved through secondary data analysis conducted by domain experts during a Focus Group Interview (FGI). Three experts participated: one specializing in systems engineering, one in sustainability, and one with expertise in both areas. All experts had both academic and

Table 3. Sample.

Industry	Company Size	Level of responders
Automotive	Large	Manager of SE
Automotive	Large	System Engineer
Automotive	Middle-sized	Engineering Director
Aviation	Large	System Engineer
Energy	Large	System Engineer
Space	Middle-sized	Manager of SE

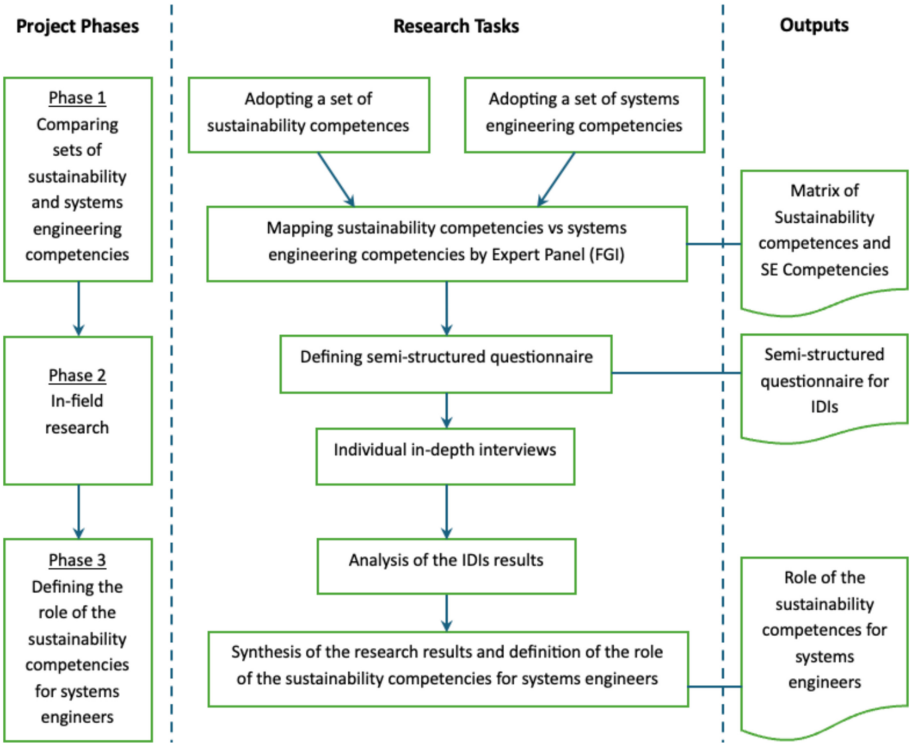

Fig. 1. Research procedure

industrial experience. The secondary data included the systems engineering competency framework provided by the International Council of Systems Engineering [16] and a synthesized list of SC [26, 27]. A 2-dimensional matrix was created to compare the lists and assess how SC are recognized within systems engineering frameworks developed by professionals. Rows represented SEC, and columns SC. The matrix used symbols to indicate the degree of alignment: '+++' for full coverage, '++' for significant overlap, and '+' for partial overlap. This analysis's results informed the questionnaire's scope

used in the next research phase. The second phase consisted of IDIs using a semi-structured questionnaire to gather the required data. Six respondents were interviewed, representing the automotive, aviation, space, and energy industries. Two respondents were involved in civil and defense projects. Five respondents were from engineering centers of large multinational companies in Poland, with extensive experience in systems engineering, embedded systems, and/or IT systems. Five were current or former members of INCOSE. Two respondents managed IT systems engineering teams. The interviews aimed to determine whether sustainability competencies are practically considered for IT systems engineers.

3 Results

The FGI and IDIs results provided material to analyze SC's role in systems engineers' daily work and development. This section presents a harmonized SEC framework, including SC, through a coverage matrix. SEC from the INCOSE handbook [17] were compared to SC [27]. Seeking stronger alignment of engineering education with the UN's SDGs, the notion of "global competence" has drawn growing attention, focusing on how engineers develop it, especially regarding sustainability goals. Section 1 discusses global competence for engineers concerning the SDGs. [35] presented the first attempts to integrate SDGs into engineering education, based on a logical framework. [21] advocate a design-based approach to enhance global competence in four areas: institutional frameworks, institutional diversity, competence training, and assessment. Figure 2 shows the results of the SC and SEC mapping. The Core SE Principles and Professional Competencies overlap with all SC. Professional Competencies correlate with extrospective-social and introspective-personal competences, while the Core SE Principles correlate with cogitative-processual competences, notably "systems thinking," which also correlates with several Technical Competencies (left of the V-model). There is a notable lack of correlations between SC and SE Management or Integrating Competencies. During the FGI, experts stressed the importance of HR processes (recruitment, evaluation, compensation, promotion), which influenced the questionnaire scope for the IDIs. Six interviews were conducted (three online). Their synthetic results, expanded in the discussion, show all respondents were aware of sustainability topics and recognized that organizations, including systems engineers, take them into account. Sustainability is often viewed through environmental protection. In large companies, formal sustainability policies are managed at the highest level, while in medium-sized companies, such policies also exist but are developed and maintained more ad hoc.

According to all respondents, sustainability-related competences are perceived as additional, while the key ones are the so-called technical competencies needed for systems design. SC, especially extrospective-social and introspective-personal, are considered during recruitment and promotions in large companies, according to responders holding managerial positions.

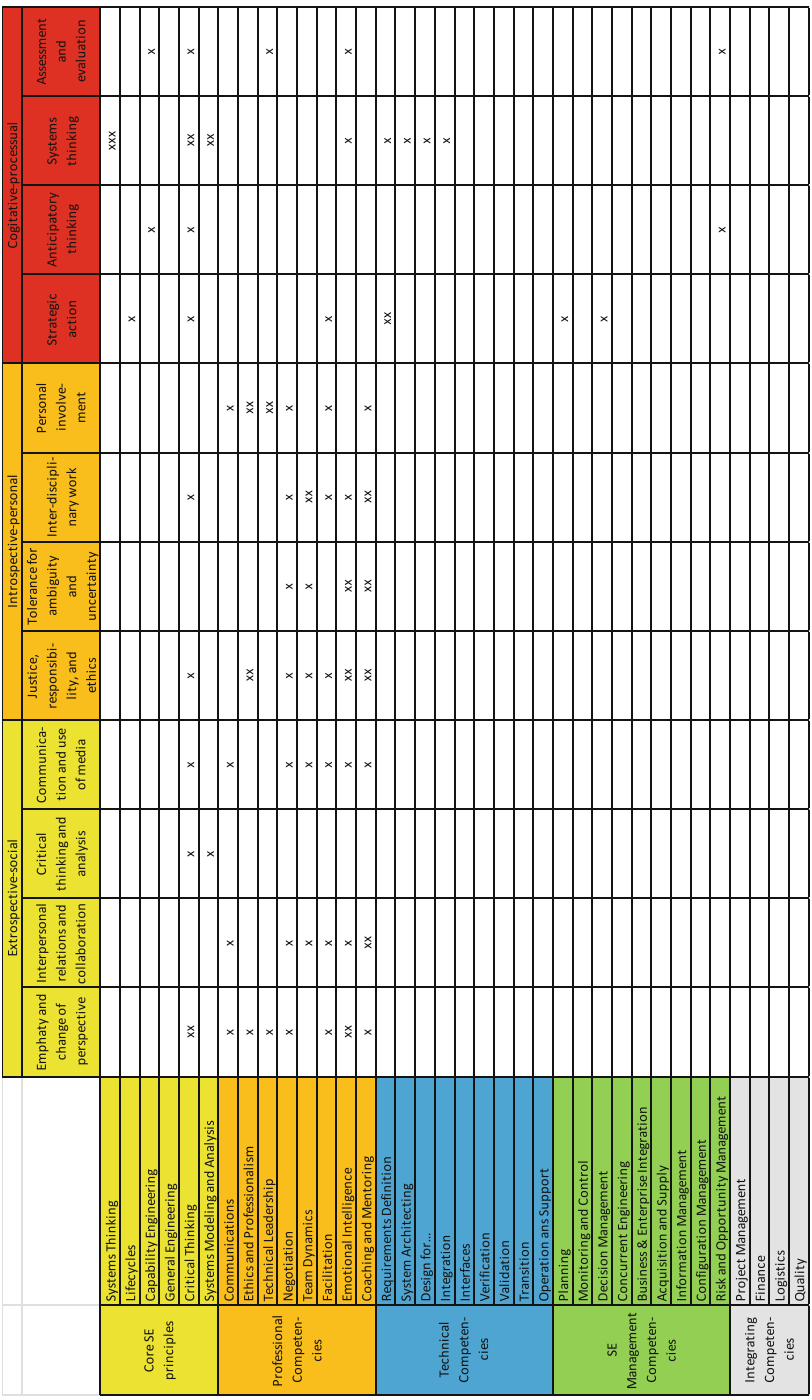

Fig. 2. Mapping sustainability competences to INCOSE competency framework

4 Discussion

4.1 Systems Engineering and Sustainability Competencies Gaps and Overlaps

SC and SEC significantly intersect, requiring an understanding of complex systems, lifecycle thinking, and long-term planning with impact assessment. The matrix (Fig. 2) shows these taxonomies overlap, and SEC includes SC, confirming that SE professionals value sustainability paradigms in SE processes. However, the taxonomies also differ significantly. There is no 1:1 match between SE and sustainability competences, and each SC overlaps partially with multiple SEC. The SEC covers most SC under "core SE principles" and "professional competencies." Analysis of relationships between systems thinking vs. strategic action outlines that systems thinking is essential for IT systems engineers, enabling them to understand how different system elements interact. It is equally critical in sustainability, where strategic actions must consider long-term environmental, social, and economic impacts. A strong relation is visible for emotional intelligence vs. empathy and change of perspective. Emotional intelligence, which includes understanding and managing one's emotions and empathy, is vital in cross-cultural and interdisciplinary collaboration in sustainable projects, where changing perspectives can lead to better understanding and acceptance of diverse interests and needs.

Table 2 may indicate the need to develop further management competencies in integrating sustainability throughout the product life cycle. It is also worth noting that technical competencies are directly linked to system design aspects, suggesting that implementing sustainability in design requires a more holistic approach at the management level. The lack of significant correlations between SE and SE management competencies and integrating competencies is particularly intriguing. SE management competencies, such as planning, risk, and information management, are crucial for guiding engineering projects toward sustainable outcomes. Weak connections with sustainability competencies may indicate that sustainability principles are not yet fully integrated into the management and decision-making processes that drive systems engineering. This gap highlights a missed opportunity to promote sustainability within the broader context of management and integration in systems engineering. The lack of connections could suggest that current management practices may be focused primarily on efficiency and effectiveness, potentially overlooking the long-term sustainability impacts of their projects. During the FGI, experts emphasized the need for a greater focus on human resource-related processes as key enablers for embedding sustainability throughout organizations. Addressing these areas could help bridge the gap, ensuring that sustainability becomes a core aspect of decision-making at all levels of systems engineering, particularly in the management and integration phases.

It should be noted that core SE principles and professional competencies cover all three areas of sustainability. The relationship between professional competencies and sustainability is particularly strong. It can be inferred that a systems engineer should be skilled in all areas of sustainability and incorporate them into professional work. The competences that intersect most strongly are empathy and change of perspective, interpersonal relations and collaboration, communication, media use, justice, responsibility, and ethics, interdisciplinary work, personal involvement, strategic action, and systems

thinking. This demonstrates that the systems engineer has highly developed interpersonal skills, can collaborate with others, is responsible, ethical, and highly committed to the tasks. Importantly, system engineers can use multiple media and think strategically and systemically.

Very few technical and management competencies overlap with the sustainability dimensions. This may be evidence that when moving from the general to operational (technical and management) level of professional competence, there is a lack of consideration of the sustainability and triple bottom line perspective. The systems engineer knows the importance of sustainability in professional work, but does not consider sustainability guidelines/recommendations in many detailed tasks. It is worth noting that none of the integrating competencies overlap with sustainability. This may indicate that it is difficult to directly demonstrate sustainability aspects with complex competences, requiring knowledge and skills in many areas (e.g., Quality, Logistics, Finance. Each competency could be broken down into smaller areas and defined in terms of the required sustainability competences. For example, in Logistics competence, interpersonal relations and collaboration with partners in the supply chain are very important. This is a research gap; further research is worthwhile to establish why these competences do not overlap. Admittedly, systems thinking and strategic action are found in technical and management competences. This is also confirmed by the fact that the systems engineer often has a strategic/systems view of the tasks performed in the context of sustainability, but without focusing on their implementation into operational activities (e.g., validation, planning, etc.). In the education of system engineers in the context of sustainability, the focus is on general professional competences (strategic level), to the extent that the development of practical competences (operational level) is lacking.

4.2 Sector- and Competence-Type-Specific Insights

IDIs confirmed differences in the perception of sustainability between large and medium-sized enterprises (SMEs). Large companies consider sustainability at the corporate level through internal policies rather than in the daily activities of systems engineers. For example, a company in the space and electronics sector applies sustainability principles mainly at the mission level, focusing on Clean Space policies. Although IT systems engineers consider these principles during the design stage, the organizational culture does not require them to implement these competencies daily. Companies from the energy sector demonstrate sustainability awareness, especially in terms of social responsibility and energy management. Still, these practices are mostly managed by HR and organizational policies, with systems engineers not directly involved in daily implementation. In companies from the aviation sector, sustainability is embedded in processes and policies related to product design. Still, the daily tasks of systems engineers focus more on following these guidelines rather than actively creating sustainable solutions. Companies operating in the automotive sector strongly emphasize the involvement of systems engineers in implementing sustainable practices, especially in team building, work environment, and individual actions. Sustainability in these companies is more visible at the operational level, with systems engineers actively applying competencies such as empathy, collaboration, and flexibility. Organizational sustainability awareness is limited, showing these practices rely more on the initiative of individual engineers than on

formal company policies. The company prefers a bottom-up approach, where engineers can incorporate sustainable practices into daily work.

Large companies addressed sustainability at the managerial level. They are mainly implemented through internal policies, while in medium-sized companies, systems engineers are directly involved in applying sustainable practices at the operational level. Responses across industries demonstrate that technical knowledge and familiarity with engineered systems are paramount for systems engineers. Systems thinking emerges as a core competency, enabling engineers to analyze and model complex interactions. Activities like stakeholder needs definition, system architecting, and integration are central to their roles, requiring detailed technical expertise. Respondents highlighted reliance on structured methodologies like the V-model and INCOSE guidelines for consistency and precision in system design and validation. Moreover, technical processes like requirements definition, interface control, and system verification are prioritized in daily operations. These tasks demand a granular understanding of system interactions and technical functionality, underscoring their criticality. Systems engineers are also expected to propose solutions to complex challenges, such as integrating new components into existing infrastructures, as noted in the energy and aerospace sectors. Career development within the field emphasizes technical accomplishments, with evaluations often centered on functional outcomes and system delivery. Interpersonal and sustainability-related competencies are acknowledged but remain secondary to technical expertise in systems design and implementation. This widespread prioritization across various domains underscores the centrality of technical knowledge for systems engineers.

The interviews reveal that soft skills are acknowledged as valuable, particularly in hiring and promotion processes. Some respondents emphasized interpersonal abilities like collaboration, communication, and leadership during recruitment. For example, one company uses critical thinking tests and assesses interpersonal dynamics in hiring. In promotion scenarios, soft skills like teamwork and emotional intelligence are often factored into evaluations, as they help build trust and foster effective team environments. Technical knowledge remains a primary determinant in performance evaluations and advancement. Respondents highlighted that assessments often focus on tangible outputs, like project delivery and adherence to technical standards. Engineers are evaluated on their ability to apply methodologies like systems thinking, requirements definition, and integration, reflecting their technical proficiency. These criteria are pivotal for advancing their roles, especially in highly technical fields like aerospace and energy systems. Computational science and AI skills are crucial for systems engineers: utilizing them daily and incorporating, in particular, AI solutions in designed systems [20]. Soft skills are increasingly recognized for supporting teamwork and leadership, and technical expertise dominates the evaluation framework. This dual emphasis ensures engineers are technically competent and can navigate interpersonal and organizational challenges critical for long-term career growth. The IDIs suggest soft skills are often more crucial than technical knowledge for management. Respondents emphasized that leadership roles prioritize fostering effective team dynamics over individual technical excellence. Managers highlighted the value of interpersonal skills like collaboration, empathy, and conflict resolution in maintaining team cohesion. For example, one respondent noted that aligning work with team

members' predispositions and ensuring a balance between work responsibilities and personal well-being enhances team trust and productivity.

4.3 Other Insights

Severe organizations stressed that a cohesive team consistently outperforms groups dominated by high-performing individuals who create conflict. Managers reported prioritizing skills such as communication, emotional intelligence, and adaptability when deciding promotions to leadership positions. These competencies enable leaders to build trust, manage uncertainty, and navigate organizational challenges effectively. In essence, technical skills remain essential for systems engineers; leadership roles require a shift in focus toward managing relationships and fostering a collaborative environment. This ensures that teams can collectively achieve their goals without being disrupted by interpersonal conflicts or siloed expertise.

IDIs support the statement that managers perceive sustainability competences as very important in their careers. Sustainability-related issues should be included in higher education programs addressed to experienced employees, including MBA programs, etc. [33]. The same applies to AI/ML solutions in designed systems [47]. Large companies are usually better prepared to develop systems engineering and sustainable development competences. They often have greater resources. That allows them to integrate a wider range of skills and practices, including sustainability-related ones. Smaller companies focus on core competences/activities that directly generate added value. Therefore, many sustainability-related competences and activities are often perceived as indirectly related to the core business activity, making it difficult to prioritize them and invest in sustainability initiatives. While systems engineers focus more on technical and project management skills within defined systems, experts with sustainability competences emphasize environmental knowledge and ethical advocacy within broader ecological and social systems. Both contribute crucially to addressing complex, interdisciplinary challenges in today's world.

5 Conclusion

The study determined the role of SC in activities performed by systems engineers. The results indicate that systems engineers' perception of SC is not uniform and particularly depends on the enterprise's size and position in the company hierarchy. The study's key findings highlight several important insights. First, sustainability competencies (SC) and systems engineering competencies intersect significantly, although the competency taxonomies for both fields show notable differences. Human resource-related processes are identified as crucial enablers for embedding sustainability throughout organizations, emphasizing their role in facilitating sustainable practices. Systems engineering principles and professional competencies encompass all three dimensions of sustainability; however, only a limited overlap exists between technical and management competencies and sustainability, and none of the integrating competencies in systems engineering align with sustainability. The research also revealed differences in the perception and

integration of sustainability between large enterprises and small-to-medium-sized enterprises (SMEs). Variations were observed across different industry sectors, highlighting the need for tailored approaches to sustainability. Managers regard SC as highly significant in their professional development and career progression. Future research should explore several key areas. One focus should be on how sustainability can be more effectively integrated into the technical, management, and integrating SEC. Another critical question is how operational and practical sustainability methods, principles, and tools can be better utilized to implement complex engineered systems. Supporting SMEs in enhancing their sustainability activities and performance is another priority, addressing smaller organizations' unique challenges. Lastly, research should investigate strategies to integrate sustainability more effectively into managers' and leaders' education and training programs, ensuring they can drive sustainable organizational initiatives.

Acknowledgements. This work was partially supported by the bilateral cooperation and mobility action between CAR CSIC-UPM – WMT WUT for 2025–2027.

Disclosure of Interests. The authors have no competing interests to declare relevant to this article's content.

References

1. Bianchi, G.: Sustainability competences - a systematic literature review (2020)
2. Blatti, J., et al.: Systems thinking in science education and outreach toward a sustainable future. J. Chem. Educ. **96** (2019)
3. Brundiers, K., et al.: Key competencies in sustainability in higher education—toward an agreed-upon reference framework. Sustain. Sci. **16**(1), 13–29 (2021)
4. Brundiers, K., Wiek, A.: Beyond interpersonal competence: teaching and learning professional skills in sustainability. Educ. Sci. **7**(1), 39 (2017)
5. Brundtland: Our Common Future. The Brundtland Report to the World Commission on Environment and Development. Oxford University Press, Oxford, New York (1987)
6. Dano, E.B.: A validated systems engineering competency methodology and functional/domain competency assessment tool. In: 2019 International Symposium on Systems Engineering (ISSE), pp. 1–7 (2019)
7. de Oliveira, A., et al.: Competencies for sustainability: a proposed method for the analysis of their interrelationships. Sustain. Prod. Consum. **14**, 82–94 (2018)
8. Eisenhardt, K.M.: Building theories from case study research. Acad. Manag. Rev. **14**(4), 532–550 (1989)
9. Eisenhardt, K.M., Graebner, M.E.: Theory building from cases: opportunities and challenges. Acad. Manag. J. **50**(1), 25–32 (2007)
10. Flyvbjerg, B.: Five misunderstandings about case-study research. Qual. Inq. **12**(2), 219–245 (2006)
11. Gelosh, D.S.: Implementing the new INCOSE systems engineering competency framework using an evidence based approach for oil and gas companies. Presented at the Offshore Technology Conference, 26 April 2019
12. Graessler, I., et al.: Systems engineering competencies in academic education : an industrial survey about skills in systems engineering. In: 2018 13th Annual Conference on System of Systems Engineering (SoSE), pp. 501–506 (2018)

13. Hahn, H.A.: Improving competence in the professional competencies for systems engineers. In: Squires, A.F., Wheaton, M.J., Feli, H.J. (eds.) Emerging Trends in Systems Engineering Leadership: Practical Research from Women Leaders. WES, pp. 89–143. Springer, Cham (2022). https://doi.org/10.1007/978-3-031-08950-3_4
14. He, B., et al.: Product sustainability assessment for product life cycle. J. Clean. Prod. **206**, 238–250 (2019)
15. Impertro, S., et al.: A competence portfolio for future leaders in advanced systems engineering. Proc. Des. Soc. **3**, 69–80 (2023)
16. INCOSE: Competency Framework (2018). https://www.incose.org/publications/products/competency-framework
17. INCOSE ed: INCOSE Systems Engineering Handbook. Wiley, Hoboken (2023)
18. INCOSE: Systems Engineering Competency Assessment Guide. Wiley, Hoboken (2023)
19. Jawahir, I., et al.: Total life-cycle considerations in product design for sustainability: a framework for comprehensive evaluation. In: Proceedings of the TMT 2006 Keynote, pp. 1–10 (2006)
20. Kasser, J., et al.: Assessing the competencies of systems engineers (2010)
21. Kjellgren, B., Richter, T.: Education for a sustainable future: strategies for holistic global competence development at engineering institutions. Sustainability **13**(20), 11184 (2021)
22. Lambrechts, W., et al.: The integration of competences for sustainable development in higher education: an analysis of bachelor programs in management. J. Clean. Prod. **48**, 65–73 (2013)
23. Li, H., et al.: Individual sustainability competence development in engineering education: community interaction open-source learning. PLoS ONE **18**, 11, e0294421 (2023)
24. Lozano, R., et al.: Adopting sustainability competence-based education in academic disciplines: insights from 13 higher education institutions. Sustain. Dev. **30**(4), 620–635 (2022)
25. Lozano, R., et al.: Connecting competences and pedagogical approaches for sustainable development in higher education: a literature review and framework proposal. Sustainability **9**(10), 1889 (2017)
26. Lozano, R., et al.: Improving sustainability teaching by grouping and interrelating pedagogical approaches and sustainability competences: evidence from 15 Worldwide Higher Education Institutions. Sustain. Dev. **31**(1), 349–359 (2023)
27. Lozano, R., Barreiro-Gen, M. (eds.): Developing Sustainability Competences Through Pedagogical Approaches. Springer, Cham (2021). https://doi.org/10.1007/978-3-030-64965-4
28. Marnewick, A.L., Handley, H.A.H.: Integration of international competencies into systems engineering graduate programs. Syst. Eng. **25**(3), 271–287 (2022)
29. McAloone, T.: A competence-based approach to sustainable innovation teaching: experiences within a new engineering program. J. Mech. Des. **129** (2007)
30. Mulder, K.F.: Strategic competences for concrete action towards sustainability: an oxymoron? Engineering education for a sustainable future. Renew. Sustain. Energy Rev. **68**, 1106–1111 (2017)
31. Muniz, R.N. et al.: The sustainability concept: a review focusing on energy. Sustainability **15**(19), 14049 (2023)
32. Ofei-Manu, P., Didham, R.: Quality education for sustainable development: a priority in achieving sustainability and well-being for all (2014)
33. Peters, A.-K., et al.: Sustainability in computing education: a systematic literature review. ACM Trans. Comput. Educ. **24**(1), 13:1–13:53 (2024)
34. Rieckmann, M.: Future-oriented higher education: which key competencies should be fostered through university teaching and learning? Futures **44**(2), 127–135 (2012)
35. Singh, N., et al.: Sustainable development by carbon emission reduction and its quantification: an overview of current methods and best practices. Asian J. Civ. Eng. **24**, 1–26 (2023)

36. Stake, R.E.: The Art of Case Study Research. SAGE, Thousand Oaks (1995)
37. Thompson, A., et al.: Applying a competency-based education approach for designing a unique interdisciplinary graduate program: a case study for a systems engineering program. In: 2023 ASEE Annual Conference & Exposition (2023)
38. Tite, C., et al.: Embedding sustainability in complex projects: a pedagogic practice simulation approach (2021)
39. Trudeau, P.N.: The process of enhancing a systems engineering training and development program. In: 2005 IEEE Aerospace Conference, Big Sky, MT, USA, pp. 4489–4500. IEEE (2005)
40. Wade, J., et al.: Systems engineering competency expectations, gaps, and program analysis. In: INCOSE International Symposium, vol. 32, no. 1, pp. 1359–1372 (2022)
41. Wasson, C.S.: System engineering competency: the missing course in engineering education. In: 2012 ASEE Annual Conference & Exposition, pp. 25–1227 (2012)
42. Whitcomb, C., et al.: The U.S. department of defense systems engineering competency model. In: INCOSE International Symposium, vol. 27, no. 1, pp. 214–228 (2017)
43. Whitcomb, C., Khan, R.: Comparing competencies for the development of engineers and systems engineers. In: IIE Annual Conference. Proceedings, pp. 1777–1782 (2017)
44. Wiek, A., et al.: Key competencies in sustainability: a reference framework for academic program development. Sustain. Sci. **6**(2), 203–218 (2011)
45. Wiek, A., et al.: Operationalising competencies in higher education for sustainable development. In: Routledge Handbook of Higher Education for Sustainable Development, pp. 241–260. Taylor and Francis (2015)
46. Yin, R.K.: Case Study Research and Applications. SAGE, Thousand Oak (2018)
47. Zhang, C., et al.: Construction of higher education teaching quality evaluation model based on scientific computing. Mob. Inf. Syst. **2022**(1), 4302348 (2022)

Smart Product-Service System for Intelligent Welding System

Mariusz Salwin(✉) and Tomasz M. Chmielewski

Faculty of Mechanical and Industrial Engineering, Warsaw University of Technology, 85 Narbutta Street, Warsaw, Poland
mariusz.salwin@onet.pl

Abstract. This paper aims to design a conceptual model of a Smart Product-Service System (SPSS) for Intelligent Welding System (IWS). To achieve this goal, a detailed literature review, analysis of the welding industry (WI), and a training-educational-design workshop on SPSS and IWS were conducted at a business partner, a welding plant. This allowed the researchers to develop an SPSS in which the tangible component is the IWS (welding robot, sensors, monitoring devices, supporting devices, network infrastructure), enriched with an intangible component, i.e., services and a digital component in the form of a platform and a mobile application. Focusing on specific problems, requirements, and needs of welding plant employees, the developed model aims to draw attention to important elements of the plant in the context of global digital transformation and environmental protection. Thanks to this solution, the WI receives several advanced innovations integrating digital technologies, services, and automation. Additionally, the approach to developing SPSS presented in the article emphasizes the need to combine theoretical knowledge with practical knowledge in welding. This contributes to developing innovative training, education, and design methods for innovative solutions in the digital era.

Keywords: Smart Product-Service System (SPSS) · Smart Product-Service System (SPSS) Design · Intelligent Welding System (IWS) · Welding Industry (WI)

1 Introduction

Modern manufacturing companies increasingly realize that providing traditional product-based solutions generates a tiny competitive advantage and value for the customer [1]. In addition, production and sales must be expanded to cover global trends related to environmental protection [2]. In addition, manufacturers must provide comprehensive solutions that include both products and services to meet market dynamics, growing technological innovations, and customer needs and requirements [3]. All this means that they are increasingly moving from traditional forms to combinations of products and services [4]. These combinations are commonly known as Product-Service System (PSS) [5]. They are defined as an integrated package of products and services that aims to create utility and functionality for the customer and generate new added value for him [6].

M. Paszynski et al. (Eds.): ICCS 2025 Workshops, LNCS 15912, pp. 285–304, 2025.
https://doi.org/10.1007/978-3-031-97573-8_20

The rapid development of information and communication technologies (ICT) has enabled the global digital transformation (DT) of the economy [1]. Digital technologies have begun to be used to create and offer new values and generate revenues [7]. DT went hand in hand with developing digital servitization by integrating intelligent technologies with PSS [8]. This has become a fundamental element of the changing environment and has led to the emergence of the Smart Product-Service System (SPSS) [9]. SPSS is a business-oriented, customer-specific suite of digitalized and well-integrated artifacts in physical hardware, services, and software that deliver more excellent value than when used separately [7]. SPSS is characterized by an interactive and iterative problem-solving process in a customer-integrated value network spanning the entire customer life cycle [10]. This solution enables continuous adjustment of its components to changing buyer needs and supplier capabilities [11]. In this way, it opens a continuum that guarantees flexibility and adaptability in a long-term business relationship and supports the diffusion of new technologies (NT), and innovative solutions [8].

DT has a significant impact on industrial production [12, 13]. Revolutionary technologies implemented in industrial practice are used to automate processes, monitor in real-time, manage integrated systems that combine computational capabilities with material resources, and reduce environmental impact and costs [14]. Many traditional industrial processes have become obsolete, while digitally based industrial processes have become an indispensable element of intelligent production [15]. An intelligent production system is a combination of automated intelligent machines that can make precise decisions based on available data and information. In addition, such a system can more accurately and independently control production processes. In addition, it contributes to eliminating problems related to waste generation and disposal, emission of pollutants, and electricity consumption [16].

Welding is one of the important areas of industry, and the issues discussed are of particular importance [17]. The development and dissemination of the Intelligent Welding System (IWS) is a fundamental factor for modern welding [18, 19]. These advanced technological innovations allow the transformation of traditional welding processes into automated, intelligent, efficient, and precise production systems that respond to the requirements of today's industry sector [20]. The development of IWS focuses on the integration of modern technologies (Artificial Intelligence (AI), Machine Learning (ML), Intelligent Digital Twin (IDT), Cyber-Physical Systems (CPS), and the Internet of Things (IoT)) [18]. The fundamental goal of IWS is to maximize the flexibility, quality, and efficiency of welding processes while minimizing costs, reducing the negative impact on the environment, and adapting to the dynamically changing needs of the market [19].

This paper aims to develop a Smart Product-Service System (SPSS) for Intelligent Welding System (IWS). The solution was developed based on research and training-educational-design workshops in a welding shop (WS) focused on producing pressure vessels and steel elements for overhead cranes, hoists, and cranes. Thanks to SPSS for IWS, several advanced innovations integrating digital technologies, services, and automation will be introduced to the welding industry (WI). This aims to increase the flexibility, quality, and efficiency of welding processes. By enabling WSs to have easier access to IWS and advanced technologies without the need for high initial costs associated with the purchase. This solution will accelerate the digitalization process of the

WI and the dissemination of innovative solutions, making them affordable for interested companies. The IWS manufacturer offers welding robots, AI-based software, sensors, and cloud services for process management and monitoring as part of SPSS. In addition, it is responsible for the supply of materials, technical support, and services. The WS, in turn, receives access to IWS, which increases welding efficiency, improves weld quality, and allows for cost optimization through real-time data analysis and predictive maintenance. Additionally, they do not have to worry about issues related to the purchase, storage, and disposal of raw materials, which allows them to focus on their core business. Thanks to its flexible financing, SPSS has introduced a revolutionary and comprehensive solution to the WI, available to every WS. This allows for implementing low-emission and energy-intensive solutions based on NT, thus supporting the protection of the natural environment.

The paper is structured as follows: the first part is the introduction. The next part presents the research methodology. The third part contains the systematic literature review (SLR). The fourth part presents the analysis of the WS. The fifth part contains Smart Product-Service System for Intelligent Welding System. The last part are the conclusions.

2 Research Methodology

The paper aims to develop a Smart Product-Service System (SPSS) for Intelligent Welding System (IWS). The paper addresses the following research questions:

- What is the potential of using SPSS for IWS in the WI?
- Will SPSS for IWS contribute to improving DT and disseminating intelligent solutions in the WI?
- What is the potential of training-educational-design workshops in developing skills to create new SPSS?

The research methodology adopted in the work included the following steps:

1. Literature analysis - a systematic literature review (SLR) was used in this step. The research was divided into three equal analyses. The first focused on reviewing the industrial application of SPSS/PSS, the second concerned SPSS/PSS design methods, and the third the need for a new business and technological solution for the WI. Leading scientific databases were used for SLR, where the phrases "SPSS/PSS in industry" and synonyms were searched. The search assumptions concerned publications from 2000–2023 in English. 150 scientific papers focusing on SPSS/PSS in industry were found.

   Then, the authors searched for "SPSS/PSS design" and synonyms in the previously indicated databases and time range and conducted SLR on SPSS/PSS design methods. This review identified 74 scientific papers presenting 70 SPSS/PSS design methods.

   Then, a study of the demand for a new business and technological solution for the WI was conducted using the same scientific databases and time range. The authors searched for the phrases "welding," "intelligent," and "businesses" and their synonyms. This analysis enabled the identification of 150 scientific papers indicating the need to develop new solutions for welding.

2. Analysis of the WI. This step focused on the analysis of manufacturers and users of welding machines. Industry reports, sector analyses, and statistical yearbooks were used here.
3. Research and analysis of a WS. A survey was conducted in a WS whose activity focuses on producing pressure vessels and steel elements for overhead cranes, hoists, and cranes. It concerns the situation related to the DT of the WS, SPSS, and IWS used there. The survey was composed of closed and open-ended questions. Some closed questions took values from 0 (very negative) to 10 (very positive).
4. Training, educational and design workshop on SPSS for IWS. In this step, interactive and multimedia training of WS employees was conducted on SPSS and IWS dedicated to the WI. Each substantive part contained a case study on SPSS, which precisely described how this model works in various industries. The method of operation and correct practices related to the use of IWS were presented. After the training, an educational exercise was conducted. It consisted of developing a solution combining SPSS and IWS. Participants worked in groups. They identified the problems that SPSS was to solve. Analyzing the WS from different perspectives, they determined its needs. Then, they identified the conventional and digital services they needed and the technologies that supported them. Finally, each group presented its solution, considering the benefits of the WS and the potential challenges associated with its implementation. After the groups' presentations, a feedback session was organized. In this session, other participants evaluated the projects, indicating areas for improvement and their strengths. Then, the recurring and most inspiring elements were selected based on the discussion. Finally, a summary discussion was held. During this session, the employees jointly concluded the SPSS design process for IWS and the knowledge and experience gained in connection with it.
5. Smart Product-Service System (SPSS) for Intelligent Welding System (IWS). This step concerned building SPSS for IWS. All the knowledge obtained in the previous research steps was used here. This allowed the researchers to develop an SPSS in which the tangible component is the IWS (welding robot, sensors and monitoring devices, supporting devices, network infrastructure), enriched with an intangible component, i.e., services, and a digital component in the form of a platform and a mobile application. Then, the researchers presented their solution to the company's employees and subjected it to a company-wide discussion and assessment. This allowed for the improvement of the presented solution and the development of the final SPSS.

3 Systematic Literature Review

3.1 Product-Service System in Industrial Practice

This stage focused on the analysis of SPSSs operating in the industry. Leading examples include Tesla, Philips Hue, Amazon Echo, John Deere, GE Predix, Apple Watch, Nest Thermostat, Siemens MindSphere, BMW ConnectedDrive, and Dyson Air Purifier. The analyzed SPSSs were developed in large corporations and used in various economic sectors. A long service life and high value characterize these solutions. They use advanced technology to collect and analyze data in real-time. They are supported by integrated digital platforms, allowing their users to access various digital services easily. Their

level of technological advancement depends on the target group and industry. They have significant potential for adapting to customer requirements and maximizing efficiency. It should be emphasized that no solution used in welding was found among the analyzed SPSSs operating in the industry [21, 22].

3.2 Product-Service System Desing

The literature on SPSS/PSS design provides 70 design methods. Their analysis indicates that only 19 have been verified in industrial practice. The most significant number, 13 methods, have been assigned to the domestic appliances, consumer electronics, and other equipment sector, while 14 of them have not been assigned to any sector of the economy. Furthermore, the analysis does not provide SPSS/PSS design methods addressed to the WI. The analysis indicates that some methods are addressed to the design of several types of SPSS/PSS. Out of the 70 methods, as many as 20 can be used to design all types of PSS. In turn, the most significant number, 64 methods, can be used in the design of service-oriented SPSS/PSS. The analyzed methods emphasize the need to maximize customer value, analyze the product life cycle, and identify points of contact between manufacturers' capabilities and customers' needs and requirements. The analysis also indicates their high universality and various readiness levels for digital solutions [23, 24].

3.3 Demand for a New Business and Technological Solution for the Welding Industry

The analyzed literature indicates that dynamic changes in technology, environmental protection, and growing requirements of industrial partners are causing revolutions in the WI [17, 25]. It concerns not only individual machines but also complex systems, enabling a significant increase in the production capacity of WS [17]. Modernizing traditional welding processes through integration with advanced digital technologies plays a fundamental role in this revolution. This sector's needs include improving the quality of welds, minimizing defects, optimizing costs, increasing production efficiency through process automation, and using real-time monitoring [18, 19].

Growing needs require implementing AI-based systems that can predict weld quality parameters (penetration, weld thickness, self-adaptation to changing working conditions) [14, 26]. ML algorithms and infrared thermography technology (IRT) can be used to monitor and control processes [27]. All this will significantly minimize the occurrence of errors and material losses. Implementing innovative solutions such as IDT, multi-sensor IoT platforms, or vision systems for quality control enables real-time data analysis and optimization of welding processes [28]. They influence the maximization of efficiency and allow for meeting restrictive standards regarding quality and safety, including EN ISO 3834, EN 15085, or ISO/IEC 62264 [29, 30].

The implementation of innovative welding solutions such as IWS requires significant initial investments [31]. These investments are mainly related to purchasing and maintaining equipment, digital infrastructure, and employee training [32]. This shows that not every company can afford this type of solution [33]. Such initial costs are harrowing and sometimes unaffordable for micro, small, and medium WS with a limited budget [34].

Implementation costs and a long payback period discourage them additionally [35]. In this context, WS expect to develop and introduce flexible solutions to the market, giving them access to innovative solutions without incurring substantial investment costs [36]. Developing such solutions will allow for a faster transformation of the WI and the dissemination of new solutions [37, 38].

4 Welding Industry and Welding Machines

The most important markets of this WI include China, the USA, South Korea, Japan, India, and the countries of the European Union. Its global value in 2022 is 23.75 billion dollars. In Europe, it is an industry with a long tradition that generates innovation and many jobs. The WI is one of the key industries of the global economy, and it integrates versatility, durability, and strength. These features make this industry an indispensable element of other sectors (industrial production, construction, automotive, energy, and many others), in which they are responsible for the production of structures and parts. Products of this sector are precise in their artistry and flexible in generating complex shapes. These features guarantee their broad application and the possibility of adapting to various customer needs. The welding process allows for the production of strong and durable connections (welds) between metals or thermoplastics, which are often characterized by strength equal to or greater than the materials they connect. Welding integrates versatility, durability, and strength.

The WI is founded on machines ranging from portable conventional welding machines to technologically advanced robotic welding stations. They are characterized by a long service life, versatility, and the possibility of implementing innovative solutions. Technological progress influences the dynamic development in welding precision and efficiency, as well as improving work safety and reducing environmental impact. Currently, the leading manufacturers of this equipment include Kemppi, Fronius International, Electric, ESAB, Miller, and Lincoln Electric. These companies offer a wide range of machines and devices in various equipment options for the WI, together with essential services during the warranty period.

In the era of dynamic DT, well-known welding processes, although practical, encounter several limitations related to efficiency, precision, environmental protection, and costs. This indicates the need for change and combating challenges to prevent stagnation. The answer to this is IWS, which revolutionizes the way welding work is performed. They introduce advanced digital technologies to the industry and allow repetitive work automation, which significantly increases quality and efficiency. Thanks to such solutions, it is changing its face, becoming environmentally friendly and modern. Implementing these solutions involves high initial costs, primarily equipment and digital infrastructure investment. The investment size can be a massive barrier for micro, small, and medium-sized WS because they usually have minimal budgets for updating their machinery. However, the long-term benefits resulting from the implementation of IWS usually outweigh the very high initial costs. Therefore, the WI is looking for solutions that will reduce financial barriers and allow for the popularization of IWS.

5 Welding Shop Analysis

5.1 Characteristics of the Analyzed Welding Shop

The analyzed WS focuses on pressure vessels and steel elements for cranes, lifts, and jib cranes. This small company has been operating on the market for over 15 years. The analyzed WS uses MAG, TIG, MIG, and MMA welding methods. In production, unalloyed steel of ordinary quality and unalloyed steel of increased strength are used. The machine park consists of 10 machines and 1 robot. There are 6 welding machines and 1 device for thermal cutting of metal materials with plasma and oxygen. The WS also has a shot-blasting plant converted into a machine for the surface treatment of metal materials using the shot. The annual mass of manufactured structures is about 240 tons, and the consumption of additional materials is about 300 kg. The structures are manufactured here by EN ISO 3834 (lift structures), and the EN ISO 3834 standard (pressure structures). The overall percentage share of welding processes in the production of the entire structure is 40%, while automated welding is 20%. The company employs 5 welders, 4 people in the welding supervision staff, and 6 people in the non-destructive testing staff. The company has used the machines for no more than 15 years. The ones currently in use are 10 years old. New machines are purchased once every 2 years for the company's funds. The company operates in a 1-shift system (8 h of work) and produces 30 products. In 2023, it achieved an annual turnover of about EUR 800,000. In recent years, the analyzed company began to invest in welding automation, as evidenced by purchasing a welding robot worth EUR 50,000, which increased production efficiency.

5.2 Survey of the Welding Shop

In the survey, the WS rated its level of use of: NT at 4, AI at 5, wearable technologies (WT) at 2. The level of satisfaction with the use of NT is 4, AI is 5, and WT is 3. Additionally, it indicates the need to develop AI-based solutions for welding (9). The company also drew attention to the need for harmonious cooperation between people and welding equipment. This factor was rated very high (9). The same rating (9) was given to support for operators and welders in the form of virtual AI consultants and the development of human-machine interfaces. Staff training is becoming a significant need in the field of NT and IWS. This is supported by a rating of 6. This fact is related to the company's concerns in using these solutions by its employees (1). The WS also indicates the need for data protection (9) and is afraid of cyberattacks (7). The study shows that the WSop shows high interest in the development of automation in welding and IWS, as evidenced by the ratings of 8 and 9. The company indicates the need to improve welding efficiency and increase the repeatability and precision of welds. It also emphasizes that this is possible thanks to the use of IWS supported by AI and ML. The company rated 9 for the use of real-time monitoring systems. This fact refers primarily to the need to optimize welding processes (7), reduce defects (8), and minimize the impact on the environment (9). In questions about the use of NT, the company rated the possibility of using IoT as 8, IDT as 7, augmented reality (AR) as 7, and Big Data as 6. The company noted that the above NT can improve resource management, connect welding equipment, and collect, simulate and analyze data and the welding process. The company draws attention to the

services accompanying the purchase of machines (7) and indicates that their purchase should be associated with a service contract (8). It rates the need to add digital services to welding equipment very high, at 7. An important factor for the WS is the reduction of material and energy consumption and the reduced waste generated. This is reflected in the rating of 7. This emphasizes the need to invest in new, low-emission technologies and business solutions that fit into the trend of environmental protection. Issues related to incurring investment costs in IWS were rated 3. This indicates concerns and difficulties in implementing such a capital-intensive investment for a company of this size. The WS indicates that support for it would be an alternative IWS financing model tailored to its needs, which it rates 8. It would eliminate high investment costs and enable the use of new solutions. The company shows a high level of interest in solutions based on SPPS, as evidenced by the rating of 7. The factors motivating the use of SPSS indicate an increase in resource management efficiency, no need to incur high investment costs, reduction of barriers related to the use of expensive NT, and quick access to consumables and spare parts.

6 Training, Educational and Design Workshop

6.1 Training and Educational Session

At this stage, training was conducted. It was designed to be a comprehensive educational program, combining practical and theoretical elements. Interactive multimedia elements with case study analysis were used here. The training aimed to improve WSop employees' competencies inf DT, SPSS, and IWS.

The first stage of the training was a theoretical introduction to SPSS and IWS. The company's employees were introduced to the concept of product and service integration and the origins of PSS/SPSS. Issues related to the classification and design of PSS/SPSS were discussed. Information about IWS, their use, application, and the possibilities and opportunities they offer in welding were presented. Issues related to digital technologies, their evolution, and their impact on welding precision, efficiency, and quality were also discussed. At this stage, multimedia presentations enriched with animations were used. Additionally, an interactive quiz was conducted after each discussed issue.

The next stage of the training concerned a case study session. It was presented how PSS/SPSS works in various industrial sectors. The focus was on the leading cases: Tesla, Philips Hue, Amazon Echo, John Deere, GE Predix, Apple Watch, Nest Thermostat, Siemens MindSphere, BMW ConnectedDrive, Dyson Air Purifier. Each case was discussed in detail, and its unique features were described. Their strengths and benefits for manufacturers and customers were indicated. In this stage, multimedia presentations were used, enriched with videos with expert statements and opinions. Additionally, after each discussed case study, a question and answer session was held to encourage WS employees to ask questions about the presented cases.

The third stage of the training focused on a detailed presentation of the IWS. It presented what the IWS consists of, how it works, and how much it costs. The WS employees were shown some of the functions, including the operation of vision systems and sensors to monitor welding parameters in real-time, automatic calibration of welding equipment, and IoT to connect it and send data for analysis in the cloud. Videos, photos, animations,

comparative studies, and simulation software supported this stage. In addition, at the end of this stage, each participant had the opportunity to familiarize themselves with the software and conduct an individual IWS simulation. Employees tested how changes in various parameters affect the quality of welds. Then, the simulations were compared with the results achieved in the company.

The fourth stage of the training concerned correct practices related to implementing IWS. Attention was focused on capital needs and the need to train staff. Methods of planning welding processes using NT and issues related to predictive maintenance and maintenance were discussed. In this case, attention was paid to analyzing operational data from sensors. Issues of data management, production optimization, and digital security were discussed. This stage presented possible errors, barriers to implementation, and methods for avoiding them. Films provided support here with examples of WS and individual interviews with WS employees.

6.2 Design Session

The next stage of the workshop was a design session with an educational exercise, which consisted of developing a solution combining SPSS and IWS. Based on the knowledge they had already acquired, the employees carried out this exercise in groups representing different areas of the company's operations. Each group began its project by identifying the WS problems. In the next step, each group identified the needs of the WS. Then, the employees identified the conventional and digital services that should be added to IWS in the developed SPSS. Then, the groups focused on NT, which would support SPSS. In the next part, they indicated financing models that would benefit the company. The results of each group's work are presented in Table 1.

Table 1. Requirements set for PSS for IWS by welding shop employees.

	Group 1	Group 2	Group 3	Group 4
Problems	Calibration difficulties	Lack of process repeatability	Insufficient surface preparation	Welding robot programming
	Production downtime	Excessive consumption of raw materials and materials	High costs of quality corrections	Long project implementation time
	Ineffective diagnostics and maintenance of equipment	Excessive energy consumption	A large number of weld defects	Long response time to emerging problems

(*continued*)

Table 1. (*continued*)

	Group 1	Group 2	Group 3	Group 4
	Insufficient use of process data	Generation of large amounts of waste	Insufficient visual inspection of welds	Lack of technical support for equipment
Needs	Automation of complex processes	Optimization of production processes	Improve equipment maintenance	Shortening project implementation time
	Access to new technological solutions	Elimination of production downtime	Minimize the risk of defects	Reduction of human errors
	Improvement of the use of process data	Comprehensive analysis of welding processes	Increase welding accuracy, precision and repeatability	Improvement of ergonomics and work safety
	Remote monitoring of welding parameters in real time	Waste disposal	Improve quality control	Welding robot programming training
Conventional Services	Monitoring and diagnostics of welding equipment	Recycling and waste management	Supply of filler metal and technical gases	Training
	Installation and commissioning	Equipment rental	Supply of raw materials and materials	Welding equipment service and maintenance
	Maintenance of tools and auxiliary equipment	Take-back	Supervision of the welding process	Analysis of failure causes
	Optimization of welding processes	Spare parts and consumables	Technical consulting	Warranty
Digital Services	Automatic calibration	Monitoring of welding process contamination	Automatic quality analysis	Training platform
	Automatic firmware updates	Automatic energy management	Remote technical support in real time	Cybersecurity services

(*continued*)

Table 1. (*continued*)

	Group 1	Group 2	Group 3	Group 4
	Offline programming for welding robots	Adjustment of machine parameters to individual needs	Access to welding parameter libraries	Predictive service
	Advanced multidimensional analyses in real time	Remote monitoring of welding parameters in real time	Automatic detection of weld defects	Cloud data analysis
New Technologies	IoT	AI	IDT	Augmented reality (AR)
	Cloud Computing (CC)	ML	CAE (Computer-Aided Engineering) platforms	Virtual reality (VR)
	Big Data (BD)	Edge Computing (EC)	Metaverse (M)	Blockchain
Forms of Financing	Subscription model with monthly fees	Rental with purchase option	Leasing	Payment for time of use

Then, a presentation session was held. During this time, each group presented the results of their work (Table 2) and discussed them in detail. Each group highlighted the unique elements of their solutions, which resulted from their experiences and analyses of the WS. The presentations showed that Group One focused on welding automation, Group Two on issues related to sustainable development, Group Three on quality issues, and Group Four on staff development.

After the presentations, a feedback session was held. Participants asked questions, discussed strengths and areas requiring improvement of the developed solutions, and indicated the benefits resulting from them. This session showed that the solutions proposed by each group complement each other. It also indicated recommendations regarding SPSS. The results of this session's work are presented in Table 2.

Table 2. Feedback session - results of the work.

Strengths	Areas for improvement	Benefits	Recommendations
Automation and digitalization of processes	Better integration of digital systems with existing infrastructure	Increased production efficiency	Combination of solutions proposed by the groups

(*continued*)

Table 2. (*continued*)

Strengths	Areas for improvement	Benefits	Recommendations
NT application	Employee training	Improved weld quality	Cooperation with the IWS manufacturer and suppliers
Minimization of energy consumption and waste reduction	Consideration of data security issues	Reuse of materials	Education of staff regarding long-term savings
Promotion of sustainable development	Adaptation to changing standards and regulations	Support for the DT of welding	Systematic analysis of the WS needs
Financial flexibility and cost reduction	Reduction of emissions and carbon footprint	Alignment with environmental protection programs	Cooperation in interdisciplinary teams

7 Smart Product-Service System for Intelligent Welding System

The final solution was developed in this chapter using the knowledge and fundamentals of PSS/SPSS design acquired so far. In the developed solution, the tangible component is the Intelligent Welding System (welding robot and welder, sensors and monitoring devices, supporting devices, network infrastructure), enriched with an intangible component, i.e. services, and a digital component in the form of a platform and mobile application. Then, the researchers presented their solution to the company's employees and subjected it to a company-wide discussion and evaluation. This allowed for the improvement of the presented solution and the development of the final SPSS. The results of the work are presented in Table 3, Fig. 1, Table 4.

The company producing the IWS makes it available to its customers and provides them access to a wide range of services. Settlements are based on a flexible financing model tailored to the needs of the WS and dependent on the period of use of the IWS. Ownership and maintenance of the IWS remain with the manufacturer; the WS only uses this solution. The priority for the WS is to use a modern solution that will positively impact its digitalization and increase the number of welded structures produced. After the specified period of use, it is possible to replace the IWS with a newer or updated model.

Table 3. Smart Product-Service System for Intelligent Welding System – Components.

Category	Component	Description
Tangible Component	Welding robot and welding machine	Welding automation, increasing welding efficiency and precision

(*continued*)

Table 3. (*continued*)

Category	Component	Description
	Sensors and monitoring devices	Collecting various types of data on the welding process and its parameters
	Support devices	Accessories that increase the functionality and capabilities of welding (welding tables, manipulators)
	Network infrastructure	Hardware and software enabling communication between devices and employees
Intangible Component	Conventional services	Analysis of failure causes, technical consulting, supply of raw materials and materials, supply of filler metal and technical gases, warranty, installation and start-up, monitoring and diagnostics of welding equipment, supervision of the welding process, optimization of welding processes, recycling and waste management, service and maintenance of welding equipment, training, take-back, maintenance of tools and auxiliary equipment, equipment rental
	Digital services	Cloud data analysis, automatic quality analysis, automatic calibration, automatic firmware updates, automatic detection of weld defects, automatic energy management, access to welding parameter libraries, adjustment of machine parameters to individual needs, monitoring of welding process contamination, offline programming for welding robots, predictive service, training on a digital platform, cybersecurity services, advanced multidimensional analyses in real-time, remote monitoring real-time welding parameters, real-time remote technical support

(*continued*)

Table 3. (*continued*)

Category	Component	Description
Digital Component	IWS digital platform	A tool that connects welding equipment, services, and data into a coherent ecosystem within SPSS
	IWS mobile application	A tool that allows access to the IWS digital platform functions from mobile devices
New Technologies	IoT	Integration of devices in the network, allowing real-time data exchange
	AI	Automatic welding parameter settings and data analysis
	AR/VR/M	Visualization of welding processes and training in a virtual environment
	IDT	Creation of digital models of IWS and welding processes for simulation and optimization
	CC	Storage and analysis of large data sets on the use of IWS and welding processes
	EC	Data processing directly on welding equipment
	ML	Identification of patterns based on welding data and optimization of processes based on data
	Blockchain	Ensuring transparency and data security during the life of the IWS
	BD	Analysis of large data sets on information on current, voltage, wire feed speed, welding speed and time, and job numbers

Implementing SPSS for IWS benefits all parties involved in the transaction. The WS focuses on its core business and does not engage in activities related to maintaining the IWS. In addition, it saves financial resources and time. It does not engage in employee training and additional equipment because it provides this as part of SPSS. Additionally, troubleshooting and replacing parts is also the manufacturer's responsibility. This approach allows the WS to maximize tasks and reduce costs. Thanks to this solution, the manufacturer no longer focuses only on producing and selling IWS but instead enters into long-term cooperation with the WS. This guarantees the stability of revenues and

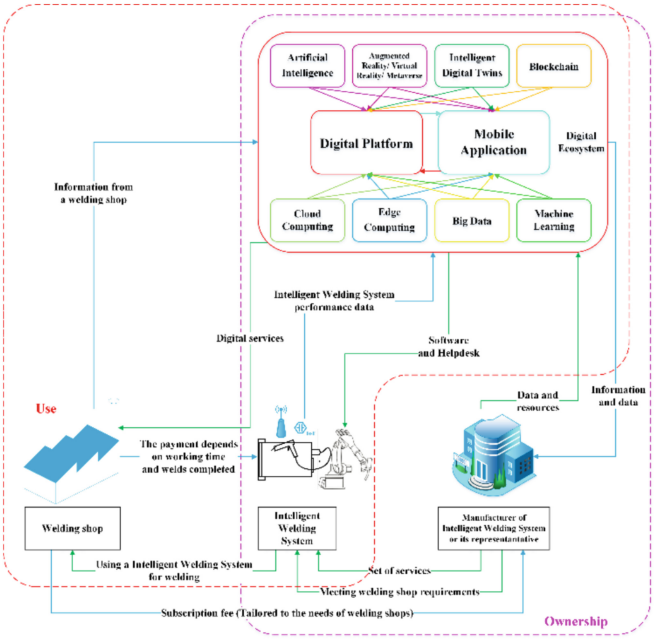

Fig. 1. Smart Product-Service System for Intelligent Welding System - Concept.

Table 4. Smart Product-Service System for Intelligent Welding System - Concept.

Area	Assumptions
Property	The manufacturer remains the owner
	The manufacturer is responsible for maintaining the IWS
	The customer uses IWS tailored to their needs in the financial model
Sales	Flexible financing model
	Additional functions or services are available for purchase on request
	Long-term cooperation between the customer and the manufacturer instead of a one-time sale
Services	Access to a broad service package
	Combination of conventional and digital solutions
	Additional services on request
Digital Transformation	Integration of NT with the customer's digital infrastructure
	Real-time data collection and analysis
	Access to a digital platform and mobile application

(*continued*)

Table 4. (*continued*)

Area	Assumptions
Customer Benefits	Elimination of high capital investments
	Tailoring the IWS to the specific needs of the WS
	Reduced responsibility for maintaining the IWS
Manufacturer Benefits	Long-term and stable revenues thanks to new financing models
	Long-term customer relationships and increased customer loyalty
	Collection and analysis of data from the IWS's service life
Environmental Benefits	Elimination of overproduction of devices thanks to long-term equipment operation
	Recycling, reduction of waste and emissions of harmful substances
	Reduction of the consumption of raw materials, materials and electricity

the availability of IWS operating data, which will allow the development of new generations of welding equipment, digital platforms, applications, and services tailored to the needs of the WS.

The SPSS proposed here plays a fundamental role in the operation and reliability of welding equipment while offering significant benefits to WS and manufacturers. Implementing SPSS in the context of IWS enables the integration of welding equipment, services, and new digital technologies, significantly improving the availability of modern solutions for the WI at an affordable price. Systematic service and real-time monitoring guarantee the diagnosis of possible failures and the implementation of preventive measures. This eliminates the occurrence of downtimes and the related costs. In addition, it allows IWS to adapt to the needs of WS through systematic technical modifications and software updates. This is aimed at dynamic adaptation to the changing market situation and working conditions and extending the service life of the IWS.

The implementation of NT in the developed solution significantly accelerates the DT of WS, which leads to changes in the management of welding processes and organizational culture. It translates into a wide range of benefits beyond conventional and well-known improvements in welding processes. The manufacturer undergoes a specific transformation of the operating model, thanks to which it can flexibly respond to market requirements and needs changes. In turn, WS gain the ability to maximize control of welding processes, as well as their efficiency and quality. NT supports the automation of repetitive tasks, thus maximizing work efficiency. NT also provides support for the manufacturer in the development of new services. This allows for offering WS broader and more complex solutions. Additionally, it supports sustainable development. This involves reducing energy consumption, raw materials, and generated waste. The implementation of NT also supports the development of knowledge and skills of WS employees. This is possible thanks to the manufacturer providing AR/VR/M-based

training via a digital platform and mobile application, which increases flexibility. Additionally, platforms and applications enable remote access to data and management of welding equipment from any location.

8 Conclusion

This paper focuses on the WI. This industry is characterized by the technical complexity of processes and the diversity of welding methods. Micro, small, and medium-sized enterprises dominate it. Recent years have been associated with its slow automation and digitalization, which was limited by barriers related to the need for massive investments, discouraging companies.

The analysis of the available literature and the welding market indicates the need for new solutions for the WI. This article fills this gap in the use of SPSS for IWS. It discusses theoretical and practical issues related to it. On the other hand, developing a new SPSS for welding was carried out through surveys and training-educational-design workshops conducted in a WS. Only the most important elements are presented here, emphasizing the importance and necessity of developing such models.

Based on the conducted surveys and training, educational and design workshops, the following conclusions can be drawn:

- Economic aspects – the model proposed in the article enables WS to access IWS without high initial investments, which is particularly important for micro, small, and medium-sized enterprises. A flexible form of financing, which is also tailored to the needs of WS, minimizes the entry barriers of modern solutions based on automation and digitization for the analyzed industry.
- SPSS development – The workshops that were conducted constitute an effective form of SPSS development. They enable identifying those consistent with WS specific requirements and needs. The involvement of the company's employees allows for the adjustment of SPSS to actual market requirements. All this maximizes the effectiveness of implementation and supports the implementation of NT in this industry.
- Knowledge and competence development – The workshops conducted significantly affect the development of knowledge and competencies of the company's employees in the SPSS, IWS, and NT fields. Additionally, they raise their awareness of new business solutions for enterprises. Finally, they support education and teach skills necessary for DT, which help to use in practice.
- SPSS for IWS introduces advanced integration of physical, service, and digital NT elements to develop a comprehensive ecosystem that meets the needs and requirements of the modern WI. This includes using a wide range of NT, thanks to which SPSS optimizes welding processes, increases welding quality and precision and improves operational efficiency by dynamically adapting to changing production conditions.
- Environmental protection - including NT elements and services in the physical element of welding equipment allows for reducing the WI impact on the environment. Additionally, it allows for extending its service life, regeneration, and reuse, reducing the need to manufacture new equipment.

- When creating SPSS for the analyzed sector, it is necessary to consider the fulfillment of restrictive standards regarding quality and safety, including EN ISO 3834, EN 15085, or ISO/IEC 62264. Compliance with them will guarantee an increase in the competitiveness of the developed solution.
- The use of NT in this solution will significantly improve welding processes, reduce the number of defects, minimize energy and material consumption, and support waste management. Additionally, their implementation will enable monitoring and optimizing processes in real-time, translating into an increase in companies' competitiveness level using SPSS.

In addition, the surveys and training-educational-design workshops provided a solid foundation for developing and implementing the SPSS model for IWS. They indicate what elements must be addressed and what factors are worth considering when designing a personalized and digitally advanced SPSS-based solution.

Our contribution to education and design is the innovative approach to creating SPSS for IWS. With an emphasis on practical aspects and experiences in PSS/SPSS and welding production, we conducted a dynamic training-educational-design workshop. It equipped the WS employees with the practical knowledge and skills to develop new SPSS solutions for the WI. It allowed the authors to develop a new solution that is unavailable in the open scientific literature so far.

Future research directions should focus on developing the approach based on the workshops presented in this article, including additional digital tools and stages of training and individual and creative projects in PSS/SPSS. They prioritize innovations in education and the design of PSS/SPSS in enterprises; it is important to continue cooperation between universities and industry. This will ensure the transfer of scientific knowledge to industry and will allow the introduction of solutions into business practices that have not been used in enterprises so far. In addition, it will enable the generation of personalized solutions for specific enterprises.

Acknowledgments. Love and praise God.

Disclosure of Interests. The authors have no competing interests to declare that are relevant to the content of this article.

References

1. Gaiardelli, P., et al.: Product-service systems evolution in the era of Industry 4.0. Serv. Bus. **15**, 177–207 (2021)
2. Vezzoli, C., et al.: Sustainable product-service system (S.PSS). In: Vezzoli, C., et al. (eds.) Designing Sustainable Energy for All. Green Energy and Technology, pp. 41–51. Springer, Cham (2018). https://doi.org/10.1007/978-3-319-70223-0_3
3. Annarelli, A., Battistella, C., Costantino, F., Di Gravio, G., Nonino, F., Patriarca, R.: New trends in product service system and servitization research: a conceptual structure emerging from three decades of literature. CIRP J. Manuf. Sci. Technol. **32**, 424–436 (2021)
4. Salwin, M., Lipiak, J., Kulesza, R.: Product-service system–a literature review. Res. Logist. Prod. **9**, 5–14 (2019)

5. Mont, O.K.: Clarifying the concept of product–service system. J. Clean. Prod. **10**, 237–245 (2002)
6. Negash, Y.T., Calahorrano Sarmiento, L.S., Tseng, M.-L., Jantarakolica, K., Tan, K.: Sustainable product-service system hierarchical framework under uncertainties: the pharmaceutical industry in Ecuador. J. Clean. Prod. **294**, 126188 (2021)
7. Ren, M., Zheng, P.: Towards smart product-service systems 2.0: a retrospect and prospect. Adv. Eng. Inform. **61**, 102466 (2024)
8. Shao, S., Xu, G., Li, M.: The design of an IoT-based route optimization system: a smart product-service system (SPSS) approach. Adv. Eng. Inform. **42**, 101006 (2019)
9. Chen, Z., Ming, X., Zhou, T., Chang, Y., Sun, Z.: A hybrid framework integrating rough-fuzzy best-worst method to identify and evaluate user activity-oriented service requirement for smart product service system. J. Clean. Prod. **253**, 119954 (2020)
10. Salwin, M., Andrzejewski, M., Kraslawski, A.: Information asymmetry in product-service system design - example of the pharmaceutical industry. Procedia Manuf. **55**, 282–289 (2021)
11. Chiu, M.-C., Chu, C.-Y., Kuo, T.C.: Product service system transition method: building firm's core competence of enterprise. Int. J. Prod. Res. **57**, 6452–6472 (2019)
12. Szala, M., Łatka, L., Awtoniuk, M., Winnicki, M., Michalak, M.: Neural modelling of APS thermal spray process parameters for optimizing the hardness, porosity and cavitation erosion resistance of Al2O3-13 wt% TiO2 coatings. Processes **8**, 1544 (2020)
13. Liu, J., et al.: Digital twin model-driven capacity evaluation and scheduling optimization for ship welding production line. J. Intell. Manuf. **35**, 3353–3375 (2024)
14. Gyasi, E.A., Kah, P., Penttilä, S., Ratava, J., Handroos, H., Sanbao, L.: Digitalized automated welding systems for weld quality predictions and reliability. Procedia Manuf. **38**, 133–141 (2019)
15. Szczucka-Lasota, B., Szymczak, T., Węgrzyn, T., Tarasiuk, W.: Superalloy—steel joint in microstructural and mechanical characterisation for manufacturing rotor components. Materials **16**, 2862 (2023)
16. Amasawa, E., Shibata, T., Sugiyama, H., Hirao, M.: Environmental potential of reusing, renting, and sharing consumer products: systematic analysis approach. J. Clean. Prod. **242**, 118487 (2020)
17. Skowrońska, B., Szulc, B., Morek, R., Baranowski, M., Chmielewski, T.M.: Selected properties of X120Mn12 steel welded joints by means of the plasma-MAG hybrid method. In: Proceedings of the Institution of Mechanical Engineers, Part L: Journal of Materials: Design and Applications, p. 14644207241256113 (2024)
18. Wang, B., Li, Y., Freiheit, T.: Towards intelligent welding systems from a HCPS perspective: a technology framework and implementation roadmap. J. Manuf. Syst. **65**, 244–259 (2022)
19. Wang, B., Hu, S.J., Sun, L., Freiheit, T.: Intelligent welding system technologies: state-of-the-art review and perspectives. J. Manuf. Syst. **56**, 373–391 (2020)
20. Skowrońska, B., Chmielewski, T., Golański, D., Szulc, J.: Weldability of S700MC steel welded with the hybrid plasma + MAG method. Manuf. Rev. **7**, 4 (2020)
21. Salwin, M., Andrzejewski, M.: Product-service system: a new opportunity for the plastics processing industry. Procedia Comput. Sci. **246**, 4541–4551 (2024)
22. Salwin, M., Kraslawski, A.: Product-service system business model for plastics industry. J. Clean. Prod. **451**, 141874 (2024)
23. Salwin, M., Chmielewski, T.: Smart product-service system for parking furniture—sale of storage space in parking places. Sustainability **16**, 8824 (2024)
24. Salwin, M., Kraslawski, A., Andrzejewski, M., Hryniewicka, M.: Product-service system design - a case study for parking furniture industry. In: Hamrol, A., Grabowska, M., Hinz, M. (eds.) MANUFACTURING 2024. LNME, pp. 41–56. Springer, Cham (2024). https://doi.org/10.1007/978-3-031-56474-1_4

25. Skowrońska, B., Chmielewski, T., Baranowski, M., Kulczyk, M., Skiba, J.: Friction weldability of ultrafine-grained titanium grade 2. J. Adv. Join. Process. **10**, 100246 (2024)
26. Gyasi, E.A., Handroos, H., Kah, P.: Survey on artificial intelligence (AI) applied in welding: a future scenario of the influence of AI on technological, economic, educational and social changes. Procedia Manuf. **38**, 702–714 (2019)
27. Skowrońska, B., Bober, M., Kołodziejczak, P., Baranowski, M., Kozłowski, M., Chmielewski, T.: Solid-state rotary friction-welded tungsten and mild steel joints. Appl. Sci. **12**, 9034 (2022)
28. Boaretto, N., Centeno, T.M.: Automated detection of welding defects in pipelines from radiographic images DWDI. NDT E Int. **86**, 7–13 (2017)
29. Węgrzyn, T., Gołombek, K., Szczucka-Lasota, B., Szymczak, T., Łazarz, B., Lukaszkowicz, K.: Docol 1300M micro-jet-cooled weld in microstructural and mechanical approaches concerning applications at cyclic loading. Materials **17**, 2934 (2024)
30. Szczucka-Lasota, B., Węgrzyn, T., Jurek, A.: Formation of oxides and sulfides during the welding process of S700MC steel by using new electrodes wires. Materials **17**, 2974 (2024)
31. Cai, W., Jiang, P., Shu, L., Geng, S., Zhou, Q.: Real-time laser keyhole welding penetration state monitoring based on adaptive fusion images using convolutional neural networks. J. Intell. Manuf. **34**, 1259–1273 (2023)
32. Fernández, J., Valerieva, D., Higuero, L., Sahelices, B.: 3DWS: reliable segmentation on intelligent welding systems with 3D convolutions. J. Intell. Manuf. **36**, 5–18 (2025)
33. Chen, C., Lv, N., Chen, S.: Data-driven welding expert system structure based on Internet of Things. In: Chen, S., Zhang, Y., Feng, Z. (eds.) Transactions on Intelligent Welding Manufacturing. TIWM, pp. 45–60. Springer, Singapore (2018). https://doi.org/10.1007/978-981-10-8330-3_3
34. Fang, H.C., Ong, S.K., Nee, A.Y.C.: Adaptive pass planning and optimization for robotic welding of complex joints. Adv. Manuf. **5**, 93–104 (2017)
35. Afian, A., Mustikowati, R.I., Sari, A.R., Halim, D.M., Khoir, N.U.: Mentoring the importance of financial literacy and digital literacy in the welding workshop business. JPM **5**, 206–210 (2024)
36. Chen, S.B.: On intelligentized welding manufacturing. In: Tarn, T.J., Chen, S.B., Chen, X.Q. (eds.) RWIA 2014. AISC, vol. 363, pp. 3–34. Springer, Cham (2015). https://doi.org/10.1007/978-3-319-18997-0_1
37. Bolotov, S.V., Zakharchenkov, K.V., Krutolevich, S.K.: Intelligent hardware and software sup-port and increasing the efficiency of welding processes. Pattern Recognit. Image Anal. **34**, 686–691 (2024)
38. Sałaciński, T., Chrzanowski, J., Chmielewski, T.: Statistical process control using control charts with variable parameters. Processes **11**, 2744 (2023). https://doi.org/10.3390/pr11092744

The Use of Artificial Intelligence and Virtual Computer Laboratories to Develop Computer Science Education

Andrzej Kamiński[1], Martyna Wybraniak-Kujawa[1(✉)], Sergio Iserte[2], and Jerzy Krawiec[1]

[1] Warsaw University of Technology, Faculty of Mechanical and Industrial Engineering, Warsaw, Poland
{andrzej.kaminski,martyna.wybraniak,jerzy.krawiec}@pw.edu.pl
[2] Barcelona Supercomputing Center (BSC-CNS), Barcelona, Spain
sergio.iserte@bsc.es

Abstract. This research introduces and evaluates a new method of teaching information and communication technology (ICT), which results in the active participation of the trainee in the sequential performance of laboratory exercises in the virtual environment. This training is carried out using a virtual educational platform - VLC. The proposed approach uses an innovative mechanism for controlling the training process, called a virtual tutor, whose task is to continuously monitor the trainee's progress and adjust the pace and level of subsequent laboratory tasks. The virtual tutor function is implemented using machine learning techniques and semantic networks. The proposed method allows the use of educational content management mechanisms, an object repository, and educational process maps. Similar studies on IT tools for e-learning are conducted to a large extent, but they often lack a holistic approach to the problem. Such aspects as career counseling in selecting an educational program based on the balance of the future trainee's competencies, individual course of study through selective selection of laboratory exercises, remote progress monitoring, and activation of people over 45 years of age constitute the innovative nature of the article. Study results prove the effectiveness of the new holistic VLC method.

Keywords: Virtual laboratories · Educational platform · E-learning · Artificial Intelligence in e-learning · Innovative teaching methods

1 Introduction

In order to ensure the effective functioning of the labor market, it would be necessary to ensure better adaptation of existing competence resources to market requirements and increase the demand for high competences. Considering the dynamic development of the ICT sector, it is recommended to create favorable conditions for the development of staff and new educational programs. Undoubtedly, modern e-learning methods can be used effectively in the process of staff

M. Paszynski et al. (Eds.): ICCS 2025 Workshops, LNCS 15912, pp. 305–319, 2025.
https://doi.org/10.1007/978-3-031-97573-8_21

development and balancing competencies in the so-called high-tech sectors, especially in ICT.

Distance learning is referred to as e-learning, e-education, or remote teaching. The latest advances in information technology are used in the e-learning process, and the transfer of teaching content and other information takes place mainly over the Internet. Online learning is becoming increasingly popular. The authors of the publications indicate that this is due to its independence from time and place, low costs, and wide educational opportunities [1]. Interfacing tools that improve interactions between students, teachers, and content are key factors influencing academic outcomes in e-learning [2].

Artificial intelligence (AI) has found wide application in almost all areas of life, including e-learning. Researchers emphasize that AI enables the rapid and efficient production of learning content as a response to the ever-increasing demand for flexible online learning [3].

This article mainly addresses the following research questions.

- What impact does the new proposed teaching method have on the training results of course participants? The authors respond to this by presenting a comparison of the results of a traditional postgraduate course and a course enriched with the use of an innovative educational platform, which is the proposed teaching solution.
- How do course participants perceive this method? This question is answered in the survey results from the participants.
- Does the proposed method facilitate a holistic approach to teaching, and if so, what are the contributing factors? The conclusions from the expert panel address this question.

Organizations involved in IT training can use these research findings to improve the quality of education and improve the planning, organization, and management of training courses.

2 Related Work

Distance learning is becoming more and more popular every year, and the breakthrough was the coronavirus pandemic when it was necessary to adapt to the prevailing conditions.

Currently, three types of application software are used in distance learning:

- LMS (Learning Management System) – a system for administering, monitoring, and reporting learning progress, managing teaching materials and permissions, and registering users for courses [4];
- LCMS (Learning Content Management System) – a training content management system, which, in addition to the functionalities available within LMS, can create, edit, deliver, and manage teaching content; provides the ability to control the process of creating didactic content and its archiving [5];

– VCS (Virtual Classroom System) – a system enabling management and conducting distance learning in synchronous ("online") mode. This solution includes several functions in the area of cooperation, communication and knowledge distribution [6].

Artificial intelligence and machine learning are widely used in education. Popular techniques include:

– Supervised learning, which personalizes the educational material and predict student progress. The algorithms most often used in supervised learning are decision trees, Support Vector Machines (SVM), and logistic regression [7].
– Unsupervised learning, which involves clustering topics and grouping students by learning style. The algorithms most often used here are: k-means clustering and Principal Component Analysis (PCA) [8].
– Reinforcement learning (RL), which may include educational games and learning systems (intelligent tutors) [9].
– Artificial neural networks in education are most often used to recognize speech and text or generate didactic content [10].
– Recommendation systems - are mainly used to recommend additional lessons or tasks [10].
– Predictive analytical models - mainly used to predict future events such as a student's exam result, problematic topics for a student, etc. [10]
– NLP (Natural Language Processing) - used mainly in language translation, text analysis and editing or educational chatbots [10].

In the educational process, it is also worth looking at pedagogical theories. We can mention the following:

– Constructivism - involves engaging students by constructing their knowledge after interacting with the environment or their experiences. The emphasis here is mainly on practical tasks, promoting student engagement [11].
– Connectivism - this is a theory that says that learning is a network process. The emphasis here is on interaction with other students, experts, and digital resources. The approach promotes the ability to use information and technology and personalized learning [11].
– Cognitive Load Theory – a theory that discusses the internal, external, and useful load in the learning process. According to this theory, students should engage in activities that deepen the deeper processing of valuable information. The aim here is to reduce external load, i.e. unnecessary knowledge, and optimize internal load by adapting the material to the student's level [12].

The key component that integrates the methods, techniques, and tools used in e-learning is the educational platform. This platform facilitates the continuous management of the teaching process and allows the modular expansion of the content accessible to students. Educational platforms are widely used for teaching at national universities. For example, Moodle, a product based on the GNU GPL license, is implemented in Poland universities, for example, at the Gdańsk

University of Technology [13], Ukraine universities [14], or the Peru National University of San Agustín (UNSA) [15]. Similarly, the ILIAS platform, also based on the GNU GPL license, is used in many universities, even African ones, ensuring the development of African students despite many adversities [16]. The ILIAS platform is gaining popularity in countries of the European Union. This platform supports the administration of various university study programs and facilitates the management of e-learning courses [17]. In addition to ILIAS, other educational platforms such as Claroline, Chamilo, Docebo, and ATutor are also widely used [18]. These are just a few examples of how software can be used to bridge distances and teach despite war or pandemics. However, research has identified several shortcomings in traditional educational platforms, such as insufficient user engagement, lack of integration with other systems, high costs for material development, a need for greater motivation, and a prolonged duration of learning [19].

Other authors highlight that a significant advantage of Artificial Intelligence in e-learning is its ability to personalize the content for each learner [20]. This contrasts with traditional e-learning systems, where only difficulty levels are defined and all students at a particular level use the same instructional material [21]. To effectively utilize AI in e-learning, it is essential to develop a comprehensive and personalized e-learning framework. Unfortunately, many of the currently proposed solutions lack this holistic approach [22]. To establish a personalized learning system, various IT challenges must be addressed [23]. Machine learning (ML) and deep learning (DL) models can be used effectively to match appropriate learning materials to individual learners according to their competencies [24]. Furthermore, the algorithm should be trained and updated in real-time [25]. Another key aspect is analyzing the learning preferences of the course participants, which should be included in the recommendation system [26]. The key dysfunctions of existing educational platforms include lack of interactivity (the software only acts as a repository of static documents), the level of training not being adjusted to the competency profile of individual participants, problems with understanding the names and messages used in the graphical user interface, and the lack of specialist solutions dedicated to the needs of the ICT sector. The response to diagnostic dysfunctions of classic solutions [27] is a research and development program, the result of which was the development of an innovative educational platform.

3 Materials and Methods

The following section describes the implementation of the project, which was the source of obtaining data for the research. It also describes the innovative VLC method proposed by the authors of the article, as well as the importance of AI in this method. At the end of the section, methods for verifying the results used in the next section are proposed.

3.1 Project Realization

The research was carried out as part of a project co-financed by the European Union. The aim of the project "Management of the transfer of information technology to enterprises" [28] - was to educate and prepare staff - specialists with interdisciplinary knowledge in the field of information technology (e-business, IT systems supporting knowledge management) and skills in the field of managing this category of enterprise. This aim was achieved by organizing postgraduate studies"Management of IT projects in the e-business environment" and "Knowledge management using modern technologies and information systems". The strategic criterion of the project was the professional activation of people over 45 years of age. The project was divided into five stages shown in Fig. 1.

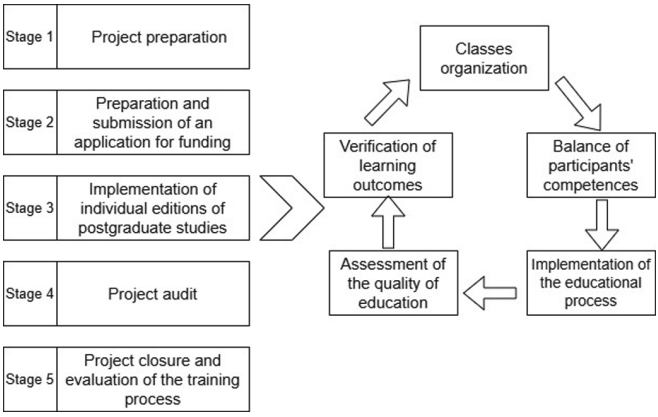

Fig. 1. Management cycle of an educational project co-financed by the European Union (source: own elaboration)

The project preparation process (stage 1) included analyzing the training needs of future participants, formulating the goal and scope of the project, and defining the target group. The work related to the development of the project funding application (stage 2) included: formulating the concept of education for postgraduate studies in the IT and management profile, conditions of participation, recruitment rules, organization of the educational process, and rules for verification of education results. As part of the project, the postgraduate studies "IT project management in the e-business environment" and "Knowledge management using modern technologies and information systems" were organized and conducted in a total of fourteen editions (stage 3). Within the fourteen editions, 560 people were trained over three years. It is worth highlighting that, in addition to meeting the substantive criteria, the organization implementing the project was required to professionally activate people over 45 years of age, as well as to observe the principle of equal opportunities for women and men in the recruitment process. In each edition of the postgraduate studies, the conditions

for participation were higher education, and the requirement was for at least 60% of women and at least 15% of people over 45 years of age. The participants showed similar characteristics, most of them were directly or indirectly related to IT. Some of them managed projects, others were analysts, still others were testers, there were also those who worked, for example, in accounting, but used data from IT systems as end users. They were certainly not programmers, but they had professional experience and an understanding of various data and processes. Their goal was to change the industry or use acquired skills in IT projects of which they were members. The turnover among instructors over the 3 years was insignificant.

The third stage of the project was cyclical. It included: the preparation of a training schedule within the individual editions of studies, development (verification) of syllabuses of didactic classes, recruitment of lecturers, promotion, recruitment and qualification of candidates, balance of participants' competencies, implementation of didactic classes, assessment of the quality of teaching and verification of education effects. As part of the project, systematic research was conducted on the analysis and evaluation of the competencies acquired by the participants. The last two stages focused on project audit and evaluation.

3.2 VLC Method Characteristic

The innovative educational platform, "Virtual Computer Laboratories" (VLC), is the result of this paper. This package includes tutoring software that supports the teaching of ICT technologies. It features typical modules specific to LMS, LCMS, and VCS software, while also introducing completely new functionalities. These include career counseling to help students select an educational program based on their competencies, personalized study paths through the selective choice of laboratory exercises, and remote progress monitoring. The individualization of the curriculum is based on the level of advancement, adapted to the specific topic determined by the system based on the tasks performed by the student. For example, for people who have basic skills in designing database systems, it is reasonable to reduce the number of exercises intended to learn the basics of SQL semantics and syntax. In return, these people may be offered advanced exercises in the field of client-server application programming, during which it will be possible to extend the classic elements of the SQL language course. In other words, the traditional concept of teaching ICT technologies containing the classic division of the group type: "basic group / advanced group" will be replaced by the method of creating original laboratory class paths.

The VLC educational platform uses virtual machines to simulate database servers and data warehouses for laboratory exercises. These exercises consist of a project description, a scenario, and step-by-step instructions. Students interact with virtual application servers, which allows them to continuously verify and control their work in a professional database management system environment. Tasks include configuring roles and authorizations, writing T-SQL scripts, and managing data migration in distributed systems. The platform provides real-time feedback on exercise performance.

The project work was focused on the following:

- Development of a new method of teaching ICT technologies, the result of which is the active participation of the course participant through sequential performance of laboratory exercises in the virtual environment. The mechanism for controlling the training process (virtual tutor) will activate subsequent laboratory tasks (educational objects) according to the current progress of the trainee and the assumed goals and effects of education (educational process maps). The adopted methodological concept of teaching advanced ICT technologies and the platform architecture therefore exclude passive participation of the course participant.
- Application of knowledge engineering systems for the development of an intelligent tutor mechanism: The research was initiated by the analysis and assessment of the possibilities of using machine learning techniques and semantic networks to implement a virtual tutor mechanism. As part of the project, a model of information flow, decisions, and control between logically and physically related educational objects (educational process maps) was developed. The possibility of a graphical representation of the educational process map using open standards was also provided including XHTML (Extensible HyperText Markup Language), SVG (Scalable Vector Graphics), and SMIL (Synchronized Multimedia Integration Language).

3.3 The Impact of Artificial Intelligence in VLC Method

Training materials are stored as educational objects, each with metadata that defines the relationship between course elements, including descriptions, complexity, recommendations, and assessment criteria. These objects are linked to their predecessors and successors, allowing the creation of personalized educational process maps. The VLC platform prototype includes tools for searching, selecting, and filtering educational objects, as well as analyzing their effectiveness for specific courses. Educational objects are described using XML, and their specifications will be freely available to future course creators.

Virtual Tutor is a mechanism controlled by artificial intelligence. Before starting to work on the VLC platform, the virtual tutor function was temporarily dormant, and the configuration of the provided content was the default (all participants used the same content). After starting to work in the platform, the output data from the individual platform modules were the input data for the AI as part of training the model. Each thematic part of the course was divided into tasks, and after training in each part, the student had to take a test to move on to the next part. The student's identifier, task number, and test result were the training data for the AI as part of the virtual tutor. These results could be binary (0 or 100% for the task) or represent the ratio of correctness of task performance according to the programmed evaluation criteria. After going through the first part of the course in the full thematic scope, the training of the output data from the partial tests was carried out. The algorithm assigns the results of the

exercises to thematic parts to propose appropriate tasks in the second part of the course. If the student demonstrates a good level of knowledge in a given subject area, tasks in this area will appear less frequently in the future. Similarly, if the algorithm identifies a subject area as problematic for the student, it is practiced by selecting more frequent tasks in this area. The next partial tests are further data training for the model, so that the student receives content appropriate to his level. Of course, course elements with which the student copes well also appear in the course, but with a much lower frequency than standard, so that the student can consolidate a given issue and not forget about it. The virtual tutor has information on the specific subject area of the tasks (type/subtype) and information about their level of difficulty. A system implemented in this way allows you to focus only on the essential elements.

The virtual tutor also works with course moderators, who can introduce their own cognitive rules based on their expertise and learning goals. This allows for the creation of personalized courses that align with both the mentor's goals and the learner's competencies.

Supervised learning techniques were used through the implementation of semantic networks to classify the students' questions and answers in a given area into a specific level of advancement. In addition, reinforcement learning was used so that the system could dynamically decide what material to offer the student at a given time. The system is designed to learn which activities bring the best results for a specific student and dynamically adapt the tasks to their needs.

3.4 Methods of Verifying Educational Results

The verification of the results after the project implementation was carried out in three ways:

– The most measurable verification method was the quantitative method, comparing the course results to the results of a previous year's course with the same thematic structure but without the support of the VLC method. The students were given an exam task that consisted of creating a database system for any company. The task included: formulating the purpose and scope of the project, specification of requirements, implementation of the physical model of the database, and the construction of T-SQL scripts (views, data validation rules, triggers, stored procedures, transactions). The exam project task was mandatory for all participants in studies. It was verified and evaluated by lecturers and external experts. An average of the student's grades was taken and compared with the average of the student's grades from the previous year. In general, the study involved 192 people - 96 students from 8 random laboratory groups in the academic year before the new method was implemented and 96 students in the academic year after it was implemented. In the previous year (before the VLC implementation), there were 63 women and 33 men, while in the following year, 65 women and 31 men. The number of people over 45 years of age - 32 and 37 people, respectively.

- A survey was conducted among the course participants and conclusions were drawn. This survey was conducted using the in-depth interview method. Due to the lack of conditions for conducting in-depth surveys among all participants, a decision was made to conduct them in two random laboratory groups, which is why it was based on the answers of 24 random people - 13 women and 11 men. The purpose of this survey was to collect opinions about working with the VLC platform as a tool to supplement education in post-graduate studies. The survey included the following prompts:
  - List the advantages of the e-learning platform.
  - List the disadvantages of this platform.
  - How many hours did you spend using the platform during the course?
  - Do you intend to use similar educational solutions in the future?
- An expert panel composed of five professionally involved experts in conducting training in the broadly understood field of IT discussed the proposed method to allow for a holistic teaching approach and what makes it so.

4 Results

As mentioned in the previous section, the method was verified by analyzing an expert panel, student satisfaction surveys, and the final test results. The summary of this is given below.

4.1 Expert Panel Results

The result of the expert panel is that the fundamental advantages of the computer-aided teaching of computer science using the VLC educational platform prototype, proving its holistic approach to e-learning, include:

- Interactive implementation of laboratory exercise programs.
- Educational content management mechanism- object repository and educational process maps.
- Leverage of artificial intelligence in the teaching process (virtual tutor).

4.2 Satisfaction Survey Results

The survey, conducted with approximately 560 students over 3 years of post-graduate studies, highlighted the effectiveness of the virtual application server environment. Students appreciated the simplicity of using an IBM PC to work in a multi-user setting, process large data sets, and test program scripts and security. Interactive laboratory exercises allowed students to create a "skeleton" of their future system and formed the basis for design tasks. The VLC platform also supported error correction, enabling students to restore previous states and continue work, which was not possible in traditional courses, where errors could result in losing progress. Furthermore, respondents indicated that the greatest

advantage of the proposed solution was the ability to create and test database systems without the need to install and configure the appropriate server infrastructure. This undoubtedly encouraged students to work on the VLC platform.

The main drawback was the limited scope of teaching materials available in the prototype version of the platform. However, the students appreciated the ability to create and test database systems without the need for server setup. They were interested in using a similar platform for both IT and non-IT training. In general, the students spent about 50% of their education using the platform.

4.3 Exam Results

The results of course completion (Table 1) indicate the following:

- When analyzing the points for all elements of the completion, the average score increased by 16%, a median rise of 18%, and a mode increase of 12% compared to the previous year.
- Focusing on elements practiced more on the VLC platform, the average score rose by 24%, the median by 25%, and the mode surged by 66%.

A detailed analysis shows that results improved significantly (over 10%) in five of the eight aspects. Table 2 summarizes grades, and Table 3 lists the completion points. The results are as follows:

- construction of data correctness control mechanisms (rules, scripts) - by an average of 25%;
- creating data views based on a set of reference tables (views) - by an average of 27%;
- data processing methods using stored procedures and triggers - by an average of 21%;
- transaction management techniques - by an average of 19%;
- security procedures (authentication, authorization, access control) - by an average of 26%.

Based on the exam results, it can be concluded that people using the VLC platform obtained significantly better final grades. The results are correlated with the appropriate course elements that were provided on the VLC platform. The results of these elements that were not included in the platform did not change significantly.

An important observation is that all of the above criteria were practiced within the VLC platform using interactive training and in total consumed almost 94% of the time of the entire training module. This may indicate the effectiveness of the VLC platform in improving competencies.

Table 1. General course completion results in points (source: own elaboration)

Result type	Each course parts		Trend	Parts of the course included in training within the VLC platform		Trend
	traditional course	trad. course + work in VLC		traditional course	trad. course + work in VLC	
Final points avg	75.36	87.71	116%	49.84	61.98	124%
Final points median	74.38	87.88	118%	49.50	61.88	125%
Final points mode	72.50	81.25	112%	38.50	63.75	166%

Table 2. Detailed course completion results presented through grades (source: own elaboration)

Criteria for evaluating course	Grades average		Trend	Grades median		Trend	Grades mode		Trend
	trad. course	trad. course + work in VLC		trad. course	trad. course + work in VLC		trad. course	trad. course + work in VLC	
Clarification of the project's purpose and scope, along with the specification of functional requirements	4.25	4.23	100%	4.00	4.00	100%	4	4	100%
Design of a physical database model (specification of tables and reference connections)	4.44	4.46	100%	4.50	4.50	100%	4.50	4.50	100%
Mechanisms for checking data correctness (rules, scripts)	3.83	4.77	125%	4.00	5.00	125%	3.00	5.00	167%
Perspectives (reporting based on a set of related data tables)	3.88	4.92	127%	4.00	5.00	125%	4.00	5.00	125%
Implementation of data processing mechanisms (stored procedures, triggers)	4.02	4.88	121%	4.00	5.00	125%	4.00	5.00	125%
Transactions	3.75	4.48	119%	4.00	4.50	113%	4.00	5.00	125%
Security procedures (authentication, authorization, access control)	3.48	4.40	126%	3.50	4.50	129%	3.00	5.00	167%
Project documentation (description of the physical model of the database and T-SQL scripts)	4.10	4.25	104%	4.00	4.25	106%	4.00	5.00	125%

Table 3. Detailed course completion results in points (source: own elaboration)

Criteria for evaluating course	Max. points	Points avg		Trend	Points median		Trend	Points mode		Trend
		trad. course	trad. course + work in VLC		trad. course	trad. course + work in VLC		trad. course	trad. course + work in VLC	
Clarification of the project's purpose and scope, along with the specification of functional requirements	6.00	4.88	4.82	99%	4.75	4.75	100%	4.50	4.50	100%
Design of a physical database model (specification of tables and reference connections)	15.00	12.88	12.88	100%	13.25	13.25	100%	13.25	13.25	100%
Mechanisms for checking data correctness (rules, scripts)	20.00	14.49	18.32	126%	14.25	18.50	130%	11.25	17.50	156%
Perspectives (reporting based on a set of related data tables)	10.00	7.32	9.38	128%	7.63	9.38	123%	7.75	9.25	119%
Implementation of data processing mechanisms (stored procedures, triggers)	17.00	13.00	15.77	121%	13.00	15.75	121%	13.00	15.75	121%
Transactions	10.00	7.15	8.54	119%	7.25	8.75	121%	7.75	8.75	113%
Security procedures (authentication, authorization, access control)	12.00	7.89	9.97	126%	8.25	10.50	127%	6.50	11.00	169%
Project documentation (description of the physical model of the database and T-SQL scripts)	10.00	7.77	8.03	103%	7.75	8.13	105%	7.75	9.25	119%

5 Conclusion

In the author's solution - in addition to the classic functionalities of LMS, LCMS, and VCS software - mechanisms using artificial intelligence techniques were implemented for the selection of educational content depending on the didactic goals set by the mentor, as well as the competency profile of the trainee. The concept of "intelligent" selection of educational content using a set of cognitive rules (virtual tutor) and activation of people over 45 years of age is characterized by innovation to classic forms of teaching. Pilot studies show that platforms such as Moodle and ILIAS are commonly used for teaching materials, but lack interactivity. In contrast, VLC enables interactive laboratory exercises in a dynamic virtual environment, helping students design IT systems and ensuring correct execution. Unlike traditional LMS, LCMS, and VCS, VLC offers flexible course design by combining educational objects to meet specific training goals and trainee needs. Unlike traditional LMS, LCMS, and VCS platforms, the VLC platform allows for dynamic, adaptive course creation, such as designing an SQL course and extending it with advanced topics such as database server programming. It is worth recalling that a large number of stationary and on-line

courses offered by commercial training companies are available on the market. However, to obtain real professional competencies, e.g. in the field of database system design, participation in a several-hour course or its online substitute is not enough. Acquiring ICT competency requires practice, performing a series of laboratory exercises, and multiple validation and testing of applications.

In summary, the new proposed teaching method:

- Has a positive impact on the quality of training, as evidenced by the course completion results;
- Is positively received by participants - as confirmed by the survey results;
- Enables a holistic teaching approach by interactive implementation of laboratory exercise programs, educational content management mechanism- object repository, educational process maps, and leverage of artificial intelligence in the teaching process.

In conclusion, tests of the educational platform prototype confirmed validity of the proposed teaching concept and set the directions for further work.

In the future, the following are planned: conducting research on the ergonomics of the graphical user interface, adapting the platform to the needs of people with disabilities following the Web Content Accessibility Guidelines, developing a commercial version of the software, increasing the number of available courses, and developing a manual for future training creators.

Acknowledgements. This paper was co-financed under the research grant of the Warsaw University of Technology supporting the scientific activity in the discipline of Civil Engineering, Geodesy and Transport.

References

1. Şimşek, A., Batar, Ş.B., Saypınar, M.S., Çakmak, F.: Evaluating the usability of a virtual classroom application from the educator perspective. Manisa Celal Bayar Üniversitesi Eğitim Fakültesi Dergisi **12**(1), 46–65 (2024)
2. Dreheeb, A.E., Basir, N., Fabil, N.: Impact of system quality on users' satisfaction in continuation of the use of e-learning system. Int. J. e-Educ. e-Bus. e-Manag. e-Learn. **6**(1), 13 (2016)
3. Robinson, B.: Harnessing AI for structured learning: the case for objective-driven design in e-learning. In: International Journal on E-Learning, pp. 457–470. Association for the Advancement of Computing in Education (AACE) (2024)
4. Vaughn Malcolm Bradley: Learning management system (LMS) use with online instruction. Int. J. Technol. Educ. **4**(1), 68–92 (2021)
5. Rustamov, S.: Conceptual basis of the development of the educational system based on modern information technologies. Int. J. Sci. Technol. **1**(2), 110–113 (2024)
6. Caglar-Ozhan, S., Altun, A., Ekmekcioglu, E.: Emotional patterns in a simulated virtual classroom supported with an affective recommendation system. Br. J. Edu. Technol. **53**(6), 1724–1749 (2022)
7. Yadav, S.K., Bharadwaj, B., Pal, S.: Data mining applications: a comparative study for predicting student's performance. arXiv preprint arXiv:1202.4815 (2012)

8. Tyagi, K., Rane, C., Sriram, R., Manry, M.: Unsupervised learning. In: Artificial intelligence and Machine Learning for EDGE Computing, pp. 33–52. Elsevier (2022)
9. Fahad Mon, B., Wasfi, A., Hayajneh, M., Slim, A., Abu Ali, N.: Reinforcement learning in education: a literature review. Informatics **10**, 74. MDPI (2023)
10. Salau, L., Hamada, M., Prasad, R., Hassan, M., Mahendran, A., Watanobe, Y.: State-of-the-art survey on deep learning-based recommender systems for e-learning. Appl. Sci. **12**(23), 11996 (2022)
11. Md Afroz Alam: From teacher-centered to student-centered learning: the role of constructivism and connectivism in pedagogical transformation. J. Educ. **11**(2), 154–167 (2023)
12. Sweller, J.: The development of cognitive load theory: replication crises and incorporation of other theories can lead to theory expansion. Educ. Psychol. Rev. **35**(4), 95 (2023)
13. Zięba, M.: Wykorzystanie platformy moodle na wydziale zarządzania i ekonomii politechniki gdańskiej-studium przypadku. e-mentor **4** 33–36 (2010)
14. Rebukha, L., Polishchuk, V.: Ukrainian society and Covid-19: the influence of the pandemic on educational processes in higher school. Postmodern Openings/Deschideri Postmoderne **11**(2) (2020)
15. Calderon-Valenzuela, J., Payihuanca-Mamani, K., Bedregal-Alpaca, N.: Educational data mining to identify the patterns of use made by the university professors of the moodle platform. Int. J. Adv. Comput. Sci. Appl. **13**(1) (2022)
16. Alabi, T.O., Thaddeus, H., Falode, O.C., Chukwuemeka, E.J.: Effects of ILIAS online learning platform on academic achievement in educational technology among university students in Nigeria (2020)
17. Castelló, A., Iserte, S., Belloch, J.A.: Accessible c-programming course from scratch using a MOOC platform without limitations. In: 4th International Conference on Higher Education Advances (HEAD'18), pp. 1197–1204. Editorial Universitat Politècnica de València (2018)
18. Campanella, P.: LMS: benchmarking Atutor, Moodle and Docebo. In: 2022 20th International Conference on Emerging eLearning Technologies and Applications (ICETA), pp. 85–90. IEEE (2022)
19. Murtaza, M., Ahmed, Y., Shamsi, J.A., Sherwani, F., Usman, M.: Ai-based personalized e-learning systems: issues, challenges, and solutions. IEEE access. 10:81323–81342 (2022)
20. Bozkurt, A., Karadeniz, A., Baneres, D., Guerrero-Roldán, A.E., Rodríguez, M.E.:Artificial intelligence and reflections from educational landscape: a review of AI studies in half a century. Sustainability **13**(2), 800 (2021)
21. Murtaza, M., Ahmed, Y., Shamsi, J.A., Sherwani, F. and Usman, M.: Ai-based personalized e-learning systems: Issues, challenges, and solutions. IEEE Access **10**, 81323–81342 (2022)
22. Mazon-Fierro, M., Mauricio, D.: Usability of e-learning and usability of adaptive e-learning: a literature review. Int. J. Hum. Fact. Ergon. **9**(1), 1–31 (2022)
23. Chookaew, S., Panjaburee, P., Wanichsan, D., Laosinchai, P.: A personalized e-learning environment to promote student's conceptual learning on basic computer programming. Proc. Soc. Behav. Sci. **116**, 815–819 (2014)
24. Panjaburee, P., Komalawardhana, N., Ingkavara, T.: Acceptance of personalized e-learning systems: a case study of concept-effect relationship approach on science, technology, and mathematics courses. J. Comput. Educ. 1–25 (2022). https://doi.org/10.1007/s40692-021-00216-6

25. Rahayu, N.W., Ferdiana, R., Kusumawardani, S.S.: A systematic review of ontology use in e-learning recommender system. Comput. Educ. Artif. Intell. **3**, 100047 (2022)
26. Alshmrany, S.: Adaptive learning style prediction in e-learning environment using levy flight distribution based CNN model. Clust. Comput. **25**(1), 523–536 (2022)
27. Iserte, S., Tomás, V.R., Pérez, M., Castillo, M., Boronat, P., García, L.A.: Complete integration of team project-based learning into a database syllabus. IEEE Trans. Educ. **66**(3), 218–225 (2022)
28. mapadotacji.gov.pl. https://mapadotacji.gov.pl/projekty/667744/. Accessed 15 Feb 2025

Exploring AI Applications in Business: Case Studies on Key Competencies for Professionals

Aleksandra Kopyto[1(✉)], Mahtab Afsari[2], and Bartosz Wachnik[1]

[1] Warsaw University of Technology, Warsaw, Poland
aleksandrakrupa811@gmail.com
[2] IU International University of Applied Sciences, Berlin, Germany

Abstract. Artificial Intelligence (AI) is transforming business operations across various industries, requiring professionals to develop new competencies. This study explores AI applications in business through case studies, identifying key competencies essential for AI project teams. The research highlights the interdisciplinary nature of AI projects, emphasizing the need for both technical and soft skills, including communication, leadership, and adaptability. Using a case study methodology, the study examines real-world AI implementations, revealing competency gaps among business professionals. The findings suggest that structured training programs and interdisciplinary collaboration are crucial for successful AI integration. Additionally, the study underscores the importance of AI governance, ethical considerations, and compliance with regulatory frameworks. The results contribute to the development of competency models for AI project teams.

Keywords: AI skills · Professional Competencies · Business Applications

1 Introduction

AI projects represent a distinct category of IT projects, characterized by several key features:

1. High Level of Uncertainty. AI projects exhibit a significantly higher degree of uncertainty compared to traditional IT projects. This is due to the fact that AI research and development outcomes are difficult to predict, and achieving the desired model accuracy often requires iterative experimentation [1].
2. Required Interdisciplinarity. AI projects necessitate collaboration between specialists from diverse fields. Effective communication and integration of knowledge from various domains are crucial for the success of AI initiatives [2].
3. Experimentation. AI projects closely resemble scientific experiments, where hypotheses are formulated and tested to verify their validity. They require an approach based on experimentation, flexibility, and a readiness to pivot based on observed results [3].

Research on AI project methodologies is still in its early stages. There is a visible trend of adapting existing IT methodologies to AI projects. However, a key area requiring further exploration is the development of methodologies that reflect the unique

M. Paszynski et al. (Eds.): ICCS 2025 Workshops, LNCS 15912, pp. 320–332, 2025.
https://doi.org/10.1007/978-3-031-97573-8_22

characteristics of AI projects. Defining the necessary competencies of AI project team members is a crucial element in developing AI project methodologies. Consequently, researchers focusing on AI project methodologies emphasize the importance of identifying the required competencies within project teams. The primary objective of this study is to identify and analyze competency gaps among AI project team members, enabling the development of recommendations regarding roles and required skills within AI project execution methodologies.

This study employs two scientific methods: literature analysis, based on a review of academic articles, industry reports, and case studies. The results of the literature analysis reveal a knowledge gap concerning the competencies required for AI project team members. Additionally, case studies highlight specific competency gaps among individual project team members, which may ultimately widen the information gap on the client side during IT project implementation [4].

The conclusions drawn from this research will contribute to both the development of recommendations regarding the necessary competencies for AI project teams within AI project methodologies and the formulation of training plans for specialists, as well as curricula for higher education institutions.

2 Literature Review

Artificial Intelligence (AI) has become a critical component in transforming business operations across various sectors. In business management, e-commerce, and finance, AI applications are extensively utilized to boost efficiency and enhance consumer interactions. By analyzing transaction data, AI systems can identify fraudulent activities and help in making informed investment decisions, ultimately maximizing profits and enhancing security measures [5]. Marketing is another domain where AI's impact is profoundly felt. As AI technologies continue to develop, they expand the scope for their application, offering competitive advantages to organizations that embrace their potential in revolutionizing traditional marketing methodologies [6].

Arman and Lamiyar [7] delve into the functions of AI within the business realm. The paper emphasizes the importance of considering both the advantages and limitations of AI adoption in business, as well as the ethical and legal implications of its use. Menzies and colleagues [8] explore the applications, benefits, and challenges associated with utilizing AI in business. The authors note that AI prompts changes in workplace configurations and necessitates organizational and staffing adjustments in response to this technology. Hamadaqa and colleagues [9] discuss the role and functionalities of AI in business. The article ultimately offers recommendations for effectively implementing AI solutions to maximize benefits while navigating potential challenges. Chowdhury [10] examines the role of AI in business. The paper discusses how the intersection of artificial intelligence (AI), machine learning (ML), and blockchain technology is reshaping contemporary business operations. The author investigates the collective impact of these technologies on enhancing efficiency, transparency, and strategic advantages within organizations. Petrescu and colleagues [11], explore the role of AI and its application in business. This research systematically examines the impacts of AI in customer-centric retail applications based on the ecosystem value creation framework. This study can

also assist managers in determining suitable conditions for AI use. Yang and colleagues [12] discuss the uses of AI in business. The findings identify six key factors in AI adoption, including technological affordances and constraints, innovation management approaches, AI readiness, the competitive environment, and regulatory environments. The findings clarify that factors such as the competitive environment and regulatory frameworks play crucial roles in the scale and depth of AI adoption. Company size has significant effects on how challenges of AI adoption are addressed.

2.1 Definition of AI

Various definitions of Artificial Intelligence (AI) have been introduced to help distinguish it from conventional information technologies. To fully understand AI, it is essential to break down its two main components: "artificial" and "intelligence". The term "intelligence" encompasses cognitive functions such as understanding, learning, and reasoning [13], while "artificial" refers to something that is manufactured by humans rather than occurring naturally [14]. AI can be described as the development of machines capable of mimicking human intelligence [15]. At its core, AI involves creating systems that imitate human-like abilities by functioning as intelligent agents, capable of processing and responding to environmental inputs in an informed manner [16]. Some scholars argue that AI should not depend on explicit programming to perform tasks considered intelligent [17]. Instead, AI must have the capacity to independently perceive, interpret, learn, plan, and take appropriate actions [17–19]. This implies that AI systems should be capable of processing external data, drawing meaningful insights, and using this knowledge to flexibly adapt in order to achieve specific objectives or complete complex tasks [20]. Crucially, this process should not be confined to rigid rules or pre-programmed sequences of actions [21].

In some contexts, AI is viewed as a type of automation in media consumption and creation [22], and it is sometimes classified as general AI, referring to intelligent systems designed for specific, limited functions, as opposed to systems exhibiting intelligence comparable to or exceeding that of humans [23].

AI is defined as "the process of creating computing machines and systems that perform operations analogous to human learning and decision-making" [24]. "Artificial intelligence (AI) is about emulating the human intelligence process by machines" [25]. AI is "a step-by-step process for performing repetitive actions, designing models, and solving technical problems without pre-existing concrete solutions" [26]. AI "refers broadly to computational systems that involve algorithms, machine learning methods, natural language processing, and other techniques that operate on behalf of an individual to improve communication outcome" [27].

Academics have explored the function of AI in business, along with developing concepts like Human-AI Interaction (HAII) and AI-driven communication, taking into account elements such as the source's perspective and social interactions enhanced by machine learning techniques [28, 29].

In this study, we conceptualize AI as the demonstrable, practical ability of non-biological machines or artificial systems to execute tasks, resolve issues, convey information, engage with their environment, and act rationally, emulating processes found in human beings.

2.2 Structure of the AI Project Team

Successful AI project implementation requires a multidisciplinary team [30]. Data scientists handle data analysis and algorithm selection. Machine learning engineers transform models into practical solutions. Business executives and analysts set goals and facilitate communication between business and tech teams. Data engineers provide clean data infrastructure, while domain experts offer industry-specific insights.

Team skills include leadership, mentoring, decision-making, and conflict resolution. A blend of soft and hard skills is crucial for effective project management [31]. Leaders should focus on skill development through training, ensuring organizational success. The structure of AI project teams should prioritize collaboration between humans and AI systems. Johnson and Vera [32] emphasize the importance of "teaming intelligence" for AI to work effectively with people. Webber et al. [33] propose using AI to improve team diagnostics and effectiveness, highlighting both advantages and challenges. Haller [34] stresses the need for efficient project management in AI teams, focusing on delivering results quickly with limited resources. Torre et al. [35] introduce a goal programming model for team formation that considers human-AI trust and technology acceptance. They propose an index measuring attitudes towards AI tools to ensure teams are receptive to machine-based decisions. Overall, these papers suggest that successful AI project teams should balance technical expertise with collaborative skills, efficient project management, and a positive attitude towards AI integration [32–35] A novel framework proposes using generative AI agents to model diverse team member roles, potentially leading to more dynamic collaborations [36]. Siemon [37] identifies four key roles for AI teammates: coordinator, creator, perfectionist, and doer. Miller [38] emphasizes the importance of considering passive stakeholders in AI projects, proposing six stakeholder roles. Ma et al. [39] investigate three AI roles in decision-making: Recommender, Analyzer, and Devil's Advocate, finding that each role has distinct strengths and limitations depending on AI performance levels.

2.3 Identification of the Knowledge Gap

While extensive research has been conducted on the operational capabilities of Artificial Intelligence (AI) in various business contexts, several gaps persist in the current theoretical frameworks used to evaluate these applications.

- **Human-AI Collaborative Dynamics:** Research on Human-AI Interaction (HAII) focuses primarily on operational efficiency [29], yet there is limited exploration of the collaborative dynamics between AI systems and human decision-makers. Theories on social interactions enhanced by AI lack empirical studies that investigate the cognitive and behavioral impacts on human teams working alongside AI.
- **Ethical and Societal Implications:** While there are definitions of AI as a technological force [26], there is insufficient theoretical grounding on the ethical considerations surrounding its use in business decisions.
- **Role of Soft Skills in AI Implementation:** While competencies such as communication and leadership are asserted as vital for AI project success, theoretical models do not fully explain how these skills interact with AI technologies to enhance team performance and project outcomes [25].

Addressing these theoretical gaps requires multidisciplinary research that merges insights from AI technology, business strategy, human-computer interaction, and ethics. Future studies should aim to build comprehensive frameworks that not only address these gaps but also offer actionable insights for businesses looking to leverage AI for competitive advantage.

3 Research Methodology

The main goal of the conducted research was to identify the key competencies of a group of business employees that are necessary for the proper execution of AI projects. The selected group of business employees can be characterized as follows:

- Employees acting as specialists, not managers.
- Employees without IT education.
- Employees working in production, logistics, finance, and marketing departments.
- Employees with basic experience in IT project implementation, i.e., ERP, CRM, DMS, BI, ECM as key users, internal consultants, project leaders in the area of functionality implementation.
- Employees without knowledge and experience in AI project implementation; most of them have not completed any AI projects.

The study posed research question:

Q1: "What key competencies should employees in the selected group of specialists possess to properly and effectively implement AI projects?".

In the research, the authors used the case study method. The research object is three IT system implementation projects that utilize AI. It should be emphasized that the authors of the research try to include the issues contained in the concept of E - environmental, S - social responsibility, G - corporate governance. The ESG concept assumes that an enterprise should not only care about its economic interest, but the business, including the projects implemented, should bring broadly understood benefits to all stakeholders, local communities, and the environment. The authors use the case study method because it allows them to develop existing theory and provide explanations for previously unrecognized issues. The choice of the research method by the authors – case study – mainly results from the early stage of development of theoretical and practical knowledge in the field of AI project implementation in business. The consequence is a knowledge gap in the areas of:

- AI project implementation methodologies.
- Understandable taxonomy of concepts used in AI projects.
- Theoretical and practical knowledge in the field of AI project implementation, including the identification of risk factors.
- Requirements resulting from EU AI Act, ISO/IEC 22989, ISO/IEC 23894, ISO/IEC TR 24030, ISO/IEC JTC 1/SC 42, ISO/IEC 25012.
- Required competencies of employees in the implementation of AI projects.

The selection of studied cases is carried out in deliberate mode. According to B. Flyvbjerg [40], there are five main criteria for selecting studied cases. Table 1 presents the criteria along with their characteristics in the context of the conducted research.

Table 1. Characteristic of the criteria for conducted research.

Criterion	Information regarding the fulfillment of the criterion
Data availability	Guaranteed
The vividness of the case clearly illustrating the examined regularities	Successfully completed projects utilizing various artificial intelligence models
Diversity of analyzed cases	The diversity of analyzed cases is expressed in the selection of: • Various artificial intelligence models • Client profile • Project implementation results • Competency diversity of employees
The critical nature of the phenomenon allowing for the formulation of a generalization	The identification and analysis of competencies required for AI project implementation should consider the main challenges in the following areas: 1. Technical knowledge regarding AI models 2. Methods for executing AI projects, which are characterized by uncertainty 3. Soft skills in communication and knowledge transfer related to AI project execution 4. Incorporating the perspective of sustainable growth (ESG) in AI project implementation
A metaphor directing the researcher's attention to a specific course of the examined phenomenon	An AI specialist in a company is like an alchemist who combines raw data, statistical models, and business principles to create valuable and unique solutions. Success depends on skillfully balancing technical knowledge, intuition, and experimentation

4 Research Findings and Interpretation

In Tables 2 and 3, we present the results of case studies conducted in three companies from the IT industry, the training and consulting sector, and a manufacturer of industrial electronics solutions. All analyzed AI projects involved either building a complete solution from scratch or utilizing available AI systems on the market.

Analyzing case studies, researchers indicate that competency gaps in AI projects primarily relate to four key areas:

- Project Management Skills in High-Uncertainty and Research-Oriented Environments. AI projects are characterized by a high degree of uncertainty and often exhibit features of research projects, where experimentation is a crucial process. According to researchers, a key competency for AI Project Managers is managing uncertainty

Table 2. Results of case study research, including the characteristics of the studied entities. Source: Own study

	Firm X	Firm Y	Firm Z
Company Profile	IT Company	Training company	Technology company
AI Project Company	An intelligent system for identifying risks and uncertainties in IT projects through financial, technical, logistical, and organizational analysis. It uses agent-based modeling to analyze formal documents and team communication (emails, online meetings), including sentiment and emotion analysis	An intelligent, integrated platform for creating online AI training programs	AI project aimed at improving industrial manufacturing through predictive maintenance, supply chain optimization, production automation, and data-driven product development
Used tools	NLP, OCR, Machine Learning, Anomaly Detection (AI), Predictive Analytics	Adaptive Learning Systems, NLP, Chatbots, sentimental analysis platforms, automated reporting tools, AI analytical tools	Machine Learning Algorithms, Computer Vision and Machine Vision Systems, Robotics and AI-driven Automation Systems, Big Data Analytics Platforms, IoT-enabled Sensors and Smart Devices
Project Duration	12 months	6 months	over multiple years
Project Methodology	Uses a hybrid AI implementation methodology combining Waterfall (for planning and integration) with Agile (for developing AI features and sentiment analysis). Enables flexibility, ongoing user feedback, and early problem detection	Focuses on a structured methodology starting with training needs analysis, target group definition, and content planning. Followed by implementation, training delivery, evaluation, and post-training support	Implements AI in manufacturing through a structured process: data collection from IoT, AI model development, deployment in production and supply chain, and ongoing performance optimization

Table 3. Results of case study research. Source: Own study

	Firm X	Firm Y	Firm Z
List of project member	Product Owner AI Engineer/Data Scientist Data Analyst Risk Management Expert Construction Expert Software Developer DevOps Specialist UX/UI Designer Sentiment Analysis Expert QA Tester Project Manager/Scrum Master	Project Manager AI Consultant Potential Trainees End User	AI Engineers & Data Scientists Experts Software Developers Supply Chain Analysts Quality Control Specialists Project Managers

(*continued*)

Table 3. (*continued*)

	Firm X	Firm Y	Firm Z
Key, prioritized Competencies for Each Role in the Analytical and Implementation Phase of IT Projects	**Product Owner** Understands business and IT, manages and prioritizes requirements, communicates with stakeholders, and bridges business and tech teams **AI Engineer/Data Scientist** Expert in ML/DL and big data analysis, runs AI experiments, optimizes models, and aligns results with business goals **Data Analyst** Skilled in SQL, Python, R, and BI tools; identifies KPIs, visualizes data clearly, and collaborates with IT/business teams **Risk Management Expert** Manages IT and cybersecurity risks, ensures regulatory compliance, analyzes risk areas, and creates mitigation strategies **Software Developer** Experienced in Python, Java, C#, JS; develops microservices, solves coding issues, and collaborates with QA and analysts **DevOps Specialist** Automates CI/CD (e.g., Jenkins), manages cloud infrastructure, improves system performance, and ensures IT security **UX/UI Designer** Designs user-friendly interfaces (Figma, Adobe XD), conducts UX research, builds prototypes, and works with front-end teams **Cybersecurity Specialist** Secures IT systems, analyzes threats, handles incidents, and ensures compliance with security standards (e.g., ISO 27001) **Sentiment Analysis Expert** Uses NLP for analyzing emails and chats, detects emotional patterns, and works with AI/analytics teams to assess communication risks **QA Tester** Performs functional and automated testing, validates software compliance, optimizes testing flows, and reports bugs **Project Manager/Scrum Master** Leads projects with Agile/Scrum/Kanban, plans sprints, tracks progress, resolves team issues, and manages priorities and stakeholders	**Project Manager** Understands business needs, prioritizes tasks, oversees training preparation and delivery, and monitors progress **AI Consultant** Provides technical expertise, answers participant questions, refines training based on data, and supports trainers **Potential trainees** Participate in training, give feedback, ensure knowledge transfer, and help tailor methods to learner needs	**AI Engineers & Data Scientists** Experts in machine learning, deep learning, neural networks, and data modeling **Industrial Automation Experts** Skilled in robotics, control sys tems, and AI-based process op timization **Software Developers** Proficient in programming (Python, Java, C++), with experience in integrating AI into industrial systems **Supply Chain Analysts** Experienced in demand forecasting, big data analytics, and AI-supported decision-making **Quality Control Specialists** Work with computer vision, defect detection, and automated quality assurance **Project Managers** Strong leadership and planning skills, with knowledge of AI implementation in industrial environments

and adopting an experimental approach. AI projects often require an iterative approach, where initial results are difficult to predict, and model effectiveness depends on data quality and tested algorithms. Therefore, AI Project Managers must be able to manage experiments, accept unpredictability, and adapt project timelines and scope based on test results.

- Managing Interdisciplinary Teams. Researchers emphasize the importance of teamwork in AI projects under conditions of strong interdisciplinarity. AI projects require collaboration between Data Scientists, AI Engineers, business experts, and data analysts, which is not typical for traditional IT projects. AI Project Managers must be able to coordinate interdisciplinary teams, understand different perspectives, and translate technical results into business language.
- Communication Skills in High-Uncertainty and Interdisciplinary Environments. In AI projects, engineers, Data Scientists, and IT specialists use technical jargon that may be incomprehensible to managers and business stakeholders. A crucial competency is the ability to simplify complex technical concepts and present them in an accessible manner to different audiences. Researchers highlight that the ability to ask the right questions and engage in active listening allows for a better understanding of business and technical needs while preventing misunderstandings. According to research, these communication skills require new competencies that are not as commonly found in traditional IT projects. Scientific studies suggest that the proportion of individuals with Asperger's syndrome may be higher among engineers and programmers compared to the general population, making communication skills particularly crucial in AI project execution [41].
- Skills related to Ethics and Regulatory Compliance. While ethics and regulatory issues are important in IT projects, they become particularly critical in AI, especially in the context of algorithmic bias, compliance with regulations (e.g., AI Act), and model interpretability. Researchers emphasize that AI Project Managers must possess the ability to identify and manage ethical risks while implementing responsible AI development principles such as XAI (Explainable AI). Additionally, they should have the competencies to lead projects in accordance with ethical and regulatory frameworks within the project team.

Researchers argue that it is necessary to develop a competency model for AI project team members as an integral part of AI project methodologies. The competency model should include:

1. Definition of Key Roles in AI Projects and Their Responsibilities. Identifying essential roles in AI project teams and specifying the required competencies for each role.
2. Determining Proficiency Levels for Each Competency. Defining the required skill levels across different levels of expertise (e.g., beginner, intermediate, expert).
3. Interdisciplinary Competency Connections. Identifying common competency areas between technical, analytical, and managerial roles that enhance collaboration efficiency in AI projects.
4. Soft and Managerial Skills. Including communication skills, the ability to work in high-uncertainty conditions, adaptability, and decision-making based on experimental outcomes.

5. Recommendations for Competency Development. Developing career paths for AI team members, outlining training methods, certifications, and best practices for improving key skills.
6. Guidelines for Competency Assessment and Validation in Practice. Establishing tools and methods for evaluating team members' competencies, such as certification systems, practical tests, pilot project assessments, and AI problem simulations.

The competency model should be integrated into AI project methodologies, including CRISP-DM, Agile AI, and Lean AI, ensuring a structured approach to AI project execution.

5 Discussion and Conclusion

The goal of the conducted research was to identify the key competencies of a group of business employees that are necessary for the proper execution of AI projects. This study identifies key competencies for AI project implementation in business, emphasizing both technical and non-technical skills. AI engineers require expertise in machine learning and programming, while business analysts and managers need analytical and communication skills. Soft skills, including leadership and adaptability, are also crucial for successful AI adoption.

A major challenge is the lack of AI-specific knowledge among business employees, leading to inefficiencies. AI governance complexity, compliance with regulations, and ethical concerns also pose significant barriers, necessitating robust frameworks. Businesses should establish cross-functional teams, combining the expertise of data scientists, IT professionals, and business leaders, to ensure a holistic implementation of AI solutions. Policymakers should establish standardized AI competency guidelines through industry-academic collaboration. Furthermore, investing in continuous learning and development programs can empower employees to effectively leverage AI tools, thereby enhancing innovation and productivity.

Interdisciplinary collaboration and governance frameworks are essential for effective AI adoption. Businesses must actively foster an AI-ready workforce by implementing skill development initiatives and fostering cross-functional cooperation. Strategic alignment of AI projects with business goals ensures better integration and maximizes benefits. Additionally, ethical considerations should remain central in AI deployment, requiring transparency, fairness, and accountability in decision-making processes. Ultimately, organizations that proactively invest in AI capabilities will gain a competitive edge, drive efficiency, and position themselves as leaders in an increasingly AI-driven business landscape. By fostering a culture of collaboration and innovation, businesses can effectively use AI to drive growth, improve customer experiences, and maintain a competitive edge in the fast-evolving digital landscape.

References

1. Forsythe, D., McDermott, R.: Managing Innovation: Learning from McKinsey and its Best Clients. Wiley, Hoboken (2017)

2. Ronanki, R., Nguyen, A.V.: Artificial intelligence for the real world. Int. Res. J. Mod. Eng. Technol. Sci. (2023)
3. Kohavi, R., Tang, D., Xu, Y.: Trustworthy Online Controlled Experiments: A Practical Guide to A/B Testing. Cambridge University Press, Cambridge (2020)
4. Wachnik, B.: Luka informacyjna w przedsięwzięciach informatycznych. Problemy i rozwiązania, Polskie Wydawnictwo Ekonomiczne, Warszawa, p. 27 (2020)
5. Pallathadka, H., Ramirez-Asis, E.H., Loli-Poma, T.P., Kaliyaperumal, K., Ventayen, R.J.M., Naved, M.: Applications of artificial intelligence in business management, e-commerce and finance. Mater. Today Proc. **80**, 2610–2613 (2021)
6. Haleem, A., Javaid, M., Qadri, M.A., Singh, R.P., Suman, R.: Artificial intelligence (AI) applications for marketing: a literature-based study. Int. J. Intell. Netw. **3,** 119–132 (2022)
7. Arman, M., Lamiyar, U.R.: Exploring the implication of ChatGPT AI for business: efficiency and challenges. Int. J. Mark. Digit. Creat. **1**(2), 64–84 (2023)
8. Menzies, J., Sabert, B., Hassan, R., Mensah, P.K.: Artificial intelligence for international business: its use, challenges, and suggestions for future research and practice. Thunderbird Int. Bus. Rev. **66**(2), 185–200 (2024)
9. Hamadaqa, M.H.M., Alnajjar, M., Ayyad, M.N., Al-Nakhal, M.A., Abunasser, B.S., Abu-Naser, S.S.: Leveraging artificial intelligence for strategic business decision-making: opportunities and challenges (2024)
10. Chowdhury, R.H.: The evolution of business operations: unleashing the potential of artificial intelligence, machine learning, and blockchain. World J. Adv. Res. Rev. **22**(3), 2135–2147 (2024)
11. Petrescu, M., Krishen, A.S., Gironda, J.T., Fergurson, J.R.: Exploring AI technology and consumer behavior in retail interactions. J. Consum. Behav. **23**(6), 3132–3151 (2024)
12. Yang, J., Blount, Y., Amrollahi, A.: Artificial intelligence adoption in a professional service industry: a multiple case study. Technol. Forecast. Soc. Change **201**, 123251 (2024)
13. Lichtenthaler, U.: An intelligence-based view of firm performance: profiting from artificial intelligence. J. Innov. Manag. **7**(1), 7–20 (2019)
14. Mikalef, P., Gupta, M.: Artificial intelligence capability: conceptualization, measurement calibration, and empirical study on its impact on organizational creativity and firm performance. Inf. Manag. (2021)
15. Wamba-Taguimdje, S.L., Wamba, S.F., Kamdjoug, J.R.K., Wanko, C.E.T.: Influence of artificial intelligence (AI) on firm performance: the business value of AI-based transformation projects. Bus. Process. Manag. J. **26**(7), 1893–1924 (2020)
16. Eriksson, T., Bigi, A., Bonera, M.: Think with me, or think for me? On the future role of artificial intelligence in marketing strategy formulation. TQM J. **32**(4), 795–814 (2020)
17. Demlehner, Q., Laumer, S.: Shall we use it or not? Explaining the adoption of artificial intelligence for car manufacturing purposes In: Proceedings of the 28th European Conference on Information Systems (ECIS) (2020)
18. Kolbjørnsrud, V., Amico, R., Thomas, R.J.: Partnering with AI: how organizations can win over skeptical managers. Strategy Leadersh. **45**(1), 37–43 (2017)
19. Wang, H., Huang, J., Zhang, Z.: The impact of deep learning on organizational agility. In: Proceedings of the 40th International Conference on Information Systems (ICIS), Munich, Germany (2019)
20. Makarius, E.E., Mukherjee, D., Fox, J.D., Fox, A.K.: Rising with the machines: a sociotechnical framework for bringing artificial intelligence into the organization. J. Bus. Res. **120**, 262–273 (2020)
21. Ninness, H.A.C., Ninness, S.K.: A scholarly definition of artificial intelligence (AI): advancing AI as a conceptual framework in communication research. Paper presented at the Annual Meeting of the Association for Education in Journalism and Mass Communication, San Francisco, California (2020)

22. Hepp, A.: Communicative robots and empathetic media: a typology of forms and their applications in everyday life. Media Cult. Soc. **42**(1), 1–13 (2020)
23. Ryan, M.: In AI we trust: ethics, artificial intelligence, and reliability. J. Responsible Innov. **7**(3), 482–486 (2020)
24. Castro, D., New, J.: The promise of artificial intelligence. Center Data Innov. **115**(10), 32–35 (2016)
25. Ng, D., Leung, M.: Challenges of emulation: AI versus human intelligence. Technol. Soc. **62**, 101296 (2020)
26. de-Lima-Santos, M.F., Ceron, W.: Artificial intelligence in news media: current perceptions and future outlook. Journal. Media **3**(1), 13–26 (2021)
27. Hancock, J.T., Naaman, M., Levy, K.: Where are we in data visualization education? Perspect. Real World **6**(4), 34–41 (2020)
28. Guzman, A.L., Lewis, S.C.: Artificial intelligence and communication: a human–machine communication research agenda. New Media Soc. **22**(1), 70–86 (2020)
29. Sundar, S.S., Lee, J.: Designing human-AI partnerships for human flourishing. In: Proceedings of the SIGCHI Conference on Human Factors in Computing Systems (CHI 2022), New Orleans, LA (2022)
30. Galsgaard, A., Doorschodt, T., Holten, A.L., Müller, F.C., Boesen, M.P., Maas, M.: Artificial intelligence and multidisciplinary team meetings; a communication challenge for radiologists' sense of agency and position as spider in a web? Eur. J. Radiol. **155**, 110231 (2022)
31. Stogiannos, N., et al.: A multidisciplinary team and multiagency approach for AI implementation: a commentary for medical imaging and radiotherapy key stakeholders. J. Med. Imaging Radiat. Sci. **55**(4), 101717 (2024)
32. Johnson, M.T., Vera, A.H.: No AI is an island: the case for teaming intelligence. AI Mag. 40 , 16–28 (2019)
33. Webber, S.S., Detjen, J., MacLean, T., Thomas, D., Team challenges: is artificial intelligence the solution? Bus. Horiz. (2019)
34. Haller, K.: Structuring and delivering AI projects. In: Haller, K. (ed.) Managing AI in the Enterprise, pp. 23–60. Apress, Berkeley (2022). https://doi.org/10.1007/978-1-4842-7824-6_2
35. Torre, D.L., Colapinto, C., Durosini, I., Triberti, S.: Team formation for human-artificial intelligence collaboration in the workplace: a goal programming model to foster organizational change. IEEE Trans. Eng. Manag., 1–11 (2021)
36. Chan, J., Li, Y.: Enhancing team diversity with generative AI: a novel project management framework. In: 2024 IEEE 48th Annual Computers, Software, and Applications Conference (COMPSAC), pp. 1648–1652 (2024)
37. Siemon, D.: Elaborating team roles for artificial intelligence-based teammates in human-AI collaboration. Group Decis. Negot. **31**, 871–912 (2022)
38. Miller, G.J.: Stakeholder roles in artificial intelligence projects. Proj. Leadersh. Soci. (2022)
39. Ma, S., Zhang, C., Wang, X., Ma, X., Yin, M.: Beyond recommender: an exploratory study of the effects of different AI roles in AI-assisted decision making. arXiv, abs/2403.01791 (2024)
40. Flyvbjerg, B.: Five misunderstandings about case-study research. In: Seale, C., Gobo, G., Gubrium, J.F., Silverman, D. (eds.) Qualitative Research Practice. Sage, Thousand Oaks (2004)
41. Migdał, P., Krawczyk, S.: Zespół Aspergera, nauki ścisłe i kultura nerdów. V Krakowska Konferencja Kognitywistyczna, 8–10 April 2011

The Use of the Chat GPT to Solve Mathematical Programming Tasks: A Didactic Experiment with the Participation of Warsaw University of Life Sciences Students

Włodzimierz Wojas(✉) and Piotr Stachura

Department of Applied Mathematics, Warsaw University of Life Sciences (SGGW), Nowoursynowska 159, 02-776 Warsaw, Poland
{wlodzimierz_wojas,piotr_stachura1}@sggw.edu.pl

Abstract. In this article, the authors present three didactic examples of using Chat GPT in mathematical programming optimization tasks: linear programming, nonlinear programming and convex programming. These examples are analyzed in terms of the correctness of the methods used and the solutions obtained. The article also describes a didactic experiment with the participation of Informatics and Econometrics students of Warsaw University of Life Sciences, consisting in solving optimization tasks on their own using Chat GPT. The final conclusions of the article also present a comparison of the approach based on the CAS methodology and the approach using Chat GPT.

Keywords: AI · Chat GPT · CAS · mathematical programming · optimization · mathematical didactic

1 Introduction

Chat GPT (Chat Generative Pre-trained Transformed) was developed by research organization OpenAI and launched in November 2022. It is available in online versions: a free version based on GPT-3.5 and more advanced commercial versions based on GPT-4 and GPT-4o [9,11]. Based on the LLM (Large Language Model), Chat GPT works by learning statistical language patterns from huge databases of online texts, which also contain various types of false information and outdated knowledge. It allows users to conduct and refine conversations, and subsequent answers, questions and suggestions are treated as context at every stage of the conversation. It can both download and create images, as well as use math and coding software [7,11,13,16]. Chatbots, in general, can generate fabricated information called hallucinations. The topic of using artificial intelligence, in particular Chat GPT, in teaching and learning various subjects - including mathematics and computer science - has been undertaken

M. Paszynski et al. (Eds.): ICCS 2025 Workshops, LNCS 15912, pp. 333–346, 2025.
https://doi.org/10.1007/978-3-031-97573-8_23

and widely discussed in recent years [1–6,10,12,14,15,17]. Assessing the usefulness of Chat GPT in learning and teaching mathematics requires solving a number of computational tasks from different areas, with different levels of difficulty, and analyzing obtained solutions. For example, in the article [15] a scan of solving a quadratic equation in a math lesson using GPT Chat is presented. The paper [17] contains scans from GPT Chat sessions presenting solving algebraic equations, calculating the limit of a function of one variable and elementary geometry tasks using the Pythagorean theorem.

Related articles highlight the educational utility of Chat GPT as a comprehensive tool that provides users with access to basic knowledge of mathematics and other fields, including access to basic definitions, methods, instructions and algorithms. On the other hand, attention was also drawn to Chat GPT's lack of deep understanding of some issues, as well as the lack of effective opportunities to correct its "false beliefs". It is also worth emphasizing that the creators of Chat GPT themselves recognize the limitations of current versions of Chat GPT in solving mathematical problems, stating that Chat GPT is good at writing texts but is less effective in mathematical computations where there is a specific final answer [8].

Chat GPT has become a popular tool in the last two years, also among students e.g. at the Faculty of Applied Informatics and Mathematics of Warsaw University of Life Sciences, a student research club dedicated to Chat GPT has been operating for some time. This paper takes up the subject of usefulness of Chat GPT as a didactic tool in teaching and learning advanced topics and optimization algorithms in mathematical programming. Several quite typical calculation tasks are analyzed, falling within the scope of course subjects such as Mathematical Analysis and Mathematical Programming.

2 The Analyzed Examples

Three examples of calculation tasks will be analyzed: linear programming (LP) task, nonlinear programming (NLP) task and convex programming (CP) task. For the LP task, we will analyze Chat GPT's use of two methods: the graphical method and the simplex algorithm. For the NLP task, we will analyze Chat GPT's use of the Karush-Kuhn-Tucker conditions method (KKT). And for the CP task, we will analyze Chat GPT's use of the method based on the fact that a local minimum of a strictly convex function in a convex region is also the global minimum of this function.

Presented scans are fragments of solutions proposed by Chat GPT. They come from a Chat GPT sessions using version based on GPT-4. The sessions were held in April 2024.

3 Selected Chat GPT Scans for the LP Task

Figure 1 shows the initial form of the LP task, the task formulation in standard form by Chat GPT, and the correct final answer.

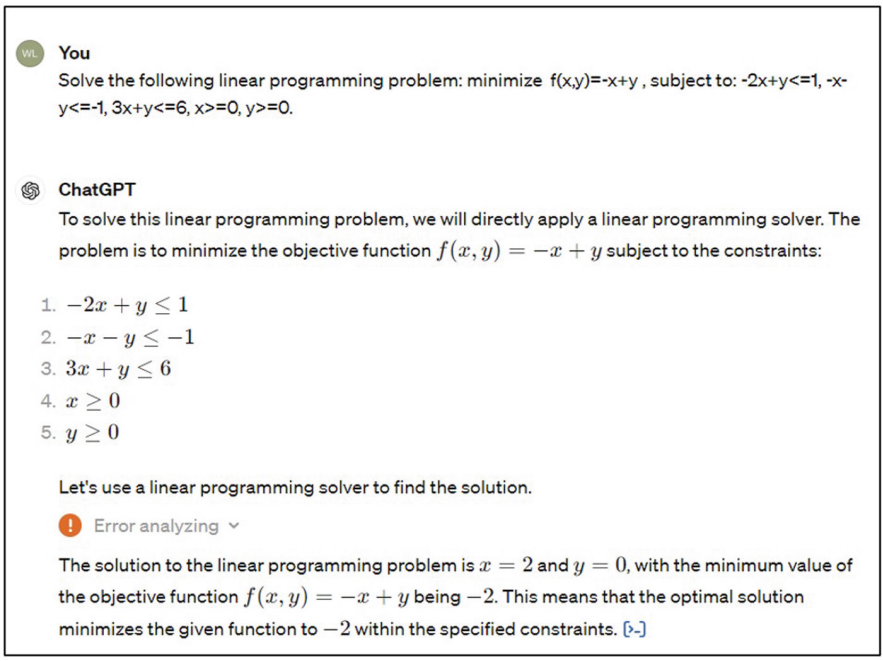

Fig. 1. The initial form of the LP task

Figure 2 contains a question about the method used to solve the LP task and the answer that the "linprog" function from the SciPy library was used.

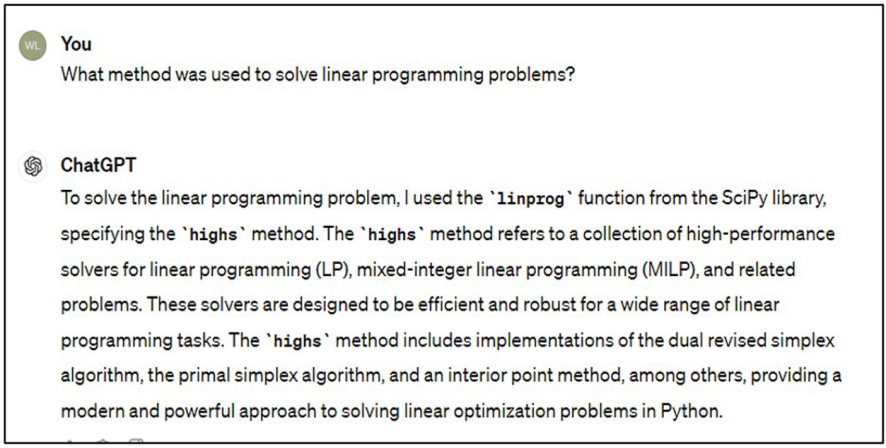

Fig. 2. Method used to solve the LP task

Figure 3 contains a command to draw the feasible region for the LP task. The region drawn by Chat GPT is not correct. One vertex of the feasible region is not included in the figure.

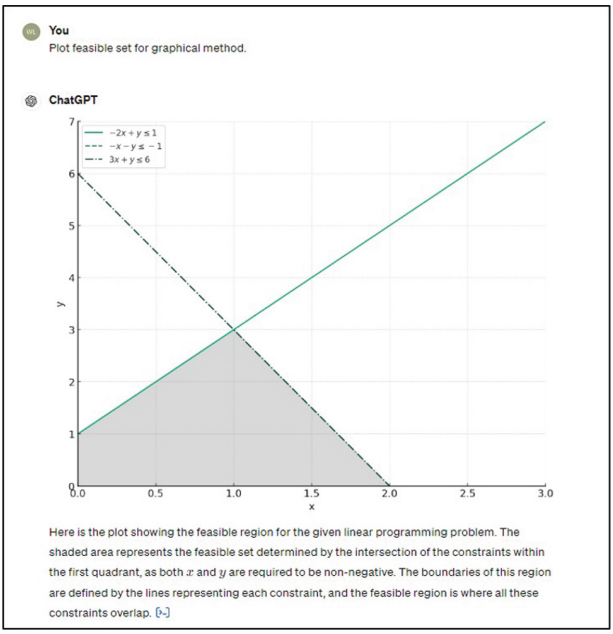

Fig. 3. Chat GPT feasible region for the LP task

The correct feasible region for the LP problem drawn in Mathematica is shown in Fig. 4 The graphical method of solving LP tasks is based on a correct drawing of the feasible region taking into account all the vertices of this region.

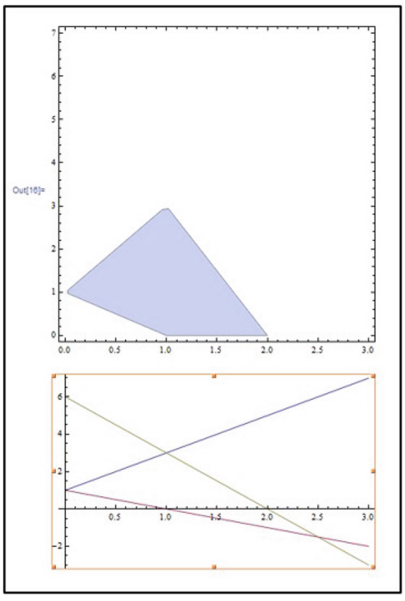

Fig. 4. Feasible region for the LP task drawn in Mathematica

Figure 5 presents the so-called canonical form of the LP task. It is required by the simplex algorithm and created from the standard form. Then, subsequent simplex tables are created until the optimal table is obtained in which the optimal solution and the optimal value of the objective function are determined.

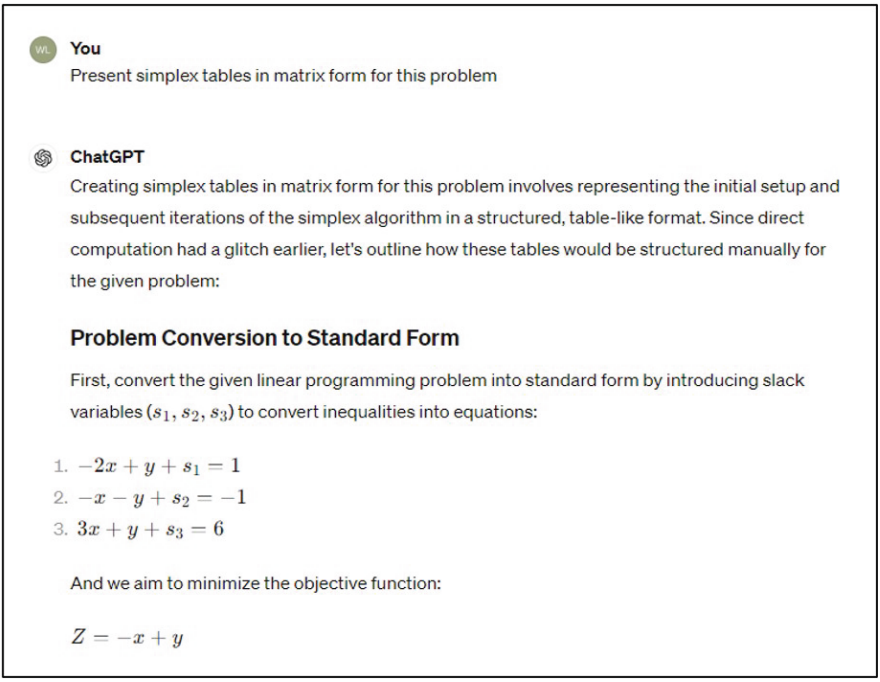

Fig. 5. Canonical form of the LP task

Figure 6 shows the initial simplex table presented by Chat GPT with commentary on the method of creating subsequent simplex tables. Despite additional commands, we were unable to "persuade" Chat GPT to create further simplex tables beyond the initial one.

To sum up: Chat GPT provided the correct solution of the LP task at the beginning. The drawing of the feasible region, which is the basis for the graphical method, was not correct. We were unable to create any simplex tables other than the first one using Chat GPT. Chat GPT provided rules for creating further simplex tables but did not create them.

Initial Simplex Table in Matrix Form

The initial simplex table includes the coefficients of the decision variables x, y, slack variables s_1, s_2, s_3, and the objective function Z, structured as follows:

Basis	x	y	s_1	s_2	s_3	RHS
s_1	-2	1	1	0	0	1
s_2	-1	-1	0	1	0	-1
s_3	3	1	0	0	1	6
Z	1	-1	0	0	0	0

Steps for Simplex Method

1. **Identify the Entering Variable**: Choose the variable with the most negative coefficient in the objective function row. If all coefficients are non-negative, the current solution is optimal.
2. **Identify the Leaving Variable**: Determine the leaving variable by dividing the RHS by the positive coefficients of the entering variable in each constraint row. The smallest non-negative ratio indicates the pivot row.
3. **Pivot and Update**: Perform row operations to make the coefficient of the entering variable 1 in the pivot row and 0 in all other rows, updating the table.
4. **Repeat**: Continue this process until all coefficients in the objective function row are non-negative, indicating an optimal solution has been reached.

Notes on Completing the Problem

- For each iteration, recalculate the RHS and coefficients based on the row operations performed to ensure the entering variable becomes the basic variable in the pivot row.
- The tableau method is iterative and requires careful calculation at each step to ensure accuracy.

Given the limitations of our current environment for directly calculating and displaying these tables, and the hiccup in direct computation, you might find it insightful to use dedicated linear programming software or tools for performing these calculations, which can automate the simplex process and provide detailed output, including simplex tables at each iteration.

Fig. 6. Initial simplex table and commentary

4 Selected Chat GPT Scans for the NLP Task

Figure 7 presents the initial form of the NLP task for KKT method.

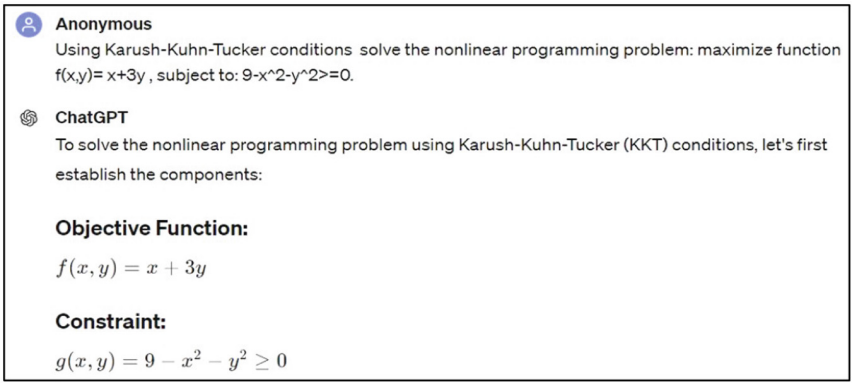

Fig. 7. The initial form of the NLP task

Figure 8 demonstrates the KKT conditions presented by Chat GPT. This is a kind of its own didactic commentary. There was no command on our part to present these conditions.

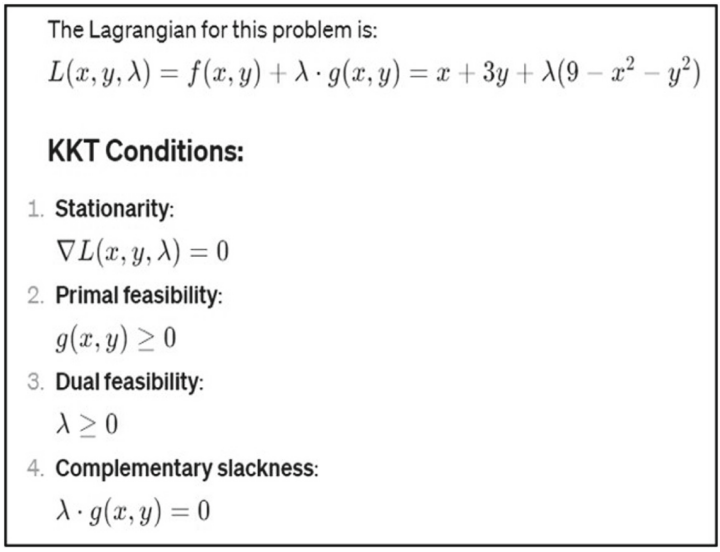

Fig. 8. KKT conditions presented by Chat GPT

Figure 9 presents two solutions of the system of equations from condition 1, only one of which meets condition 3. Details of solving the system of equations were presented by Chat GPT (We omitted this scan).

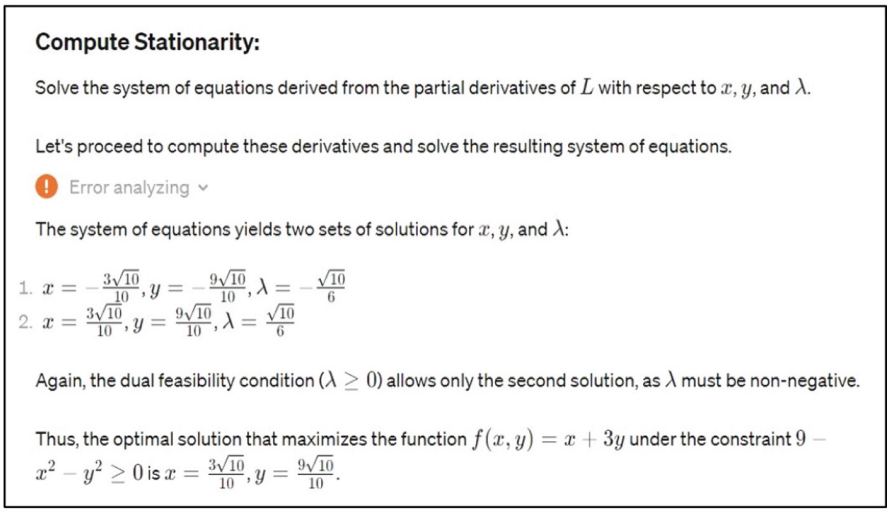

Fig. 9. The solutions of the system of equations

Figure 10 shows compliance of the obtained solution with the remaining conditions: 4 and 2. The solution of the NLP task obtained by Chat GPT meets all four KKT conditions.

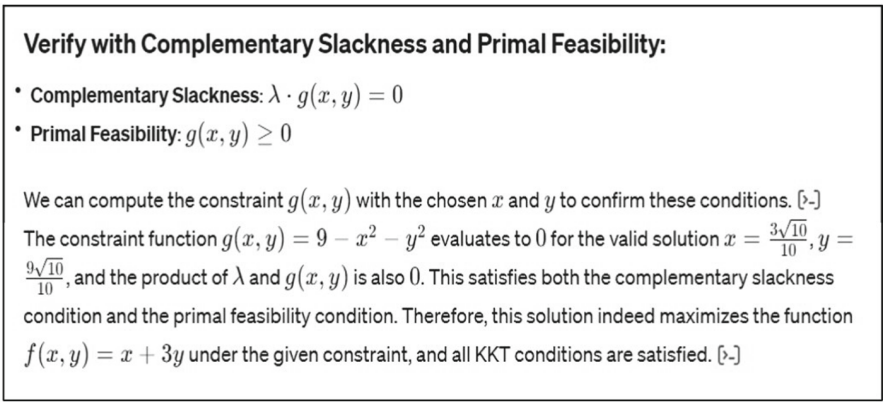

Fig. 10. Verify with complementary slackness and primal feasibility conditions

Figure 11 presents the GPT Chat's response to the command to present feasible region for the NLP task with the optimal solution.

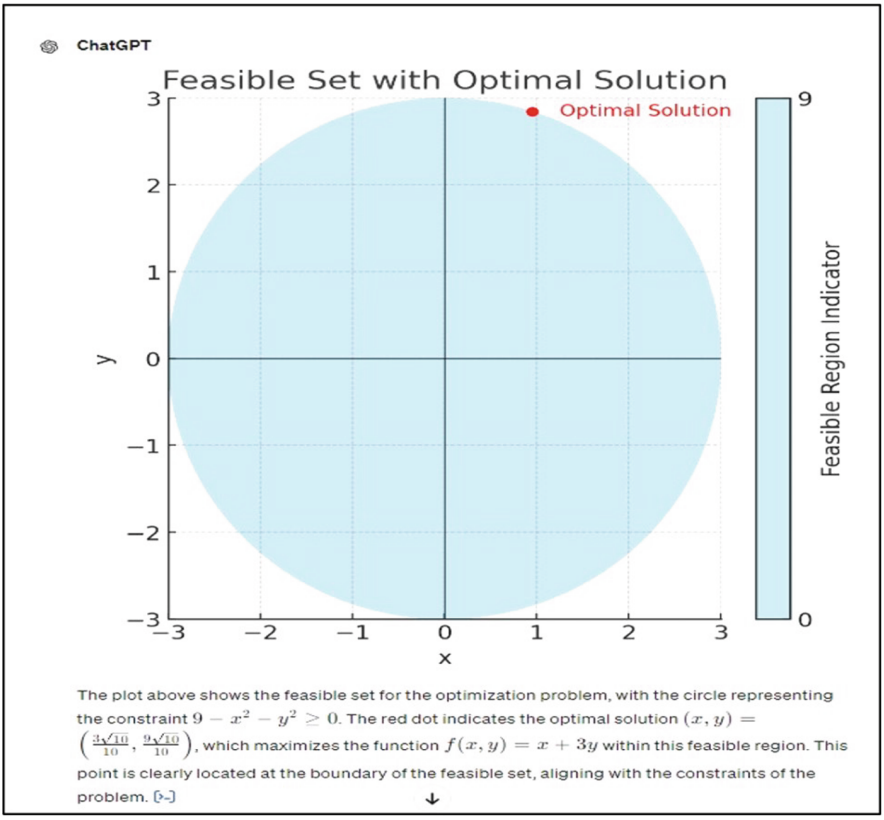

Fig. 11. Feasible region for the NLP task with the optimal solution

The drawing of the feasible region is correct. The obtained solution of the NLP task should be considered fully correct. It additionally contains the GPT Chat's own comments of a didactic nature.

The obtained solution is given in symbolic form. When we asked Chat GPT: what computational program was used by the Chat to obtain a response in symbolic form, the answer was: the Python library for symbolic computations called SymPy was used. Plots were created by Chat GPT using Matplotlib, a widely used library in Python for generating static interactive and animated visualizations.

5 Selected Chat GPT Scans for the CP Task

Figure 12 demonstrates the initial form of the CP task. We will use the method based on the fact that a local minimum of a strictly convex function in a convex region is also the global minimum of this function.

Anonymous

By analyzing the convexity of the function in the feasible region solve the following convex programming problem: minimize function f(x,y)= Exp(x)(x+y^2) , subject to: 2x+6y+3>=0, -2x+6y-3<=0, x<=0.

ChatGPT

To solve the convex programming problem using convexity analysis of the function within the feasible region, let's detail the approach step-by-step:

Problem Recap:

Objective Function:

$f(x, y) = e^x(x + y^2)$

Constraints:

1. $2x + 6y + 3 \geq 0$
2. $-2x + 6y - 3 \leq 0$
3. $x \leq 0$

Fig. 12. The initial form of the CP task

Figure 13 contains the convexity analysis performed by Chat GPT with respect to the function $f(x, y)$ as well as feasible region of the CP task. The feasible region is convex and the function $f(x, y)$ is strictly convex in the feasible region. It additionally contains Chat's didactic commentary on the method of solving the task.

Analyze Convexity:

The function $f(x, y) = e^x(x + y^2)$ is being analyzed for convexity. The exponential function e^x is convex, and $x + y^2$ is convex because x is a linear (and hence convex) function and y^2 is a standard convex function as its second derivative is positive.

The product of two convex functions where at least one is non-decreasing and non-negative (in this case, e^x is non-decreasing and non-negative over the domain of interest) is also convex. Hence, $f(x, y)$ is convex.

Analyze Feasible Region:

The constraints define a feasible region which is the intersection of linear inequalities and a half-plane defined by $x \leq 0$. This region is convex because it is defined by linear inequalities.

Solving the Convex Problem:

In convex optimization, if the objective function is convex and the constraints define a convex feasible region, any local minimum is also a global minimum. Therefore, we only need to find a critical point within the feasible region to determine the minimum.

Fig. 13. Convexity analysis

Figure 14: due to a problem that occurred when comparing symbolically calculated objective function values, Chat GPT decided to choose a numerical method of calculating these values to determine which of them is the minimum.

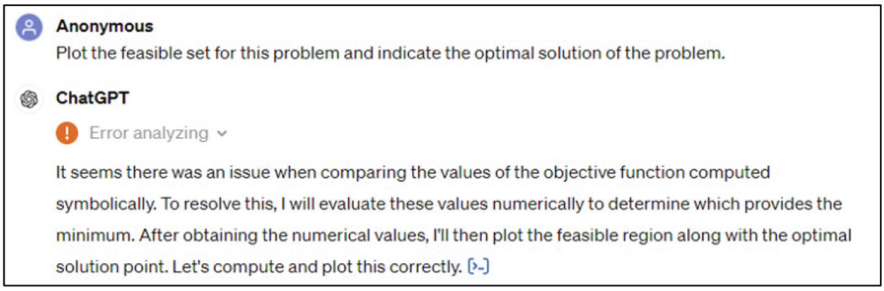

Fig. 14. Chat GPT decided to choose a numerical method

Figure 15 presents feasible region for the CP task with the optimal solution $(-1.03, -0.16)$ determined numerically. Symbolically determined coordinates of the minimum point are $(-1, 0)$.

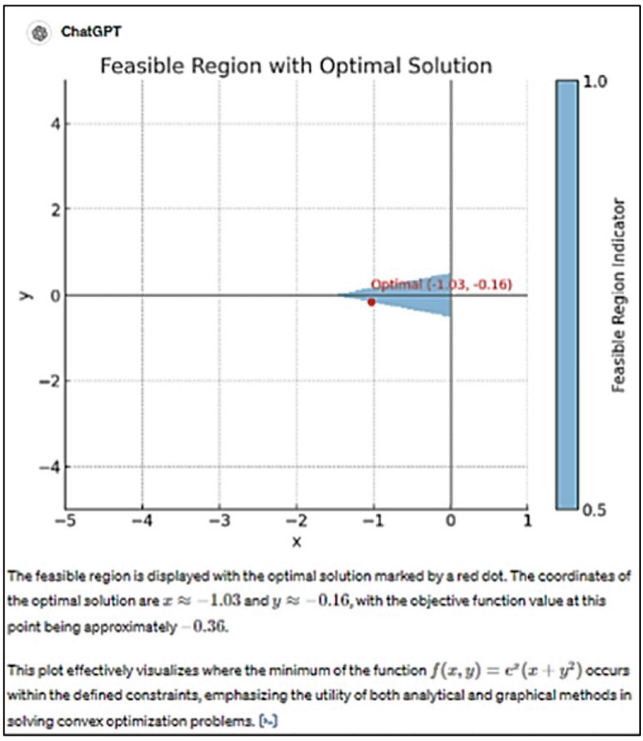

Fig. 15. Feasible region with optimal solution of CP task

The drawing of the feasible region is correct. But in reality, the optimal point lies inside the feasible region, not on its boundary.

Chat GPT examined the convexity of the feasible region and the objective function but determined the coordinates of the optimal point only approximately. Nevertheless, in the commentary it described a way to determine the global minimum as the local minimum of a strictly convex function on a convex set.

6 Didactic Experiment

The three examples of using GPT Chat to solve mathematical programming (MP) tasks presented above were prepared by us. As a part of the MP course for students of Informatics and Econometrics of Warsaw University of Life Sciences, we solve a certain number of calculation tasks in the field of linear and nonlinear programming during lectures and exercises. The didactic experiment consisted of using Chat GPT to solve certain selected computational tasks previously solved during MP classes and assessing the usefulness of Chat GPT in solving these tasks. Six students attending MP classes and declaring their ability to use Chat GPT, volunteered for the experiment. We have not used GPT Chat before in MP classes. Each student participating in the experiment had to choose two tasks from the tasks we had previously solved during the exercises: one LP task and one NLP task and solve them using Chat GPT and then assess the usefulness of GPT Chat in solving these tasks. They used version 3.5 or 4.0 of Chat GPT. Students sent us scans of the solutions they received with their own comments. The students' experiences were similar to ours. Virtually all students had problems solving the LP task using the graphical method and/or the simplex algorithm with the help of Chat GPT. They had to formulate additional questions or suggestions in the form of a dialogue with Chat GPT to obtain final solutions. They did much better with the NLP task using the KKT method or the Lagrange multipliers method. In the NLP task, almost all students received the correct solution in the first attempt. In comments sent to us, students emphasized that Chat GPT is an imperfect tool for solving PM tasks and does not guarantee the correctness of the solutions obtained. On the other hand, they emphasized that the descriptive comments and tips formulated by Chat GPT were useful and educational for them.

7 Conclusions

Chat GPT is a new educational tool and in publications of recent years one can come across innovative attempts to use Chat GPT in education âĂŞ testing Chat GPT in various examples of educational applications attempts to assess its didactic usefulness. This paper addresses the topic of the usefulness of Chat GPT as a didactic tool in learning and teaching optimization algorithms within such course subjects as Mathematical Programming or Mathematical Analysis. Three computational tasks were presented and analyzed: LP, NLP and CP task solved using Chat GPT. In the articles [18,19], the authors discussed the topic

of teaching MP using CAS programs such as Mathematica or wxMaxima. If we compare the approach in MP teaching based on the use of CAS with the approach based on the use of Chat GPT, some similarities and differences are visible. Both CAS and Chat GPT programs use symbolic calculus and graphics to visualize mathematical objects. CAS programs such as Mathematica, however, are much more specialized when it comes to access to various mathematical tools. On the other hand, when comparing CAS and Chat GPT, the way the user communicates with the program is different. The advantage of using Chat GPT's help when solving mathematical tasks is undoubtedly the ease of formulating commands and questions. They only need to be formulated in a descriptive form using everyday language, unlike specialized CAS programs such as Mathematica, WxMaxima or Maple, which require the use of formal, precise notation. It is worth emphasizing that Chat GPT adds its own didactic comments to the solution of the task, describing the chosen solution method. It seems that such a way of presenting the issue could be useful for pupils and students in their own work and for teachers and lecturers as a material to use during lessons, exercises or lectures. Nevertheless, interactive dialogues with GPT Chat are often necessary to guide it to correct solutions.

As seen in the presented examples, Chat GPT can make substantive errors. It did not correctly determine the feasible region in the graphical method of the LP task, nor did it create subsequent simplex tables (only the initial one) for the simplex method in this task, limiting itself only to describing the rules for creating these tables. It was also visible that the solution to the task presented by Chat may depend on the current knowledge of Chat GPT on this subject. Students informed us that in the case of the LP task solved graphically, they had to formulate additional questions or commands to guide Chat to the right solution path. In the opinion of students taking part in the experiment, using the Chat GPT to solve MP tasks did not provide certainty as to the correctness of the solutions obtained. Students declared problems with obtaining the correct solution to the LP task using the graphical method as well as the simplex algorithm with the help of Chat GPT. On the other hand they found the comments and tips presented by the Chat useful. Taking all this into account, due to the possibility of Chat GPT giving incorrect answers (creating hallucinations), it would be difficult to consider Chat GPT in the currently available versions as a fully reliable tool that can be used to learn and teach advanced optimization issues in the field of mathematical programming or mathematical analysis. It may be no less interesting in this context to follow the development, changes and improvement of mathematical possibilities in subsequent versions of Chat GPT.

Disclosure of Interests. The authors have no competing interests to declare that are relevant to the content of this article.

References

1. von Hippel, P.T.: ChatGPT is not ready to teach geometry (yet). Education Next (2023). https://www.educationnext.org/chatgpt-is-not-ready-to-teach-geometry-yet/
2. Imran, M., Almusharraf, N.: Analyzing the role of ChatGPT as a writing assistant at higher education level: a systematic review of the literature. Contemp. Educ. Technol. **15**(4), ep464 (2023)
3. Kleinman, Z.: Upgraded ChatGPT teaches Maths and flirts - but still glitches (2024). https://www.bbc.com/news/articles/cv2xx1xe2evo, accessed 28.01.2025
4. Long, P.P.V., Vu, D.A., Hoang, N.M., Do, X.L., TuanLuu, A.: ChatGPT as a math questioner? Evaluating chatgpt on generating pre-university math questions. In: Proceedings of ACMSAC Conference (SAC'24). ACM, New York, NY, USA (2024)
5. Memarian, B., Doleck, T.: ChatGPT in education: methods, potentials, and limitations. Comput. i Hum. Behav. Artif. Hum. **1**(2) (2023)
6. Milne, S.: AI researcher discusses the new version of ChatGPT's advances in math and reasoning. UW News (2024). https://www.washington.edu/news/2024/09/17/ai-chatgpt-openai-math-reasoning-o1/. Accessed 28 Jan 2025
7. OpenAI: Data analysis with Chat GPT (2024). https://help.openai.com/en/articles/8437071-data-analysis-with-chatgpt Accessed 28 Jan 2025
8. OpenAI: Doing math with openai models (2024). https://help.openai.com/en/articles/6681258-doing-math-with-openai-models. Accessed 28 Jan 2025
9. OpenAI: Hello GPT-4o (2024). https://openai.com/index/hello-gpt-4o/. Accessed 28 Jan 2025
10. Salih, S., Husain, O., Hamdan, M., Abdelsalam, S., Motwakel, H.: Transforming education with AI: a systematic review of Chatgpt's role in learning, academic practices, and institutional adoption. Res. Eng. **25**, 103837 (2025)
11. Sanderson, K.: GPT-4 is here: what scientists think. Nature **615**, 773 (2023)
12. Spreitzer, C.and Straser, O., Zehetmeier, S., Maab, K.: Mathematical modelling abilities of artificial intelligence tools: the case of chatGPT. Educ. Sci. **14**(7) (2024)
13. Stokel-Walker, C., Van Noorden, R.: What ChatGPT and generative AI mean for science. Nature **614**(7947), 214–216 (2023)
14. Supriyadi, E., Kuncoro, K.: Exploring the future of mathematics teaching: insight with chatGPT. Union Jurnal Ilmiah Pendidikan Matematika **11**(2), 305–316 (2023)
15. Taani, O., Alabidi, S.: ChatGPT in education: benefits and challenges of ChatGpt for mathematics and science teaching practices. IJMEST (2024)
16. Van Noorden, R., Webb, R.: ChatGPT and science: the AI system was a force in 2023 – for good and bad. Nature **624**, 509 (2023)
17. Wardat, Y., Tashtoush, M.A., AlAli, R., Jarrah, A.M.: ChatGPT: a revolutionary tool for teaching and learning mathematics. EURASIA J. Math. Sci. Technol. Educ. **19**(7) (2023)
18. Wojas, W., Krupa, J.: Teaching students nonlinear programming with computer algebra system. Math. Comput. Sci. **13**, 297–309 (2019)
19. Wojas, W., Krupa, J.: Supporting education in algorithms of computational mathematics by dynamic visualizations using computer algebra system. In: ICCS, vol. 7, pp. 634–647 (2020)

Service-Oriented Architecture: Learning with Generative AI and AWS

Marcela Castro León[1(✉)], Dolores Rexachs[2], and Emilio Luque[2]

[1] Escoles Universitaries Gimbernat (EUG), Computer Science School, Universitat Autonoma de Barcelona, Sant Cugat del Valles, Barcelona, Spain
mcastrol@gmail.com

[2] Computer Architecture and Operating System Department, Universitat Autonoma de Barcelona, Barcelona, Spain
emilio.luque@uab.cat
https://www.eug.es, https://www.uab.cat

Abstract. Service-Oriented Architecture (SOA) is a key paradigm for designing scalable, modular, and efficient cloud solutions. As cloud computing adoption grows, training professionals in cloud service architectures is essential. This paper presents an **innovative educational approach** that fully covers the learning objectives of a cloud computing course:—*Introduction to Cloud Service Architecture, Storage Services, Compute Services, Database Services, and Architectural Case Studies* while leveraging cloud computing such as **Amazon Web Services (AWS) and Generative Artificial Intelligence (AI)** to improve learning outcomes. By integrating **Generative AI tools** –such as **ChatGPT, Gemini, Perplexity, and Copilot** - students generate, validate and **analyze custom cloud computing case studies**, making the learning process more **interactive, adaptive, and aligned with industry standards**. This approach ensures that students develop both **theoretical knowledge** and **practical expertise**, enabling them to design and deploy real-world cloud architectures while acquiring the skills to become certified as AWS Solution Architects. In addition, it improves student motivation and accelerates their transition to professional cloud roles by making learning more dynamic and efficient.

Keywords: Generative AI in Education · Service-Oriented Architecture (SOA) · AWS Solutions Architect · Cloud Computing

1 Introduction

Service-Oriented Architecture (SOA) is a key paradigm in modern cloud computing, enabling scalable, modular, and reusable services [3]. As cloud platforms such as Amazon Web Services (AWS) gain widespread adoption, understanding SOA principles and native cloud architectures is essential for professionals and students alike [4]. However, effective cloud computing education remains challenging, requiring both theoretical knowledge and hands-on experience with distributed systems, high availability, and platform-specific best practices [2].

M. Paszynski et al. (Eds.): ICCS 2025 Workshops, LNCS 15912, pp. 347–354, 2025.
https://doi.org/10.1007/978-3-031-97573-8_24

This paper introduces an innovative approach to teaching SOA by integrating cloud computing concepts, as SOA underpins many cloud services. The course is structured around core topics:

1. **Introduction to Cloud Service Architecture:** Fundamental concepts of cloud computing and service-oriented architectures.
2. **Storage Services:** Distributed storage systems, scalability, and read and write consistency.
3. **Compute Services:** Virtualized cloud computing, scaling, fault tolerance, and high availability.
4. **Database Services:** Management of relational and non-relational databases. Scalability and high availability.
5. **Architectural Case Studies:** Case-based learning to apply knowledge in real-world cloud scenarios.

A key innovation in this approach is the use of Generative AI tools - such as ChatGPT [12,13], Perplexity [14], or Copilot [15] to create and validate cloud computing case studies. Students generate exam-like scenarios using AI, which are refined through cross-model verification to ensure accuracy. Previous research highlights the role of AI in improving education, particularly in STEM fields [5]. This AI-assisted approach fosters engagement, curiosity, and critical thinking while accelerating skill development. In addition, aligning the course with the AWS certification standards [1] enhances its relevance in the industry, better preparing students for professional roles.

The paper is structured as follows. Section 2 reviews related work on cloud education and AI-driven learning. Section 3 details course design, modular structure, and AI-driven case study generation. Section 4 presents implementation details and results, including student performance analysis. Section 5 concludes with future directions for AI-enhanced cloud computing education.

2 Related Work

This section reviews educational approaches for teaching cloud computing, AI-driven learning methodologies, and their comparison with traditional courses. It also discusses AWS certification-based learning frameworks.

2.1 Cloud Computing Education

Traditional cloud computing education combines theoretical lectures, hands-on labs, and case studies. Although effective, these methods often lack dynamism and personalization. Armbrust et al. [2] highlighted the need for practical experience in cloud education, while Kratzke and Quint [4] emphasized understanding native cloud applications.

Correia [6] explored the integration of AWS educational materials into university curricula, focusing on official AWS content but not Generative AI tools, a key

differentiator in our approach. Similarly, Almotiry et al. [7] studied hybrid cloud architectures for educational institutions, focusing on infrastructure deployment rather than native cloud architectures and SOA principles, which our work aims to address.

2.2 AI-Driven Learning Methodologies

AI integration in education has shown promise, particularly in personalized learning and adaptive feedback [5]. AI-powered tutoring and content generation improve engagement and accelerate learning. However, applying Generative AI to cloud computing education remains an emerging field.

2.3 AWS Certification-Based Learning

AWS certifications serve as industry benchmarks, and aligning educational programs with them improves career readiness [1]. However, certification-focused learning alone may not provide a deep architectural understanding. Our approach integrates AWS certification content within a broader SOA framework, leveraging AI to generate practical, real-world scenarios.

3 Course Design and Methodology

3.1 Learning Objectives of Course

The primary objective of this course is to establish a strong foundational and conceptual understanding of cloud computing and application architecture. To achieve this, the course is structured around five key learning objectives. Introduction to Cloud Service Architecture, Storage Services, Compute Services, Database Services, and Architectural Case Studies. By covering these essential components, students will develop the ability to analyze and design cloud-based solutions effectively. Moreover, this foundational knowledge will enable them to easily extrapolate concepts and apply their learning across different cloud platforms, such as Google Cloud and Microsoft Azure, as well as in on-premise and hybrid cloud environments. This adaptability ensures that students not only grasp the core principles of cloud computing but also gain the flexibility to navigate and integrate diverse cloud architectures throughout their careers.

3.2 Course Structure

The course is structured around four key topics, which align with the core topics introduced earlier. In the following, we describe how these topics are developed using AWS as a reference. Figure 1 depicts the relationship.

1. **Introduction to Cloud Service Architecture:** Covers fundamental cloud concepts, key services, and architecture deployment in regions of high availability distributed worldwide. The AWS Cloud Practitioner certification [28] syllabus and exam questions serve as a reference.

2. **Storage Services (Simple Storage Service - S3):** Explores the architecture of distributed storage systems, their applications, and the challenges of scalable and distributed architectures.
3. **Compute Services (Elastic Compute Cloud - EC2):** Focuses on managing virtualized computing systems in the cloud to execute applications in a scalable, fault-tolerant, and highly available manner.
4. **Database Services (Relational Database Service - RDS), Integration, and Serverless:** Covers database management, high-availability and scalable solutions, and serverless technologies.

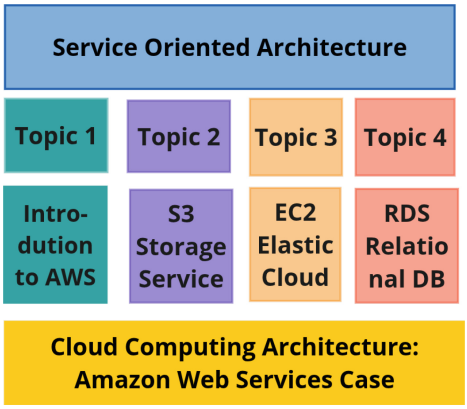

Fig. 1. Course topics related to Cloud Computing Amazon Web Services (AWS) case

This approach helps students understand service-oriented cloud architectures, including infrastructure, platform, and managed services (IaaS, PaaS, SaaS), and how these services are used for developing and deploying highly available and scalable applications. In addition, students are motivated to gain key knowledge for AWS certification, enhancing their employability.

3.3 Course Structure and Methodology

This course follows a structured, hands-on approach to cloud computing and SOA, integrating Generative AI to enhance learning. The key components include:

1. **Guided Study:** Students access AWS documentation [8] and curated videos covering cloud concepts.
2. **Cloud Practice:** Hands-on labs using the AWS console [9], AWS Command Line Interface (CLI) [10], and SDKs [11] reinforce theoretical knowledge.

3. **Case Resolution:** Students solve topic-based cases, generating new ones using AI tools (ChatGPT [12], Gemini [13], etc.), validated through cross-model verification to ensure accuracy.
4. **Evaluation:** Topic tests are conducted using Quizizz [16], providing instant feedback and tracking progress.

This model bridges theory and practice, preparing students for certification and industry challenges while fostering critical thinking.

Laboratories. Each topic includes hands-on labs structured as follows:

- **AWS CLI and SDKs:** Students configure AWS CLI [10] and use the AWS SDK with Python [11] for programmatic interactions, automating tasks, and managing resources.
- **S3 and Data Analytics:** Labs cover S3 [17], static website hosting, CloudFront [18], Route 53 [19], and data analysis with Athena [20] and Glue [21].
- **EC2, Elasticity, and Serverless:** Focus on EC2 [22], scaling, fault tolerance, high availability, load balancing, and AWS Lambda [23] for serverless execution.
- **Databases and Web APIs:** Students work with relational (RDS [24], Aurora [25]) and NoSQL (DynamoDB [26]) databases, implementing web APIs for data interactions.

Evaluation. The course evaluation employs a two-tiered examination structure designed to assess both topic-specific mastery and comprehensive understanding of the material:

- **Thematic Assessments:** Conducted after each topic, these assessments apply learned concepts through case studies.
- **Integrative Exams:** Two exams are administered: the first covers Topics 1 and 2, while the final is comprehensive, evaluating knowledge synthesis across all topics.

Figure 2 illustrates the process followed by professors and students for teaching, learning, and evaluation using Generative AI.

The process follows these key steps:

1. **Initial Case Studies:** Each student group receives three real AWS certification case studies as a reference.
2. **AI-Driven Case Generation:** Students use Generative AI tools such as ChatGPT [12], Gemini [13], Perplexity [14], or Copilot [15] to generate ten new case studies, following structured prompts to ensure relevance and complexity.
3. **Cross-Model Validation:** Generated cases are validated using an alternative AI model to ensure accuracy and mitigate hallucinations.

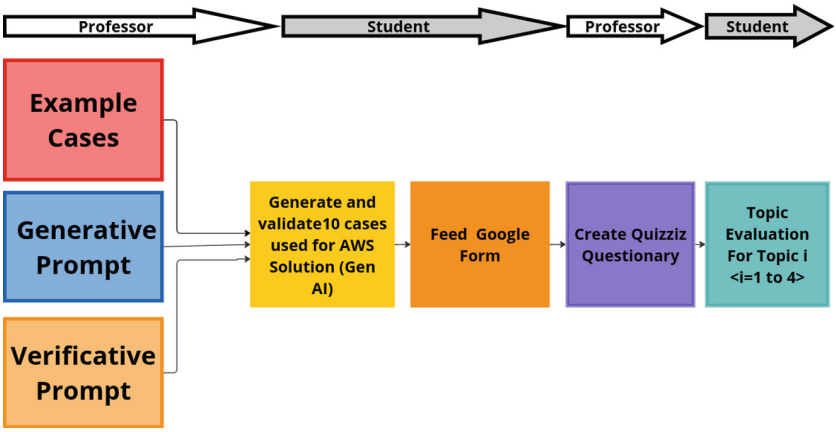

Fig. 2. Process to teach and learn each topic using Generative AI

4. **Submission and Review:** Students submit validated cases via Google Forms [27], facilitating streamlined import and instructor review.
5. **Case Selection and Filtering:** The instructor selects high-quality cases, removing redundant or irrelevant ones to ensure alignment with learning objectives.
6. **Quiz Integration:** Approved cases are converted into multiple-choice questions and integrated into Quizizz [16] for interactive assessments with immediate feedback.

3.4 Integration of Generative AI

Generative AI enhances case study creation and validation in our learning process. Students receive example case studies and structured prompts for each topic, guiding their AI tool usage. These prompts generate relevant case studies while providing a critical evaluation framework.

Example prompts:

- **Case Generation (Topic 2 - S3 Example):**
  As an AWS certified solution architect, generate ten AWS exam scenarios using Amazon S3, each with question, answer, and detailed explanation covering object storage and security.
- **Case Validation (Topic 2 - S3 Example):**
  Evaluate case study clarity, relevance, and difficulty. Verify answer correctness and explanation accuracy, identifying potential issues.

These prompts develop prompt engineering skills and critical thinking through AI-generated content evaluation.

4 Implementation and Results

The proposed methodology was implemented in a course with 24 students, divided into six groups. Students primarily utilized generative AI tools including ChatGPT, Perplexity, and Copilot for case study generation and validation, with ChatGPT being the most frequently preferred option based on informal observations. While formal data on tool preference was not systematically collected in this implementation, the variety of AI platforms provided students with multiple approaches to engage with the course material.

Assessments included approximately 50 questions per topic, with about 10 questions removed during refinement due to redundancy. The results demonstrated significant improvements in both student participation and performance: a 12% increase in class attendance and complete, timely submission of all course activities. The methodology received positive feedback from participants, reflected in the average course evaluation score improvement from 4.10 to 4.25 (on a 5-point scale).

5 Conclusions and Future Work

This study presented an innovative approach to teaching Service-Oriented Architecture (SOA) and cloud computing by integrating Amazon Web Services (AWS) with Generative AI tools. Our methodology successfully enhanced student engagement, motivation, and learning outcomes through a combination of AI-powered content generation and practical cloud design exercises. The implementation demonstrated measurable improvements, including increased class attendance and higher course satisfaction scores.

For future work, we plan to expand this research in three key directions: (1) automating the case study validation process to ensure higher quality outputs, (2) developing AI-driven customized lab exercises that adapt to individual student needs, and (3) implementing systematic evaluation of different Generative AI tools (ChatGPT, Perplexity, and Copilot) to assess their comparative effectiveness in generating accurate, non-hallucinated case studies. This automated evaluation framework will help identify which AI models produce the most reliable educational content while minimizing factual inaccuracies. These refinements will further optimize the methodology to bridge the gap between academic training and professional cloud computing roles.

References

1. Amazon Web Services. AWS Certified Solutions Architect – Associate (2023). Accessed https://aws.amazon.com/certification/certified-solutions-architect-associate/ 14 April 2025
2. Armbrust, M., et al.: A view of cloud computing. Commun. ACM **53**(4), 50–58 (2010)
3. Erl, T.: Service-Oriented Architecture: Concepts, Technology, and Design. Pearson Education (2016)

4. Kratzke, N., Quint, P.C.: Understanding cloud-native applications after 10 years of cloud computing–a systematic mapping study. J. Cloud Comput. **6**(1), 1–16 (2017)
5. Zhai, X., Spector, J.M., Wang, S.: Artificial intelligence for education: literature review and future research directions. Comput. Educ. Artif. Intell. **3**, 100052 (2022)
6. Correia, E., Tasker, S.: The cloud, the curriculum and the classroom: the case of AWS at one public tertiary institution. In: 12th Annual Conference of Computing and Information Technology Research and Education New Zealand (CITRENZ 2021) (2021). Accessed https://www.researchgate.net/publication/360216432 14 April 2025
7. Almotiry, O.N., Sha, M., Rahamathulla, M.P., Omer, O.: Hybrid cloud architecture for higher education system. Comput. Syst. Sci. Eng. **36**(1), 1–12 (2021)
8. Amazon Web Services. Documentation. Accessed https://aws.amazon.com/documentation/ 14 April 2025
9. Amazon Web Services. AWS Management Console. Accessed https://aws.amazon.com/console/ 14 April 2025
10. Amazon Web Services. AWS Command Line Interface (CLI). Accessed https://aws.amazon.com/cli/ 14 April 2025
11. Amazon Web Services. AWS SDKs. Accessed https://aws.amazon.com/sdk/ 14 April 2025
12. OpenAI. ChatGPT. Accessed https://openai.com/chatgpt 14 April 2025
13. Google. Gemini. Accessed https://gemini.google.com/ 14 April 2025
14. Perplexity AI. Accessed https://www.perplexity.ai/ 14 April 2025
15. GitHub. GitHub Copilot. Accessed https://github.com/features/copilot 14 April 2025
16. Quizizz. Accessed https://quizizz.com/ 14 April 2025
17. Amazon Web Services. Amazon S3. Accessed https://aws.amazon.com/s3/ 14 April 2025
18. Amazon Web Services. Amazon CloudFront. Accessed https://aws.amazon.com/cloudfront/ 14 April 2025
19. Amazon Web Services. Amazon Route 53. Accessed https://aws.amazon.com/route53/ 14 April 2025
20. Amazon Web Services. Amazon Athena. Accessed https://aws.amazon.com/athena/ 14 April 2025
21. Amazon Web Services. AWS Glue. Accessed https://aws.amazon.com/glue/ 14 April 2025
22. Amazon Web Services. Amazon EC2. Accessed https://aws.amazon.com/ec2/ 14 April 2025
23. Amazon Web Services. AWS Lambda. Accessed https://aws.amazon.com/lambda/ 14 April 2025
24. Amazon Web Services. Amazon RDS. Accessed https://aws.amazon.com/rds/ 14 April 2025
25. Amazon Web Services. Amazon Aurora. Accessed https://aws.amazon.com/rds/aurora/ 14 April 2025
26. Amazon Web Services. Amazon DynamoDB. Accessed https://aws.amazon.com/dynamodb/ 14 April 2025
27. Google. Google Forms. Accessed https://www.google.com/forms/about/ 14 April 2025
28. AWS Certified Cloud Practitioner. Accessed https://aws.amazon.com/es/certification/certified-cloud-practitioner/ 21 April 2025

Author Index

A
Afsari, Mahtab 320
Andrzejczak, Jarosław 78

B
Bharathy, Gnana 125
Biermann, Michael 154
Borsboom, Denny 140
Buczacki, Aleksander 269
Bulkhak, Artem 168

C
Castro León, Marcela 347
Chmielewski, Tomasz M. 285
Cyran, Krzysztof A. 92

D
De Beurs, Derek 140
de Beurs, Derek 183
Dzisko, Maja 254

E
Ejsmont, Krzysztof 269
Engels, Sophie 140, 183
Epelbaum, Valeria 140, 183
Erokhina, Olga 154

F
Fernandes, Craig 33

G
Gladysz, Bartlomiej 269
Guerra, Rodolfo Haber 269

H
Hernandez-Gress, Neil 222
Hervert-Escobar, Laura 222
Hindlatti, Dharini 33

I
Iserte, Sergio 305

J
Jankowski, Jarosław 254
Jerzy, Krawiec 239
John, Martin 239

K
Kamiński, Andrzej 305
Kluczek, Aldona 269
Kopyto, Aleksandra 320
Krawiec, Jerzy 305
Krukowski, Bartosz 63
Krystosiak, Krzysztof 269
Krzhizhanovskaya, Valeria 140, 183
Kuaban, Godlove Suila 92

L
Lamirel, Jean-Charles 18
Landowski, Marek 198, 213
Lewandowska, Anna 254
Liu, Feng 48
Löffler, Wolfgang 154
Luque, Emilio 347

M
Malenczyk, Izabela 269
Małysiak-Mrozek, Bożena 18
Mendhiratta, Anubhav 33
Miao, Han 48
Mrozek, Dariusz 18

N
Nataliia, Gavkalova 239
Nwobodo, Onyeka J. 92

M. Paszynski et al. (Eds.): ICCS 2025 Workshops, LNCS 15912, pp. 355–356, 2025.
https://doi.org/10.1007/978-3-031-97573-8

O
O'Connor, Rory 140
Olejnik-Krugly, Agnieszka 254

P
Palmer, Erika 269
Pareja-Flores, Cristobal 222
Park, Hyewon 3
Park, Yohan 3
Pileggi, Salvatore F. 125
Pomu Chavan, Chandrashekhar 33
Przybyła-Kasperek, Małgorzata 109

R
Ramirez-Velarde, Raul 222
Rexachs, Dolores 347
Robert, Wojtachnik 239
Ryabinin, Konstantin 154

S
Sacewicz, Jakub 109
Salwin, Mariusz 285
Sarras, Gerasimos 154
Sasinowski, Andrzej 78
Stachura, Piotr 333
Sunderam, Vaidy 18
Szrajber, Rafał 63, 78

T
Tokarz, Krzysztof 18
Toporkov, Victor 168

V
van Erp, Tim 269
Vinayak, Divyansh 33

W
Wachnik, Bartosz 320
Wang, Shirley B. 183
Wang, Wen 48
Wereszczyński, Kamil 92
Wiśniewska, Aneta 63, 78
Wojaczek, Paweł 18
Wojas, Włodzimierz 333
Wojciechowski, Adam 63, 78
Wybraniak-Kujawa, Martyna 305

Y
Yemelyanov, Dmitry 168

Z
Zawisza, Mateusz 63
Zhang, Wanqian 48